

Book: Chemistry of the Main Group Elements
(Barron)

This text is disseminated via the Open Education Resource (OER) LibreTexts Project (<https://LibreTexts.org>) and like the hundreds of other texts available within this powerful platform, it is freely available for reading, printing and "consuming." Most, but not all, pages in the library have licenses that may allow individuals to make changes, save, and print this book. Carefully consult the applicable license(s) before pursuing such effects.

Instructors can adopt existing LibreTexts texts or Remix them to quickly build course-specific resources to meet the needs of their students. Unlike traditional textbooks, LibreTexts' web based origins allow powerful integration of advanced features and new technologies to support learning.



The LibreTexts mission is to unite students, faculty and scholars in a cooperative effort to develop an easy-to-use online platform for the construction, customization, and dissemination of OER content to reduce the burdens of unreasonable textbook costs to our students and society. The LibreTexts project is a multi-institutional collaborative venture to develop the next generation of open-access texts to improve postsecondary education at all levels of higher learning by developing an Open Access Resource environment. The project currently consists of 14 independently operating and interconnected libraries that are constantly being optimized by students, faculty, and outside experts to supplant conventional paper-based books. These free textbook alternatives are organized within a central environment that is both vertically (from advance to basic level) and horizontally (across different fields) integrated.

The LibreTexts libraries are Powered by [NICE CXOne](#) and are supported by the Department of Education Open Textbook Pilot Project, the UC Davis Office of the Provost, the UC Davis Library, the California State University Affordable Learning Solutions Program, and Merlot. This material is based upon work supported by the National Science Foundation under Grant No. 1246120, 1525057, and 1413739.

Any opinions, findings, and conclusions or recommendations expressed in this material are those of the author(s) and do not necessarily reflect the views of the National Science Foundation nor the US Department of Education.

Have questions or comments? For information about adoptions or adaptations contact info@LibreTexts.org. More information on our activities can be found via Facebook (<https://facebook.com/Libretexts>), Twitter (<https://twitter.com/libretexts>), or our blog (<http://Blog.Libretexts.org>).

This text was compiled on 03/09/2025

Preface

The main group (*s*- and *p*-block) elements are among the most diverse in the Periodic Table. Ranging from non-metallic gases (e.g., hydrogen and fluorine), through semi-metals (e.g., metalloids such as silicon) to highly reactive metals (e.g., sodium and potassium). The study of the main group elements is important for a number of reasons. On an academic level they exemplify the trends and predictions in structure and reactivity that are the key to the Periodic Table. They represent the diversity of inorganic chemistry, and the fundamental aspects of structure and bonding that are also present for the transition metal, lanthanide and actinide elements.

The main group elements represent the most prevalent elements in the Earth's crust, as well as most of the key elements of life, and have enormous industrial, economic, and environmental importance. In this regard an understanding of the chemistry of the main group elements is vital for students within science, engineering, and medicine; however, it is hoped that those who make political and economic decisions would make better ones (or at least more responsible ones) if they had a fraction of the knowledge of the world around them.

Since the position of the main group elements within the Periodic Table defines their properties (and *visa versa*) this represents a logical organization of the topics. Prior to introducing the elements, a series of general and background topics are covered to provide the basis for further discussion. The subsequent organization is based upon a Chapter for each Group of the *s*- and *p*-block elements; however, hydrogen is given its own chapter due to its importance as an element. Although the Group 12 elements are often omitted from a discussion of main group elements they have been included herein.

Some chapters are organized with regard to individual elements (e.g., carbon, silicon, etc.) and others are arranged with regard the types of compounds (e.g., oxides, halides, etc.). This is based upon particular interest or importance of an element. An effort has been made to ensure that topics are not covered twice (unless necessary) and so in general a particular subject is covered in the Group chapter associated with the lower Group number. For example, the halides of boron are described in the Chapter on the Group 13 elements rather than Group 17 elements.

In addition to the basic synthesis, structure, properties, and reactivity of the elements and their compounds, sections describing some industrial use, as well as historical or social perspective have been added. These sections were as a result of attempts within class to put the chemistry into a context outside of the classroom. It is important that the discovery and use of elements be understood to be a human endeavor rather than a series of abstract concepts or facts. It is only by an appreciation of the past that we can advance the future.

Although this book was developed from the Rice University course Chem 360 (Inorganic Chemistry), and is not intended to be either encyclopedic or overly detailed. Thus, some topics will be covered at a greater or lesser depth depending on the relevance or interest. Given the continued expansion in the chemistry of the main group elements it is intended that appropriate modules will be added as they are developed.

Andrew R. Barron

Rice University, Houston, TX 77005. E-mail: arb@rice.edu.

TABLE OF CONTENTS

Preface

Licensing

1: General Concepts and Trends

- 1.1: Fundamental Properties - Oxidation State
- 1.2: Fundamental Properties - Ionization Energy
- 1.3: Fundamental Properties - Electron Affinity
- 1.4: Fundamental Properties - Electronegativity
- 1.5: Structure and Bonding - Valence Shell Electron Pair Repulsion (VSEPR) Theory
- 1.6: Structure and Bonding - Crystal Structure
- 1.7: Structure and Bonding - Stereochemistry
- 1.8: Acids, Bases, and Solvents - Choosing a Solvent
- 1.9: Chemical Reactivity - The Basics of Combustion
- 1.10: Periodic Trends for the Main Group Elements

2: Hydrogen

- 2.1: Discovery of Hydrogen
- 2.2: The Physical Properties of Hydrogen
- 2.3: Synthesis of Molecular Hydrogen
- 2.4: Atomic Hydrogen
- 2.5: The Proton
- 2.6: Hydrides
- 2.7: The Hydrogen Bond
- 2.8: Isotopes of Hydrogen
- 2.9: Nuclear Fusion
- 2.10: Storage of Hydrogen for Use as a Fuel

3: Group 1 - The Alkali Metals

- 3.1: The Alkali Metal Elements
- 3.2: Compounds of the Alkali Metals
- 3.3: The Anomalous Chemistry of Lithium
- 3.4: Organolithium Compounds

4: Group 2 - The Alkaline Earth Metals

- 4.1: The Alkaline Earth Elements
- 4.2: Calcium the Archetypal Alkaline Earth Metal
- 4.3: Differences for Beryllium and Magnesium
- 4.4: Organometallic Compounds of Magnesium

5: Group 12

- 5.1: The Group 12 Elements
- 5.2: Cadmium Chalcogenide Nanoparticles
- 5.3: Organometallic Chemistry of Zinc
- 5.4: Organomercury Compounds
- 5.5: The Myth, Reality, and History of Mercury Toxicity

6: Group 13

- 6.1: The Group 13 Elements
- 6.2: Trends for the Group 13 Compounds
- 6.3: Borides
- 6.4: Boron Hydrides
- 6.5: Wade's Rules
- 6.6: Trends for the Oxides of the Group 13 Elements
- 6.7: Boron Oxides, Hydroxides, and Oxyanions
- 6.8: Aluminum Oxides, Hydroxides, and Hydrated Oxides
- 6.9: Ceramic Processing of Alumina
- 6.10: Boron Compounds with Nitrogen Donors
- 6.11: Properties of Gallium Arsenide
- 6.12: Electronic Grade Gallium Arsenide
- 6.13: Chalcogenides of Aluminum, Gallium, and Indium
- 6.14: Group 13 Halides

7: Group 14

- 7.1: The Group 14 Elements
- 7.2: Carbon Black- From Copying to Communication
- 7.3: Carbon Nanomaterials
- 7.4: Nitrogen Compounds of Carbon
- 7.5: Carbon Monoxide
- 7.6: Carbon Dioxide
- 7.7: Suboxides of Carbon
- 7.8: Carbon Halides
- 7.9: Comparison Between Silicon and Carbon
- 7.10: Semiconductor Grade Silicon
- 7.11: Oxidation of Silicon
- 7.12: Applications for Silica Thin Films

8: Group 15 - The Pnictogens

- 8.1: The Group 15 Elements- The Pnictogens
- 8.2: Reaction Chemistry of Nitrogen
- 8.3: Hydrides
- 8.4: Oxides and Oxoacids
- 8.5: Halides of Phosphorous

9: Group 16

- 9.1: The Group 16 Elements- The Chalcogens
- 9.2: Ozone
- 9.3: Water - The Fuel for the Medieval Industrial Revolution
- 9.4: Hydrogen Peroxide
- 9.5: Hydrogen Peroxide Providing a Lift for 007
- 9.6: Comparison of Sulfur to Oxygen
- 9.7: Chalcogenide Hydrides
- 9.8: Oxides and Oxyacids of Sulfur
- 9.9: Sulfur Halides

10: The Halogens

- [10.1: The Group 17 Elements- The Halogens](#)
- [10.2: Compounds of Fluorine](#)
- [10.3: Compounds of Chlorine](#)
- [10.4: Oxyacids of Chlorine](#)
- [10.5: Bromine Trifluoride as a Solvent](#)

11: Group 18 - The Noble Gases

- [11.1: The Group 18 Elements- The Noble Gases](#)

[Index](#)

[Index](#)

[Glossary](#)

[Detailed Licensing](#)

Licensing

A detailed breakdown of this resource's licensing can be found in [Back Matter/Detailed Licensing](#).

CHAPTER OVERVIEW

1: General Concepts and Trends

- 1.1: Fundamental Properties - Oxidation State
- 1.2: Fundamental Properties - Ionization Energy
- 1.3: Fundamental Properties - Electron Affinity
- 1.4: Fundamental Properties - Electronegativity
- 1.5: Structure and Bonding - Valence Shell Electron Pair Repulsion (VSEPR) Theory
- 1.6: Structure and Bonding - Crystal Structure
- 1.7: Structure and Bonding - Stereochemistry
- 1.8: Acids, Bases, and Solvents - Choosing a Solvent
- 1.9: Chemical Reactivity - The Basics of Combustion
- 1.10: Periodic Trends for the Main Group Elements

This page titled [1: General Concepts and Trends](#) is shared under a [CC BY 3.0](#) license and was authored, remixed, and/or curated by [Andrew R. Barron \(CNX\)](#) via [source content](#) that was edited to the style and standards of the LibreTexts platform.

1.1: Fundamental Properties - Oxidation State

The oxidation state of an element is defined as *the formal charge on the atom if all bonds were assumed to be fully ionic*.

In an ionic compound the oxidation state is equal to the charge on the ion, e.g., in NaCl the charge on the sodium is +1 and the oxidation state is also +1. In contrast, the charge on an atom in a covalent compound never approaches the charge implied from the oxidation number, e.g., in CCl₄, the oxidation state of carbon is +4 but the charge on the carbon atom is significantly less.

Thus, while oxidation state is a simple formulism it is very useful in a number of ways:

1. Classification of compounds of elements, especially those of the transition metals.
2. Enables the balance of reduction-oxidation (redox) reactions.

To determine the oxidation state of an element within a particular compound the following steps act as a guideline:

1. The oxidation state of any atom of any element in its elemental form is zero.
2. The oxidation state of a monatomic ion is equal to its charge.
3. Any homoleptic X-X bonds (e.g., the C-C bond in H₃C-CH₃) are assumed to be non-ionic and do not contribute to the oxidation state of X.
4. Fluorine always has oxidation state of 1
5. Elements of Group 1 (IA) (except hydrogen) have an oxidation state of +1 in compounds.
6. Elements of Group 2 (IIA) have an oxidation state of +2 in compounds.
7. Elements of Group 17 (VIIA) have an oxidation state of -1 when they combine with elements below or to the left of their position in the periodic table
8. Oxygen is usually assigned the oxidation state of 2, except in compounds with uorine, oxygen has a positive oxidation number.
9. Hydrogen is assigned the oxidation state of +1 with non-metals and 1 with metals.
10. In any compound the sum of the oxidation states (oxidation numbers) is equal to the overall charge.

Exercises

Exercise 1.1.1

What is the oxidation state of sulfur in Na₂SO₄?

Solution

The two sodium atoms each have an oxidation state of +1, while the oxygen atoms have an oxidation state of 2, and the overall charge is 0.

1. overall charge = sum of oxidation states
2. $0 = (2 \times \text{oxidation state of Na}) + (\text{oxidation state of S}) + (4 \times \text{oxidation state of O})$
3. $0 = (2 \times +1) + (\text{oxidation state of S}) + (4 \times -2)$
4. oxidation state of S = $0 (2 \times +1) - (4 \times 2)$
5. oxidation state of S = +6

Exercise 1.1.2

What is the oxidation state of sulfur in Na₂SO₃?

Solution

The two sodium atoms each have an oxidation state of +1, while the oxygen atoms have an oxidation state of 2, and the overall charge is 0.

1. overall charge = sum of oxidation states
2. $0 = (2 \times \text{oxidation state of Na}) + (\text{oxidation state of S}) + (3 \times \text{oxidation state of O})$
3. $0 = (2 \times +1) + (\text{oxidation state of S}) + (3 \times -2)$
4. oxidation state of S = $0 (2 \times +1) - (3 \times 2)$
5. oxidation state of S = +4

Exercise 1.1.3

What is the oxidation state of sulfur in H_2S ?

Solution

The two hydrogen atoms each have an oxidation state of +1 and the overall charge is 0.

- overall charge = sum of oxidation states
- $0 = (2 \times \text{oxidation state of H}) + (\text{oxidation state of S})$
- $0 = (2 \times +1) + (\text{oxidation state of S})$
- oxidation state of S = $0 - (2 \times +1)$
- oxidation state of S = -2

In writing the oxidation state of an element within a compound it is common to use a Roman numeral, rather than the charge, i.e., Al(III) rather than Al^{3+} .

This page titled [1.1: Fundamental Properties - Oxidation State](#) is shared under a [CC BY 3.0](#) license and was authored, remixed, and/or curated by [Andrew R. Barron \(CNX\)](#) via [source content](#) that was edited to the style and standards of the LibreTexts platform.

1.2: Fundamental Properties - Ionization Energy

The ionization energy (IE), or more properly the ionization enthalpy, is defined as the energy required to loose an electron from a gaseous atom or ion.



Each subsequent ionization energy is greater than the previous one because of the increase in charge on the ion. For example, for any given atom or ion the 1st ionization energy is less than the 2nd ionization energy, and so on. This is shown in Table 1.2.1.1.

Table 1.2.1.1: The first three ionization energies for aluminum.

Ionization		Ionization energy (kJ/mol)
$Al^0 \rightarrow Al^+ + e^{-}$	(1.2.2)	548
$Al^+ \rightarrow Al^{2+} + e^{-}$	(1.2.3)	1823
$Al^{2+} \rightarrow Al^{3+} + e^{-}$	(1.2.4)	2751

How does the ionization energy vary with elements in the periodic table? If we consider the 1st ionization potential of the elements in a particular group of the periodic table we note that there is a decrease in ionization potential as you go down the Group. The reason for this trend is due to the increased shielding of the outer shell electrons (ns^1) by the completed (filled) inner shells. The ns^1 electron thus exhibits a lower effective nuclear charge and makes it easier to remove. For example, Table 1.2.1.2 shows the 1st ionization potential for the Group 1 alkali metals.

Table 1.2.1.2: Variation of the first ionization potential ($M^0 \rightarrow M^+$) for the Group 1 (IA) elements.

Element	Ionization energy (kJ/mol)
Li	526
Na	502
K	425
Rb	409
Cs	382

In contrast, to individual Groups, moving across a particular Period results in a general increase in the ionization potential as is shown in Figure 1.2.1.1. The lack of additional screening of filled shells across the Period means that the ionization energy for the outer shell electrons is dominated by the increase in nuclear charge (number of protons) with increased atomic number.

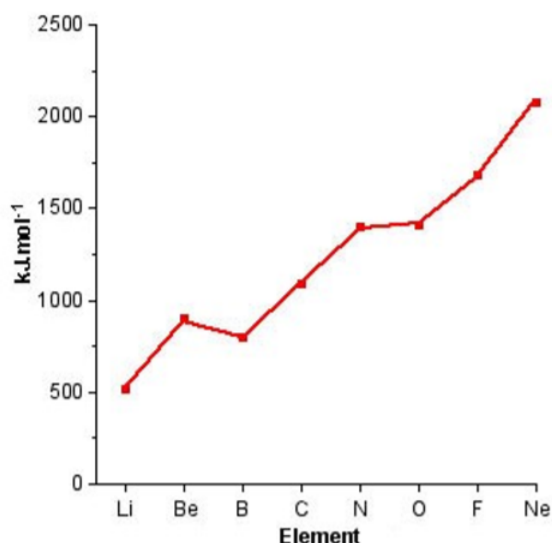


Figure 1.2.1: Plot of the first ionization potential for the elements Li to Ne.

From Figure 1.2.1.1 it can be seen that the Periodic trend is not linear, there are significant steps in the plot. Boron, for example, has a lower first ionization potential than beryllium, why? A consideration of the electron configuration for the elements provides in answer (Figure 1.2.1.2). Beryllium has a $2s^2$ outer shell configuration, while boron has a $2s^2 2p^1$ configuration. The $2p^1$ electron is easy to remove because it exhibits increased shielding from the nucleus due to the filled $2s$ orbital.

	2s	2p
Be	$\uparrow\downarrow$	$\square \square \square$
B	$\uparrow\downarrow$	$\uparrow \square \square$
C	$\uparrow\downarrow$	$\uparrow \uparrow \square$
N	$\uparrow\downarrow$	$\uparrow \uparrow \uparrow$
O	$\uparrow\downarrow$	$\uparrow\downarrow \uparrow \uparrow$

Figure 1.2.2: Outer shell electron configuration of beryllium through oxygen.

As we move from, boron to nitrogen, the $2p$ shell is filled (Figure 1.2.1.2) without additional shielding and the effect of the increased nuclear charge dominates. Finally, the $2p^4$ configuration for oxygen (Figure 1.2.1.2) results in an electron pair, which repel each other, thus making it easier to remove an electron (lower ionization potential) than expected from the increased nuclear charge. From Figure 1.2.1 we can see that the effect of electron pairing is less than that of a filled shell.

The trend for the 2^{nd} ionization potential is similar, but different, to that of the 1^{st} ionization potential. As may be seen in Figure 1.2.1.3 the steps observed for the 1^{st} ionization energy plot (i.e., between Be/B and N/O have moved one element to the right. A view of the electron configuration for the E^+ ions (Figure 1.2.1.4) shows that the rationale for the trend in the 1^{st} ionization potential trends still applies but to the ion of the element to the right in the Periodic table. Now B^+ has a $2s^2$ outer shell configuration, while C^+ has a $2s^2 2p^1$ configuration. A similar plot for the 3^{rd} ionization energy would move the steps another element to the right.

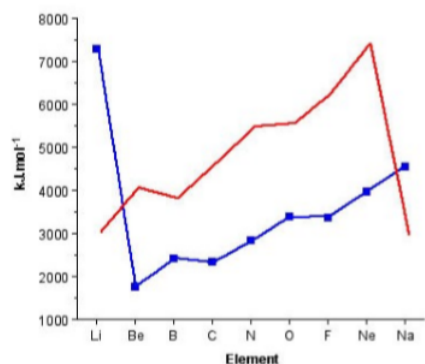


Figure 1.2.3: A plot of 2nd ionization energy (enthalpy) for elements Li to Na (blue with square data points) showing the relative trend to the 1st ionization potential (red line not to scale).

	2s	2p
Be ⁺	\uparrow	$\square \square \square$
B ⁺	$\uparrow\downarrow$	$\square \square \square$
C ⁺	$\uparrow\downarrow$	$\uparrow \square \square$
N ⁺	$\uparrow\downarrow$	$\uparrow \uparrow \square$
O ⁺	$\uparrow\downarrow$	$\uparrow \uparrow \uparrow$

Figure 1.2.4: Outer shell electron configuration of E⁺ for beryllium through oxygen.

The other observation to be made from Figure 1.2.1.3 is the very large 2nd ionization potential for lithium associated with the ionization of Li⁺ to Li²⁺. The large increase is due to the removal of an electron from the filled 1s² shell.

This page titled [1.2: Fundamental Properties - Ionization Energy](#) is shared under a [CC BY 3.0](#) license and was authored, remixed, and/or curated by [Andrew R. Barron \(CNX\)](#) via [source content](#) that was edited to the style and standards of the LibreTexts platform.

1.3: Fundamental Properties - Electron Affinity

The electron affinity (EA) of an element is defined as the energy given off when a neutral atom in the gas phase gains an extra electron to form a negatively charged ion.



Electron affinities are more difficult to measure than ionization energies and are usually less accurately known. Electron affinities are large and negative for elements such as fluorine and oxygen, and small and positive for metals.

Electron affinities generally become smaller as you go down a Group of the periodic table (Table 1.3.1.3). This is because the electron being added to the atom is placed in a larger orbital, where it spends less time near the nucleus of the atom, and also the number of electrons on an atom increases as we go down a column, so the force of repulsion between the electron being added and the electrons already present on a neutral atom becomes larger. Electron affinities are further complicated since the repulsion between the electron being added to the atom and the electrons already present on the atom depends on the volume of the atom. Thus, for the nonmetals in Groups 6 (VIA) and 7 (VIIA), this force of repulsion is largest for the very smallest atoms in these columns: oxygen and fluorine. As a result, these elements have a smaller electron affinity than the elements below them in these columns as shown in Table 1.3.1.3.

Table 1.3.1.3: The electron affinity for the non-metallic halogens.

Element	Electron affinity (kJ/mol)
F	-322
Cl	-349
Br	-325
I	-295

Although there is a general trend that for Group 1 (IA) to Group 17 (VIIA) elements the electron affinity increases across the Periodic table from left to right, the details of the trend are more complex. As may be seen from Figure 1.3.1.5, there is a cyclic trend. The explanation of this is a consequence of the unusually stable electron configurations exhibited by atoms with filled or half filled shells, i.e., helium, beryllium, nitrogen and neon (see Table 1.3.1.4). These configurations are so stable that it actually takes energy to force one of these elements to pick up an extra electron to form a negative ion.

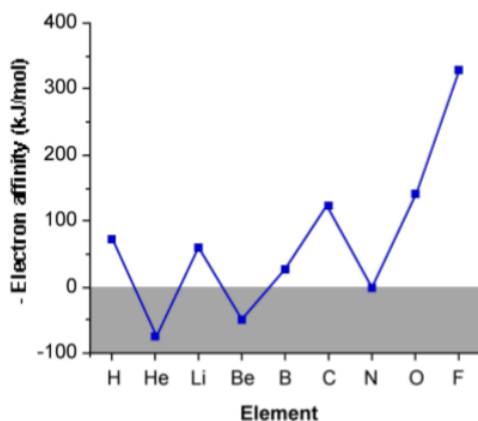


Figure 1.3.5: Plot of the electron affinity for the elements hydrogen to fluorine. N.B. Values for helium, beryllium, nitrogen, and neon are not known with any accuracy but are all positive.

Table 1.3.1.4: Electron affinities of the elements hydrogen to neon. N.B. Values for helium, beryllium, nitrogen, and neon are not known with any accuracy but are all positive.

Element	Electron affinity (kJ/mol)	Electron configuration
H	-72.8	1s ¹

He	+ve	$1s^2$
Li	-59.8	$[\text{He}] 2s^1$
Be	+ve	$[\text{He}] 2s^2$
B	-27	$[\text{He}] 2s^2 2p^1$
C	-122.3	$[\text{He}] 2s^2 2p^2$
N	+ve	$[\text{He}] 2s^2 2p^3$
O	-141.1	$[\text{He}] 2s^2 2p^4$
F	-328.0	$[\text{He}] 2s^2 2p^5$
Ne	+ve	$[\text{He}] 2s^2 2p^6$

This page titled [1.3: Fundamental Properties - Electron Affinity](#) is shared under a [CC BY 3.0](#) license and was authored, remixed, and/or curated by [Andrew R. Barron \(CNX\)](#) via [source content](#) that was edited to the style and standards of the LibreTexts platform.

1.4: Fundamental Properties - Electronegativity

An issue with ionization potential and electron affinity is that they are defined and measured as reactions in the gas phase. Although values have been determined for molecular fragments it is still difficult to correlate with reaction trends in solution. To overcome this issue the concept of electronegativity was developed.

Electronegativity is defined as *the tendency of an atom in a molecule to attract electrons to itself*. Although several electronegativity scales have been developed, that by Linus Pauling (Figure 1.4.1.6) is the most often used. Table 1.4.1.5 provides selected Pauling electronegativity values (unit less).

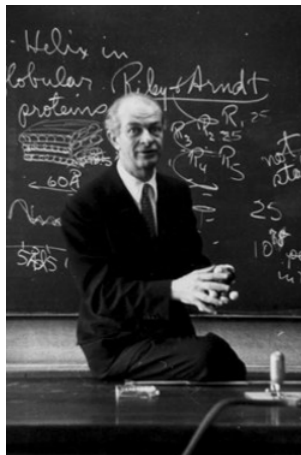


Figure 1.4.6: American chemist Linus Carl Pauling (1901 1994).

Table 1.4.1.5: Selected Pauling electronegativity values.

Element	Pauling Scale
F	4.0
O	3.5
Cl	3.0
N	3.0
S	2.5
C	2.5
H	2.1
B	2.0
Na	0.9

The advantage of the Pauling electronegativity scale is that it allows the prediction of general behavior. For example, the larger the difference in electronegativity between two elements the more ionic character or more polar the bonding interaction. Thus, a H-O bond ($3.5 - 2.1 = 1.4$) is more polar than a H-S bond ($2.5 - 2.1 = 0.4$).

This page titled [1.4: Fundamental Properties - Electronegativity](#) is shared under a [CC BY 3.0](#) license and was authored, remixed, and/or curated by [Andrew R. Barron \(CNX\)](#) via [source content](#) that was edited to the style and standards of the LibreTexts platform.

1.5: Structure and Bonding - Valence Shell Electron Pair Repulsion (VSEPR) Theory

The idea of a correlation between molecular geometry and the number of valence electrons was first presented in 1940 by Sidgwick and Powell; however, in 1957, Ronald Gillespie (Figure 1.5.1.7) and Sir Ronald Nyholm (Figure 1.5.1.8) refined this concept to build a more detailed theory. It is their work that provides the basis of the valence shell electron pair repulsion (VSEPR) theory, and as such it is also known as the Gillespie-Nyholm theory.

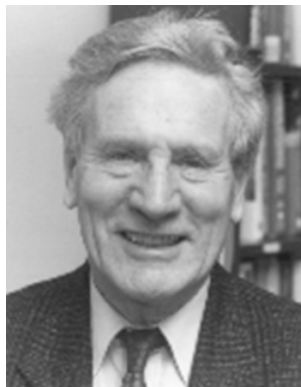


Figure 1.5.7: Chemist Ronald J. Gillespie (1924 -).



Figure 1.5.8: Australian chemist Sir Ronald Sydney Nyholm (1917 -).

One attribute of VSEPR is that with the ability to predict the shape of a molecule for a compound comes the ability to predict some of the physical and chemical properties of that compound.

The formal definition that is the basis for VSEPR is as follows: *Pairs of electrons in the valence shell of a central atom of a molecule repel each other and take up positions as far apart as possible.*

Within this definition it is implicitly assumed that the core shells are not polarized and therefore take no part in bonding, and therefore can be ignored. Since the maximum repulsion of the electron pairs (be they associated with a bonding interaction or a lone pair) control the shape of a molecule, for each number of electron pairs we can define the geometric optimum position that maximizes the distance between the electron pairs (Table 1.5.1.6). The number of electron pairs surrounding an atom, both bonding and nonbonding, is called its steric number.

Table 1.5.1.6: Shapes of molecules and ions

Number of central atom electron pairs	Bonding pairs	Non-bonding pairs	Shape	Example
2	2	0	Linear	BeCl ₂
3	3	0	Triangular	BF ₃
3	2	1	Bent	SnCl ₂
4	4	0	Tetrahedral	CCl ₄
4	3	1	Pyramidal	NH ₃
4	2	2	Bent	H ₂ O
5	5	0	Trigonal bipyramidal (tbp)	PF ₅

5	4	1	Pseudo-tdp	BrF_4^-
5	3	2	T-Shaped	BrF_3
5	2	3	Linear	XeF_2
6	6	0	Octahedral	$\text{SF}_6, \text{PF}_6^-$
6	5	1	Square pyramidal	IF_5
6	4	2	Square planar	$\text{XeF}_4, \text{IF}_4^-$

The steps for dening the molecular shape are as follows:

1. Draw a simple Lewis structure including single, double, and triple bonds where appropriate.
2. Count the number of electrons on the central atom assuming it is neutral.
3. Add one electron for each σ -bond.
4. Subtract one electron for each π -bond.
5. Subtract one electron for each positive (+) charge.
6. Add one electron for each negative (-) charge.
7. Divide the number of electrons by two to give the number of electron pairs.
8. Use the list in Table 1.5.1.6 to predict the structure of the molecule.

Example

What is the shape of NH_4^+

Solution

1. Nitrogen has 5 valence electrons
2. Add 4 electrons for the four σ -bonds: $5 + 4 = 9$
3. Subtract one electron for the positive (+) charge: $9 - 1 = 8$
4. Divide the number of electrons by two to give the number of electron pairs: $8/2 = 4$
5. Four bonding pairs and no lone pairs = tetrahedral geometry

Exercises

Exercise 1.5.1

What is the shape of HgCl_2 ?

Answer

1. Mercury has 2 valence electrons
2. Add 2 electrons for the two σ -bonds: $2 + 2 = 4$
3. Divide the number of electrons by two to give the number of electron pairs: $4/2 = 2$
4. Two bonding pairs and no lone pairs = linear geometry

Exercise 1.5.2

What is the shape of H_2CO ?

Answer

1. Carbon has 4 valence electrons
2. Add 3 electrons for the three σ -bonds: $4 + 3 = 7$
3. Subtract one electron for each π -bond: $7 - 1 = 6$
4. Divide the number of electrons by two to give the number of electron pairs: $6/2 = 3$
5. Two bonding pairs and no lone pairs = triangular geometry

Lone pairs versus bonding pairs

The prediction of the detailed molecular structure (including bond angles) is not as simple as shown in Table 1.5.1.6. In molecules with either lone pair electrons or multiple (double or triple) bonds the angles about the central atom are distorted due to the increased electron repulsion (Figure 1.5.1.9). The differences in repulsion caused by a lone pair or a bonding pair may be rationalized in a simple manner by a lone pair taking up more space than a bonding pair (Figure 1.5.1.10).

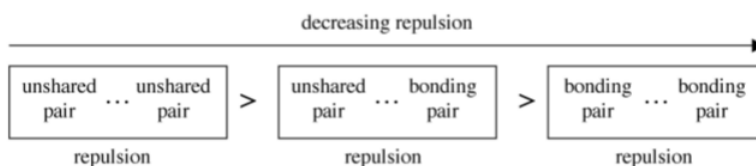


Figure 1.5.9: The order of decreasing repulsion between non-bonding (unshared) and bonding electron pairs.

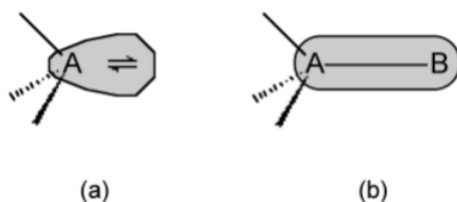


Figure 1.5.10: Representation of the relative space taken up by (a) a lone pair of electrons and (b) a bonding pair of electrons.

Water is one of the classic cases in considering the issue of non-bonding (unshared) electron pairs.

1. Oxygen has 6 valence electrons
2. Add 2 electrons for the two σ -bonds: $6 + 2 = 8$
3. Divide the number of electrons by two to give the number of electron pairs: $8/2 = 4$
4. Two bonding pairs and two lone pairs = tetrahedral geometry

From this an idealized tetrahedral geometry would give the H-O-H angle as 109.5° , however, from Figure 1.5.1.9 we know that the lone pair...lone pair repulsion is greater than the lone pair...bonding pair repulsion which is greater than the bonding pair...bonding pair repulsion, and thus, the H-O-H angle should be decreased from the ideal tetrahedral. The experimentally determined H-O-H angle in water is in fact 104.5° .

Ethylene is a good case in considering the issue of multiple bonds. Ethylene contains both σ -bond and π -bond between the carbon atoms. This combination can be thought of as a super bond, and as such its effect is similar to a lone pair.

Carbon has 4 valence electrons

Add 3 electrons for the two σ -bonds: $4 + 3 = 7$

Subtract one electron for each π -bond: $7 - 1 = 6$

Divide the number of electrons by two to give the number of electron pairs: $6/2 = 3$

Three bonding pairs and no lone pairs = triangular geometry

From this an idealized tetrahedral geometry would give the H-C-H angle as 120° , however, the π -bond repulsion is greater than the σ -bond repulsion, and thus, the H-C-H angle should be decreased from the ideal tetrahedral. The experimentally determined H-O-H angle in water is in fact 118.3° .

Resonance structures

If a molecule or ion has two or more resonance forms it is necessary to consider each form before angles are predicted. For example, the carbonate anion, CO_3^- , can be drawn as a single structure from which it would be predicted that two groups of O-C-O angles would result (Figure 1.5.1.11).

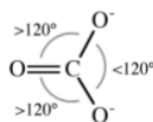


Figure 1.5.11: VSEPR predicted structure of a single resonance form of CO_3^{2-} .

However, CO_3^{2-} should actually be drawn in each of its resonance forms as in Figure 1.5.1.12.

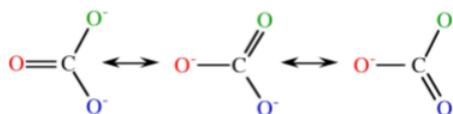


Figure 1.5.12: Resonance forms of CO_3^{2-} .

From Figure 1.5.1.12 it is clear that the real structure will be an average of the three resonance forms, and hence there will be a single O-C-O angle = 120° (Figure 1.5.1.13).

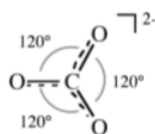


Figure 1.5.13: Structure of CO_3^{2-} .

Atom electronegativities

In an A-X bond where the atom electronegativities are very different the bonding pair is assumed to occupy less space than in bond between two atoms of similar electronegativities. As the bonding pair occupies less space it will repel neighboring electron pairs less.

For example, based on the above, a comparison of the tetrahedral compounds H_2O and F_2O would suggest that the F-O-F angle be smaller than the H-O-H angle since fluorine has a higher electronegativity than hydrogen (4.0 and 2.1, respectively). This is indeed observed (Figure 1.5.1.14).

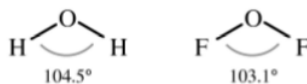


Figure 1.5.14: Structures of H_2O and F_2O .

In many cases, inter-ligand steric interactions can also be used to explain the difference in angle. For example, while fluorine is more electronegative than chlorine (4.0 versus 3.0, respectively) it is also significantly smaller (Table 1.5.1.7). Thus, a larger Cl-X-Cl angle than a F-X-F angle in the homologous compound, can be attributed to a greater steric interactions, rather than difference in electronegativities.

Table 1.5.1.7: Comparison of size between fluoride and chloride ligands.

Ligand	Covalent Radius (Å)	Van der Waal radius (Å)
F	0.57	1.35
Cl	1.02	1.80

Bent's rule

There is the potential for more than one isomer for molecules that adopt structures in which there is a symmetry difference between at least two of the ligand positions. For example a trigonal bipyramidal compound of the formula PXY_4 has two possible structures. One where the X occupies an axial position (Figure 1.5.1.15a) and the other where it occupies an equatorial position (Figure 1.5.1.15b).

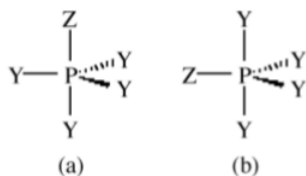


Figure 1.5.15: The two possible structures of PXY_4 .

Through the consideration of structures Henry Bent suggested a rule: *More electronegative substituents prefer hybrid orbitals with less s character, and conversely, more electropositive substituents prefer hybrid orbitals with greater s character.*

For example, in $PFCl_5$ the fluorine is the most electronegative substituent and will therefore occupy the axial (p-character only) position.

Bibliography

- H. A. Bent, *J. Chem. Educ.*, 1960, **37**, 616.
- H. A. Bent, *Chem. Rev.*, 1961, **61**, 275.
- R. J. Gillespie, *J. Chem. Educ.*, 1970, **47**, 18.
- R. J. Gillespie, *Chem. Soc. Rev.*, 1992, **21**, 59.
- R. J. Gillespie and R. S. Nyholm, *Quart. Rev.*, 1957, **11**, 339.

This page titled [1.5: Structure and Bonding - Valence Shell Electron Pair Repulsion \(VSEPR\) Theory](#) is shared under a [CC BY 3.0](#) license and was authored, remixed, and/or curated by [Andrew R. Barron \(CNX\)](#) via [source content](#) that was edited to the style and standards of the LibreTexts platform.

1.6: Structure and Bonding - Crystal Structure

Introduction

In any sort of discussion of crystalline materials, it is useful to begin with a discussion of crystallography: the study of the formation, structure, and properties of crystals. A crystal structure is defined as the particular repeating arrangement of atoms (molecules or ions) throughout a crystal. Structure refers to the internal arrangement of particles and not the external appearance of the crystal. However, these are not entirely independent since the external appearance of a crystal is often related to the internal arrangement. For example, crystals of cubic rock salt (NaCl) are physically cubic in appearance. Only a few of the possible crystal structures are of concern with respect to simple inorganic salts and these will be discussed in detail, however, it is important to understand the nomenclature of crystallography.

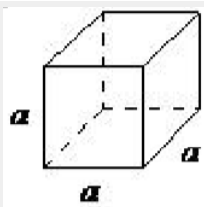
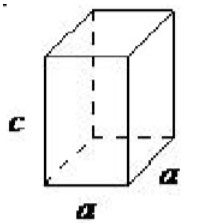
Crystallography

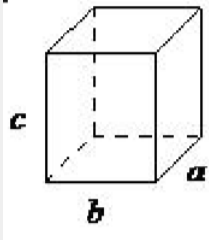
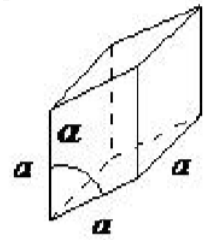
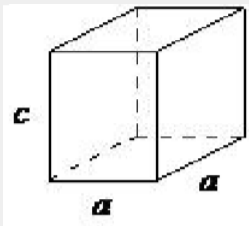
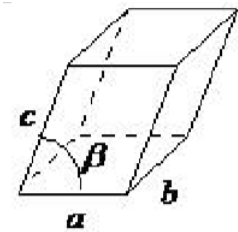
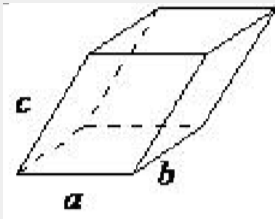
Bravais lattice

The Bravais lattice is the basic building block from which all crystals can be constructed. The concept originated as a topological problem of finding the number of different ways to arrange points in space where each point would have an identical atmosphere. That is each point would be surrounded by an identical set of points as any other point, so that all points would be indistinguishable from each other. Mathematician Auguste Bravais discovered that there were 14 different collections of the groups of points, which are known as Bravais lattices. These lattices fall into seven different "crystal systems, as differentiated by the relationship between the angles between sides of the unit cell and the distance between points in the unit cell. The unit cell is the smallest group of atoms, ions or molecules that, when repeated at regular intervals in three dimensions, will produce the lattice of a crystal system. The lattice parameter is the length between two points on the corners of a unit cell. Each of the various lattice parameters are designated by the letters a , b , and c . If two sides are equal, such as in a tetragonal lattice, then the lengths of the two lattice parameters are designated a and c , with b omitted. The angles are designated by the Greek letters α , β , and γ , such that an angle with a specific Greek letter is not subtended by the axis with its Roman equivalent. For example, α is the included angle between the b and c axis.

Table 1.6.1.8 shows the various crystal systems, while Figure 1.6.1.16 shows the 14 Bravais lattices. It is important to distinguish the characteristics of each of the individual systems. An example of a material that takes on each of the Bravais lattices is shown in Table 1.6.1.9.

Table 1.6.1.8: Geometrical characteristics of the seven crystal systems.

System	Axial lengths and angles	Unit cell geometry
cubic	$a = b = c, \alpha = \beta = \gamma = 90^\circ$	
tetragonal	$a = b \neq c, \alpha = \beta = \gamma = 90^\circ$	

orthorhombic	$a \neq b \neq c, \alpha = \beta = \gamma = 90^\circ$	
rhombohedral	$a = b = c, \alpha = \beta = \gamma \neq 90^\circ$	
hexagonal	$a = b \neq c, \alpha = \beta = 90^\circ, \gamma = 120^\circ$	
monoclinic	$a \neq b \neq c, \alpha = \gamma = 90^\circ, \beta \neq 90^\circ$	
triclinic	$a \neq b \neq c, \alpha \neq \beta \neq \gamma$	

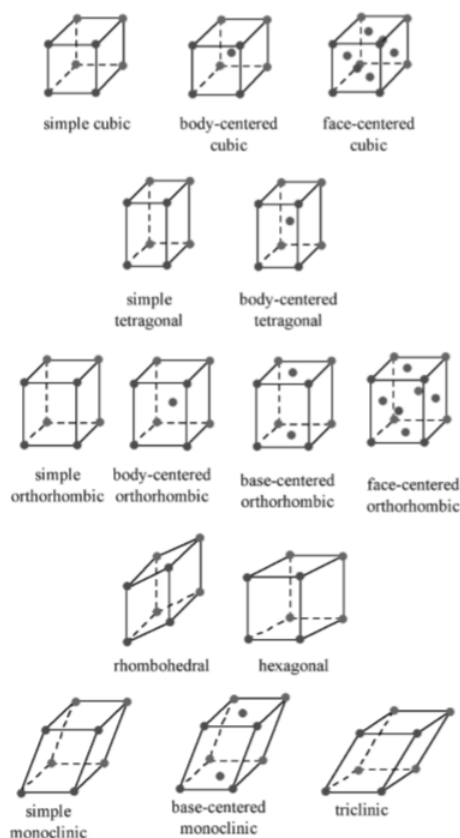


Figure 1.6.16: Bravais lattices.

Table 1.6.1.9: Examples of elements and compounds that adopt each of the crystal systems.

Crystal system	Example
triclinic	$\text{K}_2\text{S}_2\text{O}_8$
monoclinic	As_4S_4 , KNO_2
rhombohedral	Hg, Sb
hexagonal	Zn, Co, NiAs
orthorhombic	Ga, Fe_3C
tetragonal	In, TiO_2
cubic	Au, Si, NaCl

The cubic lattice is the most symmetrical of the systems. All the angles are equal to 90° , and all the sides are of the same length ($a = b = c$). Only the length of one of the sides (a) is required to describe this system completely. In addition to simple cubic, the cubic lattice also includes body-centered cubic and face-centered cubic (Figure 1.6.1.16). Body-centered cubic results from the presence of an atom (or ion) in the center of a cube, in addition to the atoms (ions) positioned at the vertices of the cube. In a similar manner, a face-centered cubic requires, in addition to the atoms (ions) positioned at the vertices of the cube, the presence of atoms (ions) in the center of each of the cubes face.

The tetragonal lattice has all of its angles equal to 90° , and has two out of the three sides of equal length ($a = b$). The system also includes body-centered tetragonal (Figure 1.6.1.16).

In an orthorhombic lattice all of the angles are equal to 90° , while all of its sides are of unequal length. The system needs only to be described by three lattice parameters. This system also includes body-centered orthorhombic, base-centered orthorhombic, and

face-centered orthorhombic (Figure 1.6.1.16). A base-centered lattice has, in addition to the atoms (ions) positioned at the vertices of the orthorhombic lattice, atoms (ions) positioned on just two opposing faces.

The rhombohedral lattice is also known as trigonal, and has no angles equal to 90° , but all sides are of equal length ($a = b = c$), thus requiring only by one lattice parameter, and all three angles are equal ($\alpha = \beta = \gamma$).

A hexagonal crystal structure has two angles equal to 90° , with the other angle (γ) equal to 120° . For this to happen, the two sides surrounding the 120° angle must be equal ($a = b$), while the third side (c) is at 90° to the other sides and can be of any length.

The monoclinic lattice has no sides of equal length, but two of the angles are equal to 90° , with the other angle (usually defined as β) being something other than 90° . It is a tilted parallelogram prism with rectangular bases. This system also includes base-centered monoclinic (Figure 1.6.1.16).

In the triclinic lattice none of the sides of the unit cell are equal, and none of the angles within the unit cell are equal to 90° . The triclinic lattice is chosen such that all the internal angles are either acute or obtuse. This crystal system has the lowest symmetry and must be described by 3 lattice parameters (a , b , and c) and the 3 angles (α , β , and γ).

Atom positions, crystal directions and Miller indices

Atom positions and crystal axes

The structure of a crystal is defined with respect to a unit cell. As the entire crystal consists of repeating unit cells, this definition is sufficient to represent the entire crystal. Within the unit cell, the atomic arrangement is expressed using coordinates. There are two systems of coordinates commonly in use, which can cause some confusion. Both use a corner of the unit cell as their origin. The first, less-commonly seen system is that of Cartesian or orthogonal coordinates (X , Y , Z). These usually have the units of Angstroms and relate to the distance in each direction between the origin of the cell and the atom. These coordinates may be manipulated in the same fashion as are used with two- or three-dimensional graphs. It is very simple, therefore, to calculate inter-atomic distances and angles given the Cartesian coordinates of the atoms. Unfortunately, the repeating nature of a crystal cannot be expressed easily using such coordinates. For example, consider a cubic cell of dimension 3.52 \AA . Pretend that this cell contains an atom that has the coordinates (1.5, 2.1, 2.4). That is, the atom is 1.5 \AA away from the origin in the x direction (which coincides with the a cell axis), 2.1 \AA in the y (which coincides with the b cell axis) and 2.4 \AA in the z (which coincides with the c cell axis). There will be an equivalent atom in the next unit cell along the x -direction, which will have the coordinates (1.5 + 3.52, 2.1, 2.4) or (5.02, 2.1, 2.4). This was a rather simple calculation, as the cell has very high symmetry and so the cell axes, a , b and c , coincide with the Cartesian axes, X , Y and Z . However, consider lower symmetry cells such as triclinic or monoclinic in which the cell axes are not mutually orthogonal. In such cases, expressing the repeating nature of the crystal is much more difficult to accomplish.

Accordingly, atomic coordinates are usually expressed in terms of fractional coordinates, (x , y , z). This coordinate system is coincident with the cell axes (a , b , c) and relates to the position of the atom in terms of the fraction along each axis. Consider the atom in the cubic cell discussion above. The atom was 1.5 \AA in the a direction away from the origin. As the a axis is 3.52 \AA long, the atom is ($1.5/3.52$) or 0.43 of the axis away from the origin. Similarly, it is ($2.1/3.52$) or 0.60 of the b axis and ($2.4/3.52$) or 0.68 of the c axis. The fractional coordinates of this atom are, therefore, (0.43, 0.60, 0.68). The coordinates of the equivalent atom in the next cell over in the a direction, however, are easily calculated as this atom is simply 1 unit cell away in a . Thus, all one has to do is add 1 to the x coordinate: (1.43, 0.60, 0.68). Such transformations can be performed regardless of the shape of the unit cell. Fractional coordinates, therefore, are used to retain and manipulate crystal information.

Crystal directions

The designation of the individual vectors within any given crystal lattice is accomplished by the use of whole number multipliers of the lattice parameter of the point at which the vector exits the unit cell. The vector is indicated by the notation $[hkl]$, where h , k , and l are reciprocals of the point at which the vector exits the unit cell. The origination of all vectors is assumed defined as $[000]$. For example, the direction along the a -axis according to this scheme would be $[100]$ because this has a component only in the a -direction and no component along either the b or c axial direction. A vector diagonally along the face defined by the a and b axis would be $[110]$, while going from one corner of the unit cell to the opposite corner would be in the $[111]$ direction. Figure 1.6.1.17 shows some examples of the various directions in the unit cell. The crystal direction notation is made up of the lowest combination of integers and represents unit distances rather than actual distances. A $[222]$ direction is identical to a $[111]$, so $[111]$ is used. Fractions are not used. For example, a vector that intercepts the center of the top face of the unit cell has the coordinates $x = 1/2$, $y = 1/2$, $z = 1$. All have to be inversed to convert to the lowest combination of integers (whole numbers); i.e., $[221]$ in Figure

1.6.1.17. Finally, all parallel vectors have the same crystal direction, e.g., the four vertical edges of the cell shown in Figure 1.6.1.17 all have the crystal direction $[hkl] = [001]$.

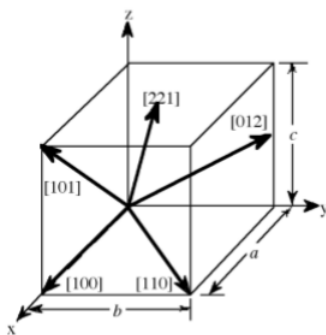


Figure 1.6.17: Some common directions in a cubic unit cell.

Crystal directions may be grouped in families. To avoid confusion there exists a convention in the choice of brackets surrounding the three numbers to differentiate a crystal direction from a family of direction. For a direction, square brackets $[hkl]$ are used to indicate an individual direction. Angle brackets $\langle hkl \rangle$ indicate a family of directions. A family of directions includes any directions that are equivalent in length and types of atoms encountered. For example, in a cubic lattice, the $[100]$, $[010]$, and $[001]$ directions all belong to the $\langle 100 \rangle$ family of planes because they are equivalent. If the cubic lattice were rotated 90° , the a , b , and c directions would remain indistinguishable, and there would be no way of telling on which crystallographic positions the atoms are situated, so the family of directions is the same. In a hexagonal crystal, however, this is not the case, so the $[100]$ and $[010]$ would both be $\langle 100 \rangle$ directions, but the $[001]$ direction would be distinct. Finally, negative directions are identified with a bar over the negative number instead of a minus sign.

Crystal planes

Planes in a crystal can be specified using a notation called Miller indices. The Miller index is indicated by the notation $[hkl]$ where h , k , and l are reciprocals of the plane with the x , y , and z axes. To obtain the Miller indices of a given plane requires the following steps:

1. The plane in question is placed on a unit cell.
2. Its intercepts with each of the crystal axes are then found.
3. The reciprocal of the intercepts are taken.
4. These are multiplied by a scalar to insure that is in the simple ratio of whole numbers.

For example, the face of a lattice that does not intersect the y or z axis would be (100) , while a plane along the body diagonal would be the (111) plane. An illustration of this along with the (111) and (110) planes is given in Figure 1.6.1.18.

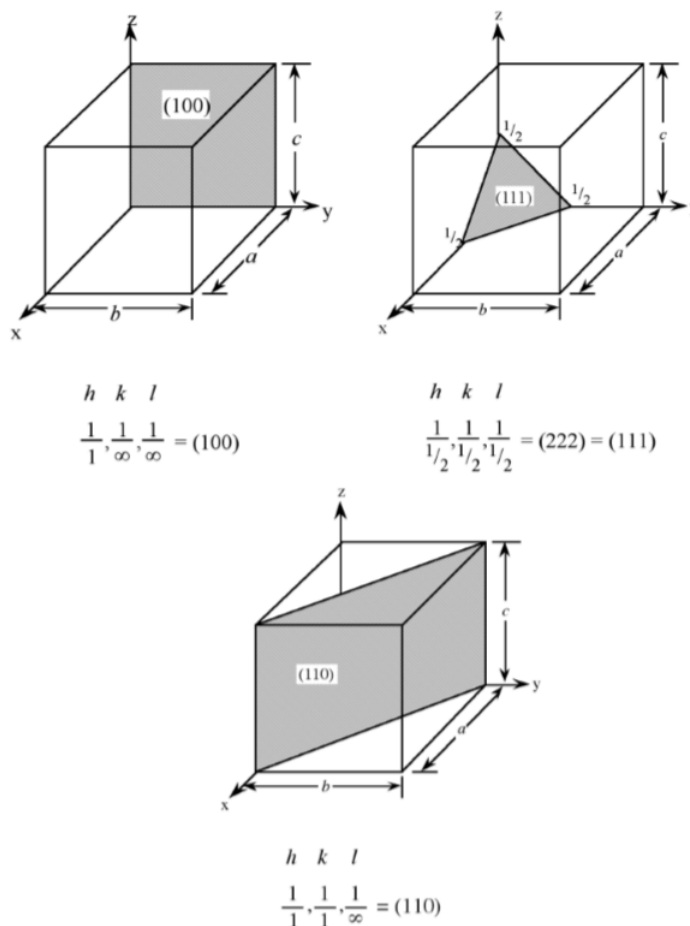


Figure 1.6.18: Examples of Miller indices notation for crystal planes.

As with crystal directions, Miller indices directions may be grouped in families. Individual Miller indices are given in parentheses (hkl) , while braces $\{hkl\}$ are placed around the indices of a family of planes. For example, (001) , (100) , and (010) are all in the $\{100\}$ family of planes, for a cubic lattice.

Description of crystal structures

Crystal structures may be described in a number of ways. The most common manner is to refer to the size and shape of the unit cell and the positions of the atoms (or ions) within the cell. However, this information is sometimes insufficient to allow for an understanding of the true structure in three dimensions. Consideration of several unit cells, the arrangement of the atoms with respect to each other, the number of other atoms they in contact with, and the distances to neighboring atoms, often will provide a better understanding. A number of methods are available to describe extended solid-state structures. The most applicable with regard to elemental and compound semiconductor, metals and the majority of insulators is the close packing approach.

Close packed structures: hexagonal close packing and cubic close packing

Many crystal structures can be described using the concept of close packing. This concept requires that the atoms (ions) are arranged so as to have the maximum density. In order to understand close packing in three dimensions, the most efficient way for equal sized spheres to be packed in two dimensions must be considered.

The most efficient way for equal sized spheres to be packed in two dimensions is shown in Figure 1.6.1.19, in which it can be seen that each sphere (the dark gray shaded sphere) is surrounded by, and is in contact with, six other spheres (the light gray spheres in Figure 1.6.1.19). It should be noted that contact with six other spheres the maximum possible is the spheres are the same size, although lower density packing is possible. Close packed layers are formed by repetition to an infinite sheet. Within these close packed layers, three close packed rows are present, shown by the dashed lines in Figure 1.6.1.19.

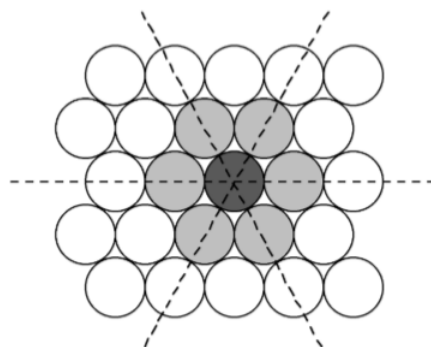


Figure 1.6.19: Schematic representation of a close packed layer of equal sized spheres. The close packed rows (directions) are shown by the dashed lines.

The most efficient way for equal sized spheres to be packed in three dimensions is to stack close packed layers on top of each other to give a close packed structure. There are two simple ways in which this can be done, resulting in either a hexagonal or cubic close packed structures.

Hexagonal close packed

If two close packed layers A and B are placed in contact with each other so as to maximize the density, then the spheres of layer B will rest in the hollow (vacancy) between three of the spheres in layer A. This is demonstrated in Figure 1.6.120. Atoms in the second layer, B (shaded light gray), may occupy one of two possible positions (Figure 1.6.120a or b) but not both together or a mixture of each. If a third layer is placed on top of layer B such that it exactly covers layer A, subsequent placement of layers will result in the following sequence ...ABABAB.... This is known as hexagonal close packing or *hcp*.

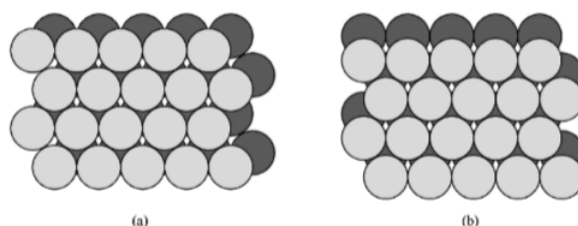


Figure 1.6.20: Schematic representation of two close packed layers arranged in A (dark grey) and B (light grey) positions. The alternative stacking of the B layer is shown in (a) and (b).

The hexagonal close packed cell is a derivative of the hexagonal Bravais lattice system (Figure 1.6.116) with the addition of an atom inside the unit cell at the coordinates $(\frac{1}{3}, \frac{2}{3}, \frac{1}{2})$. The basal plane of the unit cell coincides with the close packed layers (Figure 1.6.121). In other words the close packed layer makes-up the $\{001\}$ family of crystal planes.

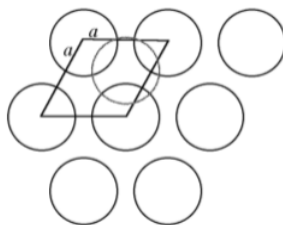


Figure 1.6.21: A schematic projection of the basal plane of the hcp unit cell on the close packed layers.

The packing fraction in a hexagonal close packed cell is 74.05%; that is 74.05% of the total volume is occupied. The packing fraction or density is derived by assuming that each atom is a hard sphere in contact with its nearest neighbors. Determination of the packing fraction is accomplished by calculating the number of whole spheres per unit cell (2 in hcp), the volume occupied by these spheres, and a comparison with the total volume of a unit cell. The number gives an idea of how open or filled a structure is. By comparison, the packing fraction for body-centered cubic (Figure 1.6.116) is 68% and for diamond cubic (an important semiconductor structure to be described later) is 34%.

Cubic close packed: face-centered cubic

In a similar manner to the generation of the hexagonal close packed structure, two close packed layers are stacked (Figure 1.6.1.19) however, the third layer (C) is placed such that it does not exactly cover layer A, while sitting in a set of troughs in layer B (Figure 1.6.1.22), then upon repetition the packing sequence will be ...ABCABCABC.... This is known as cubic close packing or *ccp*.

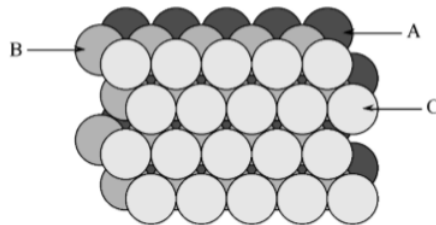


Figure 1.6.22: Schematic representation of the three close packed layers in a cubic close packed arrangement: A (dark grey), B (medium grey), and C (light grey).

The unit cell of cubic close packed structure is actually that of a face-centered cubic (*fcc*) Bravais lattice. In the *fcc* lattice the close packed layers constitute the {111} planes. As with the *hcp* lattice packing fraction in a cubic close packed (*fcc*) cell is 74.05%. Since face centered cubic or *fcc* is more commonly used in preference to cubic close packed (*ccp*) in describing the structures, the former will be used throughout this text.

Coordination number

The coordination number of an atom or ion within an extended structure is defined as the number of nearest neighbor atoms (ions of opposite charge) that are in contact with it. A slightly different definition is often used for atoms within individual molecules: the number of donor atoms associated with the central atom or ion. However, this distinction is rather artificial, and both can be employed.

The coordination numbers for metal atoms in a molecule or complex are commonly 4, 5, and 6, but all values from 2 to 9 are known and a few examples of higher coordination numbers have been reported. In contrast, common coordination numbers in the solid state are 3, 4, 6, 8, and 12. For example, the atom in the center of body-centered cubic lattice has a coordination number of 8, because it touches the eight atoms at the corners of the unit cell, while an atom in a simple cubic structure would have a coordination number of 6. In both *fcc* and *hcp* lattices each of the atoms have a coordination number of 12.

Octahedral and tetrahedral vacancies

As was mentioned above, the packing fraction in both *fcc* and *hcp* cells is 74.05%, leaving 25.95% of the volume unfilled. The unfilled lattice sites (interstices) between the atoms in a cell are called interstitial sites or vacancies. The shape and relative size of these sites is important in controlling the position of additional atoms. In both *fcc* and *hcp* cells most of the space within these atoms lies within two different sites known as octahedral sites and tetrahedral sites. The difference between the two lies in their coordination number, or the number of atoms surrounding each site. Tetrahedral sites (vacancies) are surrounded by four atoms arranged at the corners of a tetrahedron. Similarly, octahedral sites are surrounded by six atoms which make-up the apices of an octahedron. For a given close packed lattice an octahedral vacancy will be larger than a tetrahedral vacancy.

Within a face centered cubic lattice, the eight tetrahedral sites are positioned within the cell, at the general fractional coordinate of $(\frac{n}{4}, \frac{n}{4}, \frac{n}{4})$ where $n = 1$ or 3 , e.g., $(\frac{1}{4}, \frac{1}{4}, \frac{1}{4})$, $(\frac{1}{4}, \frac{1}{4}, \frac{3}{4})$, etc. The octahedral sites are located at the center of the unit cell $(\frac{1}{2}, \frac{1}{2}, \frac{1}{2})$, as well as at each of the edges of the cell, e.g., $(\frac{1}{2}, 0, 0)$. In the hexagonal close packed system, the tetrahedral sites are at $(0, 0, \frac{3}{8})$ and $(\frac{1}{3}, \frac{2}{3}, \frac{7}{8})$, and the octahedral sites are at $(\frac{1}{3}, \frac{1}{3}, \frac{1}{4})$ and all symmetry equivalent positions.

Important structure types

The majority of crystalline materials do not have a structure that fits into the one atom per site simple Bravais lattice. A number of other important crystal structures are found, however, only a few of these crystal structures are those of which occur for the elemental and compound semiconductors and the majority of these are derived from *fcc* or *hcp* lattices. Each structural type is generally defined by an archetype, a material (often a naturally occurring mineral) which has the structure in question and to which all the similar materials are related. With regard to commonly used elemental and compound semiconductors the important structures are diamond, zinc blende, Wurtzite, and to a lesser extent chalcopyrite. However, rock salt, β -tin, cinnabar and cesium chloride are observed as high pressure or high temperature phases and are therefore also discussed. The following provides a summary of these structures. Details of the full range of solid-state structures are given elsewhere.

Diamond Cubic

The diamond cubic structure consists of two interpenetrating face-centered cubic lattices, with one offset $\frac{1}{4}$ of a cube along the cube diagonal. It may also be described as face centered cubic lattice in which half of the tetrahedral sites are filled while all the octahedral sites remain vacant. The diamond cubic unit cell is shown in Figure 1.6.1.23. Each of the atoms (e.g., C) is four coordinate, and the shortest interatomic distance (C-C) may be determined from the unit cell parameter (a).

$$C-C = a \frac{\sqrt{3}}{4} \approx 0.442a$$

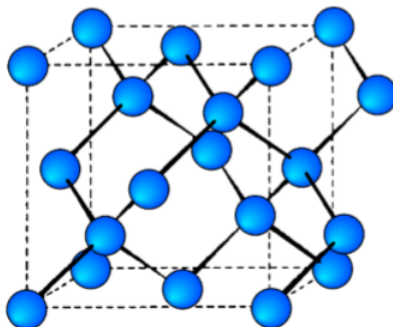


Figure 1.6.23: Unit cell structure of a diamond cubic lattice showing the two interpenetrating face-centered cubic lattices.

Zinc blende

This is a binary phase (ME) and is named after its archetype, a common mineral form of zinc sulfide (ZnS). As with the diamond lattice, zinc blende consists of the two interpenetrating fcc lattices. However, in zinc blende one lattice consists of one of the types of atoms (Zn in ZnS), and the other lattice is of the second type of atom (S in ZnS). It may also be described as face centered cubic lattice of S atoms in which half of the tetrahedral sites are filled with Zn atoms. All the atoms in a zinc blende structure are 4-coordinate. The zinc blende unit cell is shown in Figure 1.6.1.24. A number of inter-atomic distances may be calculated for any material with a zinc blende unit cell using the lattice parameter (a).

$$Zn-S = a \frac{\sqrt{3}}{4} \approx 0.442a$$

$$Zn-Zn = \frac{a}{\sqrt{2}} \approx 0.707a \quad (1.6.1)$$

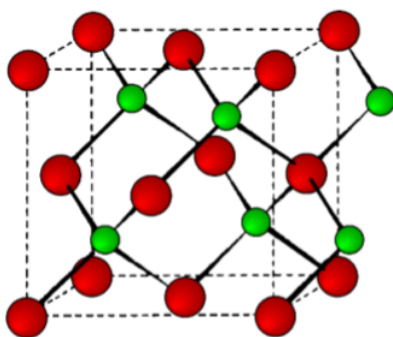


Figure 1.6.24: Unit cell structure of a zinc blende (ZnS) lattice. Zinc atoms are shown in green (small), sulfur atoms shown in red (large), and the dashed lines show the unit cell.

Chalcopyrite

The mineral chalcopyrite $CuFeS_2$ is the archetype of this structure. The structure is tetragonal ($a = b \neq c$, $\alpha = \beta = \gamma = 90^\circ$), and is essentially a superlattice on that of zinc blende. Thus, is easiest to imagine that the chalcopyrite lattice is made-up of a lattice of sulfur atoms in which the tetrahedral sites are filled in layers, ...FeCuCuFe..., etc. (Figure 1.6.1.25). In such an idealized structure $c = 2a$, however, this is not true of all materials with chalcopyrite structures.

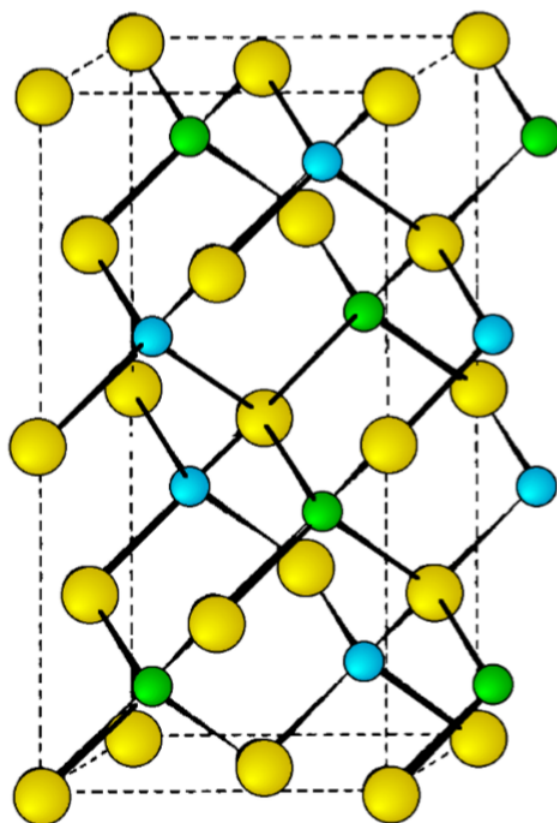


Figure 1.6.25: Unit cell structure of a chalcopyrite lattice. Copper atoms are shown in blue, iron atoms are shown in green and sulfur atoms are shown in yellow. The dashed lines show the unit cell.

Rock salt

As its name implies the archetypal rock salt structure is NaCl (table salt). In common with the zinc blende structure, rock salt consists of two interpenetrating face-centered cubic lattices. However, the second lattice is offset $1/2a$ along the unit cell axis. It may also be described as face centered cubic lattice in which all of the octahedral sites are filled, while all the tetrahedral sites remain vacant, and thus each of the atoms in the rock salt structure are 6-coordinate. The rock salt unit cell is shown in Figure 1.6.1.26. A number of inter-atomic distances may be calculated for any material with a rock salt structure using the lattice parameter (a).

$$Na - Cl = \frac{a}{2} \approx 0.5a \quad (1.6.2)$$

$$Na - Na = Cl - Cl = \frac{a}{\sqrt{2}} \approx 0.707a \quad (1.6.3)$$

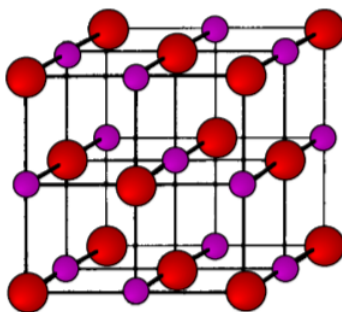


Figure 1.6.26: Unit cell structure of a rock salt lattice. Sodium ions are shown in purple (small spheres) and chloride ions are shown in red (large spheres).

Cinnabar

Cinnabar, named after the archetype mercury sulfide, HgS , is a distorted rock salt structure in which the resulting cell is rhombohedral (trigonal) with each atom having a coordination number of six.

Wurtzite

This is a hexagonal form of the zinc sulfide. It is identical in the number of and types of atoms, but it is built from two interpenetrating hcp lattices as opposed to the fcc lattices in zinc blende. As with zinc blende all the atoms in a wurtzite structure are 4-coordinate. The wurtzite unit cell is shown in Figure 1.6.1.27. A number of inter atomic distances may be calculated for any material with a wurtzite cell using the lattice parameter (a).

$$\text{Zn} - \text{S} = a\sqrt{\frac{3}{8}} \approx 0.612a = \frac{3c}{8} = 0.375c \quad (1.6.4)$$

$$\text{Zn} - \text{Zn} = \text{S} - \text{S} = a = 1.632c \quad (1.6.5)$$

However, it should be noted that these formulae do not necessarily apply when the ratio a/c is different from the ideal value of 1.632.

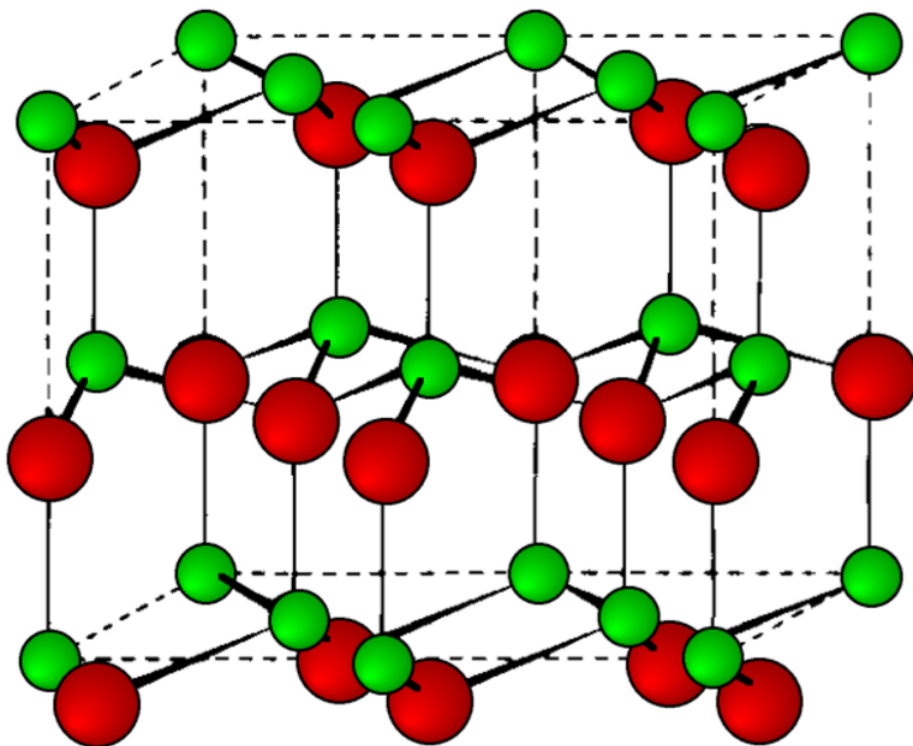


Figure 1.6.27: Unit cell structure of a wurtzite lattice. Zinc atoms are shown in green (small spheres), sulfur atoms shown in red (large spheres), and the dashed lines show the unit cell.

Cesium Chloride

The cesium chloride structure is found in materials with large cations and relatively small anions. It has a simple (primitive) cubic cell (Figure 1.6.1.16) with a chloride ion at the corners of the cube and the cesium ion at the body center. The coordination numbers of both Cs^+ and Cl^- , with the inner atomic distances determined from the cell lattice constant (a).

$$\text{Cs} - \text{Cl} = \frac{a\sqrt{3}}{2} = 0.866a \quad (1.6.6)$$

$$\text{Cs} - \text{Cs} = \text{Cl} - \text{Cl} = a \quad (1.6.7)$$

β -Tin

The room temperature allotrope of tin is β -tin or white tin. It has a tetragonal structure, in which each tin atom has four nearest neighbors ($\text{Sn-Sn} = 3.016 \text{ \AA}$) arranged in a very flattened tetrahedron, and two next nearest neighbors ($\text{Sn-Sn} = 3.175 \text{ \AA}$). The overall structure of β -tin consists of fused hexagons, each being linked to its neighbor via a four-membered Sn_4 ring.

Defects in crystalline solids

Up to this point we have only been concerned with ideal structures for crystalline solids in which each atom occupies a designated point in the crystal lattice. Unfortunately, defects ordinarily exist in equilibrium between the crystal lattice and its environment. These defects are of two general types: point defects and extended defects. As their names imply, point defects are associated with a single crystal lattice site, while extended defects occur over a greater range.

Point defects: too many or too few or just plain wrong

Point defects have a significant effect on the properties of a semiconductor, so it is important to understand the classes of point defects and the characteristics of each type. Figure 1.6.1.28 summarizes various classes of native point defects, however, they may be divided into two general classes; defects with the wrong number of atoms (deficiency or surplus) and defects where the identity of the atoms is incorrect.

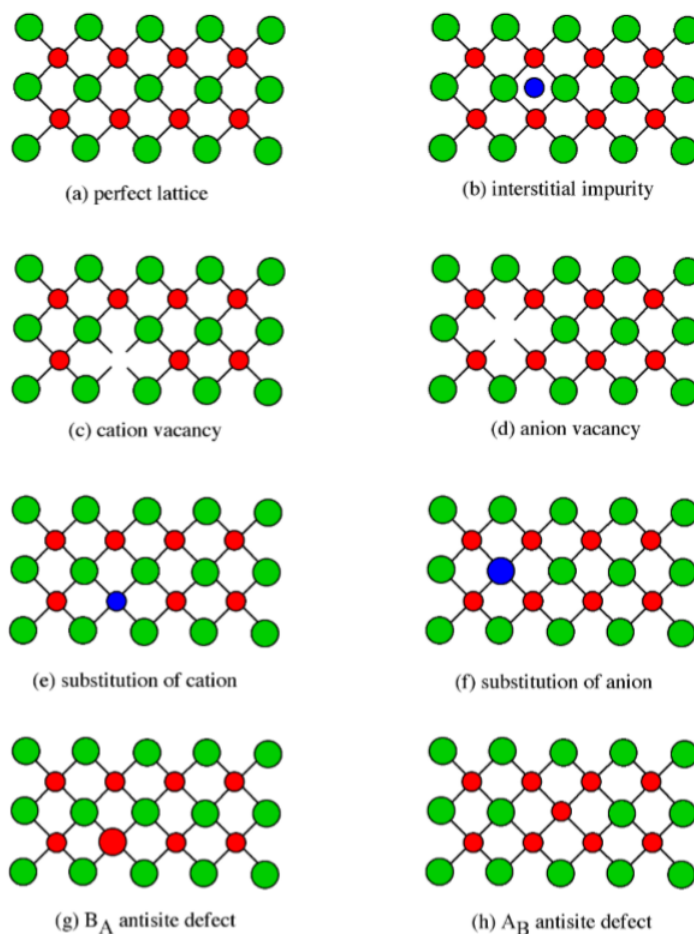


Figure 1.6.28: Point defects in a crystal lattice.

Interstitial Impurity

An interstitial impurity occurs when an extra atom is positioned in a lattice site that should be vacant in an ideal structure (Figure 1.6.1.28b). Since all the adjacent lattice sites are filled the additional atom will have to squeeze itself into the interstitial site, resulting in distortion of the lattice and alteration in the local electronic behavior of the structure. Small atoms, such as carbon, will prefer to occupy these interstitial sites. Interstitial impurities readily diffuse through the lattice via interstitial diffusion, which can

result in a change of the properties of a material as a function of time. Oxygen impurities in silicon generally are located as interstitials.

Vacancies

The converse of an interstitial impurity is when there are not enough atoms in a particular area of the lattice. These are called vacancies. Vacancies exist in any material above absolute zero and increase in concentration with temperature. In the case of compound semiconductors, vacancies can be either cation vacancies (Figure 1.6.1.28c) or anion vacancies (Figure 1.6.1.28d), depending on what type of atom are missing.

Substitution

Substitution of various atoms into the normal lattice structure is common, and used to change the electronic properties of both compound and elemental semiconductors. Any impurity element that is incorporated during crystal growth can occupy a lattice site. Depending on the impurity, substitution defects can greatly distort the lattice and/or alter the electronic structure. In general, cations will try to occupy cation lattice sites (Figure 1.6.1.28e), and anion will occupy the anion site (Figure 1.6.1.28f). For example, a zinc impurity in GaAs will occupy a gallium site, if possible, while a sulfur, selenium and tellurium atoms would all try to substitute for an arsenic. Some impurities will occupy either site indiscriminately, e.g., Si and Sn occupy both Ga and As sites in GaAs.

Antisite Defects

Antisite defects are a particular form of substitution defect, and are unique to compound semiconductors. An antisite defect occurs when a cation is misplaced on an anion lattice site or vice versa (Figure 1.6.1.28g and h). Dependent on the arrangement these are designated as either AB antisite defects or BA antisite defects. For example, if an arsenic atom is on a gallium lattice site the defect would be an AsGa defect. Antisite defects involve fitting into a lattice site atoms of a different size than the rest of the lattice, and therefore this often results in a localized distortion of the lattice. In addition, cations and anions will have a different number of electrons in their valence shells, so this substitution will alter the local electron concentration and the electronic properties of this area of the semiconductor.

Extended Defects: Dislocations in a Crystal Lattice

Extended defects may be created either during crystal growth or as a consequence of stress in the crystal lattice. The plastic deformation of crystalline solids does not occur such that all bonds along a plane are broken and reformed simultaneously. Instead, the deformation occurs through a dislocation in the crystal lattice. Figure 1.6.1.29 shows a schematic representation of a dislocation in a crystal lattice. Two features of this type of dislocation are the presence of an extra crystal plane, and a large void at the dislocation core. Impurities tend to segregate to the dislocation core in order to relieve strain from their presence.

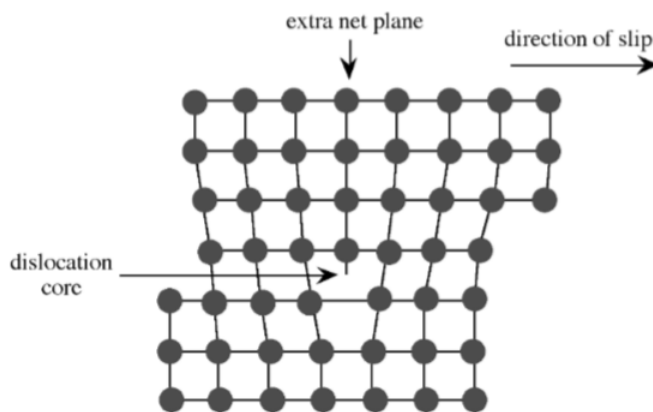


Figure 1.6.29: Dislocation in a crystal lattice.

Epitaxy

Epitaxy, is a transliteration of two Greek words *epi*, meaning "upon", and *taxis*, meaning "ordered". With respect to crystal growth it applies to the process of growing thin crystalline layers on a crystal substrate. In epitaxial growth, there is a precise crystal

orientation of the lm in relation to the substrate. The growth of epitaxial films can be done by a number of methods including molecular beam epitaxy, atomic layer epitaxy, and chemical vapor deposition, all of which will be described later.

Epitaxy of the same material, such as a gallium arsenide lm on a gallium arsenide substrate, is called homoepitaxy, while epitaxy where the lm and substrate material are different is called heteroepitaxy. Clearly, in homoepitaxy, the substrate and lm will have the identical structure, however, in heteroepitaxy, it is important to employ where possible a substrate with the same structure and similar lattice parameters. For example, zinc selenide (zinc blende, $a = 5.668 \text{ \AA}$) is readily grown on gallium arsenide (zinc blende, $a = 5.653 \text{ \AA}$). Alternatively, epitaxial crystal growth can occur where there exists a simple relationship between the structures of the substrate and crystal layer, such as is observed between Al_2O_3 (100) on Si (100). Whichever route is chosen a close match in the lattice parameters is required, otherwise, the strains induced by the lattice mismatch results in distortion of the lm and formation of dislocations. If the mismatch is significant epitaxial growth is not energetically favorable, causing a textured lm or polycrystalline untextured lm to be grown. As a general rule of thumb, epitaxy can be achieved if the lattice parameters of the two materials are within about 5% of each other. For good quality epitaxy, this should be less than 1%. The larger the mismatch, the larger the strain in the lm. As the lm gets thicker and thicker, it will try to relieve the strain in the lm, which could include the loss of epitaxy of the growth of dislocations. It is important to note that the $\langle 100 \rangle$ directions of a lm must be parallel to the $\langle 100 \rangle$ direction of the substrate. In some cases, such as Fe on MgO, the [111] direction is parallel to the substrate [100]. The epitaxial relationship is specified by giving first the plane in the film that is parallel to the substrate [100].

Bibliography

- *International Tables for X-ray Crystallography*. Vol. IV; Kynoch Press: Birmingham, UK (1974).
- B. F. G. Johnson, in *Comprehensive Inorganic Chemistry*, Pergamon Press, Vol. 4, Chapter 52 (1973).
- A. R. West, *Solid State Chemistry and its Applications*, Wiley, New York (1984).

This page titled [1.6: Structure and Bonding - Crystal Structure](#) is shared under a [CC BY 3.0](#) license and was authored, remixed, and/or curated by [Andrew R. Barron \(CNX\)](#) via [source content](#) that was edited to the style and standards of the LibreTexts platform.

1.7: Structure and Bonding - Stereochemistry

Stereo isomers

Stereo isomers have the same empirical formula or molecular formula but different structural formulas. A typical example is butane, C_4H_{10} , which can have two different possible structures: *n*-butane (Figure 1.7.130a) and iso-butane also known as 1-methylpropane (Figure 1.7.130b).

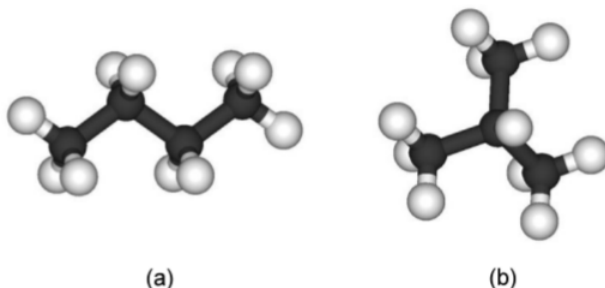


Figure 1.7.30: The two stereo isomers of butane: (a) *n*-butane and (b) iso-butane.

Geometric isomers

Geometric isomers have the same empirical formula or molecular formula and also the same structural formula, but have a different relative arrangement of the substituent groups. For example, the two geometric isomers of 1,2-dichloroethene (Figure 1.7.131) have the molecular formula of $C_2H_2Cl_2$, and the same structural formula of $Cl(H)C=C(H)Cl$, but the relative position of the two chlorine atoms can either be the same side of the $C=C$ double bond (i.e., *cis*, see Figure 1.7.131a) or on opposite sides of the $C=C$ double bond (i.e., *trans*, see Figure 1.7.131b). The use of *cis* and *trans* is not limited to organic compounds such as olefins, but can also be used in metal complexes, e.g., Figure 1.7.132.

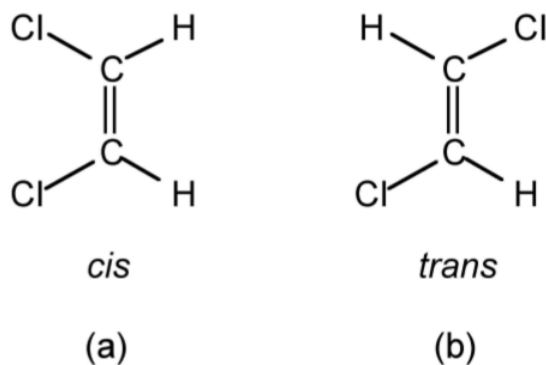


Figure 1.7.31: The two geometric isomers of 1,2-dichloroethene.

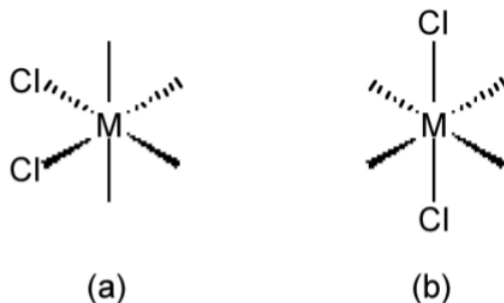


Figure 1.7.32: Examples of (a) *cis* and (b) *trans* geometric isomers for metal complexes.

When it is not possible to describe geometric isomers by the terms *cis* or *trans*, the terms facial (*fac*, Figure 1.7.1.33a) or meridinal (*mer*, Figure 1.7.1.33b) are commonly employed.

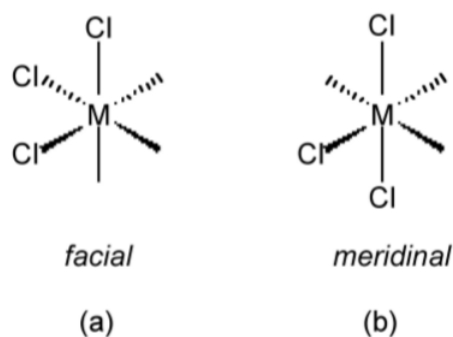


Figure 1.7.33: Examples of (a) fac and (b) mer geometric isomers for metal complexes.

Optical isomers

If the mirror object and mirror image of a molecule are not the same (i.e., they are not superimposable) they are known as *enantiomers*. If they also have optical activity they are called *chiral* and are described as having *chirality*. Enantiomers of a particular compound have the same general properties with two exceptions:

1. Their behavior to polarized light.
2. Their reaction with other chiral molecules

It is possible to determine if a molecule is chiral or not from its symmetry. Chiral molecules will have no symmetry or axis of rotation. The optical activity of a chiral molecule will turn the plane of polarized light either to the right (+) or the left (-). The former is known as *dextrorotatory* (D), while the latter is known as *levorotatory* (L).

Configuration

The configuration of a chiral molecule may be represented in a number of ways. Lactic acid ($C_3H_6O_3$) provides a suitable and simple example. The two optical isomers of lactic acid can be represented in 3-dimensional (3D) form as shown in Figure 1.7.1.34; however, it is also possible to draw the same molecules in 2D using the Fischer projection (Figure 1.7.1.35). While the Fischer projection does not appear to define the geometry about the central carbon atom, the convention is that the side chains are out of the plane of the page (towards the observer), while the top and bottom groups are into the plane of the page (away from the observer). Thus, Figure 1.7.1.35a is a representation of Figure 1.7.1.34a, and Figure 1.7.1.35b is a representation of Figure 1.7.1.34b.

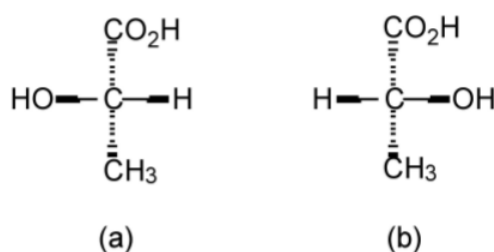


Figure 1.7.34: 3D representations of lactic acid.

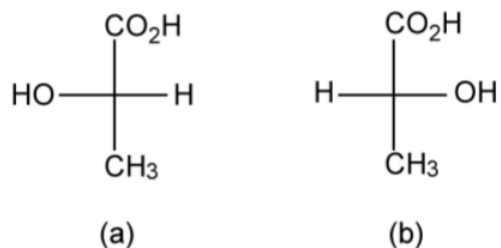


Figure 1.7.35: 2D Fischer representations of lactic acid.

Fischer-Rosenoff convention

The Fischer-Rosenoff convention defines chirality of a molecule using the Fischer projection. The convention is based upon D-(+)-glyceraldehydes (Figure 1.7.1.36).

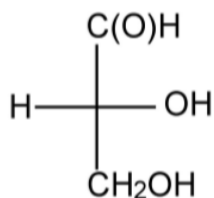


Figure 1.7.36: The Fischer projection of D-(+)-glyceraldehyde.

To determine the chiral label for a molecule, the Fischer projection is drawn with the longest carbon chain pointing away from the observer, i.e., into the plane of the page. The number 1 carbon (that of the highest substitution) is positioned at the top of the diagram. If the functional group is on the right of the diagram the isomer is given the label D (from the dextrorotatory enantiomer of glyceraldehydes rather than the molecule being dextrorotatory per se), i.e., Figure 1.7.1.36. On the other hand if the functional group is on the left of the diagram the isomer is given the label L (from the levorotatory enantiomer of glyceraldehyde rather than the molecule being levorotatory per se).

Rules

Where molecules are large and complex a number of additional rules are useful:

1. Make any alcohol substituent to be nearest to the top, e.g., a butan-2-ol (Figure 1.7.1.37a) rather than a butan-3-ol (Figure 1.7.1.37b).
2. Aldehydes and ketones are the number 1 carbon atom.
3. If there are both sets of substituents, rule 1 has precedence over rule 2.

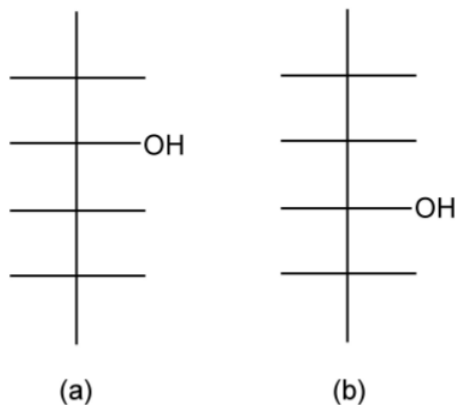


Figure 1.7.37: Preferred positioning of an alcohol substituent to be nearest the top (a) rather than at the bottom (b), according to the rules of the Fischer-Rosenoff convention.

Nomenclature in terms of R and S

The *R/S* nomenclature is a more widely used alternative to the *D/L* nomenclature, and is based upon the hierarchical order of the substituents. From the Fischer projection, the groups are ordered with the largest atom first, as shown in Figure 1.7.1.38. The lowest numbered substituent is then oriented away from the observer (i.e., H in Figure 1.7.1.38). The order of the remaining substituents 1, 2, 3 is then traced: if it goes clockwise the molecule is labeled *R*, if it goes anti-clockwise (counter-clockwise) the molecule is labeled *S*.

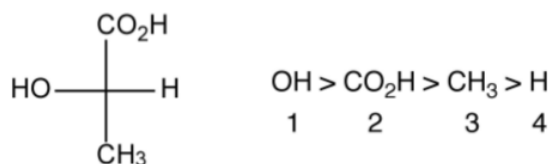


Figure 1.7.38: The structure of Lactic acid, and the ordering of the substituents.

The advantage of the *R/S* methodology is that it can also be used for geometric isomers. Thus, while *cis* and *trans* are useful when the groups either side of a C=C double bond are the same (e.g., *cis*-1,2dichloroethene, Figure 1.7.1.39a); however, when four different groups are present (e.g., A, B, X, and Y as seen in Figure 1.7.1.39b) then an alternative must be used. By taking either group A/B or X/Y and placing in order of precedence, the relative order defines the isomer. Thus, if in Figure 1.7.10b A>B and X>Y the label *Z* (*zusammen* from the German for *together*) is used. Conversely, if in Figure 1.7.10b A<B and X>Y the label *E* (*entgegen* from the German for *opposite*) is used.

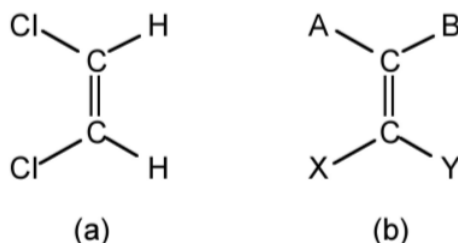


Figure 1.7.39: The structures of (a) *cis*-1,2-dichloroethene and (b) a generic olefin with four different substituent groups.

More complex molecules

As molecules become more complex with multiple functional groups and multiple chiral centers the *D/L* nomenclature has the potential to become confusing. Erythrose has two chiral centers, and based upon the Fischer projections it may be seen that since the alcohol substituents in the 2 and 3 positions are on the same side of the backbone in the Fischer projection irrespective if it is *D*-(-)-erythrose or *L*-(+)-erythrose (Figure 1.7.1.40a and b). Thus, the naming is simplified despite the presence of multiple side groups. However, in threose (Figure 1.7.1.40c) the substituents are on different sides of the Fischer projection raising the issue as to whether this should be *L* or *D*. However, in such cases the substituent at the bottom of the side chain takes priority, thus Figure 1.7.1.40c is *D*-(-)-threose.

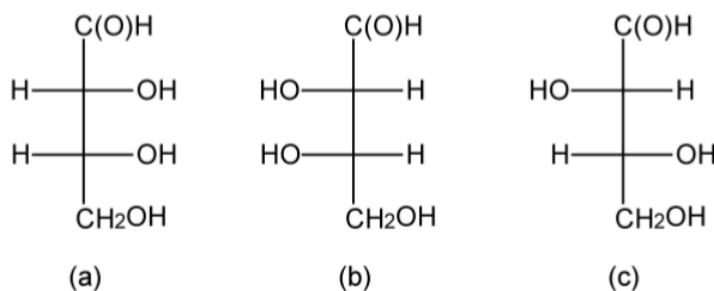


Figure 1.7.40: The Fischer projections of (a) *D*-(-)-erythrose, (b) *L*-(+)-erythrose, and (c) *D*-(-)-threose.

Note

D-(-)-erythrose and *L*-(+)-erythrose are enantiomers, and *D*-(+)-threose and *L*-(+)-threose are also enantiomers, but threose and erythrose are *diastereomers*. Enantiomers have the same physical properties (just different behavior to polarized light), while diastereomers may have different physical properties such as melting points and solubility.

Amino Acids

Amino acids (or more properly α -amino acids) are compounds containing both an amine (NH₂) group and a carboxylic acid (CO₂H) attached to the same carbon atom. The presence of both acid and base groups can result in the formation of the Zwitterionic form with ammonium (NH₃⁺) and carboxylate (CO₂⁻) groups.

In defining the labels for amino acids, the basis is D-(-)-allothreonine (Figure 1.7.1.41), whereas for an amino acid such as threonine the top substituent is used for a label, e.g., Figure 1.7.1.42.

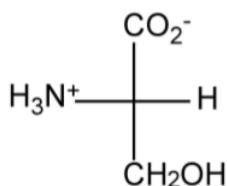


Figure 1.7.41: The Fischer projection of D-(-)-allothreonine.

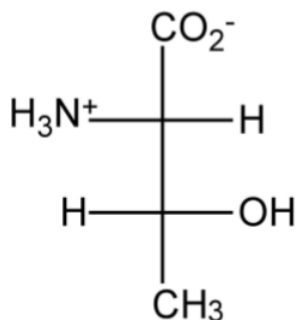


Figure 1.7.42: The Fischer projection of D-(-)-threonine.

Similar chiral centers

Just because a compound has more than one chiral center does not mean that it is optically active. A consideration of erythritol shows the presence of a mirror plane of symmetry (Figure 1.43). As such, erythritol is not optically active, i.e., there is no effect on polarized light. In contrast, while threitol has the same molecular and geometric formula, the lack of a mirror plane of symmetry (Figure 1.7.1.44) means that the *L*- and *D*⁺ forms are optically active.

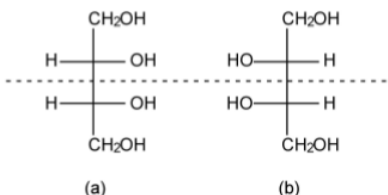


Figure 1.7.43: The Fischer projections of *D* and *L* erythritol showing the presence of a mirror plane of symmetry. N.B. The presence of a mirror plane means that erythritol is not optically active and hence there is no need to label with + or -.

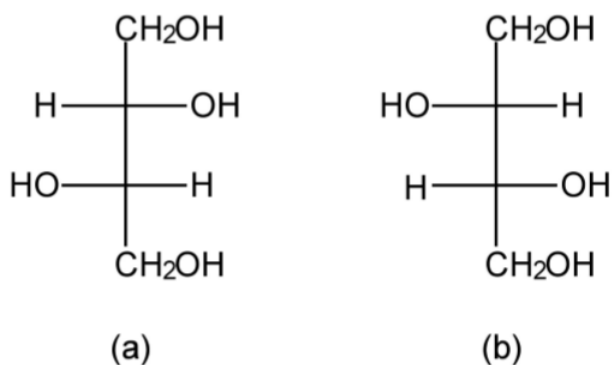


Figure 1.7.44: The Fischer projections of (a) *L*-(-)-threitol and (b) *D*-(+)-threitol.

Compounds with a *D*:*L* ratio of 1:1 are called racemic compounds and are totally optically inactive. However, it is also possible for a racemic solution of a compound to crystallize to form crystals of pure *D* or *L*, which may be manually separated.

Optical isomers that are not tetrahedral

Pyramidal molecules

Pyramidal molecules can also exhibit chirality when the three substituents are distinct, e.g., $\text{PR}_1\text{R}_2\text{R}_3$ (Figure 1.7.145). Unfortunately, most pyramidal compounds undergo an inversion of their isomers (in a similar manner to turning an umbrella inside out), such that the chiral forms interconvert rapidly. In such a case, it is not possible to resolve (separate) the different forms. Phosphines may generally be resolved because the barrier to their inversion is sufficiently large (ca. 132 kJ/mol)

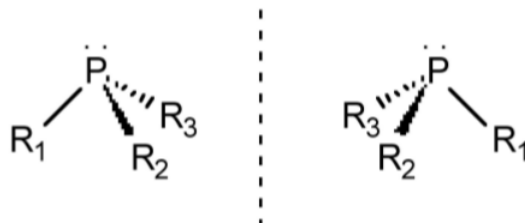


Figure 1.7.45: An example of a chiral phosphine where $\text{R}_1 \neq \text{R}_2 \neq \text{R}_3$.

The notation used for pyramidal molecules is the same as that for tetrahedral molecules, in that the individual substituents are ordered with the largest atom first. The lone pair is defined as having the lowest numbering and thus is oriented away from the observer. The order of the remaining substituents 1, 2, and 3 is then traced: if it goes clockwise the molecule is labeled R, if it goes anti-clockwise (counter-clockwise) the molecule is labeled S.

Chirality in octahedral complexes

The presence of a chelate ligand on an octahedral complex can induce chirality in the complex.

Note

A chelate ligand is a molecule or ion that is bonded to at least two points of a central atom or ion. The term chelate is from the Greek *chelè*, meaning claw.

Unlike tetrahedral based compounds, chiral octahedral compounds have their nomenclature based on the structure of a helix. For example, in the case of a bis-chelate complex (Figure 1.7.146), with one of the chelate ligands pointing straight up the helix, the direction of the other defines the chirality of the helix, i.e., if it is a left or right hand helix. If the ligand points up to the left the complex is assigned the symbol shown in Figure 1.7.146a, while if the ligand points up to the right the complex is assigned the symbol shown in Figure 1.7.146b.

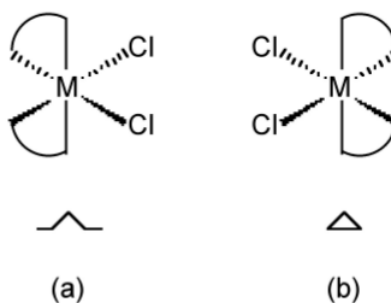


Figure 1.7.46: The two optical isomers of a bis-chelate metal complex.

In complexes with three chelate ligands (i.e., a tris-chelate complex, Figure 1.7.147), the same methodology applies, in that any two ligands can be chosen and the same rules applied.

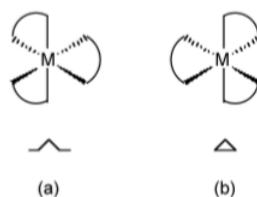


Figure 1.7.47: The two optical isomers of a tris-chelate metal complex.

Methods of resolution of racemic mixtures

A racemic mixture, or racemate, is one that has equal amounts of left- and right-handed enantiomers of a chiral molecule. The first known racemic mixture was "racemic acid," which Louis Pasteur (Figure 1.7.1.48) found to be a mixture of the two enantiomeric isomers of tartaric acid (Figure 1.7.1.49).



Figure 1.7.48: French microbiologist and chemist Louis Pasteur who is remembered for his remarkable breakthroughs in the causes and preventions of disease (1822-1895).

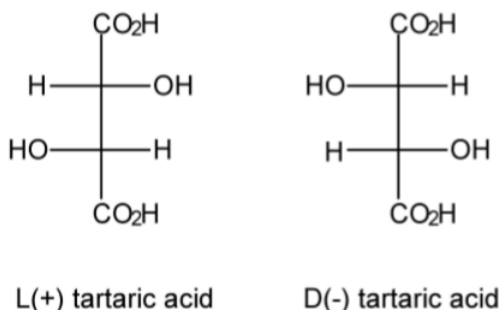


Figure 1.7.49: The Fischer projections of the two enantiomeric isomers of tartaric acid.

In nature, it is common that only one of an optical isomers is naturally produced, but in laboratory synthesis it is more common that both isomers are made in equal amounts. The separation of a racemate into its components (the pure enantiomers) is called a chiral resolution.

Mechanical separation

The crystals of enantiomerically pure compounds often have different appearances. Thus, just as Pasteur did in 1848, it is often possible to look under a microscope and physically separate the two different enantiomers.

Resolution by formation of diastereomers

One of the differentiating properties of a chiral molecule is that each enantiomer reacts with another chiral molecule to form a diastereomeric pair of compounds. For example, a racemic acid, (+)HA and (-)HA, will react with a chiral base, (-)B, to form a mixture of diastereomers, [(-)BH⁺.(+)A⁻] and [(-)BH⁺.(-)A⁻]. Because diastereomers have different physical properties they can be separated by recrystallization. Once separated by recrystallization, the addition of excess acid will liberate the enantiomerically pure compound, i.e., (+)HA or (-)HA. A typical chiral base would be a natural alkaloid base to ensure that it is pure + or -. If it is a base that is needed to be separated, then (-)malic acid is a suitable acid.

Resolution by chromatography

In a related method to resolution by the formation of diastereomers, a chiral column material will allow for the chromatographic separation of an enantiomeric mixture. Thus, the retention rate for (+)X will be different from (-)X on a column in which the

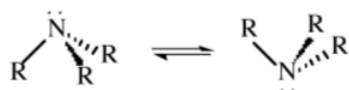
stationary phase is chiral, i.e., (-)-A. Many common chiral stationary phases are based on oligosaccharides such as cellulose or cyclodextrin (in particular with β -cyclodextrin).

Labile stereo isomers and racemization

It is only possible to separate (resolve) racemic mixtures if the molecule stays as one form for a long time. In other words, if there is a mechanism by which the two forms are interconverted, then resolution cannot be achieved.

Intramolecular rearrangement

Intramolecular rearrangements involve no bonds being broken. The classic example is the inversion of an amine, (1.12), which has a low energy barrier (24.7 kJ/mol).



Another example of an intramolecular rearrangement is the conversion of a square-based pyramidal geometry via a trigonal bipyramidal geometry to the isomeric square-based pyramidal geometry, or the alternative isomerization of one trigonal bipyramidal geometry to another via a square-based pyramidal transition state. Such a process is known as a *Berry rotation*. The Berry mechanism is a pseudorotation process for simultaneously interchanging two equatorial groups with the two axial groups, while the third equatorial group (called the pivot group) remains an equatorial group (Figure 1.7.150).

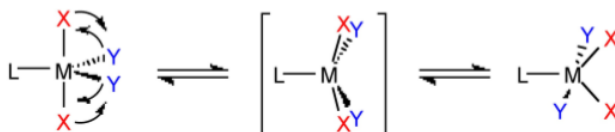


Figure 1.7.50: The Berry pseudorotation.

Intermolecular processes

Intermolecular processes involve bond breaking (and bond formation). For example a tetrahedral compound could lose one ligand, which creates a labile pyramidal compound. Rapid inversion of the pyramidal compound is followed by re-attachment of the ligand. Such a process is often so fast that resolution cannot be achieved.

Intramolecular processes

Intramolecular processes with bond breaking (and making) also lead to racemization. For example, in an octahedral complex with chelate ligands, if one of the ends of a chelate ligand detaches, it can reattach in the same configuration, or attach differently to change the chirality. In this manner the chirality can be changed from one form to another.

Conformation

The conformation of a molecule arises from the rotation of a single bond (Figure 1.7.151). However, even though there is rotation about the bond, there are energy barriers due to steric interactions of the substituents. In order to understand (and predict) these interactions, it is necessary to visualize the molecule in such a manner as to highlight the across-bond interactions; this is done by using a Newman projection.

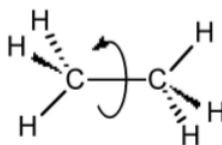


Figure 1.7.51: The rotation about the C-C single bond in ethane.

A Newman projection, useful in alkane stereochemistry, visualizes chemical conformations of a carbon-carbon chemical bond from front to back, with the front carbon represented by a dot and the back carbon as a circle (Figure 1.7.152). The front carbon atom is called proximal, while the back atom is called distal. This type of representation is useful for assessing the torsional angle between bonds. Using ethane as an example, the Newman projection along the C-C single bond results in two basic conformations: eclipsed (Figure 1.7.152a) and staggered (Figure 1.7.152b). The staggered conformation will be energetically favored since the

substituents are the most distant from each other. Conversely, the staggered will be the highest in energy. The difference in energy between the two conformations will define the barrier to rotation. In the case of ethane this is very small (12.5 kJ/mol).

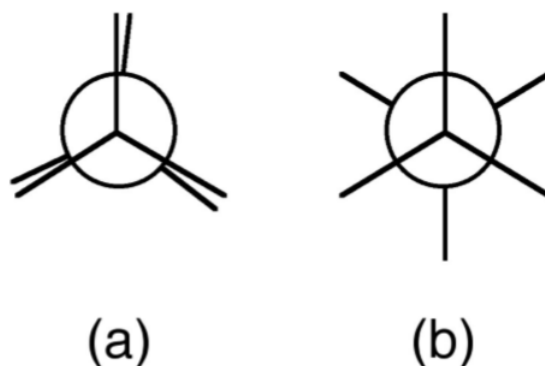


Figure 1.7.52: The Newman projection of ethane showing (a) eclipsed (E) and (b) staggered (S) conformations.

Although we often only consider the two extreme conformations, in reality there is a continuum around 360° rotation of the C-C bond. Figure 1.7.153 shows the relative energy as a function of the dihedral angle for ethane. Since each carbon in ethane has equivalent substitution (i.e., three H atoms) the energy for each staggered conformation is the same. This is not true for more complex molecules such as butane (Figure 1.7.154).

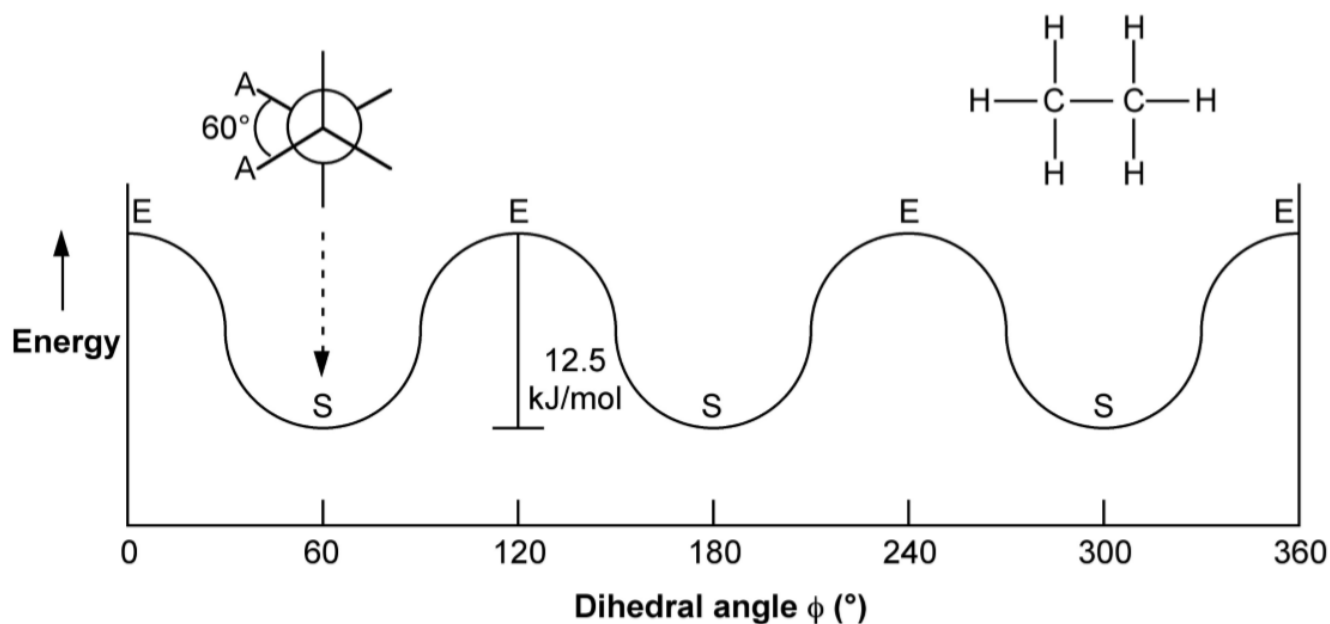


Figure 1.7.53: The relative energy as a function of the dihedral angle for ethane.

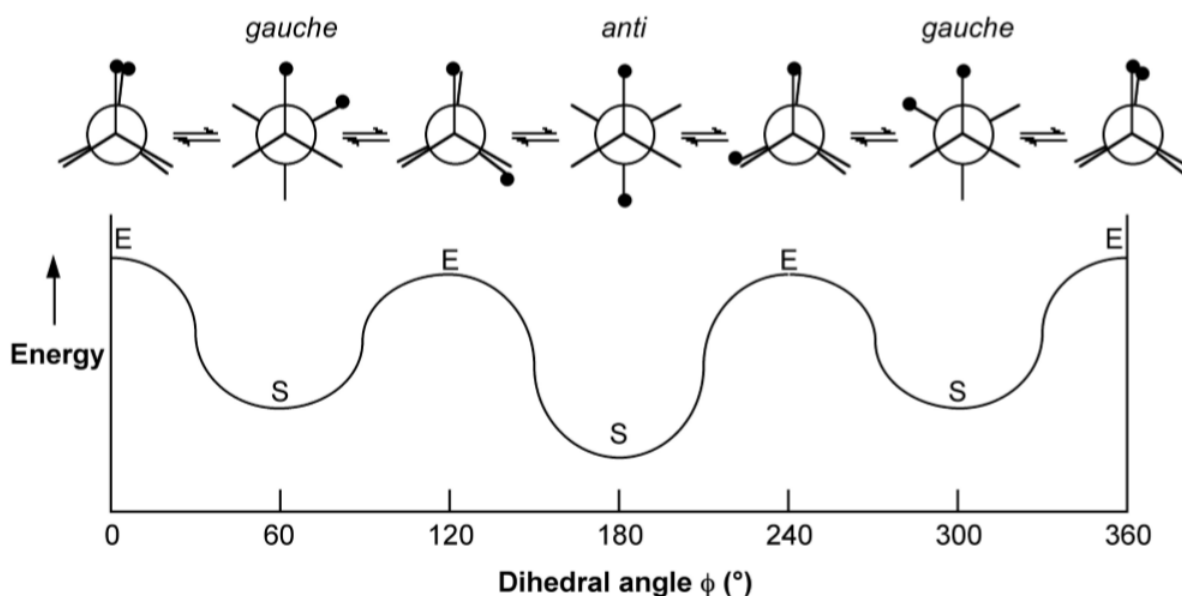


Figure 1.7.54: The relative energy as a function of the dihedral angle for butane.

As may be seen from Figure 1.7.154, the staggered conformation in which the two methyl groups (represented by the black circles) are as far away from each other (*anti*) is the most energetically favored. The other two staggered conformations (*gauche*) are mirror images of each other and are hence conformation enantiomers. It should also be noted from Figure 1.7.154 that the eclipsed conformations vary in energy since the presence of methyl···methyl near neighbors is clearly less energetically favorable than methyl···H near neighbors.

Generally the rotation about C-C bonds has a low barrier to rotation, however, if substituents are sufficiently bulky the molecule will not twist around the bond, e.g., substituted bi-phenyl with sterically bulky substituents (Figure 1.7.155).

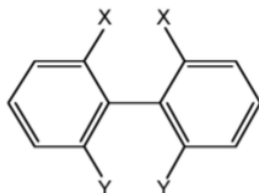


Figure 1.7.55: The ease of rotation about the C-C bond of a substituted bi-phenyl will depend on the steric bulk of X and Y.

Free rotation about a C-C bond is not fully possible when you have a ring system, e.g., in a cyclic compound such as cyclohexane, C_6H_{12} . The limited rotation about the C-C bonds results in the flipping of the ring conformation from the chair form (Figure 1.7.156a) to the boat form (Figure 1.7.156b). Since the boat form has steric hindrance between the hydrogen atoms, the chair form is the more stable.

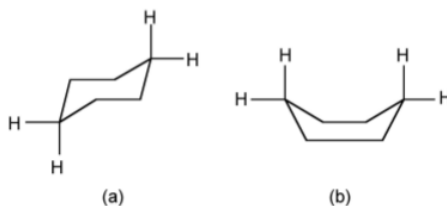


Figure 1.7.56: The chair (a) and boat (b) conformations of cyclohexane, C_6H_{12} .

Conformation of compounds with lone pairs

Lone pairs often behave in a different manner to substituents in regard to conformations. Thus, methylamine (CH_3NH_2) would be predicted to have the staggered conformation shown in Figure 1.7.157a. However, the lower steric bulk of the lone pair results in the nitrogen being 0.09 Å away from the true center of the CH_3 projection (Figure 1.7.157b).

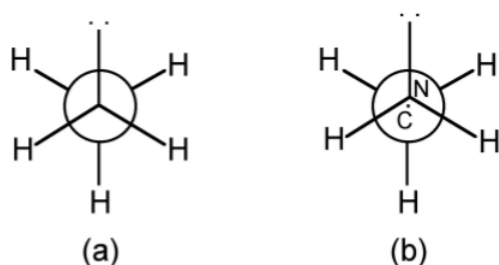


Figure 1.7.57: The ideal (a) and observed (b) conformations of methylamine, CH_3NH_2 .

In compounds with more than one lone pair, the lowest energy form is not always the *anti* conformation. For example, at 20°C hydrazine (H_2NNH_2) is 100% *gauche* (Figure 1.7.1.58a); but for substituted hydrazines (i.e., a diamine, R_2NNR_2) if the substituent groups are sufficiently large then the *anti* conformation will dominate (Figure 1.7.1.58b).

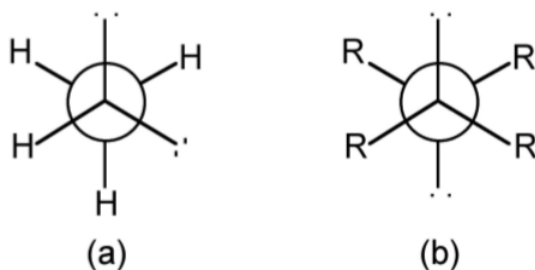


Figure 1.7.1.58: The stable conformation of hydrazine (H_2NNH_2) at 20°C (a) as compared to the *anti* conformation (b) observed for diamines (R_2NNR_2).

The conformation of hydrogen peroxide (H_2O_2) is dominated by the lone pairs rather than the hydrogen atoms. Instead of the expected *anti* conformation (c.f., Figure 1.7.1.54 where the black circles would represent the hydrogen atoms) in the free state the dihedral angle is 94° (Figure 1.7.1.59). The conformation of hydrogen peroxide is therefore neither eclipsed nor staggered but an intermediate structure. When in the solid state hydrogen bonding will cause the shape and angles to change.

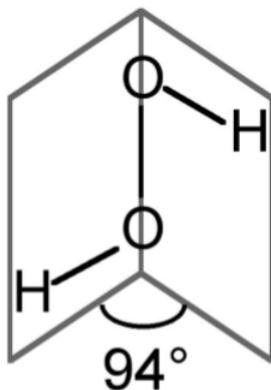


Figure 1.7.59: The structure of hydrogen peroxide in the free state.

Bibliography

- R. S. Berry, *J. Chem. Phys.*, 1960, **32**, 933.
- A. Keys, S. G. Bott, and A. R. Barron, *J. Chem. Cryst.*, 1998, **28**, 629.

This page titled [1.7: Structure and Bonding - Stereochemistry](#) is shared under a [CC BY 3.0](#) license and was authored, remixed, and/or curated by Andrew R. Barron (CNX) via [source content](#) that was edited to the style and standards of the LibreTexts platform.

1.8: Acids, Bases, and Solvents - Choosing a Solvent

The choice of solvent is an important parameter for any chemical reaction. The following provides a guide to some of the consideration to be made in choosing a solvent to ensure the desired reaction occurs.

Solvation

Solvation may be defined as the interaction between the solvent and the solute, however, two general classes of solvation have different consequences to the stability of either reagents or products in a chemical reaction, and hence the potential of a reaction to occur

- **Specific solvation** is where the solvent interacts with one of the ions (or molecules) in solution via a covalent interaction. Furthermore, there will be a specific number of solvent molecules bound to each ion (or molecule), e.g., $[\text{Cu}(\text{NH}_3)_4]^{2+}$ and $[\text{Mg}(\text{H}_2\text{O})_6]^{2+}$ (Figure 1.8.1.60a).
- **Non-specific solvation** is as a result of van der Waals or dipole-dipole forces between the solvent and an ion (or molecule). There will be no defined number of interactions and the solvent...ion interaction will be highly fluxional, e.g., while water solvates the chloride ion (Figure 1.8.1.60b) the number of water molecules around each anion is not fixed

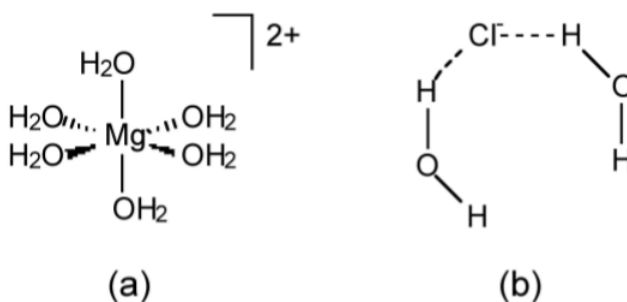
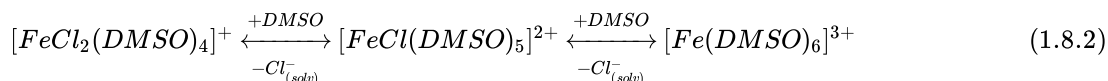
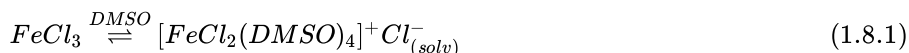


Figure 1.8.60: Examples of (a) specific and (b) non-specific solvation.

Table 1.8.1.10 shows the ability of three solvents to act with specific and non-specific solvation. The relative solvation ability of each solvent results in three different products from the dissolution of iron(III) chloride (FeCl_3).

Solvation	DMSO (Me_2SO)	Pyridine ($\text{C}_5\text{H}_5\text{N}$)	Acetonitrile (MeCN)
Specific	Good	Very good	Poor
Non-specific	Good	Poor	Moderately good

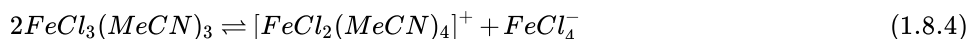
Dissolution of FeCl_3 in DMSO results in the dissociation of a chloride ligand, (1.8.1), due to both the specific solvation of the FeCl_2^+ cation and the non-specific solvation of the Cl^- anion. In fact, the good solvation properties of DMSO means that depending on the concentration (and temperature) a series of dissociations may occur, (1.8.2).



In contrast, if FeCl_3 is dissolved in pyridine (py) the neutral Lewis acid-base complex is formed, (1.8.3), because while pyridine is a very good at specific solvation (Table 1.8.1.10), it is poor at solvating the chloride anion.



In a similar manner, $\text{FeCl}_3(\text{MeCN})_3$ will be formed by the dissolution in acetonitrile, because although it is not good at specific solvation, it is not sufficiently good at non-specific solvation to stabilize the chloride anion. However, since the FeCl_4^- anion has a lower charge density than Cl^- , it can be supported by the non-specific solvation of acetonitrile and thus a disproportionation reaction occurs, (1.8.4).

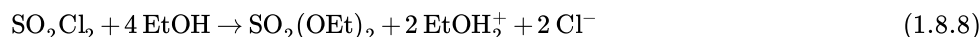
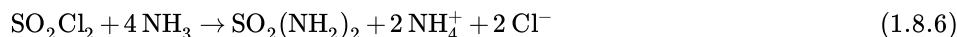
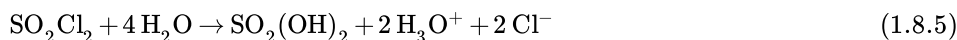


Interference by the solvent

Rather than solvating a molecule or ion, the solvent can take an active and detrimental role in the synthesis of a desired compound.

Solvolysis

The archetypal solvolysis reaction is the reaction with water, i.e., hydrolysis, (1.8.5). However, solvolysis is a general reaction, involving bond breaking by the solvent. Thus, the reaction with ammonia is **ammonolysis**, (1.8.6), the reaction with acetic acid is **acetolysis**, (1.8.7), and the reaction with an alcohol is **alcoholysis**, (1.8.8) where $Et = C_2H_5$. In each case the same general reaction takes place yielding the cation associated with the solvent.



Competition reactions

Where more than one reaction could occur the reaction involving the solvent can often compete with the desired reaction.

If it is desired to synthesis the Lewis acid-base complex between diethylether (Et_2O) and boron triuoride (BF_3) it is important to choose a solvent that will not compete with the complex formation. For example, pyridine is a poor choice because the nitrogen donor is a stronger Lewis base than the diethylether, (1.8.9), and thus no reaction would occur between diethylether and boron trifluoride. In contrast, since acetonitrile ($MeCN$) is a poor Lewis base, then the reaction will occur.



If the synthesis of $GeCl_6^{2-}$ from germanium tetrachloride ($GeCl_4$) and a source of chloride anion, then water would be a poor choice of solvent since hydrolysis of $GeCl_4$ would result. Liquid hydrogen chloride would be equally poor solvent since strong $Cl \cdots H-Cl$ hydrogen bonding would stabilize the chloride anion and preclude reaction. In contrast, nitromethane (CH_3NO_2) would be a polar enough solvent to solvate the $GeCl_4$, but it will be displaced by the chloride anion, which would be only weakly solvated.

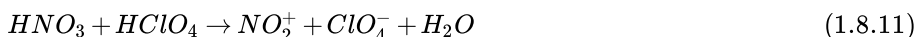
Salt formation

The formation of a salt via a double displacement reaction, (1.8.10), can be promoted by the choice of solvent by shifting the equilibrium by stabilization of one or more reagent/product.

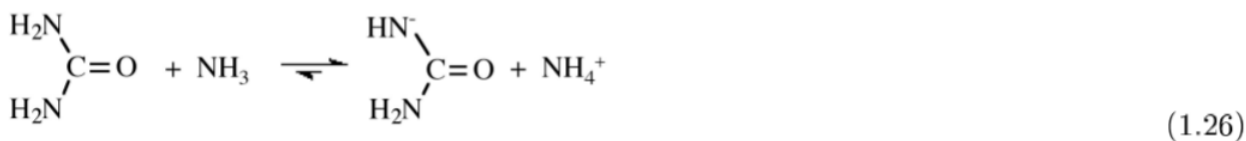
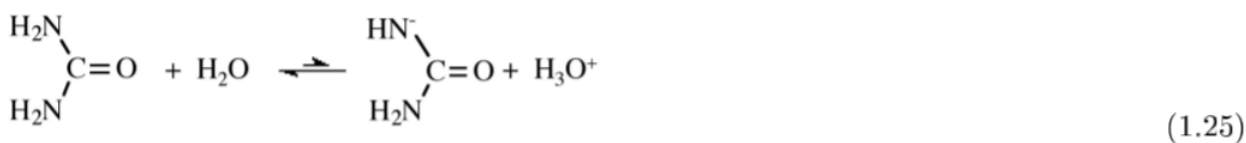


Salt stabilization through relative acidity

The attempted formation of nitronium perchlorate from nitric acid and perchloric acid, (1.8.11), in water will result in the decomposition of the NO_2^+ cation, (1.24). However, if the reaction is carried out in a stronger acid, i.e., sulfuric acid, the NO_2^+ cation is stable, and the resulting salt can be recrystallized, (1.8.12).



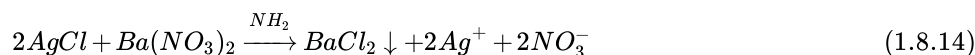
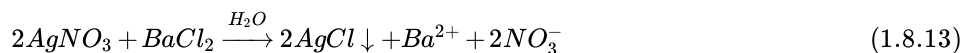
In a similar manner, the weak basic character of water means the equilibrium reaction, (1.25), has a very small equilibrium constant, K . However, if the reaction is carried out in a strongly basic solvent such as ammonia the uride anion is stabilized, (1.26), and can be precipitated by cation exchange.



Salt stabilization through solvation

The following observations may be explained by a consideration of the solvation ability of the solvent.

1. The reaction of silver nitrate with barium chloride in water yields silver chloride and barium nitrate, (1.8.13).
2. The reaction of barium nitrate with silver chloride in ammonia yields barium chloride and silver nitrate, (1.8.14).



Since silver nitrate and barium nitrate are soluble in both solvents, the differences must be due to differences in the solubility of the chlorides in each solvent. A consideration of the relative stability of solid silver chloride versus the solvated species (Figure 1.8.1.61) shows that the enthalpy of solvation in water is less than the lattice energy. Thus, if silver chloride were present as Ag^+ and Cl^- in water it would spontaneously precipitate. In contrast, the enthalpy of solvation in ammonia is greater than the lattice energy, thus solid AgCl will dissolve readily in liquid ammonia. The reason for the extra stabilization from the specific solvation of the silver cation by the ammonia, i.e., the formation of the covalent complex $[\text{Ag}(\text{NH}_3)_2]^+$.

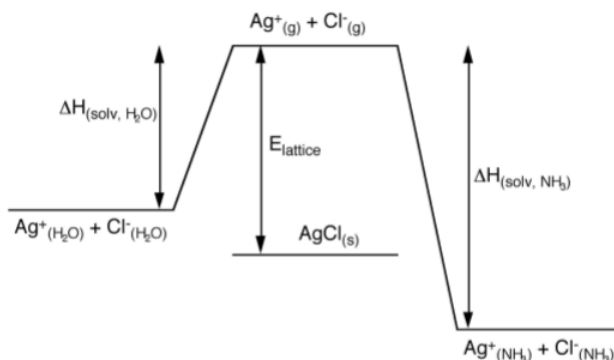


Figure 1.8.61: Enthalpy of solvation of silver chloride in water and ammonia in comparison to the lattice energy.

As may be seen from Figure 1.8.1.62, the opposite effect occurs for barium chloride. Here the enthalpy of solvation in ammonia is less than the lattice energy. Thus, if barium chloride were present as Ba^{2+} and Cl^- in ammonia it would spontaneously precipitate. In contrast, the enthalpy of solvation in water is greater than the lattice energy, thus solid BaCl_2 will dissolve readily in water. The stabilization of $\text{Ba}^{2+}(\text{aq})$ occurs because water will have a larger sphere of non-specific solvation as a consequence of having two lone pairs, allowing interaction with the Ba^{2+} as well as other water molecules (Figure 1.8.1.63).

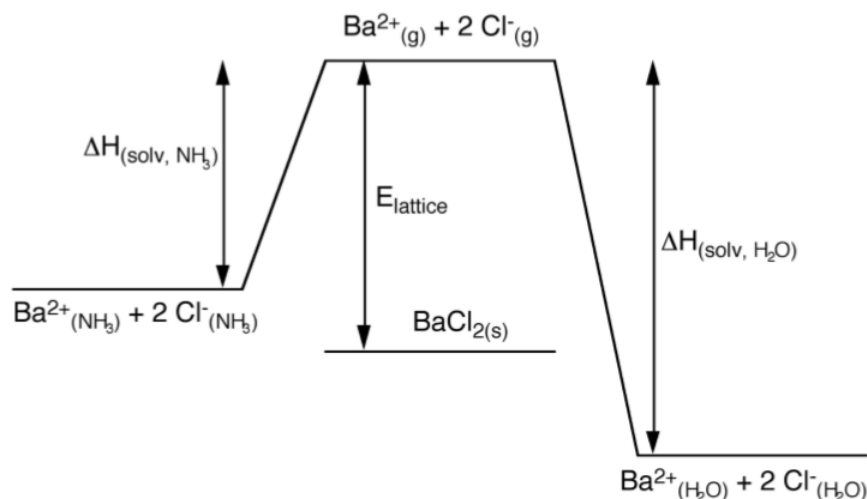


Figure 1.8.62: Enthalpy of solvation of barium chloride in water and ammonia in comparison to the lattice energy.

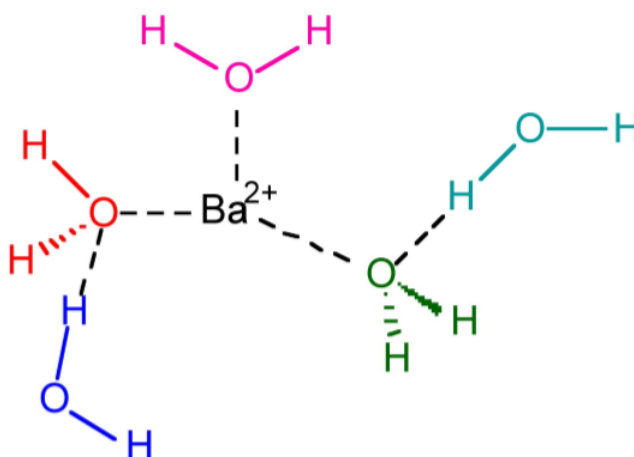
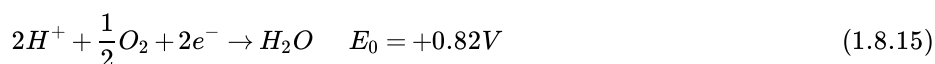


Figure 1.8.63: Schematic representation of the extended water solvation (aqua) sphere about Ba²⁺ cation.

Electron transfer reaction

A consideration of the oxidation, (1.8.15), and reduction, (1.8.16), reactions that occur for pure water at neutral pH (where $[H^+] = 10^{-7}$) would suggest that water will not tolerate oxidants whose E_0 is greater than 0.82 V nor tolerate reductants whose E_0 is less than -0.41 V.



Thus, while water has a fair range to support redox reactions it is not very good at the extremes with strong reducing agents or strong oxidizing agents. Liquid ammonia is an excellent solvent for very strong reducing agents because of the stabilization of solvated electrons, i.e., $[e^-(NH_3)_6]$. In contrast, hydrochloric acid is a good solvent for reactions involving very strong oxidizing agents.

This page titled [1.8: Acids, Bases, and Solvents - Choosing a Solvent](#) is shared under a [CC BY 3.0](#) license and was authored, remixed, and/or curated by [Andrew R. Barron \(CNX\)](#) via [source content](#) that was edited to the style and standards of the LibreTexts platform.

1.9: Chemical Reactivity - The Basics of Combustion

When discussing the combustion of a compound it is ordinarily referring to the reaction of an organic compound (hydrocarbon) with oxygen, in which the carbon is converted to carbon dioxide (CO₂) and the hydrogen forms water (H₂O) as a vapor, e.g., (1.9.1).



However, this only a narrow view of combustion, and a more general definition should be that combustion or burning is the sequence of exothermic chemical reactions between a fuel and an oxidant accompanied by the production of heat and conversion of chemical species. Based upon this definition methane can combust in the presence of fluorine (F₂) as strong oxidant, (1.9.2).



In considering the combustion of any flammable compound, for example gasoline, it should be noted that the compounds that make up gasoline are quite stable in the absence of a source of oxygen (usually from the air). Furthermore, some form of energy input (heat, flame, or spark) must be provided. Thus, the combustion of gasoline provides the archetypal example of the three component explosive system typical of a traditional chemical explosive: fuel (something that will burn), an oxidizer (usually a source of oxygen), and energy (ignition). In this regard, combustion also includes the exothermic reactions of many metals with oxygen, (1.9.3).



It is not just reactive metals that can be used as the fuel component of combustion, but many of their compounds as well. The formation of water from the hydrogen in organic compounds, in combination with an oxygen source, releases significant energy. It stands to reason therefore that any compound comprising of hydrogen and an element can be a potential fuel: a compound of hydrogen and another element is known as a [hydride](#). This is especially true for the hydrides of reactive metals such as aluminum and sodium (and metalloids such as boron, (1.9.4)), but is also true for the hydrides of silicon and phosphorus. These hydride compounds react with an oxidizer in a manner analogous to that of a hydrocarbon, as may be seen by a comparison of (1.9.5) and (1.9.1).



Figure 1.9.1.64 shows a comparison of the heat of combustion of various inorganic fuels with commonly used jet fuels (JP-10 and JP-8). Hydrocarbons heat of combustion is limited by the C:H ratio, while graphite is the limiting case. Boron and boron compounds have greater volumetric and gravimetric energy density than hydrocarbons, and therefore were studied as potential high-energy fuels.

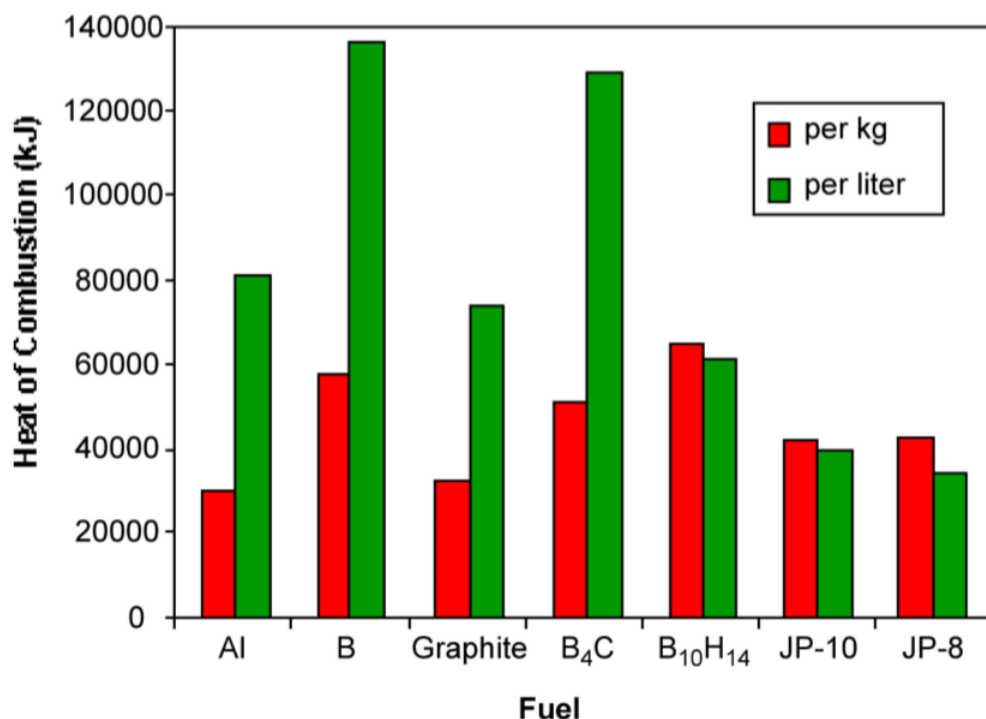


Figure 1.9.64: Heat of combustion of various fuels.

Note

Ammonia has been proposed as a practical alternative to fossil fuel for internal combustion engines. The energy value of ammonia is 22.5 MJ/kg, which is about half that of diesel. In a normal engine, in which the water vapor is not condensed, the caloric value of ammonia will be about 21% less than this value; however, it can be used in existing engines with only minor modifications to carburetors/fuel injectors.

Oxygen (O₂) from the air does not have to be the source of oxidizer. Alternatives such as hydrogen peroxide (H₂O₂), nitrous oxide (N₂O), and nitrates (e.g., ammonium nitrate, NH₄(NO₃)) are all sources of oxygen for combustion or explosions. However, this does not mean that every compound containing oxygen can be an oxidizer. For example, alcohols such as methanol will burn (in the presence of additional oxygen), but they will not act as an oxidizer. The oxygen within any compound must be reactive. By this we mean that it must be able to be released, preferentially as the more reactive oxygen atom (O) rather than O₂, or be attached (chemically bonded to an element that wants to get rid of the oxygen (i.e., an element that is readily reduced). The most likely element in this case is nitrogen, with sulfur and phosphorus also potential candidates. Almost all compounds containing nitrogen bonded to oxygen can act as an oxidizer. Generally, the more oxygen atoms attached to nitrogen the more reactive the compound.

The efficiency of a chemical reaction such as combustion is dependent on how well the fuel and oxidizer are mixed at the molecular scale. Obviously the best situation is if both components are in the same molecule. Self-oxidizers are compounds containing oxygen in a reactive form as well as a suitable fuel (carbon or hydrogen). The most common self-oxidizers are organic nitrates. It should be pointed out that in spite of the presence of reactive oxygen, self-oxidizers may still require an external source of oxygen to ensure complete reaction, and some form of energy input (ignition) is still required.

Oxygen balance

While many compounds contain oxygen that does not mean they will combust efficiently in the absence of an external oxidizer, or whether they have sufficient oxygen to completely self-combust, or whether they can act as an oxidizer for other compounds. The simplest test for a compound's potential to fulfill these roles is its oxygen balance. The oxygen balance for a chemical is the amount of oxygen needed or produced to ensure the complete oxidation of all the carbon, hydrogen, or other elements.

Compounds such as trinitrotoluene (TNT, Figure 1.9.165a) have a negative oxygen balance since extra oxygen is needed for complete formation of all the CO₂ and H₂O possible, (1.9.6). Thus, despite its reputation as an explosive, TNT is only efficient in

the presence of an external oxidant, which may be air or another compound that provides a positive oxygen balance.

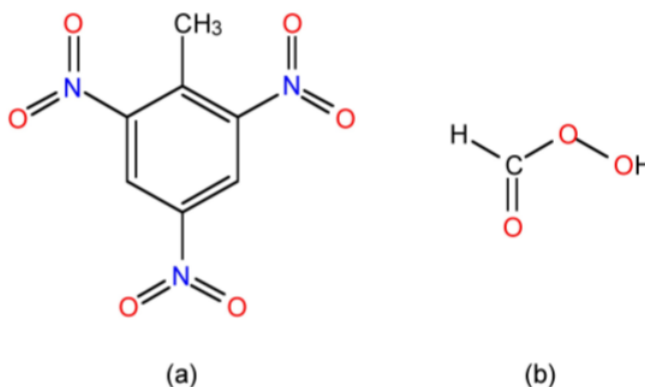
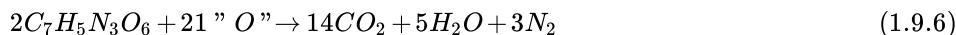


Figure 1.9.65: The structures of (a) trinitrotoluene (TNT) and (b) The structure of performic acid.

In contrast to TNT, performic acid (Figure 1.9.1.65b) is an example of a compound with a zero oxygen balance: it has all the oxygen it needs for complete combustion, (1.9.7), and hence only requires energy to detonate making it a much more dangerous compound per se than TNT.



A positive oxygen balance means that the compound liberates oxygen surplus to its own needs, for example the decomposition of ammonium nitrate provides one atom of oxygen per molecule, (1.9.8). Clearly, any compound with a positive oxygen balance makes a good oxidizer and is highly incompatible with combustible chemicals.



Quantification of oxygen balance

A quantification of oxygen balance allows for the determination of approximate ratio of reagents to optimize combustion/explosion. In this regard *oxygen balance* is defined as the number of moles of oxygen (excess or deficient) for 100 g of a compound of a known molecular weight (M_w), (1.8.9) where x = number of atoms of carbon, y = number of atoms of hydrogen, z = number of atoms of oxygen, and m = number of atoms of metal oxide produced.

$$OB\% = \frac{-1600}{M_w} \times (2x + \frac{y}{2} + m - z) \quad (1.9.9)$$

Example

In the case of TNT, the $M_w = 227.1$ g/mol, the number of carbon atoms (x) = 7, the number of hydrogen atoms (y) = 5, the number of oxygen atoms (z) = 6, and the number of atoms of metal oxide produced (m) = 0. Therefore:

$$OB\% = \frac{-1600}{227.1} \times (14 + 2.5 + 0 - 6) = -74\% \quad (1.9.10)$$

A summary of selected oxygen balance values is given in Table 1.9.1.11.

Table 1.9.1.11: Oxygen balance of selected compounds.

Element or Compound	Oxygen balance (%)
Carbon	-266.7
Sulfur	-100
Aluminum powder	-89
Trinitrotoluene	-74

Element or Compound	Oxygen balance (%)
Nitroglycerine	+3.5
Ammonium nitrate	+20
Ammonium perchlorate	+27
Potassium chlorate	+26
Sodium chlorate	+45
Sodium nitrate	+37
Tetranitromethane	+57
Lithium perchlorate	+45

This page titled [1.9: Chemical Reactivity - The Basics of Combustion](#) is shared under a [CC BY 3.0](#) license and was authored, remixed, and/or curated by [Andrew R. Barron \(CNX\)](#) via [source content](#) that was edited to the style and standards of the LibreTexts platform.

1.10: Periodic Trends for the Main Group Elements

Within the main group (s- and p-block) elements of the Periodic Table (Figure 1.10.166) there are some general trends that we can observe for the elemental form, as well as the hydrides, oxides, and halides.

1						18	
H						He	
2	13	14	15	16	17		
Li	Be	B	C	N	O	F	Ne
Na	Mg	Al	Si	P	S	Cl	Ar
K	Ca	Ga	Ge	As	Se	Br	Kr
Rb	Sr	In	Sn	Sb	Te	I	Xe
Cs	Ba						

MetalMetalloidNon-metal

Figure 1.10.66: The main group elements (Adapted from www.meta-synthesis.com).

Periodic trends for the main group elements

Within the main group (s- and p-block) elements there are some general trends that we can observe.

- The further down a given Group the elements have increased metallic character, i.e., good conductors of both heat and electricity, and exhibit delocalized bonding.
- Moving from left to right across a Period the elements have greater non-metallic character, they are insulators with localized bonding.
- Within the p-block at the boundary between the metallic elements (Figure 1.10.166, grey elements) and nonmetal elements (Figure 1.10.166, green elements) there is positioned boron and silicon that are metalloid in character (Figure 1.10.166, pink elements), i.e., they have low electrical conductivity but it increases with temperature.

As an example of these changes Table 1.10.112 shows the trends across one Period.

Table 1.10.112: Summary of trends for elements across the Periodic Table.

Element	Na	Mg	Al	Si	P	S	Cl	Ar
Properties	Electropositive metal	Electropositive metal	Metal but forms covalent bonds	Metalloid semiconductor or metal/non-metal characteristics	E-E bonding in elements	E-E bonding in elements	Simple molecule	Monoatomic gas

Periodic trends for the main group hydrides

The properties of main group hydrides are dependant on the difference in electronegativity between the element and hydrogen (Table 1.10.113). Elements on the left of the Periodic Table are highly electropositive and form ionic hydrides, while those of the center and right are covalent in character. However, of those with covalent E-H bonds, there is a change from polymeric hydrides to molecular compounds. For example, the Group 13 element hydrides (i.e., BH_3) form hydrogen-bridged oligomers (i.e., B_2H_6). In contrast, HCl is a diatomic molecule.

Table 1.10.113: Summary of properties of selected main group hydrides as a function of the relative electronegativities.

Hydride	Element electronegativity	Hydrogen electronegativity	E-H polarity	Structure	Comments
NaH	0.9	2.1	M^+H^-	Ionic	Reacts with H_2O to liberate H_2
BH_3	2.0	2.1	$B^{\delta+}-H^{\delta-}$	Oligomeric and polymeric	Reacts slowly with H_2O
CH_4	2.4	2.1	$C^{\delta-}-H^{\delta+}$	Molecular	Insoluble in H_2O
HCl	3.0	2.1	$Cl^{\delta-}-H^{\delta+}$	Molecular	Dissolves in H_2O to form H^+ and Cl^-

Periodic trends for the main group oxides

As with hydrides the properties of main group oxides are dependant on the difference in electronegativity between the element and oxygen. Highly electropositive metals form ionic oxides, while other elements form covalent bonds (albeit polar in character) with oxygen. In addition, the aggregation of covalent oxides decreased across the Period from left to right (Table 1.10.1.14). As may also be seen from Table 1.10.1.14, oxides of elements on the left of the Periodic Table dissolve in water to form basic solutions, while those on the right form acidic solutions. There is a class of oxides (especially those of Group 13 and 14) that can react as either an acid or a base. These are known as amphoteric substances.

Note

The word is from the Greek prefix *ampho* meaning "both"

Table 1.10.1.14: Comparison of oxides across the Periodic Table.

Oxide	Bonding	Reactivity with H_2O	Description
Na_2O	Ionic	Dissolves to give a strong base	Basic
Al_2O_3	Covalent polymeric	Dissolves in both acidic and basic solution	Amphoteric
SiO_2	Covalent polymeric	Dissolves in both acidic and basic solution	Amphoteric
CO_2	Covalent molecular	Dissolves to give a weak acid	Acidic
SO_3	Covalent molecular	Dissolves to give a strong acid	Acidic

In summary, oxides of the main group elements show two trends.

1. From left to right across a Period, the oxides change from ionic → oligomeric/polymeric covalent → molecular covalent
2. From left to right across a Period, the oxides change from ionic → oligomeric/polymeric covalent → molecular covalent.

Periodic trends for the main group chlorides

The trend between ionic and non-ionic/covalent in moving across a Period is also true for the chlorides of the main group elements. Those on the left (i.e., Group 1 and 2) are ionic and soluble in water, while those to the right tend to give acidic solutions due to reactions with the water and the formation of hydrochloric acid, e.g., (1.10.1).



This page titled [1.10: Periodic Trends for the Main Group Elements](#) is shared under a [CC BY 3.0](#) license and was authored, remixed, and/or curated by [Andrew R. Barron \(CNX\)](#) via [source content](#) that was edited to the style and standards of the LibreTexts platform.

CHAPTER OVERVIEW

2: Hydrogen

- 2.1: Discovery of Hydrogen
- 2.2: The Physical Properties of Hydrogen
- 2.3: Synthesis of Molecular Hydrogen
- 2.4: Atomic Hydrogen
- 2.5: The Proton
- 2.6: Hydrides
- 2.7: The Hydrogen Bond
- 2.8: Isotopes of Hydrogen
- 2.9: Nuclear Fusion
- 2.10: Storage of Hydrogen for Use as a Fuel

Thumbnail: Zeppelin the Hindenburg on fire at the mooring mast of Lakehurst (United States of America) 6 May 1937. (Public Domain; Sam Shere via [Wikipedia](#))

This page titled [2: Hydrogen](#) is shared under a [CC BY 3.0](#) license and was authored, remixed, and/or curated by [Andrew R. Barron \(CNX\)](#) via [source content](#) that was edited to the style and standards of the LibreTexts platform.

2.1: Discovery of Hydrogen

Hydrogen gas, H_2 , was first artificially synthesized by Phillip von Hohenheim (known as Paracelsus, Figure 2.1.2.1) by mixing metals with strong acids. He was unaware that the flammable gas produced by this chemical reaction was a new chemical element. In 1671, Robert Boyle (Figure 2.1.2.2) rediscovered the reaction between iron lings and dilute acids, which results in the production of hydrogen gas. He noted that these fumes were highly flammable and that the flame gave o a lot of heat but not much light.



Figure 2.1.1: Renaissance physician, botanist, alchemist, and astrologer Paracelsus (1493 1541).



Figure 2.1.2: Irish philosopher, chemist, physicist, and inventor Robert Boyle (1627 1691).

In 1766, Henry Cavendish (Figure 2.1.2.3) was the first to recognize hydrogen gas as a discrete substance, by identifying the gas from a metal-acid reaction as *flammable* air. One of the richest men in Britain at the time, he lived in London and spent his time in his private laboratory at his home. In 1781 he was the first person to nd that the gas produces water when burned. This was a key experiment in disproving the Aristotelian theory of the four elements. As a consequence of his work he is usually given credit for its discovery as an element. However, it was Antoine Lavoisier (Figure 2.1.2.4) who in 1783 named the element *hydrogen* (from the Greek *hydro* meaning water and *genes* meaning creator) after he reproduced Cavendish's findings.

The four Aristotalian elements were *Earth*, *Fire*, *Air* and *Water*. A fifth element, *Aether*, was ascribed as a divine substance that made up the heavenly spheres and heavenly bodies (stars and planets).



Figure 2.1.3: British scientist Henry Cavendish (1731 - 1810).



Figure 2.1.4: French chemist and biologist Antoine-Laurent de Lavoisier (1743 1794).

Using his invention, the vacuum flask, James Dewar (Figure 2.1.25) was the first to liquefy hydrogen in 1898. He produced solid hydrogen the next year.



Figure 2.1.5: Scottish chemist and physicist Sir James Dewar FRS (1842 1923).

This page titled [2.1: Discovery of Hydrogen](#) is shared under a [CC BY 3.0](#) license and was authored, remixed, and/or curated by [Andrew R. Barron \(CNX\)](#) via [source content](#) that was edited to the style and standards of the LibreTexts platform.

2.2: The Physical Properties of Hydrogen

Table 2.2.2.1: Physical properties of hydrogen.

Chemical Symbol	H
Atomic number	1
Electron configuration	1s ¹
Atomic weight	1.00794
Melting point	-259 °C
Boiling point	-253 °C
Density (gas)	0.090 g/L
Density (liquid)	0.70g/L
Ionization potential	13.598 eV
Pauling electronegativity	2.1
Ionic radius (H ⁻)	1.54 Å
van der Waal radius	1.2 Å
Explosive limit	4 - 75%
Ignition temperature	585 °C

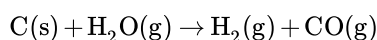
This page titled [2.2: The Physical Properties of Hydrogen](#) is shared under a [CC BY 3.0](#) license and was authored, remixed, and/or curated by [Andrew R. Barron \(CNX\)](#) via [source content](#) that was edited to the style and standards of the LibreTexts platform.

2.3: Synthesis of Molecular Hydrogen

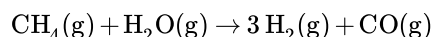
Although hydrogen is the most abundant element in the universe, its reactivity means that it exists as compounds with other elements. Thus, molecular hydrogen, H_2 , must be prepared from other compounds. The following outlines a selection of synthetic methods.

Steam reforming of carbon and hydrocarbons

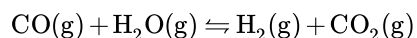
Many reactions are available for the production of hydrogen from the reaction of steam with a carbon source. The choice of reaction is guided by the availability of raw materials and the desired purity of the hydrogen. The simplest reaction involves passing steam over coke at high temperatures ($1000\text{ }^{\circ}\text{C}$).



Coke is a grey, hard, and porous carbonaceous material derived from destructive distillation of low-ash, low-sulfur bituminous coal. As an alternative to coke, methane may be used at a slightly higher temperature ($1100\text{ }^{\circ}\text{C}$).



In each case the carbon monoxide formed in the reaction can react further with steam in the presence of a suitable catalyst (usually iron or cobalt oxide) to generate further hydrogen.



This reaction is known as the water gas-shift reaction, and was discovered by Italian physicist Felice Fontana (Figure 2.3.2.6) in 1780.

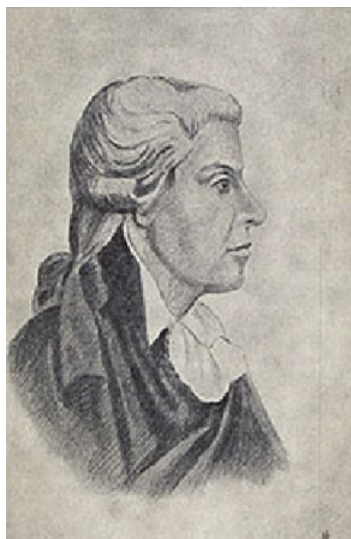
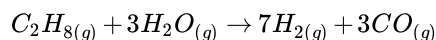


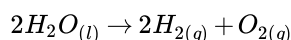
Figure 2.3.6: Italian physicist Felice Fontana (1730 - 1805).

The dominant industrial process for hydrogen production uses natural gas or oil refinery feedstock in the presence of a nickel catalyst at $900\text{ }^{\circ}\text{C}$.

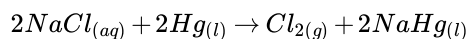


Electrolysis of water

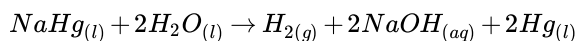
Electrolysis of acidified water in with platinum electrodes is a simple (although energy intensive) route to hydrogen.



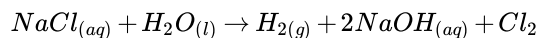
On a larger scale hydrolysis of warm aqueous solutions of barium hydroxide can yield hydrogen of purity greater than 99.95%. Hydrogen is also formed as a side product in the production of chlorine from electrolysis of brine ($NaCl$) solutions in the presence of a mercury electrode.



The sodium mercury amalgam reacts with water to yield hydrogen.



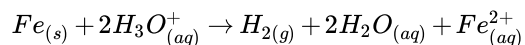
Thus, the overall reaction can be written as:



However, this method is being phased out for environmental reasons.

Reaction of metal with acid

Hydrogen is produced by the reaction of highly electropositive metals with water, and less reactive metals with acids, e.g.,



This method was originally used by Henry Cavendish (Figure 2.3.2.7) during his studies that led to the understanding of hydrogen as an element (Figure 2.3.2.8).



Figure 2.3.7: Henry Cavendish (1731 - 1810).

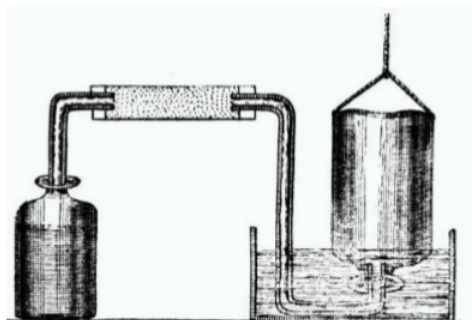


Figure 2.3.8: Cavendish's apparatus for making hydrogen in the left hand jar by the reaction of a strong acid with a metal and collecting the hydrogen gas above water in the right hand inverted jar.

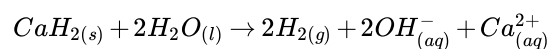
The same method was employed by French inventor Jacques Charles (Figure 2.3.2.9) for the first flight of a hydrogen balloon on 27th August 1783. Unfortunately, terrified peasants destroyed his balloon when it landed outside of Paris.



Figure 2.3.9: Jacques Alexandre César Charles (1746 1823).

Hydrolysis of metal hydrides

Reactive metal hydrides such as calcium hydride (CaH_2) undergo rapid hydrolysis to liberate hydrogen.



This reaction is sometimes used to inflate life rafts and weather balloons where a simple, compact means of generating H_2 is desired.

This page titled [2.3: Synthesis of Molecular Hydrogen](#) is shared under a [CC BY 3.0](#) license and was authored, remixed, and/or curated by [Andrew R. Barron \(CNX\)](#) via [source content](#) that was edited to the style and standards of the LibreTexts platform.

2.4: Atomic Hydrogen

Atomic hydrogen has the electron configuration of $1s^1$ and as such represents the simplest atomic configuration. However, as a consequence there is dispute as to its proper position within the Periodic Table. Its electron configuration is similar to the valence electron configuration of the alkali metals (ns^1) suggesting it be listed at the top of Group 1 (1A). However, its reaction chemistry is dissimilar to the alkali metals. Hydrogen is also one electron short of a noble gas configuration, and therefore it is possible to think of its relationship to the halogens.

Vapor phase

Atomic hydrogen (H^\cdot) is highly reactive and consequently has a short lifetime due to its reaction chemistry. Consequently, in order to generate and observe the reactivity they must be generated at low pressures.

Thermolysis of hydrogen compound (commonly halide) or photolysis at an energy above the bond dissociation energy results in the homolytic cleavage of the H-X bond to generate the appropriate radical species.



Alternatively, atomic hydrogen can be generated from elemental hydrogen.



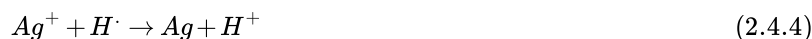
The reverse reaction (recombination of two hydrogen atoms) is highly exothermic (-434 kJ.mol^{-1}) and forms the basis of the heat generated in arc welding.

Solution

Atomic hydrogen may be generated in aqueous solution through the solvation of electrons.



The formation equilibrium constant (K_{eq}) is very small resulting in very low concentrations being generated (10^{-5} M). As expected solvated atomic hydrogen is a strong reducing agent.



Solid state

Hydrogen atoms may be trapped in the solid state lattice upon generation by photolysis of HX. Observation by electron spin resonance (esr) of a signal split by $s = 1/2$ nucleus (i.e., 1H) results in a doublet with a coupling of 1428 MHz.

This page titled 2.4: Atomic Hydrogen is shared under a CC BY 3.0 license and was authored, remixed, and/or curated by Andrew R. Barron (CNX) via source content that was edited to the style and standards of the LibreTexts platform.

2.5: The Proton

The proton, H^+ , is the name given to hydrogen in the +1 oxidation state.

Gas phase

The proton can be formed from the photolysis of atomic hydrogen in the vapor phase at low pressure.



The proton is more reactive than the hydrogen atom because of its high charge density. In addition, the proton's small ionic radius, 1.5×10^{-15} cm, means that it can get close to other atoms and hence form strong bonds.



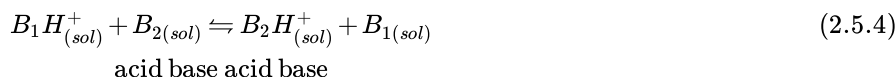
The strength of the bonding interaction is such that it is very hard to measure directly. Instead the relative bond strength between the proton and an appropriate base, B_1 , is measured in the presence of a competing base, B_2 .



In measuring the exchange reaction, the *relative proton affinity* of B_1 and B_2 is measured. This is also known as the gas phase acidity, and as such it is a measure of the inherent acidity of a species $X-H$ because it obviates any solvent effects.

Liquid and solution

The high reactivity of the proton means that it does not exist free in solution. There are however many H^+ containing species. These are generally classified as *acids*.



The reaction between the acid and the base is a proton transfer reaction. While the proton travels from B_1 to B_2 , it is never free in solution. Instead a bridged transition state or intermediate is formed, $B_1 \cdots H^+ \cdots B_2$.

Acidity and pH

The most common solvent for H^+ is water. The acid form is usually defined as the hydronium ion or H_3O^+ , (2.5.5). The terms oxonium, hydroxonium and oxidanium are also used for the H_3O^+ . Although we commonly use H_3O^+ it is known from spectroscopy that larger complexes are formed such as $H_9O_4^+$ (Figure 2.5.2.10).

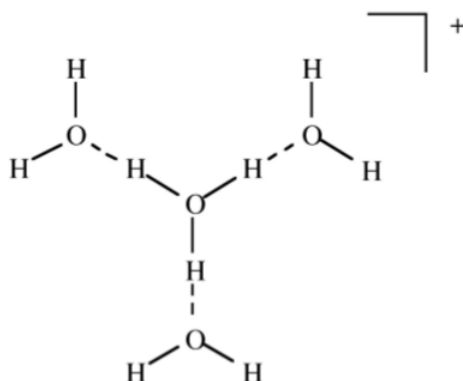


Figure 2.5.10: Structure of $H_9O_4^+$.

Acids and bases have been characterized in a number of different ways. In 1680 Robert Boyle (Figure 2.5.2.11) defined an acid as a compound that dissolved many other compounds, had a sour taste, and reacted with alkali (base).



Figure 2.5.11: Portrait of Robert Boyle (1627-1691).

Boyle's simple observational description was rationalized by Danish physical chemist Johannes Brønsted (Figure 2.5.12). Brønsted proposed that acids are *proton donors*, and bases are *proton acceptors*. An acid-base reaction is one in which a proton is transferred from a proton donor (acid) to a proton acceptor (base). Based upon Brønsted's proposal simple acids contain an ionizable proton. Examples of simple acids include neutral molecules (HCl, H₂SO₄), anions (HSO₄⁻, H₂PO₄⁻), and cations (NH₄⁺). The most common Brønsted bases include metal hydroxides (MOH).



Figure 2.5.12: Johannes Nicolaus Brønsted (1879-1947).

Brønsted noted that when an acid donates a proton it forms a conjugate base. The following are examples of an acid and its conjugate base.





Exercises

Exercise 2.5.1\

What is the conjugate base of HCl?

Answer



Exercise 2.5.2\

What is the conjugate base of HSO_4^- ?

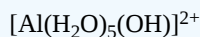
Answer



Exercise 2.5.3\

What is the conjugate base of $[Al(H_2O)_6]^{3+}$?

Answer



The same occurs when a base accepts a proton it forms a conjugate acid. The following are examples of a base and its conjugate acid.



Exercises

Exercise 2.5.4\

What is the conjugate acid of NH_3 ?

Answer



Exercise 2.5.5\

What is the conjugate acid of S^{2-} ?

Answer



Exercise 2.5.6\

What is the conjugate acid of CO_3^{2-} ?

Answer



Thus, the reaction between an acid and a base results in the formation of the appropriate conjugate base and conjugate acid.



A specific example is as follows:



Exercise

What is the conjugate acid and base formed from the reaction of NH_4^+ with S_2^{2-} ?

Answer



In the equilibrium reactions shown in (2.12) and (2.13) there is a competition between the two bases for the proton. As would be expected the strongest base wins.

When a strong acid is added to (dissolved in) water it will react with the water as a base:



In contrast, when a strong base is added to (dissolved in) water it will react with the water as an acid:



pH a measure of acidity

The acidity of a water (aqueous) solution depends on the concentration of the hydronium ion, i.e., $[H_3O^+]$. The acidity of a solution is therefore the ability of the solution to donate a proton to a base. The acidity or pH of a solution is defined as:

$$pH = -\log[H_3O^+] \quad (2.5.17)$$

It is important to note that the value is the *activity* of H_3O^+ and not the *concentration*.

Note

Activity is a measure of the effective concentration of a species in a mixture. The difference between activity and other measures of composition such as concentration arises because molecules in non-ideal gases or solutions interact with each other, either to attract or to repel each other.

The activity of the H_3O^+ ion can be measured by

- (a) A gas electrode
- (b) Acid-base indicators

Proton Transfer Reactions

The proton transfer reaction is one of the simplest reactions in chemistry. It involves no electrons and low mass transfer/change, giving it a low energy of activation. For proton transfer between O-H or N-H groups and their associated bases the reaction is very fast. The proton transfer occurs across a hydrogen-bonded pathway during which the proton is never free.

This page titled [2.5: The Proton](#) is shared under a [CC BY 3.0](#) license and was authored, remixed, and/or curated by [Andrew R. Barron \(CNX\)](#) via [source content](#) that was edited to the style and standards of the LibreTexts platform.

2.6: Hydrides

The combination of hydrogen with another element produces a hydride, E_xH_y . The formal charge or oxidation state of the hydrogen in these compounds is dependant on the relative electronegativity of the element in question.

Ionic hydrides

Hydrogen compounds with highly electropositive metals, i.e., those in which the metal has an electronegativity of less than 1.2, are ionic with the hydrogen having a s^2 configuration (H^-). Typical ionic metal hydrides are those of the Group 1 (IA) metals and the heavier Group 2 (IIA) metals.

The ionic radius of the hydride ion is in between that of fluoride and chloride and the same as oxide (Table 2.6.2.2). As a consequence, in the solid state the hydride ion replicates that of a halide ion (e.g., Cl^-), and as such similar solid state structures are observed (Table 2.6.2.3).

Table 2.6.2.2: Selected ionic radii.

Ion	Ionic Radius (Å)
H^-	1.40
F^-	1.36
Cl^-	1.81
O^{2-}	1.40

Table 2.6.2.3: Lattice parameters (Å) for hydrides, and halides of the Group 1 metal salts with cubic rock salt structures.

Metal	Hydride	Fluoride	Chloride
Li	4.085	4.0173	5.129
Na	4.880	4.620	5.640
K	5.700	5.347	6.292
Rb	6.037	5.640	6.581
Cs	6.376	6.008	7.020

Unlike the halide ions that are soluble in water, the hydride ion reacts with water, (2.32), and consequently NaH and CaH_2 are commonly used as drying agents. The liberation of hydrogen was used as a commercial source of hydrogen for small-scale applications.



WARNING

Group 1 and 2 metal hydrides can ignite in air, especially upon contact with water to release hydrogen, which is also flammable. Hydrolysis converts the hydride into the analogous hydroxide, which are caustic bases. In practice, most ionic hydrides are dispensed as a dispersion in oil, which can be safely handled in air.

Covalent Hydrides

The most common binary compounds of hydrogen are those in which hydrogen bonds have covalent bond character. The E-H bond is usually polar ranging from those in which the hydrogen is polarized positively (e.g., those with non-metals such as F, O, S, and C) to where it is negative (e.g., those with metals and metalloids such as B, Al, etc). Magnesium hydride is intermediate between covalent and ionic since it has a polymeric solid similar to AlH_3 , but reacts rapidly with water like ionic hydrides. Table 2.6.2.4 lists the important covalent hydrides of p-block elements. It should be noted that all organic hydrocarbons can be thought of as simply the hydrides of carbon!

Group 13	Group 14	Group 15	Group 16	Group 17
B_2H_6	C_nH_{2n+2} , C_nH_{2n} , C_nH_{2n-2}	NH_3 , N_2H_4	H_2O , H_2O_2	HF
$(AlH_3)_n$	Si_nH_{2n+2}	PH_3 , P_2H_4	H_2S , H_2S_n	HCl
Ga_2H_6	Ge_nH_{2n+2}	AsH_3	H_2Se	HBr
	SnH_4	SbH_3	H_2Te	HI

The elements of Group 14 to 17 all form hydrides with normal covalent bonds in which the hydrogen is bonded by a single bond to the element in question. In contrast, the elements of Group 13 (as typified by boron) all exhibit a second type of covalent bond: the electron deficient **hydrogen bridged bond**. In this type of bond the hydrogen nucleus is embedded in a molecular orbital that covers more than two atoms to create a multi-center two-electron bond. Diborane (Figure 2.6.2.13) represents the archetypal compound containing the hydrogen bridge bond. Hydrides are not limited to terminal (E-H) or those bridging two atoms (E-H-E), but are also known where the hydrogen bridges (or caps) more than two atoms, i.e., Figure 2.6.2.14.

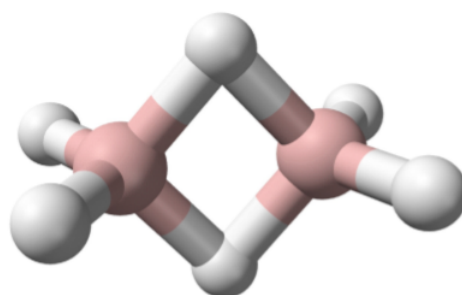


Figure 2.6.13: Structure of diborane (B_2H_6); where pink = boron; white = hydrogen.

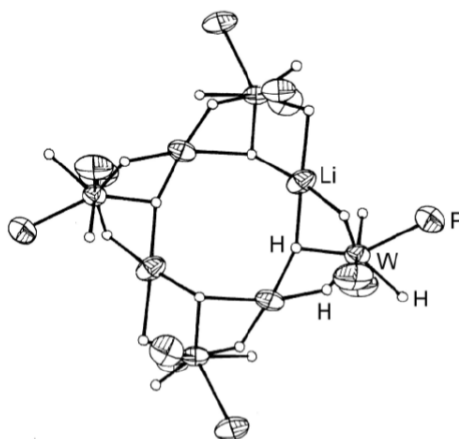


Figure 2.6.14: The structure of $\{[(Me_3P)_3WH_5]Li^+\}_4$ showing the presence of terminal, bridging, and trifurcated hydrides. The methyl groups have been omitted for clarity. Adapted from A. R. Barron, M. B. Hursthouse, M. Motevalli, and G. Wilkinson, *J. Chem. Soc., Chem. Commun.*, 1986, 81.

Synthesis of covalent hydrides

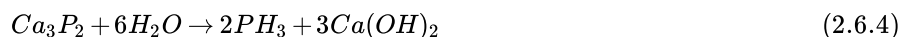
Covalent hydrides can be made by a range of synthetic routes. The simplest is direct combination of the elements (in a similar manner to that used with ionic hydrides).



The use of a hydride as a reagent to reduce a halide or oxide of the desired element



Metal phosphides, carbides, silicides, and borides result in the formation of the hydride.



Hydride compounds can be interconverted in the presence of a catalyst, heat, or an electrical discharge. This is the basis of catalytic cracking of petroleum mixtures.

Interstitial hydrides

Many transition metal, lanthanides and actinides absorb hydrogen to give a metallic hydride which retain the properties of a metal, although the presence of hydrogen does result in embrittlement of the metal. As such these hydrides are best considered as alloys since they do not have defined stoichiometries. For example, vanadium absorbs hydrogen to form an alloy with a maximum hydrogen content of $VH_{1.6}$. In a similar manner palladium forms $PdH_{0.6}$. The hydrogen atoms are present in interstitial sites in the metal's lattice; hence *interstitial hydride*. Interstitial hydrides show certain promise as a way for safe hydrogen storage.

Bibliography

- A. R. Barron, M. B. Hursthouse, M. Motevalli, and G. Wilkinson, *J. Chem. Soc., Chem. Commun.*, 1986, 81.

This page titled [2.6: Hydrides](#) is shared under a [CC BY 3.0](#) license and was authored, remixed, and/or curated by [Andrew R. Barron \(CNX\)](#) via [source content](#) that was edited to the style and standards of the LibreTexts platform.

2.7: The Hydrogen Bond

Hydrogen bonds are formed between a species with a polar $X^{\delta-}-H^{\delta+}$ bond and a species with a lone pair ($Y^{\delta-}$), i.e., $X^{\delta-}-H^{\delta+} \cdots Y^{\delta-}$. The most common species for X are oxygen and nitrogen, and to a lesser extent carbon, fluorine, and sulfur. However, as long as the X-H bond is polar then hydrogen bonding is possible. Similarly, the most common Lewis bases that hydrogen bond involve oxygen, nitrogen, and fluorine as the donor atom. Again there are many examples of other atoms, but as long as the atom has a lone pair that is chemically active, hydrogen bonding can occur.

The majority of hydrogen bonds are asymmetrical, that is the hydrogen is closer to one atom than the other (Figure 2.7.2.15), even when X and Y are the same element, i.e., O-H...O. While the typical hydrogen bond involves one Lewis base (lone pair donor), there are many examples where the hydrogen interacts with two Lewis base lone pairs (Figure 2.7.2.16).

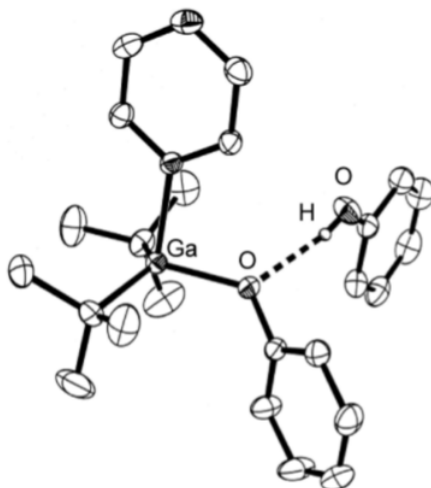


Figure 2.7.15: Structure of $(t\text{Bu})_2\text{Ga}(\text{OPh})(\text{pyz})(\text{PhOH})$ from X-ray crystallographic data showing the presence of an asymmetrical hydrogen bond. Hydrogen atoms attached to carbon are omitted for clarity. Adapted from L. H. van Poppel, S. G. Bott and A. R. Barron, *Polyhedron*, 2002, **21**, 1877.

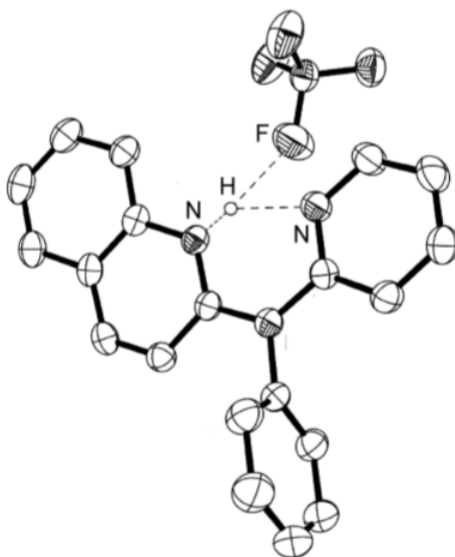


Figure 2.7.16: Structure of $[\text{H}\{\text{PhN}(\text{py})(\text{quin})\}]\text{BF}_4$ from X-ray crystallographic data showing the presence of a trifurcated asymmetrical hydrogen bond. Hydrogen atoms attached to carbon are omitted for clarity. Adapted from J. J. Allen, C. E. Hamilton, and A. R. Barron, *J. Chem. Cryst.*, 2009.

Hydrogen bonds are mostly electrostatic attractions, and as such they are weaker than covalent bonds, but stronger than van der Waal interactions. With bond strengths generally covering the range of 5–50 kJ/mol, the energy required to break a hydrogen bond is comparable to that of thermal motion within the temperature range of 0–200°C. As a consequence the number of groups involved

in hydrogen bonding decreases with increasing temperature, until few hydrogen bonds are observed in the vapor phase. One noted exception is the hydrogen bridged anion $[F-H-F]^-$, in which the strong interaction (243 kJ/mol) is covalent in character involving a three-center molecular orbital bond.

Classes of hydrogen bond

Although hydrogen bonds may be characterized with respect to the X and Y atom, it is more useful to classify them as either intramolecular or intermolecular hydrogen bonds. This is due to the difference in physical and chemical properties between these two classes.

Intramolecular

Intramolecular hydrogen bonds ($X-H\cdots Y$) arise where the X and Y atoms are in the same molecule (Figure 2.7.2.17).

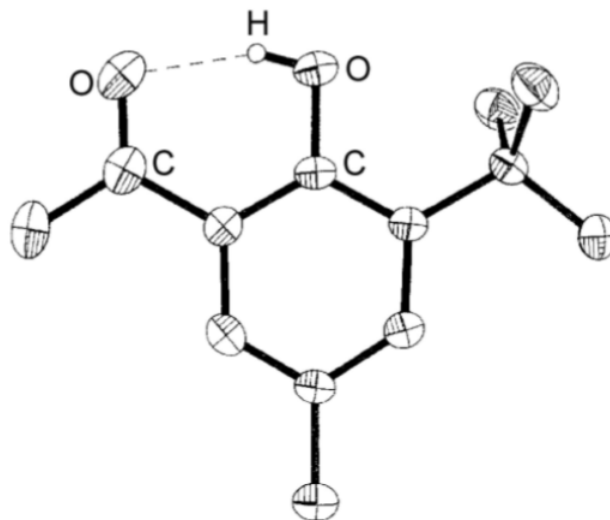


Figure 2.7.17: Structure of 3-*tert*-butyl-2-hydroxy-5-methylacetophenone showing the presence of an intramolecular hydrogen bond. Hydrogen atoms attached to carbon are omitted for clarity. Adapted from M. B. Power, A. R. Barron, S. G. Bott, E. J. Bishop, K. D. Tierce and J. L. Atwood, *J. Chem. Soc., Dalton Trans.*, 1991, 241.

Intermolecular

If the hydrogen bond ($X-H\cdots Y$) involves X and Y being from different molecules this is an intermolecular hydrogen bond. Within the range of intermolecular hydrogen bonded compounds there are two sub-categories: those involving discrete molecular species (oligomers) and those resulting in polymeric species.

Carboxylic acids are a typical example of a discrete oligomeric species that are held together by intermolecular hydrogen bonds (Figure 2.7.2.18a). A wide range of structurally analogous compounds also form head-to-tail hydrogen bonded dimers (e.g., Figure 2.7.2.19). In a polymeric hydrogen bonded species every molecule hydrogen bonds but in a random form. As an example, liquid primary alcohols form extended hydrogen networks (Figure 2.7.2.18b). Such an arrangement is labile and as such it is difficult to determine definitive speciation. Liquids that form this type of hydrogen-bonded network are known as associated liquids. In the solid state the networks generally adopt a more ordered structure. For example as is seen in the structure of ice.

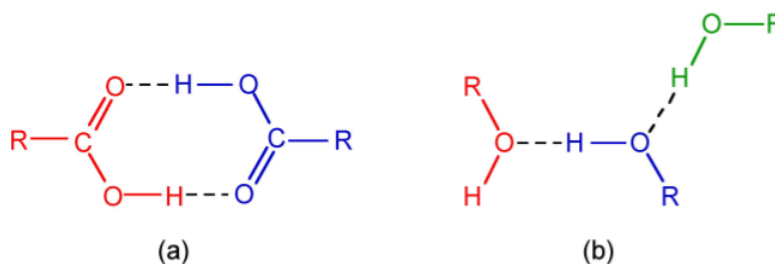


Figure 2.7.18: Structure of (a) the head-to-tail dimer formed between two carboxylic acid molecules, and (b) a typical network of a primary alcohol in the liquid phase.

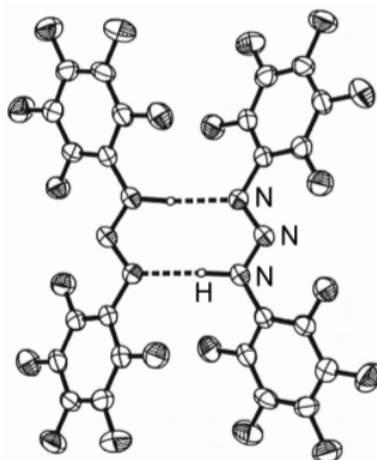


Figure 2.7.19: Structure of the hydrogen bonded dimer of $(\text{C}_6\text{H}_5)\text{NNN}(\text{H})(\text{C}_6\text{F}_5)$. Adapted from J. T. Leman, J. Braddock-Wilking, A. J. Coolong, and A. R. Barron, *Inorg. Chem.*, 1993, **32**, 4324.

Methods of study

The study of the structure arising from hydrogen bonding and the properties exhibited due to the presence of hydrogen bonds is very important.

Diffraction methods

X-ray diffraction of single crystals is the most common structural method employed to determine the presence, effect, and strength of a hydrogen bond. Unfortunately, in order for the location of the hydrogen to be determined with some degree of accuracy, diffraction data of a high quality is needed and/or low temperature (e.g., -196°C) data collection is required. Neutron scattering can be used where very accurate data is required because hydrogen atoms scatter neutrons better than they do X-rays. Figure 2.7.220 summarizes the key parameters that are obtained from X-ray (and neutron) diffraction experiments.

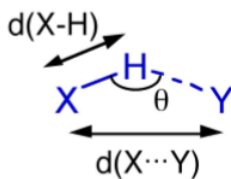


Figure 2.7.20: Structural parameters obtained from diffraction methods.

Given the electrostatic nature of a hydrogen bond between a polar X-H bond and a Lewis base it is reasonable that the X-H...Y angle (θ) is roughly linear (i.e., 180°). However, it is not always so and nonlinear interactions are known where steric or conformational restrictions limit the orientation of the X-H bond with respect to Y.

The distance between X and Y, $d(\text{X}\cdots\text{Y})$, is less than the sum of the van der Waals radii of X and Y (Table 2.7.2.5). This is in line with the relative strength of these interactions. As would be expected the shorter the X...Y distance the stronger the hydrogen bond.

Table 2.7.2.5: Comparison of the X...Y distance in hydrogen bonded species with the sum of the van der Waals radii.

X	Y	Sum of van der Waals radii (Å)	Typical X...Y distance (Å)
---	---	--------------------------------	----------------------------

X	Y	Sum of van der Waal radii (Å)	Typical X...Y distance (Å)
O	O	2.8	2.50-2.69
O	N	2.9	2.75-2.85
N	N	3.0	2.69-2.98

The bond distance to hydrogen, $d(X-H)$, is often longer in hydrogen bonded species. For example the O-H distance for an alcohol in the absence of hydrogen bonding is typically 0.97 Å. In contrast, the value typically seen for a hydrogen-bonded analog is 1.05 Å.

Spectroscopy

Spectroscopy is a simple method of comparing hydrogen-bonded systems in particular in the solution or liquid phase.

Infra red and Raman

The X-H stretching frequency in the IR (and Raman) spectrum is dependant on the identity of X, i.e., O-H = 3610 - 3640 cm^{-1} and N-H = 3400 - 3500 cm^{-1} . However, the $\nu(X-H)$ is shifted to lower energy (lower frequency) as a consequence of hydrogen bonding. In addition, while non-hydrogen bonded X-H stretches are sharp, the presence of hydrogen bonding results in the peak being broadened. Figure X demonstrates both these effects. The O-H stretch for dilute ${}^n\text{BuOH}$ in CCl_4 is a sharp peak at 3650 cm^{-1} due to the lack of hydrogen bonding between the two components (Figure 2.7.221a), and the presence of hydrogen bonding between ${}^n\text{BuOH}$ and ${}^n\text{BuOH}$ is limited by the dilution. By contrast, a dilute solution of ${}^n\text{BuOH}$ in Et_2O results in a shift to lower frequency and a significant increase of peak width (Figure 2.7.221b) as a result of fairly strong O-H...O bonds. Finally, a dilute solution of ${}^n\text{BuOH}$ in NMe_3 results in a further shift to 3250 cm^{-1} and a very broad peak (Figure 2.7.221c). The broadening of the peaks is due to the distribution of X-H distances within a X-H...Y hydrogen bond.

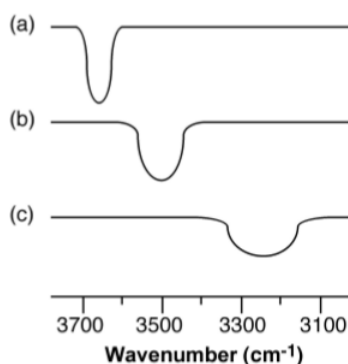


Figure 2.7.21: Schematic representation of the O-H stretch region in the IR spectra of a dilute solution of ${}^n\text{BuOH}$ in (a) CCl_4 , (b) Et_2O , and (c) NEt_3 .

NMR

The presence of hydrogen bonding results the shift to higher ppm (lower frequency) of the ${}^1\text{H}$ NMR resonance for the proton. This shift is due to the decrease in shielding of the proton. A dilute solution of ${}^n\text{BuOH}$ in CCl_4 shows a resonance typical of a non-hydrogen bonded compound (Figure 2.7.222a), while that for ${}^n\text{BuOH}$ in NMe_3 (Figure 2.7.222b) shows a significant low field shift. Very strong intra or intermolecular hydrogen bonded species show a very large ${}^1\text{H}$ NMR shift (e.g., Figure 2.7.222c).

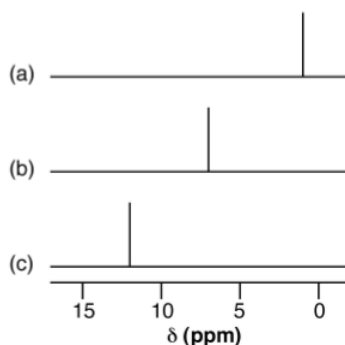


Figure 2.7.22: Schematic representation of the relative shift of the OH resonance for (a) ${}^n\text{BuOH}$ in CCl_4 , (b) ${}^n\text{BuOH}$ in NEt_3 , and (c) concentrated acetic acid.

Effects of hydrogen bonding

Physical effects

The presence of intermolecular hydrogen bonding provides additional attractive forces between molecules. Thus, properties that depend on intramolecular forces are affected.

Liquids with significant hydrogen bonding exhibit higher boiling points, higher viscosity, and higher heat of vaporization (ΔH_v) as compared to analogous compounds without extensive hydrogen bonding. For solids the presence of hydrogen bonding results in an increase in the melting point of the solid and an increase in the associated heat of fusion (ΔH_f).

The archetypal case for the effect of hydrogen bonding is the melting and boiling points of the hydrides of the Group 16 elements, i.e., H_2E . For a series of analogous compounds with the same molecular structure it would be expected that the boiling points would be related to the molecular mass. However, as can be seen from Table 2.7.2, the melting and boiling points of water are anomalously higher than those of its heavier analogs. In fact from Figure 2.7.2.23 it is clear that just considering H_2S , H_2Se , and H_2Te , the expected trend is observed, and it is similar to that for the Group 14 hydrides (CH_4 , SiH_4 , etc). Therefore, water must have additional intermolecular forces as compared to its heavier homologs. This observation is consistent with the strong hydrogen bonding in water, and the very weak if nonexistent hydrogen bonding in the sulfur, selenium, and tellurium analogs.

Table 2.7.2: Summary of physical properties for the hydrides of the Group 16 elements.

Compound	Molecular weight (g/mol)	Melting point ($^{\circ}\text{C}$)	Boiling Point ($^{\circ}\text{C}$)
H_2O	18.01	0	100
H_2S	34.08	-85.5	-60.7
H_2Se	80.98	-60.4	-41.5
H_2Te	129.62	-49	-2

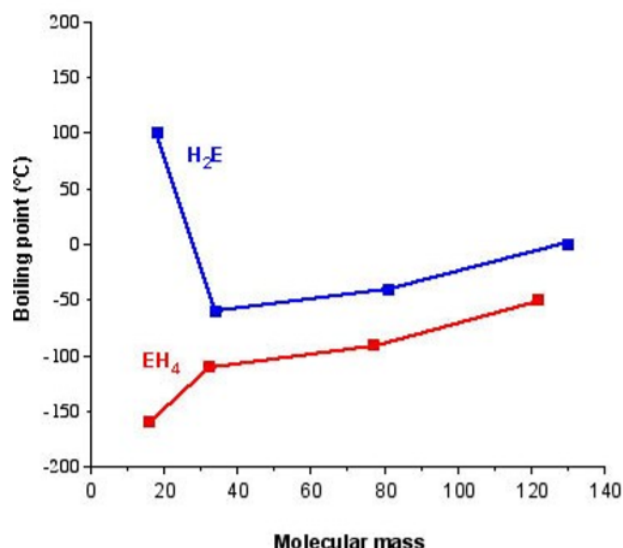


Figure 2.7.23: Plot of boiling point as a function of molecular weight for the hydrides of the Group 14 (EH_4) and 16 (H_2E) elements.

A similar but not as pronounced trend is observed for the Group 15 hydrides, where ammonia's higher values are associated with the presence of significant hydrogen bonding (Table 2.7.2.7).

Table 2.7.2: Summary of physical properties for the hydrides of the Group 15 elements.

Compound	Molecular weight (g/mol)	Melting point (°C)	Boiling Point (°C)
NH_3	17.03	-77.7	-33.35
PH_3	34.00	-133.5	-87.4
AsH_3	77.95	-113.5	-55
SbH_3	124.77	-88.5	-17

Exercise

Would you expect H_2S_2 to have a higher or lower boiling point than H_2O_2 ? Why?

Answer

The boiling point for H_2O_2 is 150.2 °C, while that of 70.7 °C. The difference in boiling point is due to the stronger intermolecular hydrogen bonding in H_2O_2 than in H_2S_2 .

The types of hydrogen bond can also have a significant effect on the physical properties of a compound. For example, the *cis* isomer of hydroxybenzaldehyde melts at 1 °C, while the *trans* isomer has melting and boiling points of 112 °C. Both compounds exhibit strong hydrogen bonding in the solid state, however, as may be seen from Figure 2.7.2.24a, *cis*-hydroxybenzaldehyde (salicylaldehyde) has a configuration that allows strong intramolecular hydrogen bonding, which precludes any intermolecular hydrogen bonding. The melting point of *cis*-hydroxybenzaldehyde is going to be controlled by the van der Waal forces between adjacent molecules. In contrast, since intramolecular hydrogen bonding is precluded in the *trans* isomer (Figure 2.7.2.24b) it can form strong intermolecular hydrogen bonds in the solid state, and thus, it is these that define the melting point. The boiling points are controlled in a similar manner.

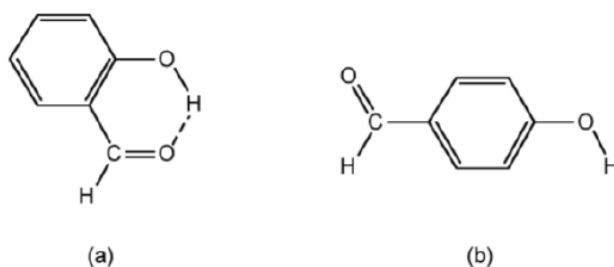


Figure 2.7.24: Structures of (a) salicylaldehyde and (b) trans-hydroxybenzaldehyde.

Exercise

4-Hydroxybenzoic acid melts at 213 °C, while 2-hydroxybenzoic acid melts at 158 °C. Explain this observation.

Answer

2-Hydroxybenzoic acid exhibits strong intramolecular hydrogen bonding while 4-hydroxybenzoic acid has strong intermolecular hydrogen bonding.

Melting and boiling are not the only physical properties that are affected by hydrogen bonding. Solubility can also be affected. Consider two isomers of $C_4H_{10}O$: n BuOH and Et_2O . The n -butanol is much more soluble in water than diethyl ether. The reason for this is that while both compounds can hydrogen bond to water, those between n BuOH and water are much stronger than those between Et_2O and water, and thus, dissolution of n BuOH in water does not disrupt the very strong hydrogen bonding in water as much as Et_2O does.

Acid strength

The acidity of a protic species can be affected by the presence of hydrogen bonding. For example, consider the di-carboxylic acid derivatives of ethylene (fumaric acid). Each of the carboxylic acid groups has sequential equilibria that may be defined by the pK values, (2.36). Table 2.7.2 lists the pK values for the *cis* and *trans* isomers. The acidity of the first and second carboxylic group for the *trans* isomer is similar, the difference being due to the increased charge on the molecule. In contrast, the second proton in the *cis* isomer is much less acidic than the first proton: why? A consideration of the structure of the mono anion of the *cis* isomer (Figure 2.7.225) shows that a very strong intramolecular hydrogen bond is formed once the first proton is removed. This hydrogen bond makes the second acidic proton much more difficult to remove and thus lowers the acidity of the proton.

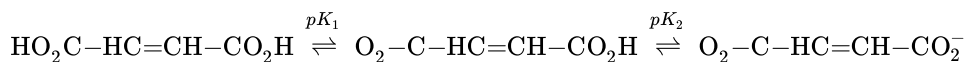


Table 2.7.2: Acidity equilibrium constants for *cis* and *trans* isomers of fumaric acid.

Isomer	pK_1	pK_2	Ratio
<i>Trans</i>	3	4.5	25:1
<i>Cis</i>	1.9	6.2	10,000:1

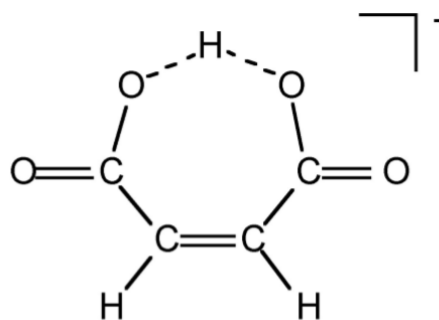


Figure 2.7.25: Structure of *cis*-[O₂C-CH=CH-CO₂H]⁻.

Solid state structure

In the solid state, molecules that can form hydrogen bonds will tend to arrange themselves so as to maximize the formation of linear hydrogen bonds. The structure of ice is a typical example, where each water molecule's hydrogen bonds to four other molecules creating a diamond-like lattice (Figure 2.7.226). However, ice isn't the only compound whose solid state structure is defined by its hydrogen bonding. Cyanuric acid forms six strong intermolecular hydrogen bonds to three other molecules in the plane of the heterocyclic ring and thus creates a graphite-like structure (Figure 2.7.227).

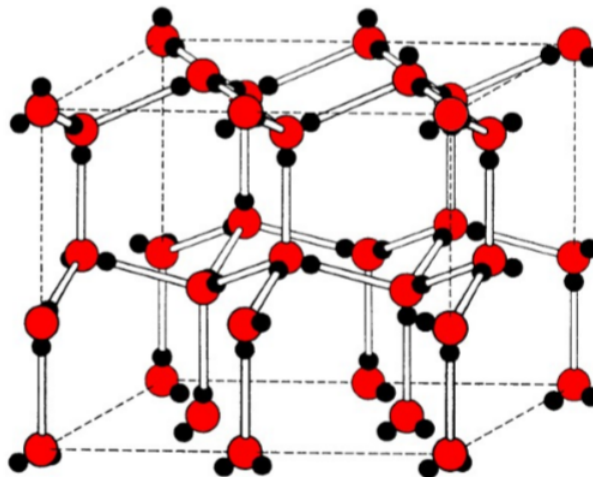


Figure 2.7.26: The diamond-like structure formed in ice by hydrogen bonding.

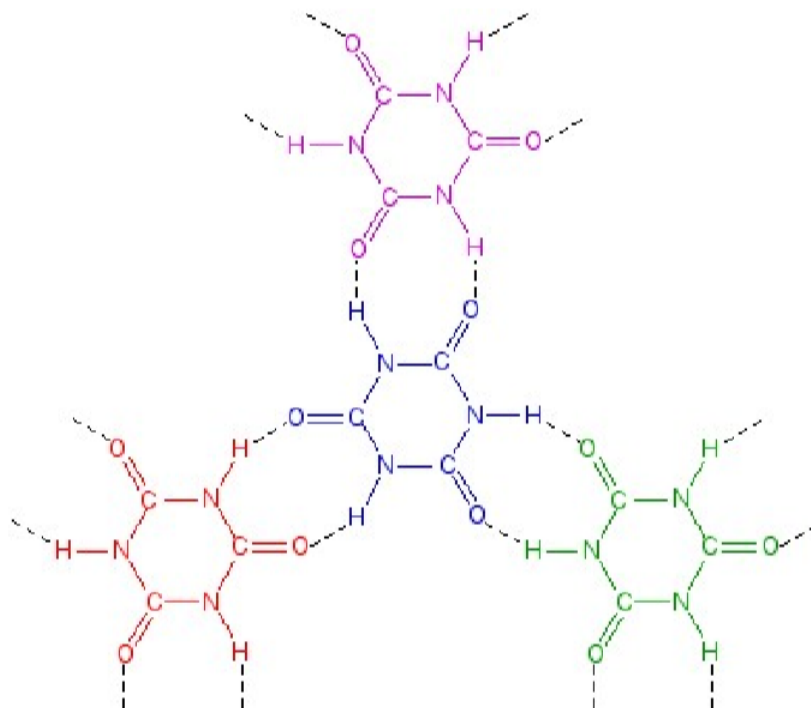


Figure 2.7.27: The hydrogen bonding of cyanuric acid.

Conformational stabilization

The presence of hydrogen bonding can stabilize certain conformations over others that in the absence of hydrogen bonding would be more favored. For example, based on steric considerations $\text{H}_2\text{NCH}_2\text{CH}_2\text{C}(\text{O})\text{H}$ would be expected to adopt a staggered conformation as is typical for compounds with free rotation about a C-C bond. However, due to the presence of a strong intramolecular hydrogen bond it adopts a sterically disfavored eclipsed conformation (Figure 2.7.28).

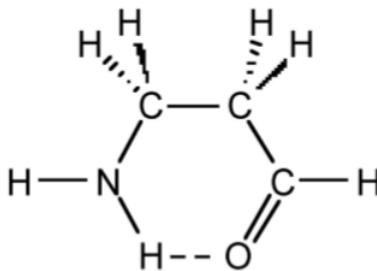


Figure 2.7.28: Stable conformation of $\text{H}_2\text{NCH}_2\text{CH}_2\text{C}(\text{O})\text{H}$.

This conformational stabilization is even more important in biopolymers such as peptides. If we assume that a peptide chain (Figure 2.7.229) made from a sequence of amino acids would not adopt any eclipsed conformations on steric grounds, and that the amide group ($\text{H}-\text{N}-\text{C}=\text{O}$) is near planar due to delocalization, then there will be 3^2 possible conformations per nitrogen in the peptide chain, i.e., three each for the C-C and C-N bonds (Figure 2.7.229). Assuming a modest peptide has 50 amino acids, there will be $3^{2 \times 50}$ potential conformations of the polymer chain, i.e., over 5×10^{47} conformations. However, in reality there are limits to the number of conformations observed since particular ones are stabilized by intramolecular hydrogen bonds. The most important of these are the α -helix (Figure 2.7.230) and β -sheet structures.

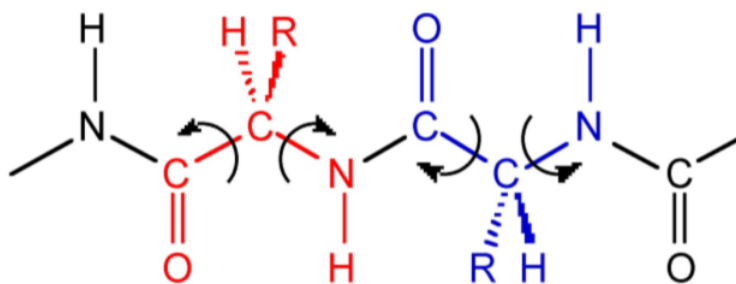


Figure 2.7.29: A section of a peptide polymer chain showing the possible rotational freedom of the C-C and C-N bonds.

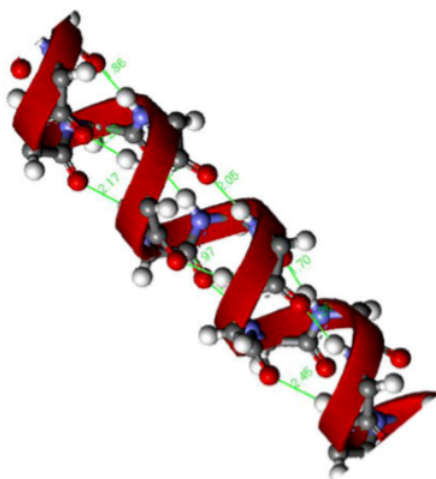


Figure 2.7.30: A representation of a peptide α -helix structure showing the stabilizing hydrogen bonds.

Bibliography

- J. T. Leman, J. Braddock-Wilking, A. J. Coolong, and A. R. Barron, *Inorg. Chem.*, 1993, **32**, 4324.
 K. Nakamoto, M. Margoshes, and R. E. Rundle, *J. Am. Chem. Soc.*, 1955, **77**, 6480.
 M. B. Power, A. R. Barron, S. G. Bott, E. J. Bishop, K. D. Tierce and J. L. Atwood, *J. Chem. Soc., Dalton Trans.*, 1991, 241.
 R. Taylor and O. Kennard, *Acc. Chem. Res.*, 1984, **17**, 320.

This page titled [2.7: The Hydrogen Bond](#) is shared under a [CC BY 3.0](#) license and was authored, remixed, and/or curated by [Andrew R. Barron \(CNX\)](#) via [source content](#) that was edited to the style and standards of the LibreTexts platform.

2.8: Isotopes of Hydrogen

Physical effects

The presence of intermolecular hydrogen bonding provides additional attractive forces between molecules. Thus, properties that depend on intramolecular forces are affected.

Table 2.8.2.9: Summary of isotopes of hydrogen.

Isotope	Hydrogen-1	Hydrogen-2	Hydrogen-3
Special name	Hydrogen	Deuterium	Tritium
Symbol	H	D	T
Atomic number	1	1	1
Number of neutrons	0	1	2
Mass number	1	2	3
Natural abundance	99.9844%	0.0156%	very small

Synthesis of deuterium compounds

Electrolysis of water

The electrolysis of hydrogen-1 water (H_2O) in the presence of an alkali results in the formation of hydrogen and oxygen.



In a similar manner the hydrolysis of deuterated water (D_2O) yields deuterium and oxygen.



However, the rate of electrolysis of D_2O is slightly slower than that of H_2O . Thus, the partial hydrolysis of water with a mixture of natural isotopes results in the slight enrichment of the water with D_2O . The level of enrichment in one step is less than 1%. In order to obtain high levels of D_2O (e.g., ca. 30%) it is necessary to reduce the original volume of water by $1/100,000^{\text{th}}$.

Chemical equilibrium

Proton exchange reactions can be used to enrich compounds in deuterium. For example, the reaction of HSD with water shown in (2.8.3) has a slight preference for the formation of H_2S , i.e., $K_{\text{eq}} = 1.012$. Thus, bubbling HSD through water results in the enrichment of the water in HOD. However, about 30% enrichment is about the best that can be achieved by this method.



Fractional distillation

The boiling point of H_2O is (by definition) 100°C , in contrast the boiling point of D_2O is 101.4°C . Thus, it is possible to separate H_2O from D_2O by fractional distillation. This method provides the most suitable route to high isotopic enrichment and D_2O of 99.8% can be produced this way.

Note

The term *heavy water* is used for D_2O of greater than 99.8% enrichment.

Uses of deuterium compounds

Possible nuclear fusion

The largest use of D_2O is as a moderator and heat exchanger for fission nuclear reactors, however, the biggest potential application will be if nuclear fusion is realized as a commercial process.

The fusion of two deuterium atoms to form a helium atom and energy would be one source of energy, (2.8.4), however, deuterium-tritium fusion is the most promising, (2.8.5).



The deuterium part of the fuel does not pose a great problem because about 1 part in 5000 of the hydrogen in seawater is deuterium. This amounts to an estimate that there is over 10^{15} tons of deuterium in the oceans. The tritium part of the fuel is more problematic since there is no significant natural source (Table 2.8.2.9), and the tritium would have to be obtained by breeding the tritium from lithium.



Since a gallon of seawater could produce as much energy as 300 gallons of gasoline, there is clearly a large amount of energy that can potentially be realized through nuclear fusion. Unfortunately, this advantage is also a disadvantage since the temperatures attained are similar to the surface of the sun, which would vaporize any conventional container. Fusion experiments therefore use a magnetic field to contain the reaction. The shape of the eld is like a bottle, hence the term "magnetic bottle".

One demonstrated fusion process is the so-called hydrogen bomb or thermonuclear bomb in which a fission atom bomb is used to initiate a fusion reaction. The atomic bomb is surrounded by a layer of lithium deuteride. Neutrons from the atomic explosion (fission) cause the lithium to be converted into helium, tritium, and energy, (2.8.6). The atomic explosion also supplies the 50,000,000 °C temperature needed for the subsequent fusion of deuterium with tritium, (2.8.5). So in-fact the hydrogen bomb is misnamed and it should be called a deuterium bomb.

Note

The original calculations to model the hydrogen bomb were performed using ENIAC (short for Electronic Numerical Integrator And Computer) that was originally designed to generate tables of trajectories of shells red from large artillery. The artillery ring tables were made by women mathematicians who were called calculators hence the name used today. Built in 1946 ENIAC is often assumed to be the first programmable electronic computer, however, it was predated by the six Colossus machines that were used to successfully crack the German Enigma code as early as 1944. However, the existence of the Colossus machines was kept secret until 1975.

Spectroscopy

In the chemical laboratory deuterium compounds are commonly used in spectroscopy for:

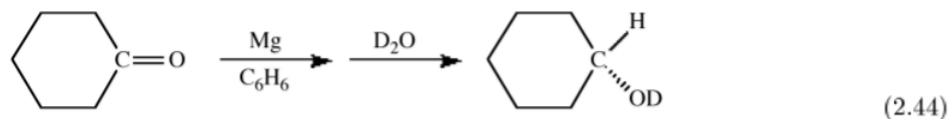
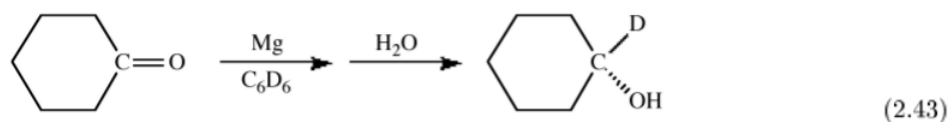
- The assignment of resonances in IR, Raman, and NMR spectroscopy.
- As a non-proton containing solvent in ${}^1\text{H}$ NMR spectroscopy.

A description of these applications is given below.

Reaction mechanism and rate determination

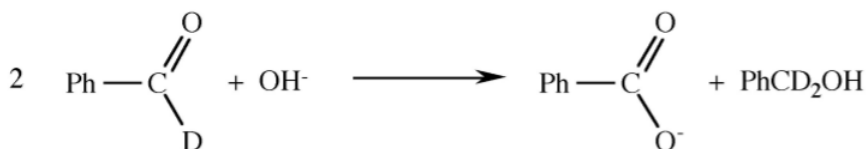
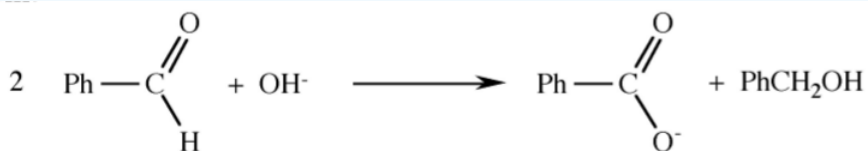
Given the larger mass of deuterium over hydrogen there is an associated difference in the rate of reactions (see below) and therefore investigations using hydrogen and deuterium analogs can provide information as to reaction mechanisms.

The spectroscopic differences between hydrogen and deuterium can also be used as a tracer to uniquely determine the source of particular substituents. For example, the magnesium (or Grignard) reduction of a ketone yields upon hydrolysis the secondary alcohol. If the reaction is carried out in a deuterated solvent and H_2O used for hydrolysis then the secondary carbon is deuterated, (2.43). In contrast, if the reaction is carried out in a non-deuterated solvent and hydrolysis is accomplished with D_2O then the deuterated alcohol is formed, (2.44). These experiments define that the initial reduction occurs at the ketone's α -carbon.

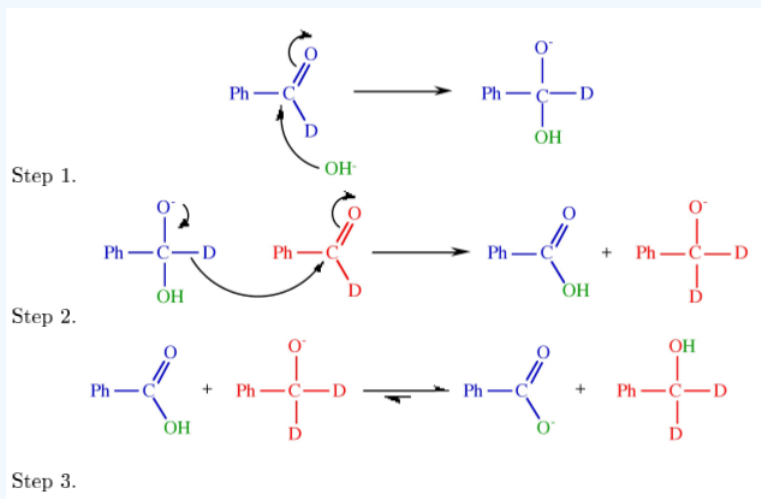


Exercise

Given the following reactions and the isotope distribution of the products suggest the reaction mechanism.



Answer



Differences between hydrogen and deuterium

Properties that depend on nuclei properties

The nuclear magnetic moment of an atomic nucleus arises from the spins of the protons and neutrons within the nucleus. As a consequence the magnetic moment for hydrogen and deuterium are very different and hence the conditions for detection by NMR are very different. Thus, in observing the ^1H NMR spectrum of a compound not only are the deuterium atoms not observed, but the coupling is now H-D rather than H-H (Figure 2.8.2.31).

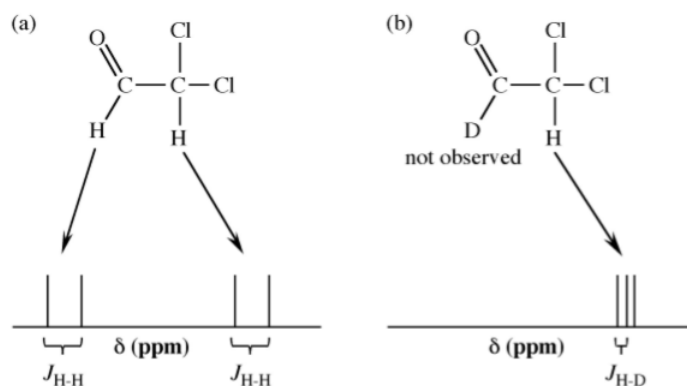


Figure 2.8.31: An example of the differences in the ^1H NMR spectrum upon deuterium substitution.

Deuterium is better at scattering neutrons than hydrogen. The H and D cross sections are very distinct and different in sign, which allows contrast variation in such experiments. Hydrogen's low electron density makes it difficult to determine its position by X-ray diffraction methods, neutron diffraction methods allow for highly accurate structure determination. Hydrogen can be seen by neutron diffraction and scattering, however, it has a large incoherent neutron cross-section. This is nil for deuterium and thus delivers much clearer signals may be obtained for deuterated samples. Neutron scattering of deuterated samples is indispensable for many studies of macromolecules in biology.

Properties that depend on mass

The difference in mass between hydrogen and deuterium obviously results in a difference in molecular mass of their analogous compounds. This difference can be used for analysis by mass spectrometry, but it also results in different densities of compounds. For example, the density of H_2O at 25°C is 0.997 g/cm^3 , while the density of D_2O at 25°C is 1.104 g/cm^3 .

The vibrational frequency for a diatomic molecule, H-X, can be defined by the equation:

$$v_{\text{H-X}} = \frac{1}{2\pi} \sqrt{\frac{f_{\text{H-X}}}{\mu_{\text{H-X}}}} \quad (2.8.7)$$

where $f_{\text{H-X}}$ is the H-X bond force constant, and $\mu_{\text{H-X}}$ is the reduced mass.

$$\mu_{\text{H-X}} = \frac{m_{\text{H}} \cdot m_{\text{X}}}{m_{\text{H}} + m_{\text{X}}} \quad (2.8.8)$$

If substitute H for D the D-X force constant is the same as the H-X force constant, but the reduced mass is twice the value for the H-X bond. As a result the ratio of the vibrational frequency of an H-X bond to that of the analogous D-X bond is given by the following equation.

$$\frac{\mu_{\text{D-X}}}{\mu_{\text{H-X}}} = \left(\frac{\mu_{\text{H-X}}}{\mu_{\text{D-X}}} \right) \frac{1}{2} = \frac{1}{\sqrt{2}} \quad (2.8.9)$$

With the change in vibrational energy there is concomitant change in the bond strength.

$$E_{\text{D-X}} > E_{\text{H-X}} \quad (2.8.10)$$

Thus, the rate of reactions will be faster for hydrogen derivative than the deuterium analog. The ratio of the rate constants will be dependant on the involvement of H-X bond breaking or forming in the rate limiting step (the slowest reaction step within the overall reaction mechanism). When an H-X bond is made or broken in the rate limiting step, then the ratio of the rate constants upon deuterium substitution will be:

$$\frac{k_{\text{H-X}}}{k_{\text{D-X}}} \approx 7 \quad (2.8.11)$$

This is known as the *primary isotope effect*. In this case where H-X bond breaking or forming is not part of the rate limiting step, then the isotope effect will be much smaller and is known as a *secondary isotope effect*.

The position of equilibrium reactions that involve hydrogen exchange, (2.8.12), will be effected by the presence of deuterium to favor the deuterium being concentrated in the more stable bond. This is the basis of the concentration of HOD from HSD and water, (2.8.3).



Bibliography

- M. B. Power, S. G. Bott, J. L. Atwood, and A. R. Barron. *J. Am. Chem. Soc.*, 1990, **112**, 3446.
- A. S. Borovik and A. R. Barron, *Main Group Chem.* 2005, **4**, 135.

This page titled [2.8: Isotopes of Hydrogen](#) is shared under a [CC BY 3.0](#) license and was authored, remixed, and/or curated by [Andrew R. Barron \(CNX\)](#) via [source content](#) that was edited to the style and standards of the LibreTexts platform.

2.9: Nuclear Fusion

The process of nuclear fission and radioactive decay are both associated with the conversion of an atom with a large nucleus to an atom (or atoms) with a smaller nucleus. In the process, mass is lost and energy is produced. However, what happens if two atoms with small nuclei are combined to give a single atom with a larger nucleus? In such a process the nuclei would be fused together, and this process is called nuclear fusion.

One of the simplest fusion processes involves the fusing of two hydrogen-2 (deuterium) atoms:



The mass of each deuterium atom is 2.0140 amu, while the mass of the resulting helium is 4.0026 amu. The mass defect of the reaction is 0.0254 amu or 0.63% of the original mass. While this percentage of the original mass may not seem much, it should be noted that the mass defect for the conversion of uranium-238 to lead-206 is only 0.026%, and that for splitting uranium-235 is 0.056%. Based upon these comparisons it is clear that fusion of hydrogen produces 24x the energy kg/kg than natural radioactivity and 11x that of nuclear fission.

In addition to being a plentiful source of energy, fusion is actually the most important process in the universe. Since the statement in 1847 of the Law of conservation of energy (the total amount of energy in an isolated system remains constant) scientists had wondered how the sun works. No source of energy was known in the 19th century that could explain the sun. Based upon the age of the earth it is known that the sun is 4,550,000,000 years old, and it was marveled at the continued source of energy over that span of time. By the 1920s nuclear energy was defined as being the most powerful source of energy, and British astrophysicist Arthur Eddington (Figure 2.9.232) suggested that the sun's energy arises from the fusion of hydrogen into helium.



Figure 2.9.32: (left) Arthur Stanley Eddington (1882 1944). (middle) Henry Norris Russell (1877 - 1957). (right) Hans Albrecht Bethe (1906 - 2005).

In 1929 American Henry Norris Russell (Figure 2.9.33) studied the spectrum of the sun. Based upon his studies he calculated the composition of the sun to be 90% hydrogen, 9% helium, and 1% of all other elements up to iron (but nothing of higher atomic number). Given the composition it became clear that the only reaction possible to account for the sun's energy was the fusion of hydrogen. In 1938 Hans Bethe (Figure 2.9.234) demonstrated a model for how the sun worked. The energy source is the fusion of hydrogen to give helium (Figure 2.9.235), while in massive stars the presence of heavier elements such as carbon, oxygen, nitrogen, neon, silicon, and iron are the result of the fusion of helium.

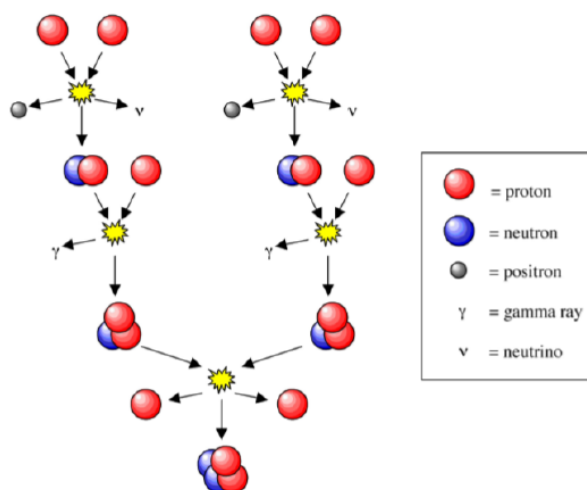


Figure 2.9.35: The proton-proton chain dominates in stars the size of the Sun or smaller.

Why is it that uranium, thorium and other radioactive elements undergo radioactive decay, but hydrogen does not undergo spontaneous fusion? The reason for this difference is that any change that uranium undergoes occurs inside a nucleus that is already formed, while fusion requires that two nuclei must come together. This process results in extremely large repulsive forces. So why does it happen in a star? The temperatures inside a star approach $15,000,000\text{ }^{\circ}\text{C}$, while the high pressure results in a density of approximately 160 g/cm^3 which for comparison is 8x that of gold. Under these conditions the nuclei are free to move in a sea of electrons. Nuclear fusion takes place in the core of the sun where the density is at the highest but an explosion does not result due to the extreme gravity of the sun: 333,000x that of Earth.

Research into controlled fusion, with the aim of producing fusion power for the production of electricity, has been conducted for over 50 years. It has been accompanied by extreme scientific and technological difficulties, but has resulted in progress. At present, break-even (self-sustaining) controlled fusion reactions have not been demonstrated, however, work continues since the fuel for such a fusion reaction is hydrogen (in its compounds including water) is the 3rd most abundant element on the Earth.

This page titled [2.9: Nuclear Fusion](#) is shared under a [CC BY 3.0](#) license and was authored, remixed, and/or curated by [Andrew R. Barron \(CNX\)](#) via [source content](#) that was edited to the style and standards of the LibreTexts platform.

2.10: Storage of Hydrogen for Use as a Fuel

Note

This module is based upon the Connexions course *Methods of Hydrogen Storage for Use as a Fuel Case Study* by Christian Cioce.

Introduction

Dihydrogen is a colorless and odorless gas at room temperature which is highly amammable, releasing a large amount of energy when combusted. As compared with combustion of the current fuels which operate automobiles, for example petrol or diesel, the energy released when hydrogen is combusted is more than three times greater. The heat of combustion for hydrogen is 141.9 kJ/mol as compared to 47.0 kJ/mol and 45.0 kJ/mol for gasoline and diesel, respectively.

Furthermore, the combustion of hydrocarbons releases the greenhouse gas carbon dioxide (CO₂) into the atmosphere, and is therefore not a "clean" fuel. When hydrogen is combusted in the presence of oxygen (from air) the only product is water, (2.52). Both its clean reactivity and the large chemical energy make H₂ extremely appealing for use as a fuel in automobiles.



If hydrogen has such a potential as a fuel why has it not been widely implemented? Dihydrogen is a gas at room temperature. Gases, compared to the other states of matter (liquid and solid), occupy the most volume of space, for a given number of molecules. Octane and the other hydrocarbons found in gasoline are liquids at room temperature, demanding relatively small fuel tanks. Liquids are therefore easier to store than compressed gases.

Hydrogen has a high energy content per weight (more than three times as much as gasoline), but the energy density per volume is rather low at standard temperature and pressure. Volumetric energy density can be increased by storing the gaseous hydrogen under increased pressure or storing it at extremely low temperatures as a liquid. Hydrogen can also be adsorbed into metal hydrides and highly porous materials (Table 2.10.2.10). The current available methods of storing hydrogen include compressed hydrogen and liquefied hydrogen, however many promising methods exist, namely metal organic materials (MOMs), metal hydrides and carbon nanostructures.

Table 2.10.2.10: Comparison of hydrogen storage ability of metal hydrides.

Material	H-atoms per cm ³ (x 10 ²²)	% of weight that is H ₂
H ₂ gas, 200 bar (2850 psi)	0.99	100
H ₂ liquid, 20 K (-253 °C)	4.2	100
H ₂ solid, 4.2 K (-269 °C)	5.3	100
MgH ₂	6.5	7.6
Mg ₂ NiH ₄	5.9	3.6
FeTiH ₂	6.0	1.89
LaNi ₅ H ₆	5.5	1.37

Liquid hydrogen

Liquid hydrogen is made possible by cryogenically cooling it to below its boiling point, -253 °C. As a liquid, the same amount of gaseous hydrogen will require much less volume, and therefore is feasible to individual automobile use. A refrigeration system is required to keep the liquid cooled, for if the system temperature rises above hydrogen's critical point (-241 °C), the liquid will become a gas. There must exist a vacuum insulation between the inner and outer walls of liquid hydrogen tank system, for heat cannot travel through a vacuum. There is a tradeo, however, because the tank must be an open system to prevent overpressure. This will lead directly to heat loss, though minimal.

The relative tank size has a broad range, with small tanks having a volume of 100 L, and large spherical tanks sizing all the way up to 2000m³. Refrigerationsystemsarenotlikelyfeatureforeveryautomobile, and open systems may pose a hazard should an accident

occur. Cooling hydrogen down to a liquid is a convenient method of storage, however, and its implementation most likely will be limited to large stationary tanks as well as mobile multi-axle trucks.

Compressed hydrogen

Compressing gas is the process of applying an external force which minimizes the distance between gas particles, therefore forcing the system to occupy less volume. This is attractive since many particles can exist in a reasonably sized tank. At room temperature and atmospheric pressure, 4 kg of hydrogen occupies a volume of 45 m³, which corresponds to a balloon with a diameter of 5 m. Clearly compression is required to store and transport the gas. When it comes to individual mobility however, these tanks are still far too large for the average sized automobile.

Compressed tanks are regularly lled to 200 atmospheres in most countries. Storing 4 kg of hydrogen still requires an internal volume of 225 L (about 60 gallons). This amount can be divided into 5 tanks with 45 L internal volume.

Metal hydrides for storage

Metal hydrides are coordinated complexes and/or crystal systems which reversibly bind hydrogen. The hydrogen is favorably incorporated into the complex and may be released by applying heat to the system. A major method to determine a particular complex's eectiveness is to measure the amount of hydrogen that can be released from the complex, rather than the amount it can store (Table 2.10.210).

Some issues with metal hydrides are low hydrogen capacity, slow uptake and release kinetics, as well as cost. The rate at which the complex accepts the hydrogen is a factor, since the time to fuel a car should ideally be minimal. Even more importantly, at the current stage of research, the rate at which hydrogen is released from the complex is too slow for automobile requirements. This technology is still a very promising method, and further research allows for the possibility of highly binding and rapid reversal rates of hydrogen gas.

This page titled [2.10: Storage of Hydrogen for Use as a Fuel](#) is shared under a [CC BY 3.0](#) license and was authored, remixed, and/or curated by [Andrew R. Barron \(CNX\)](#) via [source content](#) that was edited to the style and standards of the LibreTexts platform.

CHAPTER OVERVIEW

3: Group 1 - The Alkali Metals

[3.1: The Alkali Metal Elements](#)

[3.2: Compounds of the Alkali Metals](#)

[3.3: The Anomalous Chemistry of Lithium](#)

[3.4: Organolithium Compounds](#)

This page titled [3: Group 1 - The Alkali Metals](#) is shared under a [CC BY 3.0](#) license and was authored, remixed, and/or curated by [Andrew R. Barron \(CNX\)](#) via [source content](#) that was edited to the style and standards of the LibreTexts platform.

3.1: The Alkali Metal Elements

The Group 1 metals have a particular name: the alkali metals. This is due to the formation of alkali (basic) solutions upon their reaction with water. Table 3.1.3.1 lists the derivation of the names of the alkali metals.

Table 3.1.3.1: Derivation of the names of each of the alkali metal elements.

Element	Symbol	Name
Lithium	Li	Greek <i>lithos</i> meaning <i>stone</i>
Sodium	Na	Latin <i>natrium</i> or Arabic <i>natrun</i> meaning <i>soda</i>
Potassium	K	From the Latin <i>kalium</i> , and from Arabic <i>al-qali</i> meaning <i>plant ashes</i>
Rubidium	Rb	Latin <i>rubidus</i> meaning <i>deepest red</i>
Caesium	Cs	Latin <i>caesius</i> meaning <i>blueish grey</i>
Francium	Fr	Named after France

Note

Caesium is the international spelling standardized by the IUPAC, but in the United States it is more commonly spelled as cesium.

Discovery

Lithium

Petalite ($\text{Li}_2\text{O} \cdot \text{Al}_2\text{O}_3 \cdot 8\text{SiO}_2$) was first discovered in 1800 by José Bonifácio de Andrada e Silva (Figure 3.1.3.1), who discovered the mineral in a Swedish mine on the island of Utö. However, it was not until 1817 that Johan August Arfwedson (Figure 3.1.3.2) working in the laboratory of Jöns Jakob Berzelius (Figure 3.1.3.3), discovered the presence of a new element while analyzing petalite ore. Named from the Greek *lithos* meaning *stone* reflected its discovery in a mineral, as opposed to sodium and potassium, which had been discovered in plant tissue; its name was later standardized as lithium. The element was not isolated until 1821, when William Brande (Figure 3.1.3.4) isolated the element by performing electrolysis on lithium oxide, a process previously employed by Sir Humphry Davy to isolate potassium and sodium.



Figure 3.1.1: Portuguese statesman and naturalist José Bonifácio de Andrada e Silva (1763 - 1838).



Figure 3.1.2: Swedish chemist Johan August Arfwedson (1792 - 1841).



Figure 3.1.3: Swedish chemist Friherre Jöns Jacob Berzelius (1779 - 1848).

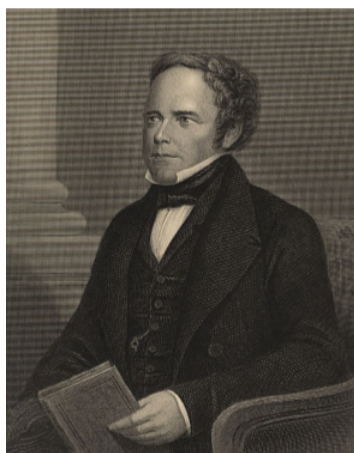


Figure 3.1.4: English chemist William Thomas Brande FRS (1788 - 1866).

Sodium

3.1.1.2 Sodium Elemental sodium was first isolated by Sir Humphry Davy (Figure 3.1.3.5) in 1806 by passing an electric current through molten sodium hydroxide.



Figure 3.1.5: British chemist and inventor Sir Humphry Davy FRS (1778 - 1829).

Potassium

The name *kalium* was taken from the word alkali, which came from Arabic *al qali* meaning the *calcined ashes*. The name potassium was made from the English word *potash*, meaning an alkali extracted in a pot from the ash of burnt wood or tree leaves. Potassium metal was discovered in 1807 by Sir Humphry Davy (Figure 3.1.3.5), who derived it from caustic potash (KOH), by the use of electrolysis of the molten salt.

Rubidium

Rubidium was discovered using spectroscopy in 1861 by Robert Bunsen (Figure 3.1.3.6) and Gustav Kirchhoff (Figure 3.1.3.7) in the mineral lepidolite. The first rubidium metal was produced by Bunsen from the reaction of rubidium chloride (RbCl) with potassium.



Figure 3.1.6: German chemist Robert Wilhelm Eberhard Bunsen (1811 - 1899).

Element	Terrestrial abundance (ppm)
Li	20 (Earth's crust), 40 (soil), 0.17 (sea water)
Na	23,000 (Earth's crust), 10,500 (sea water)
K	21,000 (Earth's crust), 14 (soil), 380 (sea water)
Rb	90 (Earth's crust), 30 - 250 (soil), 0.1 (sea water)
Cs	3 (Earth's crust), 0.0001 (soil), 0.0003 (sea water)
Fr	Essentially nil

Isotopes

The naturally abundant isotopes of the alkali metals are listed in Table 3.1.3.3. All of the isotopes of francium are radioactive. Lithium-7 and sodium-23 are both useful NMR nucleus having $I = 1/2$.

Table 3.1.3.3: Abundance of the major isotopes of the alkali metals.

Isotope	Natural abundance (%)
Lithium-6	7.5
Lithium-7	92.5
Sodium-23	100
Potassium-39	93
Potassium-40	0.0118
Potassium-41	6.9
Caesium-133	100

Potassium has three isotopes (Table 3.1.3.3), of which potassium-40 is radioactive and provides the basis for the determination of the age of rocks between 10^5 and 10^9 years old, i.e., those formed in proterozoic and cenozoic periods of geological time. The decay of potassium-40 occurs with a half life of 1.31×10^9 years, by two routes. That associated with a beta particle decay accounts for 89% of the decay:



While that associated with an electron capture and by positron emission decay accounts for 11% of the decay to give argon-40. Since many rocks contain potassium containing minerals the decay of potassium-40 after solidification of the rock will result in the formation of argon trapped in the rock. The argon-40 content is determined by mass spectrometry, while the potassium content is determined by flame spectrophotometry. The ratio of the two, (3.2), will allow for the determination of the elapsed time since the rock solidified.

$$\frac{^{40}_{18}\text{Ar}}{^{40}_{19}\text{K}} \quad (3.1.2)$$

Caesium has at least 39 known isotopes (more than any other element except francium) ranging from caesium-112 caesium-151; however, caesium-133 is the only naturally occurring stable isotope. The other isotopes have half-lives from a few days to fractions of a second. The radiogenic isotope caesium-137 is produced from the detonation of nuclear weapons and is produced in nuclear power plants, and was released to the atmosphere most notably from the 1986 Chernobyl accident.

Physical properties

Many of the physical properties of the alkali metals (Table 3.1.3.4) are typical of metals, e.g., thermal and electrical conductivity. However, due to the relatively weak inter-atomic forces (weak M-M bonding) they are soft and readily cut with a knife.

Table 3.1.3.4: Selected physical properties of the alkali metal elements.

Element	Melting point (°C)	Boiling point (°C)	Density (g/cm ³)	Electrical resistivity (Ω·cm)
Li	453	1615	0.534	12.17 @ 86 °C
Na	370	1156	0.968	5.23 @ 29 °C
K	336	1032	0.89	7.01 @ 22.8 °C
Rb	312	961	1.532	12.52 @ 53 °C
Cs	201	944	1.93	37.38 @ 28.1 °C

Reactivity

All the alkali metals are highly reactive and are as a consequence of the stability of the M^+ ion are strong reducing agents (Table 3.1.3.5). The metals react readily with hydrogen and oxygen.



Table 3.1.3.5: Electrochemical reduction potential for alkali metals.

Reduction	Reduction potential (V)
$Li^+ + e^- \rightarrow Li$	-3.045
$Na^+ + e^- \rightarrow Na$	-2.7109
$K^+ + e^- \rightarrow K$	-2.924
$Rb^+ + e^- \rightarrow Rb$	-2.925
$Cs^+ + e^- \rightarrow Cs$	-2.923

All of the alkali metals react with water to liberate hydrogen.



WARNING

The reactions of alkali metals with water are exothermic and the heat generated is sufficient to ignite the hydrogen. In addition the solutions formed are highly alkaline. Caution should be taken when handling alkali metals and storage should always be under mineral oil.

A similar, but less violent, reaction is also observed with ammonia when catalyzed by transition metal ions.



In the absence of a catalyst, the Group 1 metals dissolve in liquid ammonia to form solutions with characteristic properties.

- Highly reducing.
- Blue color.
- ESR signal due to solvated electrons.

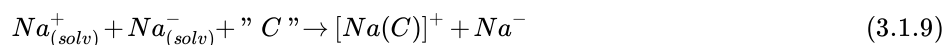
As an example, the dissolution of sodium in liquid ammonia results in the formation of solvated Na^+ cations and electrons.



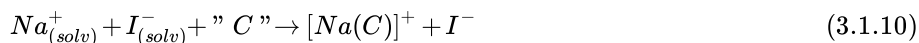
The solvated electrons are stable in liquid ammonia and form a complex: $[e^-(NH_3)_6]$. It is this solvated electron that gives the strong reducing properties of the solution as well as the characteristic signal in the ESR spectrum associated with a single unpaired electron. The blue color of the solution is often ascribed to these solvated electrons; however, their absorption is in the far infra-red region of the spectrum. A second species, $Na\text{-(solv)}$, is actually responsible for the blue color of the solution.



The formation of the sodium anion is confirmed by complexation of the cation with a cryptan ligand (C) such as a crown ether.



The resulting complex is found to be isostructural to the iodide analog in the solid state.



Vapor phase

All the alkali metals form M_2 dimers in the vapor phase in an analogous manner to hydrogen. As with dihydrogen the bonding is associated with the molecular orbital combination of the two valence s-orbitals (Figure 3.1.3.9).

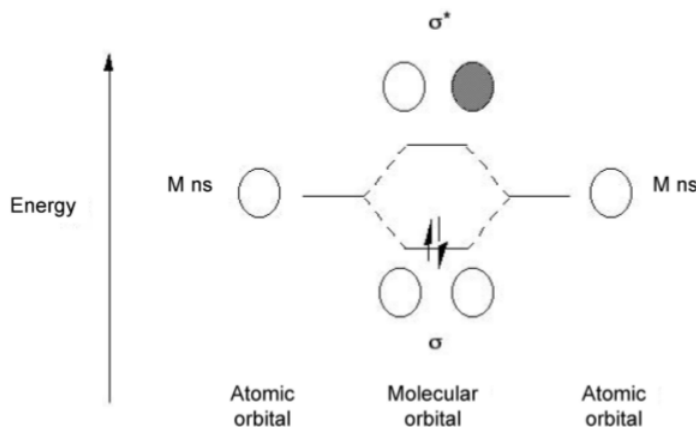


Figure 3.1.9: Molecular orbital diagram for the formation of M_2 .

Sodium vapor is commonly used for lighting in a gas discharge lamp, which uses sodium in an excited state to produce light (Figure 3.1.3.10). There are two varieties of such lamps: low pressure and high pressure.



Figure 3.1.10: A low pressure sodium streetlamp.

This page titled [3.1: The Alkali Metal Elements](#) is shared under a [CC BY 3.0](#) license and was authored, remixed, and/or curated by [Andrew R. Barron \(CNX\)](#) via [source content](#) that was edited to the style and standards of the LibreTexts platform.

3.2: Compounds of the Alkali Metals

The chemistry of the alkali metals is dominated by the stability of the +1 oxidation state and the noble gas configuration of the M^+ cation. The alkali metals all have low first ionization energies (Table 3.2.3.6) but very high second ionization energies.

Table 3.2.3.6: First ionization potentials for the alkali metals.

Element	1 st ionization energy (kJ/mol)
Li	526
Na	502
K	425
Rb	409
Cs	382

As a consequence of the stability of M^+ , the Group 1 metals have the least variation in chemistry of the any Group in the periodic table. The only exceptions are the subtle trends that exist for lithium due to its small size (Table 3.2.3.7). All of the metals are more electropositive than hydrogen (Table 3.2.3.8).

Table 3.2.3.7: Radii of alkali metals. N.B. Some values are unknown.

Element	Atomic radius (Å)	Ionic radius (Å)	Covalent radius (Å)	Van der Waals radius (Å)
Li	1.52	0.68	1.52	1.82
Na	1.86	0.97	1.53	2.27
K	2.31	1.33	1.90	2.75
Rb	2.44	1.47	2.47	-
Cs	2.62	1.67	2.65	-
Fr	-	1.80	2.70	-

Table 3.2.3.8: Pauling electronegativities of Group 1 elements.

Element	Electronegativity
H	2.20
Li	0.98
Na	0.93
K	0.82
Rb	0.82
Cs	0.79
Fr	0.70

Solid State

In the solid state, the compounds of the alkali metals generally form ionic lattices, e.g., Na^+Cl^- . These structures are essentially electrostatic in nature and the lattice energy is usually defined as the enthalpy of formation of the ionic compound from gaseous ions and as such is invariably exothermic.



In all cases the lattice energies is high and is found to be proportional to the ratio of the charges on the ions and the sum of the ionic radii (r).

$$U \propto \frac{z^+ z^-}{\sum(r)} \quad (3.2.2)$$

The ionic radii for alkali metal cations are given in Table 3.2.3.7; those for common anions are given in Table 3.2.3.9.

Table 3.2.3.9: Ionic radii of common anions.

Anion	Ionic radius (Å)
F ⁻	1.33
Cl ⁻	1.81
Br ⁻	1.96
I ⁻	2.20
H ⁻	1.54
O ²⁻	1.32

The ratio of the ionic radii (r^+/r^-) neatly defines the structural type observed for alkali metal salts (Table 3.2.3.10). The unit cells for ZnS (zinc blende), NaCl (rock salt), and CsCl are shown in Figure 3.2.3.11, Figure 3.2.3.12, and Figure 3.2.3.13, respectively.

Table 3.2.3.10: Defining MX structural types for alkali metal salts.

r^+/r^-	Structural type	Metal coordination number
0.225 - 0.414	ZnS (zinc blende)	4
0.414 - 0.732	NaCl (rock salt)	6
0.732 -	CsCl	8

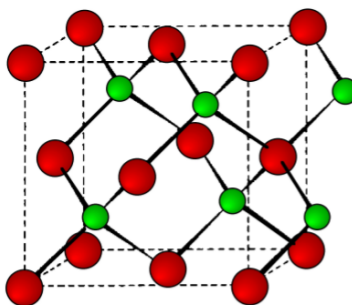


Figure 3.2.11: Unit cell structure of a zinc blende (ZnS) lattice.

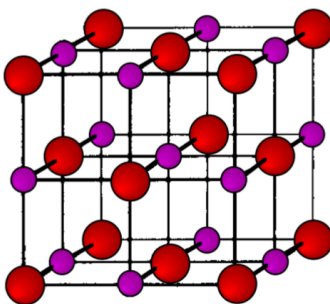


Figure 3.2.12: Unit cell structure of a rock salt lattice.

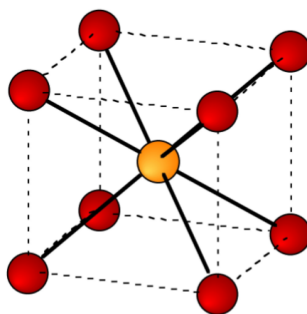


Figure 3.2.13: Unit cell of CsCl.

As an example, the structure of KBr can be predicted from the data in Table 3.2.3.7 and Table 3.2.3.9. The ionic radius of K^+ is 1.33 Å, while that for Br^- is 1.96 Å. The ratio of the ionic radii (r^+/r^-) is 0.67. Hence, KBr has a NaCl (rock salt) structure.

Exercise : Sodium Hydride

What is the structure of NaH?

Answer

The ionic radius of Na^+ is 0.97 Å, while that for H^- is 1.54 Å. The ratio of the ionic radii (r^+/r^-) is 0.67. Hence, NaH has a NaCl (rock salt) structure

Exercise : Rubidium Fluoride

What is the structure of RbF?

Answer

The ionic radius of Rb^+ is 1.47 Å, while that for F^- is 1.33 Å. The ratio of the ionic radii (r^+/r^-) is 1.10. Hence, RbF has a CsCl structure.

Complexes

The coordination complexes of the alkali metal cations (M^+) involve electrostatic, or ion-dipole, interactions (Figure 3.2.3.14) that have no preferred direction of interaction. Thus, the ionic radius of the cation (Table 3.2.3.7) controls the coordination numbers of the metal in its complexes (Table 3.2.3.11).

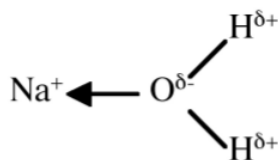
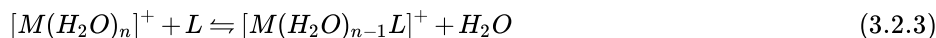


Figure 3.2.14: A schematic representation of the ion-dipole or electrostatic interaction of Na^+ with water.

Table 3.2.3.11: Coordination number for alkali metal ions in aqueous complexes.

Aqua ion	n
$[Li(H_2O)_n]^+$	4
$[Na(H_2O)_n]^+$	6
$[K(H_2O)_n]^+$	6
$[Rb(H_2O)_n]^+$	6-8
$[Cs(H_2O)_n]^+$	8

In general the alkali metal ions form complexes with hard donor such as oxygen (H_2O , ROH , RCO_2^- , etc.) or nitrogen (e.g., NH_3 , NR_3 , etc.). The aquo complexes readily exchange the water for other ligands, (3.13); however, the equilibrium constants are small when the ligand is similar in size to water.



As a consequence of the low equilibrium constants for monodentate ligands, the alkali metal cations, M^+ , favor coordination to polydentate ligands such as ethylenediaminetetraacetic acid (EDTA, Figure 3.2.3.15), polyethers, and even natural polyesters or polypeptides. In each case the polydentate ligand wraps itself around the cation.

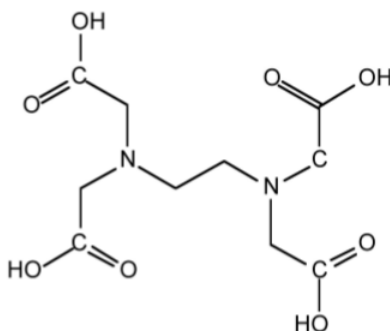


Figure 3.2.15: Structure of ethylenediaminetetraacetic acid (EDTA).

Macrocyclic ligands

Macrocyclic ligands represent a special class of polydentate ligand. They are defined as being a cyclic compound with nine or more members including all the heteroatoms and with three or more donor atoms, and are given the special name of **cryptands** when they are synthetic bi- and poly-cyclic multidentate ligands. Crown ethers is the name applied to macrocyclic ligands that consist of a ring containing several ether groups. Figure 3.2.3.16 shows several common macrocyclic ligands.

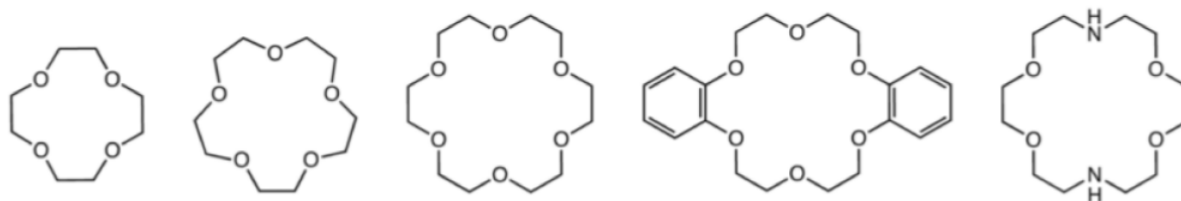


Figure 3.2.16: The structures of some common macrocyclic ligands.

Macrocyclic ligands are generally oxygen or nitrogen donor ligands, and they form highly stable 1:1 complexes with alkali metal ions in which all or most of the coordination sites on the metal are occupied, i.e., $[M(L)]^+$ rather than $[M(L)(\text{H}_2\text{O})_n]^+$. Since the external surface of the macrocyclic ligands comprises of organic residue (e.g., CH_2 groups) the complexes are soluble in organic solvents. Thus, crown ethers are commonly used to solubilize salts (e.g., NaCl) in organic solvents. They have also been used to create solutions of nanoparticles, such as carbon nanotubes (Figure 3.2.3.17), that are ordinarily highly insoluble in common organic solvents (Table 3.2.3.12).

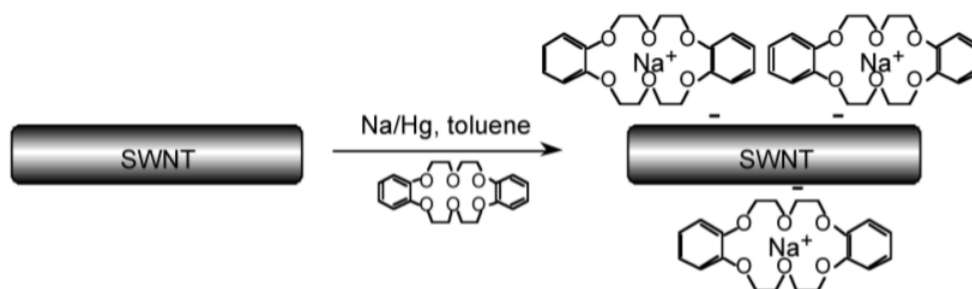


Figure 3.2.17: Representation of the reaction between Na/Hg amalgam, dibenzo-18-crown-6, and purified single walled carbon nanotubes (SWNTs) in toluene and the formation of the $[\text{Na}(\text{dibenzo-18-crown-6})]_n[\text{SWNT}]$ complex. Adapted from R. E. Anderson and A. R. Barron, *J. Nanosci. Nanotechnol.*, 2007, 7, 3436

Table 3.2.3.12: The concentration of Na/dibenzo-18-crown-6 solubilized reduced single walled carbon nanotubes (SWNTs) in various solvents.

Solvent	SWNT concentration (mg/L)
CH ₂ Cl ₂	14.05
DMF	11.42
hexane	4.65
toluene	3.79
EtOH	2.37
MeOH	2.37
CHCl ₃	0.30
H ₂ O	0.10

The most important factor in the coordination of various macrocyclic ligands to alkali metal ions is the relative size of the ion and the ligand cavity. For example, 4,7,13,16,21,24-hexaoxa-1,10diazabicyclo[8,8,8]hexacosane is a potentially octa-dentate ligand; however, the binding efficiency is very dependant on the identity of the M⁺ ion (Figure 3.2.3.18). The low binding constant for lithium is probably as a consequence that the ligand would have to distort to coordinate to the small cation. Conversely, the lower equilibrium for caesium is due to its being too large to fit completely into the ligand cavity.

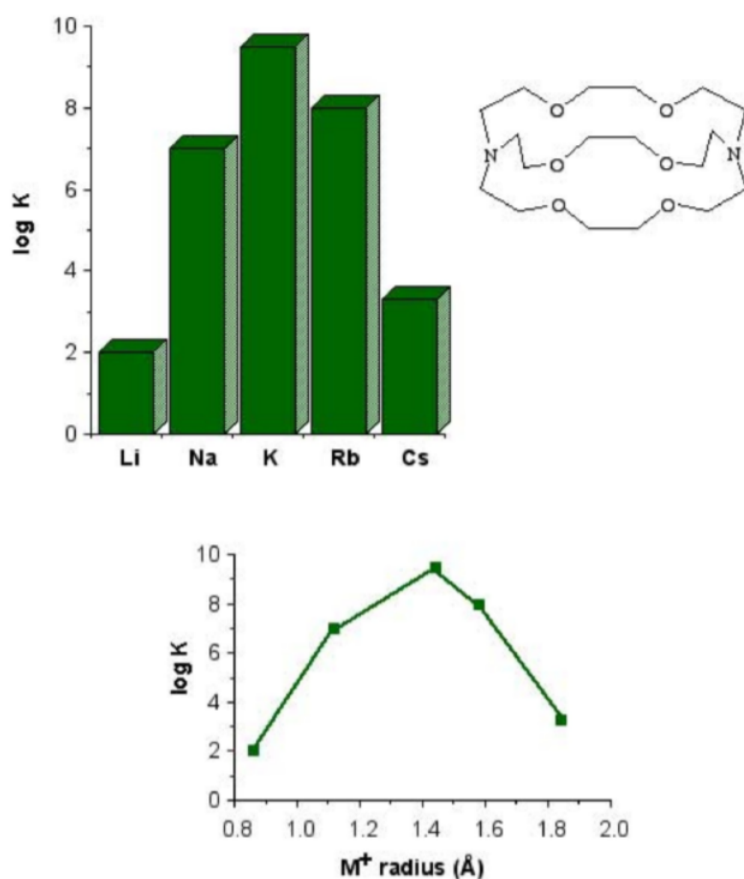


Figure 3.2.18: Relative stability constants (log K) of alkali metal ions to 4,7,13,16,21,24-hexaoxa-1,10diazabicyclo[8,8,8]hexacosane and relationship to the M⁺ ionic radius.

One application of the size effect for macrocyclic ligands is the ability to selectively bind different metals. For example, the 4,7,13,16,21-pentaoxa-1,10-diazabicyclo[8,8,5]tricosane and 4,7,13,16,21,24-hexaoxa-1,10diazabicyclo[8,8,8]hexacosane ligands

shown in Figure 3.2.3.19 have very different binding constants to Na^+ and K^+ , as a consequence of the relative size of the cation and the ligand cavity (Table 3.2.3.13).

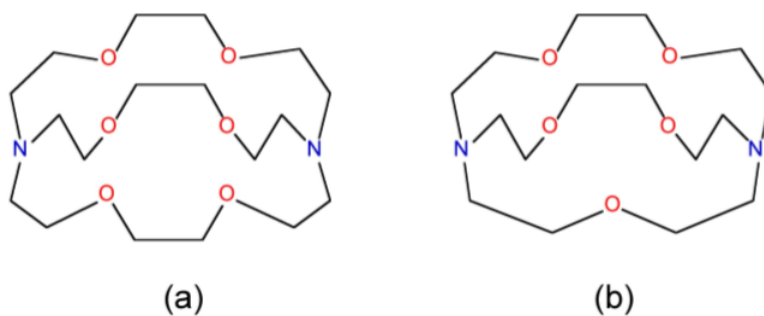


Figure 3.2.19: Structure of (a) 4,7,13,16,21-pentaoxa-1,10-diazabicyclo[8,8,5]tricosane [2,2,1] and (b) 4,7,13,16,21,24-hexaoxa-1,10-diazabicyclo[8,8,8]hexacosane [2,2,2].

Table 3.2.3.13: Equilibrium constants for the M^+ complexes for macrocyclic ligands with different cavity sizes. The structures of the ligands are shown in Figure 3.2.3.19.

Cation	[2,2,2]	[2,2,1]
Na^+	800	250,000
K^+	250,000	700

Bibliography

1. R. E. Anderson and A. R. Barron, *J. Nanosci. Nanotechnol.*, 2007, **7**, 3436.
2. J. M. Lehn, *Supramolecular Chemistry: Concepts and Perspectives*. VCH (1995).

This page titled [3.2: Compounds of the Alkali Metals](#) is shared under a [CC BY 3.0](#) license and was authored, remixed, and/or curated by [Andrew R. Barron \(CNX\)](#) via [source content](#) that was edited to the style and standards of the LibreTexts platform.

3.3: The Anomalous Chemistry of Lithium

While lithium shows many properties that are clearly consistent with its position in Group 1, it also has key differences to the other alkali metals. In fact, in many ways it is more similar to its diagonal neighbor magnesium (Mg) than the other Group 1 metals - a phenomenon known as **the diagonal effect**.

Charge/radius

The ionic radius for the +1 cation of lithium is very small in comparison with its next highest homolog, sodium (Table 3.3.14). This results in a correspondingly high value for the charge density (z/r). As may be seen from Table 3.3.1 the charge density for lithium is significantly higher than that of its Group 1 relations.

Table 3.3.1: Comparison of charge densities for lithium, sodium, potassium, and magnesium.

Element	z	r (Å)	z/r (Å ⁻¹)
Li	+1	0.68	1.47
Na	+1	0.97	1.03
K	+1	1.33	0.75
Mg	+2	0.66	3.03

As a result of the high charge density, the Li^+ ion is a highly polarizing ion. One of the main consequences of this is that lithium tends to form polar covalent bonds rather than ionic interactions. For example, alkyl lithium compounds (RLi) contain covalent Li-C bonds in a similar manner to the Mg-C bonds in Grignards (RMgX, where X = Cl, Br)

Lattice energy

Lithium compounds have high lattice energies as compared to the other Group 1 metals (Table 3.3.2). As a consequence lithium compounds would be less soluble than the highly soluble sodium compounds. In some cases (Li_2O , Li_3N) they react with water.

Table 3.3.2: Comparison of lattice energies for compounds of lithium, sodium, potassium, and magnesium.

Compound	Lattice energy (kJ/mol)
LiF	-1046
NaF	-923
KF	-821
MgF ₂	-2957

Coordination number

The small size of lithium results in a lower coordination number (4) for compounds and complexes than observed for the other Group 1 metals. However, lithium and magnesium complexes and organometallic compounds both have most commonly four-coordinate metal centers (in the absence of large steric constraints).

Chemical reactivity

A review of some of the reactions of lithium, magnesium and the other Group 1 metals shows the anomalous behavior of lithium and its similarity to magnesium. Both lithium and magnesium reacts with carbon or nitrogen to form the corresponding carbide and nitride. Whereas sodium and the other Group 1 metals show no reaction under ambient conditions. The combustion of either lithium or magnesium in air results in the formation of the oxides, Li_2O and MgO , respectively. In contrast, sodium forms the peroxide, Na_2O_2 .

It is not only in the reactivity of the elements that this relationship between lithium and its diagonal neighbor exists. Many of the compounds of lithium have a similar reactivity to those of magnesium rather than sodium. For example, the carbonates of lithium

and magnesium decompose under thermolysis to yield the oxides, (3.14) and (3.15), in contrast, sodium carbonate (Na_2CO_3) is stable to [thermolysis](#).



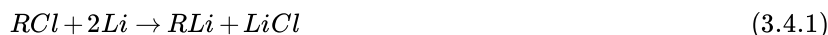
This page titled [3.3: The Anomalous Chemistry of Lithium](#) is shared under a [CC BY 3.0](#) license and was authored, remixed, and/or curated by [Andrew R. Barron \(CNX\)](#) via [source content](#) that was edited to the style and standards of the LibreTexts platform.

3.4: Organolithium Compounds

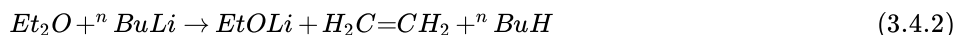
One of the major uses of lithium is in the synthesis of organolithium compounds, RLi. They have great importance and utility in industry and chemical research. Their reactivity resembles that of Grignard reagents, but they are generally more reactive.

Synthesis

The best general method for RLi synthesis involves the reaction of an alkyl or aryl chloride with lithium metal in benzene or an aliphatic hydrocarbon (e.g., hexane), (3.4.1).



While it is possible to use diethyl ether (Et₂O), the solvent slowly attack the resultant alkyl lithium compound, (3.4.2).



Metal-hydrogen exchange, (3.4.3), metal-halogen exchange, (3.19), and metal-metal exchange can also be used, (3.4.4).



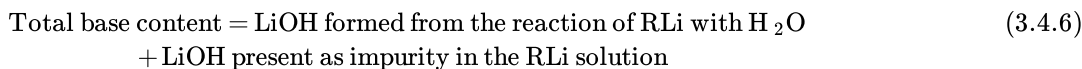
All organolithium compounds are produced as solutions and are hence used in synthetic protocols by volume of solution. It is therefore important to know the exact concentration of RLi in solution. The simplest approach to quantify the amount of organolithium is to react a known volume with water, (3.4.5), and then titrate (with acid) the resultant base that is formed.



However, while the concentration of freshly prepared samples of organolithium reagents can be theoretically measured in this way, real samples always contain some amount of LiOH or other bases. A simple titration inevitably results in an over estimation of the organolithium reagent. To overcome this a *double titration* method is used.

Gillman double titration method

The careful addition of a known volume of an organolithium reagent solution (between 0.5 and 1.5 mL) to an excess of water yields a solution of LiOH that can be titrated with a standardized solution of hydrochloric acid, using phenolphthalein as the indicator. The presence of any LiOH in the original organolithium solution will be incorporated into this titration, and thus the result will be a measure of the *total base content* in the solution, i.e., (3.4.6).



In order to determine the amount of LiOH present as impurity in the organolithium solution it is necessary to react the RLi without the formation of base, then titrate the resulting solution. To do this, an aliquot (the same amount as used before) of the organolithium is reacted slowly with 1,2-dibromoethane (BrCH₂CH₂Br) dissolved in dry diethyl ether (Et₂O). After 5 min of stirring, the solution is diluted with an excess of water and then titrated with a standardized solution of hydrochloric acid, again using phenolphthalein as the indicator. The difference of the two titrations gives the exact concentration of the organolithium.

Example

An aliquot of nBuLi in hexanes (0.50 mL) was added to degassed water (20 mL). After any visible reaction had ceased, a few drops of a phenolphthalein solution in water/methanol are added resulting in a pink color indicative of a basic pH. The resulting mixture is titrated with standardized hydrochloric acid ([HCl] = 0.1034 N) until complete disappearance of the pink color (7.90 mL).

A second aliquot of nBuLi in hexanes (0.50 mL) is added to 1,2-dibromoethane (0.20 mL, Et₂O). After 5 min of stirring, the mixture was diluted with water (20 mL) and after addition of the phenolphthalein indicator titrated (with vigorous stirring due

to the biphasic nature of the system) with standardized hydrochloric acid ($[HCl] = 0.1034\text{ N}$) until complete disappearance of the pink color (0.25 mL).

The concentration of $n\text{BuLi}$ is calculated as follows:

Step 1.

$$[\text{total base}] = \frac{\text{volume HCl} \times [HCl]}{\text{volume } n\text{BuLi}} = \frac{7.90 \times 0.1034}{0.50} = 1.633 \quad (3.4.7)$$

Step 2.

$$[\text{residual base}] = \frac{\text{volume HCl} \times [HCl]}{\text{volume } n\text{BuLi}} = \frac{0.25 \times 0.1034}{0.50} = 0.013 \quad (3.4.8)$$

Step 3.

$$[n\text{BuLi}] = [\text{total base}] - [\text{residual base}] = 1.633 - 0.013 = 1.620\text{ M} \quad (3.4.9)$$

Properties

Alkyl lithium compounds are either low melting solids or liquids, and often with high volatility (depending on the substituent) due to the covalent nature of the bonding. They are soluble in aliphatics, aromatics, and ethers. However, while the reaction with ethers is generally slow, (3.17), alkyl lithium compounds can polymerize tetrahydrofuran (THF).

Organolithium compounds react rapidly with air and water (both vapor and liquid). The reaction with water is the basis of the Gillman double titration method for determining the concentration of organolithium reagents in solution.

Structure

The structure of organolithium compounds is dominated by their highly oligomeric nature as a result of 3-center 2-electron bridging bonds. In all cases the extent of oligomerization is dependant on the identity of the alkyl (or aryl) group. The alkyl-bridged bond is similar to those found for beryllium and aluminum compounds.

In the vapor phase any particular organolithium derivative show a range of oligomeric structures. For example, the mass spectrum of EtLi shows ions associated with both tetramers (e.g., $[\text{Et}_3\text{Li}_4]^+$) and hexamers (e.g., $[\text{Et}_5\text{Li}_6]^+$). The structures of the different oligomers have been predicted by molecular orbital calculations (Figure 3.4.3.20).

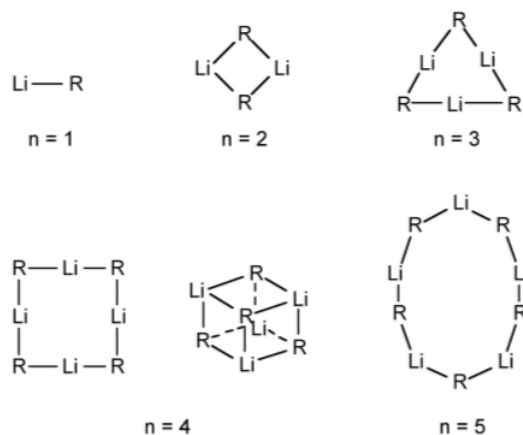


Figure 3.4.20: Proposed vapor phase structures for various oligomers of RLi .

Solution molecular weight measurements indicate the oligomerization is present (in the absence of a coordinating ligand such as Et_2O or an amine). The extent of oligomerization depends on the steric bulk of the alkyl group (Table 3.4.3.16). Oligomerization and solution structures have also been investigated by ^7Li and ^{13}C NMR spectroscopy.

Table 3.4.3.16: Extent of oligomerization (n) for organolithium compounds $[\text{RLi}]_n$ in benzene solution.

R	$[\text{RLi}]_n$	R	$[\text{RLi}]_n$
Me	4	Et	6

R	[RLi] _n	R	[RLi] _n
ⁿ Bu	6	^t Bu	4

There are a large number of X-ray crystallographically determined structures for organolithium derivatives. The archetypal example is MeLi, which exists as a tetramer in the solid state (Figure 3.4.3.21). The lithium atoms are arranged as a tetrahedron and the carbon atoms are positioned on the center of the facial planes, i.e., the carbon is equidistant from each of the lithium atoms. In contrast, EtLi has a similar tetrahedral structure, but the α -carbon of the ethyl groups are asymmetrically arranged such that it is closer to one lithium atom than the other two.

This page titled [3.4: Organolithium Compounds](#) is shared under a [CC BY 3.0](#) license and was authored, remixed, and/or curated by [Andrew R. Barron \(CNX\)](#) via [source content](#) that was edited to the style and standards of the LibreTexts platform.

CHAPTER OVERVIEW

4: Group 2 - The Alkaline Earth Metals

[4.1: The Alkaline Earth Elements](#)

[4.2: Calcium the Archetypal Alkaline Earth Metal](#)

[4.3: Differences for Beryllium and Magnesium](#)

[4.4: Organometallic Compounds of Magnesium](#)

Thumbnail: A crystal of strontianite. Both strontianite, one of the most important strontium ores, and strontium are named after the town of Strontian, Scotland, the location of one of the first mines for strontium ores.

This page titled [4: Group 2 - The Alkaline Earth Metals](#) is shared under a [CC BY 3.0](#) license and was authored, remixed, and/or curated by [Andrew R. Barron \(CNX\)](#) via [source content](#) that was edited to the style and standards of the LibreTexts platform.

4.1: The Alkaline Earth Elements

The Group 2 metals have a particular name: the alkaline earth metals. The name is derived from the observation that they have such high melting points (Table 4.1.4.1) that they remain solids (earths) in a fire. Table 4.1.4.2 lists the derivation of the names of the alkali metals.

Table 4.1.4.1: Melting points of the alkaline earth metals in comparison with the alkali metals.

Alkali metal	Melting point (°C)	Alkaline earth metal	Melting point (°C)
Li	180.54	Be	1287
Na	97.72	Mg	650
K	63038	Ca	842
Rb	39.31	Sr	777
Cs	28.44	Ba	727
Fr	27 (estimated)	Ra	700

Table 4.1.4.2: Derivation of the names of the alkaline earth metals.

Element	Symbol	Name
Beryllium	Be	From the Greek <i>berullos</i> meaning <i>to become pale</i> , in reference to the pale semiprecious gemstone beryl
Magnesium	Mg	From the <i>Magensia</i> district in Greece
Calcium	Ca	From the Latin <i>calcis</i> meaning <i>lime</i>
Strontium	Sr	From the mineral <i>strontianite</i> named after the Scottish village of <i>Strontian</i>
Barium	Ba	From the Greek <i>bary</i> , meaning <i>heavy</i>
Radium	Ra	From the Latin <i>radius</i> meaning <i>ray</i>

Discovery

Beryllium

Beryllium was discovered by Louis-Nicolas Vauquelin (Figure 4.1.4.1) in 1798 as a component in beryls and emeralds; however, Fredrich Wöhler (Figure 4.1.4.2) and Antoine Bussy (Figure 4.1.4.3) independently isolated the metal in 1828 by reacting potassium with beryllium chloride, (4.1.1).



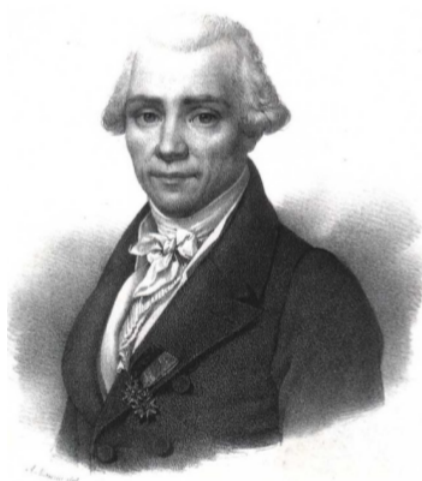


Figure 4.1.1: French pharmacist and chemist Louis Nicolas Vauquelin (1763 - 1829).

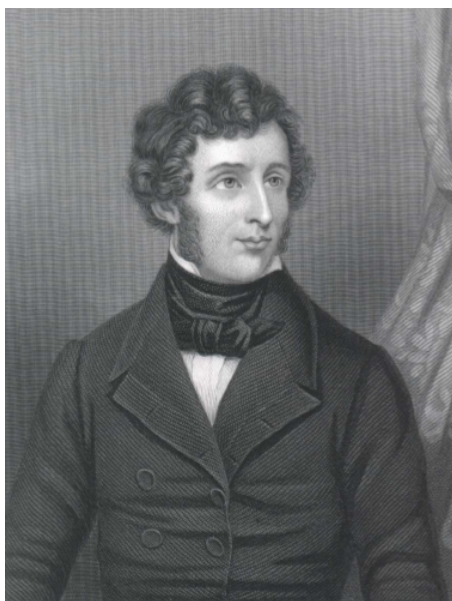


Figure 4.1.2: German chemist Friedrich Wöhler (1800 - 1882) also known for his synthesis of urea and, thus, the founding of the field of natural products synthesis.

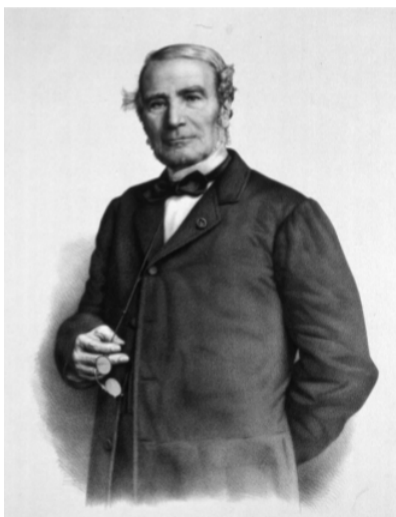


Figure 4.1.3: French chemist Antoine Alexandre Brutus Bussy (1794 - 1882).

Magnesium

Magnesium is found in large deposits of magnesite and dolomite, and in mineral waters where the Mg^{2+} ion is soluble. In 1618 a farmer at Epsom in England attempted to give his cows water from a well. The farmer noticed that the water seemed to heal scratches and rashes. These *Epsom salts* were recognized to be hydrated magnesium sulfate, MgSO_4 . The metal was first isolated in 1808 by Sir Humphry Davy (Figure 4.1.4.4) via the electrolysis of a mixture of magnesia and mercury oxide.



Figure 4.1.4: British chemist and inventor Sir Humphry Davy FRS (1778 - 1829).

Antoine Bussy (Figure 4.1.4.3) subsequently prepared magnesium by heating magnesium chloride and potassium in a glass tube, (4.1.2). When the potassium chloride was washed out, small globules of magnesium remained.



Calcium

Calcium oxide or lime was known in ancient Rome, while even in 975 AD, Plaster of Paris (calcium sulphate) was reported to be useful for setting broken bones. The element itself was not isolated until 1808 when Sir Humphry Davy (Figure 4.1.4.4) electrolyzed a mixture of lime and mercuric oxide (HgO). His work was based upon prior work by Jöns Berzelius (Figure 4.1.4.5) who had prepared calcium amalgam (an alloy of calcium and mercury) by electrolyzing lime in mercury.



Figure 4.1.5: Swedish chemist Jöns Jacob Berzelius (1779 1848).

Strontium

Discovered in lead mines in 1787 the mineral strontianite was named after the Scottish village of Strontian. Although it was realized that this mineral was different from others that contained barium, it wasn't until 1798 that Thomas Hope (Figure 4.1.46) suggested the presence of a new element. As with calcium, metallic strontium was first isolated by Sir Humphry Davy (Figure 4.1.44) in 1808 using electrolysis of a mixture containing strontium chloride and mercuric oxide.



Figure 4.1.6: Scottish chemist Thomas Charles Hope (1766 - 1844).

Barium

Barium minerals were known by alchemists in the early Middle Ages. Stones of the mineral barite found in Bologna, Italy (also known as *Bologna stones*), were known to glow after exposure to light. Carl Scheele (Figure 4.1.47) identified barite in 1774, but did not isolate barium. Barium was first isolated as Ba^{2+} in solution by Sir Humphry Davy (Figure 4.1.44) in 1808. The oxidized barium was at first called *barote*, by Guyton de Morveau, (Figure 4.1.48) which was changed by Antoine Lavoisier (Figure 4.1.49) to *baryta*, from which barium was derived to describe the metal.



Carl Wilhelm Scheele.

Figure 4.1.7: : German-Swedish pharmaceutical chemist Carl Wilhelm Scheele (1742 - 1786). Author Isaac Asimov has called him "hard-luck Scheele" because he made a number of chemical discoveries before others who are generally given the credit.

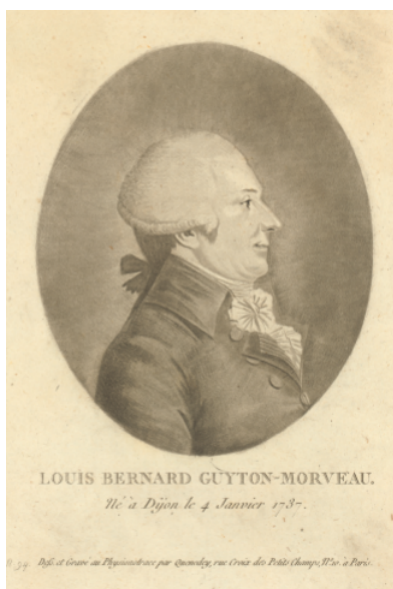


Figure 4.1.8: : French chemist and politician Louis-Bernard Guyton de Morveau (1737 - 1816) changed his name to Guyton-Morveau after the French Revolution.



Figure 4.1.9: French chemist and biologist Antoine-Laurent de Lavoisier (1743 1794).

Radium

Radium was discovered by Marie Curie (Figure 4.1.4.10) and her husband Pierre (Figure 4.1.4.11) in 1898 while studying pitchblende. After removing uranium they found that the remaining material was still radioactive. They then separated out a radioactive mixture consisting mostly of barium and an element that gave crimson spectral lines that had never been documented before. In 1910, radium was isolated as a pure metal by Curie and André-Louis Debierne (Figure 4.1.4.12) through the electrolysis of a radium chloride solution by using a mercury cathode and distilling in an atmosphere of hydrogen gas.



Figure 4.1.10: Marie Curie (1867-1934). Copyright Academy of Achievement.



Figure 4.1.11: French physicist Pierre Curie (1859 1906).



Figure 4.1.12: French chemist André-Louis Debierne (1874 - 1949).

Abundance

The abundance of the alkaline earth elements is given in Table 4.1.4.3. Beryllium is rare, but found in the mineral beryl ($\text{Be}_3\text{Al}_2\text{Si}_6\text{O}_{18}$). While magnesium is widespread within the Earth's crust, commercial sources tend to be from sea water as well as the carbonate minerals magnesite (MgCO_3) and dolomite [$(\text{Ca,Mg})\text{CO}_3$]. Calcium is also commonly found as the carbonate, however, strontium and barium are present as the sulfates celestine (SrSO_4) and barites (BaSO_4), respectively.

Table 4.1.4.3: Abundance of alkaline earth elements.

Element	Terrestrial abundance (ppm)
Be	2.6 (Earth's crust), 6 (soil), 2×10^{-7} (sea water)
Mg	23,000 (Earth's crust), 10,000 (soil), 1,200 (sea water)
Ca	41,000 (Earth's crust), 20,000 (soil), 400 (sea water)
Sr	370 (Earth's crust), 200 (soil), 8 (sea water)
Ba	500 (Earth's crust), 500 (soil), 0.001 (sea water)
Ra	6×10^{-7} (Earth's crust), 8×10^{-7} (soil), 1×10^{-10} (sea water)

Calcium is a key element for living. Not only is it present as the skeletal material for shell sh and crabs (CaCO_3) its phosphate derivative, hydroxyapatite [$\text{Ca}_5(\text{OH})(\text{PO}_4)_3$] is the structural material of bones and teeth. Calcium is also present in soft tissue at a level of ca. 22g/kg. Calcium is a vital metal for the following:

- Links large molecules together.
- Used in the activation of muscles
- Used in enzyme activation by stabilization of particular conformations of proteins to be acted upon by enzymes.

Isotopes

The naturally abundant isotopes of the alkaline earth elements are listed in Table 4.1.4.4. All of the 25 isotopes of radium are radioactive, and while radium-223, radium-224, and radium-228 are found in nature as decay products of either uranium or thorium, they are only present in trace amounts.

Table 4.1.4.4: Abundance of the major isotopes of the alkaline earth elements.

Isotope	Natural abundance (%)
Beryllium-9	100
Magnesium-24	78.99
Magnesium-25	10
Magnesium-26	11.01
Calcium-40	96.941
Calcium-42	0.647
Calcium-43	0.135
Calcium-44	2.086
Calcium-46	0.004
Calcium-48	0.187
Strontium-84	0.56
Strontium-86	9.86
Strontium-87	7.0

Isotope	Natural abundance (%)
Strontium-88	82.58
Barium-130	0.106
Barium-132	0.101
Barium-134	2.417
Barium-135	6.592
Barium-136	7.854
Barium-137	11.23
Barium-138	71.7
Radium-226	100

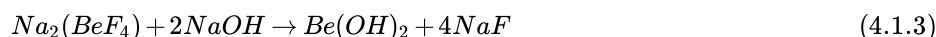
Although beryllium-7 and beryllium-10 are found as trace isotopes, they are so rare beryllium is considered mononuclidic element (a chemical element which is found essentially as a single nuclide, of only one atomic mass). Calcium has four stable isotopes plus two more isotopes (calcium-46 and calcium-48) that have such long half-lives (2.8×10^{15} and 4×10^{19} years, respectively) that for all practical purposes they can be considered stable.

Measurement of the $^{87}\text{Sr}/^{86}\text{Sr}$ ratio allows for geological dating of minerals and rocks. Strontium-90 (half-life = 28.9 years) is a by-product of nuclear fission and found in nuclear fallout. For example, the 1986 Chernobyl nuclear accident contaminated released a large amount of strontium-90. Since strontium substitutes for calcium in bones it prevents excretion from the body and thus presents a significant health risk, however, strontium-89 is a short-lived artificial radioisotope that is used in the treatment of bone cancer.

Naturally occurring barium is a mix of seven stable isotopes (Table 4.1.44), but there are a total twenty-two isotopes known, most of which are highly radioactive and have half-lives in the several millisecond to several day range. The only notable exception is barium-133 which has a half-life of 10.51 years.

Industrial production

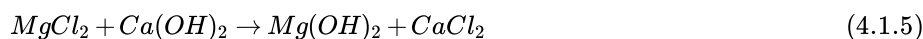
The industrial production of beryllium is usually from the reaction of beryl ($\text{Be}_3\text{Al}_2\text{Si}_6\text{O}_{18}$) with $\text{Na}_2(\text{SiF}_6)$ which yields the beryllium fluoride, $\text{Na}_2(\text{BeF}_4)$. Subsequent reactions with base give the hydroxide.



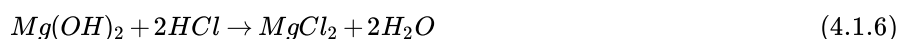
Reaction of the hydroxide with the ammonium salt of HF_2^- , followed by thermolysis gives beryllium fluoride (BeF_2). Finally, reduction of the fluoride with magnesium yields beryllium.



Although magnesium is an abundant metal in dozens of mineral the majority of commercial production comes from sea water, where it is present at about a level of 12% that of sodium. Calcium hydroxide is added to seawater to form magnesium hydroxide precipitate.



Subsequent reaction with hydrochloric acid yields concentrated magnesium chloride solution.



Electrolysis of the magnesium chloride produces magnesium. At the cathode, the Mg^{2+} ion is reduced to magnesium metal, (4.1.7), while at the anode chlorine gas is formed, (4.1.8).



Strontium metal is produced in an analogous manner; however, it may also be prepared from strontium oxide by reduction with aluminum in vacuum at a temperature at which strontium distills off.



Reactivity and toxicity

The chemistry of the Group 2 elements is dominated by the +2 oxidation state and the noble gas configuration of the M^{2+} cation.

Calcium, strontium, and barium react with water on contact to produce the hydroxide and hydrogen gas. Although the lighter alkaline earth metals do not react violently with water, they do burn in air.

Magnesium burns with a very bright white flame such that caution should be taken not to look at the flame directly. Magnesium is capable of reducing water, (4.1.10), and as a result, water cannot be used to extinguish magnesium fires; the hydrogen gas produced will only intensify the fire. In addition, magnesium also reacts with carbon dioxide, (4.1.11), precluding the use of carbon dioxide fire extinguishers. Class D dry chemical fire extinguisher or sand are used for magnesium fires.



Strontium and barium burn in air to produce both the oxide and the nitride, but since the metals do not react with nitrogen except at high temperatures they only form the oxide spontaneously at room temperature.

Beryllium is a class 1 carcinogen, i.e., it is carcinogenic to both animals and humans. Beryllium is harmful if inhaled; if the concentration in air is high enough (greater than 100 $\mu\text{g}/\text{m}^3$) an acute condition can result, called acute beryllium disease, which resembles pneumonia. Acute beryllium disease was reported as being associated with the manufacture of fluorescent lighting tubes (a practice that ceased in 1949).

The human body absorbs strontium as if it were calcium, and while stable isotopes pose no significant health threat, the uptake of radioactive strontium-90 can lead to various bone disorders and diseases, including bone cancer. All water or acid soluble barium compounds are extremely poisonous. At low doses, barium acts as a muscle stimulant, while higher doses affect the nervous system. Radium is highly radioactive and its decay product, radon gas, is also radioactive.

This page titled [4.1: The Alkaline Earth Elements](#) is shared under a [CC BY 3.0](#) license and was authored, remixed, and/or curated by [Andrew R. Barron \(CNX\)](#) via [source content](#) that was edited to the style and standards of the LibreTexts platform.

4.2: Calcium the Archetypal Alkaline Earth Metal

Calcium represents the typical Group 2 metal. The chemical properties of its compounds can be applied to all the heavier homologs.

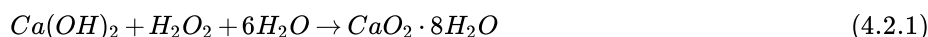
Solid state

In the solid state the compounds of the alkaline metals generally form ionic lattices. In fact (except for beryllium and to a lesser extent magnesium) the lattice parameters calculated from the ionic radii of Group 2 metals are within 1% of the experimentally determined values, indicating the highly ionic character.

Due to the increased ionic charge the cations of the alkaline earths are less than that of their alkali metal neighbors. Thus, the ionic radius of Ca^{2+} (0.99 Å) is less than that of K^+ (1.33 Å), but more similar to Na^+ (0.97 Å). This diagonal relationship is seen for the other metals in Group 2.

Oxides

Combustion of the Group 2 metals gives the monoxide, MO. In the case of SrO and BaO further reaction occurs by the absorption of oxygen under pressure to give the peroxides, MO_2 . The peroxide and superoxides are not stable for the lighter homologs because the smaller M^{2+} ions are more polarizing and cause the peroxide and superoxides to decompose to the monoxide. Calcium peroxide can be prepared by the reaction of the hydroxide with hydrogen peroxide.



As typical for the Group 2 oxides, calcium monoxide is basic and reacts with water to give the hydroxide, (4.2.2). In fact, thin films of the Group 2 oxides of calcium, barium and strontium will readily absorb water and form the hydroxides.



Carbonate

Calcium carbonate (CaCO_3) is a common substance found in rock in all parts of the world, and is the main component of shells of marine organisms, snails, pearls, and eggshells. Calcium carbonate is usually the principal cause of hard water. Most calcium carbonate used is extracted by quarrying or mining. However, pure calcium carbonate (e.g., for pharmaceutical use) can be produced from a pure quarried source (usually marble) or manufactured by the sequential reaction involving the thermal decomposition of the carbonate to the monoxide, (4.2.3), followed by the reaction with water to give the hydroxide, (4.2.2), and finally, the reaction with carbon dioxide to reform the carbonate, (4.2.4).



Calcium carbonate crystallizes as a variety of mineral forms.

- Aragonite
- Calcite (Figure 4.2.4.13)
- Vaterite
- Chalk
- Travertine
- Limestone
- Marble

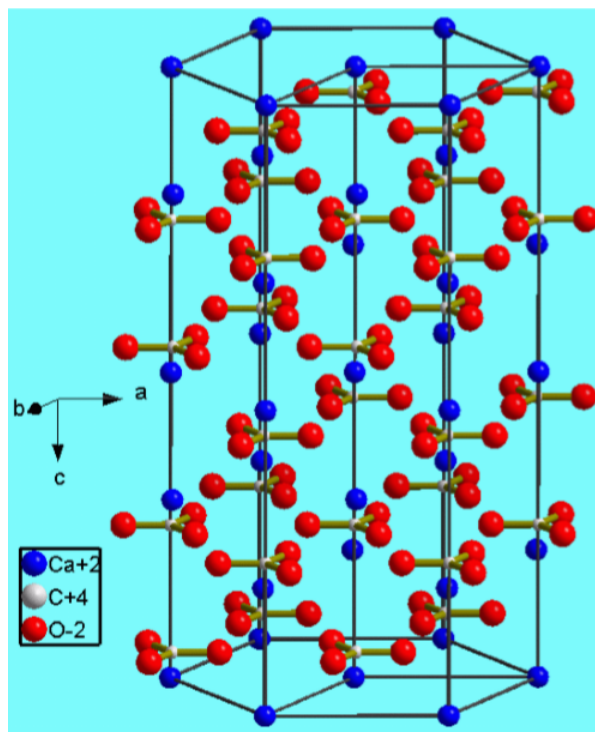


Figure 4.2.4.13: Unit cell of calcite a common form of calcium carbonate (CaCO_3).

Calcium carbonate is one of the most widely used mineral materials, the following represents a list of some of the main applications.

- Construction industry as a building material (marble) or as an ingredient of cement.
- Purification of iron from iron ore in a blast furnace.
- A drilling fluids in the oil industry.
- Filler material for latex gloves.
- Filler (extender) in paints.
- Filler in plastics.
- Babies' diapers.
- DIY adhesives, sealants, and decorating fillers.
- Whiting in ceramics/glazing application.
- The filler in glossy paper.
- The production of blackboard chalk (CaSO_4).
- An abrasive in household cleaning products.
- Dietary calcium supplement.
- Inert filler for tablets and pharmaceuticals.
- Toothpaste.

Halides

Calcium chloride, bromide, and iodide are all ionic, water-soluble salts. In contrast, due to its high lattice energy for the small fluoride ion, CaF_2 is only slightly soluble (Table 4.2.4.5). The *fluorite* structure typified for CaF_2 (Figure 4.2.4.14) is found for most of the MX_2 ionic solids.

Table 4.2.4.5: Solubility of calcium halides in water.

Compound	Solubility @ 20 °C (g/100 mL)	Solubility @ 100 °C (g/100 ml)
CaF_2	0.0016	0.0017
CaCl_2	74.5	159
CaBr_2	142	312

Compound	Solubility @ 20 °C (g/100 mL)	Solubility @ 100 °C (g/100 ml)
CaI ₂	209	426

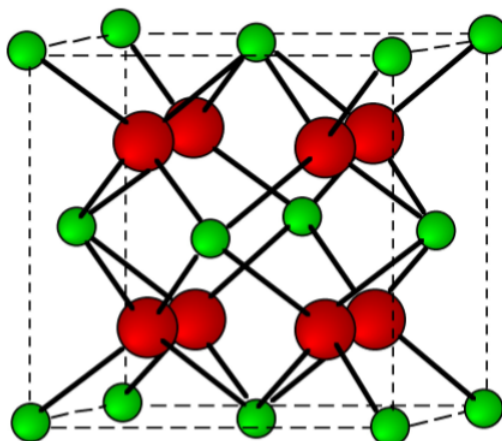


Figure 4.2.4.14 Unit cell for the fluorite (CaF₂) structure. Calcium atoms are shown in green (small), fluorine atoms are shown in red (large), and the dashed lines show the unit cell.

Complexes

The coordination complexes of the alkaline earth metal cations (M^{2+}) involve electrostatic, or ion-dipole, interactions that have no preferred direction of interaction. Calcium will tolerate a wide range of coordination numbers, however, 6 and 8 are the most common. Complexes generally form with oxygen donors in a wide range of ligands, including: ROH, R₂O, R₂C=O, RCO₂⁻, and PO₄²⁻. While complexes with nitrogen donor ligands are known they are usually present with oxygen donors as well. As with the Group 1 metals, the aquo complex readily exchanges the water for other ligands, however, since the bond energy is larger for Ca²⁺ than for Na⁺, the equilibrium constants are larger for analogous complexes.

Bibliography

- J. M. Buriak, L. K. Cheatham, R. G. Gordon, J. J. Graham, and A. R. Barron, *Euro J. Solid State Inorg. Chem.*, 1992, **29**, 43.
- R. E. Anderson and A. R. Barron, *Main Group Chem.*, 2005, **4**, 279.
- C. Lupu, R. S. Arvidson, A. Lüttge and A. R. Barron, *Chem. Commun.*, 2005, 2354.

Calcium Carbide: From Gaslight to Fertilizer

Calcium carbide has an interesting role in the societal and commercial changes that took place in the late 19th and early 20th centuries. However, in order to understand the effects of calcium carbide it is important to realize the state of the art of lighting in the late 18th century.

It was in 1792 that William Murdoch (Figure 4.2.4.15) first began experimenting with the use of gas, derived from the heating of coal and other materials, for lighting. Murdoch produced this coal gas, or manufactured gas and conveyed it through metal pipes, lighting his cottage and offices in Redruth, Cornwall (Figure 4.2.4.16).



Figure 4.2.4.15: Scottish engineer, inventor, and pioneer of gas lighting William Murdoch (1754 - 1839).



Figure 4.2.4.16: Murdoch's house at Redruth was the first domestic residence to be lit by gas.

In 1802 as part of the public celebrations of the Peace of Amiens (between England and France) Murdoch made a public exhibition of his lighting by illuminating the exterior of the Soho Foundry in Birmingham, England. Then in 1807 an entrepreneur, Fredrick Winsor (originally Friedrich Albrecht Winzer) displayed gaslights along the top of the wall between Carlton House and the Mall in London. This demonstration for city use was a revelation. By 1823 Britain had 300 miles of gas pipe and by 1850 it was 2000 miles. Gaslight had a profound impact on society. Walking the streets at night was safer, and it allowed for longer working hours. It also made evening activities easier. As a consequence reading and evening schools became popular pastimes. Unfortunately, gaslight was rather dull orange in color (Figure 4.2.4.17), but it was due to another area of chemical research that a brighter alternative was discovered.



Figure 4.2.4.17: A gas light still in use on the streets of London.

In 1895 the Frenchman Henry Moissan (Figure 4.2.4.18) was trying to make diamonds by the reaction of carbon (graphite) with almost anything he could lay his hands on. Although highly unsuccessful, one of his experiments did prove useful. By reacting carbon with lime, the common name for calcium oxide (CaO) at $2000\text{ }^{\circ}\text{C}$ (in an electric arc furnace that he had helped develop) he produced calcium carbide (CaC_2).



Figure 4.2.4.18: French chemist Ferdinand Frederick Henri Moissan (1852 - 1907).

Pure calcium carbide is colorless, but most samples have a color ranging from black to grayish-white, depending on the grade. As an ionic salt it has a high melting point ($2160\text{ }^{\circ}\text{C}$). While the structure of calcium carbide (Figure 4.2.4.19) has a tetragonal lattice, it is related to that of a cubic rock salt structure, but where the anion is the linear C_2^{2-} moiety.

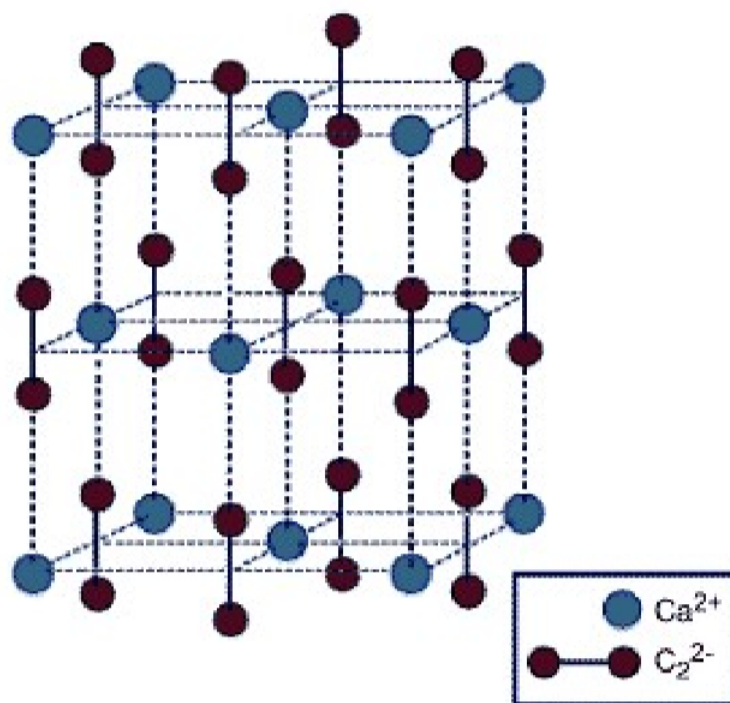


Figure 4.2.4.19: The unit cell of calcium carbide (CaC_2). Adapted from N. N. Greenwood and A. Earnshaw, *Chemistry of the Elements*, Butterworth-Heinemann (1984).

Although now used extensively, at the time of its discovery calcium carbide itself did not prove very interesting, its reaction with water had a profound effect on illumination. The reaction of calcium carbide with water yields acetylene, (4.2.5).



Unlike coal gas, acetylene burns with a very bright white flame. Although electricity was starting to become more commonly used it was very expensive and acetylene offered a cheaper alternative for domestic lighting. Thus, by 1899 there were over 250,000 acetylene gas jets in Germany alone. The reaction of calcium carbide to form acetylene was used in a variety of portable lamps. These so-called carbide lamps were used in slate, copper and tin mines, and were also used extensively as headlights in early automobiles and bikes (Figure 4.2.4.20).



Figure 4.2.4.20: The carbide lamp on a 1911 Renault.

Unfortunately for acetylene there was one discovery and one economic change that brought the use of acetylene as a light source to an end. In 1893 Auer von Welsbach (Figure 4.2.4.21) invented the gas mantle (Figure 4.2.4.22). By the impregnation of silk or cotton with a mixture of thorium dioxide and cerium(IV) oxide (99:1), and using this in combination with gas he was able to produce a very white flame.



Figure 4.2.4.21: Austrian scientist and inventor Carl Auer Freiherr von Welsbach (1858 - 1929).



Figure 4.2.4.22 Gas mantles. Copyright Science Museum, London.

The other impact on acetylene, was that by 1905 the cost of electricity was significantly lower, and as a consequence the price of CaC_2 dropped to 30%. There were stockpiles of calcium carbide all over Europe and America. This may have been the end of calcium carbide's usefulness, however, in 1895 Heinrich Caro (Figure 4.2.4.23) and Adolf Frank (Figure 4.2.4.24), at the German chemical giant Badische Anilin- und Soda-Fabrik (BASF), were trying to make hydrogen cyanide (HCN) to use in its color dye business. In 1898, one of their colleagues demonstrated that what was actually produced during the reaction at temperatures exceeding 1000 °C was not cyanide, as they had hoped. It turned out that what Caro and Frank had found was that that when calcium carbide is reacted with nitrogen at 1000 °C it forms calcium cyanamide (CaCN_2), (4.2.6). The cyanamide anion has the structure $[\text{N}=\text{C}=\text{N}]^{2-}$.



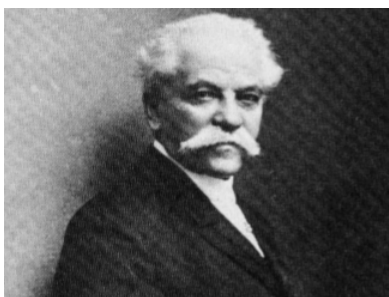


Figure 4.2.4.23: German chemist Heinrich Caro (1834 - 1910).



Figure 4.2.4.24: German chemist, engineer, and businessman Adolph Frank (1834 1916).

In contact with water calcium cyanamide decomposes and liberates ammonia:



As such, CaCN_2 is an excellent solid fertilizer that is readily plowed into the soil. By 1908 calcium cyanamide was also found to be a plant protection agent, which, at a time when all weed control was performed mechanically, represented a great step forward. Consequently, the output of calcium cyanamide grew enormously. In 1910, 30,000 tons were produced, but in 1928, global production had reached 1.2 million tons. After a temporary decline, demand has again risen in recent years owing to the ban on several pesticides due to the environmental damage they cause. Even after 100 years of use, no harmful long-term effects to the earth or environment have been observed, nor have weeds or pests developed a resistance to calcium cyanamide.

Bibliography

- N.-G. Vannerberg, *Acta Chem. Scand.*, 1962, **16**, 1212.
- M. A. Bredig, *J. Am. Chem. Soc.*, 1942, **64**, 1730.
- Y. Yamamoto, K. Kinoshita, K. Tamaru, and T. Yamanaka, *Bull. Chem. Soc. Japan*, 1958, **31**, 501.

Portland Cement

Chemical Composition of Portland Cement

There are four chief minerals present in a Portland cement grain: tricalcium silicate (Ca_3SiO_5), dicalcium silicate (Ca_2SiO_4), tricalcium aluminate ($\text{Ca}_3\text{Al}_2\text{O}_5$) and calcium aluminoferrite ($\text{Ca}_4\text{Al}_n\text{Fe}_{2-n}\text{O}_7$). The formula of each of these minerals can be broken down into the basic calcium, silicon, aluminum and iron oxides (Table 4.2.4.6). Cement chemists use abbreviated nomenclature based on oxides of various elements to indicate chemical formulae of relevant species, i.e., C = CaO , S = SiO_2 , A = Al_2O_3 , F = Fe_2O_3 . Hence, traditional cement nomenclature abbreviates each oxide as shown in Table 4.2.4.6.

Table 4.2.4.6: Chemical formulae and cement nomenclature for major constituents of Portland cement. Abbreviation notation: C = CaO , S = SiO_2 , A = Al_2O_3 , F = Fe_2O_3 .

Mineral	Chemical formula	Oxide composition	Abbreviation
---------	------------------	-------------------	--------------

Mineral	Chemical formula	Oxide composition	Abbreviation
Tricalcium silicate (alite)	Ca_3SiO_5	$3\text{CaO} \cdot \text{SiO}_2$	C3S
Dicalcium silicate (belite)	Ca_2SiO_4	$2\text{CaO} \cdot \text{SiO}_2$	C2S
Tricalcium aluminate	$\text{Ca}_3\text{Al}_2\text{O}_6$	$3\text{CaO} \cdot \text{Al}_2\text{O}_3$	C3A
Tetracalcium aluminoferrite	$\text{Ca}_4\text{Al}_n\text{Fe}_{2-n}\text{O}_7$	$4\text{CaO} \cdot \text{Al}_n\text{Fe}_{2-n}\text{O}_3$	C4AF

The composition of cement is varied depending on the application. A typical example of cement contains 50-70% C3S, 15-30% C2S, 5-10% C3A, 5-15% C4AF, and 3-8% other additives or minerals (such as oxides of calcium and magnesium). It is the hydration of the calcium silicate, aluminate, and aluminoferrite minerals that causes the hardening, or setting, of cement. The ratio of C3S to C2S helps to determine how fast the cement will set, with faster setting occurring with higher C3S contents. Lower C3A content promotes resistance to sulfates. Higher amounts of ferrite lead to slower hydration. The ferrite phase causes the brownish gray color in cements, so that white cements (i.e., those that are low in C4AF) are often used for aesthetic purposes.

The calcium aluminoferrite (C4AF) forms a continuous phase around the other mineral crystallites, as the iron containing species act as a fluxing agent in the rotary kiln during cement production and are the last to solidify around the others. Figure 4.2.4.25 shows a typical cement grain.

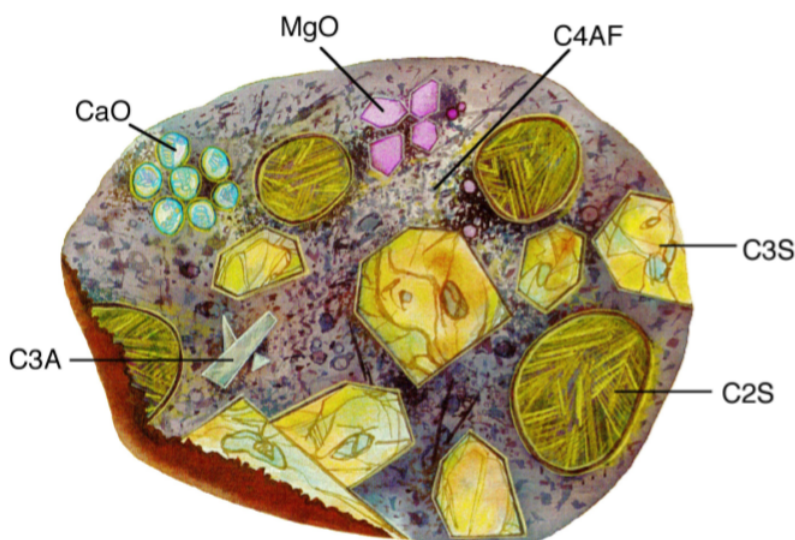


Figure 4.2.4.25: A pictorial representation of a cross-section of a cement grain. Adapted from Cement Microscopy, Halliburton Services, Duncan, OK.

It is worth noting that a given cement grain will not have the same size or even necessarily contain all the same minerals as the next grain. The heterogeneity exists not only within a given particle, but extends from grain to grain, batch-to-batch, plant to plant.

Bibliography

- H. F. W. Taylor, *Cement Chemistry*, 2nd Ed., Academic Press, London (1997).

Manufacture of Portland Cement

Portland Cement is manufactured by heating calcium carbonate and clay or shale in a kiln. During this process the calcium carbonate is converted to calcium oxide (also known as lime) and the clay minerals decompose to yield dicalcium silicate (Ca_2SiO_4 , C2S) and other inorganic oxides such as aluminate and ferrite. Further heating melts the aluminate and ferrite phases. The lime reacts with dicalcium silicate to form tricalcium silicate (Ca_3SiO_5 , C3S). As the mixture is cooled, tricalcium aluminate ($\text{Ca}_3\text{Al}_2\text{O}_6$, C3A) and tetracalcium aluminoferrite ($\text{Ca}_4\text{Al}_n\text{Fe}_{2-n}\text{O}_7$, C4AF) crystallize from the melt and tricalcium silicate and the remaining dicalcium silicate undergo phase transitions. These four minerals (C3S, C2S, C3A, and C4AF) comprise the bulk of most cement mixtures. Initially Portland cement production was carried out in a furnace, however, technological developments such as the rotary kiln have enhanced production capabilities and allowed cement to become one of the most widely used construction materials.

Cement plants generally produce various grades of cement by two processes, referred to as either the wet or dry process. The dry process uses a pneumatic kiln system which uses superheated air to convert raw materials to cement, whereas the wet process slurries the raw materials in water in preparation for conversion to cement. Cement manufacturers due to its higher energy efficiency generally favor the dry process, but the wet process tends to produce cement with properties more palatable to the energy services industry. The American Petroleum Institute (API) Class H cement used in energy service applications is produced by the wet process, and thus will be the focus of the following discussion.

The cement manufacturing process begins at the quarry (Figure 4.2.4.26), where limestone formations are ripped and crushed in two crushers to a mean particle size of 4". The quarry formation is not entirely limestone, and no attempt is made to isolate the limestone from the other minerals. On the contrary, the rippers act to blend in the impurity minerals as evenly as is feasible while still maintaining an acceptable limestone content so as not to waste the formation. This is accomplished by ripping the formation face at a 45° (Figure 4.2.4.27). The rock is quality controlled via mobile X-ray fluorescence (XRF) spectroscopy (Figure 4.2.4.28) at the starting point of a mobile covered conveyor belt system (Figure 4.2.4.29), which transports the material to a dome storage unit (Figure 4.2.4.30).



Figure 4.2.4.26: Limestone quarry face in Midlothian, TX (Copyright Halliburton Energy Services).



Figure 4.2.4.27: Limestone quarry formation, showing the 45° ripping technique (Copyright Halliburton Energy Services).



Figure 4.2.4.28: Mobile crusher and XRF unit (Copyright Halliburton Energy Services).



Figure 4.2.4.29: Covered conveyor belt for limestone transport (Copyright Halliburton Energy Services).



Figure 4.2.4.30: Exterior view of dome storage unit with conveyor loading port (Copyright Halliburton Energy Services).

The dome storage unit has a capacity of 60 kilotons, and is filled by dispensing the rock from the conveyor at the top of the dome into a pile built in a circular pattern (Figure 4.2.4.31). The rock is reclaimed from storage via a raking device (Figure 4.2.4.32) that grates over the pile at the natural angle of material slide. The raked material slides to the base of the raking unit, where a second conveyor system transfers material to either of two limestone buffer bins (Figure 4.2.4.33), each of which is dedicated to a particular kiln process. There is an additional buffer bin for mill scale from a nearby steel plant, as well as a buffer bin for sand. It

is worth noting at this point that the mill scale from the steel plant contains significant levels of boron, which acts as an innate retarder and seems to affect adversely, though not overly severely, the early compressive strength development when compared to cement from other plants.

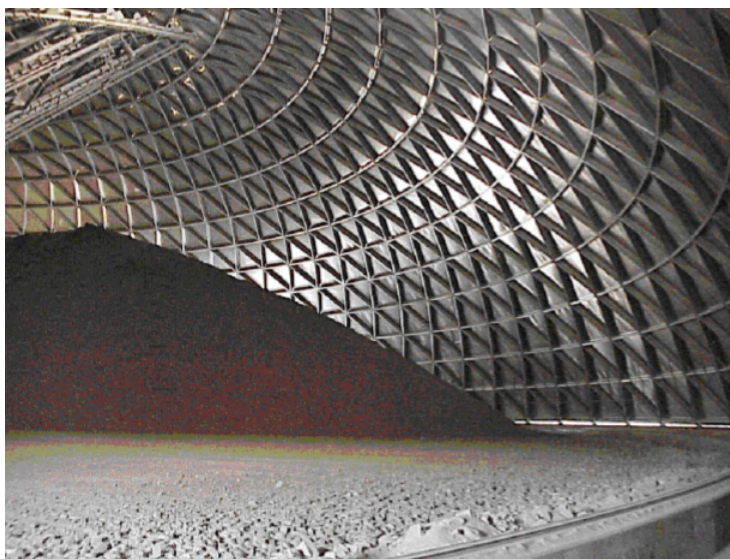


Figure 4.2.4.31: Interior view of dome storage unit, illustrating its radial piling (Copyright Halliburton Energy Services).



Figure 4.2.4.32: Raking device for reclaiming stored limestone (Copyright Halliburton Energy Services).



Figure 4.2.4.33: Buffer bin (Copyright Halliburton Energy Services).

Material leaving the buffer bins is monitored for elemental composition via XRF and feed rates are adjusted for maintaining proper flow of calcium, silicon, aluminum, and iron. The raw materials are carried to ball mills (Figure 4.2.4.34) for grinding to fine powder, which is then mixed with water. The resulting slurry is then sent to the rotary kiln for burning (Figure 4.2.4.35), or transformation into cement clinker.

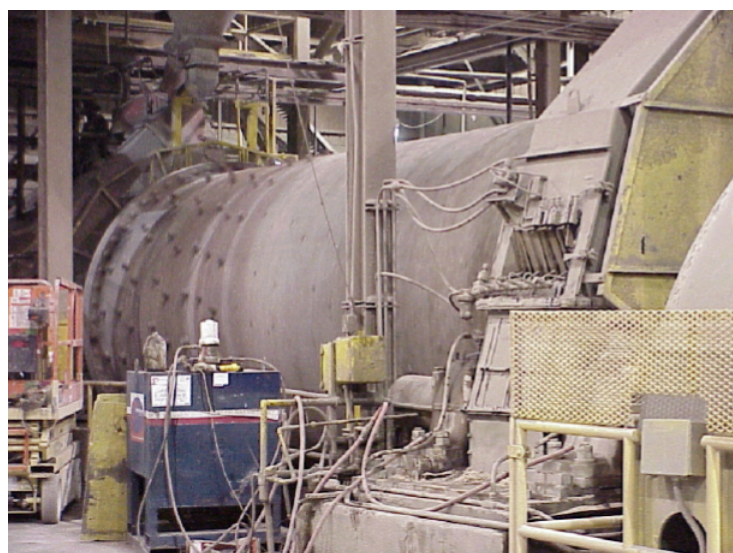


Figure 4.2.4.34: Coarse grinder (Copyright Halliburton Energy Services).



Figure 4.2.4.35: A wet rotary kiln (Copyright Halliburton Energy Services).

The kilns are red to an internal material temperature of 2700 °F (Figure 4.2.4.36) with a fuel of nely ground coal, natural gas, and/or various waste materials. Around fifty percent of the energy expenditure in the wet kiln process is dedicated to evaporating the water from the slurry, in contrast to the dry process, which spends most of its energy on the calcining process. Since the dry process only requires approximately half the energy of the wet process, it is generally more attractive to cement manufacturers. Unfortunately, the dry process in current use produces poor API Class H cement. A fuller understanding of the differences in cement synthesis via the two processes could lead to the development of a more effective dry synthesis of Class H cements, but that is beyond the scope of this work.

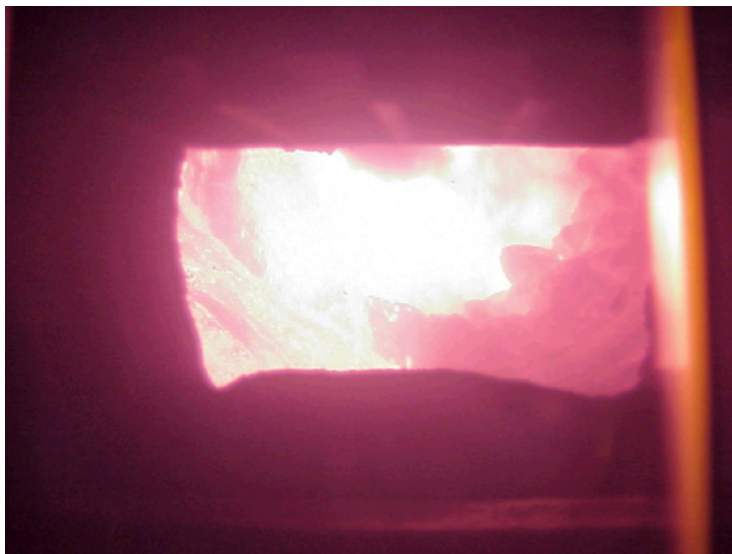


Figure 4.2.4.36: Interior view of an operational wet kiln (Copyright Halliburton Energy Services).

After the clinker leaves the kiln, it enters a cooler that uses pressurized air to cool the clinker. The energy absorbed by the air in the cooler serves to pre-heat the air for feed into the kiln. The cooled clinker is then taken to storage to await nal grinding with approximately ve percent gypsum by weight. After grinding to the specied fineness, the nal cement powder is pneumatically transferred to storage silos until it is shipped to the customer.

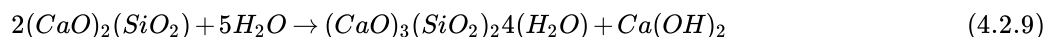
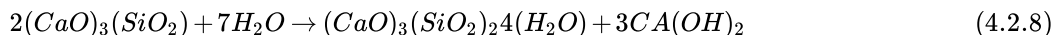
Quality control of the clinker and nal powder is handled via an automated X-ray diffraction/X-ray fluorescence (XRD/XRF) system, simple wet chemical analyses, simple optical microscopy, and periodic performance tests, including compressive strength and thickening time. This entire process results in the heterogeneous nanocomposite of calcium silicate and aluminate particles, among other materials, which make up a typical cement grain.

Hydration of Portland Cement

The addition of water to dry cement powder results in a thin cement slurry that can be easily manipulated and cast into different shapes. In time, the slurry sets and develops strength through a series of hydration reactions. Hydration of cement is not linear through time, it proceeds very slowly at first, allowing the thin mixture to be properly placed before hardening. The chemical reactions that cause the delay in hardening are not completely understood; however, they are critical to developing a rational methodology for the control of cement setting.

Tri- and di-calcium silicates

The tri- and di-calcium silicates (C_3S and C_2S , respectively) comprise over 80% by weight of most cement. It is known that C_3S is the most important phase in cement for strength development during the first month, while C_2S reacts much more slowly, and contributes to the long-term strength of the cement. Both the silicate phases react with water as shown below to form calcium hydroxide and a rigid calcium-silicate hydrate gel, CSH, (4.2.7) and (4.2.8).



The detailed structure of CSH is not completely known, however it is generally agreed upon that it consists of condensed silicate tetrahedrally sharing oxygen atoms with a central, calcium hydroxide-like CaO_2 layer. Calcium hydroxide consists of hexagonal layers of octahedrally coordinated calcium atoms and tetrahedrally coordinated oxygen atoms. Taylor has proposed that the structure is most similar to either Tobermorite or Jennite, both of which share a skeletal silicate chain Figure 4.2.437.

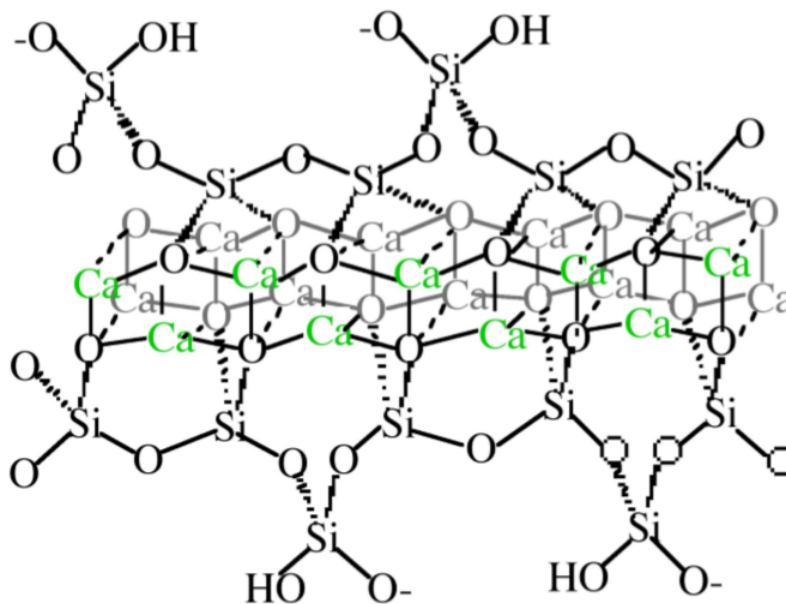


Figure 4.2.4.37: Schematic representation of Tobermorite, viewed along a polysilicate chain. Silicate ions either share oxygen atoms with a central CaO_2 core or bridge silicate tetrahedra. Interlayer calcium ions and water molecules are omitted for clarity.

Although the precise mechanism of C_3S hydration is unclear, the kinetics of hydration is well known. The hydration of the calcium silicates proceeds via four distinct phases as shown in Figure 4.2.438. The first 15-20 minutes, termed the pre-induction period (Figure 4.2.438a), is marked by rapid heat evolution. During this period calcium and hydroxyl ions are released into the solution. The next, and perhaps most important, phase is the induction period (Figure 4.2.438b), which is characterized by very slow reactivity. During this phase, calcium oxide continues to dissolve producing a pH near 12.5. The chemical reactions that cause the induction period are not precisely known; however, it is clear that some form of an activation barrier must be overcome before hydration can continue. It has been suggested that in pure C_3S , the induction period may be the length of time it takes for CSH to begin nucleation, which may be linked to the amount of time required for calcium ions to become supersaturated in solution. Alternatively, the induction period may be caused by the development of a small amount of an impermeable calcium-silicon-hydrate (CSH) gel at the surface of the particles, which slows down the migration of water to the inorganic oxides. The initial Ca/Si ratio at the surface of the particles is near 3. As calcium ions dissolve out of this CSH gel, the Ca/Si ratio in the gel becomes 0.8-

1.5. This change in Ca/Si ratio corresponds to a change in gel permeability, and may indicate an entirely new mechanism for CSH formation. As the initial CSH gel is transformed into the more permeable layer, hydration continues and the induction period gives way to the third phase of hydration, the acceleratory period (Figure 4.2.4.38c).

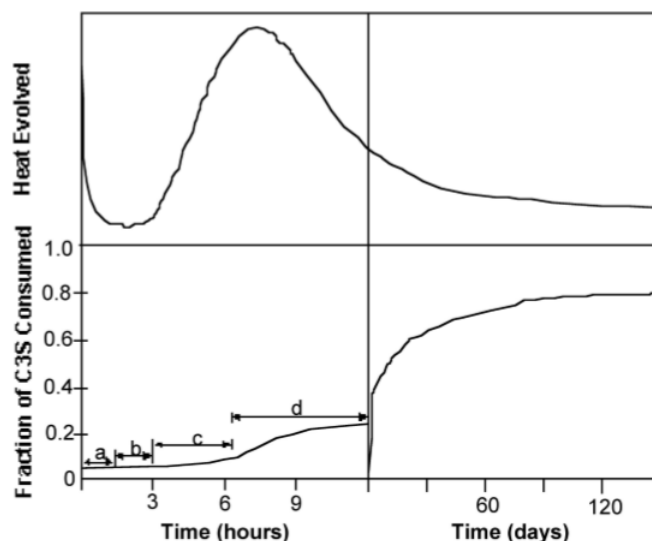
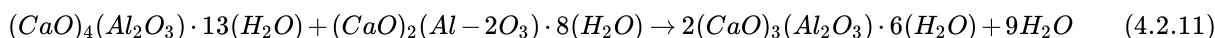
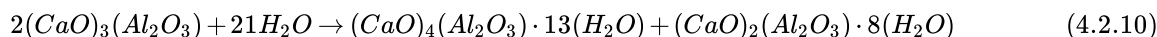


Figure 4.2.4.38: Hydration of C3S over time: (a) the preinduction period, (b) the induction, (c) period the acceleratory period, and (d) the deceleratory period.

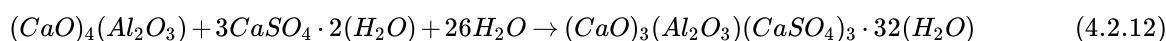
After ca. 3 hours of hydration, the rate of CSH formation increases with the amount of CSH formed. Solidification of the paste, called setting, occurs near the end of the third period. The fourth stage (Figure 4.2.4.38d) is the deceleratory period in which hydration slowly continues hardening the solid cement until the reaction is complete. The rate of hydration in this phase is determined either by the slow migration of water through CSH to the inner, unhydrated regions of the particles, or by the migration of H^+ through the CSH to the anhydrous CaO and SiO_2 , and the migration of Ca^{2+} and Si^{4+} to the OH^- ions left in solution.

Calcium aluminate and ferrite

In spite of the fact that the aluminate and ferrite phases comprise less than 20% of the bulk of cement, their reactions are very important in cement and dramatically affect the hydration of the calcium silicate phases, see below. Relative to C3S, the hydration of C3A is very fast. In the absence of any additives, C3A reacts with water to form two intermediate hexagonal phases, C2AH8 and C4AH13, (4.2.9). The structure of C2AH8 is not precisely known, but C4AH13 has a layered structure based on the calcium hydroxide structure, in which one out of every three Ca^{2+} is replaced by either an Al^{3+} or Fe^{3+} with an OH^- anion in the interlayer space to balance the charge. All of the aluminum in C4AH13 is octahedral. C2AH8 and C4AH13 are meta-stable phases that spontaneously transform into the fully hydrated, thermodynamically stable cubic phase, C3AH6, (4.2.10). In C3A, aluminum coordination is tetrahedral. The structure consists of rings of aluminum tetrahedrally linked through bridging oxygen atoms, which slightly distorts the aluminum environment. In C3AH6, aluminum exists as highly symmetrical, octahedral $Al(OH)_6$ units.



If the very rapid and exothermic hydration of C3A is allowed to proceed unhindered in cement, then the setting occurs too quickly and the cement does not develop strength. Therefore, gypsum [calcium sulfate dihydrate, $CaSO_4 \cdot 2(H_2O)$] is added to slow down the C3A hydration. In the presence of gypsum, tricalcium aluminate forms ettringite, $[Ca_3Al(OH)_6 \cdot 12(H_2O)]_2 \cdot (SO_4)_3 \cdot 2(H_2O)$, (4.2.11), which can also be written as $C_3A \cdot 3(CaSO_4) \cdot 32(H_2O)$. Ettringite grows as columns of calcium, aluminum and oxygen surrounded by water and sulfate ions, as shown in Figure 4.2.4.39.



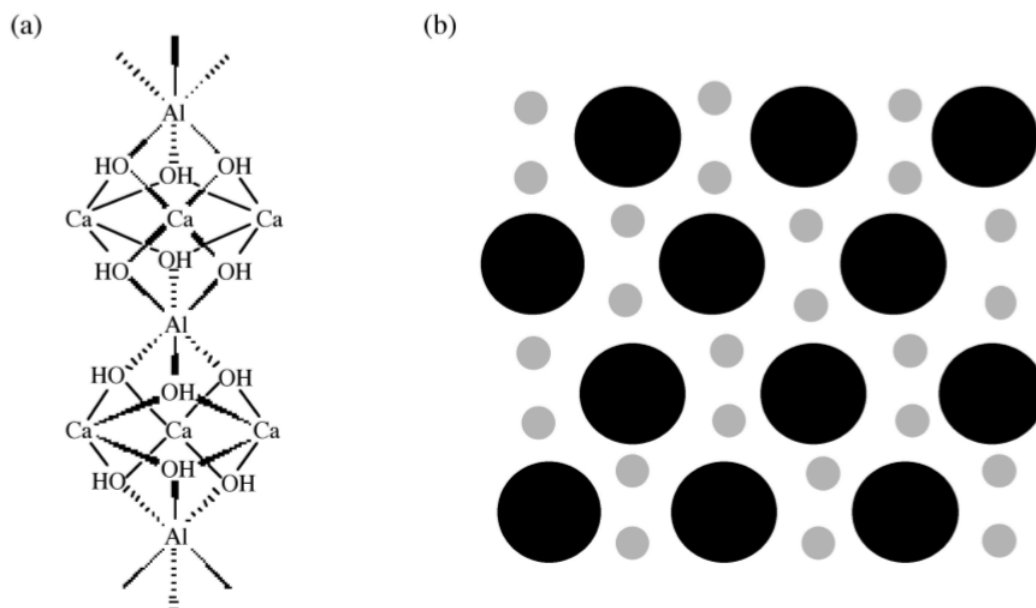


Figure 4.2.4.39: Ettringite columns (a) consisting of octahedral aluminum, tetrahedral oxygen, and 8-coordinate calcium. The coordination sphere of each calcium is filled by water and sulfate ions. The packing of the columns (b) represented by large circles, the smaller circles represent channels containing with water and sulfate ions.

Tetracalcium aluminoferrite (C4AF) reacts much like C3A, i.e., forming ettringite in the presence of gypsum. However, hydration the ferrite phase is much slower than hydration of C3A, and water is observed to bead up on the surface of C4AF particles. This may be due to the fact that iron is not as free to migrate in the pastes as aluminum, which may cause the formation of a less permeable iron rich layer at the surface of the C4AF particles and isolated regions of iron hydroxide. In cement, if there is insufficient gypsum to convert all of the C4AF to ettringite, then an iron-rich gel forms at the surface of the silicate particles which is proposed to slow down their hydration.

Portland Cement

The hydration of cement is obviously far more complex than the sum of the hydration reactions of the individual minerals. The typical depiction of a cement grain involves larger silicate particles surrounded by the much smaller C3A and C4AF particles. The setting (hydration) of cement can be broken down into several distinct periods. The more reactive aluminate and ferrite phases react first, and these reactions dramatically affect the hydration of the silicate phase. Scrivener and Pratt used TEM to develop the widely accepted model depicted in Figure 4.2.4.40.

In the first few minutes of hydration (Figure 4.2.4.40b), the aluminum and iron phases react with gypsum to form an amorphous gel at the surface of the cement grains and short rods of ettringite grow. After this initial period of reactivity, cement hydration slows down and the induction period begins. After about 3 hours of hydration, the induction period ends and the acceleratory period begins. During the period from 3 to 24 hours, about 30% of cement reacts to form calcium hydroxide and CSH. The development of CSH in this period occurs in 2 phases. After ca. 10 hours hydration (Figure 4.2.4.40c), C3S has produced outer CSH, which grows out from the ettringite rods rather than directly out from the surface of the C3S particles. Therefore, in the initial phase of the reaction, the silicate ions must migrate through the aluminum and iron rich phase to form the CSH. In the latter part of the acceleratory period, after 18 hours of hydration, C3A continues to react with gypsum, forming longer ettringite rods (Figure 4.2.4.40d). This network of ettringite and CSH appears to form a hydrating shell about 1 μm from the surface of anhydrous C3S. A small amount of inner CSH forms inside this shell. After 13 days of hydration, reactions slow down and the deceleratory period begins (Figure 4.2.4.40e). C3A reacts with ettringite to form some monosulfate. Inner CSH continues to grow near the C3S surface, narrowing the 1 μm gap between the hydrating shell and anhydrous C3S. The rate of hydration is likely to depend on the diffusion rate of water or ions to the anhydrous surface. After 2 weeks hydration (Figure 4.2.4.40f), the gap between the hydrating shell and the grain is completely filled with CSH. The original, outer CSH becomes more fibrous.

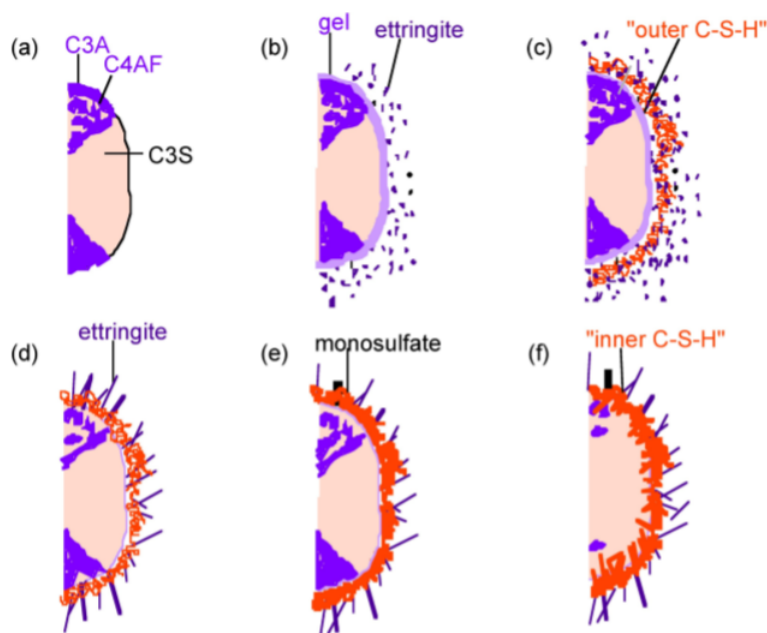


Figure 4.2.4.40: Schematic representation of anhydrous cement (a) and the effect of hydration after (b) 10 minutes, (c) 10 hours, (d) 18 hours, (e) 13 days, and (f) 2 weeks. Adapted from M. Bishop, PhD Thesis, Rice University, 2001

Bibliography

- H. F. W. Taylor, *Cement Chemistry*, 2nd Ed., Academic Press, London (1997).
- H. F. W. Taylor, *J. Am. Ceram. Soc.*, 1986, **69**, 464.
- V. S. Ramachandran, R.F. Feldman, and J. J. Beaudoin, *Concrete Science*, Heyden and Son Ltd., Philadelphia, PA, 1981.
- H. N. Stein and J. Stevels, *J. App. Chem.*, 1964, **14**, 338.
- M. Grutzeck, S. Kwan, J. Thompson, and A. Benesi, *J. Mater. Sci. Lett.*, 1999, **18**, 217.
- V. S. Ramachandran, *Concrete Admixtures Handbook, 2nd Edition*, Noyes Publications, New Jersey (1995).
- K. L. Scrivener and P. L. Pratt, *Mater. Res. Soc. Symp. Proc.*, 1984, **31**, 351.

Hydration Inhibition of Portland Cement

In the oil industry, Portland cement supports boreholes of ever increasing depth. This application requires a high degree of control over the setting kinetics to allow the cement to be pumped down in a liquid form. A number of chemical inhibitors are employed to delay the setting time. The ideal inhibitor for oil well cementing would predictably delay the setting of cement, and then suddenly allow hydration to continue at a rapid rate.

A wide range of compounds show set inhibition of the hydration of Portland cement. Some common examples include, sucrose, tartaric acid, gluconic acid δ -lactone, lignosulfonate, and organic phosphonic acids, in particular nitrilo-tris(methylene)phosphonic acid (H6ntmp). The structures of these retarders are shown in.

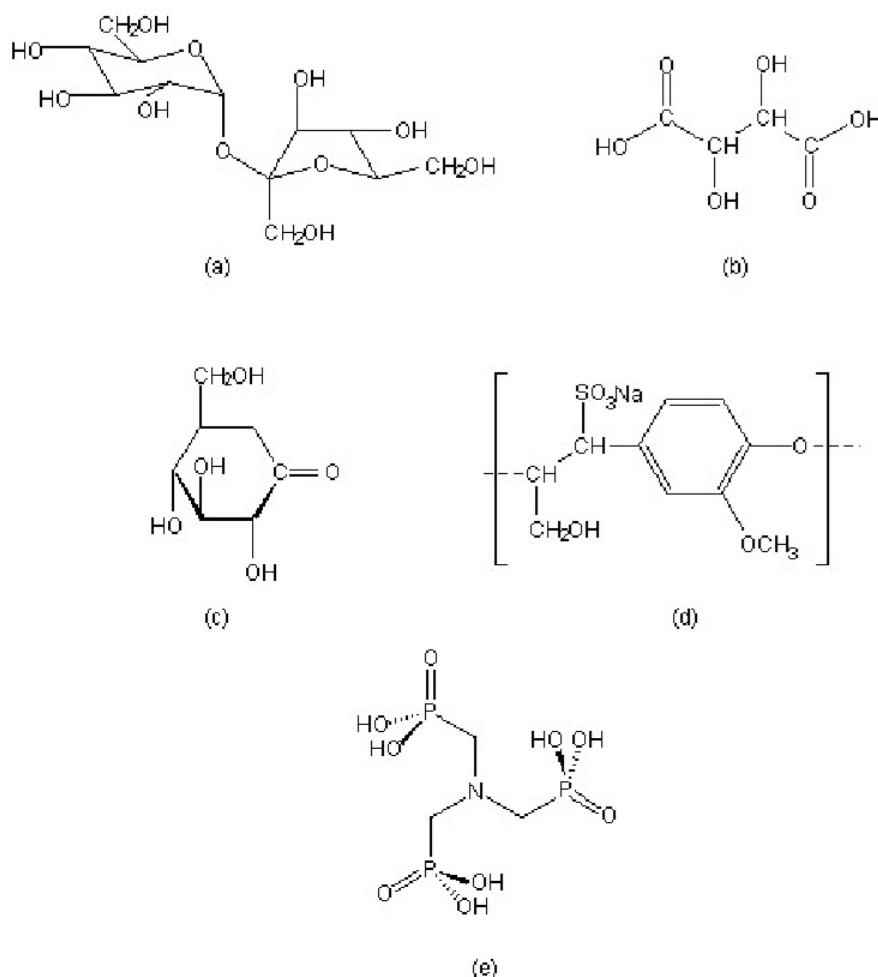


Figure 4.2.4.41: Structural formulae of common cement retarders. (a) sucrose, (b) tartaric acid, (c) gluconic acid d-lactone, (d) sodium lignosulfonate, and (e) nitrilo-tris(methylene)phosphonic acid (H₆ntmp).

In spite of the fact that the science of cement hydration inhibition has been investigated for over 40 years, the mechanistic details are still the subject of much speculation. There are ve primary models for cement hydration inhibition: calcium complexation, nucleation poisoning, surface adsorption, protective coating/osmotic bursting, and dissolution-precipitation. A summary of the characteristic behavior of selected retarders is shown in Table 4.2.4.7.

Table 4.2.4.7: Summary of the behavior of various hydration retarders.

Retarder	Characteristic behavior
sucrose	Ca binding, acts directly on silicates, accelerates ettringite formation
tartaric acid	acts via calcium complexation and calcium tartrate coating, inhibits ettringite formation
lignosulfonate	accelerates ettringite formation, calcium becomes incorporated into the polymer matrix during hydration, forms a diffusion barrier
nitrilo-tris(methylene)phosphonic acid (H ₆ ntmp)	promotes Ca dissolution, forms $[\text{Ca}(\text{H}_6\text{ntmp})]$, heterogeneous nucleation on aluminates creates a protective coating around the grain

Calcium complexation

Inhibition by calcium complexation relies largely on the requirement that small calcium oxide/hydroxide templates must form in the pore water of cement pastes before silicate tetrahedra can condense into dimeric and oligomeric silicates to form CSH. Calcium

complexation involves either removing calcium from solution by forming insoluble salts, or chelating calcium in solution. Calcium complexation lowers the amount of calcium effectively in solution, delaying the time to $\text{Ca}(\text{OH})_2$ super-saturation and preventing precipitation of the necessary templates. Simple calcium complexation should dramatically increase the amount of $\text{Si}(\text{OH})_4$ tetrahedra in solution, and indeed this is observed with most retarders. However, if the retarder were acting solely by calcium complexation, then one molecule of retarder would be required per calcium ion in solution, and good inhibitors are used in much smaller quantities, on the order of 0.1-2% by weight of cement. In addition, there is no simple correlation between either calcium binding strength or calcium salt solubility and retarding ability. Yet it has been shown that in pure systems, i.e., of C3S and C2S, that the lime concentration in solutions is the most important factor in determining the precipitation of CSH. Therefore, although calcium complexation must play some role in inhibition, other mechanisms of inhibition must be at work as well. An example of a retarder that operates primarily through calcium complexation is tartaric acid, however, the formation of insoluble calcium tartrate on cement grains suggest that dissolution/precipitation occurs in addition (Figure 4.2.4.42).

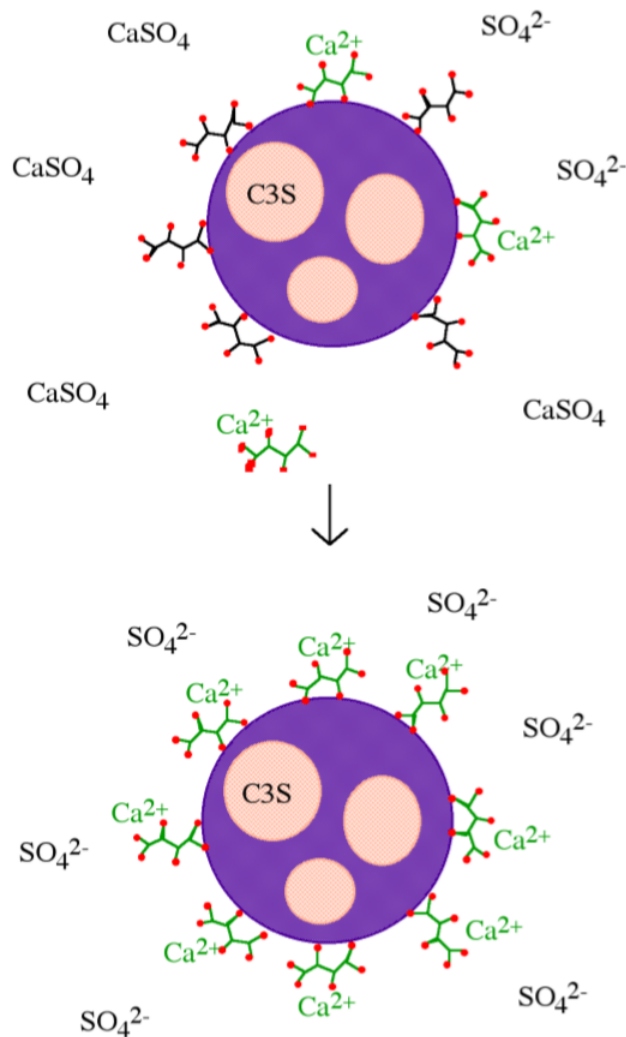


Figure 4.2.4.42: Schematic representation of cement hydration in the presence of tartaric acid. The aluminate (and aluminate ferrate) phases (shown in purple) surround the silicate phases (C3S and C2S). Tartaric acid adsorbs onto the aluminum surfaces and reacts with calcium ions from gypsum to deposit a thick calcium tartrate coating on the cement grain. Adapted from M. Bishop, PhD Thesis, Rice University, 2001.

Nucleation poisoning

As with calcium complexation, nucleation poisoning must rely on the formation of small calcium oxide/hydroxide templates in the pore water of cement pastes before silicate tetrahedra can condense into dimeric and oligomeric silicates to form CSH. Inhibition by nucleation poisoning is where the retarder blocks the growth of CSH or $\text{Ca}(\text{OH})_2$ crystals through inhibiting agglomerates of calcium ions from forming the necessary hexagonal pattern. Nucleation inhibitors act on the surface of small clusters, therefore, less than one molecule of retarder per calcium ion is required to produce dramatic results. This type of inhibition also results in an

increase in the amount of silicate ions in solution, as condensation of silicate chains onto calcium oxide templates to form the CSH is inhibited. As a retarder sucrose acts via nucleation poisoning/surface adsorption.

Surface adsorption

Surface adsorption of inhibitors directly onto the surface of either the anhydrous or (more likely) the partially hydrated mineral surfaces blocks future reactions with water. In addition, if such inhibitors are large and anionic, then they produce a negative charge at the surface of the cement grains, causing the grains to repel each other thereby reducing inter-particle interactions. Lignosulfonates are typical of retarders that act via surface adsorption.

Protective coating/osmotic bursting

The formation of a protective coating with its subsequent bursting due to the build up of osmotic pressure was originally posited to explain the existence of the induction period in C3S and cement hydration, however it may be applied to inhibition in general. In this mechanism, a semi-permeable layer at the surface of the cement grain forms and slows down the migration of water and lengthens the induction period. Osmosis will drive water through the semi-permeable membrane towards the unhydrated mineral, and eventually the flow of water creates higher pressure inside the protective coating and the layer bursts. Hydration is then allowed to continue at a normal rate.

Dissolution-precipitation

A detailed study of several retarders (in particular the organic phosphonates) has shown that they actually accelerate certain stages of the hydration process. This is unexpected since the phosphonates have been termed super retarders, due to their increased effect on cement hydration relative to the effect of conventional retarders. So how is it that a retarder can be so efficient at hydration inhibition at the same time as accelerating the process? The ability of phosphonates to retard cement setting is due to the lengthening the induction period, without slowing down the time it takes for setting to occur (once the acceleratory period has begun).

Phosphonates are known to complex calcium and other M^{2+} cations, poison the nucleation and growth of barium sulfate crystals, and inhibit the hydration of Fe_2O_3 and Al_2O_3 surfaces via direct surface adsorption, thus it was assumed that with regard to cement hydration inhibition occurred by one of these mechanisms. However, the mechanism by which phosphonates inhibit cement hydration consists of two steps. First dissolution, whereby calcium is extracted from the surface of the cement grains (Figure 4.2.4.43a) exposing the aluminum rich surface to enhanced (catalyzes) hydration and ettringite formation (Figure 4.2.4.43b). Second precipitation, whereby the soluble calcium-phosphonate oligomerizes either in solution or on the hydrate surface to form an insoluble polymeric Ca-phosphonate (Figure 4.2.4.43c). The Ca-phosphonate material binds to the surface of the cement grains inhibiting further hydration by acting as a diffusion barrier to water as well as a nucleation inhibitor.

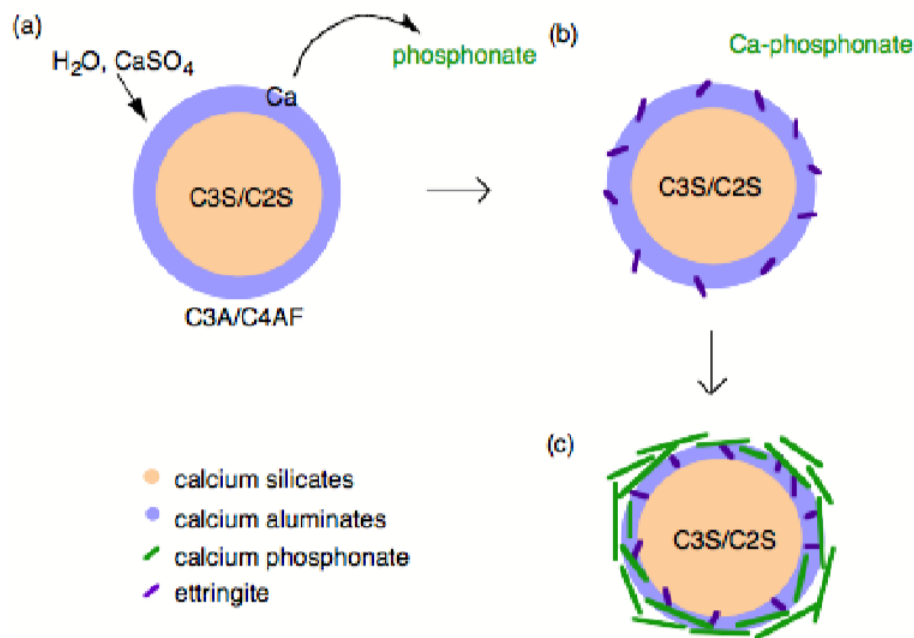


Figure 4.2.4.43: Schematic representation of the H6ntmp inhibition of cement showing (a) the phosphonic acid promoting calcium dissolution, allowing water and gypsum to react with the aluminum phases at the surface of the cement grain, (b) the formation of a meta-stable calcium phosphonate, which precipitates onto the hydrating aluminate surfaces (c), forming a barrier to water and sulfate diffusion. Adapted from M. Bishop, PhD Thesis, Rice University, 2001.

Bibliography

- N. Thomas and J. Birchall, *Cement and Concrete Research*, 1983, **13**, 830.
- D. Double, *Phil. Trans. R. Soc. London*, 1983, **A30**, 53.
- M. Bishop, S. G. Bott, and A. R. Barron, *Chem. Mater.*, 2003, **15**, 3074.
- M. Bishop and A. R. Barron, *Ind. Eng. Chem. Res.*, 2006, **45**, 7042.

This page titled [4.2: Calcium the Archetypal Alkaline Earth Metal](#) is shared under a [CC BY 3.0](#) license and was authored, remixed, and/or curated by [Andrew R. Barron \(CNX\)](#) via [source content](#) that was edited to the style and standards of the LibreTexts platform.

4.3: Differences for Beryllium and Magnesium

While the chemistry of strontium, barium (and radium) is similar to that of calcium, magnesium and beryllium show marked differences. In both cases these differences are due to the small size of the ions.

Beryllium

Beryllium can be thought of as being even more covalent than magnesium. The small size (ca. 0.3 Å) results in a very high charge density of Be^{2+} . In addition, the ionization energy for beryllium is a large positive value (1st ionization energy = 899.5 kJ/mol, 2nd ionization energy = 14,848.7 kJ/mol). Both of these factors means that the free ion does not exist. Instead, beryllium forms covalent compounds in a similar manner to its diagonal analog aluminum. Both beryllium and aluminum form covalent compounds or strongly solvated cations, and both form polymeric hydrides, chlorides, and alkyls.

Beryllium chloride is not a lattice structure with a concomitantly high melting and boiling point as observed for the other Group 2 metals (Table 4.8). Instead BeCl_2 is a polymer in the solid state (Figure 4.3.44a), and an equilibrium between a monomer (Figure 4.3.44b) and dimer (Figure 4.3.44c) in the vapor phase.

Table 4.3.4.8: Summary of structures for alkaline earth chlorides (MCl_2).

M	Structure
Be	Polymer (4-coordinate Be)
Mg	Cadmium chloride structure (6-coordinate Mg)
Ca	Deformed rutile structure (6-coordinate Ca)
Sr	Deformed rutile structure (6-coordinate Sr)
Ba	PbCl_2 structure (9-coordinate Ba) or fluorite structure (8-coordinate Ba)

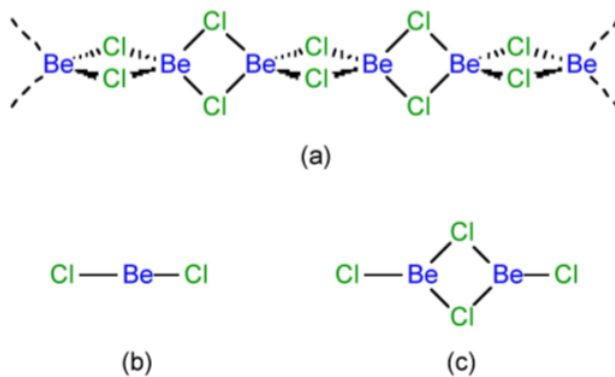


Figure 4.3.4.44: Structures of BeCl_2 .

Magnesium

The ionic radius for the +2 cation of magnesium is fairly small (0.65 Å). As a consequence the charge density (z/r) is high, which results in a high polarizing power of the Mg^{2+} ion. Thus, magnesium tends to form polar covalent bonds rather than ionic complexes. As with lithium there is a wide range of organometallic derivatives of magnesium, especially the Grignards (RMgX , where $\text{X} = \text{Cl}, \text{Br}$).

A further consequence of the covalent character of the bonding is that magnesium tends to form either 4-coordinate (tetrahedral) or 6-coordinate (octahedral) complexes with well-defined geometries.

This page titled 4.3: Differences for Beryllium and Magnesium is shared under a CC BY 3.0 license and was authored, remixed, and/or curated by Andrew R. Barron (CNX) via source content that was edited to the style and standards of the LibreTexts platform.

4.4: Organometallic Compounds of Magnesium

While beryllium makes a range of organometallic compounds, their hazardous nature has limited their study. In contrast, the ionic nature of calcium, strontium, and barium compounds limits the number of stable organometallic derivatives. However, the organometallic chemistry of magnesium is rich and extensive. The importance of Grignards (RMgX , where X = halide) and dialkyl magnesium compounds (R_2Mg) is due to their use in organic synthesis and as synthons for a range of organometallic compounds.

Grignard reagents

Grignard reagents (and the Grignard reaction using these compounds) are named after Victor Grignard (Figure 4.4.445). After studying mathematics at Lyon he transferred to chemistry, becoming a professor at the University of Nancy in 1910. During World War I, he was involved in the field of chemical warfare; however, it is for his major contribution to organic chemistry he is remembered.



Figure 4.4.445: French chemist and Nobel Prize winner François Auguste Victor Grignard (1871 1935).

Preparation

The general the synthesis of a Grignard reagent involves the reaction of an alkyl halide (RX , where X = Cl, Br, I) with magnesium metal in a suitable ether solvent, (4.4.1).



While diethyl ether (Et_2O) and tetrahydrofuran (THF) are commonly used as solvents, other polar nonprotic solvents are suitable, including: triethylamine (NEt_3), dimethylsulphide (Me_2S), dimethylselenide (Me_2Se), and dimethyltelluride (Me_2Te).

In general the alkyl halide is added to an excess of magnesium suspended in the solvent. In most cases it is necessary to activate the magnesium, by the addition of iodine (I_2), 1,2-dibromoethane, or sonication. If the halide is very inert reaction can be promoted by the co-condensation of magnesium and THF under vacuum.

There is often an induction period after the initial addition of alkyl halide. However, since the reaction, (4.4.1), is highly exothermic care should be taken to ensure that the reaction does not run-away. For this reason it is normal to initially add a small quantity of the alkyl halide to ensure the reaction initiates. Once reaction is initiated, the addition of alkyl halide is maintained at a suitable rate to ensure the reaction is maintained until all the alkyl halide is consumed. The excess reaction magnesium is removed from the reaction mixture by filtration.

It is not always necessary to use a liquid or solid halide dissolved in the solvent. Bubbling methyl chloride (MeCl) through an Et_2O suspension of magnesium yields MeMgCl . The advantage of a gaseous alkyl halide is that the reaction is very clean as all the magnesium is consumed and the excess alkyl halide is bubbled away.

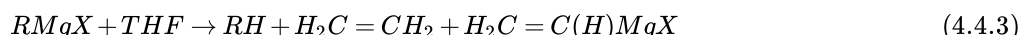
The purity of the magnesium is very important. For his original experiments Grignard used magnesium of a purity of 99.2%. However, it is now more typical to use 99.8% pure magnesium. It is important that the magnesium not be too pure since it is thought that the transition metal impurities catalyze the reaction.

The relative order of reactivity of the alkyl halide follows the trend:



In fact alkyl uorides are suciently inert that highly coordinating polar solvents such as THF or dimethylformamide (DMF) must be used.

If the reaction is allowed to get too hot then several possible side reactions can occur. In THF reaction with the solvent occurs:



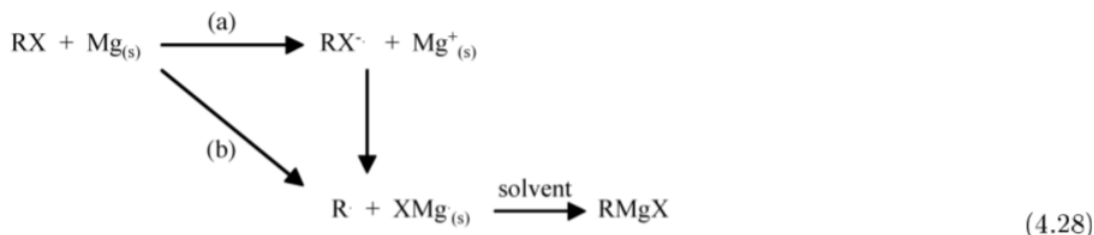
Alternatively, a transition metal catalyzed radical coupling between the Grignard and unreacted alkyl halide is observed irrespective of the identity of the solvent, (4.4.4).



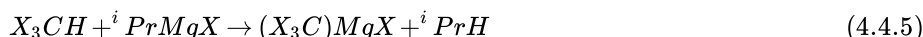
The mechanism for Grignard formation is thought to be radical in nature; however, a study of the surface of the magnesium during the reaction has shown the presence of corrosion pits. It is generally agreed that initiation occurs at surface dislocations, but the major reaction occurs at a polished surface.

The kinetics of the reaction is 1st order with respect to the alkyl halide concentration, but it has also been claimed to be 1st order with respect to the solvent concentration. It has therefore been concluded that the rate-determining step involves the metal solvent interface.

The reaction of magnesium with aryl bromides has been studied and is proposed to occur by two reactions. The first involves electron transfer between the aryl halide and the metal, while the second involves aryl radical formation.



A number of alternative synthetic routes are used with polyhalogenated hydrocarbons, (4.4.5) and (4.4.6), and where the alkyl radical is unstable, (4.4.7).



Structure

The solid state structure of Grignard reagents is controlled by the presence and identity of the solvent used in the synthesis. In this regard the size and the basicity of the solvent is important. For example, the structure of EtMgBr crystallized from diethyl ether exists as a 4-coordinate monomer (Figure 4.4.446a), while the use of the sterically less demanding THF results in a 5-coordinate monomeric structure (Figure 4.4.446b). In contrast, the use of triethylamine yields a dimeric bromide bridged structure (Figure 4.4.446c), and the use of a chelate bidentate amine gives a structure (Figure 4.4.446d) similar to that observed with diethyl ether (Figure 4.4.446a).

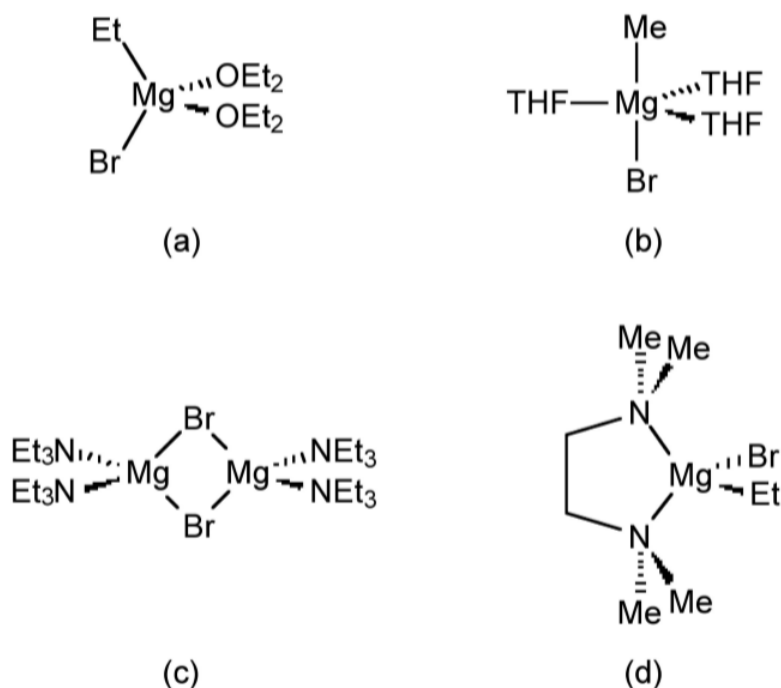


Figure 4.4.4.46: Molecular structure of EtMgBr in (a) diethyl ether, (b) THF, (c) triethyl amine, and (d) tetramethylethylenediamine (TMED).

In solution, Grignards are fluxional such that no single defined structure is present. The series of exchange reactions are known as an extended Schlenk equilibrium (Figure 4.4.4.47).

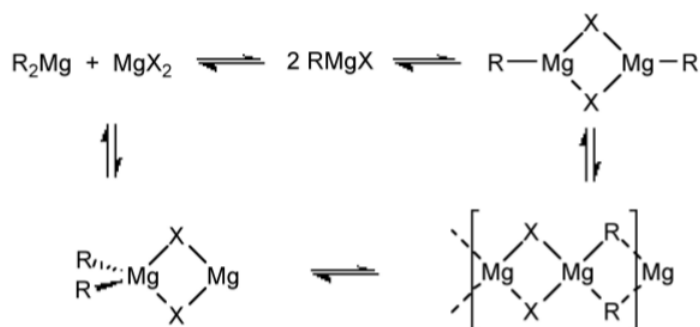


Figure 4.4.4.47: Schematic representation of the extended Schlenk equilibrium observed for Grignard compounds in solution.

It is observed that Grignard solutions are also slightly conducting, and magnesium is deposited at both the anode and cathode suggesting the formation of RMg^+ and $[RMgX_2]^-$. The alkyl/halide exchange is thought to occur through a bridging intermediate (Figure 4.4.4.48).

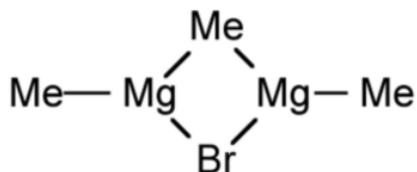


Figure 4.4.4.48: Proposed structure for the alkyl/halide exchange bridging intermediate.

Dialkyl magnesium (R_2Mg)

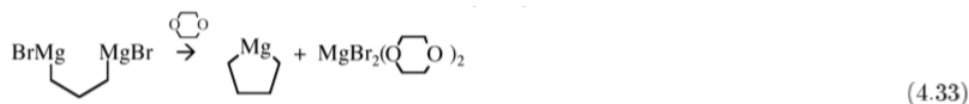
Dialkyl magnesium compounds are involatile white solids. They generally have similar reactivity to their Grignard analogs.

Synthesis

The most common synthesis of R_2Mg is by the reaction of a Grignard with dioxane ($C_4H_8O_2$), (4.32), where the precipitation of the dihalide is the reaction driving force.



This method is useful for the synthesis of cyclic compounds, (4.33).



An alternative synthesis that does not require dioxane involves the metal exchange reaction between magnesium metal and a dialkyl mercury compound.



Finally, in selected cases, magnesium will react with acidic hydrocarbons such as cyclopentadienyl at high temperatures (600 °C).

Structure

In the vapor phase dialkyl magnesium compounds are generally monomeric linear compounds. In solution, in the absence of coordinating solvents R_2Mg form a variety of oligomers (Figure 4.4.49a-c) in solution as determined by molecular weight measurements. In the presence of coordinating solvents 4-coordinate monomers predominate (Figure 4.4.49d).

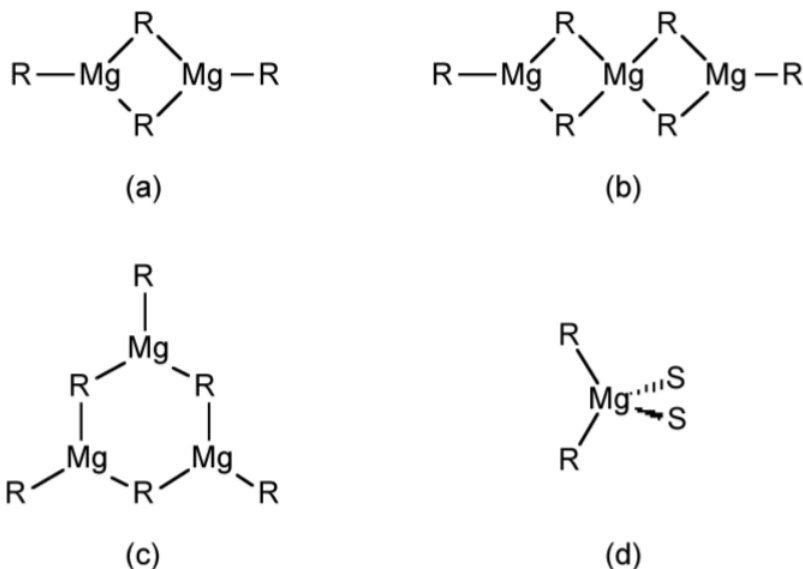


Figure 4.4.4.49: Solution structure of R_2Mg ($R = \text{Me}, \text{Et}$) in (a c) non-coordinating solvents, and (d) diethyl ether.

As similar trend is observed in the solid state, where polymers have been characterized in the absence of coordinating solvents (Figure 4.4.4.50a), while monomers or dimmers are generally observed when crystallized from a coordinating solvent (Figure 4.4.4.50b and c).

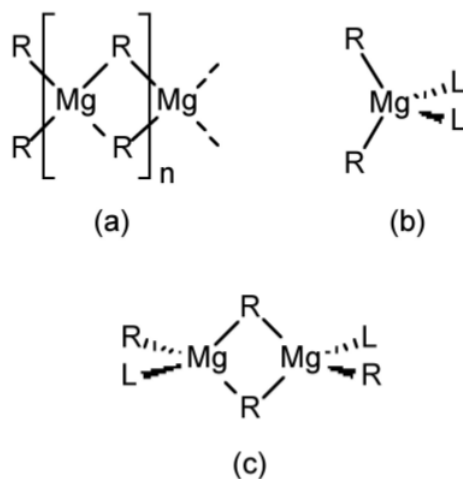
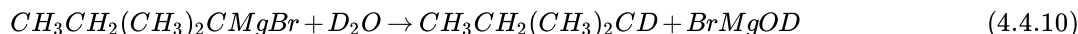


Figure 4.4.4.50: Solid state structure of R_2Mg ($R = Me, Et$) crystallized in (a) the absence and (b and c) the presence of a coordinating solvents.

The use of organomagnesium compounds in organic synthesis

Hydrolysis and related reactions

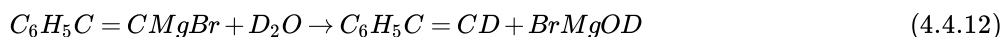
Grignard compounds react with water to give the hydrocarbon, (4.4.9), they also react with other hydroxylic compounds such as alcohols and carboxylic acids. One important use of the hydrolysis reaction is specifically deuteration, (4.4.10).



The hydrogen atom on a terminal alkyne is sufficiently acidic that the reaction with Grignards occurs in an analogous manner to that of hydrolysis.

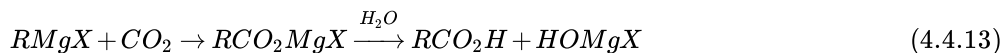


Once formed the alkynyl Grignard undergoes the same hydrolysis reaction.



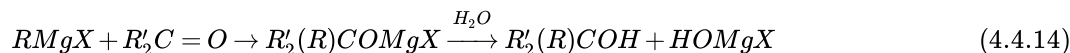
Reaction with CO_2

Grignards react readily with carbon dioxide to form the carboxylate, which yields the associated carboxylic acid upon hydrolysis, (4.4.13).

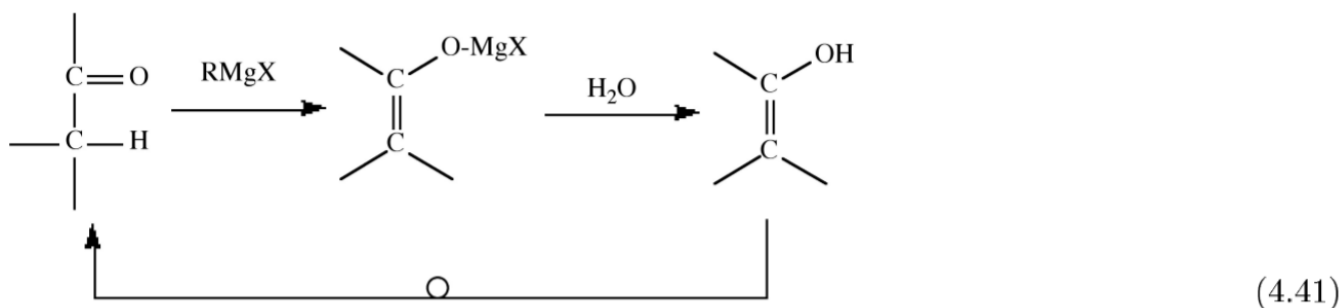


Reaction with carbonyls

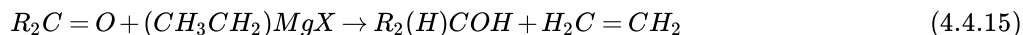
Organomagnesium compounds react with organic carbonyls (aldehydes, ketones, and esters) to yield the alcohol on hydrolysis, (4.4.14). This synthetic route is useful for the formation of primary, secondary and terminal alcohols.



Unfortunately, for some carbonyls there is a competing side reaction of enolization, where the starting ketone is reformed upon hydrolysis.



When the Grignard reagent has a β -hydrogen another side reaction occurs in which the carbonyl group is reduced and an alkene is formed.



Both the enolization and reduction occur via similar 6-membered cyclic transition states (Figure 4.4.4.51).

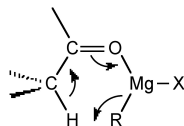
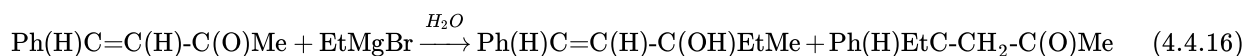


Figure 4.4.4.51: Representation of the 6-membered transition state reaction for enolization of a ketone.

Grignards react with α,β -unsaturated ketones to give either the 1,2-addition product or the 1,4-addition product, or both.



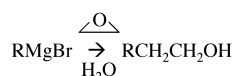
Reaction with acyl halides

Acyl halides react with Grignards to give ketones (4.4.16). Best results are obtained if the reaction is carried out at low temperature and in the presence of a Lewis acid catalysts (e.g., FeCl_3).



Reaction with epoxides

Oxirane (epoxide) rings are opened by Grignards in a useful reaction that extends the carbon chain of the Grignard by two carbon atoms. This reaction is best performed with ethylene oxide since the magnesium halide formed is a Lewis acid catalyst for further reactions in the case of substituted oxiranes.

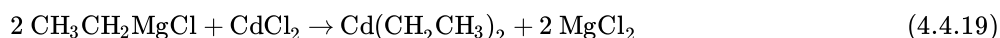


Reaction with salts

One of the most useful methods of preparing organometallic compounds is the exchange reaction of one organometallic compound with a salt of a different metal, Equation. This is an equilibrium process, whose equilibrium constant is defined by the reduction potential of both metals. In general the reaction will proceed so that the more electropositive metal will form the more ionic salt (usually chloride).



Grignard reagents are particularly useful in this regard, and may be used to prepare a wide range of organometallic compounds. For example:



The reaction with a Grignard is milder than the analogous reaction with lithium reagents, and leads to a lower incident of side-products.

Bibliography

- H. Bader and N. M. Smyth, *J. Org. Chem.*, 1964, **29**, 953.
- C. L. Hill, J. B. Vander Sande, G. M. Whitesides, *J. Org. Chem.*, 1980, **45**, 1020.
- E. Weiss, *J. Organomet. Chem.*, 1964, **2**, 314.
- A. R. Barron, *J. Chem. Soc., Dalton Trans.*, 1989, 1625.

This page titled [4.4: Organometallic Compounds of Magnesium](#) is shared under a [CC BY 3.0](#) license and was authored, remixed, and/or curated by [Andrew R. Barron \(CNX\)](#) via [source content](#) that was edited to the style and standards of the LibreTexts platform.

CHAPTER OVERVIEW

5: Group 12

[5.1: The Group 12 Elements](#)

[5.2: Cadmium Chalcogenide Nanoparticles](#)

[5.3: Organometallic Chemistry of Zinc](#)

[5.4: Organomercury Compounds](#)

[5.5: The Myth, Reality, and History of Mercury Toxicity](#)

This page titled [5: Group 12](#) is shared under a [CC BY 3.0](#) license and was authored, remixed, and/or curated by [Andrew R. Barron \(CNX\)](#) via [source content](#) that was edited to the style and standards of the LibreTexts platform.

5.1: The Group 12 Elements

Although the Group 12 metals (Table 5.1.1) are formally part of the d-block elements from their position in the Periodic Table, their electronic configuration in both their elemental form ($d^{10}s^2$) and the vast majority of their compounds (d^{10}) is that of the main group elements. The common oxidation state for all the Group 12 elements is +2, and the chemistry of zinc and cadmium compounds in particular is very similar to the analogous magnesium derivatives.

Note

The IUPAC (International Union of Pure and Applied Chemistry) definition of a transition metal (or transition element) states that a transition metal is "an element whose atom has an incomplete d sub-shell, or which can give rise to cations with an incomplete d sub-shell." Thus, Group 12 elements are not transition metals.

Element	Symbol	Name
Zinc	Zn	From German <i>zinke</i> , meaning <i>tooth-like</i> , <i>pointed</i> or <i>jagged</i> (metallic zinc crystals have a needle-like appearance), or meaning <i>tin-like</i> because of its relation to German word <i>zinn</i> meaning <i>tin</i> , or from Persian <i>seng</i> meaning <i>stone</i> .
Cadmium	Cd	From the Latin <i>cadmia</i> , meaning <i>calamine</i>
Mercury	Hg	From the Latin <i>hydrargyrum</i> , meaning <i>watery</i> or <i>liquid silver</i>

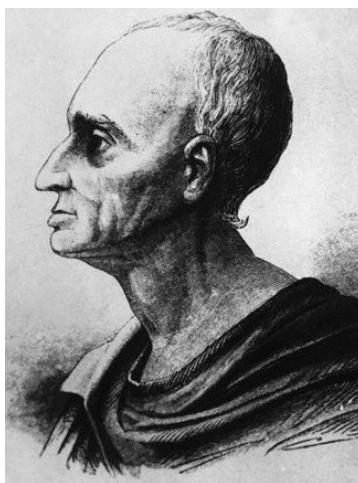
Table 5.1.1: Derivation of the names of the Group 12 metals.

Discovery

Zinc

Artifacts with a high zinc content (as much as 90%) have been found to be over 2500 years old, and possibly older. As such it is clear that several cultures had the knowledge of working with zinc alloys, in particular brass (a zinc/copper alloy). Zinc mines at Zawar, near Udaipur in India, have been active since the late 1st millennium BC. However, the smelting of metallic zinc appears to have begun around the 12th century AD.

The isolation of purified metallic zinc was reported concurrently by several people. The extraction of zinc from its oxide (ZnO) was reported as early as 1668, while John Lane is supposed to have smelted zinc in 1726. The first Patent for zinc smelting was granted to English metallurgist William Champion in 1738; however, the credit for discovering pure metallic zinc is often given to Andreas Marggraf in 1746.



Engraving of German chemist Andreas Sigismund Marggraf (1709–1782).

Cadmium

Cadmium was discovered in 1817 by Friedrich Stromeyer as an impurity in calamine (zinc carbonate, ZnCO_3). Stromeyer observed that impure samples of calamine changed color when heated but pure calamine did not. Eventually he was able to isolate cadmium metal by roasting and reduction of the sulfide.



German chemist Friedrich Stromeyer (1776 - 1835).

Mercury

Mercury was known to the ancient Chinese and was found in Egyptian tombs that date from 1500 BC. In China and Tibet, mercury use was thought to prolong life, heal fractures, and maintain generally good health. The ancient Greeks used mercury in ointments; the ancient Egyptians and the Romans used it in cosmetics that sometimes deformed the face.

Abundance

The Group 12 elements mainly occur in sulfide ores, however, as with their Group 2 analogs, carbonate are known, but not as economically viable. The major zinc containing ore is zinc blende (also known as sphalerite), which is zinc sulfide (ZnS). Other important ores include, wurtzite (ZnS), smithsonite (zinc carbonate, ZnCO_3), and hemimorphite (calamine, Zn_2SiO_4). The basic form of zinc carbonate (hydrozincite, $\text{Zn}_5(\text{CO}_3)_2(\text{OH})_6$) is also mined where economically viable. The main source of cadmium is as an impurity in zinc blende; however, there are several other ores known, e.g., cadmoselite (cadmium selenide, CdSe) and otavite (CdCO_3). Mercury sulfide (cinnabar, HgS) is the major source of mercury, and in fact metallic liquid mercury droplets are often found in the ore. The terrestrial abundance of the Group 12 elements is given in Table 5.1.2.

Element	Terrestrial abundance (ppm)
Zn	75 (Earth's crust), 64 (soil), 30×10^{-6} (sea water)
Cd	0.1 (Earth's crust), 1 (soil), 1×10^{-6} (sea water)
Hg	50×10^{-6} (Earth's crust), 2×10^{-8} (soil), 40×10^{-12} (sea water)

Table 5.1.2: Abundance of Group 12 elements.

Isotopes

The naturally abundant isotopes of the Group 12 metals are listed in Table 5.1.3.

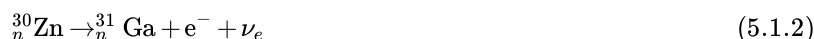
Isotope	Natural abundance (%)
Zinc-64	48.6
Zinc-66	27.9
Zinc-67	4.1
Zinc-68	18.8
Zinc-70	0.6
Cadmium-106 *	1.25
Cadmium-108 *	0.89
Cadmium-110	12.49
Cadmium-111	12.8
Cadmium-112	24.13
Cadmium-113 *	12.22
Cadmium-114 *	28.73
Cadmium-116 *	7.49
Mercury-196	0.15
Mercury-198	9.97
Mercury-199	16.87
Mercury-200	23.1
Mercury-201	13.18
Mercury-202	29.86
Mercury-204	6.87

Table 5.1.3: Abundance of the major (non-synthetic) isotopes of the Group 12 metals. Isotopes labeled with * are radioactive.

Many radioisotopes of zinc have been characterized. Zinc-65 that has a half-life of 244 days, is the most long-lived isotope, followed by ^{72}Zn with a half-life of 46.5 hours. The most common decay mode of an isotope of zinc with a mass number lower than 64 is electron capture, producing an isotope of copper, (Equation 5.1.1).



The most common decay mode of an isotope of zinc with mass number higher than 64 is beta decay (β^{-}), which produces an isotope of gallium, (Equation 5.1.2).



Naturally occurring cadmium is composed of 8 isotopes. For two of them, natural radioactivity was observed, and three others are predicted to be radioactive but their decay is not observed, due to extremely long half-life times. The two natural radioactive isotopes are ${}^{113}\text{Cd}$ (half-life = 7.7×10^{15} years) and ${}^{116}\text{Cd}$ (half-life = 2.9×10^{19} years).

There are seven stable isotopes of mercury with the longest-lived radioisotopes being ${}^{194}\text{Hg}$ (half-life = 444 years) and ${}^{203}\text{Hg}$ (half-life = 47 days). ${}^{199}\text{Hg}$ and ${}^{201}\text{Hg}$ are the most often studied NMR-active nuclei, having spins of $1/2$ and $3/2$ respectively.

Properties

A summary of the physical properties of the Group 12 metals is given in Table 5.1.4. Because of the ns electron in the Group 12 metals are tightly bound, and hence relatively unavailable for metallic bonding, the metals are volatile with low boiling points, as compared to the Group 2 metals.

Element	Mp (°C)	Bp (°C)	Density (g/cm ³)
Zn	419.53	907	7.14
Cd	321.07	767	8.65
Hg	-38.83	356.73	13.534 (liquid)

Table 5.1.4: Selected physical properties of the Group 12 metals.

The most notable anomaly in the Group 12 metals is the low melting point of mercury compared to zinc and cadmium. In order to completely understand the reasons for mercury's low melting point quantum physics is required; however, the key point is that mercury has a unique electronic configuration, i.e., $[\text{Xe}] 5d 6s$. The stability of the 6s shell is due to the presence of a filled 4f shell, because an f shell poorly screens the nuclear charge that increases the attractive coulomb interaction of the 6s shell and the nucleus. Such a configuration strongly resists removal of an electron and as such mercury behaves similarly to noble gas elements, which form weakly bonded and thus easily melting solids.



Liquid mercury.

Industrial production

The vast majority (95%) of zinc is mined from the zinc sulfide ores. The zinc is most often mixed with copper, lead, and iron. Zinc metal is produced by extraction, in which the ore is ground and then the minerals are separated from the gangue (commercially worthless mineral matter) by froth flotation (a process for selectively separating hydrophobic materials from hydrophilic). Roasting converts the zinc sulfide concentrate produced to zinc oxide (Equation 5.1.3). Reduction of the zinc oxide with carbon (5.1.4) or carbon monoxide (5.1.5) at 950 °C into the metal is followed by distillation of the metal. Since cadmium is a common impurity in zinc ores, it is most often isolated during the production of zinc. Cadmium is isolated from the zinc metal by vacuum distillation if the zinc is smelted, or cadmium sulfate is precipitated out of the electrolysis solution.



Mercury is extracted by heating cinnabar (HgS) in a current of air, [Equation](#), and condensing the vapor.



This page titled [5.1: The Group 12 Elements](#) is shared under a [CC BY 3.0](#) license and was authored, remixed, and/or curated by [Andrew R. Barron \(CNX\)](#) via [source content](#) that was edited to the style and standards of the LibreTexts platform.

5.2: Cadmium Chalcogenide Nanoparticles

The most studied non-oxide semiconductors are cadmium chalcogenides (CdE, with E = sulfide, selenide and telluride). CdE nanocrystals were probably the first material used to demonstrate quantum size effects corresponding to a change in the electronic structure with size, i.e., the increase of the band gap energy with the decrease in size of particles. These semiconductors nanocrystals are commonly synthesized by thermal decomposition of an organometallic precursor dissolved in an anhydrous solvent containing the source of chalcogenide and a stabilizing material (polymer or capping ligand). Stabilizing molecules bound to the surface of particles control their growth and prevent particle aggregation.

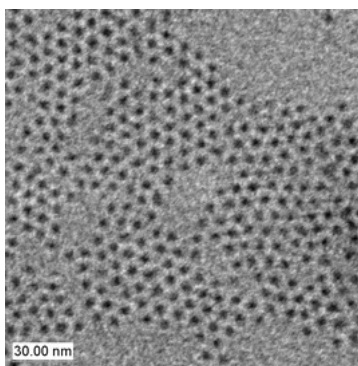


Picture of cadmium selenide (CdSe) quantum dots, dissolved in toluene, fluorescing brightly, as they are exposed to an ultraviolet lamp, in three noticeable different colors (blue ~481 nm, green ~520 nm, and orange ~612 nm) due to the quantum dots' bandgap (and thus the wavelength of emitted light) depends strongly on the particle size; the smaller the dot, the shorter the emitted wavelength of light. The "blue" quantum dots have the smallest particle size, the "green" dots are slightly larger, and the "orange" dots are the largest.

Although cadmium chalcogenides are the most studied semiconducting nanoparticles, the methodology for the formation of semiconducting nanoparticles was first demonstrated independently for InP and GaAs, e.g. Equation 5.1.1. This method has been adapted for a range of semiconductor nanoparticles.



In the case of CdE, dimethylcadmium $\text{Cd}(\text{CH}_3)_2$ is used as a cadmium source and bis(trimethylsilyl)sulfide, $(\text{Me}_3\text{Si})_2\text{S}$, trioctylphosphine selenide or telluride (TOPSe, TOPTe) serve as sources of selenide in trioctylphosphine oxide (TOPO) used as solvent and capping molecule. The mixture is heated at 230-260 °C over a few hours while modulating the temperature in response to changes in the size distribution as estimated from the absorption spectra of aliquots removed at regular intervals. These particles, capped with TOP/TOPO molecules, are non-aggregated and easily dispersible in organic solvents forming optically clear dispersions. When similar syntheses are performed in the presence of surfactant, strongly anisotropic nanoparticles are obtained, e.g., rod-shaped CdSe nanoparticles can be obtained.



TEM image of CdSe nanoparticles.

Because $\text{Cd}(\text{CH}_3)_2$ is extremely toxic, pyrophoric and explosive at elevated temperature, other Cd sources have been used. CdO appears to be an interesting precursor. CdO powder dissolves in TOPO and HPA or TDPA (tetradecylphosphonic acid) at about 300 °C giving a colorless homogeneous solution. By introducing selenium or tellurium dissolved in TOP, nanocrystals grow to the desired size.

Nanorods of CdSe or CdTe can also be produced by using a greater initial concentration of cadmium as compared to reactions for nanoparticles. This approach has been successfully applied for synthesis of numerous other metal chalcogenides including ZnS, ZnSe, and $\text{Zn}_{1-x}\text{Cd}_x\text{S}$. Similar procedures enable the formation of MnS, PdS, NiS, Cu_2S nanoparticles, nano rods, and nano disks.

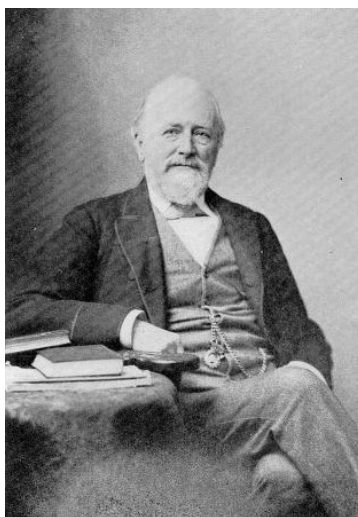
Bibliography

- C. R. Berry, *Phys. Rev.*, 1967, **161**, 848.
- M. D. Healy, P. E. Laibinis, P. D. Stupik, and A. R. Barron, *J. Chem. Soc., Chem. Commun.*, 1989, 359.
- L. Manna, E. C. Scher, and A. P. Alivisatos, *J. Am. Chem. Soc.*, 2000, **122**, 12700.
- C. B. Murray, D. J. Norris, and M. G. Bawendi, *J. Am. Chem. Soc.*, 1993, **115**, 8706.
- Z. A. Peng and X. Peng, *J. Am. Chem. Soc.*, 2002, **12**, 3343.
- R. L. Wells, C. G. Pitt, A. T. McPhail, A. P. Purdy, S. R. B. Shafieezad, and Hallock *Chem. Mater.*, 1989, **1**, 4.
- X. Zong, Y. Feng, W. Knoll, and H. Man, *J. Am. Chem. Soc.*, 2003, **125**, 13559.

This page titled [5.2: Cadmium Chalcogenide Nanoparticles](#) is shared under a [CC BY 3.0](#) license and was authored, remixed, and/or curated by [Andrew R. Barron \(CNX\)](#) via [source content](#) that was edited to the style and standards of the LibreTexts platform.

5.3: Organometallic Chemistry of Zinc

The first dialkyl zinc derivatives, Me_2Zn and Et_2Zn , were prepared in 1848 by Edward Franklin. He also prepared the monoalkyl derivatives, RZnX .



British chemist Sir Edward Franklin FRS (1825–1899).

Initially alkyl zinc compounds were used in organic synthesis, however, their use diminished significantly once Grignard reagents had been discovered. Little further was investigated of their chemistry until their use in the growth of electronic materials developed in the 1980's.

RZnX

The monoalkyl derivatives are not widely used, but were historically the first to be prepared (Equation 5.3.1).



While the iodide derivatives can be isolated as unsolvated derivatives, the chloride and bromides need to be prepared in the presence of dimethylformamide (DMF) or dimethyl sulfoxide (DMSO). Alternative methods of synthesis involve the reaction with a Grignard reagent, (Equation 5.3.2), or electrochemical synthesis with a zinc electrode.



In the solid state RZnI exists as cage oligomers or polymeric chain structures. These structures are broken by the addition of strong Lewis bases to form Lewis acid-base complexes. In solution there exists a Schlenk equilibrium (equation 5.3.3) whose presence has been determined by IR and Raman spectroscopy (Table 5.3.1).

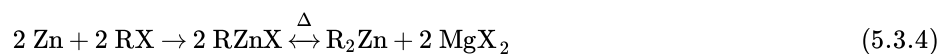


Stretch	IR (cm^{-1})	Raman (cm^{-1})
symmetric C-Zn-C	Not observed	477
asymmetric C-Zn-C	551	Not observed
C-Zn-I	510	510

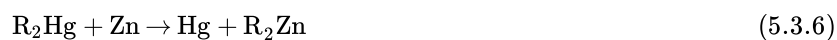
Table 5.3.1: IR and Raman spectroscopic characterization of the components of the Schlenk equilibrium,

R_2Zn

Dialkyl zinc compounds are prepared via the monoalkyl derivatives (Equation 5.3.4). The Schlenk equilibrium is shifted at high temperatures by the distillation of the volatile R_2Zn derivative. The zinc is usually alloyed with copper (10%) to improve the reaction rate.



Alternative preparation methods include the reaction of ZnX_2 with a Grignard (Equation 5.3.5) or by metal-metal exchange (Equation 5.3.6).



Bibliography

- E. von Frankland. *Justus Liebigs Ann. Chem.*, 1849, **71**, 171.
- J. J. Habeeb, A. Osman, and D. G. Tuck. *J. Organomet. Chem.*, 1980, **185**, 117

This page titled [5.3: Organometallic Chemistry of Zinc](#) is shared under a [CC BY 3.0](#) license and was authored, remixed, and/or curated by [Andrew R. Barron \(CNX\)](#) via [source content](#) that was edited to the style and standards of the LibreTexts platform.

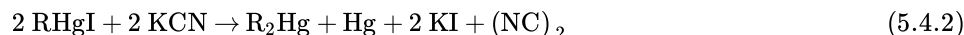
5.4: Organomercury Compounds

Synthesis

The most common routes to organomercury compounds involve the direct reaction of mercury with an alkyl iodide (Equation 5.4.1) to form the mercury analog of a Grignard reagent.

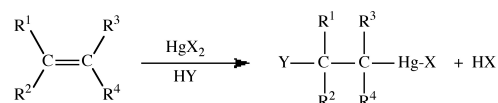


The subsequent reaction of RHgI with potassium cyanide yields the appropriate dialkyl mercury derivative (Equation 5.4.2).

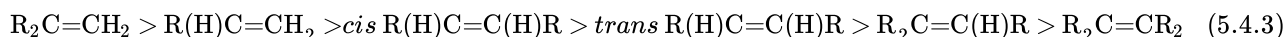


Solvomercuration

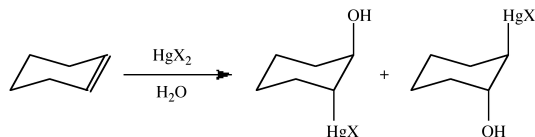
The general process of solvomercuration involves the addition of HgX_2 across an alkene double (or alkyne triple) bond in the presence of a solvent. Solvomercuration applies where HY , from Equation 5.4.3, are part of the solvent system, e.g., in water the process can be described as hydroxymercuration.



The addition to the alkene occurs with Markovnikoff addition, i.e., through the formation of the most stable carbonium ion resulting with the mercury adding to the less substituted carbon. The Hg-C bond can be cleaved by the addition of NaBH_4 to yield the C-H bond. It is common to employ mercury acetate, $\text{Hg}(\text{OAc})_2$ ($\text{OAc} = \text{O}_2\text{CCH}_3$), with subsequent reaction with NaCl or NaI to form the halide, rather than the mercury halide directly. However, the acetate can also act as a nucleophile resulting in a mixture of products. The order of reactivity for alkenes follows the trend:



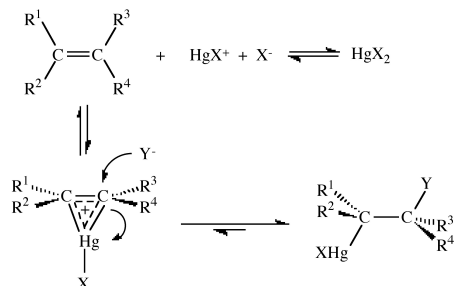
This is due to a combination of steric and electronic effects. The addition occurs in a *trans/anti* fashion.



Mercury(II) halides dissociate in polar solvents (Equation 5.4.4) and this species is commonly associated with the initial reaction step.



The mechanism of solvomercuration is best described by the reaction shown in.

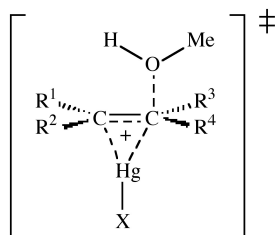


Mechanism of solvomercuration.

Evidence for the mechanism is twofold:

1. The addition is exclusively *trans*.
2. No rearrangement is observed even for $^t\text{Bu}(\text{H})\text{C}=\text{C}(\text{H})^t\text{Bu}$ whose carbonium ion is known to undergo rearrangement.

Isotope studies indicate that the C-O bond formation is present in the transition state. The mercury bridge in the transition state may not be symmetrical, but the structure is similar to the addition of Br^+ and AuX^+ to alkenes.



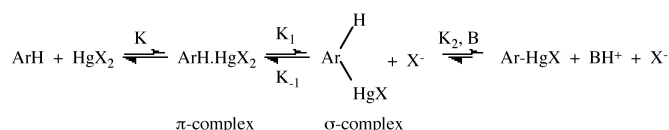
Proposed transition state for the solvomercuration reaction where the solvent is methanol.

The actual reaction was originally carried out with $\text{Hg}(\text{OAc})_2$ in benzene at 110 °C for several hours in acetic acid solution. It was found that the reaction was catalyzed by the presence of HClO_4 , H_2SO_4 , and HNO_3 , which were found to replace the acetate ion. The reaction rate is also increased by 690,000 times by the use of $\text{Hg}(\text{O}_2\text{CCF}_3)_2$ in HO_2CCF_3 .

The solvomercuration of alkynes gives alkenylmercury compounds, but the reaction is more sluggish than for the reaction with alkenes, and the product is always the *trans* isomer.

Mercuriation of aromatic compounds

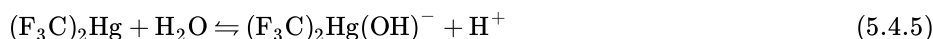
Mercuriation is an electrophilic aromatic substitution reaction that is possible for most $2n+2$ π -electron species. Evidence for the π -complex intermediate is indicated by UV spectroscopy, which shows an increase in the region 280 – 320 nm for the reaction of aromatic compounds with $\text{Hg}(\text{O}_2\text{CCF}_3)_2$ in HO_2CCF_3 . The σ -complex has detected in liquid SO_2 .



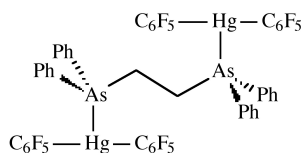
As a preparative method mercuriation suffers from alack of selectivity, including an isomerization from *para* substitution at low temperature to *meta* substitution at high temperatures.

Structure

Dialkyl mercury compounds, R_2Hg , are generally air stable and show little Lewis acid behavior. They are monomeric colorless liquids or low melting solids, e.g., Bp = 92.5 °C for Me_2Hg . No solubility is observed in water, except for $(\text{F}_3\text{C})_2\text{Hg}$ (Equation 5.4.5).



The hybridization at mercury involves the 6s and 6p orbitals; however, the 5d may be involved. X-ray crystal structures for both R_2Hg and RHgX show linear structures. In general R_2Hg compounds are very weak Lewis acids, but adduct are formed if the alkyl group is sufficiently electron withdrawing, e.g., $(\text{C}_6\text{F}_5)_2\text{Hg}$. The geometry of the Lewis acid-base complex is not triangular as predicted from VSEPR theory, but a *T-shape*. The distortion from a linear C-Hg-C unit is minor. For example, in $(\text{C}_6\text{F}_5)_2\text{Hg}$ the C-Hg-C angle is 176.2°, while in $[(\text{C}_6\text{F}_5)_2\text{Hg}]_2$ (diars), where diars = $\text{Ph}_2\text{AsCH}_2\text{CH}_2\text{AsPh}_2$, the same angle is 173°. Furthermore, the donor atom-Hg bond distance (e.g., As-Hg = 3.4 Å) is only slightly shorter than the sum of the van der Waal radii (e.g., 3.5 Å).



The structure of $[(\text{C}_6\text{F}_5)_2\text{Hg}]_2$ (diars).

Bibliography

- L. C. Damude and P. A. W. Dean. *J. Organomet. Chem.*, 1979, **181**, 1.
- L. C. Damude and P. A. W. Dean. *J. Chem. Soc., Chem. Commun.*, 1978, 1083.
- J. L. Courtneidge, A. G. Davies, P. S. Gregory, D. C. McGuchan, and S. N. Yazdi. *J. Chem. Soc., Chem. Commun.*, 1987, 1192.
- P. B. Hitchcock, J. M. Keates, and G. A. Lawless, *J. Am. Chem. Soc.*, 1998, **120**, 599.

This page titled [5.4: Organomercury Compounds](#) is shared under a [CC BY 3.0](#) license and was authored, remixed, and/or curated by [Andrew R. Barron \(CNX\)](#) via [source content](#) that was edited to the style and standards of the LibreTexts platform.

5.5: The Myth, Reality, and History of Mercury Toxicity

Mercury has a reputation for being a dangerous element, but is its reputation deserved? Given the large-scale use of mercury today it is important to understand the risks and issues related to mercury exposure. Nowhere is this now important than with the use of mercury for small low energy fluorescent lights that are being advocated by everyone from the electricity companies to Greenpeace.



An example of a modern low energy mercury vapor fluorescent light.

When considering the issue of mercury toxicity it is important to separate the effects of mercury metal (as a liquid or vapor) from the compounds of mercury.

Mercury metal

It was found very early on that people who worked with mercury, in mining for example, had very bad health. Other jobs that exposed people to mercury were mirror makers and hatters (people who manufactured hats). The problems in this latter occupation will forever live on with one of the central characters in Lewis Carroll's *Alice's Adventures in Wonderland*; the Mad Hatter.

Hats were made from felt, which is a non-woven textile of animal hair. Wool interlocks naturally due to the surface texture of the individual hairs, but rabbit and beaver have to be artificially roughened. This process was usually accomplished with nitric acid (HNO_3). It was found that if mercury was added to the nitric acid, a better quality of felt was produced. Unfortunately, when the felt was dried a fine dust was formed containing mercury. The hatters who shaped the felt inhaled large quantities of this dust were found to suffer from excessive salivation, erethism (presenting with excessive shyness, timidity and social phobia), and shaking of the limbs, which became known as *hatter's shakes*. The madness that was observed is the derivation of the phrase “mad as a hatter”.

Note

It is interesting that while Carroll's Mad Hatter is mad, he does not show the classic symptoms of mercury poisoning. In particular he can be in no way described as shy!

Hatters were not the only people that mercury caused a problem for. Chemists doing research using large quantities of mercury were also affected. They were given to violent headaches, tremors of the hands, “socially troublesome inflammation of the bladder”, loss of memory, and slow mental processes. In 1926 Alfred Stock ([Figure](#)) and his research group all suffered from symptoms. However, when the lab was cleaned of mercury the symptoms went away.



German chemist Alfred Stock (1876 –1946).

Many other notable scientists have also suffered from mercury poisoning. Faraday (Figure), Pascal (Figure), and most probably Sir Isaac Newton (Figure) were affected. As part of his research studies, Newton boiled several pounds of mercury a day just before his period of insanity between 1692 and 1693. It is likely that the mercury vapor was the cause of his malady. However, in each case, the symptoms (and insanity) abated once the source of mercury was removed.



An engraving by John Cochran of English chemist and physicist Michael Faraday, FRS (1791 –1867).



French mathematician, physicist, and religious philosopher Blaise Pascal (1623 – 1662).



English physicist, mathematician, astronomer, natural philosopher, alchemist, and theologian Sir Isaac Newton FRS (1643 –1727).
Portrait by Godfrey Kneller.

Note

It is important to remember that in all the cases described above it is the inhalation of the mercury vapor that was the cause of the trouble. Solid alloys of mercury such as those found in dental fillings have never been shown to cause any medical issues directly. Despite this the US banned the use of Cu/Hg dental amalgams until 1850! More recently, it has been suggested that dentists are exposed at higher levels during the placing and removal of fillings. Dentists as a group have higher mercury levels than those associated with people with amalgam restorations, but experience no increase in disease or death rates, and in fact tend to be healthier than the general population.

Although elemental mercury was clearly toxic, this did not stop its use in pharmacy for hundreds of years. In the 1500's mercury was used in the treatment (albeit ineffective) of syphilis. Syphilis was a new disease in Europe; it had been brought back from America by Columbus' sailors, and was promptly spread through Europe by the French army, amongst others! Syphilis was much more fatal and had more dramatic symptoms than today.

Initially mercury was used as an ointment, but the patients often got worse. Then there was *the tub*, which was a mercury vapor bath, and even calomel (Hg_2Cl_2) was used, but with little effect. These treatments were used for over four centuries, but none provided a cure, despite claims at the time. For example, John Hunter, a doctor who gave himself syphilis by mistake (!) claimed he had been cured, but he actually died of a heart attack during an argument, so it is unlikely the mercury worked. Despite this it became known that "a night with Venus results in a lifetime with Mercury".

The reasons that mercury was thought erroneously to cure syphilis are twofold:

1. Until 1906 it was difficult to diagnose syphilis. It was often confused with gonorrhea, and therefore it is likely that some people did not have the far more deadly syphilis.
2. Syphilis occurs in three phases, each with remission between the phases. The period of remission between secondary and tertiary phases can be two to three years, and therefore it may appear that a cure is found. Especially as many patients (like John Hunter) died of other deaths during this remission phase.

The prevalent use of mercury and its presence in many cadavers, led some doctors to assume that mercury was a natural part of the body. It was not just humans that were treated with mercury, cattle were also treated, and one druggist sold 25 tons of mercury to a single farmer in one year!

The density of mercury and its liquid state at room temperature led to another unusual application that was somewhat more successful, although equally dangerous: constipation. In medical texts of the time it was noted that "mercury is given in the disease called *Miserere*, unto two or three pounds, and is voided again by siege to the same weight; it is better to take a great deal of it than a little, because a small quantity might be apt to stop in the circinvolutions of the guts, and if some acid humors should happen to join with it, a *sublimate corrosive* would be made; but when a large quantity of it is taken, there's no need to fearing this accident, because it passes through by its own weight."

It is interesting that the mention of the *corrosive sublimate*; this is in fact mercury(II) dichloride (HgCl_2) which unlike mercury(I) chloride (Hg_2Cl_2), is a very violent poison. Death is caused by renal failure. So while there is no evidence for elemental mercury

itself causing fatalities, its compounds are another matter to be considered.

Organomercury compounds

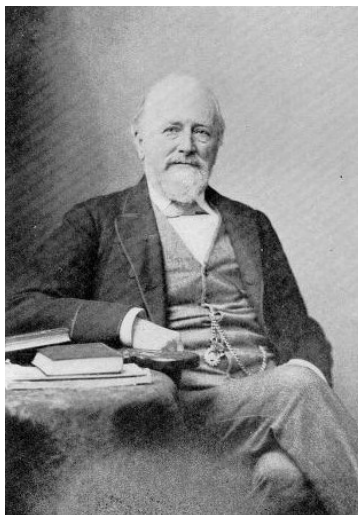
In 1953 it was noted that the fishing village of Minamata in Japan had an epidemic in which a large number of people died. Initial thoughts of either an infectious disease or malnutrition were discounted; then it was found that the fish eaten by the villagers was highly contaminated by mercury.

It was found that the mercury came from the Chisso Corporation chemical plant that made acetaldehyde from acetylene using a mercury catalyst. The plant was losing 1 Kg of mercury metal for every ton of acetaldehyde being produced. As a consequence it was originally assumed that the poisoning of the village was due to inorganic mercury. Based upon prior incidents, an obvious response was to ban consumption of all fish and shellfish. As a consequence no new cases were reported, however, people already effected continued to die. This was unlike any previous mercury poisoning.

Further analysis showed small quantities of water soluble methyl mercury (MeHg^+) was present and sequestered by the shellfish to give MeHgSMe . While the lethal effects of organomercury compounds were known, the source of the methyl mercury was a mystery. A group of Swedish researchers showed that the bacterial action in river sediment or rotting fish converted inorganic mercury to either volatile Me_2Hg or water soluble MeHg^+ . With this discovery, it was understood how the anaerobic mud of the estuary near Minamata could perform this methylation.

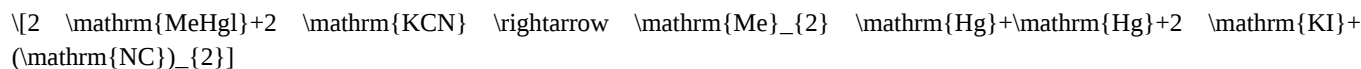
Of course Minamata was not the first report of an organomercury compound, but it was the first time that it was shown that mercury metal could be converted to a highly toxic organometallic derivative in the environment. The hazardous nature of organomercurials was found almost as soon as the first compounds were reported!

While working in Bunsen's research group in Marburg, Edward Franklin discovered the synthesis of the zinc analog of a Grignard reagent. Subsequently, in 1851 Franklin moved to Owens College in Manchester where he extended his work to mercury. In his publication he noted that these organomercury compounds had a "nauseous taste", but didn't realize they were toxic.



British chemist Sir Edward Franklin FRS (1825 – 1899).

In 1858 George Buckton working at the then Royal College of Chemistry (now Imperial College) reported the synthesis of dimethyl mercury as a volatile liquid.





British chemist George Buckton (1818 - 1905).

When Frankland moved his research to St Bartholomew's Hospital ("Barts") London he started looking into the chemistry of R_2Hg with an assistant called Bill Odling in collaboration with Dr Carl Ulrich.

Ulrich died in 1865 as a consequence of exposure to Me_2Hg . In his own statement, he had inhaled a large quantity of the volatile compound without having taken the proper precautions. The following day "his countenance had attained a dull, anxious, and confused expression" and he was admitted to the hospital in a weak condition on 3rd February. On the 9th he became noisy and had to be put under mechanical restraint. The next day his breath and body began to smell offensively and he was in a coma. He would rise from the coma periodically to utter incoherent howls. He died on the 14th of February.

A technician from the same research group (who is only identified as 'T. C.') was also admitted to the hospital on 28th March of the same year. His symptoms were initially milder than Ulrich's, but soon developed. By that summer he was completely demented, with no control over his body functions. He stayed in this state for many months, only dying on 7th April 1866. Records indicate that a third assistant was also taken ill, but there was no further mention of him, so it is unknown if he died.

Summary and the "green" future

Metallic mercury causes severe symptoms, but all records show that if the patient is removed from the source they recover. Thus, short term exposure to metallic mercury, while dangerous, is not fatal if proper precautions are taken. In contrast, mercury compounds offer different risks. As a general rule, inorganic mercury(I) compounds are far less toxic than their mercury(II) analogs, however, all should be treated with care.

Where mercury compounds offer the greatest risk of fatality is their organometallic derivatives. There is no known cure for exposure to even modest doses of organomercury compounds. Furthermore, the ability of elemental mercury to be transformed into water-soluble organomercury compounds such as $MeHg^+$, offers a future threat to public health.

The new generation of low energy consumption light bulbs contain mercury vapor. While they last longer than a traditional tungsten filament light bulb (Figure), they do have a lifetime. The presence of mercury means that they should be disposed-off separately from household waste to ensure that when the glass is broken the mercury is not released; however, this is unlikely. Most will be disposed off along with household waste which may be subsequently land filled. The lesson from Minamata should be that the bacterial action under anaerobic condition allows for the formation of water soluble $MeHg^+$, that can diffuse into the water table. Although the amount of mercury in each bulb is very small, the highly lethal nature (low LD_{50}) of organomercury compounds should be considered in efforts to conserve energy by the use of the low energy light bulbs. At the very minimum protocols for their efficient disposal and recycling should be in place.

Bibliography

- S. Jensen and A. Jernelöv, *Nature*, 1969, **223**, 753.
- J. C. Clifton II, *Pediatr. Clin. North Am.*, 2007, **54**, 237.
- H. A. Waldron, *Br. Med. J.*, 1983, **287**, 24:
- C. Naleway, R. Sakaguchi, E. Mitchell, T. Muller, W. A. Ayer, and J. J. Hefferren, *J. Amer. Dent. Assoc.*, 1985, **111**, 37.
- D. McComb, *J. Can. Dent. Assoc.*, 1997, **63**, 372.
- T. G. Duplinsky1 and D. V. Cicchetti, *Int. J. Stats. Med. Res.*, 2012, **1**, 1.

- M. Aucott, M. McLinden, and M. Winka, *J. Air. Waste Manag. Assoc.*, 2003, **53**, 143.

This page titled [5.5: The Myth, Reality, and History of Mercury Toxicity](#) is shared under a [CC BY 3.0](#) license and was authored, remixed, and/or curated by [Andrew R. Barron \(CNX\)](#) via [source content](#) that was edited to the style and standards of the LibreTexts platform.

CHAPTER OVERVIEW

6: Group 13

- [6.1: The Group 13 Elements](#)
- [6.2: Trends for the Group 13 Compounds](#)
- [6.3: Borides](#)
- [6.4: Boron Hydrides](#)
- [6.5: Wade's Rules](#)
- [6.6: Trends for the Oxides of the Group 13 Elements](#)
- [6.7: Boron Oxides, Hydroxides, and Oxyanions](#)
- [6.8: Aluminum Oxides, Hydroxides, and Hydrated Oxides](#)
- [6.9: Ceramic Processing of Alumina](#)
- [6.10: Boron Compounds with Nitrogen Donors](#)
- [6.11: Properties of Gallium Arsenide](#)
- [6.12: Electronic Grade Gallium Arsenide](#)
- [6.13: Chalcogenides of Aluminum, Gallium, and Indium](#)
- [6.14: Group 13 Halides](#)

Thumbnail: Crystals of 99.999% gallium. (CC-SA-BY 3.0; Foobar)

This page titled [6: Group 13](#) is shared under a [CC BY 3.0](#) license and was authored, remixed, and/or curated by [Andrew R. Barron \(CNX\)](#) via [source content](#) that was edited to the style and standards of the LibreTexts platform.

6.1: The Group 13 Elements

Table 6.1.1 lists the derivation of the names of the Group 13 (IIIA) elements.

Element	Symbol	Name
Boron	B	From the Arabic word <i>buraq</i> or the Persian word <i>burah</i> for the mineral <i>borax</i>
Aluminium (Aluminum)	Al	From <i>alum</i>
Gallium	Ga	From Named after the Latin word for France (Gaul) <i>Gallia</i>
Indium	In	Latin <i>rubidus</i> meaning <i>deepest red</i>
Thallium	Tl	From the Latin <i>thallus</i> meaning <i>sprouting green twig</i>

Table 6.1.1: Derivation of the names of each of the alkali metal elements.

Note

Aluminium is the international spelling standardized by the IUPAC, but in the United States it is more commonly spelled as aluminum.

Discovery

Boron

Borax (a mixture of $\text{Na}_2\text{B}_4\text{O}_7 \cdot 4\text{H}_2\text{O}$ and $\text{Na}_2\text{B}_4\text{O}_7 \cdot 10\text{H}_2\text{O}$) was known for thousands of years. In Tibet it was known by the Sanskrit name of *tincal*. Borax glazes were used in China in 300 AD, and the writings of the Arabic alchemist Geber appear to mention it in 700 AD. However, it is known that Marco Polo brought some borax glazes back to Italy in the 13th century. In 1600 Agricola in his treatise *De Re Metallica* reported the use of borax as a flux in metallurgy.



A drawing of the *father of chemistry* Abu Musa Jābir ibn Hayyān al azdi known by Geber; the Latinized form of Jabir (721 - 815). Geber was a chemist and alchemist, astronomer and astrologer, engineer, geologist, philosopher, physicist, and pharmacist and physician.



A painting of German author Georg Bauer (1494 - 1555), whose pen-name was the Latinized Georgius Agricola, was most probably the first person to be environmentally conscious.

Boron was not recognized as an element until its isolation by Sir Humphry Davy, Joseph Louis Gay-Lussac and Louis Jacques Thénard in 1808 through the reaction of boric acid and potassium. Davy called the element *boracium*. Jöns Jakob Berzelius identified boron as an element in 1824.



British chemist and inventor Sir Humphry Davy FRS (1778 - 1829).



French chemist and physicist Joseph Louis Gay-Lussac (1778 –1850).



French chemist Louis Jacques Thénard (1777 - 1857).



Swedish chemist Friherre Jöns Jacob Berzelius (1779 - 1848).

Aluminum

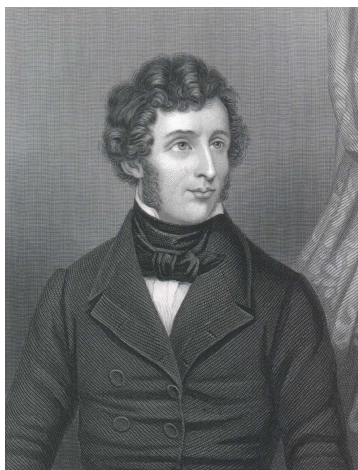
Ancient Greeks and Romans used aluminum salts as dyeing mordants and as astringents for dressing wounds; alum ($\text{KAl}(\text{SO}_4)_2 \cdot 12\text{H}_2\text{O}$) is still used as a styptic (an antihemorrhagic agent). In 1808, Sir Humphry Davy identified the existence of a metal base of alum, which he at first termed *alumium* and later aluminum.

The metal was first produced in 1825 (in an impure form) by Hans Christian Ørsted by the reaction of anhydrous aluminum chloride with potassium amalgam. Friedrich Wöhler repeated the experiments of Ørsted but suggested that Ørsted had only isolated potassium. By the use of potassium (Equation 6.1.1), he is credited with isolating aluminum in 1827. While Wöhler is generally credited with isolating aluminum, Ørsted should also be given credit.





Danish physicist and chemist Hans Christian Ørsted (1777 - 1851).



German chemist Friedrich Wöhler (1800 - 1882) also known for his synthesis of urea and, thus, the founding of the field of natural products synthesis.

In 1846 Henri Deville improved Wöhler's method, and described his improvements in particular the use of sodium in place of the expensive potassium

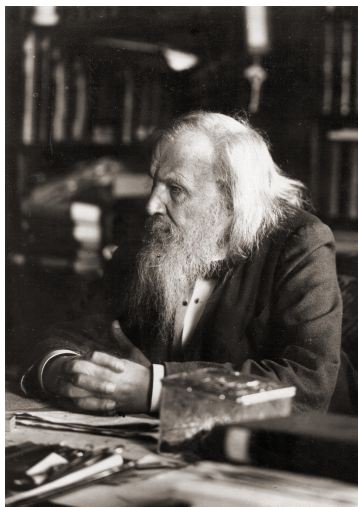


French chemist Henri Etienne Sainte-Claire Deville (1818 - 1881).

Gallium

The element gallium was predicted, as eka-aluminum, by Mendeleev in 1870, and subsequently discovered by Lecoq de Boisbaudran in 1875; in fact de Boisbaudran had been searching for the missing element for some years, based on his own

independent theory. The first experimental indication of gallium came with the observation of two new violet lines in the spark spectrum of a sample deposited on zinc. Within a month of these initial results de Boisbaudran had isolated 1 g of the metal starting from several hundred kilograms of crude zinc blende ore. The new element was named in honor of France (Latin *Gallia*), and the striking similarity of its physical and chemical properties to those predicted by Mendeleev did much to establish the general acceptance of the periodic Law; indeed, when de Boisbaudran first stated that the density of Ga was 4.7 g cm^{-3} rather than the predicted 5.9 g/cm^3 , Mendeleev wrote to him suggesting that he redetermine the value (the correct value is 5.904 g/cm^3).



Russian chemist and inventor Dmitri Ivanovich Mendeleev (1834 – 1907).



French chemist Paul Émile (François) Lecoq de Boisbaudran (1838 – 1912).

Indium

While testing ores from the mines around Freiberg, Saxony, Ferdinand Reich and Hieronymous Theodor Richter when they dissolved the minerals pyrite, arsenopyrite, galena and sphalerite in hydrochloric acid, and since it was known that ores from that region contained thallium they searched for the green emission lines by spectroscopy. Although the green lines were absent, a blue line was present in the spectrum. As no element was known with a bright blue emission they concluded that a new element was present in the minerals. They named the element with the blue spectral line indium. Richter went on to isolate the metal in 1864.



German chemist Ferdinand Reich (1799 - 1882).



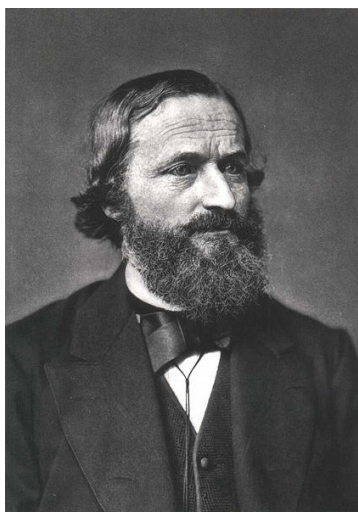
German chemist Hieronymus Theodor Richter (1824 - 1898).

Thallium

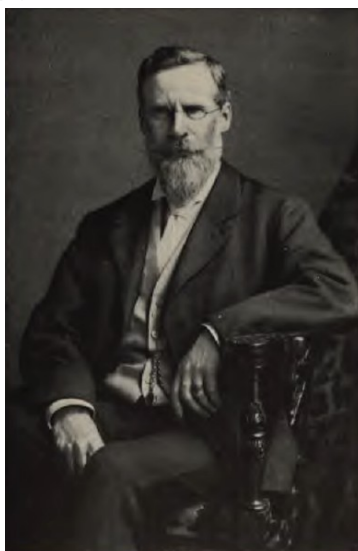
After the publication of their improved method of flame spectroscopy by Robert Bunsen and Gustav Kirchhoff this method became an accepted method to determine the composition of minerals and chemical products. Two chemists, William Crookes and Claude-Auguste Lamy, both started to use the new method and independently employed it in their discovery of thallium.



German chemist Robert Wilhelm Eberhard Bunsen (1811 - 1899).



German physicist Gustav Robert Kirchhoff (1824 - 1887).



English chemist and physicist Sir William Crookes, FRS (1832 –1919) attended the Royal College of Chemistry (now Imperial College) in London.

Crookes was making spectroscopic determinations on selenium compounds deposited in the lead chamber of a sulfuric acid production plant near Tilkerode in the Harz mountains. Using a similar spectrometer to Crookes', Lamy was determining the composition of a selenium-containing substance that was deposited during the production of sulfuric acid from pyrite. Using spectroscopy both researchers both observed a new green line the atomic absorption spectrum and assigned it to a new element. Both set out to isolate the new element. Fortunately for Lamy, he had received his material in larger quantities and thus he was able to isolate sufficient quantities of thallium to determine the properties of several compounds and prepare a small ingot of metallic thallium. At the same time Crookes was able to isolate small quantities of elemental thallium and determine the properties of a few compounds. The claim by both scientists resulted in significant controversy during 1862 and 1863; interestingly this ended when Crookes was elected Fellow of the Royal Society in June 1863.

Abundance

The abundance of the Group 13 elements is given in Table 6.1.2. Aluminum is the most abundant metal in the Earth's crust and is found in a wide range of minerals. While boron is not as common it is also found in a range of borate minerals. In contrast, gallium, indium, and thallium are found as impurities in other minerals. In particular indium and thallium are found in sulfide or selenide mineral rather than oxides, while gallium is found in both sulfides (ZnS) and oxides (bauxite). Although indium and thallium minerals are known, they are rare: indite (FeIn_2S_4), lorandite (TlAsS_2), crookesite (Cu_7TlSe_4).

Table 6.1.2: Abundance of Group 13 elements.

Element	Terrestrial abundance (ppm)
B	10 (Earth's crust), 20 (soil), 4 (sea water)
Al	82,000 (Earth's crust), 100,000 (soil), 5×10^{-4} (sea water)
Ga	18 (Earth's crust), 28 (soil), 30×10^{-6} (sea water)
In	0.1 (Earth's crust), 0.01 (soil), 0.1×10^{-6} (sea water)
Tl	0.6 (Earth's crust), 0.2 (soil), 10×10^{-6} (sea water)

Isotopes

The naturally abundant isotopes of the Group 13 elements are listed in Table 6.1.3. Thallium has 25 isotopes that have atomic masses that range from 184 to 210. Thallium-204 is the most stable radioisotope, with a half-life of 3.78 years.

Table 6.1.3: Abundance of the major isotopes of the Group 13 elements.

Isotope	Natural abundance (%)
Boron-10	19.9
Boron-11	80.1
Aluminum-27	100
Gallium-69	60.11
Gallium-71	39.89
Indium-113	4.3
Indium-115	95.7
Thallium-203	29.52
Thallium-205	70.48

The Group 13 elements offer potential as NMR nuclei (Table 6.1.4). In particular ^{11}B and ^{27}Al show promise for characterization in both solution and solid state.

Table 6.1.4: Isotopes of Group 13 elements for NMR spectroscopy.

Isotope	Spin	Natural abundance (%)	Quadrupole moment (10^{-30} m^2)	NMR frequency (MHz) at a field of 2.3488 T	Reference
Boron-10	3	19.58	8.459	-10.746	$\text{BF}_3 \cdot \text{Et}_2\text{O}$
Boron-11	$3/2$	80.42	4.059	-32.084	$\text{BF}_3 \cdot \text{Et}_2\text{O}$
Aluminum-27	$5/2$	100	14.66	-26.057	$\text{Al}(\text{NO}_3)_3$
Gallium-69	$3/2$	60.4	17.1	-24.003	$\text{Ga}(\text{NO}_3)_3$
Gallium-71	$3/2$	39.6	10.7	-30.495	$\text{Ga}(\text{NO}_3)_3$
Indium-113	$9/2$	4.28	79.9	-21.866	$\text{In}(\text{NO}_3)_3$
Indium-115	$9/2$	95.72	81.0	-21.914	$\text{In}(\text{NO}_3)_3$

Industrial production

Borax is mined as a mixture of $\text{Na}_2\text{B}_4\text{O}_7 \cdot 4\text{H}_2\text{O}$ and $\text{Na}_2\text{B}_4\text{O}_7 \cdot 10\text{H}_2\text{O}$. Acidification gives boric acid, $\text{B}(\text{OH})_3$, which can be reduced with sodium amalgam (Na/Hg) to give amorphous boron. Pure boron can be prepared by reducing boron halides (e.g., BF_3 and

BCl₃) with hydrogen at high temperatures. Ultrapure boron, for the use in semiconductor industry, is produced by the decomposition of diborane (B₂H₆) and then further purified with the zone melting or Czochralski processes.

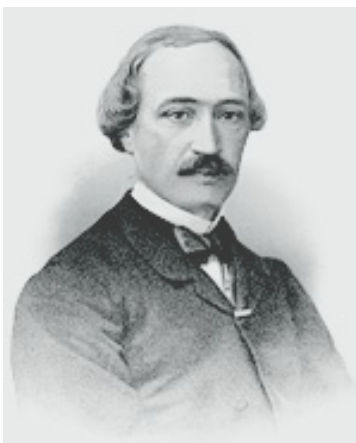
The only two economic sources for gallium are as byproduct of aluminum and zinc production. Extraction during the Bayer process followed by mercury cell electrolysis and hydrolysis of the amalgam with sodium hydroxide leads to sodium gallate. Electrolysis then gives gallium metal.

The lack of indium mineral deposits and the fact that indium is enriched in sulfides of lead, tin, copper, iron and zinc, makes the zinc production the main source for indium. The indium is leached from slag and dust of zinc production. Up until 1924, there was only about a gram of isolated indium on the planet, however, today worldwide production is currently greater 476 tons per year from mining and a 650 tons per year from recycling. This massive increase in demand is due to applications in LCD displays and solar cell applications.

Aluminum

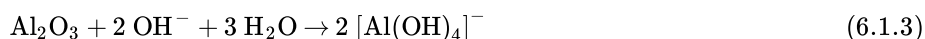
Due to aluminum's position as the most abundant metallic element in the Earth's crust (7.5 - 8.1%) and its enormous industrial importance warrants detailed discussion of its industrial production. Aluminum only appears in its elemental form in nature in oxygen-deficient environments such as volcanic mud. Ordinarily, it is found in a variety of oxide minerals.

In comparison to other metals aluminum is difficult to extract from its ores. Unlike iron, aluminum oxides cannot be reduced by carbon, and so purification is only possible on an economic scale using electrolysis. Prior to electrolysis purified aluminum oxide is obtained by refining bauxite in the process of developed by Karl Bayer.



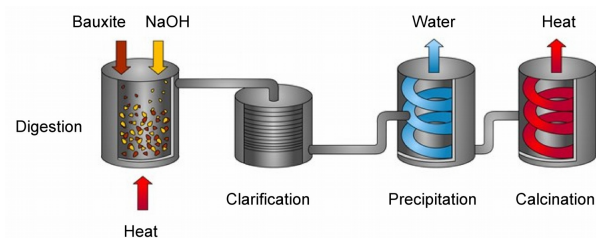
Austrian chemist Karl Josef Bayer (1847 –1904) whose father, Friedrich, founded the Bayer chemical and pharmaceutical company.

Bauxite, the most important ore of aluminum, contains only 30-50% alumina, Al₂O₃, the rest being a mixture of silica, iron oxide, and titanium dioxide. Thus, the alumina must be purified before it can be used as the oxide or refined into aluminum metal. In the Bayer process, bauxite is digested in hot (175 °C) sodium hydroxide (NaOH) solution (Figure). This converts the alumina to aluminum hydroxide, Al(OH)₃, which dissolves in the hydroxide solution.



The other components do not dissolve and are filtered off. The hydroxide solution is cooled, and the dissolved aluminum hydroxide precipitates, which when heated to 1050 °C is calcined into alumina.





Schematic representation of the Bayer process. Copyright: Andrew Perchard, Alcan Aluminium UK and courtesy of Glasgow University Archives (2007).

Once a pure alumina is formed, it is dissolved in molten cryolite (Na_3AlF_6) and reduced to the pure metal at elevated temperatures (950 - 980 °C) using the Hall-Héroult process, developed independently Charles Hall and Paul Héroult.



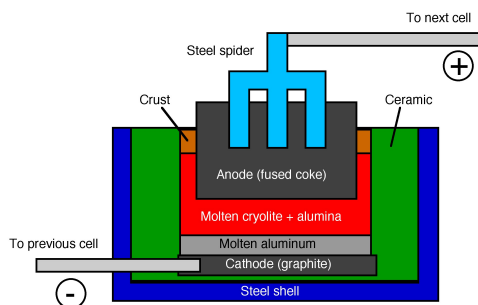
American inventor and engineer Charles Martin Hall (1863 – 1914).



French scientist Paul (Louis-Toussaint) Héroult (1863 – 1914).

Both of the electrodes used in the electrolysis of aluminum oxide are carbon. The reaction at the cathode involves the reduction of the Al^{3+} . The aluminum metal then sinks to the bottom and is tapped off, where it is usually cast into large blocks called aluminum billets.





Schematic of the Hall-Héroult cell.

At the anode oxygen is formed, (6.1.6), where it reacts with the carbon anode is then oxidized to carbon dioxide, (6.1.7). The anodes must be replaced regularly, since they are consumed. While the cathodes are not oxidized they do erode due to electrochemical processes and metal movement.



Although the Hall-Héroult process consumes a lot of energy, alternative processes have always found to be less economically and ecologically viable.

Physical properties

Table summarizes the physical properties of the Group 13 elements. While, aluminum, indium, and thallium have typical metal properties, gallium has the largest liquid range of any element. Boron exists as a molecular compound in the solid state, hence its high melting point.

Element	Mp (°C)	Bp (°C)	Density (g/cm ³)
B	2300	3658	2.3
Al	661	2467	2.7
Ga	30	2403	5.9 (solid), 6.1 (liquid)
In	156	2080	7.3
Tl	304	1457	11.9

Table 6.1.5: Selected physical properties of the Group 13 elements.

Bibliography

- C. M. Hall. *Process of reducing aluminum from its fluoride salts by electrolysis*. US Patent 400,664 (1886).
- L. B. Alemany, S. Steuarnagel, J.-P. Amoureux, R. L. Callender, and A. R. Barron. *Solid State Nuclear Magnetic Resonance*, 1999, **14**, 1.
- L. B. Alemany, R. L. Callender, A. R. Barron, S. Steuarnagel, D. Iuga, and A. P. M. Kentgens, *J. Phys. Chem., B.*, 2000, **104**, 11612.
- M. Bishop, N. Shahid, J. Yang, and A. R. Barron, *Dalton Trans.*, 2004, 2621.

This page titled [6.1: The Group 13 Elements](#) is shared under a [CC BY 3.0](#) license and was authored, remixed, and/or curated by [Andrew R. Barron \(CNX\)](#) via [source content](#) that was edited to the style and standards of the LibreTexts platform.

6.2: Trends for the Group 13 Compounds

Boron is a non-metal with metalloid tendencies. The higher ionization energies for boron than for its other Group homologs are far more than would be compensated by lattice energies, and thus, the B^{3+} ion plays no part in the chemistry of boron, and its chemistry is dominated by the formation of covalent compounds. In contrast, the elements aluminum through thallium each has a low electronegativity and the chemistry of their compounds reflects this characteristic. Each of the Group 13 metals forms both covalent compounds and ionic coordination complexes.

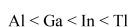
All of the Group 13 (IIIA) elements have a valence shell electron configuration of ns^2np^1 . As a consequence all of the Group 13 elements form compounds in which they adopt a +3 oxidation state. While the lighter elements do form compounds with lower oxidation state, they are not the norm; however, the +1 oxidation state is more prevalent for the heavier elements in particular thallium. The rationale for this is described as the *inert pair effect*. The inert pair effect is usually explained by the energy of the ns orbital is lower making it harder to ionize and stabilizing a ns^2np^0 valence shell. However, as may be seen from Table 6.2.1 the sum of the second and third ionization enthalpies is lower for indium (4501 kJ/mol), than for gallium (4916 kJ/mol), but with thallium intermediate (4820 kJ/mol). The true source of the inert pair effect is that the lower bond strengths observed for the heavier elements (due to more diffuse orbitals and therefore less efficient overlap) cannot compensate for the energy needed to promote the ns^2 electrons. For example, the bond energies for gallium, indium, and thallium in MCl_3 are 242, 206, and 153 kJ/mol, respectively. It has also been suggested that relativistic effects make a contribution to the inert pair effect.

Table 6.2.1: Summary of first three ionization enthalpies for the Group 13 metals.

Ionization enthalpy (kJ/mol)	Al	Ga	In	Tl
1	576.4	578.3	558.1	589.0
2	1814.1	1969.3	1811.2	1958.7
3	2741.4	2950.0	2689.3	2868.8

In summary, it may be stated that while the chemistry of gallium, indium and thallium is very similar, that of aluminum is slightly different, while boron's chemistry is very different from the rest of the Group.

A second effect is noticed in the transition from aluminum, to gallium, to indium. Based upon their position in the Group it would be expected that the ionic radius and associated lattice parameters should follow the trend:



However, as may be seen from Table 6.2.2 the values for gallium are either the same as, or smaller, than that of aluminum. In a similar manner, the covalent radius and covalent bond lengths as determined by X-ray crystallography for a range of compounds (Table 6.2.3).

Table 6.2.2: Lattice parameter (a) for zinc blende forms of the Group 13 phosphides and arsenides. Data from *Semiconductors: Group IV Elements and III-V Compounds*, Ed. O. Madelung, Springer-Verlag, Berlin (1991).

Element	Phosphide lattice parameter (Å)	Arsenide lattice parameter (Å)
Al	5.4635	5.6600
Ga	5.4505	5.6532
In	5.8687	6.0583

Table 6.2.3: Comparative crystallographically determined bond lengths.

Element	M-C (Å)	M-N (Å)	M-O (Å)	M-Cl (Å)
Al	1.96 – 2.02	2.03 – 2.19	1.74 – 1.93	2.09 – 2.11
Ga	1.97 – 2.01	1.95 – 2.12	1.89 – 1.94	2.12 – 2.23
In	2.14 – 2.17	2.23 – 2.31	2.19 – 2.20	2.39 – 2.47

Gallium is significantly smaller than expected from its position within the Group 13 elements (Table 6.2.4). The rationale for this may be attributed to an analogous effect as seen in the *lanthanide contraction* observed for the lanthanides and the 3rd row of transition elements. In multi-electron atoms, the decrease in radius brought about by an increase in nuclear charge is partially offset by increasing electrostatic repulsion among electrons. In particular, a “shielding effect” results when electrons are added in outer shells, electrons already present shield the outer electrons from nuclear charge, making them experience a lower effective charge on the nucleus. The shielding effect exerted by the inner electrons decreases in the order $s > p > d > f$. As a sub-shell is filled in a period the atomic radius decreases. This effect is particularly pronounced in the case of lanthanides, as the 4*f* sub-shell is not very effective at shielding the outer shell ($n = 5$ and $n = 6$) electrons. However, a similar, but smaller effect should be observed with the post-transition metal elements, i.e., gallium. This is indeed observed (Table 6.2.4).

Table 6.2.4: Comparison of the covalent and ionic radii of Group 13 elements.

Element	Covalent radius (Å)	Ionic radius (Å)
Aluminum	1.21	0.53
Gallium	1.22	0.62
Indium	1.42	0.80
Iron (low spin)	1.32	0.55
Iron (high spin)	1.52	0.64

The anomalous size of gallium has two positive effects.

1. The similarity in size of aluminum and gallium means that their Group 15 derivatives have near identical lattice parameters (Table 6.2.3). This allows for both epitaxial growth of one material on the other, and also the formation of ternary mixtures (i.e., $\text{Al}_x\text{Ga}_{1-x}\text{As}$) with matched lattice parameters. The ability to grow heterojunction structures of Group 13-15 compounds (III-V) is the basis for the fabrication of a wide range of important optoelectronic devices, including: LEDs and laser diodes.
2. The similarity in size of gallium(III) to iron(III) (Table 6.2.4) means that gallium can substitute iron in a range of coordination compounds without alteration of the structure. Because of a similar size and charge as Fe^{3+} , Ga^{3+} is widely used as a non-redox-active Fe^{3+} substitute for studying metal complexation in proteins and bacterial populations.

Bibliography

- K. S. Pitzer, *Acc. Chem. Res.*, 1979, **12**, 271.
- K. D. Weaver, J. J. Heymann, A. Mehta, P. L. Roulhac, D. S. Anderson, A. J. Nowalk, P. Adhikari, T. A. Mietzner, M. C. Fitzgerald, and A. L. Crumbliss, *J. Biol. Inorg. Chem.*, 2008, **13**, 887.
- *Semiconductors: Group IV Elements and III-V Compounds*, Ed. O. Madelung, Springer-Verlag, Berlin (1991).

This page titled [6.2: Trends for the Group 13 Compounds](#) is shared under a [CC BY 3.0](#) license and was authored, remixed, and/or curated by [Andrew R. Barron \(CNX\)](#) via [source content](#) that was edited to the style and standards of the LibreTexts platform.

6.3: Borides

The non-metallic nature of boron means that it makes a number of binary compounds with elements more electropositive than itself (i.e., metals). These compounds are called, *borides*, and some are also formed with metalloid elements as well (e.g., arsenic). In this regard, borides may be considered similar to carbides, silicides, and some phosphides.

Borides are prepared in a number of ways, however, direct combination of the elements, (6.3.1), is the simplest. Other routes include, electrolysis of the fused salts, and the reduction of the metal oxide with a mixture of carbon and boron carbide.



Metal borides are generally refractory in character and chemically inert, while they often have properties better than that of the constituent elements. For example, the thermal conductivity of TiB_2 is about ten times greater than that of titanium, and the melting point is significantly higher (Table 6.3.1).

Table 6.3.1: The melting points of Group 4 metals and their borides.

Element	Melting point (°C)	Boride	Melting point (°C)
Ti	1725	TiB_2	3225
Zr	1855	ZrB_2	2990
Hf	2233	HfB_2	3100

The structures of metal borides depends on the M:B ratio. Borides with an isolated boron atom have a low B:M ratio: M_4B , M_3B , M_2B , M_5B_2 , and M_7B_3 . In such compounds the boron atom is normally in a triangular-prismatic or square-antiprismatic hole in a metal lattice. Borides with equal or near equal metal and boron ratio have structures with either pairs of boron atoms (as in V_3B_2), single boron chains (seen in all MB compounds), or double boron chains (observed for many M_3B_4 compounds). Increasing the boron content results in two-dimensional structures. For example, MB_2 usually consists of alternate hexagonal layers of metal and boron (Figure 6.3.1). Finally, boron rich borides (e.g., MB_4 , MB_6 , and MB_{12}) all have three-dimensional structures.

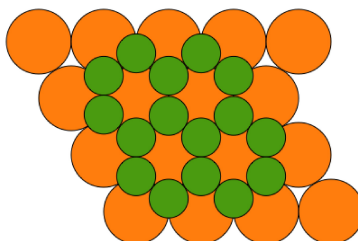


Figure 6.3.1: Alternate layers of metal atoms (large circles) and boron (small circles) in MB_2 .

This page titled 6.3: Borides is shared under a CC BY 3.0 license and was authored, remixed, and/or curated by Andrew R. Barron (CNX) via source content that was edited to the style and standards of the LibreTexts platform.

6.4: Boron Hydrides

Borane and diborane

Borane (BH_3) formed in the gaseous state from decomposition of other compounds, (6.4.2) but cannot be isolated except as a Lewis acid-base complex (6.4.1). As such many borane adducts are known.



In the absence of a Lewis base the dimeric diborane (B_2H_6) is formed. Diborane is generally synthesized by the reaction of BF_3 with a hydride source, such as NaBH_4 , (6.4.4), or LiAlH_4 , (6.4.3).



The structure of diborane (Figure 6.4.1 a) is considered to be electron deficient, and has been confirmed by IR spectroscopy and electron diffraction. The four terminal B-H bonds are normal covalent bonds, however, the bridging B-H-B unit consists of two three-centered two-electron bonds, each ordinarily considered to be formed by the combination of two boron sp^3 orbitals and one hydrogen s orbital (Figure 6.4.1 b). However, a consideration of the H-B-H bond angle associated with the terminal hydrides (120°) it is perhaps better to consider the BH_2 fragment to be sp^2 hybridized, and the B-H-B bridging unit to be a linear combination of one sp^2 orbital and one p orbital from each boron atom with the two hydrogen s orbitals. Diborane represents the archetypal electron deficient dimeric compound, of which Al_2Me_3 is also a member of this class of electron deficient molecules.

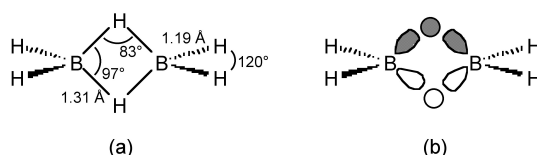


Figure 6.4.1: The structure (a) and the typical view of the three-centered two-electron bonds (b) in diborane, B_2H_6 .

B_2H_6 is spontaneously and highly exothermically inflammable above 25°C ($\Delta H = -2137.7 \text{ kJ/mol}$), (6.4.5). It is often used as one of a range of solvate forms for safety for both its flammability and toxicity.



Most reactions of diborane involve the cleavage of the dimeric structure. Hydrolysis of diborane yields boric acid, (6.4.6), while alcoholysis yields the appropriate borate ester, (6.4.7). Diborane reacts with Lewis bases to form the appropriate Lewis acid-base complex, (6.4.8).



Borohydride

The borohydride anion (or more properly the tetrahydridoborate anion), BH_4^- , can be considered as the Lewis acid-base complex between borane and H^- . A typical synthesis involves the reaction of a borate ester with a hydride source, (6.4.9).



Sodium borohydride is a stable white crystalline solid that is stable in dry air and is non-volatile. The boron in borohydride (BH_4^-) is tetrahedral. Although it is insoluble in Et_2O , it is soluble in water (in which it reacts slowly), THF, ethylene glycol, and pyridine. Interestingly, NaBH_4 reacts rapidly with MeOH , but dissolves in EtOH . Sodium borohydride has extensive uses in organic chemistry as a useful reducing agent in which it donates a hydride (H^-).

Higher Boranes

Higher boron hydrides contain, in addition to the bridging B-H-B unit, one or more B-B bonds. The higher boranes are usually formed by the thermal decomposition of diborane, (6.4.10) and (6.4.11).



These higher boranes have 'open' cluster structures, e.g., Figure 6.4.2 - Figure 6.4.4. Tetraborane, or to be more precise tetraborane(10) or *arachno*-B₄H₁₀, is a foul-smelling toxic gas. Pentaborane (9) is a toxic liquid (with a distinctive garlic odor) that can detonate in air, and like decaborane(14) was at one time considered as a potential rocket fuel. Because simple boron compounds burn with a characteristic green flame, the nickname for these fuels in the US military was *Green Dragon*. Problems with using boranes as a fuel included their toxicity and the characteristic of bursting into flame on contact with the air; furthermore, the exhaust would also be toxic. The US program resulted in a stockpile of borane fuels, in particular pentaborane(9), which was not destroyed until 2000. The system for the destroying the boranes was appropriately known as *Dragon Slayer*.

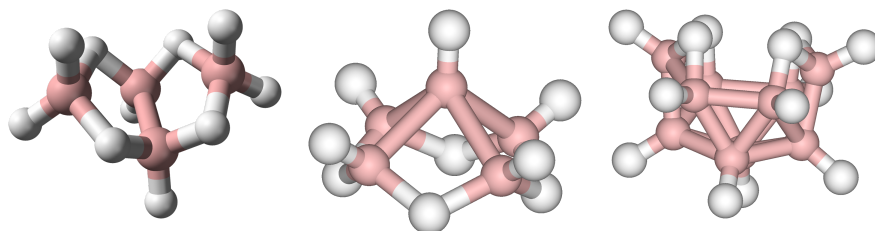


Figure 6.4.2: The molecular structure of tetraborane(10), B₄H₁₀, pentaborane(9), B₅H₉, and decaborane(14), B₁₀H₁₄. Boron atoms are represented by pink spheres, and hydrogen by white spheres.

Bibliography

- D. F. Gaines, *Acc. Chem. Res.*, 1973, **6**, 416.
- C. E. Housecroft, *Boranes and metalboranes: structure, bonding and reactivity*, Ellis Horwood, Chichester (1990).
- C. F. Lane, *Chem. Rev.*, 1976, **76**, 773.

This page titled 6.4: Boron Hydrides is shared under a CC BY 3.0 license and was authored, remixed, and/or curated by Andrew R. Barron (CNX) via source content that was edited to the style and standards of the LibreTexts platform.

6.5: Wade's Rules

Ken Wade (Figure 6.5.1) developed a method for the prediction of shapes of borane clusters; however, it may be used for a wide range of substituted boranes (such as carboranes) as well as other classes of cluster compounds.



Figure 6.5.1: Chemist Ken Wade FRS.

Wade's rules are used to rationalize the shape of borane clusters by calculating the total number of **skeletal electron pairs (SEP)** available for cluster bonding. In using Wade's rules it is key to understand structural relationship of various boranes (Figure 6.5.2).

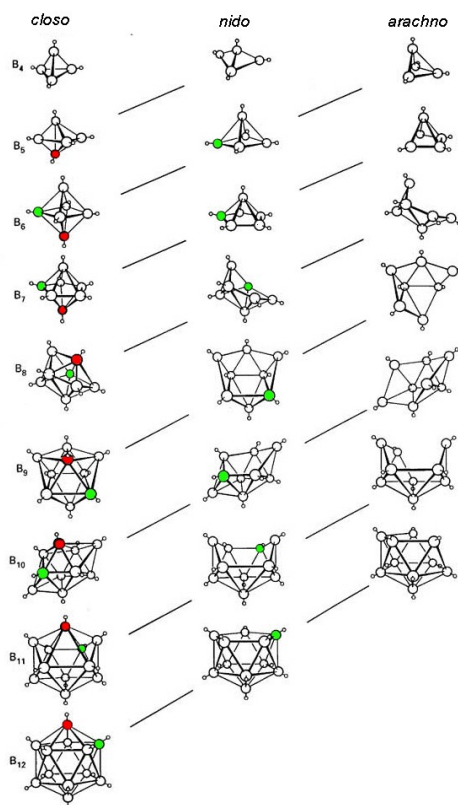


Figure 6.5.2: Structural relationship between *closo*, *nido*, and *arachno* boranes (and hetero-substituted boranes). The diagonal lines connect species that have the same number of skeletal electron pairs (SEP). Hydrogen atoms except those of the B-H framework are omitted. The red atom is omitted first, the green atom removed second. Adapted from R. W. Rudolph, *Acc. Chem. Res.*, 1976, **9**, 446.

The general methodology to be followed when applying Wade's rules is as follows:

1. Determine the total number of valence electrons from the chemical formula, i.e., 3 electrons per B, and 1 electron per H.

2. Subtract 2 electrons for each B-H unit (or C-H in a carborane).
3. Divide the number of remaining electrons by 2 to get the number of skeletal electron pairs (SEP).
4. A cluster with n vertices (i.e., n boron atoms) and $n+1$ SEP for bonding has a *closo* structure.
5. A cluster with $n-1$ vertices (i.e., $n-1$ boron atoms) and $n+1$ SEP for bonding has a *nido* structure.
6. A cluster with $n-2$ vertices (i.e., $n-2$ boron atoms) and $n+1$ SEP for bonding has an *arachno* structure.
7. A cluster with $n-3$ vertices (i.e., $n-3$ boron atoms) and $n+1$ SEP for bonding has an *hypho* structure.
8. If the number of boron atoms (i.e., n) is larger than $n+1$ SEP then the extra boron occupies a capping position on a triangular phase.

What is the structure of B_5H_{11} ?

1. Total number of valence electrons = $(5 \times B) + (11 \times H) = (5 \times 3) + (11 \times 1) = 26$
2. Number of electrons for each B-H unit = $(5 \times 2) = 10$
3. Number of skeletal electrons = $26 - 10 = 16$
4. Number SEP = $16/2 = 8$
5. If $n+1 = 8$ and $n-2 = 5$ boron atoms, then $n = 7$
6. Structure of $n = 7$ is pentagonal bipyramid (Figure 6.5.2), therefore B_5H_{11} is an *arachno* based upon a pentagonal bipyramid with two apexes missing (Figure 6.5.3).

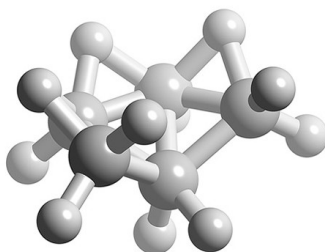


Figure 6.5.3: Ball and stick representation of the structure of B_5H_{11} .

What is the structure of B_5H_9 ?

1. Total number of valence electrons = $(5 \times B) + (9 \times H) = (5 \times 3) + (9 \times 1) = 24$
2. Number of electrons for each B-H unit = $(5 \times 2) = 10$
3. Number of skeletal electrons = $24 - 10 = 14$
4. Number SEP = $14/2 = 7$
5. If $n+1 = 7$ and $n-1 = 5$ boron atoms, then $n = 6$
6. Structure of $n = 6$ is octahedral (Figure 6.5.2), therefore B_5H_9 is a *nido* structure based upon an octahedral structure with one apex missing (Figure 6.5.4).

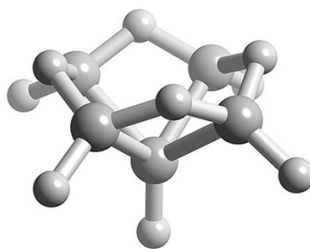


Figure 6.5.4: Ball and stick representation of the structure of B_5H_9 .

Example

What is the structure of $B_6H_6^{2-}$?

Solution

1. Total number of valence electrons = $(6 \times B) + (3 \times H) = (6 \times 3) + (6 \times 1) + 2 = 26$
2. Number of electrons for each B-H unit = $(6 \times 2) = 12$

3. Number of skeletal electrons = $26 - 12 = 14$
4. Number SEP = $14/2 = 7$
5. If $n+1 = 7$ and n boron atoms, then $n = 6$
6. Structure of $n = 6$ is octahedral (Figure 6.5.2), therefore $B_6H_6^{2-}$ is a *closo* structure based upon an octahedral structure (Figure 6.5.5).

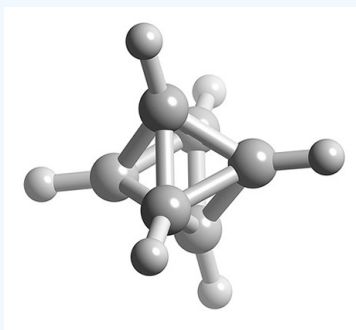


Figure 6.5.5: Ball and stick representation of the structure of $B_6H_6^{2-}$.

Table 6.5.1 provides a summary of borane cluster with the general formula $B_nH_n^{x-}$ and their structures as defined by Wade's rules.

Table 6.5.1: Wade's rules for boranes.

Type	Basic formula	Example	# of vertices	# of vacancies	# of e- in B + charge	# of bonding MOs
<i>Closo</i>	$B_nH_n^{2-}$	$B_6H_6^{2-}$	n	0	$3n + 2$	$n + 1$
<i>Nido</i>	$B_nH_n^{4-}$	B_5H_9	$n + 1$	1	$3n + 4$	$n + 2$
<i>Arachno</i>	$B_nH_n^{6-}$	B_4H_{10}	$n + 2$	2	$3n + 6$	$n + 3$
<i>Hypho</i>	$B_nH_n^{8-}$	$B_5H_{11}^{2-}$	$n + 3$	3	$3n + 8$	$n + 4$

Bibliography

- R. W. Rudolph, *Acc. Chem. Res.*, 1976, **9**, 446.
- K. Wade, *Adv. Inorg. Chem. Radiochem.*, 1976, **18**, 1.

This page titled [6.5: Wade's Rules](#) is shared under a [CC BY 3.0](#) license and was authored, remixed, and/or curated by [Andrew R. Barron \(CNX\)](#) via [source content](#) that was edited to the style and standards of the LibreTexts platform.

6.6: Trends for the Oxides of the Group 13 Elements

All of the Group 13 elements form a trivalent oxide (M_2O_3). The chemical properties of the oxides follow the trend acidic to basic going down the Group (Table 6.6.1). The physical properties are consistent with the electronegativities and covalent character in the M-O bonds. Thallium oxide is unique in that it decomposes above 100 °C to yield the thallium(I) oxide, Tl_2O . The other oxides are all stable to high temperatures.

Table 6.6.1: Properties of the Group 13 oxides.

Oxide	Color	Chemical property	Melting point (°C)
B_2O_3	White/colorless	Weak acid	450 (trigonal), 510 (tetrahedral)
Al_2O_3	White/colorless	Amphoteric	2072 (α)
Ga_2O_3	White/colorless	Amphoteric	1900 (α), 1725 (β)
In_2O_3	Yellow	Weakly basic	1910
Tl_2O_3	Brown-black	Basic, oxidizing	100 (decomposes)

Bibliography

- G. E. Jellison, Jr., L. W. Panek, P. J. Bray, and G. B. Rouse, Jr., *J. Chem. Phys.*, 1977, **66**, 802.

This page titled [6.6: Trends for the Oxides of the Group 13 Elements](#) is shared under a [CC BY 3.0](#) license and was authored, remixed, and/or curated by [Andrew R. Barron \(CNX\)](#) via [source content](#) that was edited to the style and standards of the LibreTexts platform.

6.7: Boron Oxides, Hydroxides, and Oxyanions

Oxides

Boron oxide, B_2O_3 , is made by the dehydration of boric acid, (6.7.1). It is a glassy solid with no regular structure, but can be crystallized with extreme difficulty. The structure consists of infinite chains of triangular BO_3 unit (Figure 6.7.1). Boron oxide is acidic and reacts with water to reform boric acid, (6.7.1).

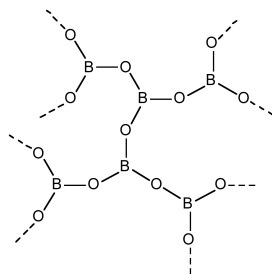


Figure 6.7.1: Glassy structure of B_2O_3 .

The reaction of B_2O_3 with hydroxide yields the metaborate ion, (6.7.2), whose planar structure (Figure 6.7.2) is related to metaboric acid. Boron oxide fuses with a wide range of metal and non-metal oxides to give borate glasses.

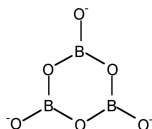
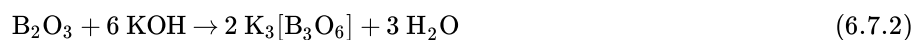


Figure 6.7.2: Structure of the metaborate anion, $[B_3O_6]^{3-}$.

Boric acid

Boric acid, $B(OH)_3$, usually obtained from the dissolution of borax, $Na_2[B_4O_5(OH)_4]$, is a planar solid with intermolecular hydrogen bonding forming a near hexagonal layered structure, broadly similar to graphite (Figure 6.7.3). The inter layer distance is 3.18 Å.

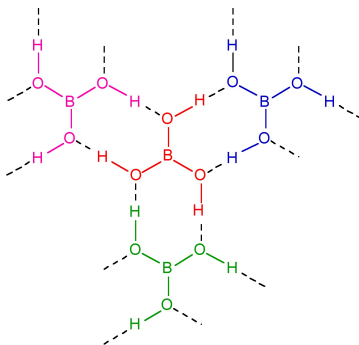


Figure 6.7.3: The hydrogen bonded structure of boric acid.

A summary of reactions of the reactivity of boric acid is shown in Figure 6.7.4.

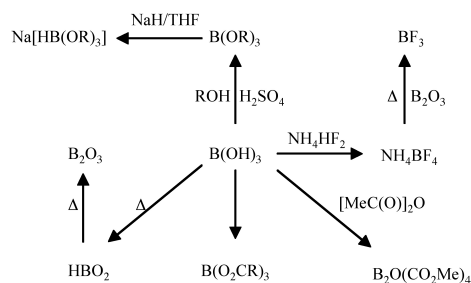


Figure 6.7.4: Selected reactions of boric acid. Adapted from F. A. Cotton and G. Wilkinson, *Advanced Inorganic Chemistry*, 4th Ed. Wiley Interscience (1980).

Upon dissolution of boric acid in water, boric acid does not act as a proton acid, but instead reacts as a Lewis acid, (6.7.3).



The reaction may be followed by ^{11}B NMR spectroscopy from the change in the chemical shift (Figure 6.7.5).

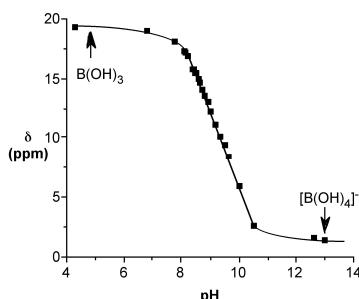


Figure 6.7.5: The ^{11}B NMR chemical shift (ppm) of boric acid as a function of pH. Adapted from M. Bishop, N. Shahid, J. Yang, and A. R. Barron, *Dalton Trans.*, 2004, 2621.

Since the ^{11}B NMR shift is directly proportional to the mole fraction of the total species present as the borate anion (e.g., $[\text{B(OH)}_4]^-$) the ^{11}B NMR chemical shift at a given temperature, $\delta_{\text{(obs)}}$, may be used to calculate both the mole fraction of boric acid and the borate anion, i.e., (6.7.4) and (6.7.5), respectively. Using these equations the relative speciation as a function of pH may be calculated for both boric acid (Figure 6.7.6). The pH at which a 50:50 mixture of acid and anion for boric acid is *ca.* 9.4.

$$\chi_{\text{(acid)}} = \frac{\delta_{\text{(obs)}} - \delta_{\text{(anion)}}}{\delta_{\text{(acid)}} - \delta_{\text{(anion)}}} \quad (6.7.4)$$

$$\chi_{\text{(acid)}} = \frac{\delta_{\text{(acid)}} - \delta_{\text{(obs)}}}{\delta_{\text{(acid)}} - \delta_{\text{(anion)}}} \quad (6.7.5)$$

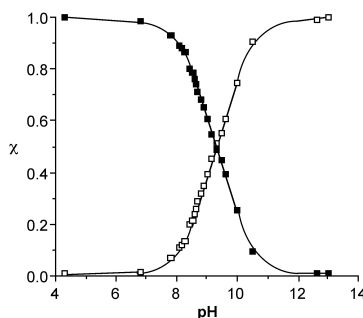
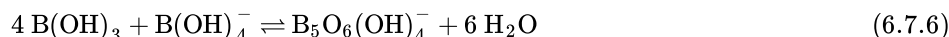


Figure 6.7.6: The mole fraction of acid (black squares) and anion (white squares) forms of boric acid as a function of pH. Adapted from M. Bishop, N. Shahid, J. Yang, and A. R. Barron, *Dalton Trans.*, 2004, 2621.

In concentrated solutions, the borate ion reacts further to form polyborate ions. The identity of the polyborate is dependent on the pH. With increasing pH, $\text{B}_5\text{O}_6(\text{OH})_4^-$, (6.7.5), $\text{B}_3\text{O}_3(\text{OH})_4^-$, (6.7.6), and $\text{B}_4\text{O}_5(\text{OH})_4^{2-}$, (6.7.7), are formed. The structure of each borate is shown in Figure 6.7.7. Once the ratio of B(OH)_3 to B(OH)_4^- is greater than 50%, only the mono-borate is observed.



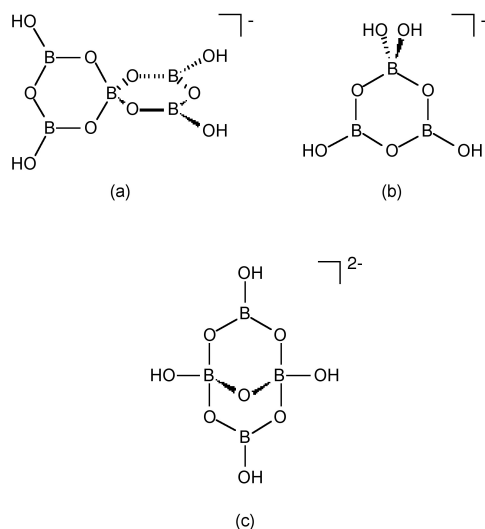
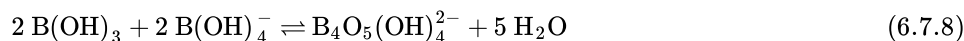
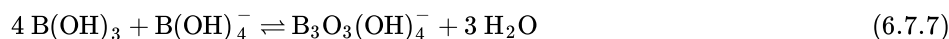


Figure 6.7.7: The structures of the borate anions (a) $\text{B}_5\text{O}_6(\text{OH})_4^-$, (b) $\text{B}_3\text{O}_3(\text{OH})_4^-$, and (c) $\text{B}_4\text{O}_5(\text{OH})_4^{2-}$.

Borax, the usual mineral form of boric acid, is the sodium salt, $\text{Na}_2[\text{B}_4\text{O}_5(\text{OH})_4]$, which upon dissolution in water re-equilibrates to B(OH)_3 .

Enough to make your hair curl

In 1906, a German hairdresser, Charles Nessler who was living in London, decided to help his sister who was fed-up with having to put her straight hair in curlers. While looking for a solution, Nessler noticed that a clothesline contracted in a wavy shape when it was wet. Nessler wound his sister's hair on cardboard tubes; then he covered the hair with borax paste. After wrapping the tubes with paper (to exclude air) he heated the entire mass for several hours. Removing the paper and tubes resulted in curly hair. After much trial and error (presumably at his sister's discomfort) Nessler perfected the method by 1911, and called the process a *permanent wave* (or perm). The process involved the alkaline borax softening the hair sufficiently to be remodeled, while the heating stiffened the borax to hold the hair into shape. The low cost of borax meant that Nessler's method was an immediate success.

Metaboric acid

Heating boric acid results in the partial dehydration to yield metaboric acid, HBO_2 , (6.7.8). Metaboric acid is also formed from the partial hydrolysis of B_2O_3 .



If the heating is carried out below 130 °C, HBO_2 -III is formed in which B_3O_3 rings are joined by hydrogen bonding to the hydroxide on each boron atom (Figure 6.7.8). Continued heating to 150 °C results in HBO_2 -II, whose structure consists of BO_4 tetrahedra and B_2O_5 groups chain linked by hydrogen bonding. Finally, heating above 150 °C yields cubic HBO_2 -I with all the boron atoms tetrahedral.

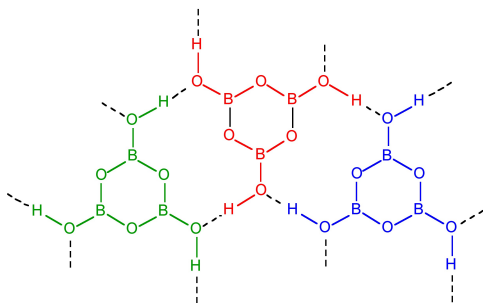


Figure 6.7.8: Structure of the layered structure of HBO_2 -III.

Borate esters

Boric acid reacts with alcohols in the presence of sulfuric acid to form $B(OR)_3$ (Figure 6.7.4). This is the basis for a simple flame test for boron. Treatment of a compounds with methanol/sulfuric acid, followed by placing the reaction product in a flame results in a green flame due to $B(OMe)_3$.

In the presence of diols, polyols, or polysaccharides, boric acid reacts to form alkoxide complexes. In the case of diols, the mono-diol $[B(OH)_2L]^-$ (Figure 6.7.9a) and the bis-diol $[BL_2]^-$ (Figure 6.7.9b) complexes.

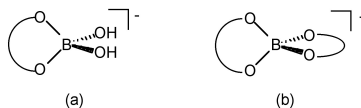
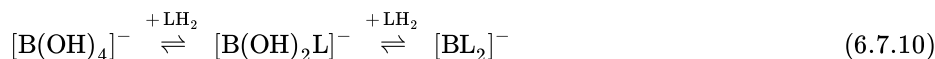


Figure 6.7.9: Structure of (a) the $[B(OH)_2L]^-$ and (b) the $[BL_2]^-$ anions formed by the reaction of boric acid (or borate) with a diol.

Originally it was proposed that diols react with the anion rather than boric acid, (6.7.9). In contrast, it was suggested that the optimum pH for the formation of carboxylic acid complexes is under the condition where pK_a (carboxylic acid) $< pH < pK_a$ (boric acid). Under these conditions it is the boric acid, $B(OH)_3$, not the borate anion, $[B(OH)_4]^-$, that reacts to form the complex.



The conversion of boric acid to borate (6.7.3) must occur through attack of hydroxide or the deprotonation of a coordinated water ligand, either of which is related to the pK_a of water. The formation of $[B(OH)_2L]^-$ from $B(OH)_3$ would be expected therefore to occur via a similar initial reaction (attack by RO^- or deprotonation of coordinated ROH) followed by a subsequent elimination of H_2O and the formation of a chelate coordination, and would therefore be related to the pK_a of the alcohol. Thus the pH at which $[B(OH)_2L]^-$ is formed relative to $[B(OH)_4]^-$ will depend on the relative acidity of the alcohol. The pK_a of a simple alcohol (e.g., MeOH = 15.5, EtOH = 15.9) are close to the value for water (15.7) and the lowest pH at which $[B(OH)_2L]^-$ is formed should be comparable to that at which $[B(OH)_4]^-$ forms. Thus, the formation of $[B(OH)_2L]^-$ as compared to $[B(OH)_4]^-$ is a competition between the reaction of $B(OH)_3$ with RO^- and OH^- (Figure 6.7.10), and as with carboxylic acids it is boric acid not borate that reacts with the alcohol, (6.7.10).

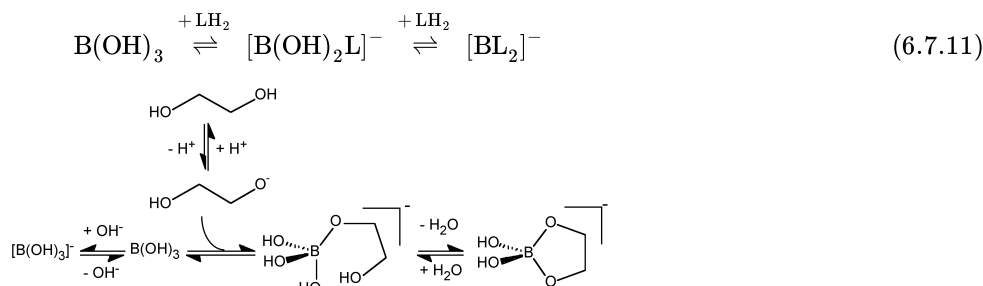


Figure 6.7.10: Competition between hydroxide and 1,2-diol for complexation to boron in the aqueous boric acid/diol system.

A key issue in the structural characterization and understanding of the diol/boric acid system is the assignment of the ^{11}B NMR spectral shifts associated with various complexes. A graphical representation of the observed shift ranges for boric acid chelate systems is shown in Figure 6.7.11.

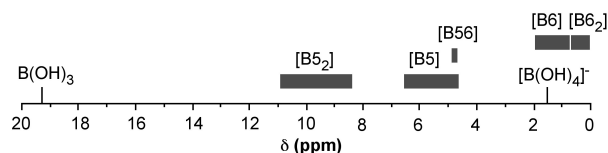


Figure 6.7.11: ^{11}B NMR spectroscopic shifts of chelate alkoxide compounds in comparison with boric acid and borate anion. The acronyms [B5] and [B6] are used to denote a borate complex of a 1,2-diol and 1,3-diol forming a chelate 5-membered and 6-membered ring cycle, respectively. Similarly, [B5₂] and [B6₂] denotes a borate complex of two 1,2-diols or 1,3-diols both forming $[BL_2]^-$. Adapted from M. Bishop, N. Shahid, J. Yang, and A. R. Barron, *Dalton Trans.*, 2004, 2621.

Boric acid cross-linking of guar gum for hydraulic fracturing fluids

Thick gels of guar gum cross-linked with borax or a transition metal complex are used in the oil well drilling industry as hydraulic fracturing fluids. The polysaccharide guaran ($M_w \approx 10^6$ Da) is the major (>85 wt%) component of guar gum, and consists of a (1 → 4)-β-D-mannopyranosyl backbone with α-D-galactopyranosyl side chain units attached via (1 → 6) linkages. Although the

exact ratio varies between different crops of guar gum the general structure is consistent with about one galactose to every other mannose (Figure 6.7.12).

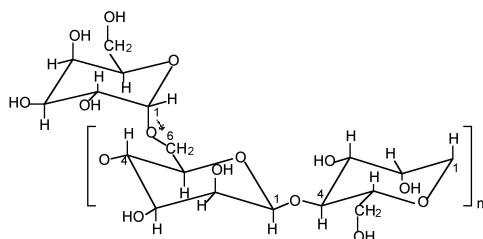


Figure 6.7.12: The repeat unit of guaran, a naturally occurring polysaccharide, consisting of (1 → 4)-β-D-mannopyranosyl units with α-D-galactopyranosyl side chains attached to about every other mannose via (1 → 6) linkages.

The synthesis of a typical boric acid cross-linked guar gel, with viscosity properties suitable for use as a fracturing fluid, involves mixing guar gum, water and boric acid, $B(OH)_3$, in a 10:2000:1 wt/wt ratio. Adjusting the pH to between 8.5 and 9 results in a viscous gel. The boron:guaran ratio corresponds to almost 2 boron centers per 3 monosaccharide repeat units. Such a large excess of boric acid clearly indicates that the system is not optimized for cross-linking, i.e., a significant fraction of the boric acid is ineffective as a cross-linking agent.

The reasons for the inefficiency of boric acid to cross-link guaran (almost 2 borate ions per 3 monosaccharide repeat unit are required for a viscous gel suitable as a fracturing fluid): the most reactive sites on the component saccharides (mannose and galactose) are precluded from reaction by the nature of the guar structure; the comparable acidity (pK_a) of the remaining guaran alcohol substituents and the water solvent, results in a competition between cross-linking and borate formation; a significant fraction of the boric acid is ineffective in cross-linking guar due to the modest equilibrium (K_{eq}).

Bibliography

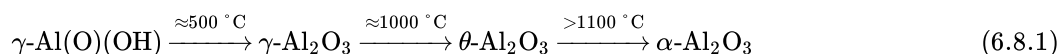
- F. A. Cotton and G. Wilkinson, *Advanced Inorganic Chemistry*, 4th Ed. Wiley Interscience (1980).
- M. Bishop, N. Shahid, J. Yang, and A. R. Barron, *Dalton Trans.*, 2004, 2621.
- M. Van Duin, J. A. Peters, A. P. G. Kieboom, and H. Van Bekkum, *Tetrahedron*, 1984, **40**, 2901.
- *Zonal Isolation*, "Borate Crosslinked Fluids," by R. J. Powell and J. M Terracina, Halliburton, Duncan, OK (1998).
- R. Schechter, *Oil Well Stimulation*, Prentice-Hall Inc., Englewood Cliffs, NJ (1992).
- S. Kesavan and R. K. Prud'homme, *Macromolecules*, 1992, **25**, 2026.

6.7: Boron Oxides, Hydroxides, and Oxyanions is shared under a CC BY 1.0 license and was authored, remixed, and/or curated by LibreTexts.

6.8: Aluminum Oxides, Hydroxides, and Hydrated Oxides

The many forms of aluminum oxides and hydroxides are linked by complex structural relationships. Bauxite has the formula $\text{Al}_x(\text{OH})_{3-2x}$ ($0 < x < 1$) and is thus a mixture of Al_2O_3 (α -alumina), $\text{Al}(\text{OH})_3$ (gibbsite), and $\text{AlO}(\text{OH})$ (boehmite). The latter is an industrially important compound that is used in the form of a gel as a pre-ceramic in the production of fibers and coatings, and as a fire-retarding agent in plastics.

Knowledge of microstructural evolution in ceramic systems is important in determining their end-use application. In this regard alumina has been the subject of many studies in which the phase, morphology, porosity and crystallinity are controlled by physical and chemical processing. The transformation from boehmite [$\gamma\text{-Al}(\text{O})(\text{OH})$] to corundum ($\alpha\text{-Al}_2\text{O}_3$) has been well characterized and is known to go through the following sequence:



The phase changes from boehmite through $\theta\text{-Al}_2\text{O}_3$ are known to be topotactic (i.e., changes in crystal structure are accomplished without changes in crystalline morphology), however, each phase change is accompanied by a change in porosity. The θ - to $\alpha\text{-Al}_2\text{O}_3$ phase transition occurs through nucleation and growth of the $\theta\text{-Al}_2\text{O}_3$ crystallites. The $\alpha\text{-Al}_2\text{O}_3$ phase transition temperature can be altered by the addition of certain additives. For example, because the $\alpha\text{-Al}_2\text{O}_3$ phase occurs by nucleation, the addition of small seed crystals can lower the transition temperature between 100 and 200 $^\circ\text{C}$. The addition of certain transition metals (chromium, manganese, iron, cobalt, nickel, and copper) has also been shown to decrease the transition temperature, while lanthanum or rare earth metals tend to increase the temperature. Finally, the addition of metal oxides has also shown to affect the growth rate in $\alpha\text{-Al}_2\text{O}_3$.

A third form of Al_2O_3 forms on the surface of the clean aluminum metal, (6.8.2). This oxide skin is rapidly self-repairing because its heat of formation is so large ($\Delta H = 3351\text{ kJ/mol}$). The thin, tough, transparent oxide layer is the reason for much of the usefulness of aluminum.



Bibliography

- K. Wefers and C. Misra, *Oxides and Hydroxides of Aluminum*, Alcoa Laboratories (1987).
- H. L. Wen and F. S. Yen, *J. Cryst. Growth*, 2000, **208**, 696.
- G. K Priya, P. Padmaja, K. G. K. Warriar, A. D. Damodaran, and G. Aruldas, *J. Mater. Sci. Lett.*, 1997, **16**, 1584.
- E. Prouzet, D. Fargeot, and J. F. Baumard, *J. Mater. Sci. Lett.*, 1990, **9**, 779.

6.8: Aluminum Oxides, Hydroxides, and Hydrated Oxides is shared under a [CC BY 1.0](https://creativecommons.org/licenses/by/1.0/) license and was authored, remixed, and/or curated by LibreTexts.

6.9: Ceramic Processing of Alumina

Introduction

While aluminum is the most abundant metal in the earth's crust (*ca.* 8%) and aluminum compounds such as alum, $K[Al(SO_4)_2] \cdot 12(H_2O)$, were known throughout the world in ancient times, it was not until the isolation of aluminum in the late eighteenth century by the Danish scientist H. C. Ørsted that research into the chemistry of the Group 13 elements began in earnest. Initially, metallic aluminum was isolated by the reduction of aluminum trichloride with potassium or sodium; however, with the advent of inexpensive electric power in the late 1800's, it became economically feasible to extract the metal *via* the electrolysis of alumina (Al_2O_3) dissolved in cryolite, Na_3AlF_6 , (the Hall-Heroult process). Today, alumina is prepared by the Bayer process, in which the mineral bauxite (named for Les Baux, France, where it was first discovered) is dissolved with aqueous hydroxides, and the solution is filtered and treated with CO_2 to precipitate alumina. With availability of both the mineral and cheap electric power being the major considerations in the economical production of aluminum, it is not surprising that the leading producers of aluminum are the United States, Japan, Australia, Canada, and the former Soviet Union.

Aluminum oxides and hydroxides

The many forms of aluminum oxides and hydroxides are linked by complex structural relationships. Bauxite has the formula $Al_x(OH)_{3-2x}$ ($0 < x < 1$) and is thus a mixture of Al_2O_3 (α -alumina), $Al(OH)_3$ (gibbsite), and $AlO(OH)$ (boehmite). The latter is an industrially important compound which is used in the form of a gel as a pre-ceramic in the production of fibers and coatings, and as a fire retarding agent in plastics.

Heating boehmite and diaspore to 450 °C causes dehydration to yield forms of alumina which have structures related to their oxide-hydroxide precursors. Thus, boehmite produces the low-temperature form γ -alumina, while heating diaspore will give α -alumina (corundum). γ -alumina converts to the hcp structure at 1100 °C. A third form of Al_2O_3 forms on the surface of the clean aluminum metal. The thin, tough, transparent oxide layer is the reason for much of the usefulness of aluminum. This oxide skin is rapidly self-repairing because its heat of formation is so large ($\Delta H = -3351$ kJ/mol).



Ternary and mixed-metal oxides

A further consequence of the stability of alumina is that most if not all of the naturally occurring aluminum compounds are oxides. Indeed, many precious gemstones are actually corundum doped with impurities. Replacement of aluminum ions with trace amounts of transition-metal ions transforms the formerly colorless mineral into ruby (red, Cr^{3+}), sapphire (blue, $Fe^{2+/3+}$, Ti^{4+}), or topaz (yellow, Fe^{3+}). The addition of stoichiometric amounts of metal ions causes a shift from the α - Al_2O_3 hcp structure to the other common oxide structures found in nature. Examples include the perovskite structure for ABO_3 type minerals (e.g., $CeTiO_7$ or $LaAlO_3$) and the spinel structure for AB_2O_4 minerals (e.g., beryl, $BeAl_2O_4$).

Aluminum oxide also forms ternary and mixed-metal oxide phases. Ternary systems such as mullite ($Al_6Si_2O_{13}$), yttrium aluminum garnet (YAG, $Y_3Al_5O_{12}$), the β -aluminas (e.g., $NaAl_3O_8$) and aluminates such as hibonite ($CaAl_{12}O_{19}$) possessing β -alumina or magnetoplumbite-type structures can offer advantages over those of the binary aluminum oxides.

Applications of these materials are found in areas such as engineering composite materials, coatings, technical and electronic ceramics, and catalysts. For example, mullite has exceptional high temperature shock resistance and is widely used as an infrared-transparent window for high temperature applications, as a substrate in multilayer electronic device packaging, and in high temperature structural applications. Hibonite and other hexaaluminates with similar structures are being evaluated as interfacial coatings for ceramic matrix composites due to their high thermal stability and unique crystallographic structures. Furthermore, aluminum oxides doped with an alkali, alkaline earth, rare earth, or transition metal are of interest for their enhanced chemical and physical properties in applications utilizing their unique optoelectronic properties.

Synthesis of aluminum oxide ceramics

In common with the majority of oxide ceramics, two primary synthetic processes are employed for the production of aluminum oxide and mixed metal oxide materials:

1. The traditional ceramic powder process.
2. The solution-gelation, or "sol-gel" process.

The environmental impact of alumina and alumina-based ceramics is in general negligible; however, the same cannot be said for these methods of preparation. As practiced commercially, both of the above processes can have a significant detrimental environmental impact.

Traditional ceramic processing

Traditional ceramic processing involves three basic steps generally referred to as powder-processing, shape-forming, and densification, often with a final mechanical finishing step. Although several steps may be energy intensive, the most direct environmental impact arises from the shape-forming process where various binders, solvents, and other potentially toxic agents are added to form and stabilize a solid ("green") body (Table 6.9.1).

Table 6.9.1: Typical composition of alumina green body

Function	Composition	Volume (%)
Powder	alumina (Al ₂ O ₃)	27
Solvent	1,1,1-trichloroethane/ethanol	58
Deflocculant	menhaden oil	1.8
Binder	poly(vinyl butyrol)	4.4
Plasticizer	poly(ethylene glycol)/octyl phthalate	8.8

The component chemicals are mixed to a slurry, cast, then dried and fired. In addition to any innate health risk associated with the chemical processing these agents are subsequently removed in gaseous form by direct evaporation or pyrolysis. The replacement of chlorinated solvents such as 1,1,1-trichloroethylene (TCE) must be regarded as a high priority for limiting environmental pollution. The United States Environmental Protection Agency (EPA) included TCE on its 1991 list of 17 high-priority toxic chemicals targeted for source reduction. The plasticizers, binders, and alcohols used in the process present a number of potential environmental impacts associated with the release of combustion products during firing of the ceramics, and the need to recycle or discharge alcohols which, in the case of discharge to waterways, may exert high biological oxygen demands in the receiving communities. It would be desirable, therefore, to be able to use aqueous processing; however, this has previously been unsuccessful due to problems associated with batching, milling, and forming. Nevertheless, with a suitable choice of binders, etc., aqueous processing is possible. Unfortunately, in many cast-parts formed by green body processing the liquid solvent alone consists of over 50 % of the initial volume, and while this is not directly of an environmental concern, the resultant shrinkage makes near net shape processing difficult.

Sol-gel

Whereas the traditional sintering process is used primarily for the manufacture of dense parts, the solution-gelation (sol-gel) process has been applied industrially primarily for the production of porous materials and coatings.

Sol-gel involves a four stage process: dispersion, gelation, drying, and firing. A stable liquid dispersion or *sol* of the colloidal ceramic precursor is initially formed in a solvent with appropriate additives. By changing the concentration (aging) or pH, the dispersion is "polymerized" to form a solid dispersion or *gel*. The excess liquid is removed from this gel by drying and the final ceramic is formed by firing the gel at higher temperatures.

The common sol-gel route to aluminum oxides employs aluminum hydroxide or hydroxide-based material as the solid colloid, the second phase being water and/or an organic solvent, however, the strong interactions of the freshly precipitated alumina gels with ions from the precursor solutions makes it difficult to prepare these gels in pure form. To avoid this complication, alumina gels are also prepared from the hydrolysis of aluminum alkoxides, Al(OR)₃.



The exact composition of the gel in commercial systems is ordinarily proprietary, however, a typical composition will include an aluminum compound, a mineral acid, and a complexing agent to inhibit premature precipitation of the gel, e.g., Table 6.9.2.

Table 6.9.2: Typical composition of an alumina sol-gel for slipcast ceramics.

Function	Composition
Boehmite precursor	ASB [aluminum <i>sec</i> -butoxide, $\text{Al}(\text{OC}_4\text{H}_9)_3$]
Electrolyte	HNO_3 0.07 mole/mole ASB
Complexing agent	glycerol <i>ca.</i> 10 wt.%

The principal environmental consequences arising from the sol-gel process are those associated with the use of strong acids, plasticizers, binders, solvents, and *sec*-butanol formed during the reaction. Depending on the firing conditions, variable amounts of organic materials such as binders and plasticizers may be released as combustion products. NO_x 's may also be produced in the off-gas from residual nitric acid or nitrate salts. Moreover, acids and solvents must be recycled or disposed of. Energy consumption in the process entails "upstream" environmental emissions associated with the production of that energy.

Bibliography

- *Advances in Ceramics*, Eds. J. A. Mangels and G. L. Messing, American Ceramic Society, Westville, OH, 1984, Vol. 9.
- Adkins, *J. Am. Chem. Soc.*, 1922, **44**, 2175.
- A. R. Barron, *Comm. Inorg. Chem.*, 1993, **14**, 123.
- M. K. Cinibulk, *Ceram. Eng. Sci., Proc.*, 1994, **15**, 721.
- F. A. Cotton and G. Wilkinson, *Advanced Inorganic Chemistry*, 5th Ed., John Wiley and Sons, New York (1988).
- N. N. Greenwood and A. Earnshaw, *Chemistry of the Elements*, Pergamon Press, Oxford (1984).
- P. H. Hsu and T. F. Bates, *Mineral Mag.*, 1964, **33**, 749.
- W. D. Kingery, H. K. Bowen, and D. R. Uhlmann, *Introduction to Ceramics*, 2nd Ed. Wiley, New York (1976).
- H. Schneider, K. Okada, and J. Pask, *Mullite and Mullite Ceramics*, Wiley (1994).
- R. V. Thomas, *Systems Analysis and Water Quality Management*, McGraw-Hill, New York (1972).
- J. C. Williams, in *Treatise on Materials Science and Technology*, Ed. F. F. Y. Wang, Academic Press, New York (1976).

6.9: Ceramic Processing of Alumina is shared under a [CC BY 1.0](https://creativecommons.org/licenses/by/1.0/) license and was authored, remixed, and/or curated by LibreTexts.

6.10: Boron Compounds with Nitrogen Donors

The “B-N” unit is isoelectronic (3 + 5 valence electrons) to the “C-C” unit (4 + 4 valence electrons). The two moieties are also isolobal, and as such there are many of the compound types formed by carbon have analogous derivatives in the chemistry of boron-nitrogen.

Lewis acid-base addition compounds

Boron compounds, BX_3 , are strong Lewis acids and as such form stable addition compounds with Lewis bases, in particular those with nitrogen donor ligands.



In principle these Lewis acid-base complexes should be similar to their isolobal hydrocarbon analogs, however, whereas the dipole in ethane is zero (by symmetry) the dipole in H_3NBH_3 is 5.2 D as a consequence of the difference in the Pauling electronegativities (i.e., B = 2.04 and N = 3.04). It is this dipole that generally differentiates the B-N compounds from their C-C analogs.

Homolytic cleavage of the C-C bond in ethane will yield two neutral methyl radicals, (6.7.2). In contrast, heterolytic cleavage will result in the formation of two charged species, (6.7.3). Thus, the products either have a net spin, (6.7.2), or a net charge, (6.7.3). By contrast, cleavage of the B-N bond in H_3N-BH_3 either yields products with both spin and charge, (6.7.5), or neither, (6.7.4). Heterolytic cleavage of the B-N bond yields neutral compounds, (6.7.4), while homolytic cleavage results in the formation of radical ions, (6.7.5).



The difference in bond strength between H_3N-BH_3 and ethane is reflected in the difference in bond lengths (Table 6.10.1).

Table 6.10.1: A comparison of bonding in $H_3E-E'H_3$.

Compound	Bond length (Å)	Bond strength (kcal/mol)
H_3C-CH_3	1.533	89
H_3N-BH_3	1.658	31

Aminoboranes

The group R'_2N-BR_2 is isoelectronic and isolobal to the olefin sub-unit $R'_2C=CR_2$, and there is even appreciable π -bonding character (Figure 6.10.1). A measure of the multiple bond character can be seen from a comparison of the calculated B-N bond in H_2NBN_2 (1.391 Å) as compared to a typical olefin (1.33 Å). It is interesting that a consideration of the possible resonance form (Figure 6.10.1) suggest the dipole in the σ -bond is in the opposite direction of that of the π -bond.

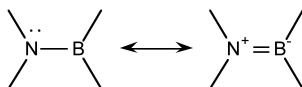


Figure 6.10.1: Resonance forms for $X_2N-BX'_2$.

Unlike olefins, borazines oligomerize to form dimers and trimers (Figure 6.10.2) in the absence of significant steric hindrance. Analogous structures are also observed for the other Group 13-15 homologs ($R_2AlNR'_2$, $R_2GaPR'_2$, etc.).

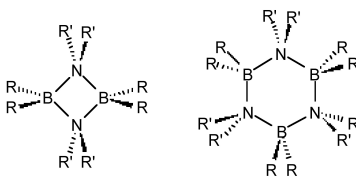
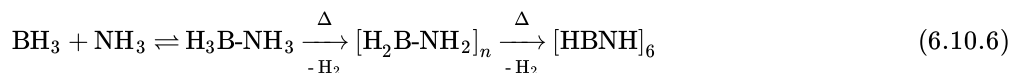


Figure 6.10.2: Typical structures of aminoboranes.

Borazines

The condensation of boron hydride with ammonia results in the formation of a benzene analog: borazine, (6.7.6). Substituted derivatives are formed by the reaction with primary amines.



Despite the cyclic structure (Figure 6.10.3), borazine is not a true analog of benzene. Despite all the B-N bond distances being equal (1.44 Å) consistent with a delocalized structure, the difference in electronegativity of boron and nitrogen (2.04 and 3.04, respectively) results in a polarization of the bonds (i.e., $\text{B}^{\delta+}\text{-N}^{\delta-}$) and hence a limit to the delocalization. The molecular orbitals of the π -system in borazine are lumpy in appearance (Figure 6.10.4 a) compared to benzene (Figure 6.10.4 b). This uneven distribution makes borazine prone to addition reactions, making it as a molecule less stable than benzene.

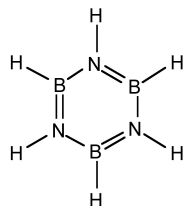


Figure 6.10.3: Structure of borazine, the inorganic analog to benzene.

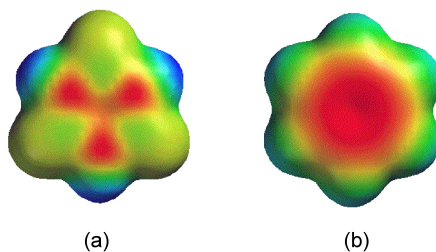


Figure 6.10.4: Probability distributions for the π -bond orbitals in (a) borazine and (b) benzene.

Iminoboranes: analogs of acetylene

Iminoboranes, $\text{RB=NR}'$, are analogs of alkynes, but like aminoboranes are only isolated as monomers with sterically hindered substituents. In the absence of sufficient steric bulk oligomerization occurs, forming substituted benzene analogs.

Boron nitrides: analogs of elemental carbon

The fusion of borax, $\text{Na}_2[\text{B}_4\text{O}_5(\text{OH})_4]$ with ammonium chloride (NH_4Cl) results in the formation of hexagonal boron nitride (h-BN). Although h-BN has a planar, layered structure consisting of six-membered rings similar to graphite (Figure 6.10.5), it is a white solid. The difference in color is symptomatic of the more localized bonding in BN than in graphite.

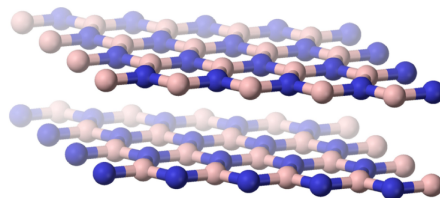


Figure 6.10.5: Structure of h-BN.

As is found for its carbon analog, hexagonal boron nitride (h-BN or α -BN) is converted at high temperatures (600 – 2000 °C) and pressures (50 – 200 kbar) to a cubic phase (c-BN or β -BN). In a similar manner to diamond, cubic-BN is very hard being actually able to cut diamond, and as a consequence its main use is as an industrial grinding agent. The cubic form has the sphalerite crystal structure (Figure 6.10.6). Finally, a wurtzite form of boron nitride (w-BN) is known that has similar structure as lonsdaleite, rare hexagonal polymorph of carbon. Table 6.10.2 shows a comparison of the properties of the hexagonal and cubic phases of BN with their carbon analogs.

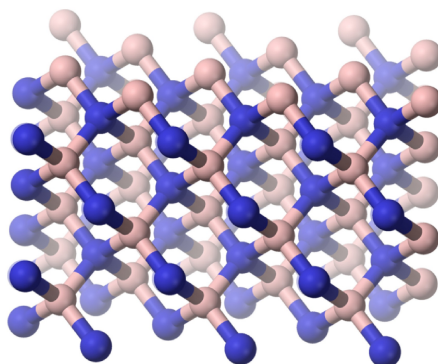


Figure 6.10.6: Structure of c-BN.

Table 6.10.2: Comparison of structural and physical properties of carbon and boron nitride analogs.

Phase	Carbon	Boron nitride
Cubic	Colorless, hard, mp = 3550 °C. C-C = 1.514 Å	Colorless, hard, B-N = 1.56 Å
Hexagonal	Black solid, planar layers, conductor, mp = 3652 – 3697 °C (sublimes), C-C = 1.415 Å	White solid, planar layers, semiconductor (Eg = 5.2 eV), mp = 2973 °C (sublimes), B-N = 1.45 Å

The partly ionic structure of BN layers in h-BN reduces covalency and electrical conductivity, whereas the interlayer interaction increases resulting in higher hardness of h-BN relative to graphite.

Bibliography

- K. M. Bissett and T. M. Gilbert, *Organometallics*, 2004, **23**, 850.
- P. Paetzold, *Adv. Inorg. Chem.*, 1987, **31**, 123.
- L. R. Thorne, R. D. Suenram, and F. J. Lovas, *J. Chem. Phys.*, 1983, **78**, 167.

6.10: Boron Compounds with Nitrogen Donors is shared under a [CC BY 1.0](https://creativecommons.org/licenses/by/1.0/) license and was authored, remixed, and/or curated by LibreTexts.

6.11: Properties of Gallium Arsenide

Gallium: the element

The element gallium was predicted, as eka-aluminum, by Mendeleev in 1870, and subsequently discovered by Lecoq de Boisbaudran in 1875; in fact de Boisbaudran had been searching for the missing element for some years, based on his own independent theory. The first experimental indication of gallium came with the observation of two new violet lines in the spark spectrum of a sample deposited on zinc. Within a month of these initial results de Boisbaudran had isolated 1 g of the metal starting from several hundred kilograms of crude zinc blende ore. The new element was named in honor of France (Latin *Gallia*), and the striking similarity of its physical and chemical properties to those predicted by Mendeleev (Table 6.11.1) did much to establish the general acceptance of the periodic Law; indeed, when de Boisbaudran first stated that the density of Ga was 4.7 g/cm^3 rather than the predicted 5.9 g/cm^3 , Mendeleev wrote to him suggesting that he redetermine the value (the correct value is 5.904 g/cm^3).

Table 6.11.1: Comparison of predicted and observed properties of gallium.

Property	Mendeleev's prediction (1871) for eka-aluminum, M	Observed properties of gallium (discovered 1875)
Atomic weight	ca. 68	69.72
Density, $\text{g}\cdot\text{cm}^{-3}$	5.9	5.904
Melting point	Low	29.78
Vapor pressure	Non-volatile	10^{-3} mmHg , 1000 °C
Valence	3	3
Oxide	M_2O_3	Ga_2O_3
Density of oxide (g/cm^3)	5.5	5.88
Properties of metal	M should dissolve slowly in acids and alkalis and be stable in air	Ga metal dissolves slowly in acids and alkalis and is stable in air
Properties of hydroxide	$\text{M}(\text{OH})_3$ should dissolve in both acids and alkalis	$\text{Ga}(\text{OH})_3$ dissolves in both acids and alkalis
Properties of salts	M salts will tend to form basic salts; the sulfate should form alums; M_2S_3 should be precipitated by H_2S or $(\text{NH}_4)_2\text{S}$; anhydrous MCl_3 should be more volatile than ZnCl_2	Ga salts readily hydrolyze and form basic salts; alums are known; Ga_2S_3 can be precipitated under special conditions by H_2S or $(\text{NH}_4)_2\text{S}$, anhydrous GaCl_3 is more volatile than ZnCl_2 .

Gallium has a beautiful silvery blue appearance; it wets glass, porcelain, and most other surfaces (except quartz, graphite, and Teflon®) and forms a brilliant mirror when painted on to glass. The atomic radius and first ionization potential of gallium are almost identical with those of aluminum and the two elements frequently resemble each other in chemical properties. Both are amphoteric, but gallium is less electropositive as indicated by its lower electrode potential. Differences in the chemistry of the two elements can be related to the presence of a filled set of 3d orbitals in gallium.

Gallium is very much less abundant than aluminum and tends to occur at low concentrations in sulfide minerals rather than as oxides, although gallium is also found associated with aluminum in bauxite. The main source of gallium is as a by-product of aluminum refining. At 19 ppm of the earth's crust, gallium is about as abundant as nitrogen, lithium and lead; it is twice as abundant as boron (9 ppm), but is more difficult to extract due to the lack of any major gallium-containing ore. Gallium always occurs in association either with zinc or germanium, its neighbors in the periodic table, or with aluminum in the same group. Thus, the highest concentrations (0.1 - 1%) are in the rare mineral germanite (a complex sulfide of Zn, Cu, Ge, and As); concentrations in sphalerite (ZnS), bauxite, or coal, are a hundred-fold less.

Gallium pnictides

Gallium's main use is in semiconductor technology. For example, GaAs and related compounds can convert electricity directly into coherent light (laser diodes) and is employed in electroluminescent light-emitting diodes (LED's); it is also used for doping other semiconductors and in solid-state devices such as heterojunction bipolar transistors (HBTs) and high power high speed metal semiconductor field effect transistors (MESFETs). The compound MgGa_2O_4 is used in ultraviolet-activated powders as a brilliant green phosphor used in Xerox copying machines. Minor uses are as high-temperature liquid seals, manometric fluids and heat-transfer media, and for low-temperature solders.

Undoubtedly the binary compounds of gallium with the most industrial interest are those of the Group 15 (V) elements, GaE (E = N, P, As, Sb). The compounds which gallium forms with nitrogen, phosphorus, arsenic, and antimony are isoelectronic with the Group 14 elements. There has been considerable interest, particularly in the physical properties of these compounds, since 1952 when Welker first showed that they had semiconducting properties analogous to those of silicon and germanium.

Gallium phosphide, arsenide, and antimonide can all be prepared by direct reaction of the elements; this is normally done in sealed silica tubes or in a graphite crucible under hydrogen. Phase diagram data is hard to obtain in the gallium-phosphorus system because of loss of phosphorus from the bulk material at elevated temperatures. Thus, GaP has a vapor pressure of more than 13.5 atm at its melting point; as compared to 0.89 atm for GaAs. The physical properties of these three compounds are compared with those of the nitride in Table 6.11.2 All three adopt the zinc blende crystal structure and are more highly conducting than gallium nitride.

Table 6.11.2: Physical properties of 13-15 compound semiconductors. ^a Values given for 300 K. ^b Dependent on photon energy; values given for 1.5 eV incident photons. ^c Dependent on temperature; values given for 300 K.

Property	GaN	GaP	GaAs	GaSb
Melting point (°C)	> 1250 (dec)	1350	1240	712
Density (g/cm ³)	ca. 6.1	4.138	5.3176	5.6137
Crystal structure	Würtzite	zinc blende	zinc blende	zinc blende
Cell dimen. (Å) ^a	$a = 3.187, c = 5.186$	$a = 5.4505$	$a = 5.6532$	$a = 6.0959$
Refractive index ^b	2.35	3.178	3.666	4.388
k (ohm ⁻¹ cm ⁻¹)	$10^{-9} - 10^{-7}$	$10^{-2} - 10^2$	$10^{-6} - 10^3$	6 - 13
Band gap (eV) ^c	3.44	2.24	1.424	0.71

Gallium arsenide versus silicon

Gallium arsenide is a compound semiconductor with a combination of physical properties that has made it an attractive candidate for many electronic applications. From a comparison of various physical and electronic properties of GaAs with those of Si (Table 6.11.3) the advantages of GaAs over Si can be readily ascertained. Unfortunately, the many desirable properties of gallium arsenide are offset to a great extent by a number of undesirable properties, which have limited the applications of GaAs based devices to date.

Table 6.11.3: Comparison of physical and semiconductor properties of GaAs and Si.

Properties	GaAs	Si
Formula weight	144.63	28.09
Crystal structure	zinc blende	diamond
Lattice constant	5.6532	5.43095
Melting point (°C)	1238	1415
Density (g/cm ³)	5.32	2.328
Thermal conductivity (W/cm.K)	0.46	1.5
Band gap (eV) at 300 K	1.424	1.12

Properties	GaAs	Si
Intrinsic carrier conc. (cm^{-3})	1.79×10^6	1.45×10^{10}
Intrinsic resistivity (ohm.cm)	10^8	2.3×10^5
Breakdown field (V/cm)	4×10^5	3×10^5
Minority carrier lifetime (s)	10^{-8}	2.5×10^{-3}
Mobility ($\text{cm}^2/\text{V.s}$)	8500	1500

Band gap

The band gap of GaAs is 1.42 eV; resulting in photon emission in the infra-red range. Alloying GaAs with Al to give $\text{Al}_x\text{Ga}_{1-x}\text{As}$ can extend the band gap into the visible red range. Unlike Si, the band gap of GaAs is direct, i.e., the transition between the valence band maximum and conduction band minimum involves no momentum change and hence does not require a collaborative particle interaction to occur. Photon generation by inter-band radiative recombination is therefore possible in GaAs. Whereas in Si, with an indirect band-gap, this process is too inefficient to be of use. The ability to convert electrical energy into light forms the basis of the use of GaAs, and its alloys, in optoelectronics; for example in light emitting diodes (LEDs), solid state lasers (light amplification by the stimulated emission of radiation).

A significant drawback of small band gap semiconductors, such as Si, is that electrons may be thermally promoted from the valence band to the conduction band. Thus, with increasing temperature the thermal generation of carriers eventually becomes dominant over the intentionally doped level of carriers. The wider band gap of GaAs gives it the ability to remain 'intentionally' semiconducting at higher temperatures; GaAs devices are generally more stable to high temperatures than a similar Si devices.

Carrier density

The low intrinsic carrier density of GaAs in a pure (undoped) form indicates that GaAs is intrinsically a very poor conductor and is commonly referred to as being semi-insulating. This property is usually altered by adding dopants of either the p- (positive) or n- (negative) type. This semi-insulating property allows many active devices to be grown on a single substrate, where the semi-insulating GaAs provides the electrical isolation of each device; an important feature in the miniaturization of electronic circuitry, i.e., VLSI (very-large-scale-integration) involving over 100,000 components per chip (one chip is typically between 1 and 10 mm square).

Electron mobility

The higher electron mobility in GaAs than in Si potentially means that in devices where electron transit time is the critical performance parameter, GaAs devices will operate with higher response times than equivalent Si devices. However, the fact that hole mobility is similar for both GaAs and Si means that devices relying on cooperative electron and hole movement, or hole movement alone, show no improvement in response time when GaAs based.

Crystal growth

The bulk crystal growth of GaAs presents a problem of stoichiometric control due the loss, by evaporation, of arsenic both in the melt and the growing crystal ($> ca. 600^\circ\text{C}$). Melt growth techniques are, therefore, designed to enable an overpressure of arsenic above the melt to be maintained, thus preventing evaporative losses. The loss of arsenic also negates diffusion techniques commonly used for wafer doping in Si technology; since the diffusion temperatures required exceed that of arsenic loss.

Crystal Stress

The thermal gradient and, hence, stress generated in melt grown crystals have limited the maximum diameter of GaAs wafers (currently 6" diameter compared to over 12" for Si), because with increased wafer diameters the thermal stress generated dislocation (crystal imperfections) densities eventually becomes unacceptable for device applications.

Physical strength

Gallium arsenide single crystals are very brittle, requiring that considerably thicker substrates than those employed for Si devices.

Native oxide

Gallium arsenide's native oxide is found to be a mixture of non-stoichiometric gallium and arsenic oxides and elemental arsenic. Thus, the electronic band structure is found to be severely disrupted causing a breakdown in 'normal' semiconductor behavior on the GaAs surface. As a consequence, the GaAs MISFET (metal-insulator-semiconductor-field-effect-transistor) equivalent to the technologically important Si based MOSFET (metal-oxide-semiconductor-field-effect-transistor) is, therefore, presently unavailable.

The passivation of the surface of GaAs is therefore a key issue when endeavoring to utilize the FET technology using GaAs. Passivation in this discussion means the reduction in mid-gap band states which destroy the semiconducting properties of the material. Additionally, this also means the production of a chemically inert coating which prevents the formation of additional reactive states, which can effect the properties of the device.

Bibliography

- S. K. Ghandhi, *VLSI Fabrication Principles: Silicon and Gallium Arsenide*. Wiley-Interscience, New York, (1994).
- *Properties of Gallium Arsenide*. Ed. M. R. Brozel and G. E. Stillman. 3rd Ed. Institution of Electrical Engineers, London (1996).

6.11: Properties of Gallium Arsenide is shared under a [CC BY 1.0](https://creativecommons.org/licenses/by/1.0/) license and was authored, remixed, and/or curated by LibreTexts.

6.12: Electronic Grade Gallium Arsenide

Introduction

The synthesis and purification of bulk polycrystalline semiconductor material represents the first step towards the commercial fabrication of an electronic device. This polycrystalline material is then used as the raw material for the formation of single crystal material that is processed to semiconductor wafers.

In contrast to electronic grade silicon (EGS), whose use is a minor fraction of the global production of elemental silicon, gallium arsenide (GaAs) is produced exclusively for use in the semiconductor industry. However, arsenic and its compounds have significant commercial applications. The main use of elemental arsenic is in alloys of Pb, and to a lesser extent Cu, while arsenic compounds are widely used in pesticides and wood preservatives and the production of bottle glass. Thus, the electronics industry represents a minor user of arsenic. In contrast, although gallium has minor uses as a high-temperature liquid seal, manometric fluids and heat transfer media, and for low temperature solders, its main use is in semiconductor technology.

Isolation and purification of gallium metal

At 19 ppm gallium (L. Gallia, France) is about as abundant as nitrogen, lithium and lead; it is twice as abundant as boron (9 ppm), but is more difficult to extract due to the lack of any major gallium-containing ore. Gallium always occurs in association either with zinc or germanium, its neighbors in the periodic table, or with aluminum in the same group. Thus, the highest concentrations (0.1-1%) are in the rare mineral germanite (a complex sulfide of Zn, Cu, Ge, and As), while concentrations in sphalerite (ZnS), diasporite [AlO(OH)], bauxite, or coal, are a hundred-fold less. Industrially, gallium was originally recovered from the flue dust emitted during sulfide roasting or coal burning (up to 1.5% Ga), however, it is now obtained as side product of vast aluminum industry and in particular from the Bayer process for obtaining alumina from bauxite.

The Bayer process involves dissolution of bauxite, $\text{Al}_2\text{O}_3 \cdot x\text{H}_2\text{O}$, in aqueous NaOH, separation of insoluble impurities, partial precipitation of the trihydrate, $\text{Al}(\text{OH})_3$, and calcination at 1,200 °C. During processing the alkaline solution is gradually enriched in gallium from an initial weight ratio Ga/Al of about 1/5000 to about 1/300. Electrolysis of these extracts with a Hg cathode results in further concentration, and the solution of sodium gallate thus formed is then electrolyzed with a stainless steel cathode to give Ga metal. Since bauxite contains 0.003-0.01% gallium, complete recovery would yield some 500-1000 tons per annum, however present consumption is only 0.1% of this about 10 tons per annum.

A typical analysis of the 98-99% pure gallium obtained as a side product from the Bayer process is shown in Table 6.12.1. This material is further purified to 99.99% by chemical treatment with acids and O_2 at high temperatures followed by crystallization. This chemical process results in the reduction of the majority of metal impurities at the ppm level, see Table 6.12.1. Purification to seven nines 99.9999% is possible through zone refining, however, since the equilibrium distribution coefficient of the residual impurities $k_0 \approx 1$, multiple passes are required, typically > 500. The low melting point of gallium ensures that contamination from the container wall (which is significant in silicon zone refining) is minimized. In order to facilitate the multiple zone refining in a suitable time, a simple modification of zone refining is employed shown in Figure 6.12.1. The gallium is contained in a plastic tube wrapped around a rotating cylinder that is half immersed in a cooling bath. A heater is positioned above the gallium plastic coil. Thus, establishing a series of molten zones that pass upon rotation of the drum by one helical segment per revolution. In this manner, 500 passes may be made in relatively short time periods. The typical impurity levels of gallium zone refined in this manner are given in Table 6.12.1.

Table 6.12.1: Typical analysis of gallium obtained as a side product from the Bayer process.

Element	Bayer process (ppm)	After acid/base leaching (ppm)	500 zone passes (ppm)
aluminum	100-1,000	7	< 1
calcium	10-100	not detected	not detected
copper	100-1,000	2	< 1
iron	100-1,000	7	< 1
lead	< 2000	30	not detected

Element	Bayer process (ppm)	After acid/base leaching (ppm)	500 zone passes (ppm)
magnesium	10-100	1	not detected
mercury	10-100	not detected	not detected
nickel	10-100	not detected	not detected
silicon	10-100	≈ 1	not detected
tin	10-100	≈ 1	not detected
titanium	10-100	1	< 1
zinc	30,000	≈ 1	not detected

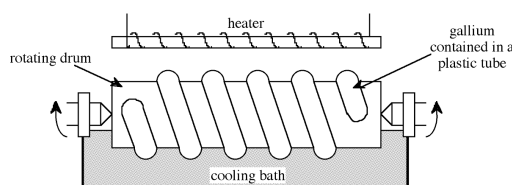


Figure 6.12.1: Schematic representation of a zone refining apparatus.

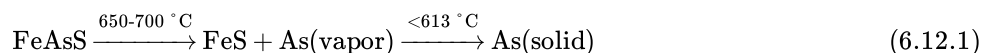
Isolation and purification of elemental arsenic

Elemental arsenic (L. arsenicum, yellow orpiment) exists in two forms: yellow (cubic, As_4) and gray or metallic (rhombohedral). At a natural abundance of 1.8 ppm arsenic is relatively rare, however, this is offset by its presence in a number of common minerals and the relative ease of isolation. Arsenic containing minerals are grouped into three main classes: the sulfides realgar (As_4S_4) and orpiment (As_2S_3), the oxide arsenolite (As_2O_3), and the arsenides and sulfaresenides of the iron, cobalt, and nickel. Minerals in this latter class include: loellinginite (FeAs_2), saffrolite (CoAs), niccolite (NiAs), rammelsbergite (NiAs_2), arsenopyrite or mispickel (FeAsS), cobaltite (CoAsS), enargite (Cu_3AsS_4), gersdorffite (NiAsS), and the quarternary sulfide glaucodot [$(\text{Co,Fe})\text{AsS}$]. Table 6.12.2 shows the typical impurities in arsenopyrite.

Table 6.12.2: Typical impurities in arsenopyrite.

Element	Concentration (ppm)	Element	Concentration (ppm)
silver	90	nickel	< 3,000
gold	8	lead	50
cobalt	30,000	platinum	0.4
copper	200	rhenium	50
germanium	30	selenium	50
manganese	3,000	vanadium	300
molybdenum	60	zinc	400

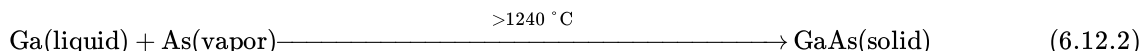
Arsenic is obtained commercially by smelting either FeAs_2 or FeAsS at 650-700 °C in the absence of air and condensing the sublimed element ($T_{\text{sub}} = 613\text{ °C}$), (6.12.1).



The arsenic thus obtained is combined with lead and then sublimed ($T_{\text{sub}} = 614\text{ °C}$) which binds any sulfur impurities more strongly than arsenic. Any residual arsenic that remains trapped in the iron sulfide is separated by forming the oxide (As_2O_3) by roasting the sulfide in air. The oxide is sublimed into the flue system during roasting from where it is collected and reduced with charcoal at 700-800 °C to give elemental arsenic. Semiconductor grade arsenic (> 99.9999%) is formed by zone refining.

Synthesis and purification of gallium arsenide.

Gallium arsenide can be prepared by the direct reaction of the elements, (6.12.2). However, while conceptually simple the synthesis of GaAs is complicated by the different vapor pressures of the reagents and the highly exothermic nature of the reaction. Furthermore, since the synthesis of GaAs at atmospheric pressure is accompanied by its simultaneous decomposes due to the loss by sublimation, of arsenic, the synthesis must be carried out under an overpressure of arsenic in order to maintain a stoichiometric composition of the synthesized GaAs.



In order to overcome the problems associated with arsenic loss, the reaction is usually carried out in a sealed reaction tube. However, if a stoichiometric quantity of arsenic is used in the reaction a constant temperature of 1238 °C must be employed in order to maintain the desired arsenic overpressure of 1 atm. Practically, it is easier to use a large excess of arsenic heated to a lower temperature. In this situation the pressure in the tube is approximately equal to the equilibrium vapor pressure of the volatile component (arsenic) at the lower temperature. Thus, an over pressure of 1 atm arsenic may be maintained if within a sealed tube elemental arsenic is heated to 600-620 °C while the GaAs is maintained at 1240-1250 °C.

Figure 6.12.2 shows the sealed tube configuration that is typically used for the synthesis of GaAs. The tube is heated within a two-zone furnace. The boats holding the reactants are usually made of quartz, however, graphite is also used since the latter has a closer thermal expansion match to the GaAs product. If higher purity is required then pyrolytic boron nitride (PBN) is used. One of the boats is loaded with pure gallium the other with arsenic. A plug of quartz wool may be placed between the boats to act as a diffuser. The tube is then evacuated and sealed. Once brought to the correct reaction temperatures (Figure 6.12.2), the arsenic vapor is transported to the gallium, and they react to form GaAs in a controlled manner. Table 6.12.3 gives the typical impurity concentrations found in polycrystalline GaAs.

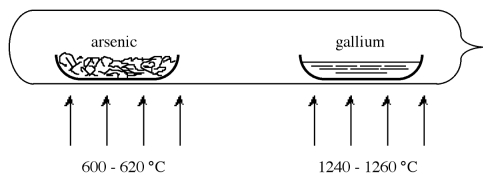


Figure 6.12.2: Schematic representation of a sealed tube synthesis of GaAs.

Table 6.12.3: Impurity concentrations found in polycrystalline GaAs.

Element	Concentration (ppm)	Element	Concentration (ppm)
boron	0.1	silicon	0.02
carbon	0.7	phosphorus	0.1
nitrogen	0.1	sulfur	0.01
oxygen	0.5	chlorine	0.08
fluorine	0.2	nickel	0.04
magnesium	0.02	copper	0.01
aluminum	0.02	zinc	0.05

Polycrystalline GaAs, formed in from the direct reaction of the elements is often used as the starting material for single crystal growth via Bridgeman or Czochralski crystal growth. It is also possible to prepare single crystals of GaAs directly from the elements using in-situ, or direct, compounding within a high-pressure liquid encapsulated Czochralski (HPLEC) technique.

Growth of gallium arsenide crystals

When considering the synthesis of Group 13-15 compounds for electronic applications, the very nature of semiconductor behavior demands the use of high purity single crystal materials. The polycrystalline materials synthesized above are, therefore, of little use for 13-15 semiconductors but may, however, serve as the starting material for melt grown single crystals. For GaAs, undoubtedly the most important 13-15 (III - V) semiconductor, melt grown single crystals are achieved by one of two techniques: the Bridgman technique, and the Czochralski technique.

Bridgman growth

The Bridgman technique requires a two-zone furnace, of the type shown in Figure 6.12.3. The left hand zone is maintained at a temperature of *ca.* 610 °C, allowing sufficient overpressure of arsenic within the sealed system to prevent arsenic loss from the gallium arsenide. The right hand side of the furnace contains the polycrystalline GaAs raw material held at a temperature just above its melting point (*ca.* 1240 °C). As the furnace moves from left to right, the melt cools and solidifies.

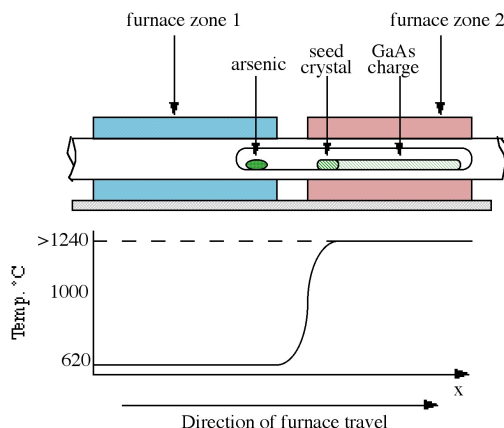


Figure 6.12.3: A schematic diagram of a Bridgman two-zone furnace used for melt growths of single crystal GaAs.

If a seed crystal is placed at the left hand side of the melt (at a point where the temperature gradient is such that only the end melts), a specific orientation of single crystal may be propagated at the liquid-solid interface eventually to produce a single crystal.

Czochralski growth

The Czochralski technique, which is the most commonly used technique in industry, is shown in Figure 6.12.4. The process relies on the controlled withdrawal of a seed crystal from a liquid melt. As the seed is lowered into the melt, partial melting of the tip occurs creating the liquid-solid interface required for crystal growth. As the seed is withdrawn, solidification occurs and the seed orientation is propagated into the grown material. The variable parameters of rate of withdrawal and rotation rate can control crystal diameter and purity. As shown in Figure 6.12.4 the GaAs melt is capped by boron trioxide (B_2O_3). The capping layer, which is inert to GaAs, prevents arsenic loss when the pressure on the surface is above atmospheric pressure. The growth of GaAs by this technique is thus termed liquid encapsulated Czochralski (LEC) growth.

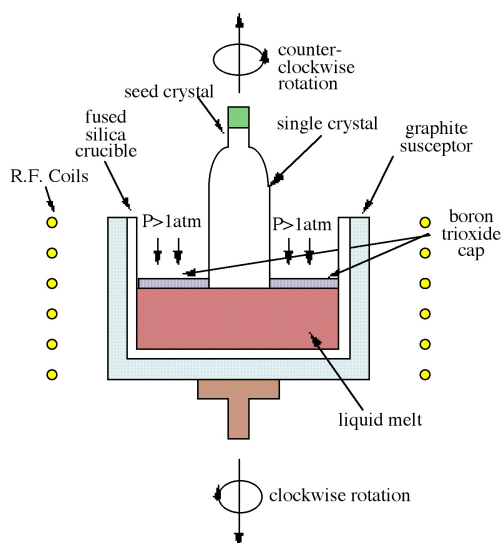


Figure 6.12.4: A schematic diagram of the Czochralski technique as used for growth of GaAs single crystal bond.

While the Bridgman technique is largely favored for GaAs growth, larger diameter wafers can be obtained by the Czochralski method. Both of these melt techniques produce materials heavily contaminated by the crucible, making them suitable almost exclusively as substrate material. Another disadvantage of these techniques is the production of defects in the material caused by the melt process.

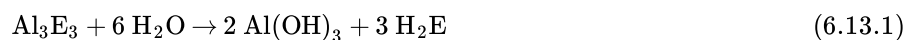
Bibliography

- S. K. Ghandhi, *VLSI Fabrication Principles: Silicon and Gallium Arsenide*. Wiley-Interscience, New York, (1994).
- J. Krauskopf, J. D. Meyer, B. Wiedemann, M. Waldschmidt, K. Bethge, G. Wolf, and W. Schültze, *5th Conference on Semi-insulating III-V Materials*, Malmo, Sweden, 1988, Eds. G. Grossman and L. Ledebo, Adam-Hilger, New York (1988).
- W. G. Pfann, *Zone Melting*, John Wiley & Sons, New York (1966).
- R. E. Williams, *Gallium Arsenide Processing Techniques*. Artech House (1984).
- *Properties of Gallium Arsenide*. Ed. M. R. Brozel and G. E. Stillman. 3rd Ed. Institution of Electrical Engineers, London (1996).

6.12: Electronic Grade Gallium Arsenide is shared under a [CC BY 1.0](#) license and was authored, remixed, and/or curated by LibreTexts.

6.13: Chalcogenides of Aluminum, Gallium, and Indium

The only stable chalcogenides of aluminum are Al_2S_3 (white), Al_2Se_3 (grey), and Al_2Te_3 (dark grey). They are each prepared by the direct reaction of the elements (100 °C) and hydrolyze rapidly in aqueous solution, (6.13.1). All the chalcogenides have a hexagonal ZnS structure in which $\frac{2}{3}$ of the metal sites are occupied.



The chalcogenides of gallium and indium are more numerous than those of aluminum, and are listed in Table 6.13.1 and Table 6.13.2 along with selected physical properties.

Table 6.13.1: Stoichiometries, structures and selected physical properties of the crystalline chalcogenides of gallium. ^a dir = direct, ind = indirect, opt = optical.

Compound	Structural type	Crystallographic system	Cell parameters (Å, °)	Band Gap (eV) ^a
GaS		Hexagonal	$a = 3.587, c = 15.492$	3.05 (dir.), 2.593 (ind.)
GaS	ZnS or NaCl	Cubic	$a = 5.5$	4.0 (opt.)
β-GaSe	GaS	Hexagonal	$a = 3.742, c = 15.919$	2.103 (dir.), 2.127 (ind.)
γ-GaSe	GaS	Rhombohedral	$a = 3.755, c = 23.92$	
δ-GaSe	GaS	Hexagonal	$a = 3.755, c = 31.99$	
β-GaTe	GaS	Hexagonal	$a = 4.06, c = 16.96$	
GaTe	GaS	Monoclinic	$a = 17.44, b = 4.077, c = 10.456, \beta = 104.4$	1.799 (dir.)
α-Ga ₂ S ₃	Wurtzite	Cubic	$a = 5.181$	
α-Ga ₂ S ₃	Wurtzite	Monoclinic	$a = 12.637, b = 6.41, c = 7.03, \beta = 131.08$	3.438 (opt.)
β-Ga ₂ S ₃	Defect wurtzite	Hexagonal	$a = 3.685, c = 6.028$	2.5 - 2.7 (opt.)
α-Ga ₂ Se ₃	Sphalerite	Cubic	$a = 5.429$	2.1 (dir.), 2.04 (ind.)
α-Ga ₂ Te ₃	Sphalerite	Cubic	$a = 5.886$	1.22 (opt.)

Table 6.13.2: Stoichiometries, structures and selected physical properties of the crystalline chalcogenides of indium. ^a dir = direct, ind = indirect, opt = optical. ^b High pressure phase.

Compound	Structural type	Crystallographic system	Cell parameters (Å, °)	Band gap (eV) ^a
β-InS	GaS	Orthorhombic	$a = 3.944, b = 4.447, c = 10.648$	2.58 (dir.), 2.067 (ind.)
InS ^b	Hg ₂ Cl ₂	Tetragonal		
InSe	GaS	Rhombohedral	$a = 4.00, c = 25.32$	1.3525 (dir.), 1.32 (ind.)
β-InSe	GaS	Hexagonal	$a = 4.05, c = 16.93$	
InTe	TlSe	Tetragonal	$a = 8.437, c = 7.139$	Metallic
InTe ^b	NaCl	Cubic	$a = 6.18$	
α-In ₂ S ₃	γ-Al ₂ O ₃	Cubic	$a = 5.36$	
β-In ₂ S ₃	Spinel	Tetragonal	$a = 7.618, c = 32.33$	2.03 (dir.), 1.1 (ind.)

$\alpha\text{-In}_2\text{Se}_3$	Defect wurtzite	Hexagonal	$a = 16.00, c = 19.24$	
$\beta\text{-In}_2\text{Se}_3$	Defect wurtzite	Rhombohedral	$a = 4.025, c = 19.222$	1.2 - 1.5 (ind.)
$\alpha\text{-In}_2\text{Te}_3$	Sphalerite	Cubic	$a = 6.158$	0.92 - 1.15 (opt.)
In_6S_7		Monoclinic	$a = 9.090, b = 3.887, c = 17.705, \beta = 108.20$	0.89 (dir.), 0.7 (ind.)
In_6Se_7	In_6S_7	Monoclinic	$a = 9.430, b = 4.063, c = 18.378, \beta = 109.34$	0.86 (dir.), 0.34 (ind.)
In_4Se_3		Orthorhombic	$a = 15.297, b = 12.308, c = 4.081$	0.64 (dir.)
In_4Te_3	In_4Se_3	Orthorhombic	$a = 15.630, b = 12.756, c = 4.441$	0.48 (dir.)

The hexagonal β -form of Ga_2S_3 is isostructural with the aluminum analogue; however, while the α -phase was proposed to be hexagonal it was later shown to be monoclinic. A cubic α -phase has been reported. Cubic Sphalerite structures are found for Ga_2Se_3 , Ga_2Te_3 , and In_2Te_3 , in which the structure is based on a cubic close packing of the chalcogenides and the metal atoms occupying $1/3$ of the tetrahedral sites. These structures are all formed with rapid crystallization; slow crystallization and/or thermal annealing leads to ordering and the formation of more complex structures. The indium sulfides, and selenides derivatives are spinel ($\gamma\text{-Al}_2\text{O}_3$), and defect Würtzite, respectively.

Unlike the chalcogenides of aluminum, those of gallium and indium also form subvalent compounds, i.e., those in which the metal is formally of an oxidation state less than +3. Of these subvalent chalcogenides the (formally) divalent materials are of the most interest. The thermodynamically stable phase of GaS has a hexagonal layer structure (Figure 6.13.1) with Ga-Ga bonds (2.48 Å). The compound can, therefore, be considered as an example of Ga(II). Each Ga is coordinated by three sulfur atoms and one gallium, and the sequence of layers along the z-axis is $\cdots\text{S-Ga-Ga-S}\cdots\text{S-Ga-Ga-S}\cdots$.

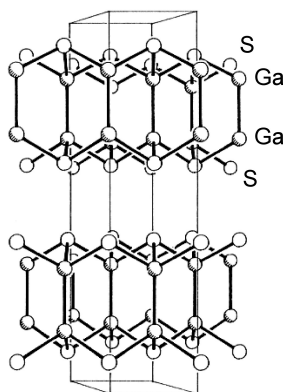


Figure 6.13.1: The $\cdots\text{S-Ga-Ga-S}\cdots\text{S-Ga-Ga-S}\cdots$ structure of hexagonal GaS. Gallium atoms are shown shaded.

The structures of $\beta\text{-GaSe}$, and $\beta\text{-InSe}$ are similar to hexagonal GaS. The layered structure of GaTe is similar in that it consists of $\cdots\text{TeGaGaTe}\cdots$ layers, but is monoclinic, while InS is found in both a (high pressure) tetragonal phase (Figure 6.13.2a) as well as an orthorhombic phase (Figure 6.13.2b). By contrast to these M-M bonded layered compounds InTe (Figure 6.13.3) has a structure formalized as $\text{In(I)[In(III)Te}_2]$; each In(III) is tetrahedrally coordinated to four Te and these tetrahedra are linked *via* shared edges; the In(I) centers lying between these chains.

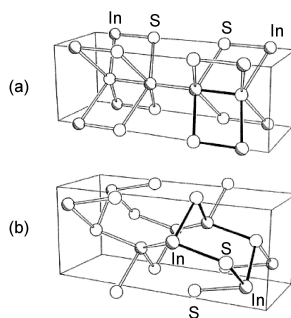


Figure 6.13.2: Unit cell of (a) tetragonal InS and (b) orthorhombic InS. Indium atoms are shown shaded, and the solid bonds represent the smallest cyclic structural fragment.

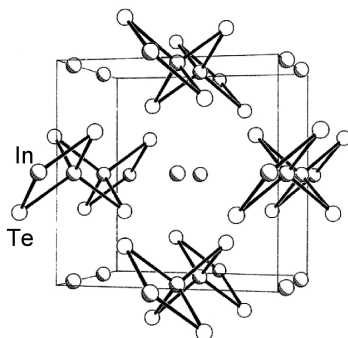


Figure 6.13.3: Unit cell of tetragonal InTe. Indium atoms are shown shaded, and the solid bonds represent the $[\text{InTe}_2]_\infty$ chains.

Further sub-chalcogenides are known for indium, e.g.; In_4Se_3 , which contains $[\text{In(III)}_3\text{Se}_2]^{5+}$ groups (Figure 6.13.4). While the formally In(I) molecule In_2S has been detected in the gas phase, it is actually a mixture of In and InS in the solid state.

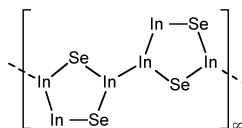


Figure 6.13.4: Structure of $[\text{In(III)}_3\text{Se}_2]^{5+}$ groups in In_4Se_3 .

Bibliography

- W. J. Duffin and J. H. C. Hogg, *Acta Crystallogr.*, 1966, **20**, 566.
- J. Goodyear and G. Steigman, *Acta Crystallogr.* 1963, **16**, 946.
- H. Hahn and G. Frank, *Z. Anorg. Allgem. Chem.*, 1955, **278**, 340.
- S. Kabalkina, V. G. Losev, and N. M. Gasanly, *Solid State Commun.*, 1982, **44**, 1383.
- A. Keys, S. G. Bott, and A. R. Barron, *Chem. Mater.*, 1999, **11**, 3578.
- A. N. MacInnes, M. B. Power, and A. R. Barron, *Chem. Mater.*, 1992, **4**, 11.
- A. N. MacInnes, W. M. Cleaver, A. R. Barron, M. B. Power, and A. F. Hepp, *Adv. Mater. Optics. Electron.*, 1992, **1**, 229.
- K. Schubert, E. Dörre, and E. Günzel, *Naturwissenschaften*, 1954, **41**, 488.

6.13: Chalcogenides of Aluminum, Gallium, and Indium is shared under a CC BY 1.0 license and was authored, remixed, and/or curated by LibreTexts.

6.14: Group 13 Halides

Trihalides, MX_3

As shown in Table 6.14.1 all the combinations of Group 13 element (M) and halogen (X) exist for the trihalides (MX_3), except thallium(III) iodide. It should be noted that while there is a compound with the general formula TlI_3 , it is actually a thallium(I) compound of I_3^- .

Table 6.14.1: Selected physical properties of the Group 13 trihalides, MX_3 .

Element	Mp (°C)	Bp (°C)
BF_3	-126.8	-100.3
BCl_3	-107.3	12.6
BBr_3	-46.3	91.3
BI_3	49.9	210
AlF_3	1291	-
$AlCl_3$	192.4 (anhydrous), 0.0 (hexahydrate)	120 (hexahydrate)
$AlBr_3$	97.8	265
AlI_3	189.4 (anhydrous) 185 dec. (hexahydrate)	300 subl.
GaF_3	800	1000
$GaCl_3$	77.9	201
$GaBr_3$	121.5	278.8
GaI_3	212	345
InF_3	1172	-
$InCl_3$	586	800
$InBr_3$	220	-
InI_3	210 subl.	-
TlF_3	300 dec.	-
$TlCl_3$	40 dec.	-
$TlBr_3$	40 dec.	-

The trihalides of boron are all monomers with a coordination number of 3 (Table 6.14.2), as evidence from their low melting points (Table 6.14.1). In contrast, the fluorides and chlorides of the heavier Group 13 elements (except $GaCl_3$) are generally ionic or have a high ionic character, with a coordination number of 6 (Table 6.14.2 Figure 6.14.1 and Figure 6.14.2). The bromides and iodides (except $InBr_3$) are generally dimeric with a coordination number of 4 (Table 6.14.2) and have molecular structures involving halide bridging ligands (Figure 6.14.3 and Table 6.14.3). $AlCl_3$ is unusual in that in the solid state it has an ionic structure, but it is readily sublimed, and in the vapor phase (and liquid phase) it has a dimeric structure (Figure 6.14.3).

Table 6.14.2: The Group 13 element coordination numbers for the trihalides, MX_3 .

Element	Fluoride	Chloride	Bromide	Iodide
B	3	3	3	3
Al	6	6 (4)	4	4
Ga	6	4	4	4

In	6	6	6	4
Tl	6	6	4	-

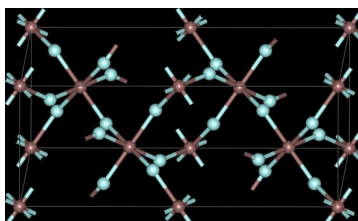


Figure 6.14.1: Solid state structure of MF_3 ($\text{M} = \text{Al}, \text{Ga}, \text{In}$). Grey spheres represent the metal, while pale blue spheres represent fluorine.

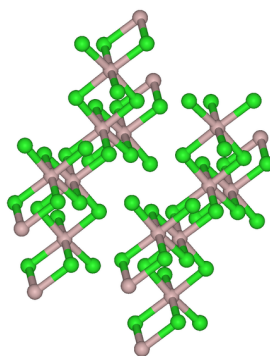


Figure 6.14.2: Solid state structure of MCl_3 ($\text{M} = \text{Al}, \text{In}, \text{Tl}$) and MBr_3 ($\text{M} = \text{In}$). Grey spheres represent the metal, while green spheres represent the halogen.

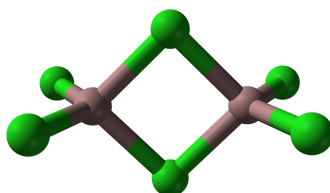


Figure 6.14.3: Structure of GaCl_3 , MBr_3 ($\text{M} = \text{Al}, \text{Ga}, \text{Tl}$), and MI_3 ($\text{M} = \text{Al}, \text{Ga}, \text{In}$). Grey spheres represent the metal, while green spheres represent the halogen.

Table 6.14.3: Selected bond lengths and angles for dimeric M_2X_6 compounds. ^a X_t and X_b indicate terminal and bridging halides, respectively.

Compound	$\text{M}-\text{X}_t$ (Å) ^a	$\text{M}-\text{X}_b$ (Å) ^a	$\text{X}_t-\text{M}-\text{X}_t$ (°) ^a	$\text{X}_b-\text{M}-\text{X}_b$ (°) ^a	$\text{M}-\text{X}-\text{M}$ (°)
Al_2Br_6	2.21	2.33	115	93	87
In_2I_6	2.64	2.84	125.1	93.7	86.3

Synthesis

Boron trifluoride (BF_3) is manufactured commercially by the reaction of boron oxides with hydrogen fluoride, (6.14.1). The HF is produced *in-situ* from sulfuric acid and fluorite (CaF_2). On smaller scales, BF_3 is prepared by the thermal decomposition of diazonium salts, (6.14.2).



Boron trichloride is also made from boron oxide, but in the presence of carbon, (6.14.3).



Many of the trihalides are readily prepared by either the direct reaction of the metal with the appropriate halogen, (6.14.4) - (6.14.6), or the acid, (6.14.7) and (6.14.8). Thallium tribromide can be prepared in CH_3CN by treating a solution of the

monobromide with bromine gas, (6.14.9).

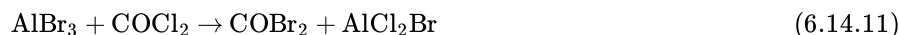


Reactivity

The reaction chemistry of the Group 13 trihalides tends to fall into two categories:

- Lewis acid-base complex formation.
- Hydrolysis.

There are, however, a number of reactions involving halide exchange reactions. Aluminum tribromide reacts with carbon tetrachloride at 100 °C to form carbon tetrabromide, (6.14.10), and with phosgene yields carbonyl bromide and aluminum chlorobromide, (6.14.11).



Group 13 halides are used as synthons for their organometallic derivatives, (6.14.12) and (6.14.13).



Lewis acid-base complexes

All of the trihalides are strong Lewis acids, and as such react with Lewis base compounds to form Lewis acid-base complexes, (6.14.12). The extent of the equilibrium is dependant on the Lewis acidity of the trihalide and the basicity of the Lewis base. For example, with BCl_3 , oxygen donor ligands result in approximately 50:50 ratio of BCl_3 and BCl_3L , while for nitrogen donor ligands the equilibrium is shifted to the formation of the complex.



The general structure of the Lewis acid-base complexes is such that the Group 13 element is close to tetrahedral (Figure 6.14.4). However, for aluminum and the heavier Group 13 elements, more than one ligand can coordinate (Figure 6.14.5) up to a maximum of six.

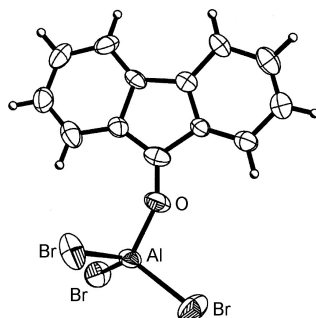


Figure 6.14.4: Molecular structure of a typical Group 13 metal trihalide Lewis acid-base complex: AlBr_3 (9-fluorenone). Adapted from C. S. Branch, S. G. Bott, and A. R. Barron, *J. Organomet. Chem.*, 2003, **666**, 23.

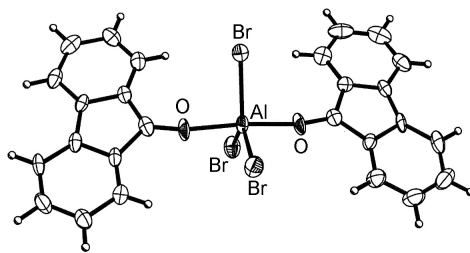
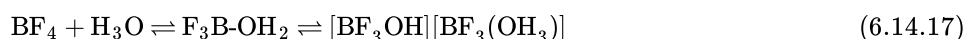


Figure 6.14.5: Molecular structure of $\text{AlBr}_3(9\text{-fluorenone})_2$. Adapted from C. S. Branch, S. G. Bott, and A. R. Barron, *J. Organomet. Chem.*, 2003, **666**, 23.

It should be noted that the dimeric form of MX_3 (Figure 6.14.3) can be thought of as mutual Lewis acid-base complexes, in which a Lewis basic lone pair of a halide on one MX_3 unit donates to the Lewis acidic metal on another MX_3 unit.

Hydrolysis

Generally the fluorides are insoluble in water while the heavier halides are more soluble. However, BF_3 , BCl_3 , and BBr_3 all decompose in the presence of water, (6.14.13). In the case of the fluoride, the HF formed reacts with BF_3 to form fluoroboric acid, (6.14.14). However, there is also a minor equilibrium (2-3%) resulting in the formation of the BF_3 complex of OH^- and H_3O^+ , (6.14.15).



While the boron compounds (and AlBr_3) decompose even in moist air, AlCl_3 reacts more slowly to make aluminum chlorohydrate (ACH) which has the general formula $\text{Al}_n\text{Cl}_{3n-m}(\text{OH})_m$. While ACH has been proposed to exist as a number of cluster species, it is actually a range of nanoparticles.

ACH is also known as polyaluminum chloride (PAC). The latter name is often used in water purification, where ACH is preferred over alum derivatives ($\text{Al}_2(\text{SO}_4)_3$). The combination of ACH and a high molecular weight quaternized ammonium polymer (e.g., diallyl dimethyl ammonium chloride (DADMAC)), has been known as an effective combination as a flocculant in water treatment process to remove dissolved organic matter and colloidal particles present in suspension.

Aluminum chlorohydrate (ACH) and aluminum-zirconium compounds, are frequently used as the active ingredient in antiperspirants. The mode of action of most aluminum-based compounds involves the dramatic change in the particle size from nano to micro as a function of pH and electrolyte changes on the skin (as compared to the antiperspirant stick or suspension) and hence forming a gel plug in the duct of the sweat gland. The plugs prevent the gland from excreting liquid and are removed over time by the natural sloughing of the skin. A further mechanism of action involves the absorption of 3-methyl-2-hexenoic acid (Figure 6.14.6). Human perspiration is odorless until bacteria ferment it. Bacteria thrive in hot, humid environments such as the underarm. When adult armpits are washed with alkaline pH soaps, the skin loses its acid mantle ($\text{pH} = 4.5 - 6$), raising the skin pH and disrupting the skin barrier. The bacteria thrive in the basic environment, and feed on the sweat from the apocrine glands and on dead skin and hair cells, releasing 3-methyl-2-hexenoic acid, which is the primary cause of body odor. As with all carboxylic acids, 3-methyl-2-hexenoic acid, reacts in a facile manner with the surface of the alumina nanoparticles. Aluminum chloride salts also have a slight astringent effect on the pores; causing them to contract, further preventing sweat from reaching the surface of the skin.

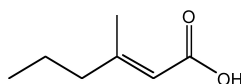
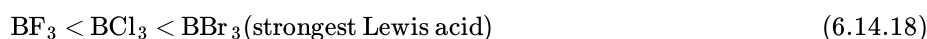


Figure 6.14.6: The structure of 3-methyl-2-hexenoic acid.

Boron trihalides: a special case

The three lighter boron trihalides, BX_3 ($\text{X} = \text{F}, \text{Cl}, \text{Br}$) form stable adducts with common Lewis bases. Their relative Lewis acidities can be evaluated in terms of the relative exothermicity of the adduct-forming reaction:



This trend is opposite to that expected based upon the electronegativity of the halogens. The best explanation of this trend takes into account the extent of π -donation that occurs between the filled lone pair orbital on the halogens and the empty p-orbital on the

planar boron (Figure 6.14.7). As such, the greater the π -bonding the more stable the planar BX_3 configuration as opposed to the pyramidalization of the BX_3 moiety upon formation of a Lewis acid-base complex, (6.4.12).

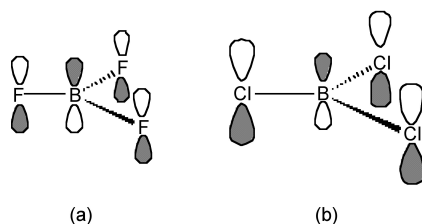


Figure 6.14.7: Schematic representation of π -donation from filled halogen p-orbitals into empty p-orbital in the halides BX_3 .

The criteria for evaluating the relative strength of π -bonding are not clear, however, one suggestion is that the F atom is small compared to the Cl atom, and the lone pair electron in p_z of F is readily and easily donated and overlapped to empty p_z orbital of boron (Figure 6.14.7a). In contrast, the overlap for the large (diffuse) p-orbitals on the chlorine is poorer (Figure 6.14.7b). As a result, the π -donation of F is greater than that of Cl. Interestingly, as may be seen from Table 6.14.4 any difference in B-X bond length does not follow the expected trend associated with shortening of the B-X bond with stronger π -bonding. In fact the B-Br distance is the most shortened as compared to that expected from the covalent radii (Table 6.14.4).

Table 6.14.4: The B-X bond distances in the boron trihalides, BX_3 , as compared to the sum of the covalent radii. ^aCovalent radius of B = 0.84(3) Å.

Compound	B-X (Å)	X covalent radius (Å)	Sum of covalent radii (Å) ^a	Δ (Å)
BF_3	1.313	0.57(3)	1.41	0.097
BCl_3	1.75	1.02(4)	1.86	0.11
BBr_3	1.898	1.20(3)	2.04	0.142
BI_3	2.125	1.39(3)	2.23	0.105

At the simplest level the requirements for bonding to occur based upon the molecular or atomic orbital are:

- Directional relationship of the orbitals.
- Relative symmetry of the orbitals.
- Relative energy of the orbitals.
- Extent of orbital overlap

In the case of the boron trihalides, the direction (parallel) and symmetry (p-orbitals) are the same, and the only significant difference will be the relative energy of the donor orbitals (i.e., the lone pair on the halogen) and the extent of the overlap. The latter will be dependant on the B-X bond length (the shorter the bond the greater the potential overlap) and the diffusion of the orbitals (the less diffuse the orbitals the better the overlap). Both of these factors will benefit B-F over B-Cl and B-Br. Thus, the extent of potential overlap would follow the order: (6.14.16). Despite these considerations, it is still unclear of the exact details of the rationalization of the low Lewis basicity of BF_3 as compared to BCl_3 and BBr_3 .

Anionic halides

The trihalides all form Lewis acid-base complexes with halide anions, (6.14.17), and as such salts of BF_4^- , AlCl_4^- , GaCl_4^- , and InCl_4^- are common.



In the case of gallium the Ga_2Cl_7^- anion (Figure 6.14.8) is formed from the equilibrium:



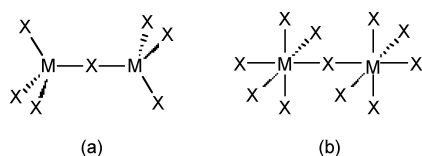


Figure 6.14.8: Structures of the (a) $M_2X_7^-$ and (b) $M_2X_9^{3-}$ anions.

As a consequence of its larger size indium forms a wide range of anionic halides addition compounds with trigonal bipyramidal, square pyramidal, and octahedral coordination geometries. For example, salts of $InCl_5^{2-}$, $InBr_5^{2-}$, InF_6^{3-} , $InCl_6^{3-}$ and $InBr_6^{3-}$ have all been made. The $InCl_5^{2-}$ ion has been found to be square pyramidal in the salt $[NEt_4]_2InCl_5$, but is trigonal bipyramidal in the acetonitrile solvate of $[Ph_4P]_2InCl_5$. The oligomeric anionic halides $In_2X_7^-$ and $In_2X_9^{3-}$ ($X = Cl$ and Br) contain binuclear anions with tetrahedral and octahedrally coordinated indium atoms, respectively (Figure 6.14.8).

Low valent halides

Oxidation state +2

Boron forms a series of low oxidation halides containing B-B bonds a formal oxidation state of +2. Passing an electric discharge through BCl_3 using mercury electrodes results in the synthesis of B_2Cl_4 , (6.14.19). An alternative route is by the co-condensation of copper as a reducing agent with BCl_3 , (6.14.20).



B_2F_4 has a planar structure (Figure 6.14.9) with D_{2h} symmetry, while B_2Cl_4 has the same basic structure it has a staggered geometry (Figure 6.14.10). The energy for bond rotation about the B-B bond is very low (5 kJ/mol) that can be compared to ethane (12.5 kJ/mol). The bromide, B_2Br_4 , is also observed to be staggered in the solid state. The staggered conformation is favorable on steric grounds, however, for B_2F_4 the planar geometry is stabilized by the smaller size of the halide, and more importantly the presence of strong delocalized π -bonding.

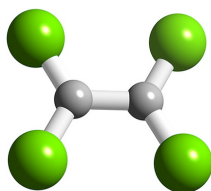


Figure 6.14.9: The planar structure of B_2F_4 .

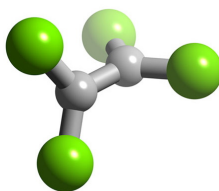


Figure 6.14.10: The staggered structure of B_2Cl_4 .

Oxidation state +1

Boron forms a number of halides with cluster structures, B_nCl_n where $n = 4$ (Figure 6.14.11), 8, 9, 10, 11, and 12. Each compound is made by the decomposition of B_2Cl_4 . For gallium, none of the monohalides are stable at room temperature, but $GaCl$ and $GaBr$ have been produced in the gas form from the reaction of HX and molten gallium. The stability of thallium(I) as compared to thallium(III) results in the monohalides, $TlCl$, $TlBr$, and TlI being stable. Each compound is insoluble in water, and photosensitive.

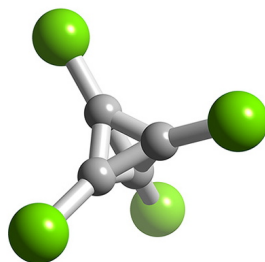


Figure 6.14.11: Structure of B_4Cl_4 .

Intermediate halides

The dihalides (MX_2) of gallium, indium, and thallium do not actually contain the metal in the +2 oxidation state. Instead they are actually mixed valence compound, i.e., $M^+[MX_4]^-$. The dihalides of gallium are unstable in the presence of water disproportionating to gallium metal and gallium(III) entities. They are soluble in aromatic solvents, where arene complexes have been isolated and the arene is η^6 -coordinated to the Ga^+ ion. $InBr_2$ and InI_2 are greenish and yellow crystalline solids, respectively, which are formulated $In(I)[In(III)X_4]$. $TlCl_2$ and $TlBr_2$ both are of similar formulations.

Ga_2X_3 ($X = Br, I$) and In_2Br_3 are formulated $M(I)_2[M(II)_2X_6]$. Both anions contain a M-M bond where the metal has a formal oxidation state of +2. The $Ga_2Br_6^{2-}$ anion is eclipsed like the $In_2Br_6^{2-}$ anion, whereas the $Ga_2I_6^{2-}$ anion is isostructural with Si_2Cl_6 with a staggered conformation. In_2Cl_3 is colorless and is formulated $In(I)_3[In(III)Cl_6]$.

Ga_3Cl_7 contains the $Ga_2Cl_7^-$ ion, which has a structure similar to the dichromate, $Cr_2O_7^{2-}$, ion with two tetrahedrally coordinated gallium atoms sharing a corner (Figure). The compound can be formulated as gallium(I) heptachlorodigallate(III), $Ga(I)[Ga(III)_2Cl_7]$.

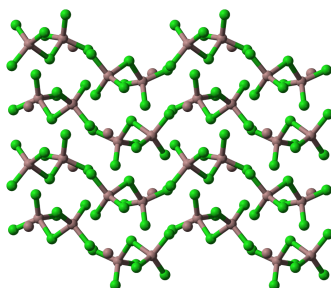


Figure 6.14.12: The crystal structure of Ga_3Cl_7 , better described as gallium(I) heptachlorodigallate(III), $Ga(I)[Ga(III)_2Cl_7]$. Grey spheres represent the gallium, while green spheres represent the chlorine.

In_4Br_7 is light sensitive (like $TlCl$ and $TlBr$) decaying to $InBr_2$ and In metal. It is a mixed salt containing the $InBr_4^-$ and $InBr_6^{3-}$ anions balanced by In^+ cations. It is formulated $In(I)_5[In(III)Br_4]_2[In(III)Br_6]$. In_5Br_7 is a pale yellow solid formulated as $In(I)_3[In(II)_2Br_6]Br$. The $In(II)_2Br_6^{2-}$ anion has an eclipsed ethane like structure with an In-In bond length of 2.70 Å. In_5Cl_9 is formulated $In(I)_3[In(III)_2Cl_9]$, with the $In_2Cl_9^{2-}$ anion having two 6 coordinate indium atoms with 3 bridging chlorine atoms, face sharing bioctahedra. Finally, In_7Cl_9 and In_7Br_9 have a structure formulated as $InX_6[In(III)X_6]X_3$.

Bibliography

- P. M. Boorman and D. Potts, *Can. J. Chem.*, 1974, **52**, 2016.
- A. Borovik and A. R. Barron, *J. Am. Chem. Soc.*, 2002, **124**, 3743.
- A. Borovik, S. G. Bott, and A. R. Barron, *J. Am. Chem. Soc.*, 2001, **123**, 11219.
- C. S. Branch, S. G. Bott, and A. R. Barron, *J. Organomet. Chem.*, 2003, **666**, 23.
- W. M. Brown and M. Trevino, *US Patent* 5,395,536 (1995).
- S. K. Dentel, *CRC Critical Reviews in Environmental Control*, 1991, **21**, 41.
- D. E. Hassick and J. P. Mikneovich, *US Patent* 4,800,039 (1989).
- M. D. Healy, P. E. Laibinis, P. D. Stupik and A. R. Barron, *J. Chem. Soc., Chem. Commun.*, 1989, 359.
- K. Hedberg and R. Ryan, *J. Chem. Phys.*, 1964, **41**, 2214.
- Y. Koide and A. R. Barron, *Organometallics*, 1995, **14**, 4026.
- G. Santiso-Quiñones and I. Krossing, *Z. Anorg. Allg. Chem.*, 2008, **634**, 704.

6.14: Group 13 Halides is shared under a [CC BY 1.0](#) license and was authored, remixed, and/or curated by LibreTexts.

CHAPTER OVERVIEW

7: Group 14

- [7.1: The Group 14 Elements](#)
- [7.2: Carbon Black- From Copying to Communication](#)
- [7.3: Carbon Nanomaterials](#)
- [7.4: Nitrogen Compounds of Carbon](#)
- [7.5: Carbon Monoxide](#)
- [7.6: Carbon Dioxide](#)
- [7.7: Suboxides of Carbon](#)
- [7.8: Carbon Halides](#)
- [7.9: Comparison Between Silicon and Carbon](#)
- [7.10: Semiconductor Grade Silicon](#)
- [7.11: Oxidation of Silicon](#)
- [7.12: Applications for Silica Thin Films](#)

This page titled [7: Group 14](#) is shared under a [CC BY 3.0](#) license and was authored, remixed, and/or curated by [Andrew R. Barron \(CNX\)](#) via [source content](#) that was edited to the style and standards of the LibreTexts platform.

7.1: The Group 14 Elements

The group was once also known as the *tetrels* (from Greek *tetra* meaning *four*), stemming from the earlier naming convention of this group as Group IVA. [Table](#) lists the derivation of the names of the Group 14 elements.

Table 7.1.1: Derivation of the names of each of the Group 14 elements.

Element	Symbol	Name
Carbon	C	From the Latin <i>carbo</i> meaning <i>coal</i>
Silicon	Si	From the Latin <i>silicis</i> meaning <i>flints</i>
Germanium	Ge	From the Latin <i>Germania</i> for <i>Germany</i>
Tin	Sn	From the Anglo-Saxon and from the Latin <i>stannum</i> meaning <i>melts easily</i>
Lead	Pb	From the Anglo-Saxon, and from the Latin <i>plumbum</i> meaning <i>soft metal</i>

Discovery

Carbon

Carbon was known in prehistory in the form of soot; while charcoal was made in Roman times (by heating wood while exclude air) and diamonds were known as early as 2500 BC in China. In 1772, Antoine Lavoisier (Figure 7.1.1) showed that diamonds were a form of carbon, when he burned samples of carbon and diamond and showed that both formed the same amount of carbon dioxide per gram of material. Carl Scheele (Figure 7.1.2) showed that graphite was a form of carbon rather a form of lead.



Figure 7.1.1: French chemist and biologist Antoine-Laurent de Lavoisier (1743 – 1794).



Carl Wilhelm Scheele.

Figure 7.1.2: German-Swedish pharmaceutical chemist Carl Wilhelm Scheele (1742 - 1786). Author Isaac Asimov has called him "hard-luck Scheele" because he made a number of chemical discoveries before others who are generally given the credit.

A new allotrope of carbon, fullerene, was discovered in 1985 by Robert Curl, Harry Kroto, and Richard Smalley (Figure 7.1.3) who subsequently shared the Nobel Prize in Chemistry in 1996. Fullerenes have been revealed to include nanostructured forms such as buckyballs and nanotubes. The renewed interest in new forms lead to the discovery of further exotic allotropes, including glassy carbon, and the realization that *amorphous carbon* is not amorphous.

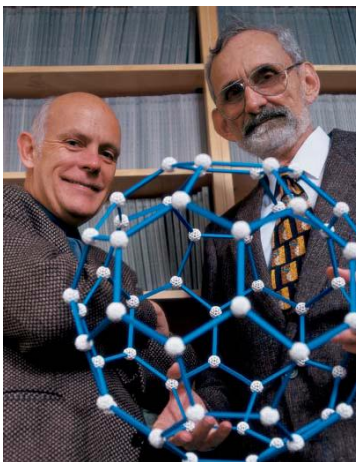


Figure 7.1.3: Rice University chemists Richard E. Smalley (1943 - 2005) and Robert F. Curl (1933 -).

Silicon

Silicon was first identified by Antoine Lavoisier (Figure 7.1.1) in 1787 as a component of flints, and was later mistaken by Humphry Davy (Figure 7.1.4) for a compound rather than an element. In 1824, Berzelius (Figure 7.1.5) prepared amorphous silicon by the reaction of potassium with silicon tetrafluoride, (7.1.1).



Figure 7.1.4: British chemist and inventor Sir Humphry Davy FRS (1778 - 1829).



Figure 7.1.5: Swedish chemist Jöns Jacob Berzelius (1779 – 1848).

Germanium

In 1869 Dmitri Mendeleev (Figure 7.1.6) predicted the existence of several unknown elements, including ekasilicon (Es) between silicon and tin.

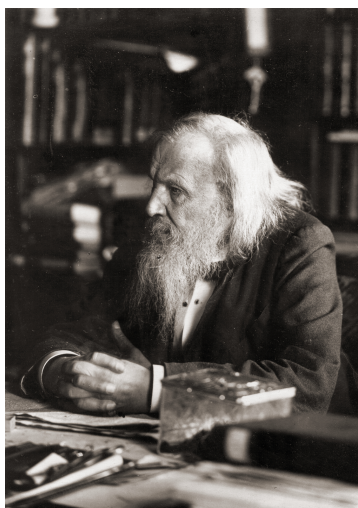


Figure 7.1.6: Russian chemist and inventor Dmitri Ivanovich Mendeleev (1834 – 1907).

In 1885 a new mineral (named *argyrodite* because of its high silver content) was found in a mine near Freiberg, Saxony. Clemens Winkler (Figure 7.1.7) isolated Mendeleev's missing element. He originally was going to name neptunium because like this element, because like ekasilicon, the planet Neptune had been preceded by mathematical prediction of its existence. However, the name neptunium had already been given to an element and so Winkler named the new metal germanium in honor of his fatherland.



Figure 7.1.7: German chemist Clemens Alexander Winkler (1838–1904).

Winkler was able to isolate sufficient germanium from 500 kg of ore to determine a number properties, including an atomic weight of 72.32 g/mol by analyzing pure germanium tetrachloride (GeCl_4). Winkler prepared several new compounds of germanium, including the fluorides, chlorides, sulfides, germanium dioxide, and tetraethylgermane ($\text{Ge}(\text{C}_2\text{H}_5)_4$). The physical data from these compounds, corresponded with Mendeleev's predictions (Table 7.1.2).

Table 7.1.2: Properties predicted for ekasilicon compared those determined for germanium.

Property	Ekasilicon	Germanium
Atomic mass	72	72.59
Density (g/cm^3)	5.5	5.35
Melting point ($^{\circ}\text{C}$)	High	947
Color	Gray	Gray
Oxide type	Refractory dioxide	Refractory dioxide
Oxide density (g/cm^3)	4.7	4.7
Oxide activity	Feebly basic	Feebly basic
Chloride boiling point ($^{\circ}\text{C}$)	Under 100	86 (GeCl_4)
Chloride density (g/cm^3)	1.9	1.9

Tin

Tin is one of the earliest metals known. When the addition of about 5% tin to molten copper produced an alloy (bronze) that was easier to work and much harder than copper, it revolutionized civilization. The widespread use of bronze to make tools and weapons became part of what archaeologists call the Bronze Age. The Bronze Age arrived in Egypt, Mesopotamia and the Indus Valley culture by around 3000 BC.

Lead

Lead has been commonly used for thousands of years because of its ease of extraction, and its ease of smelting. Lead beads dating back to 6400 BC have been found in Çatalhöyük in modern-day Turkey, while lead was used during the Bronze Age.

Abundance

Carbon and silicon are amongst the most abundant elements (Table 7.1.3). Silicon is the second most abundant element (after oxygen) in the Earth's crust, making up 28% of the crust. Carbon is the fourth most abundant chemical element in the universe after hydrogen, helium, and oxygen. In combination with oxygen in carbon dioxide, carbon is found in the Earth's atmosphere (in quantities of approximately 810 gigatonnes) and dissolved in all water bodies (approximately 36,000 gigatons). Around 1,900

gigatons are present in the biosphere. Hydrocarbons (such as coal, petroleum, and natural gas) contain carbon amounts to around 900 gigatons. Natural diamonds occur in the rock kimberlite, found in ancient volcanic "necks," or "pipes". Most diamond deposits are in Africa but there are also deposits in Canada, the Russian Arctic, Brazil, and Australia.

Table 7.1.3: Abundance of Group 14 elements.

Element	Terrestrial abundance (ppm)
C	480 (Earth's crust), 28 (sea water), 350 (atmosphere CO ₂), 1.6 (atmosphere, CH ₄), 0.25 (atmosphere, CO)
Si	28,000 (Earth's crust), 2 (sea water)
Ge	2 (Earth's crust), 1 (soil), 5×10^{-7} (sea water)
Sn	2 (Earth's crust), 1 (soil), 4×10^{-6} (sea water)
Pb	14 (Earth's crust), 23 (soil), 2×10^{-6} (sea water)

Isotopes

Table 7.1.4 summarizes the naturally occurring isotopes of the Group 14 elements.

Table 7.1.4: Abundance of the major isotopes of the Group 14 elements.

Isotope	Natural abundance (%)
Carbon-12	98.9
Carbon-13	1.1
Carbon-14	trace
Silicon-28	92.23
Silicon-29	4.67
Silicon -30	3.1
Germanium-70	21.23
Germanium-72	27.66
Germanium-73	7.73
Germanium-74	35.94
Germanium-76	7.44
Tin-112	0.97
Tin-114	0.66
Tin-115	0.34
Tin-116	14.54
Tin-117	7.68
Tin-118	24.22
Tin-119	8.59
Tin-120	32.58
Tin-122	4.63
Tin-124	5.79
Lead-204	1.4

Lead-24.1	24.1
Lead-207	22.1
Lead-208	52.4

Although radioactive, carbon-14 is formed in upper layers of the troposphere and the stratosphere, at altitudes of 9–15 km. Thermal neutrons produced by cosmic rays collide with the nuclei of nitrogen-14, forming carbon-14 and a proton. Because of its relatively short half-life of 5730 years, carbon-14 is absent in ancient rocks, but is incorporated in living organisms.

Carbon dating

Carbon dating is a process whereby the age of a material that contains carbon can be determined by comparing the decay rate of that material with that of living material.

Carbon-14 has a half life ($t_{1/2}$) of 5.73×10^3 years for its decay to nitrogen-14 by the loss of a β particle, (7.1.2).



The rate of radioactive decay can be expressed as a rate constant (k):

$$k = \frac{\ln[2]}{t_{1/2}} = \frac{0.693}{t_{1/2}} \quad (7.1.3)$$

For carbon-14, using (7.1.3),

$$k = \frac{0.693}{5.73 \times 10^3} = 1.21 \times 10^{-4} \text{ year}^{-1} \quad (7.1.4)$$

In 1947 samples of the Dead Sea Scrolls were analyzed by carbon dating. It was found that the carbon-14 present had an activity of d/min.g (where d = disintegration); by contrast in living material the activity is 14 d/min.g. Thus,

$$\ln \frac{14}{11} = (1.21 \times 10^{-4}) t \quad (7.1.5)$$

$$t = \frac{\ln 1.272}{1.21 \times 10^{-4}} = 2.0 \times 10^3 \text{ years} \quad (7.1.6)$$

From the measurement performed in 1947 the Dead Sea Scrolls were determined to be 2000 years old giving them a date of 53 BC, and confirming their authenticity. This discovery is in contrast to the carbon dating results for the Turin Shroud that was supposed to have wrapped Jesus' body. Carbon dating has shown that the cloth was made between 1260 and 1390 AD. Thus, the Turin Shroud is clearly a fake having been made over a thousand years after its supposed manufacture.

Industrial production

Due to the industrial importance of carbon and silicon, as well as the wide range of fullerene materials, the production of these elements is discussed elsewhere. However, the diamond supply chain is controlled by a limited number of commercial concerns, the largest of which is DeBeers in London (Figure). Diamonds make up only a very small fraction of ore bearing rock. The ore is crushed and subsequently the particles are sorted by density. Diamonds are located in the diamond-rich fraction by X-ray fluorescence, after which the final sorting steps are done by hand.

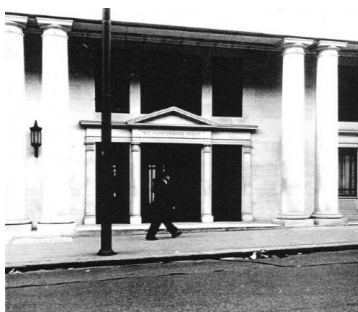


Figure 7.1.8: The Charterhouse Street Entrance of the offices of De Beers in London, are the venue for the 10 sights that are held during the year. Sightholders, both manufacturers (of polished diamonds) and dealers (in rough diamonds), meet in London, once every 5 weeks, 10 times a year, to inspect their diamond allocations.

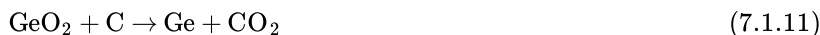
Germanium ore concentrates are mostly sulfidic, e.g., as an impurity in zinc blende. They are converted to the oxides by heating under air (roasting), (7.1.7).



Part of the germanium ends up in the dust produced during this process, while the rest is converted to germanates which are leached together with the zinc by sulfuric acid. After neutralisation the germanium and other metals are precipitated (leaving the Zn^{2+} in solution). Germanium dioxide is obtained as a precipitate and converted with chlorine gas or hydrochloric acid to germanium tetrachloride, (7.1.8) (7.1.9), which has a low boiling point and can be purified by distillation.



The germanium tetrachloride is hydrolyzed to give pure oxide (GeO_2), which is then converted to germanium glass for the semiconductor industry, (7.1.10). Germanium used in steel production and other applications that do not require the high purity is produced by reduction with carbon, (7.1.11).



Tin is mined and subsequently smelted, and its production has changed little. In contrast, lead-rich ores contain less than 10% lead, but ores containing as little as 3% lead can be economically exploited. Ores are crushed and concentrated to 70%. Sulfide ores are roasted, producing lead oxide and a mixture of sulfates and silicates of lead. Lead oxide from the roasting process is reduced in a coke-fired blast furnace. This converts most of the lead to its metallic form. Metallic lead that results from the roasting and blast furnace processes still contains significant contaminants of arsenic, antimony, bismuth, zinc, copper, silver, and gold. The melt is treated in a reverberatory furnace (Figure 7.1.9) with air, steam, and sulfur, which oxidizes the contaminants except silver, gold, and bismuth.

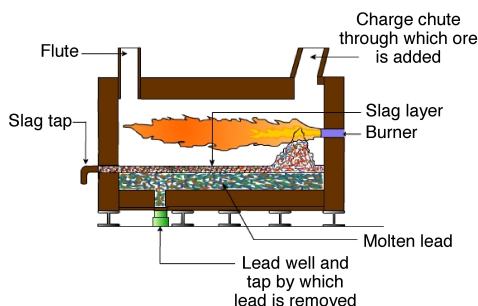


Figure 7.1.9: Schematic of a reverberatory furnace.

Physical properties

Table 7.1.5 provides a summary of the physical properties of the Group 14 elements.

Table 7.1.5: Selected physical properties of the Group 14 elements.

--	--

Element	Mp (°C)	Bp (°C)	Density (g/cm ³)
C	642 (sublimes)		2.267 (graphite), 3.515 (diamond), 1.8 - 2.1 (amorphous)
Si	1414	3265	2.3290
Ge	938	2833	5.323
Sn	232	2602	7.365 (white), 5.769 (gray)
Pb	327	1749	11.34

Cubic structure

The elements carbon through tin (in its α form) all exist in diamond cubic structure (Figure 7.1.10a), while lead crystallizes in a cubic close packed structure (Figure 7.1.10b). As expected the lattice parameter (a) increases with increased atomic radius (Table 7.1.6). The switch from diamond cubic to close packed cubic may be rationalized by the relative atomic sizes. The diamond cubic structure comprises of two interpenetrating cubic close packed lattices. As the atomic size increases large interstitial vacancies would result, resulting in an unfavorable low-density structure.

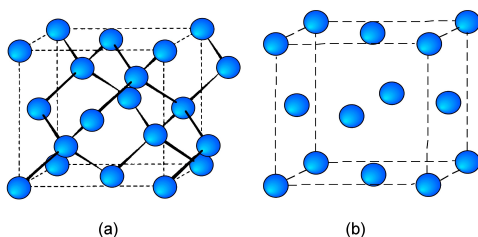


Figure 7.1.10: Unit cell structure of (a) the diamond cubic lattice showing the two interpenetrating face-centered cubic lattices, and (b) the cell of cubic close packed structure for comparison.

Table 7.1.6: Lattice parameter and crystal density for Group 14 elements.

Element	Structure	a (Å)	Atomic radius (Å)
C	diamond cubic	3.566	0.70
Si	diamond cubic	5.431	1.10
Ge	diamond cubic	5.657	1.25
α -Sn (gray)	diamond cubic	6.489	1.45
Pb	cubic close packed	4.951	1.80

This page titled [7.1: The Group 14 Elements](#) is shared under a [CC BY 3.0](#) license and was authored, remixed, and/or curated by [Andrew R. Barron \(CNX\)](#) via [source content](#) that was edited to the style and standards of the LibreTexts platform.

7.2: Carbon Black- From Copying to Communication

It is a commonly held fallacy that James Watt (Figure 7.2.1) was the inventor of the steam engine. This actually honor belongs to Thomas Newcomen (Figure 7.2.2). Watt's actual achievement was to improve Newcomen's design of a steam pump. While Watt was working in the repair shop at the University of Glasgow he was fixing a Newcomen pump when he developed several key improvements on the original design.



Figure 7.2.1: Scottish inventor and mechanical engineer James Watt FRS (1736 –1819).



Figure 7.2.2: English ironmonger and inventor of the steam engine Thomas Newcomen (1664 - 1729).

The reason for Watt's success was that Britain was going through a major industrial boom and was in need of significant quantities of raw material including coal. Many of the coalmines, especially those in Devon were prone to flooding. Unfortunately, Newcomen's engine (which was actually a steam pump) could not pump the water out fast enough, whereas Watt's engine was powerful enough to drain the mines. As a result Watt's career as a manufacturer was assured. However, Watt did not see the full potential of his invention, this was left to an employee of his, William Murdock (Figure 7.2.3), whose invention of the gearing to allow the steam engine to be used for powering machinery.



Figure 7.2.3: Scottish engineer and inventor William Murdoch (1754 - 1839).

One outcome that Watt found from his increased business was an increase in paperwork! While he was living in Redruth, Cornwall, close to where many of the mines were situated he told a friend that he was having “excessive difficulty in finding intelligent managing clerks”. In 1780 Watt solved his paperwork problems by inventing the first method of making copies. This was the subject of a Patent entitled “A new method of copying letters and writing expeditiously”. Watt’s invention involved making ink out of gum Arabic and carbon black.

Note

Gum arabic, also known as *gum acacia*, is a natural gum made of the hardened sap taken from two species of the acacia tree; *acacia senegal* and *acacia seyal*. Carbon black is a form of amorphous carbon that has a high surface area to volume ratio it is commonly produced by the incomplete combustion of heavy petroleum products such as coal tar.

Watt’s ink would stay wet for 24 hours. Writing with the ink and then pressing the result against another piece of paper created a copy. Initially there was great resistance to the copy paper. In particular banks believed that this form of copying could result in forgeries. However, by the end of its first year on sale, Watt sold over 200 examples. The real commercial push came after Watt demonstrated his process to the House of Parliament. The resultant consternation amongst the Members of Parliament resulted in their having to be reminded that Parliament was still in session! By 1785 copies were in general use, however, Cyrus P. Dalkin made the biggest advance in 1823. By using a mixture of carbon black and hot paraffin wax the back of a piece of paper was coated. The carbon black was transferred to another piece of paper underneath by the pressure of the pen. Dalkin had created *carbon copies*. Both Ralph Wedgwood in England and Pellegrino Turri in Italy had developed forms of carbon paper between 1806 and 1808, but it was Dalkin’s version of carbon copy paper that found usage.



Figure 7.2.4: Modern carbon paper.

Initially there was almost no market for this new carbon copy paper, until in 1868 when American Lebbeus Rogers was talking part in a balloon ascent. Rogers was an owner of biscuit and greengrocer companies, and was intrigued when a reporter for the Associated Press who was interviewing him used Dalkin’s carbon paper. Rogers gave up his biscuit business and founded a firm to

sell carbon paper. In 1873 he talked with E. Remington and Sons the typewriter manufacturer, and it was this application that created a success out of the carbon paper business.

Note

The term “CC” commonly used in e-mail programs today grew from the use of carbon paper and means *carbon copy*.

Interestingly, carbon black is still used today in modern photocopiers and laser printers. One of the attributes that allow its use is the ability for carbon black particles to become charged. This is related to another application of carbon black in early communications: its ability to conduct electric, and the changes that occur as a function of external pressure.

While Alexander Graham Bell was the first to be awarded a US patent for the electric telephone in March 1876, it was an invention by Thomas Edison (Figure 7.2.5) that provided significant improvements. Early telephones relied on a metal diaphragm that was attached to an electromagnet. Speaking into the metal diaphragm caused its vibration, which in turn vibrated the electromagnetic and hence created a current. Unfortunately, the current was very low and subsequent clarity was poor. Between 1877 and 1878 Edison investigated methods to improve the clarity of the signal. The key development was the carbon microphone (Figure 7.2.6).

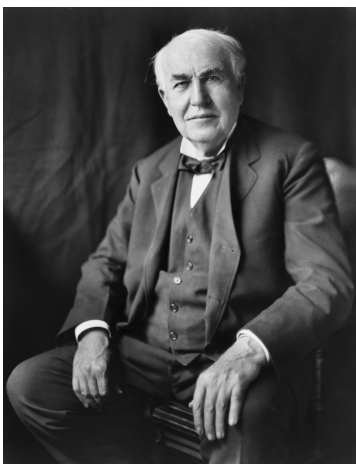


Figure 7.2.5: American inventor, scientist and businessman Thomas Alva Edison (1847 –1931).

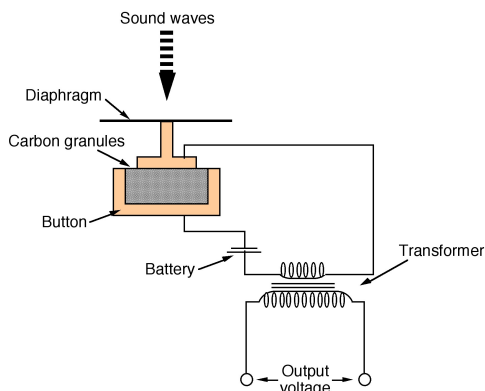


Figure 7.2.6: A schematic of a simple carbon “button” microphone.

The carbon microphone, also known as a carbon button microphone consisting of two metal plates separated by granules of carbon. One plate faces outward and acts as a diaphragm. When sound waves strike this plate, the pressure on the granules changes, which in turn changes the electrical resistance between the plates. A direct current is passed from one plate to the other, and the changing resistance results in a changing current, which can be passed through a telephone system. The carbon microphone was used in all telephones until the 1980s.

It was one of Edison’s researchers, Edward Acheson (Figure 7.2.7) whose discovery allowed for the extension of communication on a global scale. While trying to make artificial diamonds, Acheson began mixing clay and coke (carbon) at very high temperatures. In an electric furnace at high temperatures he found hexagonal crystals of silicon carbide (SiC) attached to the carbon

electrode. He called this material carborundum. When, by mistake, he overheated the mixture to 4150 °C he found that the silicon evaporated (boiling point 3265 °C) leaving pure and highly crystalline carbon: graphite.

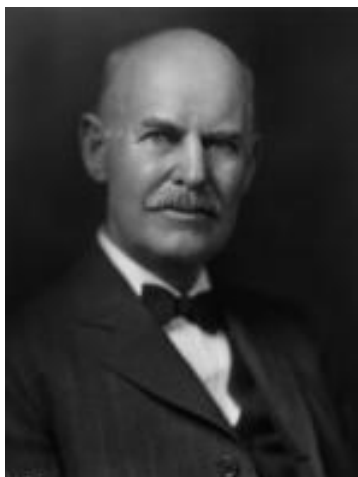


Figure 7.2.7: American chemist Edward Goodrich Acheson (1856 – 1931).

Graphite is a natural mineral normally associated with other minerals, although an enormous deposit of graphite was discovered in Cumbria, England, which the locals found very useful for marking sheep! Graphite was named by Abraham Werner (Figure 7.2.8) in 1789 from the Greek *graphein* meaning *to draw/write* due to its use in pencils. However, its use was limited due to the cost. The ability to manufacture high purity graphite resulted in its use in electrodes, dynamo brushes, and batteries. The most terrifying application of graphite was as a result of a material problem associated with the V-2 rocket built by Germany during the Second World War.



Figure 7.2.8: German geologist Abraham Gottlob Werner (1749 –1817).

The V-2 rockets or Vergeltungswaffen-2 (vengeance weapon-2) was 47 feet long, and reached 3,600 mph with an altitude of 300,000 feet (Figure 7.2.9). In order to control the direction of flight the V-2 was guided by four external rudders on the tail fins, and four internal vanes at the exit of the jet (Figure 7.2.10). These vanes were made of graphite, it being the only material that would survive the extreme temperatures.



Figure 7.2.9: A V-2 rocket at the Peenemünde Museum.



Figure 7.2.10: View of the V-2 rocket showing the graphite vanes for directional control.

Of course it was as a result of the same German scientists who worked on the V-2, working for NASA, that allowed rockets of sufficient power to escape the Earth's gravitational pull and send man to the moon, and position many of the satellites that are now vital for global communication.

This page titled [7.2: Carbon Black- From Copying to Communication](#) is shared under a [CC BY 3.0](#) license and was authored, remixed, and/or curated by [Andrew R. Barron \(CNX\)](#) via [source content](#) that was edited to the style and standards of the LibreTexts platform.

7.3: Carbon Nanomaterials

Fullerenes and Nanotubes

Introduction

Although nanomaterials had been known for many years prior to the report of C_{60} the field of nanoscale science was undoubtedly founded upon this seminal discovery. Part of the reason for this explosion in nanochemistry is that while carbon materials range from well-defined nano sized molecules (i.e., C_{60}) to tubes with lengths of hundreds of microns, they do not exhibit the instabilities of other nanomaterials as a result of the very high activation barriers to their structural rearrangement. As a consequence they are highly stable even in their unfunctionalized forms. Despite this range of carbon nanomaterials possible they exhibit common reaction chemistry: that of organic chemistry.

The previously unknown allotrope of carbon: C_{60} , was discovered in 1985, and in 1996, Curl, Kroto, and Smalley were awarded the Nobel Prize in Chemistry for the discovery. The other allotropes of carbon are graphite (sp^2) and diamond (sp^3). C_{60} , commonly known as the “buckyball” or “Buckminsterfullerene”, has a spherical shape comprising of highly pyramidalized sp^2 carbon atoms. The C_{60} variant is often compared to the typical soccer football, hence buckyball. However, confusingly, this term is commonly used for higher derivatives. Fullerenes are similar in sheet structure to graphite but they contain pentagonal (or sometimes heptagonal) rings that prevent the sheet from being planar. The unusual structure of C_{60} led to the introduction of a new class of molecules known as fullerenes, which now constitute the third allotrope of carbon. Fullerenes are commonly defined as “any of a class of closed hollow aromatic carbon compounds that are made up of twelve pentagonal and differing numbers of hexagonal faces.”

The number of carbon atoms in a fullerene range from C_{60} to C_{70} , C_{76} , and higher. Higher order fullerenes include carbon nanotubes that can be described as fullerenes that have been stretched along a rotational axis to form a tube. As a consequence of differences in the chemistry of fullerenes such as C_{60} and C_{70} as compared to nanotubes, these will be dealt with separately herein. In addition there have also been reports of nanohorns and nanofibers, however, these may be considered as variations on the general theme. It should be noted that fullerenes and nanotubes have been shown to be in flames produced by hydrocarbon combustion. Unfortunately, these naturally occurring varieties can be highly irregular in size and quality, as well as being formed in mixtures, making them unsuitable for both research and industrial applications.

Fullerenes

Carbon-60 (C_{60}) is probably the most studied individual type of nanomaterial. The spherical shape of C_{60} is constructed from twelve pentagons and twenty hexagons and resembles a soccer ball (Figure 7.3.1a). The next stable higher fullerene is C_{70} (Figure 7.3.1b) that is shaped like a rugby or American football. The progression of higher fullerenes continues in the sequence C_{74} , C_{76} , C_{78} , etc. The structural relationship between each involves the addition of six membered rings. Mathematically (and chemically) two principles define the existence of a stable fullerene, i.e., Euler’s theorem and isolated pentagon rule (IPR). Euler’s theorem states that for the closure of each spherical network, n ($n \geq 2$) hexagons and 12 pentagons are required while the IPR says no two pentagons may be connected directly with each other as destabilization is caused by two adjacent pentagons.

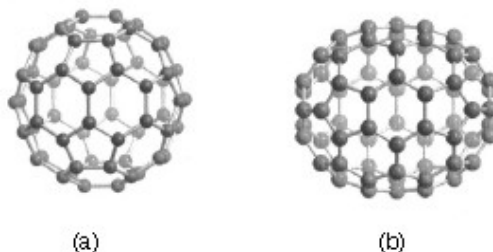


Figure 7.3.1: Molecular structures of (a) C_{60} and (b) C_{70} .

Although fullerenes are composed of sp^2 carbons in a similar manner to graphite, fullerenes are soluble in various common organic solvents. Due to their hydrophobic nature, fullerenes are most soluble in CS_2 ($C_{60} = 7.9$ mg/mL) and toluene ($C_{60} = 2.8$ mg/mL). Although fullerenes have a conjugated system, their aromaticity is distinctive from benzene that has all C-C bonds of equal lengths, in fullerenes two distinct classes of bonds exist. The shorter bonds are at the junctions of two hexagons ([6, 6] bonds) and the longer bonds at the junctions of a hexagon and a pentagon ([5,6] bonds). This difference in bonding is responsible for some of the observed reactivity of fullerenes.

Synthesis of fullerenes

The first observation of fullerenes was in molecular beam experiments at Rice University. Subsequent studies demonstrated that C_{60} it was relatively easy to produce grams of fullerenes. Although the synthesis is relatively straightforward fullerene purification remains a challenge and determines fullerene's commercial price. The first method of production of measurable quantities of fullerenes used laser vaporization of carbon in an inert atmosphere, but this produced microscopic amounts of fullerenes. Laboratory scales of fullerene are prepared by the vaporization of carbon rods in a helium atmosphere. Commercial production ordinarily employs a simple ac or dc arc. The fullerenes in the black soot collected are extracted in toluene and purified by liquid chromatography. The magenta C_{60} comes off the column first, followed by the red C_{70} , and other higher fullerenes. Even though the mechanism of a carbon arc differs from that of a resistively heated carbon rod (because it involves a plasma) the He pressure for optimum C_{60} formation is very similar.

A ratio between the mass of fullerenes and the total mass of carbon soot defines fullerene yield. The yields determined by UV-Vis absorption are approximately 40%, 10-15%, and 15% in laser, electric arc, and solar processes. Interestingly, the laser ablation technique has both the highest yield and the lowest productivity and, therefore, a scale-up to a higher power is costly. Thus, fullerene commercial production is a challenging task. The world's first computer controlled fullerene production plant is now operational at the MER Corporation, who pioneered the first commercial production of fullerene and fullerene products.

Endohedral fullerenes

Endohedral fullerenes are fullerenes that have incorporated in their inner sphere atoms, ions or clusters. Endohedral fullerenes are generally divided into two groups: endohedral metallofullerenes and non-metal doped fullerenes. The first endohedral metallofullerenes was called $La@C_{60}$. The @ sign in the name reflects the notion of a small molecule trapped inside a shell.

Doping fullerenes with metals takes place *in-situ* during the fullerene synthesis in an arc reactor or via laser evaporation. A wide range of metals have been encased inside a fullerene, i.e., Sc, Y, La, Ce, Ba, Sr, K, U, Zr, and Hf. Unfortunately, the synthesis of endohedral metallofullerenes is unspecific because in addition a high yield of unfilled fullerenes, compounds with different cage sizes are prepared (e.g., $La@C_{60}$ or $La@C_{82}$). A characteristic of endohedral metallofullerenes is that electrons will transfer from the metal atom to the fullerene cage and that the metal atom takes a position off-center in the cage. The size of the charge transfer is not always simple to determine, but it is usually between 2 and 3 units (e.g., $La_2@C_{80}$) but can be as high as 6 electrons (e.g., $Sc_3N@C_{80}$). These anionic fullerene cages are very stable molecules and do not have the reactivity associated with ordinary empty fullerenes (see below). This lack of reactivity is utilized in a method to purify endohedral metallofullerenes from empty fullerenes.

The endohedral $He@C_{60}$ and $Ne@C_{60}$ form when C_{60} is exposed to a pressure of around 3 bar of the appropriate noble gases. Under these conditions it was possible to dope 1 in every 650,000 C_{60} cages with a helium atom. Endohedral complexes with He, Ne, Ar, Kr and Xe as well as numerous adducts of the $He@C_{60}$ compound have also been proven with operating pressures of 3000 bars and incorporation of up to 0.1 % of the noble gases. The isolation of $N@C_{60}$, $N@C_{70}$ and $P@C_{60}$ is very unusual and unlike the metal derivatives no charge transfer of the pnictide atom in the center to the carbon atoms of the cage takes place.

Chemically functionalized fullerenes

Although fullerenes have a conjugated aromatic system all the carbons are quaternary (i.e., containing no hydrogen), which results in making many of the characteristic substitution reactions of planar aromatics impossible. Thus, only two types of chemical transformations exist: redox reactions and addition reactions. Of these, addition reactions have the largest synthetic value. Another remarkable feature of fullerene addition chemistry is the thermodynamics of the process. Since the sp^2 carbon atoms in a fullerene are pyramidalized there is significant strain energy. For example, the strain energy in C_{60} is ca 8 kcal/mol, which is 80% of its heat of formation. So the relief of this strain energy leading to sp^3 hybridized C atoms is the major driving force for addition reactions (Figure 7.3.2). As a consequence, most additions to fullerenes are exothermic reactions.

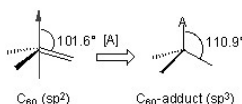


Figure 7.3.2: Strain release after addition of reagent A to a pyramidalize carbon of C_{60} .

Cyclic voltammetry (CV) studies show that C_{60} can be reduced and oxidized reversibly up to 6 electrons with one-electron transfer processes. Fulleride anions can be generated by electrochemical method and then be used to synthesize covalent organofullerene derivatives. Alkali metals can chemically reduce fullerene in solution and solid state to form M_xC_{60} ($x = 3 - 6$). C_{60} can also be

reduced by less electropositive metals like mercury to form C_{60}^- and C_{60}^{2-} . In addition, salts can also be synthesized with organic molecules, for example $[TDAE^+][C_{60}^-]$ possesses interesting electronic and magnetic behavior.

Geometric and electronic analysis predicted that fullerene behaves like an electro-poor conjugated polyolefin. Indeed C_{60} and C_{70} undergo a range of nucleophilic reactions with carbon, nitrogen, phosphorous and oxygen nucleophiles. C_{60} reacts readily with organolithium and Grignard compounds to form alkyl, phenyl or alkanyl fullerenes. Possibly the most widely used additions to fullerene is the Bingel reaction (Figure 7.3.3), where a carbon nucleophile, generated by deprotonation of α -halo malonate esters or ketones, is added to form a cyclopropanation product. The α -halo esters and ketones can also be generated *in situ* with I_2 or CBr_4 and a weak base as 1,8-diazabicyclo[5.4.0]undec-7-ene (DBU). The Bingel reaction is considered one of the most versatile and efficient methods to functionalize C_{60} .

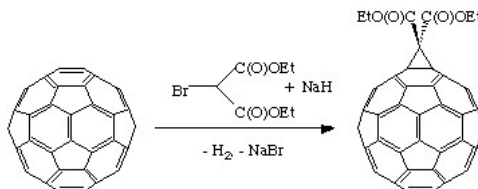


Figure 7.3.3: Bingel reaction of C_{60} with 2-bromoethylmalonate.

Cycloaddition is another powerful tool to functionalize fullerenes, in particular because of its selectivity with the 6,6 bonds, limiting the possible isomers (Figure 7.3.4). The dienophilic feature of the [6,6] double bonds of C_{60} enables the molecule to undergo various cycloaddition reactions in which the monoadducts can be generated in high yields. The best studied cycloaddition reactions of fullerene are [3+2] additions with diazoderivatives and azomethine ylides (Prato reactions). In this reaction, azomethine ylides can be generated *in situ* from condensation of α -amino acids with aldehydes or ketones, which produce 1,3 dipoles to further react with C_{60} in good yields (Figure 7.3.5). Hundreds of useful building blocks have been generated by those two methods. The Prato reactions have also been successfully applied to carbon nanotubes.

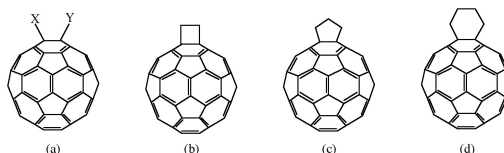


Figure 7.3.4: Geometrical shapes built onto a [6,6] ring junction: a) open, b) four-membered ring, c) five-membered ring, and d) six-membered ring.

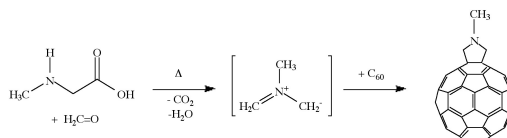


Figure 7.3.5: Prato reaction of C_{60} with N-methylglycine and paraformaldehyde.

The oxidation of fullerenes, such as C_{60} , has been of increasing interest with regard to applications in photoelectric devices, biological systems, and possible remediation of fullerenes. The oxidation of C_{60} to $C_{60}O_n$ ($n = 1, 2$) may be accomplished by photooxidation, ozonolysis, and epoxidation. With each of these methods, there is a limit to the isolable oxygenated product, $C_{60}O_n$ with $n < 3$. Highly oxygenated fullerenes, $C_{60}O_n$ with $3 \leq n \leq 9$, have been prepared by the catalytic oxidation of C_{60} with $ReMeO_3/H_2O_2$.

Carbon nanotubes

A key breakthrough in carbon nanochemistry came in 1993 with the report of needle-like tubes made exclusively of carbon. This material became known as carbon nanotubes (CNTs). There are several types of nanotubes. The first discovery was of multi walled tubes (MWNTs) resembling many pipes nested within each other. Shortly after MWNTs were discovered single walled nanotubes (SWNTs) were observed. Single walled tubes resemble a single pipe that is potentially capped at each end. The properties of single walled and multi walled tubes are generally the same, although single walled tubes are believed to have superior mechanical strength and thermal and electrical conductivity; it is also more difficult to manufacture them.

Single walled carbon nanotubes (SWNTs) are by definition fullerene materials. Their structure consists of a graphene sheet rolled into a tube and capped by half a fullerene (Figure 7.3.6). The carbon atoms in a SWNT, like those in a fullerene, are sp^2 hybridized. The structure of a nanotube is analogous to taking this graphene sheet and rolling it into a seamless cylinder. The

different types of SWNTs are defined by their diameter and chirality. Most of the presently used single-wall carbon nanotubes have been synthesized by the pulsed laser vaporization method, however, increasingly SWNTs are prepared by vapor liquid solid catalyzed growth.

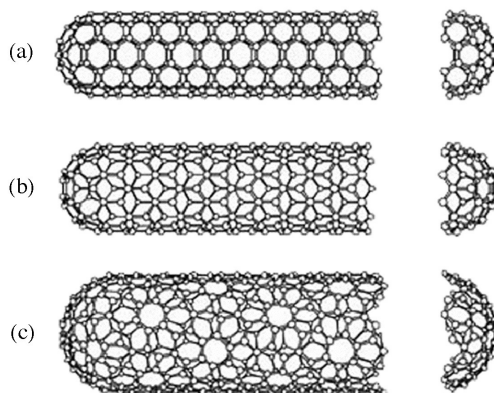


Figure 7.3.6: Structure of single walled carbon nanotubes (SWNTs) with (a) armchair, (b) zig-zag, and (c) chiral chirality.

The physical properties of SWNTs have made them an extremely attractive material for the manufacturing of nano devices. SWNTs have been shown to be stronger than steel as estimates for the Young's modulus approaches 1 Tpa. Their electrical conductance is comparable to copper with anticipate current densities of up to 10^{13} A/cm² and a resistivity as low as 0.34×10^{-4} Ω .cm at room temperatures. Finally, they have a high thermal conductivity (3000 - 6000 W.m/K).

The electronic properties of a particular SWNT structure are based on its chirality or twist in the structure of the tube which is defined by its n,m value. The values of n and m determine the chirality, or "twist" of the nanotube. The chirality in turn affects the conductance of the nanotube, its density, its lattice structure, and other properties. A SWNT is considered metallic if the value $n-m$ is divisible by three. Otherwise, the nanotube is semi-conducting. The external environment also has an effect on the conductance of a tube, thus molecules such as O₂ and NH₃ can change the overall conductance of a tube, while the presence of metals have been shown to significantly effect the opto-electronic properties of SWNTs.

Multi walled carbon nanotubes (MWNTs) range from double walled NTs, through many-walled NTs (Figure 7.3.7) to carbon nanofibers. Carbon nanofibers are the extreme of multi walled tubes (Figure 7.3.8) and they are thicker and longer than either SWNTs or MWNTs, having a cross-sectional of ca. 500 Å² and are between 10 to 100 μ m in length. They have been used extensively in the construction of high strength composites.

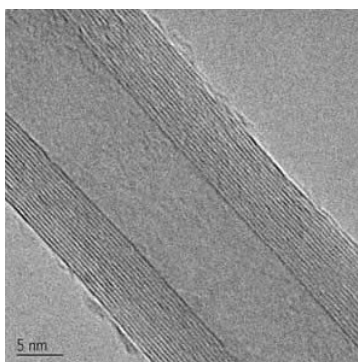


Figure 7.3.7: TEM image of an individual multi walled carbon nanotube (MWNTs). Copyright of Nanotech Innovations.

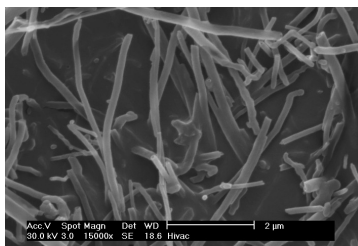


Figure 7.3.8: SEM image of vapor grown carbon nanofibers.

Synthesis of carbon nanotubes

A range of methodologies have been developed to produce nanotubes in sizeable quantities, including arc discharge, laser ablation, high pressure carbon monoxide (HiPco), and vapor liquid solid (VLS) growth. All these processes take place in vacuum or at low pressure with a process gases, although VLS growth can take place at atmospheric pressure. Large quantities of nanotubes can be synthesized by these methods; advances in catalysis and continuous growth processes are making SWNTs more commercially viable.

The first observation of nanotubes was in the carbon soot formed during the arc discharge production of fullerenes. The high temperatures caused by the discharge caused the carbon contained in the negative electrode to sublime and the CNTs are deposited on the opposing electrode. Tubes produced by this method were initially multi walled tubes (MWNTs). However, with the addition of cobalt to the vaporized carbon, it is possible to grow single walled nanotubes. This method it produces a mixture of components, and requires further purification to separate the CNTs from the soot and the residual catalytic metals. Producing CNTs in high yield depends on the uniformity of the plasma arc, and the temperature of the deposit forming on the carbon electrode.

Higher yield and purity of SWNTs may be prepared by the use of a dual-pulsed laser. SWNTs can be grown in a 50% yield through direct vaporization of a Co/Ni doped graphite rod with a high-powered laser in a tube furnace operating at 1200 °C. The material produced by this method appears as a mat of “ropes”, 10 - 20 nm in diameter and up to 100 μm or more in length. Each rope consists of a bundle of SWNTs, aligned along a common axis. By varying the process parameters such as catalyst composition and the growth temperature, the average nanotube diameter and size distribution can be varied. Although arc-discharge and laser vaporization are currently the principal methods for obtaining small quantities of high quality SWNTs, both methods suffer from drawbacks. The first is that they involve evaporating the carbon source, making scale-up on an industrial level difficult and energetically expensive. The second issue relates to the fact that vaporization methods grow SWNTs in highly tangled forms, mixed with unwanted forms of carbon and/or metal species. The SWNTs thus produced are difficult to purify, manipulate, and assemble for building nanotube-device architectures for practical applications.

In order to overcome some of the difficulties of these high-energy processes, the chemical catalysis method was developed in which a hydrocarbon feedstock is used in combination with a metal catalyst. The catalyst is typically, but not limited to iron, cobalt, or iron/molybdenum, it is heated under reducing conditions in the presence of a suitable carbon feedstock, e.g., ethylene. This method can be used for both SWNTs and MWNTs; the formation of each is controlled by the identity of the catalyst and the reaction conditions. A convenient laboratory scale apparatus is available from Nanotech Innovations, Inc., for the synthesis of highly uniform, consistent, research sample that uses pre-weighed catalyst/carbon source ampoules. This system, allows for 200 mg samples of MWNTs to be prepared for research and testing. The use of CO as a feedstock, in place of a hydrocarbon, led to the development of the high-pressure carbon monoxide (HiPco) procedure for SWNT synthesis. By this method, it is possible to produce gram quantities of SWNTs, unfortunately, efforts to scale beyond that have not met with complete success.

Initially developed for small-scale investigations of catalyst activity, vapor liquid solid (VLS) growth of nanotubes has been highly studied, and now shows promise for large-scale production of nanotubes. Recent approaches have involved the use of well-defined nanoparticle or molecular precursors and many different transition metals have been employed, but iron, nickel, and cobalt remain to be the focus of most research. The nanotubes grow at the sites of the metal catalyst; the carbon-containing gas is broken apart at the surface of the catalyst particle, and the carbon is transported to the edges of the particle, where it forms the nanotube. The length of the tube grown in surface supported catalyst VLS systems appears to be dependent on the orientation of the growing tube with the surface. By properly adjusting the surface concentration and aggregation of the catalyst particles it is possible to synthesize vertically aligned carbon nanotubes, i.e., as a carpet perpendicular to the substrate.

Of the various means for nanotube synthesis, the chemical processes show the greatest promise for industrial scale deposition in terms of its price/unit ratio. There are additional advantages to the VLS growth, which unlike the other methods is capable of growing nanotubes directly on a desired substrate. The growth sites are controllable by careful deposition of the catalyst. Additionally, no other growth methods have been developed to produce vertically aligned SWNTs.

Chemical functionalization of carbon nanotubes

The limitation of using carbon nanotubes in any practical applications has been its solubility; for example SWNTs have little to no solubility in most solvent due to the aggregation of the tubes. Aggregation/roping of nanotubes occurs as a result of the high van der Waals binding energy of *ca.* 500 eV per mm of tube contact. The van der Waals force between the tubes is so great, that it take tremendous energy to pry them apart, making it very to make combination of nanotubes with other materials such as in composite applications. The functionalization of nanotubes, i.e., the attachment of “chemical functional groups” provides the path to

overcome these barriers. Functionalization can improve solubility as well as processibility, and has been used to align the properties of nanotubes to those of other materials. The clearest example of this is the ability to solubilize nanotubes in a variety of solvents, including water. It is important when discussing functionalization that a distinction is made between covalent and non-covalent functionalization.

Current methods for solubilizing nanotubes without covalent functionalization include highly aromatic solvents, super acids, polymers, or surfactants. Non-covalent “functionalization” is generally on the concept of supramolecular interactions between the SWNT and some macromolecule as a result of various adsorption forces, such as van der Waals’ and π -stacking interactions. The chemical speciation of the nanotube itself is not altered as a result of the interaction. In contrast, covalent functionalization relies on the chemical reaction at either the sidewall or end of the SWNT. As may be expected the high aspect ratio of nanotubes means that sidewall functionalization is much more important than the functionalization of the cap. Direct covalent sidewall functionalization is associated with a change of hybridization from sp^2 to sp^3 and a simultaneous loss of conjugation. An alternative approach to covalent functionalization involves the reaction of defects present (or generated) in the structure of the nanotube. Defect sites can be the open ends and holes in the sidewalls, and pentagon and heptagon irregularities in the hexagon graphene framework (often associated with bends in the tubes). All these functionalizations are exohedral derivatizations. Taking the hollow structure of nanotubes into consideration, endohedral functionalization of SWNTs is possible, i.e., the filling of the tubes with atoms or small molecules. It is important to note that covalent functionalization methods have one problem in common: extensive covalent functionalization modifies SWNT properties by disrupting the continuous π -system of SWNTs.

Various applications of nanotubes require different, specific modification to achieve desirable physical and chemical properties of nanotubes. In this regard, covalent functionalization provides a higher degree of fine-tuning the chemistry and physics of SWNTs than non-covalent functionalization. Until now, a variety of methods have been used to achieve the functionalization of nanotubes (Figure 7.3.9).

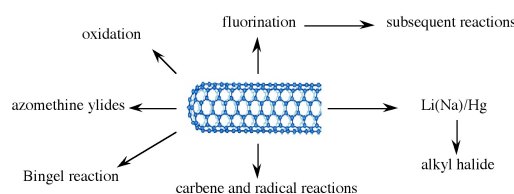


Figure 7.3.9: Schematic description of various covalent functionalization strategies for SWNTs.

Taking chemistry developed for C_{60} , SWNTs may be functionalized using 1,3 dipolar addition of azomethine ylides. The functionalized SWNTs are soluble in most common organic solvents. The azomethine ylide functionalization method was also used for the purification of SWNTs. Under electrochemical conditions, aryl diazonium salts react with SWNTs to achieve functionalized SWNTs, alternatively the diazonium ions may be generated *in-situ* from the corresponding aniline, while a solvent free reaction provides the best chance for large-scale functionalization this way. In each of these methods it is possible to control the amount of functionalization on the tube by varying reaction times and the reagents used; functionalization as high as 1 group per every 10 - 25 carbon atoms is possible.

Organic functionalization through the use of alkyl halides, a radical pathway, on tubes treated with lithium in liquid ammonia offers a simple and flexible route to a range of functional groups. In this reaction, functionalization occurs on every 17 carbons. Most success has been found when the tubes are dodecylated. These tubes are soluble in chloroform, DMF, and THF.

The addition of oxygen moieties to SWNT sidewalls can be achieved by treatment with acid or wet air oxidation, and ozonolysis. The direct epoxidation of SWNTs may be accomplished by the direct reaction with a peroxide reagent, or catalytically. Catalytic de-epoxidation (Figure 7.3.10) allows for the quantitative analysis of sidewall epoxide and led to the surprising result that previously assumed “pure” SWNTs actually contain *ca.* 1 oxygen per 250 carbon atoms.

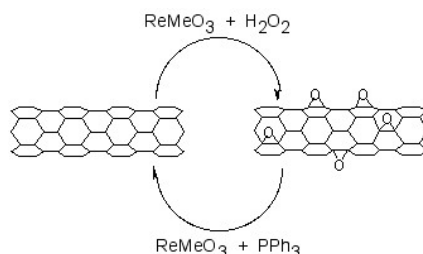


Figure 7.3.10: Catalytic oxidation and de-epoxidation of SWNTs.

One of the easiest functionalization routes, and a useful synthon for subsequent conversions, is the fluorination of SWNTs, using elemental fluorine. Importantly, a C:F ratios of up to 2:1 can be achieved without disruption of the tubular structure. The fluorinated SWNTs (F-SWNTs) proved to be much more soluble than pristine SWNTs in alcohols (1 mg/mL in *iso*-propanol), DMF and other selected organic solvents. Scanning tunneling microscopy (STM) revealed that the fluorine formed bands of approximately 20 nm, while calculations using DFT revealed 1,2 addition is more energetically preferable than 1,4 addition, which has been confirmed by solid state ^{13}C NMR. F-SWNTs make highly flexible synthons and subsequent elaboration has been performed with organolithium, Grignard reagents, and amines.

Functionalized nanotubes can be characterized by a variety of techniques, such as atomic force microscopy (AFM), transmission electron microscopy (TEM), UV-vis spectroscopy, and Raman spectroscopy. Changes in the Raman spectrum of a nanotube sample can indicate if functionalization has occurred. Pristine tubes exhibit two distinct bands. They are the radial breathing mode (230 cm^{-1}) and the tangential mode (1590 cm^{-1}). When functionalized, a new band, called the disorder band, appears at *ca.* 1350 cm^{-1} . This band is attributed to sp^3 -hybridized carbons in the tube. Unfortunately, while the presence of a significant D mode is consistent with sidewall functionalization and the relative intensity of D (disorder) mode versus the tangential G mode ($1550 - 1600\text{ cm}^{-1}$) is often used as a measure of the level of substitution. However, it has been shown that Raman is an unreliable method for determination of the extent of functionalization since the relative intensity of the D band is also a function of the substituents distribution as well as concentration. Recent studies suggest that solid state ^{13}C NMR are possibly the only definitive method of demonstrating covalent attachment of particular functional groups.

Coating carbon nanotubes: creating inorganic nanostructures

Fullerenes, nanotubes and nanofibers represent suitable substrates for the seeding other materials such as oxides and other minerals, as well as semiconductors. In this regard, the carbon nanomaterial acts as a seed point for the growth as well as a method of defining unusual aspect ratios. For example, silica fibers can be prepared by a number of methods, but it is only through coating SWNTs that silica nano-fibers with micron lengths with tens of nanometers in diameter may be prepared.

While C_{60} itself does not readily seed the growth of inorganic materials, liquid phase deposition of oxides, such as silica, in the presence of fullereneol, $\text{C}_{60}(\text{OH})_n$, results in the formation of uniform oxide spheres. It appears the fullereneol acts as both a reagent and a physical point for subsequent oxide growth, and it is C_{60} , or an aggregate of C_{60} , that is present within the spherical particle. The addition of fullereneol alters the morphology and crystal phase of CaCO_3 precipitates from aqueous solution, resulting in the formation of spherical features, 5-pointed flower shaped clusters, and triangular crystals as opposed to the usual rhombic crystals. In addition, the meta-stable vaterite phase is observed with the addition of $\text{C}_{60}(\text{OH})_n$.

As noted above individual SWNTs may be obtained in solution when encased in a cylindrical micelle of a suitable surfactant. These individualized nanotubes can be coated with a range of inorganic materials. Liquid phase deposition (LPD) appears to have significant advantages over other methods such as incorporating surfactant-coated SWNTs into a preceramic matrix, *in situ* growth of the SWNT in an oxide matrix, and sol-gel methods. The primary advantage of LPD growth is that individual SWNTs may be coated rather than bundles or ropes. For example, SWNTs have been coated with silica by liquid phase deposition (LPD) using a silica/ H_2SiF_6 solution and a surfactant-stabilized solution of SWNTs. The thickness of the coating is dependent on the reaction mixture concentration and the reaction time. The SWNT core can be removed by thermolysis under oxidizing conditions to leave a silica nano fiber. It is interesting to note that the use of a surfactant is counter productive when using MWNTs and VGFs, in this case surface activation of the nanotube offers the suitable growth initiation. Pre-oxidation of the MWNT or VGF allows for uniform coatings to be deposited. The coated SWNTs, MWNTs, and VGFs can be subsequently reacted with suitable surface reagents to impart miscibility in aqueous solutions, guar gels, and organic matrixes. In addition to simple oxides, coated nanotubes have been prepared with minerals such as carbonates and semiconductors.

Bibliography

- S. M. Bachilo, M. S. Strano, C. Kittrell, R. H. Hauge, R. E. Smalley, and R. B. Weisman, *Science*, 2002, **298**, 2361.
- D. S. Bethune, C. H. Klang, M. S. deVries, G. Gorman, R. Savoy, J. Vazquez, and R. Beyers, *Nature*, 1993, **363**, 605.
- J. J. Brege, C. Gallaway, and A. R. Barron, *J. Phys. Chem., C*, 2007, **111**, 17812.
- C. A. Dyke and J. M. Tour, *J. Am. Chem. Soc.*, 2003, **125**, 1156.
- Z. Ge, J. C. Duchamp, T. Cai, H. W. Gibson, and H. C. Dorn, *J. Am. Chem. Soc.*, 2005, **127**, 16292.
- L. A. Girifalco, M. Hodak, and R. S. Lee, *Phys. Rev. B*, 2000, **62**, 13104.
- T. Guo, P. Nikolaev, A. G. Rinzler, D. Tománek, D. T. Colbert, and R. E. Smalley, *J. Phys. Chem.*, 1995, **99**, 10694.
- J. H. Hafner, M. J. Bronikowski, B. R. Azamian, P. Nikolaev, A. G. Rinzler, D. T. Colbert, K. A. Smith, and R. E. Smalley, *Chem. Phys. Lett.*, 1998, **296**, 195.

- A. Hirsch, *Angew. Chem. Int. Ed.*, 2002, **40**, 4002.
- S. Iijima and T. Ichihashi, *Nature*, 1993, **363**, 603.
- H. R. Jafry, E. A. Whitsitt, and A. R. Barron, *J. Mater. Sci.*, 2007, **42**, 7381.
- H. W. Kroto, J. R. Heath, S. C. O'Brien, R. F. Curl, and R. E. Smalley, *Nature*, 1985, **318**, 162.
- F. Liang, A. K. Sadana, A. Peera, J. Chattopadhyay, Z. Gu, R. H. Hauge, and W. E. Billups, *Nano Lett.*, 2004, **4**, 1257.
- D. Ogrin and A. R. Barron, *J. Mol. Cat. A: Chem.*, 2006, **244**, 267.
- D. Ogrin, J. Chattopadhyay, A. K. Sadana, E. Billups, and A. R. Barron, *J. Am. Chem. Soc.*, 2006, **128**, 11322.
- R. E. Smalley, *Acc. Chem. Res.*, 1992, **25**, 98.
- M. M. J. Treacy, T. W. Ebbesen, and J. M. Gibson, *Nature*, 1996, **381**, 678.
- E. A. Whitsitt and A. R. Barron, *Nano Lett.*, 2003, **3**, 775.
- J. Yang and A. R. Barron, *Chem. Commun.*, 2004, 2884.
- L. Zeng, L. B. Alemany, C. L. Edwards, and A. R. Barron, *Nano Res.*, 2008, **1**, 72.

Graphene

Introduction

Graphene is a one-atom-thick planar sheet of sp^2 -bonded carbon atoms that are densely packed in a honeycomb crystal lattice (Figure 7.3.11). The name comes from “graphite” and “alkene”; graphite itself consists of many graphene sheets stacked together.

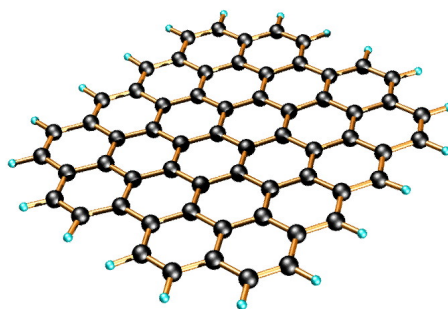


Figure 7.3.11: Idealized structure of a single graphene sheet.

Single-layer graphene nanosheets were first characterized in 2004, prepared by mechanical exfoliation (the “scotch-tape” method) of bulk graphite. Later graphene was produced by epitaxial chemical vapor deposition on silicon carbide and nickel substrates. Most recently, graphene nanoribbons (GNRs) have been prepared by the oxidative treatment of carbon nanotubes and by plasma etching of nanotubes embedded in polymer films.

Physical properties of graphene

Graphene has been reported to have a Young’s modulus of 1 TPa and intrinsic strength of 130 GP; similar to single walled carbon nanotubes (SWNTs). The electronic properties of graphene also have some similarity with carbon nanotubes. Graphene is a zero-bandgap semiconductor. Electron mobility in graphene is extraordinarily high ($15,000 \text{ cm}^2/\text{V}\cdot\text{s}$ at room temperature) and ballistic electron transport is reported to be on length scales comparable to that of SWNTs. One of the most promising aspects of graphene involves the use of GNRs. Cutting an individual graphene layer into a long strip can yield semiconducting materials where the bandgap is tuned by the width of the ribbon.

While graphene’s novel electronic and physical properties guarantee this material will be studied for years to come, there are some fundamental obstacles yet to overcome before graphene based materials can be fully utilized. The aforementioned methods of graphene preparation are effective; however, they are impractical for large-scale manufacturing. The most plentiful and inexpensive source of graphene is bulk graphite. Chemical methods for exfoliation of graphene from graphite provide the most realistic and scalable approach to graphene materials.

Graphene layers are held together in graphite by enormous van der Waals forces. Overcoming these forces is the major obstacle to graphite exfoliation. To date, chemical efforts at graphite exfoliation have been focused primarily on intercalation, chemical derivatization, thermal expansion, oxidation-reduction, the use of surfactants, or some combination of these.

Graphite oxide

Probably the most common route to graphene involves the production of graphite oxide (GO) by extremely harsh oxidation chemistry. The methods of Staudenmeier or Hummers are most commonly used to produce GO, a highly exfoliated material that is dispersible in water. The structure of GO has been the subject of numerous studies; it is known to contain epoxide functional groups along the basal plane of sheets as well as hydroxyl and carboxyl moieties along the edges (Figure 7.3.12). In contrast to other methods for the synthesis of GO, the the *m*-peroxybenzoic acid (*m*-CPBA) oxidation of microcrystalline synthetic graphite at room temperature yields graphite epoxide in high yield, without significant additional defects.

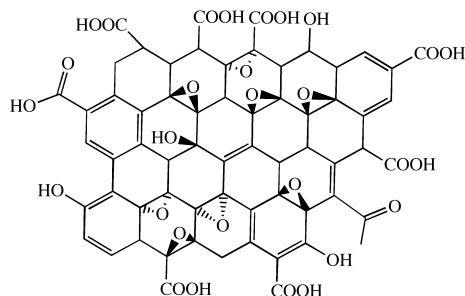


Figure 7.3.12: Idealized structure proposed for graphene oxide (GO). Adapted from C. E. Hamilton, PhD Thesis, Rice University (2009).

As graphite oxide is electrically insulating, it must be converted by chemical reduction to restore the electronic properties of graphene. Chemically converted graphene (CCG) is typically reduced by hydrazine or borohydride. The properties of CCG can never fully match those of graphene for two reasons:

1. Oxidation to GO introduces defects.
2. Chemical reduction does not fully restore the graphitic structure.

As would be expected, CCG is prone to aggregation unless stabilized. Graphene materials produced from pristine graphite avoid harsh oxidation to GO and subsequent (incomplete) reduction; thus, materials produced are potentially much better suited to electronics applications.

A catalytic approach to the removal of epoxides from fullerenes and SWNTs has been applied to graphene epoxide and GO. Treatment of oxidized graphenes with methyltrioxorhenium (MeReO₃, MTO) in the presence of PPh₃ results in the oxygen transfer, to form O=PPh₃ and allow for quantification of the C:O ratio.

Homogeneous graphene dispersions

An alternate approach to producing graphene materials involves the use of pristine graphite as starting material. The fundamental value of such an approach lies in its avoidance of oxidation to GO and subsequent (incomplete) reduction, thereby preserving the desirable electronic properties of graphene. There is precedent for exfoliation of pristine graphite in neat organic solvents without oxidation or surfactants. It has been reported that *N,N*-dimethylformamide (DMF) dispersions of graphene are possible, but no detailed characterization of the dispersions were reported. In contrast, Coleman and coworkers reported similar dispersions using *N*-methylpyrrolidone (NMP), resulting in individual sheets of graphene at a concentration of ≤ 0.01 mg/mL. NMP and DMF are highly polar solvents, and not ideal in cases where reaction chemistry requires a nonpolar medium. Further, they are hygroscopic, making their use problematic when water must be excluded from reaction mixtures. Finally, DMF is prone to thermal and chemical decomposition.

Recently, dispersions of graphene has been reported in *ortho*-dichlorobenzene (ODCB) using a wide range of graphite sources. The choice of ODCB for graphite exfoliation was based on several criteria:

1. ODCB is a common reaction solvent for fullerenes and is known to form stable SWNT dispersions.
2. ODCB is a convenient high-boiling aromatic, and is compatible with a variety of reaction chemistries.
3. ODCB, being aromatic, is able to interact with graphene *via* π - π stacking.
4. It has been suggested that good solvents for graphite exfoliation should have surface tension values of 40 – 50 mJ/m². ODCB has a surface tension of 36.6 mJ/m², close to the proposed range.

Graphite is readily exfoliated in ODCB with homogenization and sonication. Three starting materials were successfully dispersed: microcrystalline synthetic, thermally expanded, and highly ordered pyrolytic graphite (HOPG). Dispersions of microcrystalline

synthetic graphite have a concentration of 0.03 mg/mL, determined gravimetrically. Dispersions from expanded graphite and HOPG are less concentrated (0.02 mg/mL).

High resolution transmission electron microscopy (HRTEM) shows mostly few-layer graphene ($n < 5$) with single layers and small flakes stacked on top (Figure 7.3.13). Large graphitic domains are visible; this is further supported by selected area electron diffraction (SAED) and fast Fourier transform (FFT) in selected areas. Atomic force microscope (AFM) images of dispersions sprayed onto silicon substrates shows extremely thin flakes with nearly all below 10 nm. Average height is 7 - 10 nm. The thinnest are less than 1 nm, graphene monolayers. Lateral dimensions of nanosheets range from 100 – 500 nm.

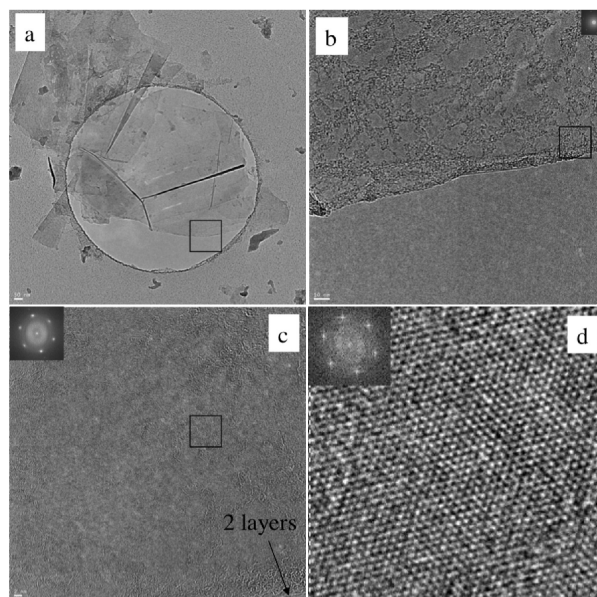


Figure 7.3.13: TEM images of single layer graphene from HOPG dispersion. (a) monolayer and few layer of graphene stacked with smaller flakes; (b) selected edge region from (a), (c) selected area from (b) with FFT inset, (d) HRTEM of boxed region in (c) showing lattice fringes with FFT inset. Adapted from C. E. Hamilton, PhD Thesis, Rice University (2009).

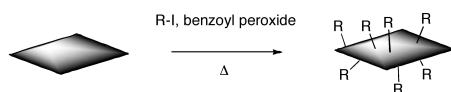
As-deposited films cast from ODCB graphene show poor electrical conductivity, however, after vacuum annealing at 400 °C for 12 hours the films improve vastly, having sheet resistances on the order of 60 Ω /sq. By comparison, graphene epitaxially grown on Ni has a reported sheet resistance of 280 Ω /sq.

Covalent functionalization of graphene and graphite oxide

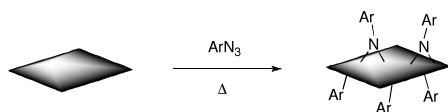
The covalent functionalization of SWNTs is well established. Some routes to covalently functionalized SWNTs include esterification/ amidation, reductive alkylation (Billups reaction), and treatment with azomethine ylides (Prato reaction), diazonium salts, or nitrenes. Conversely, the chemical derivatization of graphene and GO is still relatively unexplored.

Some methods previously demonstrated for SWNTs have been adapted to GO or graphene. GO carboxylic acid groups have been converted into acyl chlorides followed by amidation with long-chain amines. Additionally, the coupling of primary amines and amino acids via nucleophilic attack of GO epoxide groups has been reported. Yet another route coupled isocyanates to carboxylic acid groups of GO. Functionalization of partially reduced GO by aryldiazonium salts has also been demonstrated. The Billups reaction has been performed on the intercalation compound potassium graphite (C_8K), as well as graphite fluoride, and most recently GO. Graphene alkylation has been accomplished by treating graphite fluoride with alkyl lithium reagents.

ODCB dispersions of graphene may be readily converted to covalently functionalize graphene. Thermal decomposition of benzoyl peroxide is used to initiate radical addition of alkyl iodides to graphene in ODCB dispersions.



Additionally, functionalized graphene with nitrenes generated by thermal decomposition of aryl azides



Bibliography

- P. Blake, P. D. Brimicombe, R. R. Nair, T. J. Booth, D. Jiang, F. Schedin, L. A. Ponomarenko, S. V. Morozov, H. F. Gleeson, E. W. Hill, A. K. Geim, and K. S. Novoselov, *Nano Lett.*, 2008, **8**, 1704.
- J. Chattopadhyay, A. Mukherjee, C. E. Hamilton, J.-H. Kang, S. Chakraborty, W. Guo, K. F. Kelly, A. R. Barron, and W. E. Billups, *J. Am. Chem. Soc.*, 2008, **130**, 5414.
- G. Eda, G. Fanchini, and M. Chhowalla, *Nat. Nanotechnol.*, 2008, **3**, 270.
- M. Y. Han, B. Ozyilmaz, Y. Zhang, and P. Kim, *Phys. Rev. Lett.*, 2008, **98**, 206805.
- Y. Hernandez, V. Nicolosi, M. Lotya, F. M. Blighe, Z. Sun, S. De, I. T. McGovern, B. Holland, M. Byrne, Y. K. Gun'Ko, J. J. Boland, P. Niraj, G. Duesberg, S. Krishnamurthy, R. Goodhue, J. Hutchinson, V. Scardaci, A. C. Ferrari, and J. N. Coleman, *Nat. Nanotechnol.*, 2008, **3**, 563.
- W. S. Hummers and R. E. Offeman, *J. Am. Chem. Soc.*, 1958, **80**, 1339.
- L. Jiao, L. Zhang, X. Wang, G. Diankov, and H. Dai, *Nature*, 2009, **458**, 877.
- D. V. Kosynkin, A. L. Higginbotham, A. Sinitskii, J. R. Lomeda, A. Dimiev, B. K. Price, and J. M. Tour, *Nature*, 2009, **458**, 872.
- D. Li, M. B. Mueller, S. Gilje, R. B. Kaner, and G. G. Wallace, *Nat. Nanotechnol.*, 2008, **3**, 101.
- S. Niyogi, E. Bekyarova, M. E. Itkis, J. L. McWilliams, M. A. Hamon, and R. C. Haddon, *J. Am. Chem. Soc.*, 2006, **128**, 7720.
- Y. Si and E. T. Samulski, *Nano Lett.*, 2008, **8**, 1679.
- L. Staudenmaier, *Ber. Dtsch. Chem. Ges.*, 1898, **31**, 1481.

This page titled [7.3: Carbon Nanomaterials](#) is shared under a [CC BY 3.0](#) license and was authored, remixed, and/or curated by [Andrew R. Barron \(CNX\)](#) via [source content](#) that was edited to the style and standards of the LibreTexts platform.

7.4: Nitrogen Compounds of Carbon

There are a myriad of organic compounds containing carbon-nitrogen bonds, including: amines, imines, and nitriles. However, here we are concerned with the simplest carbon-nitrogen compounds.

Cyanogen

Cyanogen, $(\text{CN})_2$, may be considered the smallest molecular fragment containing carbon and nitrogen (Figure 7.4.1a). The reaction chemistry of cyanogen is related to that of the halogens, i.e., F_2 , Cl_2 , etc. Consequently, cyanogen is called a *pseudo halogen*.

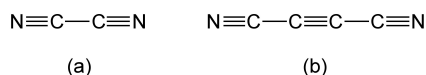


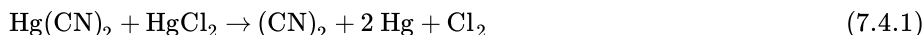
Figure 7.4.1: The structures of (a) cyanogen, $(\text{CN})_2$ and (b) dicyanoacetylene (carbon subnitride, C_4N_2).

As shown in Table 7.4.1 the bonding in cyanogen is consistent with localization of the π -bonding between carbon and nitrogen given the similarity of the C-N bond distance in cyanogens and acetonitrile. However, there is clearly some π -delocalization associated with the C-C distance given its shortening as compared to ethane.

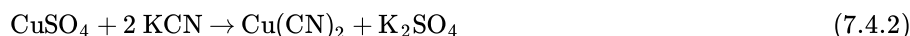
Table 7.4.1: A comparison of the bond distances in selected carbon nitrogen compounds.

Compound	Formula	C-C bond distance (Å)	C-N bond distance (Å)
Cyanogen	$(\text{CN})_2$	1.393	1.163
Hydrogen cyanide	HCN	-	1.154
Acetonitrile	CH_3CN	1.46	1.16
Ethane	C_2H_6	1.535	-
Ethylene	C_2H_4	1.339	-

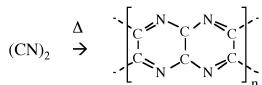
Cyanogen is produced by the reaction of a mixture of the cyanide and chloride of mercury, (7.4.1).



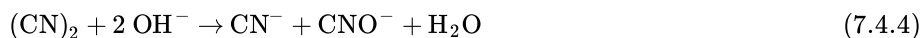
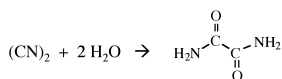
Alternatively, the decomposition of unstable copper(II) cyanide, formed from a copper(II) salts with a Group 1 cyanide, (7.4.2), yields cyanogens, (7.4.3).



Cyanogen is a flammable gas (Mp = -28°C and Bp = -21°C) that produces the second hottest flame natural flame (after carbon subnitride, C_4N_2) with a temperature of over 4525°C when burnt in oxygen. Heating cyanogen in the absence of oxygen results self polymerizes.



Hydrolysis of cyanogen results in addition across the carbon-nitrogen triple bonds and the formation of oxamide. Cleavage of the C-C bond does occur in the presence of base (e.g., KOH), with the formation of cyanide (CN^-) and cyanate (CNO^-) salts, (7.4.4).



Dicyanoacetylene

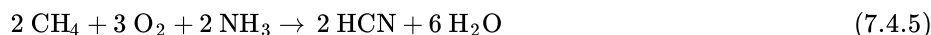
Dicyanoacetylene (also known as carbon subnitride or by its IUPAC name but-2-ynedinitrile) has the structure shown in Figure 7.4.1b, and may be thought of as a dicyanide substituted acetylene.

At room temperature, dicyanoacetylene is a clear liquid, however, solid dicyanoacetylene has been detected in the atmosphere of Titan (the largest moon of the planet Saturn) by infrared spectroscopy. Dicyanoacetylene is an entropic explosive giving carbon powder and nitrogen gas. In the presence of oxygen it burns with a bright blue-white flame at a temperature of 4990 °C.

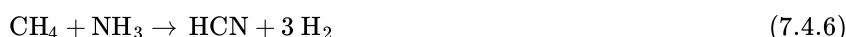
Hydrogen cyanide

Hydrogen cyanide (HCN) is a colorless, highly poisonous, gas (Mp = -13.5 °C and Bp = 25.6 °C). Due to its original isolation from Prussian blue (hydrated ferric ferrocyanide), hydrogen cyanide is also known by the name of *prussic acid*.

The synthesis of hydrogen cyanide is accomplished commercially by the partial oxidation of methane in the presence of ammonia, (7.4.5), using a platinum catalyst. The heat to activate the reaction is derived from the partial combustion of the methane and ammonia. The resulting aqueous solution is dried by distilled from phosphorus pentoxide (P₂O₅) to yield anhydrous hydrogen cyanide.



Hydrogen cyanide may also be formed in the absence of oxygen, (7.4.6); however, in this case the reaction must be heated externally.



Small quantities of hydrogen cyanide for laboratory use may be prepared by the reaction of an acid with a cyanide salt (either potassium or sodium), (7.4.7).



The structure of hydrogen cyanide is shown in Figure 7.4.2 along with its isomeric form, hydrogen isocyanide (HNC). While hydrogen cyanide is present in the pits of many fruits, and is generated by burnet moths and some millipedes, hydrogen isocyanide is only found in interstellar space. It is postulated, however, that along with HCN, HNC is an important building block for amino acids and hence life.

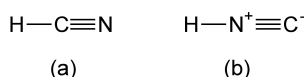


Figure 7.4.2: The structures of (a) hydrogen cyanide (HCN) and (b) its isomer hydrogen isocyanide (HNC).

In the liquid state hydrogen cyanide forms strong hydrogen bonds (Figure 7.4.3). Hydrogen cyanide is a good solvent for polar compounds due to its high permittivity (ε_r) and high dipole moment (2.98 D).

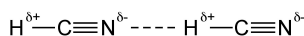
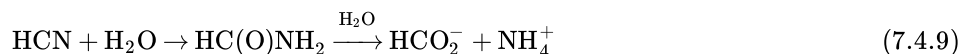


Figure 7.4.3: The hydrogen bonding in liquid hydrogen cyanide.

In aqueous solution hydrogen cyanide is a weak acid, (7.4.7), and several salts are known. However, HCN also reacts with water to give ammonium formate via formamide, (7.4.8).



In a similar manner to cyanogen's relationship to the halogens, the cyanide anion (CN⁻) is considered a *pseudo halide* (i.e., F⁻, Cl⁻, etc), and as such forms many coordination compounds, e.g., [Fe(CN)₆]³⁻ and [Ag(CN)₂]⁻.

Assassination, execution, and the Holocaust

Hydrogen cyanide is fatal to humans due to its inhibition of the enzyme cytochrome c oxidase by the cyanide ion (CN⁻), which results in the halting of cellular respiration. A concentration of 300 mg/m³ will kill within 10 minutes, while 3200 mg/m³ (ca. 3500 ppm) will be fatal in about 1 minute.

The symptoms of cyanide poisoning appear similar to a heart attack and this has led to it being the poison of choice for both fictional murder mystery writers as well as the former KGB (*Konitet gosudarstvennoy bezopasnosti* or Committee for State Security) and its predecessor SMERSH (from the contraction *smert shpionam* meaning *death to spies*) in real life. Possibly the most famous use of hydrogen cyanide for assassination was the use of an atomizer mist gun by KGB agent Bohdan Stashynsky for

the killing of the Ukrainian political writer and anti-communist Lev Rebet in 1957, and later in 1959 that of fellow Ukrainian, Stepan Bandera. In both cases the intention was to induce cardiac arrest and make it look like the victim had died of a heart attack.

Without doubt the most notorious use of hydrogen cyanide is in the form of the product Zyklon B, which was originally developed as an insecticide. Dr. Walter Heerdt found that hydrogen cyanide could be absorbed onto substrates such as absorbent pellets (e.g., silica), fibers, or diatomaceous earth (Figure 7.4.4). While stable in an airtight container, once opened the hydrogen cyanide is released. The “B” in the trade name comes from the German name for prussic acid (the common name for hydrogen cyanide), i.e., *Blausäure* meaning *blue acid*.

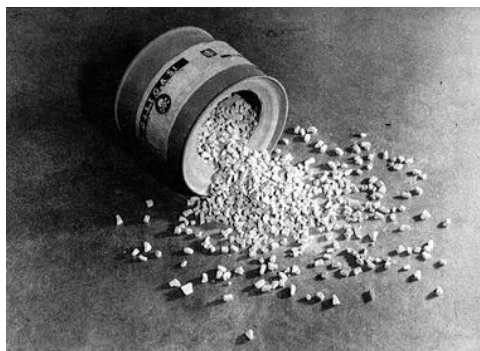


Figure 7.4.4: A can of Zyklon B granules.

The first wholesale use of Zyklon B was actually in the US where it was used as early as 1929 to disinfect the freight trains and cloths of Mexican immigrants entering the US. The first use of Zyklon B in the concentration camps during World War II was for a similar purpose (in particular for delousing to control typhus); however, for its use as an insecticide, Zyklon B contained a warning odorant. The deliberate manufacture of Zyklon B without the odorant resulted in the material that was used on a group of 250 gypsy children at the Buchenwald concentration camp in early 1940. Subsequently in September 1940, a similar number of sick Polish prisoners of war and 600 Soviet prisoners of war were killed at Auschwitz (Figure 7.4.5). Once these horrific tests were performed, the systematic murder of millions of people, including Jews, gypsies, and homosexuals, was accomplished using Zyklon B at Auschwitz, Majdanek, Sachsenhausen, and one of the Operation Reinhard camps. It is only fitting that many of the architects of the Holocaust themselves died from cyanide, including: Adolf Hitler (in addition to a bullet), Joseph Goebbles, Hermann Göring, and Heinrich Himmler.



Figure 7.4.5: The main gate at Auschwitz, through which an estimated two million victims of Nazi genocide passed.

Despite the horror associated with the use of hydrogen cyanide for the Holocaust, it was used by 11 US states for the death penalty (Figure 7.4.6). Arizona, Maryland, and Missouri retain the gas chamber as a secondary method of execution though they have lethal injection as the primary method. Potassium cyanide (KCN) pellets are placed into a compartment directly below the chair in the gas chamber. The condemned person is then strapped into the chair, and the airtight chamber sealed. Concentrated sulfuric acid (H_2SO_4) is then poured down a tube onto the cyanide pellets to generate hydrogen cyanide, (7.4.7). Execution by gas chamber is especially unpleasant for the witnesses to the execution due to the physical responses exhibited during the process of dying, including: convulsions and excessive drooling.



Figure 7.4.6: The former gas chamber in San Quentin State Prison, now an execution chamber for lethal injection, in which the State of California executed 192 men and 4 women.

Bibliography

- J. Wu and N. J. Evans, *Astrophys. J.*, 2003, **592**, L79.

This page titled [7.4: Nitrogen Compounds of Carbon](#) is shared under a [CC BY 3.0](#) license and was authored, remixed, and/or curated by [Andrew R. Barron \(CNX\)](#) via [source content](#) that was edited to the style and standards of the LibreTexts platform.

7.5: Carbon Monoxide

Carbon monoxide (CO) is iso-electronic with nitrogen (N₂) and formed through the incomplete combustion of carbon, (7.5.1), or hydrocarbon compounds.



Carbon monoxide may also be made from steam and coal as part of synthesis gas, (7.4.2). A convenient laboratory preparation of CO is the dehydration of formic acid by sulfuric acid, (7.4.3).



Hazards and toxicity

Carbon monoxide is flammable, (7.4.4), and has an explosive limit of 12.5 – 74% with an auto ignition temperature of 609 °C.



Carbon monoxide is also very toxic; however, it is colorless, odorless, tasteless and non-irritating all of which increase its danger. The incomplete combustion of hydrocarbon (natural gas or heating oil) or carbon sources (coal or charcoal) is a common hazard in the home. In a closed environment (e.g., charcoal grill in room with no, or poor, ventilation) as carbon uses up oxygen in room the formation of toxic carbon monoxide results instead of carbon dioxide (CO₂). Typical sources of CO in the home are shown in Figure 7.5.1.

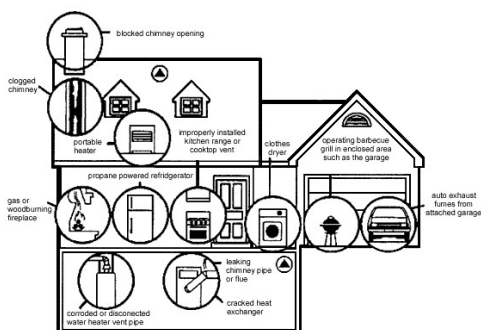


Figure 7.5.1: Potential sources of carbon in the home. Copyright: Fire Safety Council.

The toxicity of CO is due to its competition with oxygen at the heme binding site in hemoglobin. The binding affinity for CO is 200 times greater than that for oxygen, meaning that just small amounts of CO dramatically reduces hemoglobin's ability to transport oxygen around the body. The bright red color of the CO-heme complex is the reason that chronic exposure results in the skin adopting a bright red color. The symptoms of CO poisoning include headache, nausea, weakness, and eventually death. When air contains CO levels as low as 0.02%, headache and nausea occur; if the CO concentration is increased to 0.1%, unconsciousness will follow.

Note

Cigarette smoke containing large amounts of carbon monoxide and as a result heavy smokers can have up to 20% of the oxygen-active sites in their blood blocked by CO. However, despite this hazard, cigarettes would be even more deadly if they were not burnt. A key (and often engineered) ingredient in cigarettes is the addictive drug nicotine. Nicotine is an alkaloid (Figure 7.5.2a) as is caffeine (Figure 7.5.2b) that is in coffee and tea. The lethal dose of caffeine is approximately 10 g, which relates to approximately 70 – 100 cups of coffee (assuming a concentration of 100- 150 mg per cup). Alternatively, a lethal dose of caffeine from cola would require approximately 180 – 280 12 oz bottles, each containing 35 – 44 mg. In comparison nicotine has a lethal dose of 50 mg. This means that 12 cigarettes can provide a lethal dose if consumed. The only reason smoking 12 cigarettes do not kill immediately is that the majority of the nicotine is burnt in the smoking of the cigarette. If this were not true smokers would be killed before they could develop a habit!

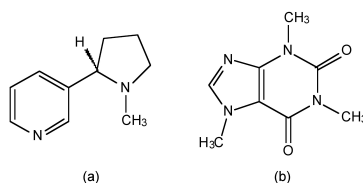


Figure 7.5.2: The molecular structures of (a) nicotine and (b) caffeine.

Structure and bonding

The bonding in CO involves 1 σ -bond and 2 sets of π -bonds (Figure 7.5.3). The C-O bond distance in carbon monoxide is 1.1 Å and therefore consistent with a triple bond. In comparison a typical C-O single bond is *ca.* 1.43 Å, and an average C-O double bond is *ca.* 1.23 Å. The major absorption band in the infra red spectrum for CO is 2143 cm^{-1} , while for ^{13}CO it is 2099.2 cm^{-1} .

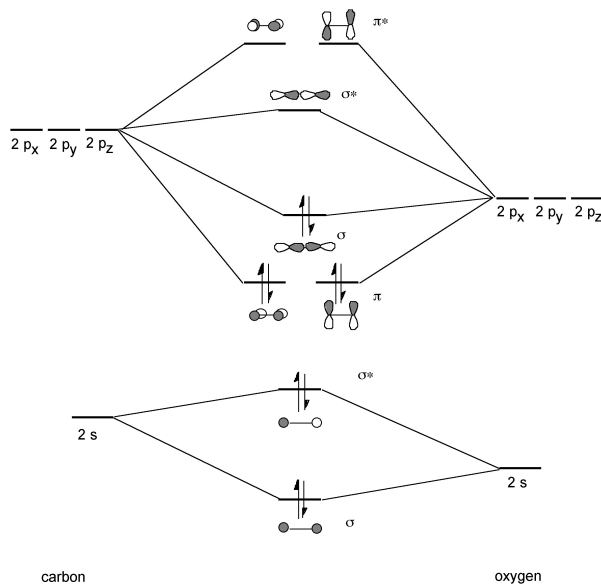


Figure 7.5.3: The carbon monoxide molecular orbital diagram.

This page titled [7.5: Carbon Monoxide](#) is shared under a [CC BY 3.0](#) license and was authored, remixed, and/or curated by [Andrew R. Barron \(CNX\)](#) via [source content](#) that was edited to the style and standards of the LibreTexts platform.

7.6: Carbon Dioxide

Carbon dioxide (CO₂) is the most stable oxide of carbon and is formed from the burning of carbon or carbon containing compounds in air or an excess of oxygen, (7.6.1). For industrial applications it is usually prepared from the decomposition of calcium carbonate (limestone), (7.6.2), rather than separation from combustion products.



Phase chemistry of carbon dioxide

Carbon dioxide does not exist as a liquid under normal atmospheric pressure, but solid CO₂ (also known as *dry ice*) sublimates at -78.5 °C (Figure 7.6.1). Dry ice (Figure 7.6.2) is commonly used as a refrigerant for food or biological sample preservation.

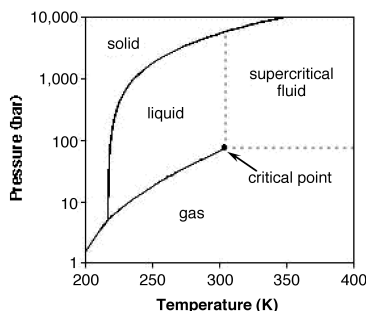


Figure 7.6.1: The phase diagram for carbon dioxide.



Figure 7.6.2: Photograph of a solid block of *dry ice*.

Note

When dry ice is placed in water (especially heated) sublimation is accelerated, and a low-sinking dense cloud of fog (smoke-like) is created. This is used in fog machines, at theaters, concerts, haunted houses, and nightclubs for dramatic effects (Figure 7.6.3). Fog from dry ice hovers above the ground unlike other artificial fog machines (that use partial combustion of oil) where the fog rises like smoke.



Figure 7.6.3: Dry ice generated smoke being used during Iron Maiden's *Somewhere Back in Time World Tour*. Copyright: Pyrotek.

Supercritical carbon dioxide

As noted above carbon dioxide usually behaves as a gas in air at standard temperature and pressure (STP = 25 °C and 1 atm) or as a solid when frozen. However, if the temperature and pressure are both increased from STP to be at or above the critical point (Figure 7.6.1), carbon dioxide adopts properties midway between a gas and a liquid ($T_c = 31.1\text{ °C}$ and $P_c = 72.9\text{ atm}$).

Supercritical CO₂ has become an important industrial solvent due to its role in chemical extraction in addition to its low toxicity and environmental impact. In this regard it is seen as a promising green solvent. One of the biggest applications is the decaffeination of coffee and tea without leaving any residue and allowing the caffeine to be separated and used in other beverage products.

Structure and bonding

Carbon dioxide is a linear molecule due to π -localization. The bonding in CO₂ involves 2 σ -bond and 2 sets of 3 center π -bonds (Figure 7.6.4). The C-O bond length of 1.2 Å should be compared to the value observed for organic carbonyls (e.g., ketones, esters, aldehydes) of 1.2 – 1.3 Å.

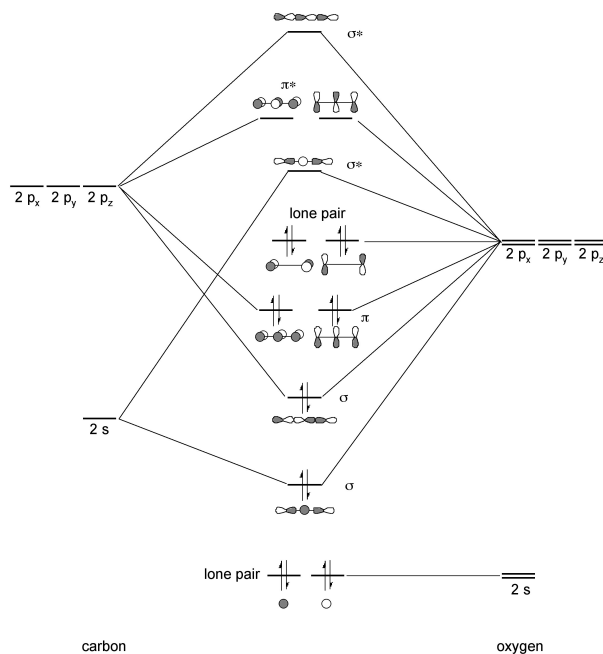


Figure 7.6.4: The carbon dioxide molecular orbital diagram.

Dissolution and reaction with water

Although CO₂ has no dipole moment it is very polar (dielectric constant = 1.60 at 0 °C, 50 atm) and consequently dissolves in polar solvents such as water up to a concentration of 18% (0.04 M). Most of it (+99%) is present as solvated CO₂ (Figure 7.6.5), and only ca. 0.2% is reacted to form carbonic acid, (7.6.1), with subsequent equilibria resulting in the formation of bicarbonate (HCO₃⁻) and carbonate (CO₃²⁻).

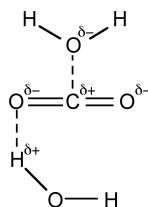


Figure 7.6.5: Typical water solvation of carbon dioxide.

The overall reaction involves a series of equilibria. The first equilibrium is the formation of carbonic acid, (7.6.4). The reaction rates, (7.6.5), are on the magnitude of 1 second (i.e., slow), and as a consequence when carbon dioxide is carried in the body an enzyme is present to speed up the reaction.



$$K = \frac{k_{\text{H}_2\text{CO}_3}}{k_{\text{CO}_2}} = \frac{25}{0.04} = 600 \quad (7.6.5)$$

The 2nd equilibrium is as a consequence of first ionization of carbonic acid to form bicarbonate (HCO_3^-), (7.6.6). In contrast to the first reaction, (7.6.4), this reaction is very fast with a $K_{\text{eq}} = 1.6 \times 10^{-4}$ @ 25 °C.



The 3rd equilibrium involves the formation of the carbonate ion (7.6.7), and has a $K_{\text{eq}} = 4.84 \times 10^{-11}$. Carbonate (CO_3^{2-}) is a delocalized ligand, which can act as a mono or bidentate or bridging group.

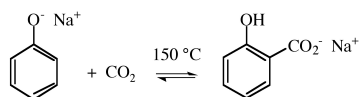
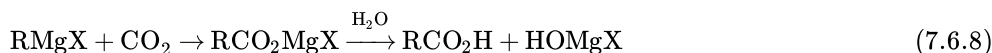


The formation of carbonic acid is the reason that even in the absence of pollutants (such as SO_2) natural rain water is slightly acidic due to dissolved CO_2 . The equilibrium associated with carbonic acid is also responsible for the buffering of the pH in blood.

Reaction chemistry

Photosynthesis in plants reduces CO_2 to organic matter but similar reactions have yet to be developed in non-living systems.

Grignards react readily with carbon dioxide to form the carboxylate, which yields the associated carboxylic acid upon hydrolysis, (7.6.8). Similar reactions occur with other organometallic compounds. In addition, CO_2 reacts with alkali metal salts of phenols (phenolates) to yield the hydroxy-carboxylate.



A number of complexes of CO_2 with transition metals are known in which the coordination can occur via the central carbon (Figure 7.6.6a) or the C=O bond (Figure 7.6.6b). Alternatively, CO_2 can bridge two metal centers.

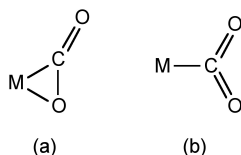


Figure 7.6.6: Bonding modes of CO_2 to transition metals.

Global warming and carbon dioxide

Global warming is the process of the observed increase in the average temperature of the Earth's near-surface air and oceans since the mid-20th century. Global surface temperature increased 0.74 °C (1.33 °F) between the start and the end of the 20th century (Figure 7.6.7). It is generally agreed that the majority of this temperature increase has occurred since the middle of the 20th century and was caused by increasing concentrations of greenhouse gases resulting from burning fossil fuels (the generation of additional CO_2) and deforestation (the loss of a mechanism for the consumption of CO_2), see Figure 7.6.7. While it is appreciated that natural phenomena (including solar radiation and volcanoes) produced most of the warming from pre-industrial times, the magnitude of the changes brought on by global industrialization is more significant.

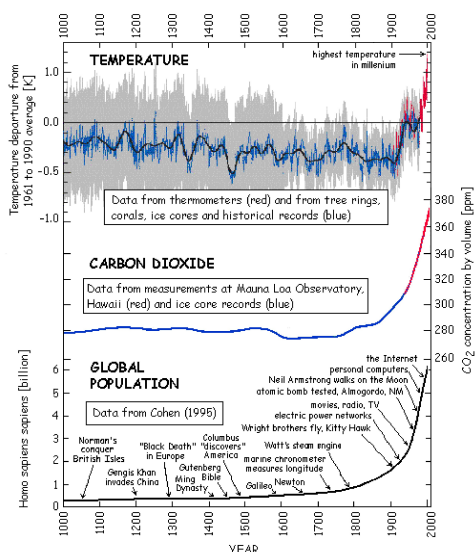


Figure 7.6.7: Correlation of Earth average temperature with carbon dioxide and global population.

The Earth's atmosphere has two functions. First, the ozone (O_3) in the upper atmosphere screens harmful UV from reaching the surface of the Earth. Second, as solar radiation penetrates the atmosphere a portion of the heat is then retained as a consequence of the CO_2 in the atmosphere. It is this process that modulates the surface temperature and provides a stable environment for life. The failure or alteration of either of these processes can have a dramatic effect on the livability of a planet.

Consider the relative position of Venus, Earth, and Mars to the Sun (Figure 7.6.8). The closer a planet is to the sun the greater the UV radiation and the greater the heating of the planet; however, the temperature is also greatly modulated by the atmosphere. Venus has an atmosphere comprising 95% CO_2 and has a surface temperature of approximately $450^\circ C$. In contrast, while Mars' atmosphere is also 95% CO_2 , it is only 1% as dense as that of Earth's, and thus the surface temperatures range from $40^\circ C$ during the day (due to radiative heating) to $-80^\circ C$ at night (due to the lack of retained heat because of the thin atmosphere). These should be compared to Earth's atmosphere which is 0.038% CO_2 , which allows for the correct amount of heat to be retained to sustain life. Clearly any significant change in the CO_2 content of the atmosphere will change the global temperatures of a planet.



Figure 7.6.8: The relative size and position of the planets from the sun.

Bibliography

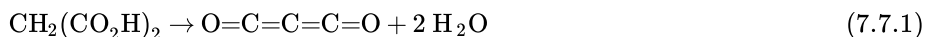
- N. Stern, *The Stern Review: The Economics of Climate Change*, HM Treasury, London.
- R. B. Gupta and J.-J. Shim, *Solubility in Supercritical Carbon Dioxide*, CRC Press (2006).
- Carbon Dioxide Capture and Storage: Special Report of the Intergovernmental Panel on Climate Change*, Cambridge University Press (2005).

This page titled [7.6: Carbon Dioxide](#) is shared under a [CC BY 3.0](#) license and was authored, remixed, and/or curated by [Andrew R. Barron \(CNX\)](#) via [source content](#) that was edited to the style and standards of the LibreTexts platform.

7.7: Suboxides of Carbon

Carbon suboxide

Carbon suboxide is the third oxide of carbon, C_3O_2 . It is made from the dehydration of malonic acid, (7.7.1), with P_4O_{10} above 140 °C. Like carbon dioxide, the C_3O_2 molecule is linear, with $p\pi-p\pi$ bonding.



Gaseous carbon suboxide has an evil smell and while stable at -78 °C it polymerizes at 25 °C. Photolysis of C_3O_2 yields the unstable C_2O . As expected from its synthesis, carbon suboxide reacts slowly with water to form malonic acid, i.e., the reverse of (7.7.1); however, the reaction with stronger nucleophiles such as amines is rapid, (7.7.2).



Mellitic acid anhydride

The anhydride of mellitic acid (Figure 7.7.1a) may be considered as an oxide of carbon since its chemical formula contains only carbon and oxygen, i.e., $C_{12}O_9$ (Figure 7.7.1b).

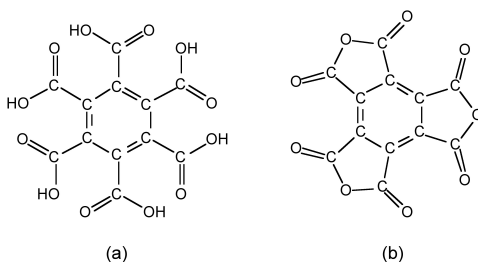


Figure 7.7.1: Structures of (a) mellitic acid and (b) its anhydride.

7.7: Suboxides of Carbon is shared under a [CC BY 1.0](https://creativecommons.org/licenses/by/1.0/) license and was authored, remixed, and/or curated by LibreTexts.

7.8: Carbon Halides

There are two general classes of carbon halides.

1. Homoleptic halides, e.g., CCl_4 , CCl_2F_2 , C_6Cl_6 , etc.
2. Carbonyl halides, e.g., $\text{Cl}_2\text{C}=\text{O}$.

A summary of some simple carbon halides is given in Table 7.8.1.

Table 7.8.1: Physical properties of simple halogen compounds of carbon.

Compound	Mp (°C)	Bp (°C)	Remarks
CF_4	-185	-128	Very stable gas
CCl_4	-23	76	Colorless liquid, stable
CBr_4	93	190	Pale yellow solid, decomposes upon boiling
CI_4	171	-	Bright red solid, decomposes prior to boiling, sublimed at low pressure
$\text{F}_2\text{C}=\text{O}$	-114	-83	Decomposed by H_2O
$\text{Cl}_2\text{C}=\text{O}$	-118	8	Phosgene, highly toxic
$\text{Br}_2\text{C}=\text{O}$	-	65	Fumes in air

Carbon tetrahalides

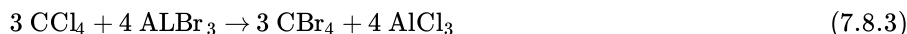
The carbon tetrahalides are generally prepared by the direct (thermal) reaction of carbon with the appropriate halogen, (7.8.1); however, specific syntheses are possible for each derivative.



In addition to the direct reaction of fluorine with carbon, CF_4 can be prepared from SiC , (7.8.2). The SiF_4 side product is removed by passing the reaction mixture through NaOH solution, in which SiF_4 reacts to form silicate. The difference in reactivity of SiF_4 and CF_4 is attributable to the lack of an energetically accessible five-coordinate intermediate required for the associative mechanism.



Carbon tetrabromide can be obtained by bromination of CH_4 with HBr or Br_2 , or by the reaction of CCl_4 with AlBr_3 , (7.8.3). Carbon tetraiodide (CI_4) can be made by the Lewis acid catalyzed halogen exchange reaction, (7.8.4).



CF_4 is very stable. In fact, it is so stable that it does not even react with molten sodium. In contrast to CF_4 , carbon tetrachloride (CCl_4) reacts readily with alkali metals (K and Na) or other strong reducing agents (e.g., F_2 , Al, Ba, Be, and Zn). While CCl_4 is thermodynamically unstable with respect to hydrolysis, it is kinetically stable, and thus finds extensive use as a solvent. Photolysis can result in the transfer of a chloride radical to various substrates. It is also used in the conversion of metal oxides to the chlorides. Carbon tetrabromide (CBr_4) is insoluble in water and other polar solvents, but soluble in benzene. Carbon tetraiodide (CI_4) decomposes thermally, (7.8.5).



The decreasing stability of CX_4 , from fluorine to iodine, is directly related to the C-X bond energy.

Table 7.8.2: Bond energies for carbon-halide bonds.

C-X	Bond energy (kJ/mol)

C-F	485
C-Cl	327
C-Br	285
C-I	213

Hazards

Despite its use as a solvent CCl_4 has significant hazardous effects. Inhalation of carbon tetrachloride vapor can cause headaches, mental confusion, depression, fatigue, loss of appetite, nausea, vomiting, and coma. The symptoms can take many hours to appear. The vapor and liquid irritate the eyes, and internal irritation, nausea, and vomiting are caused when taken orally. Chronic effects from prolonged inhalation include bronchitis and jaundice, while skin exposure can cause dermatitis.

Carbon tetrabromide is toxic by inhalation, and the vapor is narcotic if taken in high concentrations. As with CCl_4 , CBr_4 can react explosively with alkali metals.

Higher homoleptic halides

Organic compounds that contain only carbon and a halogen are called halocarbons, and these include fluorocarbons and chlorocarbons. The easiest route to fluorocarbons involves the reaction of a hydrocarbon with a high valent fluoride (e.g., CoF_3) or the reaction of a chlorocarbon with SbF_3 . In general, chlorocarbons with sp^3 carbon atoms are more stable than those with sp^2 carbon centers. The exception to this is aromatic compounds such as C_6Cl_6 .

The physical properties of fluorocarbons range from inert to toxic. Thus, poly(tetrafluoroethylene), $(\text{C}_2\text{F}_4)_n$, known by either its acronym (PTFE) or its trade name (Teflon), is chemically inert and has a low coefficient of friction (Table 7.8.3). As a consequence its uses include coatings on armor-piercing bullets (to stop the wear on the gun barrel), laboratory containers and magnetic stirrers, tubing for corrosive chemicals, and thread seal tape in plumbing applications (plumbers tape). A summary of the physical properties of PTFE is given in Table 7.8.3. PTFE is synthesized by the emulsion polymerization of tetrafluoroethylene monomer under pressure through free radical catalyst.

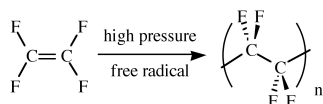


Table 7.8.3: Physical properties of poly(tetrafluoroethylene) (PTFE).

Property	Value
Density	2.2 g/cm ³
Melting point	327 °C
Young's modulus	0.5 GPa
Yield strength	23 MPa
Coefficient of friction	0.05 - 0.10
Dielectric constant	2.1
Dielectric strength (1 MHz)	60 MV/m

In contrast with PTFE, octafluoroisobutylene, $(\text{CF}_3)_2\text{C}=\text{CF}_2$, is highly toxic, while perfluorodecahydronaphthalene (C_{10}F_8 , Figure 7.8.1) is used as a blood substitute component.

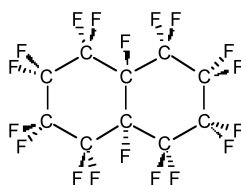
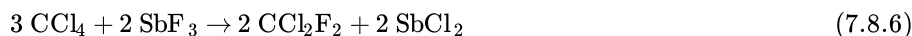


Figure 7.8.1: Structure of perfluorodecahydronaphthalene.

Mixed halides

Mixed halides are an important class of halocarbon compound. They are synthesized by halide exchange, (7.8.6). The high cost of SbF_3 means that the reaction is generally run with an excess of the chloride.



The ordinary name for mixed carbon halide is halon or Freon, although Freon is actually a Du Pont trademark. A list of selected Freon compounds are given in Table 7.8.4. Halons are non-toxic, non-flammable, and have no odor. However, it is their very lack of reactivity that has caused a problem.

Table 7.8.4: Selected Freons and their applications.

Freon	Formula	Uses
12	CCl_2F_2	Refrigerant
11	CCl_3F	Refrigerant
114	$\text{ClF}_2\text{C}-\text{CClF}_2$	Refrigerant
113	$\text{Cl}_3\text{C}-\text{CF}_3$	Solvent
13B1	CBrF_3	Fire extinguisher
1211	CBrClF_2	Fire extinguisher

Environmental impact of chlorofluorocarbon compounds (CFCs)

Chlorofluorocarbon compounds (CFCs) are very stable and are not degraded in the environment. As a consequence they are transported to the stratosphere where they decomposed upon photolysis, (7.8.7). The resulting chloride radical is a catalyst for the decomposition of ozone, (7.8.8), as well as a catalyst for the reaction of ozone with molecular oxygen, (7.8.9).



The widespread use of CFCs as refrigerants and propellants meant that by 1986 there were 2.5 billion pounds of CFC being liberated to the atmosphere. This was equivalent to $\frac{1}{2}$ lb per person on the planet. Since the ozone layer provides the vital protection to life on the Earth's surface from high energy UV radiation the release of CFC (along with other chemicals) caused a dramatic change in the ozone layer, including the increase in the polar hole in the ozone layer. As a result of the EU called for a complete ban of CFCs (which was followed by other countries). In their place new chemicals with similar refrigerant properties were developed. These compounds contained C-H bonds (e.g., $\text{C}_2\text{HCl}_2\text{F}_3$ and $\text{C}_2\text{H}_3\text{Cl}_2\text{F}$) that are readily broken in the lower atmosphere, thus limiting the transport to the stratosphere.

Carbonyl halides

All the carbonyl halides ($\text{X}_2\text{C}=\text{O}$, $\text{X} = \text{F}, \text{Cl}, \text{Br}, \text{I}$) are known (Table 7.8.1). Phosgene ($\text{Cl}_2\text{C}=\text{O}$) was first synthesized by John Davy (Figure 7.8.2) in 1812 by exposing a mixture of carbon monoxide and chlorine to sunlight, (7.8.10). He named it phosgene from the Greek, *phos* (light) and *gene* (born), in reference to use of light to promote the reaction. The fluoride is also prepared by the reaction of carbon monoxide with the halogen, while the bromide is prepared by the partial hydrolysis of CBr_4 with sulfuric acid.

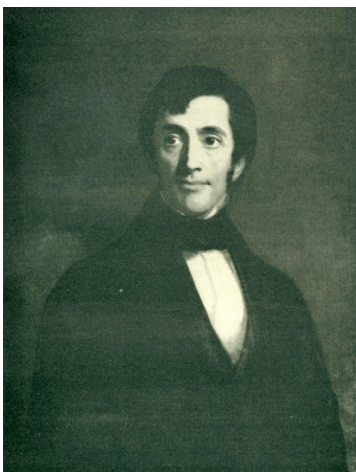
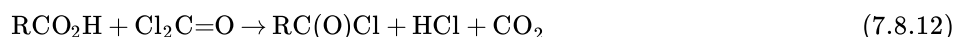


Figure 7.8.2: British doctor and chemist John Davy FRS (1790 – 1868) was also the brother of the noted chemist Sir Humphry Davy.

The synthesis of isocyanates from alkyl or aryl amines illustrates the electrophilic character of phosgene and its ability to introduce the equivalent of " CO^{2+} ", (7.8.11). This reaction is conducted in the presence of a base such as pyridine that absorbs the hydrogen chloride. Phosgene may also be used to produce acyl chlorides from carboxylic acids, (7.8.12). However, thionyl chloride is more commonly and more safely used in this reaction.



Phosgene as a weapon of war

Phosgene is a toxic gas with the smell of "new-mown hay" and was used in chemical warfare during the First World War (Figure 7.8.3) where it was a more potent weapon than chlorine. While chlorine was potentially deadly it caused the victim to violently cough and choke (the bodies natural defense to limiting inhalation), in contrast, phosgene caused much less coughing with the result that more of it was inhaled. Phosgene often had a delayed effect; apparently healthy soldiers were taken down with phosgene gas poisoning up to 48 hours after inhalation. A fatal dose of phosgene eventually led to shallow breathing and retching, pulse up to 120, an ashen face and the discharge of four pints of yellow liquid from the lungs each hour for the 48 of the drowning spasms.



Figure 7.8.3: Australian infantry from the 45th Battalion, Australian 4th Division wearing Small Box Respirators (SBR) as protection of chemical warfare agents. Photograph taken at Zonnebeke, on the Ypres sector, 27th September 1917. Copyright: Australian War Memorial.

Although phosgene's boiling point (7.6 °C) meant that it was a vapor, the so-called "white star" mixture of phosgene and chlorine was commonly used on the Somme, because the chlorine supplied the necessary vapor with which to carry the phosgene. A summary of the casualties inflicted by chemical warfare agents during the Great War is shown in Table 7.8.5.

Table 7.8.5: Casualties from gas attacks during the First World War (including chlorine, phosgene, and mustard gas). British Empire includes troops from United Kingdom, Australia, Canada, India, New Zealand, and South Africa.

Country	Total casualties	Deaths
Russia	419,340	56,000
Germany	200,000	9,000
France	190,000	8,000
British Empire	188,706	8,109
Austria-Hungary	100,000	3,000
USA	72,807	1,462
Italy	60,000	4,627
Others	10,000	1,000

7.8: Carbon Halides is shared under a [CC BY 1.0](#) license and was authored, remixed, and/or curated by LibreTexts.

7.9: Comparison Between Silicon and Carbon

An understanding of the differences between carbon and silicon is important in understanding the relative chemistry of these Group 14 elements.

Size

As expected silicon is larger than carbon due to the presence of a second shell: i.e., $C = 1s^2 2s^2 2p^2$ while $Si = 1s^2 2s^2 2p^6 3s^2 3p^2$. A comparison of the relative sizes of carbon and silicon are given in Table 7.9.1.

Table 7.9.1: Atomic, covalent, and van der Waals radii of carbon and silicon.

Element	Atomic radius (Å)	Covalent radius sp^3 (Å)	van der Waal radius (Å)
C	0.70	0.75	1.70
Si	1.10	1.14	2.10

Covalent and van der Waal radii from [Royal Society of Chemistry Online Periodic Table](#). [Webelements](#) has a more detailed discussion of all three types of radii, the atomic radii quoted here are empirical.

Coordination number

Carbon is known to have a coordination number of 2, 3, and 4 in its compounds depending on the hybridization. A coordination number of 1 can also be considered for CO and CN^- . Four-coordinate carbon may be considered to be coordinatively saturated. In contrast, in the absence of overwhelming steric bulk, silicon is observed to have coordination numbers of 3, 4, 5, and 6. Examples of five and six-coordinate silicon include $Si(acac)_2Cl$ and SiF_6^{2-} , respectively. Coordination numbers of higher than 4 have been ascribed to the use of low-lying d orbitals; however, calculations show these are not significant. Instead, hypervalent silicon is better described by the formation of 3-center molecular orbitals, e.g., Figure 7.9.1.

Note

A hypervalent molecule is a molecule that contains one or more typical elements (Group 1, 2, 13-18) formally bearing more than eight electrons in their valence shells.

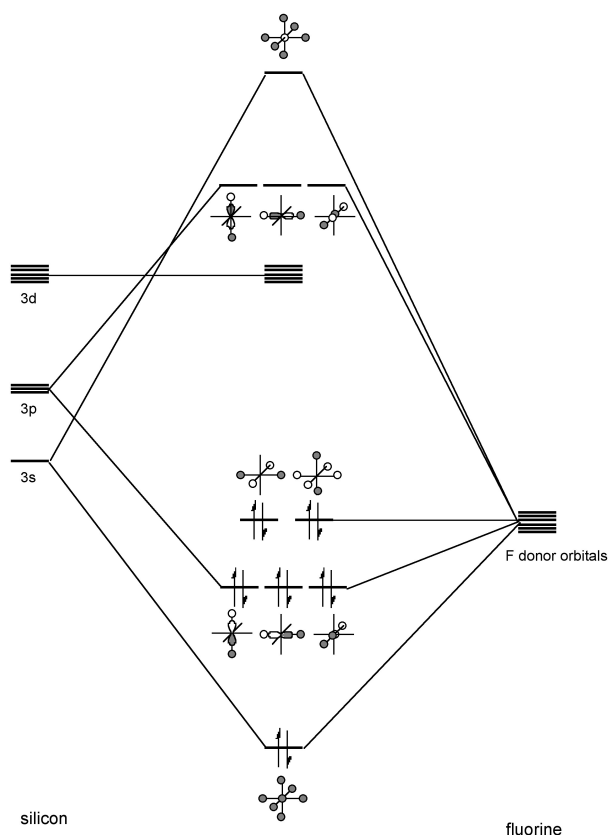


Figure 7.9.1: Molecular orbital diagram for SiF_6^{2-} .

Electronegativity

The electronegativities of silicon and carbon are given in Table along with hydrogen. Since carbon is more electronegative than hydrogen the C-H bond is polarized towards carbon resulting in a more protic hydrogen (Figure 7.9.2a). In contrast, the lower electronegativity of silicon results in a more hydridic hydrogen (Figure 7.9.2b). This difference is reflected in the reaction chemistry of SiH_4 versus CH_4 .

Table 7.9.2: Selected Pauling electronegativity values. [Royal Society of Chemistry Online Periodic Table](#)

Element	Pauling scale
C	2.55
H	2.20
Si	1.90

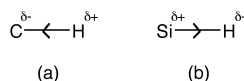


Figure 7.9.2: Relative polarization of C-H and Si-H bonds.

Bond energies

The E-E and E-O bond energies for carbon and silicon are given in Table 7.9.3. The bond energy for a C-C bond is slightly greater than for a C-O bond, while the Si-O bond is significantly stronger than the Si-Si bond. This difference is reflected in the chemistry of silicon versus carbon compounds. The chemistry of carbon is dominated by catenation: the ability of a chemical element to form a long chain-like structure via a series of covalent bonds. Although silicon does form Si-Si bonds, they are far more reactive than their C-C analogs, and polymers of silicon are predominantly comprised of Si-O chains (as a result of the very strong bond).

Table 7.9.3: Selected bond energies for carbon and silicon. [Royal Society of Chemistry Online Periodic Table](#)

Element	E-E bond energy (kJ/mol)	E-O bond energy (kJ/mol)
C	345.6	357.7
Si	222	462

Multiple bonds

While unsaturated compounds for carbon (i.e., alkenes and alkynes) are common, the analogous silicon compounds (disilenes) were only reported in 1981, and disilynes in 2004. The Si=Si double bond lengths are 2.14 - 2.29 Å which is 5 - 10% shorter than the Si-Si single bond lengths. This bond shortening is less than *ca.* 13% in carbon compounds.

Note

The traditional lack of multiple bonds for the Period 3 elements and lower led to the formulation of the double bond rule which states that *chemical elements with a principal quantum number greater than 2 do not form multiple bonds (e.g., double bonds and triple bonds) with themselves or with other elements*. This rule was made obsolete starting from 1981 with the discovery of silicon and phosphorus double bonds. Double bonds that would ordinarily not form can be stabilized with proper functional groups through kinetic stabilization, i.e., either electronically or sterically.

Bibliography

- R. West, M. J. Fink, and J. Michl, *Science*, 1981, **214**, 1343.
- A. Sekiguchi, R. Kinjo, and M. Ichinohe, *Science*, 2004, **305**, 1755.

7.9: Comparison Between Silicon and Carbon is shared under a [CC BY 1.0](#) license and was authored, remixed, and/or curated by LibreTexts.

7.10: Semiconductor Grade Silicon

Introduction

The synthesis and purification of bulk polycrystalline semiconductor material represents the first step towards the commercial fabrication of an electronic device. This polycrystalline material is then used as the raw material for the formation of single crystal material that is processed to semiconductor wafers. The strong influence on the electric characteristics of a semiconductors exhibited by small amounts of some impurities requires that the bulk raw material be of very high purity ($> 99.9999\%$). Although some level of purification is possible during the crystallization process it is important to use as high a purity starting material as possible.

Following oxygen (46%), silicon (L. silicis flint) is the most abundant element in the earth's crust (28%). However, silicon does not occur in its elemental form, but as its oxide (SiO_2) or as silicates. Sand, quartz, amethyst, agate, flint, and opal are some of the forms in which the oxide appears. Granite, hornblende, asbestos, feldspar, clay and mica, etc. are a few of the numerous silicate minerals. With such boundless supplies of the raw material, the costs associated with the production of bulk silicon is not one of abstraction and conversion of the oxide(s), but of purification of the crude elemental silicon. While 98% elemental silicon, known as metallurgical-grade silicon (MGS), is readily produced on a large scale, the requirements of extreme purity for electronic device fabrication require additional purification steps in order to produce electronic-grade silicon (EGS). Electronic-grade silicon is also known as semiconductor-grade silicon (SGS). In order for the purity levels to be acceptable for subsequent crystal growth and device fabrication, EGS must have carbon and oxygen impurity levels less than a few parts per million (ppm), and metal impurities at the parts per billion (ppb) range or lower. Table 7.10.1 and Table 7.10.2 give typical impurity concentrations in MGS and EGS, respectively. Besides the purity, the production cost and the specifications must meet the industry desires.

Table 7.10.1: Typical impurity concentrations found in metallurgical-grade silicon (MGS).

Element	Concentration (ppm)	Element	Concentration (ppm)
aluminum	1000-4350	manganese	50-120
boron	40-60	molybdenum	< 20
calcium	245-500	nickel	10-105
chromium	50-200	phosphorus	20-50
copper	15-45	titanium	140-300
iron	1550-6500	vanadium	50-250
magnesium	10-50	zirconium	20

Table 7.10.2: Typical impurity concentrations found in electronic-grade silicon (EGS).

Element	Concentration (ppb)	Element	Concentration (ppb)
arsenic	< 0.001	gold	< 0.00001
antimony	< 0.001	iron	0.1-1.0
boron	≤ 0.1	nickel	0.1-0.5
carbon	100-1000	oxygen	100-400
chromium	< 0.01	phosphorus	≤ 0.3
cobalt	0.001	silver	0.001
copper	0.1	zinc	< 0.1

Metallurgical-grade silicon (MGS)

The typical source material for commercial production of elemental silicon is quartzite gravel; a relatively pure form of sand (SiO_2). The first step in the synthesis of silicon is the melting and reduction of the silica in a submerged-electrode arc furnace. An

example of which is shown schematically in Figure 7.10.1, along with the appropriate chemical reactions. A mixture of quartzite gravel and carbon are heated to high temperatures (ca. 1800 °C) in the furnace. The carbon bed consists of a mixture of coal, coke, and wood chips. The latter providing the necessary porosity such that the gases created during the reaction (SiO and CO) are able to flow through the bed.

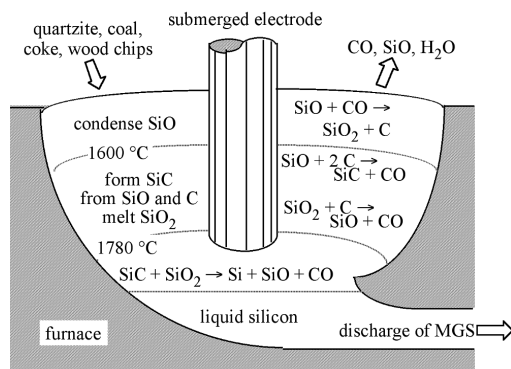
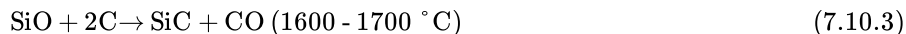
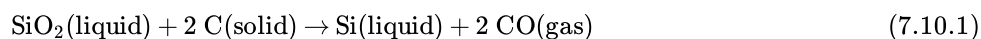


Figure 7.10.1: Schematic of submerged-electrode arc furnace for the production of metallurgical-grade silicon (MGS).

The overall reduction reaction of SiO_2 is expressed in (7.10.1), however, the reaction sequence is more complex than this overall reaction implies, and involves the formation of SiC and SiO intermediates. The initial reaction between molten SiO_2 and C, (7.10.2), takes place in the arc between adjacent electrodes, where the local temperature can exceed 2000 °C. The SiO and CO thus generated flow to cooler zones in the furnace where SiC is formed, (7.10.3), or higher in the bed where they reform SiO_2 and C, (7.10.2). The SiC reacts with molten SiO_2 , (7.10.4), producing the desired silicon along with SiO and CO. The molten silicon formed is drawn-off from the furnace and solidified.



The as-produced MGS is approximately 98-99% pure, with the major impurities being aluminum and iron (Table 7.10.1), however, obtaining low levels of boron impurities is of particular importance, because it is difficult to remove and serves as a dopant for silicon. The drawbacks of the above process are that it is energy and raw material intensive. It is estimated that the production of one metric ton (1,000 kg) of MGS requires 2500 - 2700 kg quartzite, 600 kg charcoal, 600 - 700 kg coal or coke, 300 - 500 kg wood chips, and 500,000 kWh of electric power. Currently, approximately 500,000 metric tons of MGS are produced per year, worldwide. Most of the production (ca. 70%) is used for metallurgical applications (e.g., aluminum-silicon alloys are commonly used for automotive engine blocks) from whence its name is derived. Applications in a variety of chemical products such as silicone resins account for about 30%, and only 1% or less of the total production of MGS is used in the manufacturing of high-purity EGS for the electronics industry. The current worldwide consumption of EGS is approximately 5×10^6 kg per year.

Electronic-grade silicon (EGS)

Electronic-grade silicon (EGS) is a polycrystalline material of exceptionally high purity and is the raw material for the growth of single-crystal silicon. EGS is one of the purest materials commonly available, see Table 7.10.2 The formation of EGS from MGS is accomplished through chemical purification processes. The basic concept of which involves the conversion of MGS to a volatile silicon compound, which is purified by distillation, and subsequently decomposed to re-form elemental silicon of higher purity (i.e., EGS). Irrespective of the purification route employed, the first step is physical pulverization of MGS followed by its conversion to the volatile silicon compounds.

A number of compounds, such as monosilane (SiH_4), dichlorosilane (SiH_2Cl_2), trichlorosilane (SiHCl_3), and silicon tetrachloride (SiCl_4), have been considered as chemical intermediates. Among these, SiHCl_3 has been used predominantly as the intermediate compound for subsequent EGS formation, although SiH_4 is used to a lesser extent. Silicon tetrachloride and its lower chlorinated derivatives are used for the chemical vapor deposition (CVD) growth of Si and SiO_2 . The boiling points of silane and its chlorinated products (Table 7.10.3) are such that they are conveniently separated from each other by fractional distillation.

Table 7.10.3: Boiling points of silane and chlorosilanes at 760 mmHg (1 atmosphere).

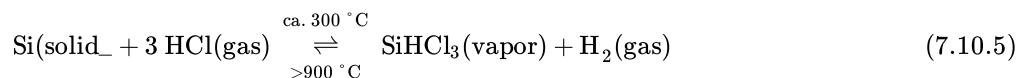
Compound	Boiling point (°C)
SiH ₄	-112.3
SiH ₃ Cl	-30.4
SiH ₂ Cl ₂	8.3
SiHCl ₃	31.5
SiCl ₄	57.6

The reasons for the predominant use of SiHCl₃ in the synthesis of EGS are as follows:

1. SiHCl₃ can be easily formed by the reaction of anhydrous hydrogen chloride with MGS at reasonably low temperatures (200 - 400 °C);
2. it is liquid at room temperature so that purification can be accomplished using standard distillation techniques;
3. it is easily handled and if dry can be stored in carbon steel tanks;
4. its liquid is easily vaporized and, when mixed with hydrogen it can be transported in steel lines without corrosion;
5. it can be reduced at atmospheric pressure in the presence of hydrogen;
6. its deposition can take place on heated silicon, thus eliminating contact with any foreign surfaces that may contaminate the resulting silicon; and
7. it reacts at lower temperatures (1000 - 1200 °C) and at faster rates than does SiCl₄.

Chlorosilane (Seimens) process

Trichlorosilane is synthesized by heating powdered MGS with anhydrous hydrogen chloride (HCl) at around 300 °C in a fluidized-bed reactor, (7.10.5).



Since the reaction is actually an equilibrium and the formation of SiHCl₃ highly exothermic, efficient removal of generated heat is essential to assure a maximum yield of SiHCl₃. While the stoichiometric reaction is that shown in (7.10.5), a mixture of chlorinated silanes is actually prepared which must be separated by fractional distillation, along with the chlorides of any impurities. In particular iron, aluminum, and boron are removed as FeCl₃ (b.p. = 316 °C), AlCl₃ (m.p. = 190 °C subl.), and BCl₃ (b.p. = 12.65 °C), respectively. Fractional distillation of SiHCl₃ from these impurity halides result in greatly increased purity with a concentration of electrically active impurities of less than 1 ppb.

EGS is prepared from purified SiHCl₃ in a chemical vapor deposition (CVD) process similar to the epitaxial growth of Si. The high-purity SiHCl₃ is vaporized, diluted with high-purity hydrogen, and introduced into the Seimens deposition reactor, shown schematically in Figure 7.10.2 Within the reactor, thin silicon rods called slim rods (ca. 4 mm diameter) are supported by graphite electrodes. Resistance heating of the slim rods causes the decomposition of the SiHCl₃ to yield silicon, as described by the reverse reaction shown in (7.10.5).

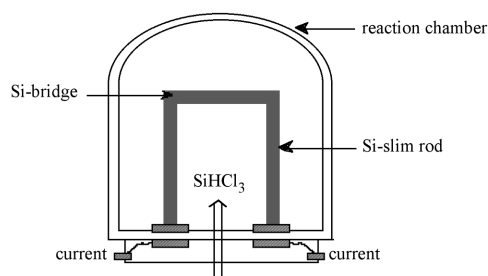


Figure 7.10.2: Schematic representation of a Seimens deposition reactor.

The shift in the equilibrium from forming SiHCl₃ from Si at low temperature, to forming Si from SiHCl₃ at high temperature is as a consequence of the temperature dependence, (7.10.6), of the equilibrium constant, (7.10.7) where p = partial pressure, for (7.10.5).

Since the formation of SiHCl_3 is exothermic, i.e., $\Delta H < 0$, an increase in the temperature causes the partial pressure of SiHCl_3 to decrease. Thus, the Siemens process is typically run at ca. 1100 °C, while the reverse fluidized bed process is carried out at 300 °C.

$$\ln K_p = \frac{-\Delta H}{RT} \quad (7.10.6)$$

$$K_p = \frac{p_{\text{SiHCl}_3} p_{\text{H}_2}}{p_{\text{HCl}}} \quad (7.10.7)$$

The slim rods act as a nucleation point for the deposition of silicon, and the resulting polycrystalline rod consists of columnar grains of silicon (polysilicon) grown perpendicular to the rod axis. Growth occurs at less than 1 mm per hour, and after deposition for 200 to 300 hours high-purity (EGS) polysilicon rods of 150 - 200 mm in diameter are produced. For subsequent float-zone refining the polysilicon EGS rods are cut into long cylindrical rods. Alternatively, the as-formed polysilicon rods are broken into chunks for single crystal growth processes, for example Czochralski melt growth.

In addition to the formation of silicon, the HCl coproduct reacts with the SiHCl_3 reactant to form silicon tetrachloride (SiCl_4) and hydrogen as major byproducts of the process, (7.10.8). This reaction represents a major disadvantage with the Siemens process: poor efficiency of silicon and chlorine consumption. Typically, only 30% of the silicon introduced into CVD reactor is converted into high-purity polysilicon.



In order to improve efficiency the HCl, SiCl_4 , H_2 , and unreacted SiHCl_3 are separated and recovered for recycling. Figure 7.10.3 illustrates the entire chlorosilane process starting with MGS and including the recycling of the reaction byproducts to achieve high overall process efficiency. As a consequence, the production cost of high-purity EGS depends on the commercial usefulness of the byproduct, SiCl_4 . Additional disadvantages of the Siemens process are derived from its relatively small batch size, slow growth rate, and high power consumption. These issues have led to the investigation of alternative cost efficient routes to EGS.

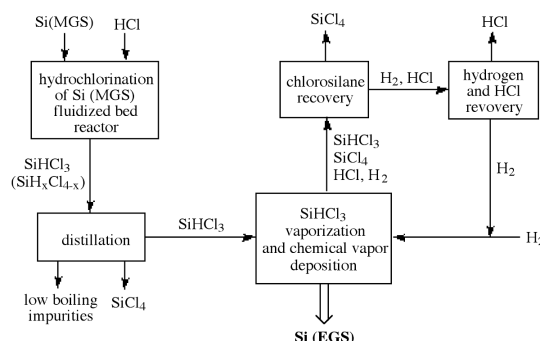


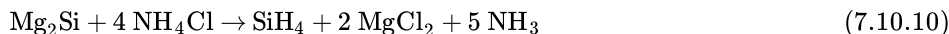
Figure 7.10.3: Schematic representation of the reaction pathways for the formation of EGS using the chlorosilane process.

Silane process

An alternative process for the production of EGS that has begun to receive commercial attention is the pyrolysis of silane (SiH_4). The advantages of producing EGS from SiH_4 instead of SiHCl_3 are potentially lower costs associated with lower reaction temperatures, and less harmful byproducts. Silane decomposes < 900 °C to give silicon and hydrogen, (7.10.9).

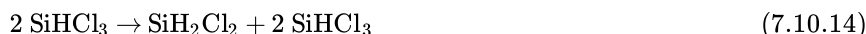
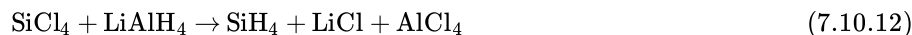


Silane may be prepared by a number of routes, each having advantages with respect to purity and production cost. The simplest process involves the direct reaction of MGS powders with magnesium at 500 °C in a hydrogen atmosphere, to form magnesium silicide (Mg_2Si). The magnesium silicide is then reacted with ammonium chloride in liquid ammonia below 0 °C, (7.10.10).



This process is ideally suited to the removal of boron impurities (a p-type dopant in Si), because the diborane (B_2H_6) produced during the reaction forms the Lewis acid-base complex, $\text{H}_3\text{B}(\text{NH}_3)$, whose volatility is sufficiently lower than SiH_4 , allowing for the purification of the latter. It is possible to prepare EGS with a boron content of ≤ 20 ppt using SiH_4 synthesized in this manner. However, phosphorus (another dopant) in the form of PH_3 may be present as a contaminant requiring subsequent purification of the SiH_4 .

Alternative routes to SiH_4 involve the chemical reduction of SiCl_4 by either lithium hydride, (7.10.11), lithium aluminum hydride, (7.10.12), or via hydrogenation in the presence of elemental silicon, (7.10.13) - (7.10.16). The hydride reduction reactions may be carried-out on relatively large scales (ca. 50 kg), but only batch processes. In contrast, Union Carbide has adapted the hydrogenation to a continuous process, involving disproportionation reactions of chlorosilanes, (7.10.14) - (7.10.16), and the fractional distillation of silane, Table 7.10.3



Pyrolysis of silane on resistively heated polysilicon filaments at 700 - 800 °C yields polycrystalline EGS. As noted above, the EGS formed has remarkably low boron impurities compared with material prepared from trichlorosilane. Moreover, the resulting EGS is less contaminated with transition metals from the reactor container because SiH_4 decomposition does not cause as much of a corrosion problem as is observed with halide precursor compounds.

Granular polysilicon deposition

Both the chlorosilane (Seimens) and silane processes result in the formation of rods of EGS. However, there has been increased interest in the formation of granular polycrystalline EGS. This process was developed in 1980's, and relies on the decomposition of SiH_4 in a fluidized-bed deposition reactor to produce free-flowing granular polysilicon.

Tiny silicon particles are fluidized in a SiH_4/H_2 flow, and act as seed crystal onto which polysilicon deposits to form free-flowing spherical particles. The size distribution of the particles thus formed is over the range from 0.1 to 1.5 mm in diameter with an average particle size of 0.7 mm. The fluidized-bed seed particles are originally made by grinding EGS in a ball (or hammer) mill and leaching the product with acid, hydrogen peroxide, and water. This process is time-consuming and costly, and tended to introduce undesirable impurities from the metal grinders. In a new method, large EGS particles are fired at each other by a high-speed stream of inert gas and the collision breaks them down into particles of suitable size for a fluidized bed. This process has the main advantage that it introduces no foreign materials and requires no leaching or other post purification.

The fluidized-bed reactors are much more efficient than traditional rod reactors as a consequence of the greater surface area available during CVD growth of silicon. It has been suggested that fluidized-bed reactors require $1/5$ to $1/10$ the energy, and half the capital cost of the traditional process. The quality of fluidized-bed polysilicon has proven to be equivalent to polysilicon produced by the conventional methods. Moreover, granular EGS in a free-flowing form, and with high bulk density, enables crystal growers to obtain the high, reproducible production yields out of each crystal growth run. For example, in the Czochralski crystal growth process, crucibles can be quickly and easily filled to uniform loading with granular EGS, which typically exceed those of randomly stacked polysilicon chunks produced by the Siemens silane process.

Zone refining

The technique of zone refining is used to purify solid materials and is commonly employed in metallurgical refining. In the case of silicon may be used to obtain the desired ultimate purity of EGS, which has already been purified by chemical processes. Zone refining was invented by Pfann, and makes use of the fact that the equilibrium solubility of any impurity (e.g., Al) is different in the solid and liquid phases of a material (e.g., Si). For the dilute solutions, as is observed in EGS silicon, an equilibrium segregation coefficient (k_0) is defined by $k_0 = C_s/C_l$, where C_s and C_l are the equilibrium concentrations of the impurity in the solid and liquid near the interface, respectively.

If k_0 is less than 1 then the impurities are left in the melt as the molten zone is moved along the material. In a practical sense a molten zone is established in a solid rod. The zone is then moved along the rod from left to right. If $k_0 < 1$ then the frozen part left on the trailing edge of the moving molten zone will be purer than the material that melts in on the right-side leading edge of the moving molten zone. Consequently the solid to the left of the molten zone is purer than the solid on the right. At the completion of the first pass the impurities become concentrated to the right of the solid sample. Repetition of the process allows for purification to

exceptionally high levels. Table 7.10.4 lists the equilibrium segregation coefficients for common impurity and dopant elements in silicon; it should be noted that they are all less than 1.

Table 7.10.4: Segregation coefficients for common impurity and dopant elements in silicon.

Element	k_0	Element	k_0
aluminum	0.002	iron	8×10^{-6}
boron	0.8	oxygen	0.25
carbon	0.07	phosphorus	0.35
copper	4×10^{-6}	antimony	0.023

Bibliography

- K. G. Baraclough, K. G., in *The Chemistry of the Semiconductor Industry*, Eds. S. J. Moss and A. Ledwith, Blackie and Sons, Glasgow, Scotland (1987).
- L. D. Crossman and J. A. Baker, *Semiconductor Silicon 1977*, Electrochem. Soc., Princeton, New Jersey (1977).
- W. C. O'Mara, Ed. *Handbook of Semiconductor Silicon Technology*, Noyes Pub., New Jersey (1990).
- W. G. Pfann, *Zone Melting*, John Wiley & Sons, New York, (1966).
- F. Shimura, *Semiconductor Silicon Crystal Technology*, Academic Press (1989).

7.10: Semiconductor Grade Silicon is shared under a [CC BY 1.0](https://creativecommons.org/licenses/by/1.0/) license and was authored, remixed, and/or curated by LibreTexts.

7.11: Oxidation of Silicon

Note

This module was developed as part of the Rice University course CHEM-496: *Chemistry of Electronic Materials*. This module was prepared with the assistance of Andrea Keys.

Introduction

In the fabrication of integrated circuits (ICs), the oxidation of silicon is essential, and the production of superior ICs requires an understanding of the oxidation process and the ability to form oxides of high quality. Silicon dioxide has several uses:

1. Serves as a mask against implant or diffusion of dopant into silicon.
2. Provides surface passivation.
3. Isolates one device from another (dielectric isolation).
4. Acts as a component in MOS structures.
5. Provides electrical isolation of multi-level metallization systems.

Methods for forming oxide layers on silicon have been developed, including thermal oxidation, wet anodization, chemical vapor deposition (CVD), and plasma anodization or oxidation. Generally, CVD is used when putting the oxide layer on top of a metal surface, and thermal oxidation is used when a low-charge density level is required for the interface between the oxide and the silicon surface.

Oxidation of silicon

Silicon's surface has a high affinity for oxygen and thus an oxide layer rapidly forms upon exposure to the atmosphere. The chemical reactions which describe this formation are:



In the first reaction a dry process is utilized involving oxygen gas as the oxygen source and the second reaction describes a wet process which uses steam. The dry process provides a "good" silicon dioxide but is slow and mostly used at the beginning of processing. The wet procedure is problematic in that the purity of the water used cannot be guaranteed to a suitable degree. This problem can be easily solved using a pyrogenic technique which combines hydrogen and oxygen gases to form water vapor of very high purity. Maintaining reagents of high quality is essential to the manufacturing of integrated circuits, and is a concern which plagues each step of this process.

The formation of the oxide layer involves shared valence electrons between silicon and oxygen, which allows the silicon surface to rid itself of "dangling" bonds, such as lone pairs and vacant orbitals. These vacancies create mid-gap states between the valence and conduction bands, which prevents the desired band gap of the semiconductor. The Si-O bond strength is covalent (strong), and so can be used to achieve the loss of mid-gap states and passivate the surface of the silicon.

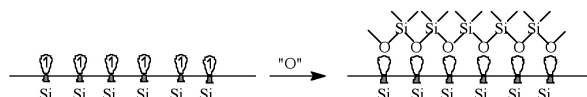


Figure 7.11.1: Removal of dangling bonds by oxidation of surface.

The oxidation of silicon occurs at the silicon-oxide interface and consists of four steps:

1. Diffusive transport of oxygen across the diffusion layer in the vapor phase adjacent to the silicon oxide-vapor interface.
2. Incorporation of oxygen at the outer surface into the silicon oxide film.
3. Diffusive transport across the silicon oxide film to its interface with the silicon lattice.
4. Reaction of oxygen with silicon at this inner interface.

As the Si-SiO₂ interface moves into the silicon its volume expands, and based upon the densities and molecular weights of Si and SiO₂, 0.44 Å Si is used to obtain 1.0 Å SiO₂.

Pre-oxidation cleaning

The first step in oxidizing a surface of silicon is the removal of the native oxide which forms due to exposure to open air. This may seem redundant to remove an oxide only to put on another, but this is necessary since uncertainty exists as to the purity of the oxide which is present. The contamination of the native oxide by both organic and inorganic materials (arising from previous processing steps and handling) must be removed to prevent the degradation of the essential electrical characteristics of the device. A common procedure uses a $\text{H}_2\text{O}-\text{H}_2\text{O}_2-\text{NH}_4\text{OH}$ mixture which removes the organics present, as well as some group I and II metals. Removal of heavy metals can be achieved using a $\text{H}_2\text{O}-\text{H}_2\text{O}_2-\text{HCl}$ mixture, which complexes with the ions which are formed. After removal of the native oxide, the desired oxide can be grown. This growth is useful because it provides: chemical protection, conditions suitable for lithography, and passivation. The protection prevents unwanted reactions from occurring and the passivation fills vacancies of bonds on the surface not present within the interior of the crystal. Thus the oxidation of the surface of silicon fulfills several functions in one step.

Thermal oxidation

The growth of oxides on a silicon surface can be a particularly tedious process, since the growth must be uniform and pure. The thickness wanted usually falls in the range 50 - 500 Å, which can take a long time and must be done on a large scale. This is done by stacking the silicon wafers in a horizontal quartz tube while the oxygen source flows over the wafers, which are situated vertically in a slotted paddle (boat). This procedure is performed at 1 atm pressure, and the temperature ranges from 700 to 1200 °C, being held to within ± 1 °C to ensure uniformity. The choice of oxidation technique depends on the thickness and oxide properties required. Oxides that are relatively thin and those that require low charge at the interface are typically grown in dry oxygen. When thick oxides are required (> 0.5 mm) are desired, steam is the source of choice. Steam can be used at wide range of pressures (1 atm to 25 atm), and the higher pressures allow thick oxide growth to be achieved at moderate temperatures in reasonable amounts of time.

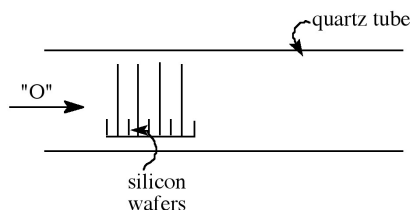


Figure 7.11.2: Horizontal diffusion tube showing the oxidation of silicon wafers at 1 atm pressure.

The thickness of SiO_2 layers on a Si substrate is readily determined by the color of the film. Table 7.11.1 provides a guideline for thermal grown oxides.

Table 7.11.1: Color chart for thermally grown SiO_2 films observed under daylight fluorescent lighting.

Film thickness (μm)	Color	Film thickness (μm)	Color
0.05	tan	0.63	violet-red
0.07	brown	0.68	"bluish"
0.10	dark violet to red-violet	0.72	blue-green to gree
0.12	royal blue	0.77	"yellowish"
0.15	light blue to metallic blue	0.80	orange
0.17	metallic to light yellow-green	0.82	salmon
0.20	light gold	0.85	light red-violet
0.22	gold	0.86	violet
0.25	orange to melon	0.87	blue violet
0.27	red-violet	0.89	blue
0.30	blue to violet blue	0.92	blue-green

0.31	blue	0.95	yellow-green
0.32	blue to blue-green	0.97	yellow
0.34	light green	0.99	orange
0.35	green to yellow-green	1.00	carnation pink
0.36	yellow-green	1.02	violet red
0.37	green-yellow	1.05	red-violet
0.39	yellow	1.06	violet
0.41	light orange	1.07	blue-violet
0.42	carnation pink	1.10	green
0.44	violet-red	1.11	yellow-green
0.46	red-violet	1.12	green
0.47	violet	1.18	violet
0.48	blue-violet	1.19	red-violet
0.49	blue	1.21	violet-red
0.50	blue green	1.24	carnation pink to salmon
0.52	green	1.25	orange
0.54	yellow-green	1.28	"yellowish"
0.56	green-yellow	1.32	sky blue to green-blue
0.57	"yellowish"	1.40	orange
0.58	light orange to pink	1.46	blue-violet
0.60	carnation pink	1.50	blue

High pressure oxidation

High pressure oxidation is another method of oxidizing the silicon surface which controls the rate of oxidation. This is possible because the rate is proportional to the concentration of the oxide, which in turn is proportional to the partial pressure of the oxidizing species, according to Henry's law, (7.11.3), where C is the equilibrium concentration of the oxide, H is Henry's law constant, and p_O is the partial pressure of the oxidizing species.

$$C = H_{(pO)} \quad (7.11.3)$$

This approach is fast, with a rate of oxidation ranging from 100 to 1000 nm/h, and also occurs at a relatively low temperature. It is a useful process, preventing dopants from being displaced and also forms a low number of defects, which is most useful at the end of processing.

Plasma oxidation

Plasma oxidation and anodization of silicon is readily accomplished by the use of activated oxygen as the oxidizing species. The highly reactive oxygen is formed within an electrical discharge or plasma. The oxidation is carried out in a low pressure (0.05 - 0.5 Torr) chamber, and the plasma is produced either by a DC electron source or a high-frequency discharge. In simple plasma oxidation the sample (i.e., the silicon wafer) is held at ground potential. In contrast, anodization systems usually have a DC bias between the sample and an electrode with the sample biased positively with respect to the cathode. Platinum electrodes are commonly used as the cathodes.

There have been at least 34 different reactions reported to occur in an oxygen plasma, however, the vast majority of these are inconsequential with respect to the formation of active species. Furthermore, many of the potentially active species are sufficiently

short lived that it is unlikely that they make a significant contribution. The primary active species within the oxygen plasma are undoubtedly O^- and O^{2+} . Both being produced in near equal quantities, although only the former is relevant to plasma anodization. While these species may be active with respect to surface oxidation, it is more likely that an electron transfer occurs from the semiconductor surface yields activated oxygen species, which are the actual reactants in the oxidation of the silicon.

The significant advantage of plasma processes is that while the electron temperature of the ionized oxygen gas is in excess of 10,000 K, the thermal temperatures required are significantly lower than required for the high pressure method, i.e., $< 600^\circ\text{C}$. The advantages of the lower reaction temperatures include: the minimization of dopant diffusion and the impediment of the generation of defects. Despite these advantages there are two primary disadvantages of any plasma based process. First, the high electric fields present during the processes cause damage to the resultant oxide, in particular, a high density of interface traps often result. However, post annealing may improve film quality. Second, the growth rates of plasma oxidation are low, typically 1000 Å/h. This growth rate is increased by about a factor of 10 for plasma anodization, and further improvements are observed if 1 - 3% chlorine is added to the oxygen source.

Masking

A selective mask against the diffusion of dopant atoms at high temperatures can be found in a silicon dioxide layer, which can prove to be very useful in integrated circuit processing. A predeposition of dopant by ion implantation, chemical diffusion, or spin-on techniques typically results in a dopant source at or near the surface of the oxide. During the initial high-temperature step, diffusion in the oxide must be slow enough with respect to diffusion in the silicon that the dopants do not diffuse through the oxide in the masked region and reach the silicon surface. The required thickness may be determined by experimentally measuring, at a particular temperature and time, the oxide thickness necessary to prevent the inversion of a lightly doped silicon substrate of opposite conductivity. To this is then added a safety factor, with typical total values ranging from 0.5 to 0.7 mm. The impurity masking properties result when the oxide is partially converted into a silica impurity oxide "glass" phase, and prevents the impurities from reaching the SiO_2 -Si interface.

Bibliography

- M. M. Atalla, in *Properties of Elemental and Compound Semiconductors*, Ed. H. Gatos, Interscience: New York (1960).
- S. K. Ghandhi, *VLSI Fabrication Principles, Silicon and Gallium Arsenide*, Wiley, Chichester, 2nd Ed. (1994).
- S. M. Sze, *Physics of Semiconductor Devices*, 2nd Edition, John Wiley & Sons, New York (1981).
- D. L. Lile, *Solid State Electron.*, 1978, **21**, 1199.
- W. E. Spicer, P. W. Chye, P. R. Skeath, and C. Y. Su, *J. Vac. Sci. Technol.*, 1979, **16**, 1422.
- V. Q. Ho and T. Sugano, *IEEE Trans. Electron Devices*, 1980, **ED-27**, 1436.
- J. R. Hollanhan and A. T. Bells, *Techniques and Applications of Plasma Chemistry*, Wiley, New York (1974).
- R. P. H. Chang and A. K. Sinha, *Appl. Phys. Lett.*, 1976, **29**, 56.

7.11: Oxidation of Silicon is shared under a [CC BY 1.0](https://creativecommons.org/licenses/by/1.0/) license and was authored, remixed, and/or curated by LibreTexts.

7.12: Applications for Silica Thin Films

Introduction

While the physical properties of silica make it suitable for use in protective and optical coating applications, the biggest application of insulating SiO₂ thin films is undoubtedly in semiconductor devices, in which the insulator performs a number of specific tasks, including: surface passivation, field effect transistor (FET) gate layer, isolation layers, planarization and packaging.

The term insulator generally refers to a material that exhibits low thermal or electrical conductivity; electrically insulating materials are also called dielectrics. It is in regard to the high resistance to the flow of an electric current that SiO₂ thin films are of the greatest commercial importance. The dielectric constant (ϵ) is a measure of a dielectric materials ability to store charge, and is characterized by the electrostatic energy stored per unit volume across a unit potential gradient. The magnitude of ϵ is an indication of the degree of polarization or charge displacement within a material. The dielectric constant for air is 1, and for ionic solids is generally in the range of 5 - 10. Dielectric constants are defined as the ratio of the material's capacitance to that of air, i.e., (7.12.1). The dielectric constant for silicon dioxide ranges from 3.9 to 4.9, for thermally and plasma CVD grown films, respectively.

$$\epsilon = \frac{C_{\text{material}}}{C_{\text{air}}} \quad (7.12.1)$$

An insulating layer is a film or deposited layer of dielectric material separating or covering conductive layers. Ideally, in these application an insulating material should have a surface resistivity of greater than 10¹³ Ω/cm² or a volume resistivity of greater than 10¹¹ Ω.cm. However, for some applications, lower values are acceptable; an electrical insulator is generally accepted to have a resistivity greater than 10⁵ Ω.cm. CVD SiO₂ thin films have a resistivity of 10⁶ - 10¹⁶ Ω.cm, depending on the film growth method.

As a consequence of its dielectric properties SiO₂, and related silicas, are used for isolating conducting layers, to facilitate the diffusion of dopants from doped oxides, as diffusion and ion implantation masks, capping doped films to prevent loss of dopant, for gettering impurities, for protection against moisture and oxidation, and for electronic passivation. Of the many methods used for the deposition of thin films, chemical vapor deposition (CVD) is most often used for semiconductor processing. In order to appreciate the unique problems associated with the CVD of insulating SiO₂ thin films it is worth first reviewing some of their applications. Summarized below are three areas of greatest importance to the fabrication of contemporary semiconductor devices: isolation and gate insulation, passivation, and planarization.

Device isolation and gate insulation

A microcircuit may be described as a collection of devices each consisting of "an assembly of active and passive components, interconnected within a monolithic block of semiconducting material". Each device is required to be isolated from adjacent devices in order to allow for maximum efficiency of the overall circuit. Furthermore within a device, contacts must also be electrically isolated. While there are a number of methods for isolating individual devices within a circuit (reverse-biased junctions, mesa isolation, use of semi-insulating substrates, and oxide isolation), the isolation of the active components in a single device is almost exclusively accomplished by the deposition of an insulator.

In [Figure](#) is shown a schematic representation of a silicon MOSFET (metal-oxide-semiconductor field effect transistor). The MOSFET is the basic component of silicon-CMOS (complimentary metal-oxide-semiconductor) circuits which, in turn, form the basis for logic circuits, such as those used in the CPU (central processing unit) of a modern personal computer. It can be seen that the MOSFET is isolated from adjacent devices by a reverse-biased junction (p⁺-channel stop) and a thick oxide layer. The gate, source and drain contact are electrically isolated from each other by a thin insulating oxide. A similar scheme is used for the isolation of the collector from both the base and the emitter in bipolar transistor devices.

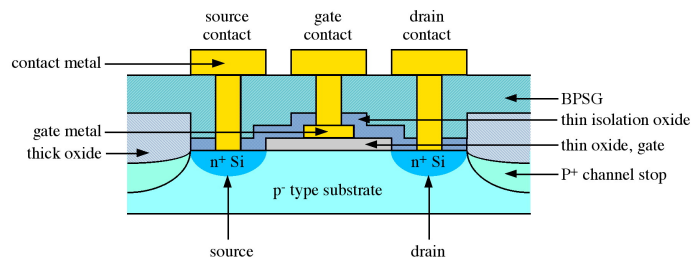


Figure 7.12.1: Schematic diagrams of a Si-MOSFET (metal-oxide-semiconductor field effect transistor).

As a transistor, a MOSFET has many advantages over alternate designs. The key advantage is low power dissipation resulting from the high impedance of the device. This is a result of the thin insulation layer between the channel (region between source and drain) and the gate contact, see Figure 7.12.1. The presence of an insulating gate is characteristic of a general class of devices called MISFETs (metal-insulator-semiconductor field effect transistor). MOSFETs are a subset of MISFETs where the insulator is specifically an oxide, e.g., in the case of a silicon MISFET device the insulator is SiO_2 , hence MOSFET. It is the fabrication of MOSFET circuits that has allowed silicon technology to dominate digital electronics (logic circuits). However, increases in computing power and speed require a constant reduction in device size and increased complexity in device architecture.

Passivation

Passivation is often defined as a process whereby a film is grown on the surface of a semiconductor to either (a) chemically protect it from the environment, or (b) provide electronic stabilization of the surface.

From the earliest days of solid state electronics it has been recognized that the presence or absence of surface states plays a decisive role in the usefulness of any semiconducting material. On the surface of any solid state material there are sites in which the coordination environment of the atoms is incomplete. These sites, commonly termed "dangling bonds", are the cause of the electronically active states which allow for the recombination of holes and electrons. This recombination occurs at energies below the bulk value, and interferes with the inherent properties of the semiconductor. In order to optimize the properties of a semiconductor device it is desirable to covalently satisfy all these surface bonds, thereby shifting the surface states out of the band gap and into the valence or conduction bands. Electronic passivation may therefore be described as a process which reduces the density of available electronic states present at the surface of a semiconductor, thereby limiting hole and electron recombination possibilities. In the case of silicon both the native oxide and other oxides admirably fulfill these requirements.

Chemical passivation requires a material that inhibits the diffusion of oxygen, water, or other species to the surface of the underlying semiconductor. In addition, the material is ideally hard and resistant to chemical attack. A perfect passivation material would satisfy both electronic and chemical passivation requirements.

Planarization

For the vast majority of electronic devices, the starting point is a substrate consisting of a flat single crystal wafer of semiconducting material. During processing, which includes the growth of both insulating and conducting films, the surface becomes increasingly non-planar. For example, a gate oxide in a typical MOSFET (see Figure 7.12.1) may be typically 100 - 250 Å thick, while the isolation or field oxide may be 10,000 Å. In order for the successful subsequent deposition of conducting layers (metallization) to occur without breaking metal lines (often due to the difficulty in maintaining step coverage), the surface must be flat and smooth. This process is called planarization, and can be carried out by a technique known as sacrificial etchback. An abrupt step (Figure 7.12.2a) is coated with a conformal layer of a low melting dielectric, e.g., borophosphosilicate glass, BPSG (Figure 7.12.2b), and subsequently a sacrificial organic resin (Figure 7.12.2c). The sample is then plasma etched such that the resin and dielectric are removed at the same rate. Since the plasma etch follows the contour of the organic resin, a smooth surface is left behind (Figure 7.12.2d). The planarization process thus reduces step height differentials significantly. In addition regions or valleys between individual metallization elements (vias) can be completely filled allowing for a route to producing uniformly flat surfaces, e.g., the BPSG film shown in Figure 7.12.1.

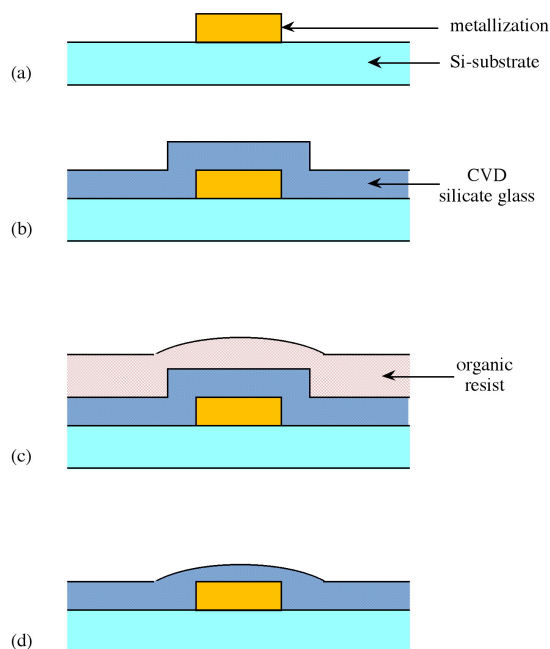


Figure 7.12.2: Schematic representation of the planarization process. A metallization feature (a) is CVD covered with silicate glass (b), and subsequently coated with an organic resin (c). After etching the resist a smooth silicate surface is produced (d).

The processes of planarization is vital for the development of multilevel structures in VLSI circuits. To minimize interconnection resistance and conserve chip area, multilevel metallization schemes are being developed in which the interconnects run in 3-dimensions.

Bibliography

- J. L. Vossen and W. Kern, *Phys. Today*, 1980, **33**, 26.
- S. K. Ghandhi, *VLSI Fabrication Principles, Silicon and Gallium Arsenide*, Wiley, Chichester, 2nd Ed. (1994).
- S. M. Sze, *Physics of Semiconductor Devices*, 2nd Edition, John Wiley & Sons, New York (1981).
- W. E. Beadle, J. C. C. Tsai, R. D. Plummer, *Quick Reference Manual for Silicon Integrated Circuit Technology*, Wiley, Chichester (1985).
- A. C. Adams and C. D. Capio, *J. Electrochem. Soc.*, 1981, **128**, 2630.

7.12: Applications for Silica Thin Films is shared under a [CC BY 1.0](https://creativecommons.org/licenses/by/1.0/) license and was authored, remixed, and/or curated by LibreTexts.

CHAPTER OVERVIEW

8: Group 15 - The Pnictogens

[8.1: The Group 15 Elements- The Pnictogens](#)

[8.2: Reaction Chemistry of Nitrogen](#)

[8.3: Hydrides](#)

[8.4: Oxides and Oxoacids](#)

[8.5: Halides of Phosphorous](#)

This page titled [8: Group 15 - The Pnictogens](#) is shared under a [CC BY 3.0](#) license and was authored, remixed, and/or curated by [Andrew R. Barron \(CNX\)](#) via [source content](#) that was edited to the style and standards of the LibreTexts platform.

8.1: The Group 15 Elements- The Pnictogens

The elements

The Group 15 elements have a particular name *pnictogens*. Despite the modern IUPAC notation, the Group 15 elements are still referred to as Group V elements in particular by the semiconductor industry. Table 8.1.1 lists the derivation of the names of the Group 15 elements.

Table 8.1.1: Derivation of the names of each of the Group 15 (V) elements.

Element	Symbol	Name
Nitrogen	N	Latin <i>nitrogenium</i> , where <i>nitrum</i> (derived from Greek <i>nitron</i>) means <i>saltpetre</i>
Phosphorus	P	From the Greek <i>phosphoros</i> meaning <i>bringer of light</i>
Arsenic	As	Derived from Syriac <i>zarniqa</i> and Persian <i>zarnikh</i> , meaning <i>yellow orpiment</i>
Antimony	Sb	Greek <i>anti</i> and <i>monos</i> meaning <i>not alone</i> . The symbol Sb from Latin <i>stibium</i>
Bismuth	Bi	New Latin <i>bisemutum</i> from German <i>Wismuth</i> , meaning <i>white mass</i>

Note

According to the Oxford English Dictionary, the correct spelling of the element is phosphorus. The word phosphorous is the adjectival form of the P^{3+} valence. In the same way that sulfur forms sulfurous and sulfuric compounds, phosphorus forms phosphorous compounds (e.g., phosphorous acid) and P^{5+} valency phosphoric compounds (e.g., phosphoric acids and phosphates).

Discovery

Nitrogen

Nitrogen was discovered by Rutherford (Figure 8.1.1) in 1772. He called it *noxious air* or *fixed air* because there it had been known since the late 18th century that there was a fraction of air that did not support combustion. Nitrogen was also studied by Scheele (Figure 8.1.2), Cavendish (Figure 8.1.3), and Priestley (Figure 8.1.4), who referred to it as *burnt air* or *phlogisticated air*.



Figure 8.1.1: Scottish chemist and physician Daniel Rutherford (1749 - 1819).



Carl Wilhelm Scheele.

Figure 8.1.2: Swedish chemist Carl Wilhelm Scheele (1742 – 1786). Isaac Asimov called him "hard-luck Scheele" because he made a number of chemical discoveries before others who are generally given the credit.



Figure 8.1.3: British scientist Henry Cavendish FRS (1731 - 1810).



Figure 8.1.4: Portrait (by Ellen Sharples) of British clergyman natural philosopher, educator, and political theorist Joseph Priestley (1733 - 1804).

Phosphorus

German alchemist Hennig Brand (Figure 8.1.5) was experimenting with urine (which contains dissolved phosphates) in 1669. While attempting to create the fabled philosopher's stone (the legendary alchemical substance capable of turning base metals, such as lead, into gold) by the distillation of salts from urine, he produced a white material that glowed in the dark and burned with a brilliant light. He gave the substance the name *phosphorus mirabilis* (*miraculous bearer of light*). His process involved letting the urine stand for days then boiling it down to a paste which led to a white waxy substance, white phosphorus.



Figure 8.1.5: The discovery of phosphorus by German merchant and alchemist Hennig Brand (1630 - 1710) as depicted by Joseph Wright (with significant artistic license with regard to the brightness of the chemiluminescence).

Brand sold the recipe for 200 thaler (a silver coin from whose name the dollar is derived) to D Krafft who toured much of Europe showing it. During his journeys he met Robert Boyle (Figure 8.1.6) who without learning the details of the synthesis recreated and improved it by using sand in the reduction of the phosphate, (8.1.1).

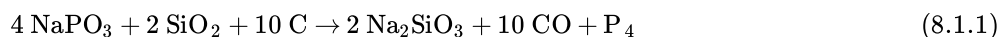


Figure 8.1.6: British natural philosopher, chemist, physicist, and inventor Robert Boyle (1627 - 1691).

Arsenic

Arsenic sulfides and oxides were known since ancient times. Zosimos (*ca.* 300 AD) describes roasting *sandarach* (realgar, $\alpha\text{-As}_4\text{S}_4$) to obtain cloud of arsenious oxide (As_2O_3) that he reduced to metallic arsenic (Figure 8.1.7).

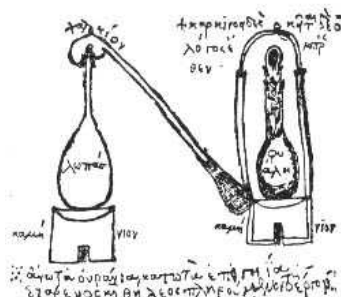


Figure 8.1.7: The distillation apparatus of Zosimos.

Antimony

Antimony(III) sulfide, Sb_2S_3 was known as early as 3000 BC. Pastes of Sb_2S_3 powder in fat were used as eye cosmetics in the Middle East. An artifact made of antimony dating to about 3000 BC was found at Tello (part of present-day Iraq), and copper

objects plated with antimony from 2500 - 2200 BC have been found in Egypt. The first European description of a procedure for isolating antimony is in the book *De la pirotechnia* by Vannoccio Biringuccio (1480 - 1539).

Bismuth

Since bismuth was known in ancient times, no one person is credited with its discovery. However, the French chemist Claude François Geoffroy (1729 - 1753) demonstrated in 1753 that this metal is distinct from lead and tin.

Abundance

The abundance of the Group 15 elements is given in Table 8.1.2.

Table 8.1.2: Abundance of the Group 15 elements.

Element	Terrestrial abundance (ppm)
N	25 (Earth's crust), 5 (soil), 0.5 (sea water), 78×10^4 (atmosphere)
P	1000 (Earth's crust), 0.65 (soil), 60×10^{-3} (sea water), trace (atmosphere)
As	1.5 (Earth's crust), 10 (soil), 16×10^{-3} (sea water), trace (atmosphere)
Sb	0.2 (Earth's crust), 1 (soil), 0.3×10^{-3} (sea water)
Bi	48×10^{-3} (Earth's crust), 0.25 (soil), 400×10^{-6} (sea water)

Isotopes

The naturally abundant isotopes of the Group 15 elements are listed in Table 8.1.3.

Table 8.1.3: Abundance of the non-synthetic isotopes of the Group 15 elements.

Isotope	Natural abundance (%)
Nitrogen-14	99.634
Nitrogen-15	0.0366
Phosphorus-31	100
Arsenic-75	100
Antimony-121	57.36
Antimony-123	42.64
Bismuth-209	100%

Two radioactive isotopes of phosphorus (^{32}P and ^{33}P) have half-lives that make them useful for scientific experiments (14.262 and 25.34 days, respectively). ^{32}P is a β -emitter (1.71 MeV) and is used to produce radiolabeled DNA and RNA probes. Due to the high energy of the β particles which can penetrate skin and corneas, and because any ^{32}P ingested, inhaled, or absorbed is incorporated into bone and nucleic acids extreme care needs to be taken in handling. The lower energy β particles emitted from ^{33}P (0.25 MeV) make it useful for applications such as DNA sequencing.

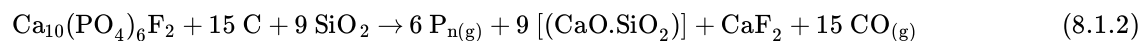
While bismuth is traditionally regarded as the element with the heaviest stable isotope, ^{209}Bi , it had long been suspected to be unstable on theoretical grounds. In 2003 researchers at the Institut d'Astrophysique Spatiale in Orsay, France, measured the alpha emission half-life of ^{209}Bi to be 1.9×10^{19} years, over a billion times longer than the current estimated age of the universe!

Industrial production of the elements

Nitrogen is the largest constituent of the Earth's atmosphere (78.082% by volume, 75.3% by weight). It is created by fusion processes in stars, and is estimated to be the 7th most abundant element by mass in the universe. Industrial gas produced is by the fractional distillation of liquid air, or by mechanical means using gaseous air (i.e., pressurized reverse osmosis membrane or

pressure swing adsorption). Commercial nitrogen is often a byproduct of air processing for industrial concentration of oxygen for steelmaking, etc.

White phosphorus was originally made commercially for the match industry in the 19th century, by distilling off phosphorus vapor from precipitated phosphates, mixed with ground coal or charcoal, (8.1.2). The precipitated phosphates were made from ground-up bones that had been de-greased and treated with strong acids. This process is, however, obsolete due to the submerged-arc furnace for phosphorus production was introduced to reduce phosphate rock. Calcium phosphate (phosphate rock) is heated to 1200 - 1500 °C with SiO₂ and coke (impure carbon) to produce vaporized tetraphosphorus, P₄.



Physical properties

The physical properties of the Group 15 elements (Table 8.1.3) encompasses a gas (N₂), a non-metallic solid (P₄), metalloids (As and Sb), and a metal (Bi).

Table 8.1.3: Selected physical properties of the Group 15 elements.

Element	Mp (°C)	Bp (°C)	Density (g/cm ³)
N	-210.00	-195.79	1.251 g/L (0 °C @ 101.325 kPa)
P	44.2 (white), 610 (black)	280.5 (white), 416 - 590 (sub., red), 620 (sub, violet)	1.823 (white), 2.2 - 2.34 (red), 2.36 (violet), 2.69 (black)
As	817	615 (sub.)	5.727
Sb	630.63	1587	6.697 (solid), 6.53 (liquid)
Bi	271.5	1564	9.78 (solid), 10.05 (liquid)

Vapor phase

Nitrogen forms a dimer in the vapor phase with a triple bond (Figure 8.1.8). In the vapor phase above 800 °C tetraphosphorus (P₄) is partially dissociated to P₂.

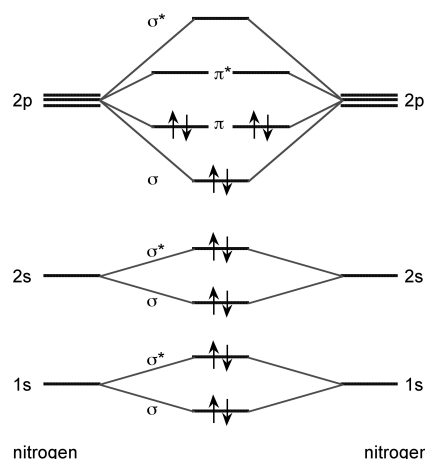


Figure 8.1.8: Molecular orbital diagram for the formation of N₂.

Solid state

Phosphorus forms a number of allotropes with very different properties (Figure 8.1.9). Red phosphorus is an intermediate phase between the white and violet forms. Scarlet phosphorus is obtained by allowing a solution of white phosphorus in carbon disulfide to evaporate in sunlight. Black phosphorus is formed by heating white phosphorus under high pressures (ca. 12,000 atmospheres).



Figure 8.1.9: Images of (left to right) white, red, violet and black allotropes of phosphorus.

White phosphorus has two forms, low-temperature β form and high-temperature α form; both of which contain the P_4 tetrahedron (Figure 8.1.10). White phosphorus is the least stable, the most reactive, most volatile, less dense, and most toxic of the allotropes.

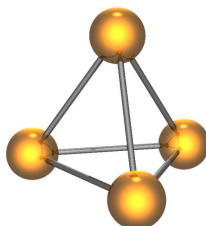


Figure 8.1.10: The structure of the P_4 molecule in white phosphorus.

The structural relationship between white and red phosphorus involves breaking one of the P-P bonds in the P_4 unit and forming a bond with a neighboring tetrahedron to give a chain structure (Figure 8.1.11). Red phosphorus is formed by heating white phosphorus to 250 °C or by exposing white phosphorus to sunlight. Actually red phosphorus is not a single allotrope, but rather an intermediate phase between the white and violet phosphorus, and most of its properties have a range of values (Table 8.1.3).

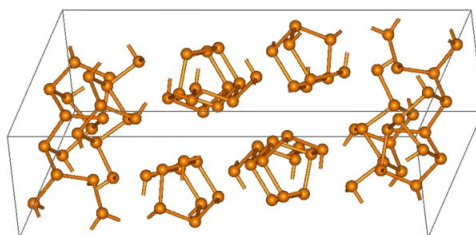


Figure 8.1.11: Crystal unit cell of red phosphorus.

Violet phosphorus (Figure 8.1.12) is the thermodynamic stable form of phosphorus that is produced by heating red phosphorus above 550 °C. Due to the synthesis being developed by Johann Hittorf (Figure 8.1.13) it is sometimes known as *Hittorf's phosphorus*.

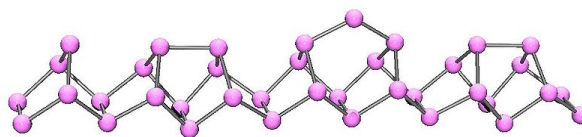


Figure 8.1.12: Structure of violet (Hittorf's) phosphorus.



Figure 8.1.13: German physicist Johann Wilhelm Hittorf (1824 - 1914).

Black phosphorus is the least reactive allotrope and the thermodynamic stable form below 550 °C. It is also known as β -metallic phosphorus and has a structure somewhat resembling that of graphite (Figure 8.1.14).

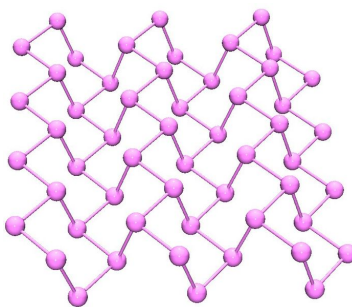


Figure 8.1.14: Crystal structure of black phosphorus.

In a similar manner to phosphorus, arsenic has several allotropes some of which are structurally related to those of phosphorus. Grey arsenic has a structure similar to black phosphorus (Figure 8.1.10). Yellow arsenic (As_4) is soft and waxy with a structure similar to P_4 (Figure 8.1.14). Finally, black arsenic is similar in structure to red phosphorus (Figure 8.1.11). Antimony and bismuth are both traditional metals and have trigonal hexagonal structures ($a = 4.299$, $c = 11.25$ Å, and $a = 4.537$, $c = 11.838$ Å, respectively).

Bibliography

- V. Biringuccio, *The Pirotechnia of Vannoccio Biringuccio: The Classic Sixteenth-Century Treatise on Metals and Metallurgy*, Dover Publications (1990).

This page titled [8.1: The Group 15 Elements- The Pnictogens](#) is shared under a [CC BY 3.0](#) license and was authored, remixed, and/or curated by [Andrew R. Barron \(CNX\)](#) via [source content](#) that was edited to the style and standards of the LibreTexts platform.

8.2: Reaction Chemistry of Nitrogen

Despite nitrogen being the inert component of the Earth's atmosphere, dinitrogen undergoes a range of reactions, although it only reacts with a few reagents under standard temperature and pressure. Nitrogen reacts with oxygen in an electric arc, (8.2.1), both in the laboratory and within lightening strikes.



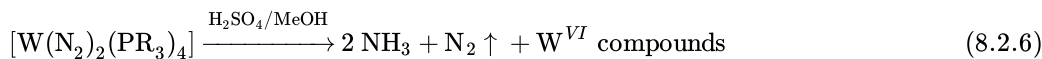
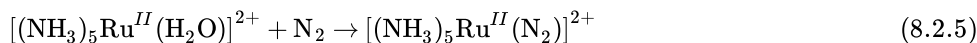
The synthesis of ammonia is accomplished by the Harber process, using an iron oxide (Fe_3O_4) catalyst, (8.2.2), at about 500 °C and 200 atmospheres pressure.



Nitrogen reacts with lithium metal at room temperature to form the nitride, (8.2.3). Magnesium also burns in nitrogen, forming magnesium nitride, (8.2.4).



Nitrogen forms complexes with transition metals yielding nitrogeno complexes, (8.2.5). Under some conditions these complexes react to give ammonia, (8.2.6), and as such may give a hint to the action of nitrogenase in which molybdenum is the active site.



This page titled [8.2: Reaction Chemistry of Nitrogen](#) is shared under a [CC BY 3.0](#) license and was authored, remixed, and/or curated by [Andrew R. Barron \(CNX\)](#) via [source content](#) that was edited to the style and standards of the LibreTexts platform.

8.3: Hydrides

Trihydrides of the Group 15 Elements

All five of the Group 15 elements form hydrides of the formula EH_3 . Table 8.3.1 lists the IUPAC names along with those in more common usage.

Table 8.3.1: Traditional and IUPAC (International Union of Pure and Applied Chemistry) names for the Group 15 hydrides.

Compound	Traditional name	IUPAC name
NH_3	Ammonia	Azane
PH_3	Phosphine	Phosphane
AsH_3	Arsine	Arsane
SbH_3	Stibine	Stibane
BiH_3	Bismuthine	Bismuthane

The boiling point and melting point increase increases going down the Group (Table 8.3.2) with increased molecular mass, with the exception of NH_3 whose anomalously high melting and boiling points (Figure 8.3.1) are a consequence of strong $\text{N-H}\cdots\text{H}$ hydrogen bonding. A similar (and stronger) effect is observed for the Group 16 hydrides (H_2E).

Table 8.3.2: Selected physical properties of Group 15 hydrides.

Compound	Mp ($^{\circ}\text{C}$)	Bp ($^{\circ}\text{C}$)	ΔH_f (kJ/mol)	E-H bond energy (kJ/mol)	H-E-H bond angle ($^{\circ}$)
NH_3	-77.7	-33.35	-46.2	391	107
PH_3	-133	-87.7	9.3	322	93.5
AsH_3	-116.3	-55	172.2	247	92
SbH_3	-88	-17.1	142.8	255	91.5

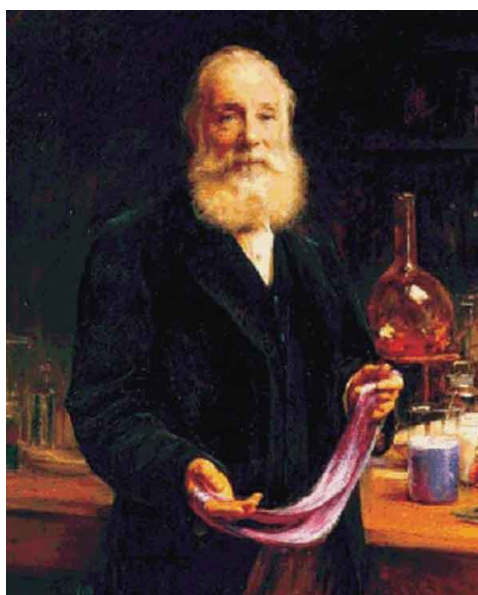


Figure 8.3.1: Plot of melting and boiling points of EH_3 (E = N, P, As, and Sb) as a function of molecular mass.

The E-H bond strengths decrease down the group and this correlates with the overall stability of each compound (Table 8.3.2). The H-E-H bond angles (Table 8.3.2) also decrease down the Group. The H-E-H bond angle is expected to be a tetrahedral ideal of

109.5°, but since lone pairs repel more than bonding pairs, the actual angle would be expected to be slightly smaller. Two possible explanations are possible for the difference between NH₃ and the other hydrides.

1. The N-H bond is short (1.015 Å) compared to the heavier analogs, and nitrogen is more electronegative than hydrogen, so the bonding pair will reside closer to the central atom and the bonding pairs will repel each other opening the H-N-H angle more than observed for PH₃, etc.
2. The accessibility of the 2s and 2p orbitals on nitrogen allows for hybridization and the orbitals associated with N-H bonding in NH₃ are therefore close to sp³ in character, resulting in a close to tetrahedral geometry. In contrast, hybridization of the ns and np orbitals for P, As, etc., is less accessible, and as a consequence the orbitals associated with P-H bonding in PH₃ are closer to p in character resulting in almost 90° H-P-H angle. The lower down the Group the central atom the less hybridization that occurs and the closer to pure p-character the orbitals on E associated with the E-H bond.

Ammonia

Ammonia (NH₃) is a colorless, pungent gas (bp = -33.5 °C) whose odor can be detected at concentrations as low 20 – 50 ppm. Its high boiling point relative to its heavier congeners is indicative of the formation of strong hydrogen bonding. The strong hydrogen bonding also results in a high heat of vaporization (23.35 kJ/mol) and thus ammonia can be conveniently used as a liquid at room temperature despite its low boiling point.

WARNING

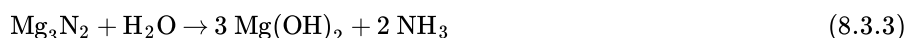
Ammonia solution causes burns and irritation to the eyes and skin. The vapor causes severe irritation to the respiratory system. If swallowed the solution causes severe internal damage.

Synthesis

Ammonia is manufactured on the industrial scale by the Haber process using the direct reaction of nitrogen with hydrogen at high pressure (10² – 10³ atm) and high temperature (400 – 550 °C) over a catalyst (e.g., α-iron), (8.3.1).



On the smaller scale ammonia is prepared by the reaction of an ammonium salt with a base, (8.3.2), or hydrolysis of a nitride, (8.3.3). The latter is a convenient route to ND₃ by the use of D₂O.



Structure

The nitrogen in ammonia adopts sp³ hybridization, and ammonia has an umbrella structure (Figure 8.3.2) due to the stereochemically active lone pair.

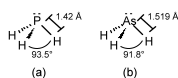
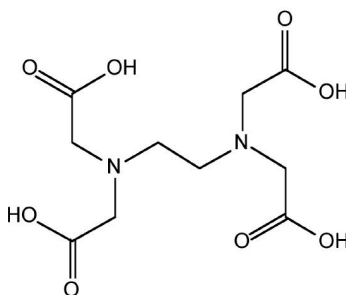
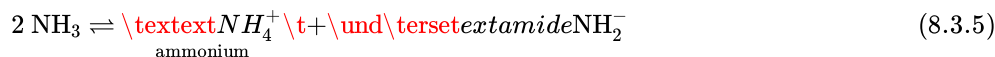


Figure 8.3.2: The structure of ammonia.

The barrier to inversion of the umbrella is very low ($E_a = 24$ kJ/mol) and the inversion occurs 100's of times a second. As a consequence it is not possible to isolate chiral amines in the same manner that is possible for phosphines.



In a similar manner to water, (8.3.4), ammonia is a self-ionizing, (8.3.5); however, the equilibrium constant ($K = 10^{-33}$) is much lower than water ($K = 10^{-14}$). The lower dielectric constant of ammonia (16.5 @ 20 °C) as compared to water (80.4 @ 20 °C) means that ammonia is not as good as water as a solvent for ionic compounds, but is better for covalent organic compounds.



Reactions

The similarity of ammonia and water means that the two compounds are miscible. In fact, ammonia forms a series of solid hydrates, analogous to ice in which hydrogen bonding defines the structures (Figure 8.3.3). Several hydrates of ammonia are known, including: $\text{NH}_3 \cdot 2\text{H}_2\text{O}$ (ammonia dihydrate, ADH), $\text{NH}_3 \cdot \text{H}_2\text{O}$ (ammonia monohydrate, AMH), and $2\text{NH}_3 \cdot 2\text{H}_2\text{O}$ (ammonia hemihydrate, AHH).

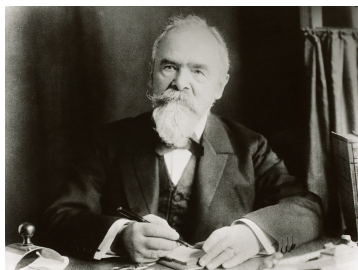


Figure 8.3.3: The crystal structure of ammonia monohydrate (ANH-II) with hydrogen atoms omitted. Adapted from A. D. Fortes, E. Suard, M. -H. Lemée-Cailleau, C. J. Pickard, and R. J. Needs, *J. Am. Chem. Soc.*, 2009, **131**, 13508. Copyright: American Chemical Society (2009).

It should be noted that these hydrates do not contain discrete NH_4^+ or OH^- ions, indicating that ammonium hydroxide does not exist as a discrete species despite the common useage of the name. In aqueous solution, ammonia is a weak base ($\text{pK}_b = 4.75$), (8.3.6).



Note

Ammonia solutions commonly used in the laboratory is a 35% solution in water. In warm weather the solution develops pressure and the cap must be released with care. The 25% solution sold commercially (for home use) is free from this problem.

Ammonia is a Lewis base and readily forms Lewis acid-base complexes with both transition metals, (8.3.7), and main group metals (Figure 8.3.4).

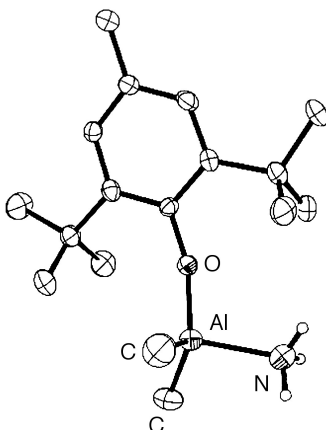
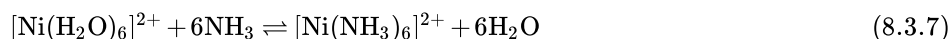


Figure 8.3.4: The molecular structure of $\text{AlMe}_2(\text{BHT})\text{NH}_3$. Hydrogen atoms, except those attached to nitrogen, are omitted for clarity. Adapted from M. D. Healy, J. T. Leman, and A. R. Barron, *J. Am. Chem. Soc.*, 1991, **113**, 2776. Copyright: American Chemical Society.

The formation of stable ammonia complexes is the basis of a simple but effective method of detection: Nessler's reagent, (8.3.8). Using a 0.09 mol/L solution of potassium tetraiodomercurate(II), $K_2[HgI_4]$, in 2.5 mol/L potassium hydroxide. A yellow coloration indicates the presence of ammonia: at higher concentrations, a brown precipitate may form. The sensitivity as a spot test is about 0.3 μg NH_3 in 2 μL .



Ammonia forms a blue solution with Group 1 metals. As an example, the dissolution of sodium in liquid ammonia results in the formation of solvated Na^+ cations and electrons, (8.3.9) where $\text{solv} = \text{NH}_3$. The solvated electrons are stable in liquid ammonia and form a complex: $[\text{e}^-(\text{NH}_3)_6]$.



It is this solvated electron that gives the strong reducing properties of the solution as well as the characteristic signal in the ESR spectrum associated with a single unpaired electron. The blue color of the solution is often ascribed to these solvated electrons; however, their absorption is in the far infra-red region of the spectrum. A second species, $\text{Na}^-(\text{solv})$, is actually responsible for the blue color of the solution.



The reaction of ammonia with oxygen is highly favored, (8.3.11), and the flammability limit of ammonia is 16 – 25 vol%. If the reaction is carried out in the presence of a catalyst (Pt or Pd) the reaction can be limited to the formation of nitric oxide (NO), (8.3.12).



Ammonium salts

The ammonium cation (NH_4^+) behaves in a similar manner to the Group 1 metal ions. The solubility and structure of ammonium salts particularly resembles those of potassium and rubidium because of their relative size (Table 8.3.3). One difference is that ammonium salts often decompose upon heating, (8.3.13).



Table 8.3.3: Ionic radius of the ammonium ion compared to those of potassium and rubidium.

Cation	Ionic radius (Å)
K^+	1.33
NH_4^+	1.43
Rb^+	1.47

The decomposition of ammonium salts of oxidizing acids can often be violent to highly explosive, and they should be treated with care. For example, while ammonium dichromate, $(\text{NH}_4)_2\text{Cr}_2\text{O}_7$, decomposes to give a volcano (Figure 8.3.5), ammonium permanganate, $\text{NH}_4[\text{MnO}_4]$, is friction sensitive and explodes at 60 °C. Ammonium nitrate, $\text{NH}_4[\text{NO}_3]$, can cause fire if contacted with a combustible material and is a common ingredient in explosives since it acts as the oxygen source due to its positive oxygen balance, i.e., the compound liberates oxygen surplus to its own needs upon decomposition, (8.3.14).





Figure 8.3.5: A laboratory demonstration of an ammonium dichromate volcano.

Bibliography

- A. R. Barron, *The Detonator*, 2009, **36**, 60.
- A. D. Fortes, E. Suard, M. -H. Lemée-Cailleau, C. J. Pickard, and R. J. Needs, *J. Am. Chem. Soc.*, 2009, **131**, 13508.
- M. D. Healy, J. T. Leman, and A. R. Barron, *J. Am. Chem. Soc.*, 1991, **113**, 2776.
- A. I. Vogel and G. Svehla, *Textbook of Macro and Semimicro Qualitative Inorganic Analysis*, Longman, London (1979).

Liquid Ammonia as a Solvent

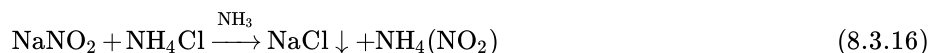
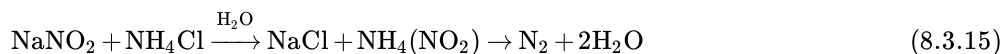
Ammonia has a reasonable liquid range (-77 to -33 °C), and as such it can be readily liquefied with dry ice (solid CO₂, T_{sub} = -78.5 °C), and handled in a thermos flask. Ammonia's high boiling point relative to its heavier congeners is indicative of the formation of strong hydrogen bonding, which also results in a high heat of vaporization (23.35 kJ/mol). As a consequence ammonia can be conveniently used as a liquid at room temperature despite its low boiling point.

Liquid ammonia is a good solvent for organic molecules (e.g., esters, amines, benzene, and alcohols). It is a better solvent for organic compounds than water, but a worse solvent for inorganic compounds. The solubility of inorganic salts is highly dependant on the identity of the counter ion (Table 8.3.4).

Table 8.3.4: General solubility of inorganic salts in liquid ammonia as a function of the counter ion.

Soluble in liquid NH ₃	Generally insoluble in liquid NH ₃
SCN ⁻ , I ⁻ , NH ₄ ⁺ , NO ₃ ⁻ , NO ₂ ⁻ , ClO ₄ ⁻	F ⁻ , Cl ⁻ , Br ⁻ , CO ₃ ²⁻ , SO ₄ ²⁻ , O ²⁻ , OH ⁻ , S ²⁻

The difference in solubility of inorganic salts in ammonia as compared to water, as well as the lower temperature of liquid ammonia, can be used to good advantage in the isolation of unstable compounds. For example, the attempted synthesis of ammonium nitrate by the reaction of sodium nitrate and ammonium chloride in water results in the formation of nitrogen and water due to the decomposition of the nitrate, (8.3.15). By contrast, if the reaction is carried out in liquid ammonia, the sodium chloride side product is insoluble and the ammonium nitrate may be isolated as a white solid after filtration and evaporation below its decomposition temperature of 0 °C, (8.3.16).



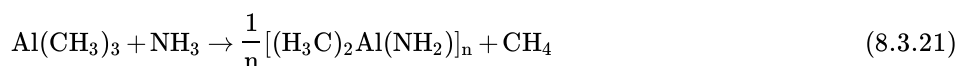
Ammonation

Ammonation is defined as a reaction in which ammonia is added to other molecules or ions by covalent bond formation utilizing the unshared pair of electrons on the nitrogen atom, or through ion-dipole electrostatic interactions. In simple terms the resulting *ammine* complex is formed when the ammonia is acting as a Lewis base to a Lewis acid, (8.3.17) and (8.3.18), or as a ligand to a cation, e.g., [Pt(NH₃)₄]²⁺, [Ni(NH₃)₆]²⁺, [Cr(NH₃)₆]³⁺, and [Co(NH₃)₆]³⁺.

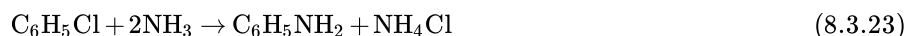


Ammonolysis

Ammonolysis with ammonia is an analogous reaction to hydrolysis with water, i.e., a dissociation reaction of the ammonia molecule producing H⁺ and an NH₂⁻ species. Ammonolysis reactions occur with inorganic halides, (8.3.18) and (8.3.19), and organometallic compounds, (8.3.20). In both case the NH₂⁻ moiety forms a substituent or ligand.



The reaction of esters, (8.3.21), and aryl halides, (8.3.22), are also examples of ammonolysis reactions.



Homoleptic amides

A homoleptic compound is a compound with all the ligands being identical, e.g., $\text{M}(\text{NH}_2)_n$. A general route to homoleptic amide compounds is accomplished by the reaction of a salt of the desired metal that is soluble in liquid ammonia (Table 8.3.4) with a soluble Group 1 amide. The solubility of the Group 1 amides is given in Table 8.3.5. Since all amides are insoluble (except those of the Group 1 metals) are insoluble in liquid ammonia, the resulting amide may be readily isolated, e.g., (8.3.23) and (8.3.24).



Table 8.3.5: Solubility of Group amides in liquid ammonia.

Amide	Solubility in liquid ammonia
LiNH_2	Sparingly soluble
NaNH_2	Sparingly soluble
KNH_2	Soluble
RbNH_2	Soluble
CsNH_2	Soluble

Redox reactions

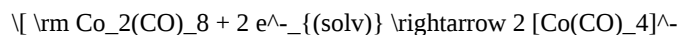
Ammonia is poor as an oxidant since it is relatively easily oxidized, e.g., (8.3.25) and (8.3.26). Thus, if it is necessary to perform an oxidation reaction ammonia is not a suitable solvent; however, it is a good solvent for reduction reactions.



Liquid ammonia will dissolve Group 1 (alkali) metals and other electropositive metals such as calcium, strontium, barium, magnesium, aluminum, europium, and ytterbium. At low concentrations (ca. 0.06 mol/L), deep blue solutions are formed: these contain metal cations and solvated electrons, (8.3.27). The solvated electrons are stable in liquid ammonia and form a complex: $[\text{e}^-(\text{NH}_3)_6]$.



The solvated electrons provide a suitable and powerful reducing agent for a range of reactions that are not ordinarily accomplished, e.g., (8.3.28) and (8.3.29).



Ammonia: From Uses in Agriculture and Beer Production to Prolonging the First World War

One of the cornerstones of the industrial expansion in Germany between 1870 and 1910 (when the population grew from 41 million to 66 million) was the chemicals industry. In particular companies such as Badische Anilin und Soda Fabrik (Baden Aniline and Soda Factory or BASF) had developed their business on the formation of synthetic dyes derived from the chemicals in coal tar.

Coal tar was formed as a by-product of the gasification of coal. A key ingredient of coal tar is naphtha (Table 8.3.6) that was used by the rubber industry; however, the remainder was disposed off. It was not long before chemists started to investigate the constituents present in coal tar. One of the first discoveries was by a chemistry student at the Royal College of Chemistry (now Imperial College) in London, William Perkin (Figure 8.3.6), who isolated the first synthetic dye: mauveine (Figure 8.3.7). This discovery led to an explosion in the chemical industry based on the extraction of compounds from coal tar, which was an essentially free waste product from every gasworks. Nowhere was this research more commercially driven than in Germany.

Table 8.3.6: The typical physical properties of naphtha.

Property	Typical value
Molecular weight	100 - 215 g/mol
Specific gravity	0.75 - 0.85 g/cm ³
Boiling point	160 - 220 °C
Vapor pressure	5 mmHg
Solubility in water	Insoluble

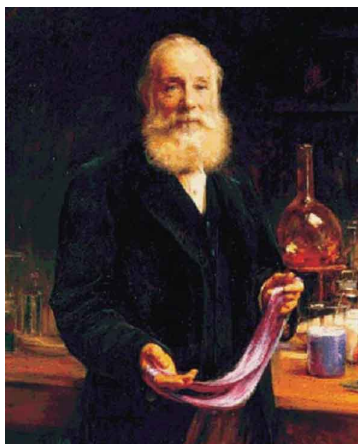


Figure 8.3.6: A portrait of English chemist Sir William Perkin (1838 - 1907) holding a sample of cloth dyed with his discovery, mauveine, which is often called *Perkin's purple*.

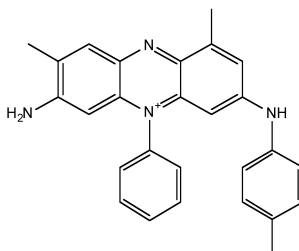


Figure 8.3.7: The structure of mauveine-B.

The rapid increase in the German population also put a strain on the country's food resources. What compounded this issue was that the aristocratic Junker families of East Prussia who owned much of the land in what was known as *Germany's breadbasket*. Junkers grew rye on their estates because the soil was too light for wheat, and since rye was fertilized with potash (potassium oxide, K₂O) of which Germany had vast resources. However, in 1870 grain from the US was becoming cheaper and thus competitive with German rye. To protect their profits the Junkers demanded both subsidies for the export of rye and tariffs for the import of wheat. The result of this was that all the German rye was leaving the country and there was not enough wheat being produced to satisfy the needs of the local population. Sufficient wheat could be grown in Germany if a suitable fertilizer was available.

Sodium nitrate (NaNO₃), also known as *Chile saltpeter*, was the most common fertilizer. Unfortunately, by 1900 the deposits looked to be depleted and an alternative was needed. The alternative was found as a component in coal tar. It was known that one of the chemicals that caused the *stink* associated with coal gas and coal tar was ammonia (NH₃). Chemist George Fownes (Figure

8.3.8) had suggested that ammonia be turned into a salt and used as a fertilizer. Unfortunately, the amount of ammonia that could be separated from coal tar was still insufficient, so if ammonia could be made on a large enough scale, then large-scale manufacture of a fertilizer could be realized.



Figure 8.3.8: British chemist George Fownes, FRS (1815 – 1849).

In 1909 Fritz Haber (Figure 8.3.9) presented a method of ammonia synthesis to BASF. His work in collaboration with Carl Bosch (Figure 8.3.10) resulted in the process known as the Haber-Bosch process in which nitrogen and hydrogen are mixed at high temperature (600 °C) under pressure (200 atm) over an osmium catalyst, (8.3.30).

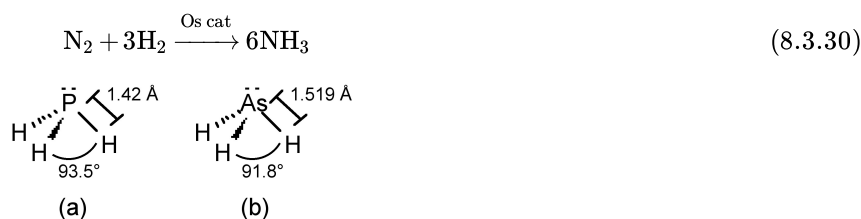


Figure 8.3.9: German chemist Fritz Haber (1868 –1934) who received the Nobel Prize in Chemistry in 1918 for his development for synthesizing ammonia.



Figure 8.3.10: German chemist Carl Bosch (1874 –1940) who received the Nobel Prize in Chemistry in 1931 for his work in high-pressure chemistry.

It is interesting to note that the realization of the Haber-Bosch process required not only high-pressure vessels to be constructed by the steel industry, but also the liquid forms of nitrogen and hydrogen. As it turned out ammonia was a necessary component for enabling the production of liquid nitrogen and hydrogen, and involved a false hypothesis of what caused malaria, which led to a desire to keep drinks cold.

Long before it was understood the real cause of malaria, John Gorrie (Figure 8.3.11), a doctor working in Apalachicola on the Gulf Coast of Florida, was obsessed with finding a cure for malaria. The term *malaria* originated from Medieval Italian: *mala aria* (bad air), and it was associated with swamps and marshlands. Gorrie noticed that malaria was connected to hot humid weather so he began hanging bowl of ice in wards and circulating the air with a fan. However, ice was cut from frozen lakes and rivers in the North East of the US, stored and then shipped all over the world, and Apalachicola was so small that ice was seldom delivered. Gorrie started looking into methods of making ice. It was well known that when a compressed gas expands it takes heat from its surroundings. Gorrie made a steam engine that compressed air in a piston, which when the piston retracted the air cooled. On the next compression stroke the cold air was pushed out across a brine solution (saturated aqueous NaCl) cooling it. When he brought water in contact with the cold brine, it froze creating the first man made ice. On 14 July 1850 Gorrie produced ice for the French Consul to cool the champagne for the celebration of Bastille Day. Just before he died, Gorrie suggested that his (by then) Patented process could be used for cooling food for transport, and it was this application that was used extensively by British merchants to bring meat from Australia to Britain. However, in Germany, Gorrie's invention was more useful for beer.

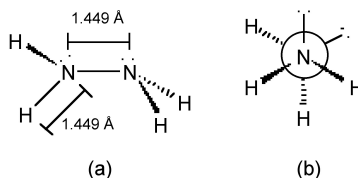


Figure 8.3.11: Portrait of American physician and scientist John Gorrie (1803 –1855) is considered the father of refrigeration and air conditioning.

Whereas the British traditionally brewed beer in which the yeast ferments on the surface (*top fermentation*) at a temperature of 60 – 70 °F, in Germany beer was made using *bottom fermentation*. This style of fermentation requires a temperature just above freezing. Traditionally, cold cellars were used to store the fermenting beer, and it is from here the name lager is derived from the German verb *lagern*: to store. There had been a law in Germany preventing brewing in the summer, but with Gorrie's process the possibility was to be able to brew beer all year. Carl von Linde (Figure 8.3.12) was asked to develop a refrigeration system. He used ammonia instead of air in Gorrie's system, and in 1879 he set up a company to commercialize his ideas. The success of his refrigerator was such that by 1891 there were over 12,000 fridges being used, and more importantly there was now a convenient method of liquefying gases such as hydrogen and nitrogen; both of which were needed for the Haber-Bosch process.

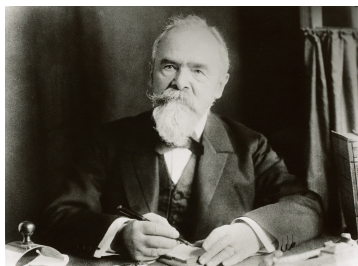


Figure 8.3.12: German engineer Carl Paul Gottfried von Linde (1842 - 1934).

As a consequence of the use of ammonia as a refrigerant, it was possible to prepare ammonia on a large industrial scale. Ammonia prepared by the Haber-Bosch process can be converted to nitric acid by the Ostwald process developed by Wilhelm Ostwald (Figure 8.3.13). Treatment of ammonia with air over a platinum catalyst yields initially nitric oxide, (8.3.31), and subsequently to nitrogen dioxide, (8.3.32), which dissolves in water to give nitric acid, (8.3.33).



Addition of soda (sodium hydroxide, NaOH) to nitric acid results in the formation of sodium nitrate, (8.3.34), which was the same fertilizer produced from the deposits in Chile.





Figure 8.3.13: German chemist Friedrich Wilhelm Ostwald (1853 – 1932) received the Nobel Prize in 1909 for his work on catalysis.

Unfortunately, for the Haber-Bosch and Ostwald processes, an even cheaper form of fertilizer was synthesized around the same time using calcium carbide to prepare calcium cyanamide (CaCN_2), (8.3.35). As a consequence, the Haber-Bosch process was forgotten until the outbreak of the First World War in 1914.



Within weeks of the outbreak Germany realized it had only enough explosives for about a year of conflict. This was because the main source of explosives, sodium nitrate was the same source that gave fertilizer, i.e., Chile. Realizing this, the Royal Navy effectively blockaded the supply lines. If Germany did not find another source of Great War would have been over early in 1916, however, it was remembered that the Haber-Bosch process in combination with the Ostwald processes would allow the synthesis of nitric acid, which when mixed with cotton, made nitrocellulose (Figure 8.3.14), also known as gun cotton, an explosive, (8.3.36).

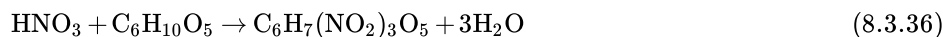


Figure 8.3.14: The structure of nitrocellulose.

As a result of the industrial synthesis of ammonia Germany was able to manufacture sufficient explosives to fight until 11 November 1918, by which time almost 10 million were dead, almost 7 million missing, and over 21 million were wounded (Figure 8.3.15).



Figure 8.3.15: The Douamont Ossuary cemetery and World War I memorial in Verdun, France.

Hydrazine

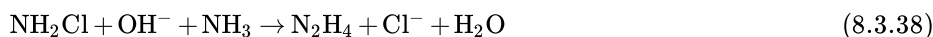
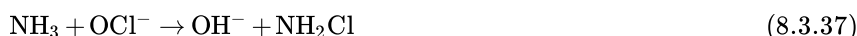
Hydrazine (N_2H_4) is a colorless liquid with an odor similar to ammonia. Hydrazine has physical properties very close to water, with a melting point of 2°C and a boiling point of 114°C . The similarity in its chemistry to water is as a result of strong intermolecular hydrogen bonding.

WARNING

Hydrazine is highly toxic and dangerously unstable, and is usually handled as aqueous solution for safety reasons. Even so, hydrazine hydrate causes severe burns on the skin and eyes. Contact with transition metals, their oxides (e.g., rust), or salts cause catalytic decomposition and possible ignition of evolved hydrogen. Reactions with oxidants are violent.

Synthesis

Hydrazine is manufactured on the industrial scale by the Olin Raschig process using the reaction of a sodium hypochlorite solution with ammonia at 5°C to form chloramine (NH_2Cl) and sodium hydroxide, (8.3.37). The chloramines solution is then reacted with ammonia under pressure at 130°C , (8.3.38). Ammonia is used in a 33 fold excess.



If transition metals are present then decomposition occurs, (8.3.38), and therefore, ethylenediaminetetraacetic acid (EDTA, Figure 8.3.16) is added to complex the transition metal ions. The as produced hydrazine solution can be concentrated by distillation to give a 65% solution. Anhydrous hydrazine is formed by the distillation from NaOH.

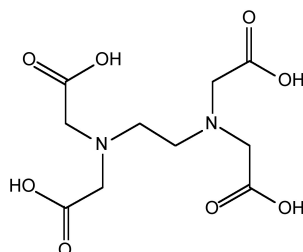
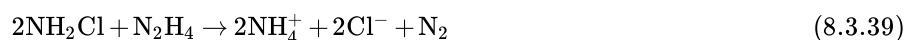
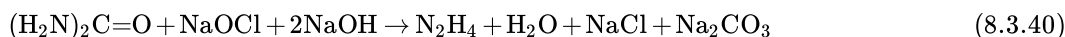


Figure 8.3.16: The structure of ethylenediaminetetraacetic acid (EDTA).

Alternative routes to hydrazine include the oxidation of urea with sodium hypochlorite, (8.3.40), and the reaction of ammonia and hydrogen peroxide, (8.3.41).



Structure

The nitrogen atoms in hydrazine adopt sp^3 hybridization (Figure 8.3.17a), and molecule adopts a *gauche* conformation in the vapor, liquid and solid states (Figure 8.3.17b).

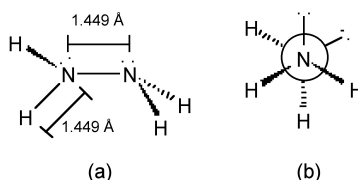
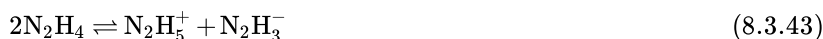


Figure 8.3.17: The structure of hydrazine.

In a similar manner to ammonia, (8.3.42), hydrazine is a self-ionizing, (8.3.43). While there is a wide range of salts of the N_2H_5^+ cation, only the sodium and potassium salts of N_2H_3^- are stable.





Reaction chemistry and uses

Hydrazine is polar, highly ionizing, and forms stable hydrogen bonds, and its resemblance to water is reflected in the formation of aqueous solutions and hydrates. In the solid state the monohydrate is formed, i.e., $\text{N}_2\text{H}_4 \cdot \text{H}_2\text{O}$. In solution hydrazine acts as a base to form the hydrazinium ion, (8.3.44) where $K_b = 8.5 \times 10^{-7}$. The presence of a second Lewis base site means that hydrazine can be protonated twice to form the hydrazonium ion, (8.3.45) where $K_b = 8.9 \times 10^{-16}$. Salts of the cation N_2H_5^+ are stable in water; however, the salts of the dication are less stable.

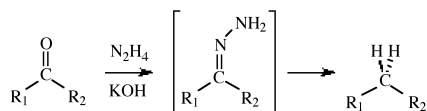
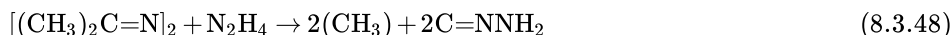
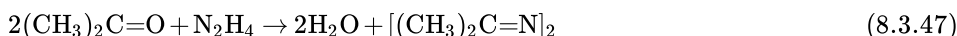


The reaction of hydrazine with oxygen is highly favored, (8.3.46), and the explosive limit is 1.8 – 100 vol%.



Hydrazine is useful in a number of organic reactions for the synthesis of a wide range of compounds used in pharmaceuticals, textile dyes, and in photography, including:

- Hydrazone formation, (8.3.47) and (8.3.48).
- Alkyl-substituted hydrazine synthesis via direct alkylation with alkyl halides.
- Reaction with 2-cyanopyridines to form amide hydrazides, which can be converted using 1,2-diketones into triazines.
- Use in the Wolff-Kishner reduction that transforms the carbonyl group of a ketone or aldehyde into a methylene (or methyl) group via a hydrazone intermediate, (shown below).
- As a building block for the preparation of many heterocyclic compounds via condensation with a range of difunctional electrophiles.
- Cleavage N-alkylated phthalimide derivatives.
- As a convenient reductant because the by-products are typically nitrogen gas and water.



Messerschmitt Me 163 Komet

Designed by Alexander Lippisch (Figure 8.3.18), the Messerschmitt Me 163B Komet (Figure 8.3.19) was the first rocket-powered fighter plane. With a top speed of around 596 mph (Mach 0.83) and a service ceiling of 40,000 ft, the Komet's performance of the Me 163B far exceeded that of contemporary piston engine fighters. However, despite its impressive performance, it was only produced in limited numbers (*ca.* 370 as compared to the 1,430 built of its jet powered compatriot the Me 262) and was not an effective combat airplane.



Figure 8.3.18: German pioneer of aerodynamics Alexander Martin Lippisch (1894 – 1976).



Figure 8.3.19: The Messerschmitt Me 163B-1.

The Komet was powered by the HWK 109-509 *hot engine* (Figure 8.3.20) that used a mixture of a fuel and an oxidizer. The fuel was a mixture of hydrazine hydrate (30%), methanol (57%), and water (13%) that was designated by the code name, *C-Stoff*, that burned with the oxygen-rich exhaust from hydrogen peroxide (*T-Stoff*) used as the oxidizer. The *C-Stoff* was stored in a glass tank on the plane, while the *T-Stoff* was stored in an aluminum container. An oxidizing agent cocktail of CaMnO_4 and/or K_2CrO_4 was added to the *T-Stoff* generating steam and high temperatures, this in turn reacted violently with the *C-Stoff*. The flow of reagents was controlled by two pumps, to regulate the rate of combustion and thereby the amount of thrust. The violent combustion process resulted in the formation of water, carbon dioxide and nitrogen, and a huge amount of heat sending out a superheated stream of steam, nitrogen and air that was drawn in through the hole in the mantle of the engine, thus providing a forward thrust of approximately 3,800 lbf. Because of the potential hazards of mixing the fuels, they were stored at least $\frac{1}{2}$ mile apart, and the plane was washed with water between fueling steps and after missions.

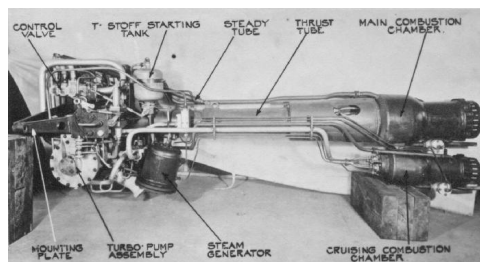


Figure 8.3.20: A photograph taken by Professor A. D. Baxter of the HWK 109-509 *hot engine*.

Phosphine and Arsine

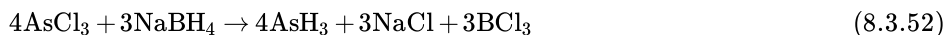
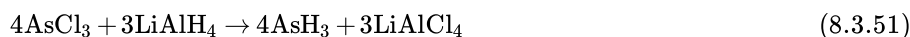
Because of their use in metal organic chemical vapor deposition (MOCVD) of 13-15 (III-V) semiconductor compounds phosphine (PH_3) and arsine (AsH_3) are prepared on an industrial scale.

Synthesis

Phosphine (PH_3) is prepared by the reaction of elemental phosphorus (P_4) with water, (8.3.49). Ultra pure phosphine that is used by the electronics industry is prepared by the thermal disproportionation of phosphorous acid, (8.3.50).



Arsine can be prepared by the reduction of the chloride, (8.3.51) or (8.3.52). The corresponding syntheses can also be used for stibine and bismuthine.



The hydrolysis of calcium phosphide or arsenide can also generate the trihydrides.

Structure

The phosphorus in phosphine adopts sp^3 hybridization, and thus phosphine has an umbrella structure (Figure 8.3.21a) due to the stereochemically active lone pair. The barrier to inversion of the umbrella ($E_a = 155 \text{ kJ/mol}$) is much higher than that in ammonia ($E_a = 24 \text{ kJ/mol}$). Putting this difference in context, ammonia's inversion rate is 10^{11} while that of phosphine is 10^3 . As a consequence it is possible to isolate chiral organophosphines (PRR'R''). Arsine adopts the analogous structure (Figure 8.3.21b).

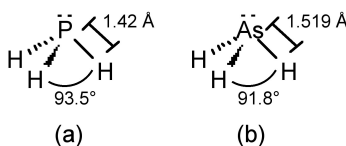
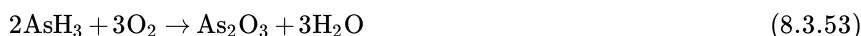


Figure 8.3.21: The structures of (a) phosphine and (b) arsine.

Reactions

Phosphine is only slightly soluble in water (31.2 mg/100 mL) but it is readily soluble in non-polar solvents. Phosphine acts as neither an acid nor a base in water; however, proton exchange proceeds via the phosphonium ion (PH_4^+) in acidic solutions and via PH_2^- at high pH, with equilibrium constants $K_b = 4 \times 10^{-28}$ and $K_a = 41.6 \times 10^{-29}$, respectively.

Arsine has similar solubility in water to that of phosphine (i.e., 70 mg/100 mL), and AsH_3 is generally considered non-basic, but it can be protonated by superacids to give isolable salts of AsH_4^+ . Arsine is readily oxidized in air, (8.3.53).



Arsine will react violently in presence of strong oxidizing agents, such as potassium permanganate, sodium hypochlorite or nitric acid. Arsine decomposes to its constituent elements upon heating to 250 - 300 °C.

Gutzeit test

The Gutzeit test is the characteristic test for arsenic and involves the reaction of arsine with Ag^+ . Arsine is generated by reduction of aqueous arsenic compounds, typically arsenites, with Zn in the presence of H_2SO_4 . The evolved gaseous AsH_3 is then exposed to silver nitrate either as powder or as a solution. With solid AgNO_3 , AsH_3 reacts to produce yellow Ag_4AsNO_3 , while with a solution of AgNO_3 black Ag_3As is formed.

Hazards

Pure phosphine is odorless, but technical grade phosphine has a highly unpleasant odor like garlic or rotting fish, due to the presence of substituted phosphine and diphosphine (P_2H_4). The presence of P_2H_4 also causes spontaneous combustion in air. Phosphine is highly toxic; symptoms include pain in the chest, a sensation of coldness, vertigo, shortness of breath, and at higher concentrations lung damage, convulsions and death. The recommended limit (RL) is 0.3 ppm.

Arsine is a colorless odorless gas that is highly toxic by inhalation. Owing to oxidation by air it is possible to smell a slight, garlic-like scent when arsine is present at about 0.5 ppm. Arsine attacks hemoglobin in the red blood cells, causing them to be destroyed by the body. Further damage is caused to the kidney and liver. Exposure to arsine concentrations of 250 ppm is rapidly fatal: concentrations of 25 – 30 ppm are fatal for 30 min exposure, and concentrations of 10 ppm can be fatal at longer exposure times. Symptoms of poisoning appear after exposure to concentrations of 0.5 ppm and the recommended limit (RL) is as low as 0.05 ppm.

Bibliography

- R. Minkwitz, A. Kornath, W. Sawodny, and H. Härtner, *Z. Anorg. Allg. Chem.*, 1994, **620**, 753.

This page titled 8.3: Hydrides is shared under a CC BY 3.0 license and was authored, remixed, and/or curated by Andrew R. Barron (CNX) via source content that was edited to the style and standards of the LibreTexts platform.

8.4: Oxides and Oxoacids

Oxides of Nitrogen

A summary of the physical properties of the oxides of nitrogen is given in Table 8.4.1.

Table 8.4.1: Physical properties of the oxides of nitrogen.

Oxide	Formula	Mp (°C)	Bp (°C)
Nitrous oxide	N ₂ O	-90.8	-88.5
Nitric oxide	NO	-163.6	-161.8
Dinitrogen trioxide	N ₂ O ₃	-100.6	3.5 (dec.)
Nitrogen dioxide (dinitrogen tetroxide)	NO ₂ /N ₂ O ₄	-11.2 (NO ₂)	21.2 (N ₂ O ₄)
Nitrogen pentoxide	N ₂ O ₅	30	47

Nitrous oxide

Gaseous nitrous oxide (N₂O) is prepared by the careful thermal decomposition of ammonium nitrate (NH₄NO₂), (8.4.1). Nitrous oxide is a linear molecule (Figure 8.4.1a) that is isoelectronic (and isostructural) with carbon dioxide. Despite its use as a power enhancement for automobiles, nitrous oxide is actually not very reactive and a major use is as an aerosol propellant.

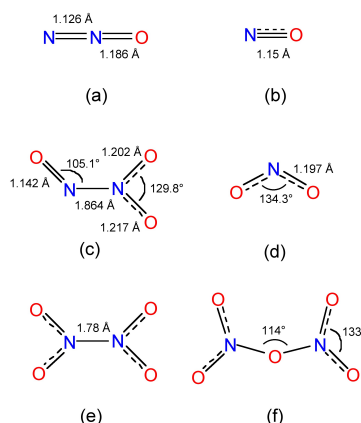


Figure 8.4.1: Structures of (a) nitrous oxide, (b) nitric oxide, (c) dinitrogen trioxide, (d) nitrogen dioxide, (e) nitrogen tetroxide, and (f) nitrogen pentoxide.

Nitrous oxide as an anesthetic drug

Nitrous oxide is known as "laughing gas" due to the euphoric effects of inhaling it, a property that has led to its recreational use as a hallucinogen. However, it is as an anesthetic that it has a legitimate application.

The first use of nitrous oxide as anesthetic drug was when dentist Horace Wells (Figure 8.4.2) with assistance by Gardner Quincy Colton (Figure 8.4.3) and John Mankey Riggs (Figure 8.4.4), demonstrated insensitivity to pain from a dental extraction in December 1844. Wells subsequently treated 12-15 patients, and according to his own record it only failed as an anesthetic in two cases. In spite of these results, the method was not immediately adopted, probably because during his first public demonstration was only partly successful.



Figure 8.4.2: American dentist Horace Wells (1815 - 1848).

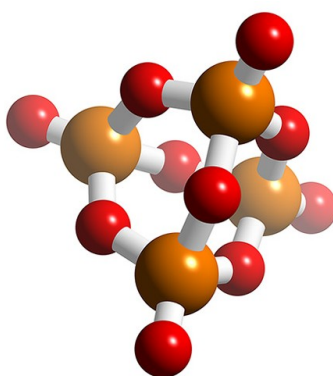


Figure 8.4.3: American showman, lecturer, and former medical student Gardner Quincy Colton (1814 - 1898).

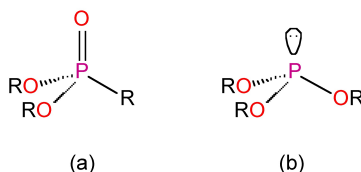


Figure 8.4.4: John Mankey Riggs (1811 - 1885) was the leading authority on periodontal disease in the United States, to the point that periodontal disease was known as *Riggs disease*.

The method did not come into general use until 1863, when Colton successfully used it for more than 25,000 patients. As such, the usage of nitrous oxide rapidly became the preferred anesthetic method in dentistry. Because the gas is mild enough to keep a patient in a conscious and conversational state, and yet in most cases strong enough to suppress the pain caused by dental work, it remains the preferred gas anesthetic in today's dentistry.

Nitrous: the secret to more power.

In motorsports, nitrous oxide (often referred to as *nitrous* or *NOS*) allows the engine to burn more fuel, resulting in a more powerful combustion, and hence greater horsepower. The gas itself is not flammable, but it delivers more oxygen (33%) than atmospheric air (21%) by breaking down at elevated temperatures. When N_2O breaks down during fuel combustion, the decomposition of nitrous is exothermic, contributing to the overall power increase.

Nitrous oxide is stored as a compressed liquid (Figure 8.4.5); the evaporation and expansion of liquid nitrous oxide in the intake manifold causes a large drop in intake charge temperature, resulting in a denser charge, further allowing more air/fuel mixture to enter the cylinder. Nitrous oxide is sometimes injected into (or prior to) the intake manifold, whereas other systems directly inject right before the cylinder (direct port injection) to increase power.

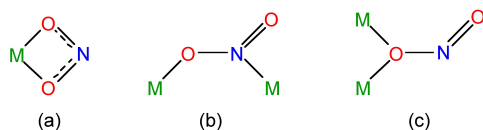


Figure 8.4.5: A typical NOS system for automotive use.

One of the major problems of using nitrous oxide in a reciprocating engine is that it can produce enough power to damage or destroy the engine. Very large power increases are possible, and if the mechanical structure of the engine is not properly reinforced, the engine may be severely damaged or destroyed during this kind of operation.

Automotive-grade liquid nitrous oxide differs slightly from medical-grade nitrous oxide in that a small amount of sulfur is added to prevent substance abuse.

Nitric oxide

Nitric oxide (NO) is formed by the high temperature oxidation of nitrogen, (8.4.2), or the platinum catalyzed oxidation of ammonia at 800 °C, (8.4.3).



Nitric oxide (Figure 8.4.6b) is electronically equivalent to dinitrogen (N_2) plus an electron, and as a consequence it is paramagnetic with one unpaired electron in the π^* orbital (Figure 8.4.6a) results in a bond order of 2.5 rather than the triple bond observed for N_2 (Figure 8.4.6b). The N-O distance of 1.15 Å is intermediate between the triple bond distance in NO^+ (1.06 Å) and the typical double bond distance (ca. 1.20 Å). Furthermore, because of the location of the electron it is easy to oxidize nitric oxide to the nitrosonium ion (NO^+), (8.4.4).

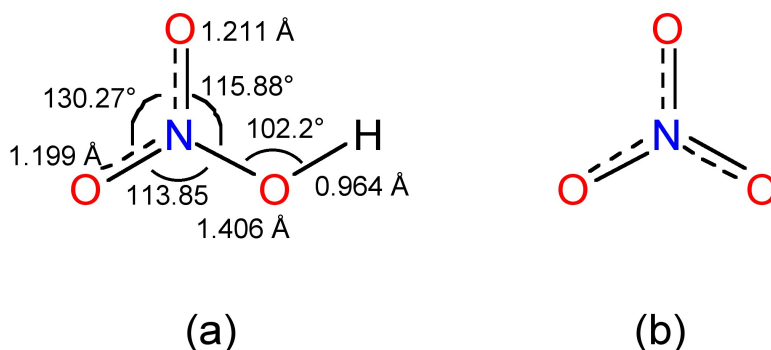


Figure 8.4.6: Molecular orbital diagrams for (a) nitric oxide and (b) dinitrogen.

Nitric oxide is unstable to heat, (8.4.6), and oxidation, (8.4.5). It will also react with halogens to form the nitrosyl halides, XNO .



Dinitrogen trioxide

Dinitrogen trioxide (N_2O_3) is formed from the stoichiometric reaction between NO and O_2 or NO and N_2O_4 . Dinitrogen trioxide has an intense blue color in the liquid phase and a pale blue color in the solid state. Thermal dissociation of N_2O_3 , (8.4.7), occurs above -30 °C, and some self-ionization of the pure liquid is observed, (8.4.8). The asymmetric structure of N_2O_3 (Figure 8.4.1c) results in a polar molecule (Figure 8.4.7).

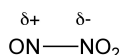


Figure 8.4.7: The polarization of the N-N bond in dinitrogen trioxide.

Nitrogen dioxide (and tetroxide)

Formed from the oxidation of nitric oxide, (8.4.9), brown nitrogen dioxide is actually in equilibrium with its colorless dimeric form, nitrogen tetroxide (N_2O_4), (8.4.10).



Nitrogen dioxide (Figure 8.4.1d) is electronically equivalent to the nitrate anion (NO_2^-) less one electron, and as such it is paramagnetic with one unpaired electron. The location of the unpaired electron in a nitrogen sp^2 orbital, and a consequently it forms a dimer through a N-N bond (Figure 8.4.1e). Furthermore, it is easy to oxidize nitrogen dioxide to the nitronium ion (NO_2^+), (8.4.11).



Nitrogen dioxide dissolves in water to form a mixture of nitric and nitrous acids, (8.4.12). Nitrogen dioxide acts as an oxidizing agent with the formation of nitrate anion, (8.4.13).



The most common structural form of N_2O_4 (Figure 8.4.1e) is planar with a long N-N bond (1.78 Å) that is significantly longer than observed in hydrazine (1.47 Å). Rationalization of this structural effect is obtained from a consideration of the molecular orbitals, which show that the electrons in the σ -bond are actually delocalized over the whole molecule. The rotation about the N-N bond is 9.6 kJ/mol.

Nitrogen pentoxide

The dehydration of nitric acid, with P_2O_5 , yields nitrogen pentoxide, (8.4.14), which is an unstable solid at room temperature (Table 8.4.1). In the solid state nitrogen pentoxide is actually nitronium nitrate ($\text{NO}_2^+\text{NO}_3^-$), however, in the vapor phase it exists as a molecular species (Figure 8.4.1f) with a bent N-O-N unit. Nitrogen pentoxide is a very powerful nitrating and oxidation agent.



Nitrogen oxides as precursors to smog and acid rain

Nitrogen oxides (NO_x) emissions are estimated to be in the range of 25 - 100 megatonnes of nitrogen per year. Natural sources are thought to make up approximately $\frac{1}{3}$ of the total. The generations of NO_x (primarily a mixture of NO_2 and NO) is the main source of smog and a significant contribution to atmospheric pollution; however, NO_x is also responsible for much of the acidity in acid rain.

Atmospheric reactions leading to acid rain

In the dry atmosphere, nitric oxide reacts is oxidized rapidly in sunlight by ozone, (8.4.15). The nitrogen dioxide reacts with the hydroxide radical, formed by the photochemical decomposition of ozone, (8.4.16) and (8.4.17), in the presence of a non-reactive gas molecule such as nitrogen to form nitric acid vapor, (8.4.18). The conversion rate for NO_x to HNO_3 is approximately ten times faster than the equivalent reaction for sulfur dioxide. For example, conversion is essentially complete for a NO_x plume by the time it transverses the North Sea from the UK to Scandinavia.



At night, conversion takes place via the formation of a nitrate radical, (8.4.19), which subsequently photochemically unstable under sunlight forming nitrogen pentoxide, (8.4.20), that reacts with water on the surface of aerosol particles to form nitric acid, (8.4.21).





Both NO and NO₂ are only slightly soluble in water and it is therefore more probable that the nitric acid content of rain is more likely due to the dissolution of nitric acid vapor into raindrops, (8.4.22), rather than a separate reaction.



Oxoacids of Nitrogen

Nitrous acid

In the gas phase nitrous acid can be made by the following reaction:



The gas phase structure as determined by IR spectroscopy is shown in Figure 8.4.8a, in which the nitrogen is planar with *sp*² hybridization.



Figure 8.4.8

In basic aqueous solution the same reaction results in the formation of the nitrite ion, (8.4.24), which can be precipitated as the Ba²⁺ salt. After separation the addition to sulfuric acid yields a solution of nitrous acid. However, it is not possible to concentrate by heating since decomposition occurs, (8.4.25).



Nitrous acid is a fairly weak acid in water (pK = 5.22); however, many salts are known of the nitrite ion, NO₂[−] (Figure 8.4.8b). Complexes of the nitrite ion can be monodentate with bonding via nitrogen (nitro) or an oxygen (nitrito). Both isomers can be isolated in the case of an inert metal, i.e., substitutionally inert *d*⁶ octahedral complexes (Figure 8.4.9). Bidentate and bridging modes of coordination are also known for the nitrite anion (Figure 8.4.10).

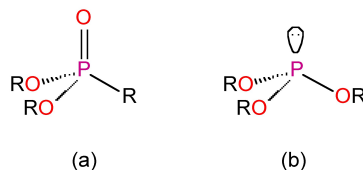


Figure 8.4.9: Structures of (a) orange nitro and (b) pink nitrito isomers of [Co^{III}(NH₃)₅(NO₂)]²⁺.

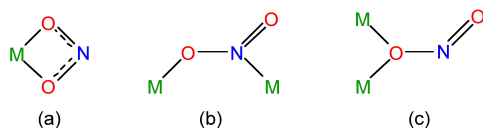
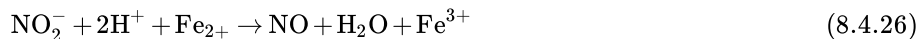


Figure 8.4.10: Bidentate (a) and bridging (b and c) modes of coordination of the nitrite anion.

Nitrite can act as either an oxidizing agent, (8.4.26), or a reducing agent, (8.4.27).



The most important use of nitrous acid is in the diazotization reactions in which nitrous acid is generated by acidifying nitrite solution.

Nitric acid

Nitric acid (HNO₃), also known as *aqua fortis* and *spirit of nitre*, is made by the dissolution of nitrogen dioxide in water, (8.4.28). Nitric acid can be concentrated by distillation from concentrated sulfuric acid.



The structure of HNO_3 in the gas phase is planar at the sp^2 nitrogen (Figure 8.4.11a).

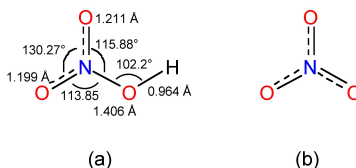
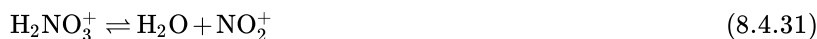


Figure 8.4.11: The structures of (a) nitric acid and (b) the nitrate anion.

Pure 100% nitric acid is a very corrosive liquid that is strongly acidic and protonates and dissolves organic species. In the liquid phase it is slightly dissociated, (8.4.29). It is also a powerful oxidizing agent, converting non-metal elements to either the oxide or oxoacid. In contrast with metals it forms either salts or complexes in which the metal is in its highest oxidation state. It is unstable and decomposes upon heating or photolysis.



The pure acid has the highest self ionization of pure liquid acids, (8.4.30). However, the loss of water results, (8.4.31), such that the overall reaction can be described by (8.4.32).



The common concentration of nitric acid is 70%. While the pure acid is colorless, samples often take on a yellow color due to the photochemical decomposition of nitric acid to give brown NO_2 .



Note

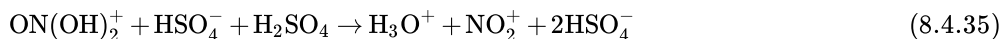
The term the “acid test” is derived from the medieval practice of debasing of gold and silver currencies (often by the Monarchs who issued them) by debasing with copper. With ducats (Milan), livres (France), florins (Florence), maravedies (Spain) and bezants (Constantinople) in widespread use, and each with a nominal gold or silver content, it was important for a merchant to be able verify the worth of any particular coin. If a drop of dilute nitric acid was placed onto a silver coin adulterated with copper, it turned green, due to the formation of copper(II) nitrate. Conversely, if a gold coin reacted in any way with the nitric acid it was not pure. In both cases the coins failed the “acid test”.

Aqua regia (so called because it dissolves gold) is a mixture of 70% nitric acid and hydrochloric acid in a 1:3 ratio. *Aqua regia* is a very powerful oxidizing agent (it contains Cl_2) and stabilizes some metals as their chloro complexes (Table 8.4.2). If HF is added in place of HCl , tantalum may be dissolved with the formation of $[\text{TaF}_2]^-$.

Table 8.4.2: Metal chloride salts formed by the dissolution of metals in *aqua regia*.

Metal	Chloride salt formed
Au	$[\text{AuCl}_4]^-$
Pt	$[\text{PtCl}_6]^{2-}$

Fuming nitric acid (100% nitric) is exceedingly corrosive and should not be used. In 100% sulfuric acid, nitric acid acts as a base and gets protonated, (8.4.34) and (8.4.35), and acts as a powerful nitrating agent.



In water dilute nitric acid is fully ionized, (8.4.36).



The nitrate ion is planar (Figure 8.4.11b) and forms many salts and complexes. The nitrate anion is most commonly a monodentate ligand, but can also be a bidentate ligand (Figure 8.4.12a) or a bridging ligand (Figure 8.4.12b and 12c).

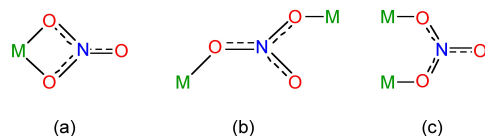


Figure 8.4.12: Coordination modes of the nitrate anion.

Phosphorous Oxides

Phosphorous trioxide

The stoichiometric oxidation of white phosphorus yields phosphorous trioxide, (8.4.37).



Several structural forms of phosphorous trioxide are known, but P_4O_6 is a stable molecule structure (Figure 8.4.13), while the rest are polymers.

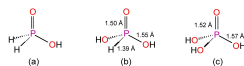


Figure 8.4.13: The structure of P_4O_6 . Phosphorus atoms are represented by the large spheres, and oxygen atoms by the small spheres (Copyright: Karl Harrison, 2005).

Phosphorous pentoxide

The reaction of white phosphorus with excess oxygen (or the oxidation of phosphorous trioxide) yields phosphorous pentoxide, (8.4.38).



The structure of hexagonal phosphorous pentoxide is actually that of the dimeric form, P_4O_{10} , and is based upon the structure of P_4O_6 , but with $\text{P}=\text{O}$ units instead of lone pairs (Figure 8.4.14). The structure is maintained in the vapor phase; however, other crystalline and glassy forms comprise of a sheet-like structure (Figure 8.4.15).

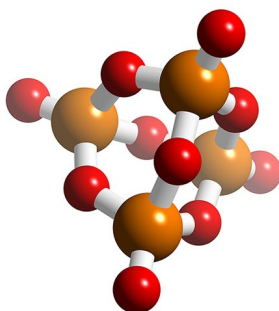


Figure 8.4.14: The structure of hexagonal P_4O_{10} . Phosphorus atoms are represented by the large spheres, and oxygen atoms by the small spheres (Copyright: Karl Harrison, 2005).

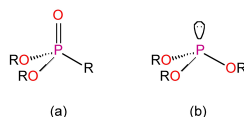


Figure 8.4.15: The structure of a sheet in glassy P_4O_{10} .

Phosphorous pentoxide is an excellent drying agent below 100 °C. It reacts with water to form various phosphoric acids, and it will extract water from other 'drying agents', e.g., (8.4.39) and (8.4.40). Phosphorous pentoxide will dehydrate amides to give nitriles, (8.4.41).



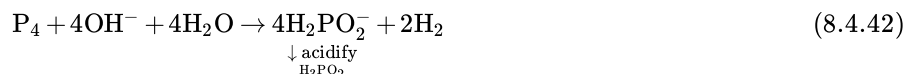


Oxoacids of Phosphorus

Phosphorous pentoxide (P_2O_5) is an excellent drying agent, and its action is a result of the formation of a range of oxoacids.

Hypophosphorous acid

Hypophosphorous acid, H_3PO_2 , is easily prepared pure by the reaction of white phosphorous with base, followed by acidification, (8.4.42). The pure acid is a solid (Mp = 27 °C) and very soluble in water.



The structure of H_3PO_2 is determined by X-ray crystallography to be tetrahedral with two hydride ligands and a hydroxide (Figure 8.4.16a). The presence of two hydrides is confirmed by NMR spectroscopy. The ^1H NMR resonance shows an OH line and a doublet from the P-H with a large one-bond coupling constant to the ^{31}P nucleus. The non-decoupled ^{31}P NMR spectrum shows a triplet ($\delta = 13$ ppm, $JP\text{-H} = 530$ Hz) due to the two hydrides.

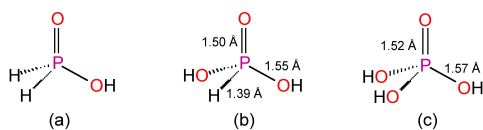
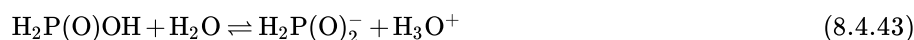


Figure 8.4.16: Oxoacids of phosphorous: (a) hypophosphorous acid, (b), phosphorous acid, and (c) phosphoric acid.

In water hypophosphorous acid is a monobasic acid ($\text{pK} = 1.2$), (8.4.43), and it forms a wide range of salts. It is also a powerful reducing agent, but its reaction kinetics is slow.



Phosphorous acid

The reaction of P_4O_6 or PCl_3 with water yields phosphorous acid, H_3PO_3 ; which like hypophosphorous acid is a solid (Mp = 70.1 °C) and very soluble in water. The structure is shown by X-ray crystallography to be comprised of a tetrahedral phosphorus with one hydride and two hydroxides (Figure 8.4.16b). ^{31}P NMR spectroscopy demonstrates the presence of a single hydride by the presence of a doublet as a consequence of the phosphorous center being split by a single hydride ($\delta = 4$ ppm, $JP\text{-H} = 700$ Hz). The ^1H NMR spectrum shows a doublet for the hydride and a single resonance of twice the intensity for the hydroxide.

As expected, in water phosphorous acid is dibasic, (8.4.44). The acid (and the anions) are strong reducing agents, yielding phosphoric acid. They actually react very slowly, and it is thought that this may be due to the reaction being in the tautomeric form, P(OH)_3 . Although this has not been isolated, the trialkyl derivatives exist in both forms, i.e., esters of phosphoric acids (Figure 8.4.17a) and trialkyl phosphates (Figure 8.4.17b).

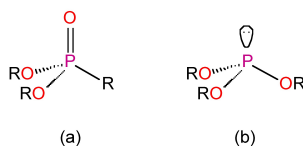
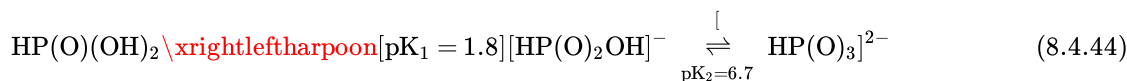


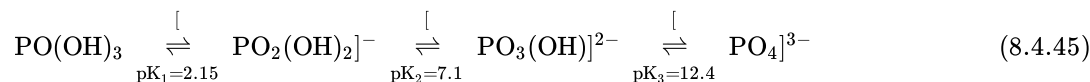
Figure 8.4.17: Structures of two tautomeric forms; (a) an ester of phosphoric acid and (b) a trialkyl phosphate.

Ortho phosphoric acid

Orthophosphoric acid (H_3PO_4) is the most common oxoacid of phosphorus (Figure c). The term acid phosphoric acid is commonly used. It is made from the reaction of phosphates with sulfuric acid (H_2SO_4), or from the hydrolysis of P_4O_{10} . The pure acid is a

colorless crystalline solid (Mp = 42.35 °C) with extensive hydrogen bonding. The inter-phosphoric acid hydrogen bonding is partially maintained in aqueous solutions above 50% solutions.

Phosphoric acid is very stable and shows no oxidation chemistry below 350 °C. As expected, phosphoric acid is tribasic, (8.4.45). The anions H_2PO_4^- and HPO_4^{2-} have particular names, dihydrogen phosphate and monohydrogen phosphate, respectively.

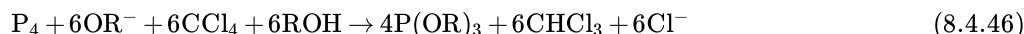


Many salts of are known for all three anions; those with phosphate (PO_4^{2-}) are often insoluble in water. Many coordination complexes are known, especially with M^{3+} and M^{4+} ions.

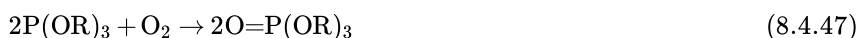
Phosphorous esters

The alkyl and aryl homologs of phosphoric acid (i.e., the phosphate triester $\text{O}=\text{P}(\text{OR})_3$) are prepared by the reaction of P_4O_{10} with the appropriate alcohol. The triesters are good solvents and Lewis basic ligands with coordination via the oxide moiety. The diesters and monoesters can also be made, and they are important in biochemical processes.

Phosphite triesters, $\text{P}(\text{OR})_3$, may be made by the reaction of PCl_3 with alcohols or phenols in the presence of an organic base as the acceptor for the HCl formed. Alternatively, they can be prepared directly from white phosphorous, (8.4.46).



Phosphite triesters are readily oxidized to the appropriate phosphate triester, (8.4.47). They also react with alkyl halides to form the dialkyl phosphonate via the Michaelis-Arbusov reaction (8.4.48).



Polyphosphates

Polyphosphates contain the PO_4 unit, and the simplest example (pyrophosphate or diphosphate, (Figure 8.4.18a)) can be considered as condensation products of monohydrogen phosphate, (8.4.49). Longer chains can be formed, e.g., the triphosphate $\text{P}_3\text{O}_{10}^{5-}$ (Figure 8.4.18b). The formation and reverse (hydrolysis) reaction are slow, but are readily catalyzed, e.g., by enzymes.

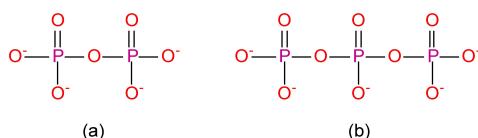
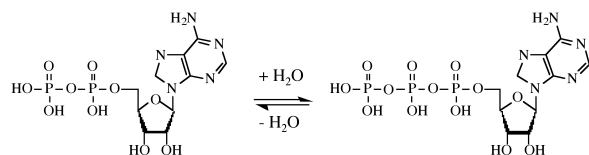


Figure 8.4.18: The structures of the (a) diphosphate and (b) triphosphate anions.

The monoesters of the diphosphate and triphosphate are very important in biological processes. In particular the conversion of the triphosphate ATP (adenosine triphosphate) to the diphosphate ADP (adenosine diphosphate) by the transfer of a phosphate group is important in the energetics of biological reactions.



Cyclic polyphosphates

Also known as meta phosphates, cyclic phosphates are also made from fused PO_4 units. The simplest, $\text{P}_3\text{O}_9^{3-}$, is shown in Figure 8.4.19. Slow addition of water to P_4O_{10} results in the formation of the tetrameric polyphosphate, $\text{P}_4\text{O}_{12}^{4-}$ (Figure 8.4.20), which is known as *calgon* due to its ability to complex Ca^{2+} as well as other metals.

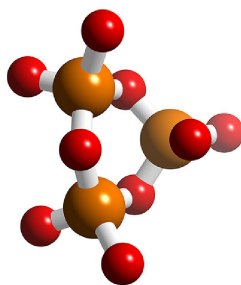


Figure 8.4.19: The structure of $\text{P}_3\text{O}_9^{3-}$. Phosphorus atoms are represented by the large spheres, and oxygen atoms by the small spheres (Copyright: Karl Harrison, 2005).

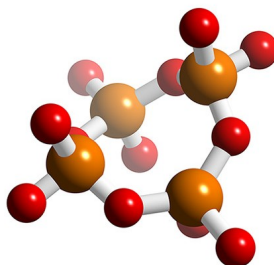


Figure 8.4.20: The structure of $\text{P}_4\text{O}_{12}^{4-}$ *calgon*. Phosphorus atoms are represented by the large spheres, and oxygen atoms by the small spheres (Copyright: Karl Harrison, 2005).

This page titled [8.4: Oxides and Oxoacids](#) is shared under a [CC BY 3.0](#) license and was authored, remixed, and/or curated by [Andrew R. Barron \(CNX\)](#) via [source content](#) that was edited to the style and standards of the LibreTexts platform.

8.5: Halides of Phosphorous

Phosphorous trihalides

Phosphorous trihalides, PX_3 , are produced from the direct reaction of phosphorous with the appropriate halogen, (8.5.1). The fluoride is readily made from the halide exchange reaction of PCl_3 with fluoride salts, (8.5.2). Mixed trihalides are formed by halide exchange, (8.5.3).



A summary of the physical properties of the phosphorous trihalides is given in Table 8.5.1. All the compounds have a pyramidal structure in the vapor phase and in solution.

Table 8.5.1: Selected physical properties of the phosphorous trihalides.

Compound	Mp (°C)	Bp (°C)	P-X (Å)	X-P-X (°)
PF ₃	-151.5	-101.8	1.56	96.3
PCl ₃	-93.6	76.1	2.04	100
PBr ₃	-41.5	173.2	2.22	101
PI ₃	61.2	200 (dec.)	2.43	102

The phosphorous trihalides hydrolyze to phosphoric acid, (8.5.4), and undergo alcoholysis to form the trialkyl phosphite derivative, (8.5.5). Phosphorous trifluoride is only slowly hydrolyzed by water, but reacts readily with alkaline solutions. In contrast, phosphorus triiodide is an unstable red solid that reacts violently with water. Phosphorous trichloride in particular is an excellent synthon for most trialkyl phosphines, (8.5.6).



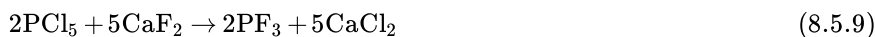
As with other P(III) compounds such as trialkyl phosphines, phosphorous trihalides can be oxidized to the analogous phosphene oxide, e.g., (8.5.7).



Phosphorous trihalides form Lewis acid-base complexes with main group metals, but the bonding to d^n ($n \neq 0$) transition metals occurs in the same manner to that of trialkyl phosphine, i.e., with $d\pi$ - $p\pi$ back donation. In fact one of the first examples of complexation of phosphorous to a low oxidation metal was the formation of PF_3 complexes with Fe-porphyrin.

Phosphorous pentahalides

The reaction of white phosphorous with excess halogen yields the pentahalides, (8.5.8). However, the pentafluoride is best prepared by halide exchange, (8.5.9).



The pentaiodide is unknown, however, selected physical properties are given for the others in Table 8.5.2.

Table 8.5.2: Selected physical properties of phosphorous pentahalides.

Compound	Mp (°C)	Bp (°C)
PF ₅	-93.78	-84.5

PCl ₅	166.8	160 (subl.)
PBr ₅	100	106.0

The structures of the phosphorous pentahalides are all trigonal bipyramidal in the gas phase (Figure 8.5.1). Phosphorous pentafluoride maintains the trigonal bipyramidal structure in solid state, but the chloride and bromide are ionic solids, [PCl₄]⁺ [PCl₆]⁻ and [PBr₄]Br (Figure 8.5.2), respectively. The tetrahedral [PCl₄]⁺ ion is also formed with the reaction of PCl₅ with other chloride ion acceptors, (8.5.10) and (8.5.11).

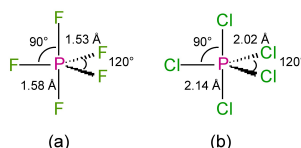


Figure 8.5.1: The structures of (a) PF₅ and (b) PCl₅.

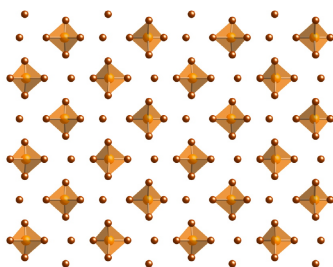


Figure 8.5.2: The crystal structure of phosphorous pentabromide.

All of the pentahalides undergo thermal decomposition, (8.5.12).



Careful hydrolysis of the pentahalides yields the oxide of the appropriate trihalide, (8.5.13), while excess hydrolysis yields phosphoric acid, (8.5.14).



This page titled [8.5: Halides of Phosphorous](#) is shared under a [CC BY 3.0](#) license and was authored, remixed, and/or curated by [Andrew R. Barron \(CNX\)](#) via [source content](#) that was edited to the style and standards of the LibreTexts platform.

CHAPTER OVERVIEW

9: Group 16

- 9.1: The Group 16 Elements- The Chalcogens
- 9.2: Ozone
- 9.3: Water - The Fuel for the Medieval Industrial Revolution
- 9.4: Hydrogen Peroxide
- 9.5: Hydrogen Peroxide Providing a Lift for 007
- 9.6: Comparison of Sulfur to Oxygen
- 9.7: Chalcogenide Hydrides
- 9.8: Oxides and Oxyacids of Sulfur
- 9.9: Sulfur Halides

Thumbnail: A sample of sulfur a member of the oxygen group of elements. (Public Domain; [Ben Mills](#)).

This page titled [9: Group 16](#) is shared under a [CC BY 3.0](#) license and was authored, remixed, and/or curated by [Andrew R. Barron \(CNX\)](#) via [source content](#) that was edited to the style and standards of the LibreTexts platform.

9.1: The Group 16 Elements- The Chalcogens

The elements

The Group 16 elements have a particular name chalcogenes. Table 1 lists the derivation of the names of the halogens.

Table 9.1.1: Derivation of the names of each of the Group 16(VI) elements.

Element	Symbol	Name
Oxygen	O	Greek <i>oxys</i> (<i>sharp</i> , from the taste of acids) and <i>genēs</i> (producer)
Sulfur (sulphur)	S	From the Latin <i>sulphurium</i>
Selenium	Se	Greek <i>selene</i> meaning <i>Moon</i>
Tellurium	Te	Latin <i>tellus</i> meaning <i>earth</i>
Polonium	Po	Named after Poland, Latin <i>Polonia</i>

Note

In Latin, the word is variously written *sulpur*, *sulphur*, and *sulfur*. It is an original Latin name and not a classical Greek loan, so the *ph* variant does not denote the Greek letter ϕ . Sulfur in Greek is *thion*, whence comes the prefix *thio-* to denote a sulfur derivative, e.g., a thioketone, $R_2C=S$. The simplification of the Latin words *p* or *ph* to an *f* appears to have taken place towards the end of the classical period. The element has traditionally been spelled sulphur in the United Kingdom, India, Malaysia, South Africa, Australia, Ireland, and Canada, but sulfur in the United States. IUPAC adopted the spelling “sulfur” in 1990, as did the Royal Society of Chemistry Nomenclature Committee in 1992.

Discovery

Oxygen

The 2nd century BC Greek writer, Philo of Byzantium, observed that inverting a jar over a burning candle and surrounding the jar's neck with water resulted in some water rising into the neck. He incorrectly ascribed this to the idea that part of the air in the vessel were converted into the element *fire* and thus were able to escape through pores in the glass. Much later Leonardo da Vinci (Figure 9.1.1) suggested that this effect was actually due to a portion of air being consumed during combustion.

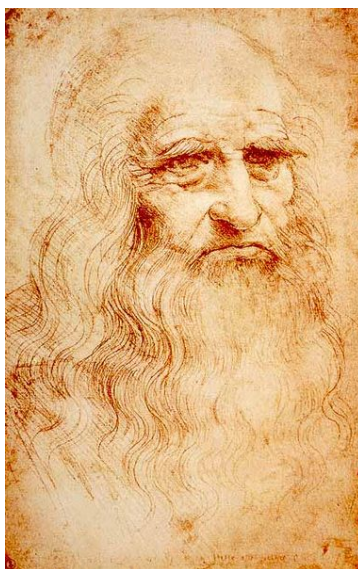


Figure 9.1.1: Italian painter, sculptor, architect, musician, scientist, mathematician, engineer, inventor, anatomist, geologist, cartographer, botanist and writer Leonardo di ser Piero da Vinci (1452 - 1519).

By the late 17th century, Robert Boyle (Figure 9.1.2) showed that air is necessary for combustion. His work was expanded by English chemist John Mayow (Figure 9.1.3) by showing that fire requires only a part of air that he called *spiritus nitroaereus* or just *nitroaereus*.



Figure 9.1.2: British natural philosopher, chemist, physicist, and inventor Robert Boyle (1627 - 1691).



Figure 9.1.3: English chemist, physician, and physiologist John Mayow FRS (1641–1679).

The reactive nature of nitroaereus was implied by Mayow from his observation that antimony (Sb) increased in weight when heated in air. He also suggested that the lungs separate nitroaereus from air and pass it into the blood and that animal heat and muscle movement result from the reaction of nitroaereus with certain substances in the body; both concepts that were proven to be correct.

Robert Hooke (Figure 9.1.4), Ole Borch (Figure 9.1.5), Mikhail Lomonosov (Figure 9.1.6), and Pierre Bayen (Figure 9.1.7) all produced oxygen in experiments in the 17th and the 18th century but none of them recognized it as an element, probably since the prevalence at that time of the phlogiston, and their attempts to fit their experimental observations to that theory.



Figure 9.1.4: Portrait of English natural philosopher, architect Robert Hooke FRS (1635 - 1703).



Figure 9.1.5: Danish scientist, physician, grammarian, and poet Ole Borch (1626 - 1690).



Figure 9.1.6: Russian scientist and writer Mikhail Vasilyevich Lomonosov (1711 - 1765).



Figure 9.1.7: French chemist and pharmacist Pierre Bayen (1725 - 1798).

Note

The phlogiston theory was postulated in 1667 by the German alchemist J. J. Becher, and modified in 1731 by the chemist Georg Ernst Stahl. Phlogiston theory stated that all combustible materials were made of two parts. One part, called *phlogiston*, was given off when the substance containing it was burned, while the *dephlogisticated* component was thought to be its true form, or *calx*. Highly combustible materials that leave little residue (e.g., wood) were thought to mostly comprise of phlogiston, while non-combustible substances that corrode (e.g., iron) contained very little phlogiston. Air did not play a role in phlogiston theory, instead, it was based on observations of what happens when something burns, that most common objects appear to become lighter and seem to lose something in the process. However, one observation that overturned phlogiston theory was that metals, gain weight in rusting when they were supposedly losing phlogiston!

Oxygen was first discovered by Carl Wilhelm Scheele (Figure 9.1.9) by heating mercuric oxide (HgO). Scheele called the gas *fire air* because it was the only known supporter of combustion. He wrote an account of this discovery in a manuscript (*Treatise on Air and Fire*) submitted in 1775. Unfortunately for Scheele his work was not published until 1777. In August 1774, an experiment conducted by Joseph Priestley (Figure 9.1.9) sunlight on mercuric oxide (HgO) inside a glass tube, which liberated a gas he named *dephlogisticated air*. Priestley noted that candles burned brighter in this gas. He even went as far as breathing the gas himself, after which he wrote: "The feeling of it to my lungs was not sensibly different from that of common air, but I fancied that my breast felt peculiarly light and easy for some time afterwards." Priestley published his findings in 1775. Because he published his findings first, Priestley is usually given credit for the discovery of what became known as oxygen.



Carl Wilhelm Scheele.

Figure 9.1.8: Swedish chemist Carl Wilhelm Scheele (1742 – 1786). Isaac Asimov called him "hard-luck Scheele" because he made a number of chemical discoveries before others who are generally given the credit.



Figure 9.1.9: Portrait (by Ellen Sharples) of British clergyman natural philosopher, educator, and political theorist Joseph Priestley (1733 - 1804).

Interestingly, Lavoisier (Figure 9.1.10) claimed to have discovered this new substance independently. However, Priestley visited Lavoisier in October 1774 and told him about his experiment and how he liberated the new gas. Furthermore, Scheele also posted a letter to Lavoisier on September 30, 1774 that described his own discovery. Lavoisier never acknowledged receiving it, however, a copy of the letter was found in Scheele's belongings after his death.



Figure 9.1.10: Line engraving (by Louis Jean Desire Delaistre) of the French chemist and biologist Antoine-Laurent de Lavoisier (1743 - 1794) often referred to as the *father of modern chemistry* due to his extensive contributions.

Raoul Pictet (figure 11) showed that by the evaporation of liquid sulfur dioxide (SO_2), carbon dioxide could be liquefied, which in turn was evaporated to cool oxygen gas enough to liquefy it. Pictet reported his results on December 22, 1877. Two days later, Louis Cailletet (Figure 9.1.12) announced his own method of liquefying oxygen. In both cases only a few drops could be produced, making analysis difficult. In 1891 James Dewar (Figure 9.1.13) was able to produce enough liquid oxygen to study. However, it was the process developed independently by Carl von Linde (Figure 9.1.14) and William Hampson (1854 - 1926).

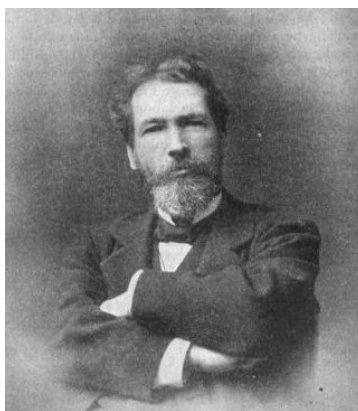


Figure 9.1.11: Swiss chemist and physicist Raoul Pierre Pictet (1846 - 1929).

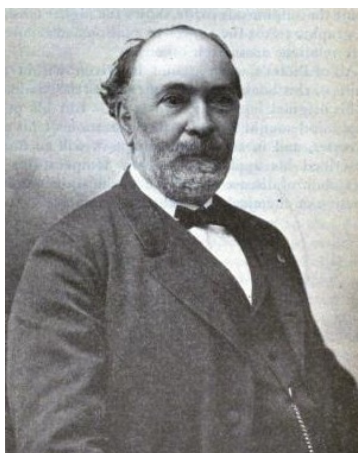


Figure 9.1.12: French physicist Louis Paul Cailletet (1832 - 1913).



Figure 9.1.13: Scottish chemist and physicist Sir James Dewar FRS (1842 - 1923).

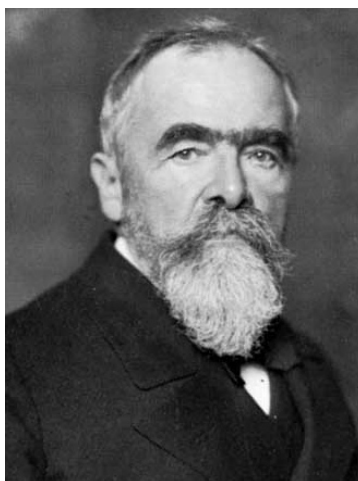


Figure 9.1.14: German engineer Carl Paul Gottfried von Linde (1842 - 1934).

Sulfur

Sulfur was known in ancient times and is referred to in the Bible. English translations of the Bible commonly referred to burning sulfur as *brimstone*, giving rise to the name of *fire-and-brimstone* sermons, in which listeners are reminded of the fate of eternal damnation that await the unbelieving and unrepentant. It is from this part of the Bible that Hell is implied to *smell of sulfur* (likely due to its association with volcanic activity). Sulfur ointments were used in ancient Egypt, while it was used for fumigation in Greece. A natural form of sulfur known as *shilihuang* was known in China since the 6th century BC. However, it was not until 1777 that Lavoisier (Figure 9.1.10) convinced the scientific community that sulfur was an element and not a compound.

Selenium

The element was discovered in 1817 by Berzelius (Figure 9.1.15), who found the element associated with tellurium. It was discovered as a byproduct of sulfuric acid production.



Figure 9.1.15: Swedish chemist Jöns Jacob Berzelius (1779 - 1848).

Tellurium

Tellurium was discovered in the 18th century in gold ore from the mines in Zlatna, Transylvania. In 1782 Müller von Reichenstein (Figure 9.1.16), the Hungarian chief inspector of mines in Transylvania, concluded that the ore was bismuth sulfide. However, the following year, he reported that this was erroneous and that the ore contained mostly gold and an unknown metal very similar to antimony. After three years of work Müller determined the specific gravity of the mineral and noted the radish-like smell of the white smoke evolved when the new metal was heated. Nevertheless, he was not able to identify this metal and gave it the names *aurum paradoxium* and *metallum problematicum*, as it did not show the properties predicted for the expected antimony.



Figure 9.1.16: A stamp showing Hungarian mineralogist Franz-Joseph Müller von Reichenstein (1742 - 1825).

In 1789 Kitaibel (Figure 9.1.17) also discovered the element independently in an ore from Deutsch-Pilsen which had been regarded as *argentiferous molybdenite*, but later he gave the credit to Müller. In 1798, the name was chosen by Klaproth (Figure 9.1.18) who earlier isolated it from the mineral calaverite.



Figure 9.1.17: Hungarian botanist and chemist Pál Kitaibel (1757 - 1817).



Figure 9.1.18: Figure. German chemist Martin Heinrich Klaproth (1743 –1817).

Polonium

Temporarily called *radium F*, polonium was discovered by Marie Curie and her husband Pierre Curie (Figure 9.1.19) in 1898, but it was later named after Marie Curie's native land of Poland. At the time Poland was not an independent country, but partitioned under Russian, Prussian, and Austrian. It was Curie's hope that naming the element after her native land would publicize its lack of independence. Polonium was the first chemical element named to highlight a political controversy.

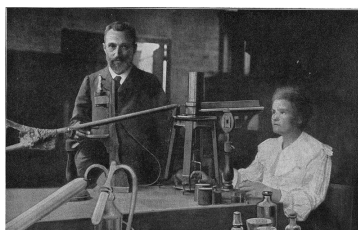


Figure 9.1.19: Pierre (1859 - 1906) and Marie Skłodowska-Curie (1867 - 1934) in their Paris laboratory.

Abundance

The abundance of the chalcogenes is given in Table 9.1.2.

Table 9.1.2: Abundance of Group 16 elements.

Element	Terrestrial abundance (ppm)
O	47×10^4 (Earth's crust), constituent of water, 21×10^4 (atmosphere)
S	260 (Earth's crust), 870 (sea water), 10^{-3} (atmosphere)
Se	0.05 (Earth's crust), 5 (soil), 0.2×10^{-3} (sea water)
Te	5×10^{-3} (Earth's crust), 0.03 (soil), 0.15×10^{-6} (sea water)
Po	Trace (Earth's crust)

Isotopes

The naturally abundant isotopes of the Group 16 elements are listed in Table 9.1.3. All of the isotopes of polonium are radioactive.

Table 9.1.3: Abundance of the non-synthetic isotopes of the Group 16 elements.

Isotope	Natural abundance (%)
Oxygen-16	99.76
Oxygen-17	0.039
Oxygen-18	0.201
Sulfur-32	95.02
Sulfur-33	0.75
Sulfur-34	4.21
Sulfur-36	0.02
Selenium-74	0.87
Selenium-76	9.36
Selenium-77	7.63
Selenium-78	23.78
Selenium-80	49.61
Tellurium-120	0.09
Tellurium-122	2.55
Tellurium-123	0.89
Tellurium-124	4.74
Tellurium-125	7.07

Tellurium-126	18.84
Tellurium-128	31.74
Tellurium-130	34.08

There are 38 known nuclear isomers of tellurium with atomic masses that range from 105 to 142. Tellurium is the lightest element known to undergo alpha decay, with isotopes ^{106}Te to ^{110}Te being able to undergo this mode of decay.

Cigarettes: it is not only the smoke that kills, but also the radioactivity

Ever since the early 1960s, the presence of polonium-210 in tobacco smoke has been known. The world's biggest tobacco firms spent over 40 years trying to find ways to remove the polonium-210 without success: even to this day. However, they also never published the results, keeping the facts of the radioactive hazards from the consumer.

Radioactive polonium-210 is contained in phosphate fertilizers and is absorbed by the roots of plants (such as tobacco) and stored in its tissues. Tobacco plants fertilized by rock phosphates contain polonium-210, which emits alpha radiation estimated to cause about 11,700 lung cancer deaths annually worldwide.

Industrial production of the elements

Sulfur

Elemental sulfur is found near hot springs and volcanic regions in many parts of the world. Volcanic deposits are mined in Indonesia, Chile, and Japan. Significant deposits of sulfur also exist in salt domes along the coast of the Gulf of Mexico, and in eastern Europe and western Asia. The sulfur in these deposits is believed to come from the action of anaerobic bacteria on sulfate minerals. However, fossil-based sulfur deposits from salt domes are the basis for commercial production in the United States, Poland, Russia, Turkmenistan, and Ukraine. Sulfur is mainly extracted from natural sources by two processes: the Sicilian process and the Frasch process.

Sicilian process

First used in Sicily from where it takes its name, the Sicilian process was used in ancient times to get sulfur from rocks present in volcanic regions. The sulfur deposits are piled and stacked in brick kilns built on sloping hillsides, and with airspaces between them (Figure 9.1.20). Then powdered sulfur is put on top of the sulfur deposit and ignited. As the sulfur burns, the heat melts the sulfur deposits, causing the molten sulfur to flow down the sloping hillside. The molten sulfur can then be collected in wooden buckets. The sulfur produced by the Sicilian process must be purified by distillation.

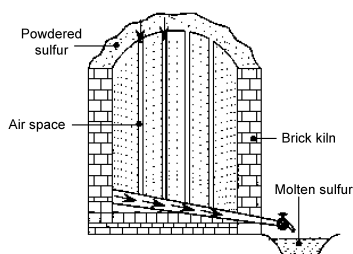


Figure 9.1.20: Extraction of sulfur by the Sicilian process.

Frasch process

In 1867, sulfur was discovered in the caprock of a salt dome in Louisiana; however, it was beneath quicksand, which prevented mining. In 1894 Herman Frasch (Figure 9.1.21), devised a method of sulfur removal using pipes to bypass the quicksand. The process proved successful, but the high cost of fuel needed to heat the water made the process uneconomic until the 1901 discovery of the Spindletop oil field in Texas (Figure 9.1.22) provided cheap fuel oil to the region.



Figure 9.1.21: German-born American chemist Herman Frasch (1851 - 1914).

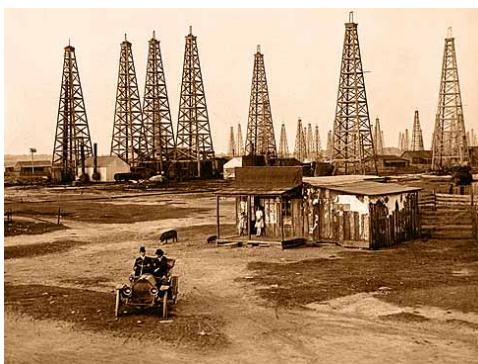


Figure 9.1.22: Spindletop oil field in Beaumont, Texas.

In the Frasch process three concentric pipes to extract sulfur at high purity directly out of the ground (Figure 9.1.23). Superheated steam ($160\text{ }^{\circ}\text{C}$) is pumped down the outermost pipe, which melts the sulfur. Hot compressed air is pumped down the innermost pipe, which serves to create foam and pressure. The resulting molten sulfur foam is then expelled through the middle pipe. The Frasch process produces sulfur with 99.5% purity, which needs no further purification.

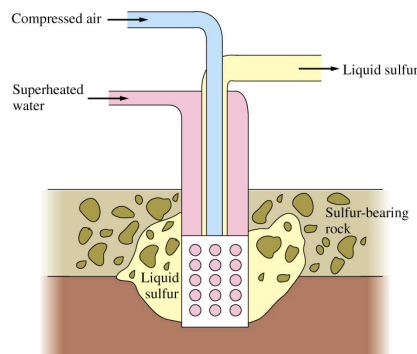


Figure 9.1.23: Schematic diagram of the Frasch process.

Most of the world's sulfur was obtained using the Frasch process until the late 20th century, when sulfur recovered from petroleum sources (recovered sulfur) became more commonplace.

Selenium

Elemental selenium is a rare mineral, and most elemental selenium comes as a byproduct of refining copper or producing sulfuric acid. Isolation of selenium begins by oxidation with sodium carbonate to produce selenium dioxide. The selenium dioxide is then mixed with water and the solution is acidified to form selenous acid (oxidation step). Selenous acid is bubbled with sulfur dioxide (reduction step) to give elemental selenium.

Elemental selenium produced by chemical reactions appears as the amorphous red form. When the red form is rapidly melted, it forms the black, vitreous form. The most thermodynamically stable and dense form of selenium is the electrically conductive gray (trigonal) form, which is composed of long helical chains of selenium atoms (Figure 9.1.24). The conductivity of this form is

notably light sensitive. Selenium also exists in three different deep-red crystalline monoclinic forms, which is composed of Se_8 molecules, similar to many allotropes of sulfur.

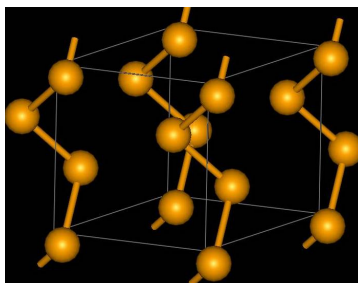
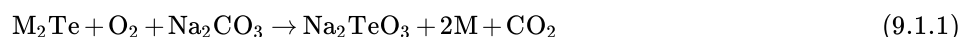


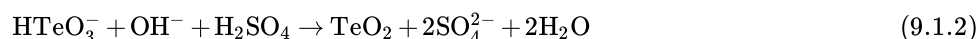
Figure 9.1.24: The structure of trigonal selenium.

Tellurium

The principal source of tellurium is from anode sludges produced during the electrolytic refining of copper. Treatment of 500 tons of copper ore typically yields 1 lb (0.45 kg) of tellurium. The anode sludges contain the selenides and tellurides of the noble metals in compounds with the formula M_2Se or M_2Te ($\text{M} = \text{Cu}, \text{Ag}, \text{Au}$). At temperatures of 500 °C the anode sludges are roasted with sodium carbonate (Na_2CO_3) under air. The metals are reduced to the metals, while the tellurium is converted to sodium tellurite, (9.1.1).



Tellurites can be extracted from the mixture with water and are normally present as hydrotellurites HTeO_3^- in solution. Selenates are also formed during this process, but they can be separated by adding sulfuric acid. The hydrotellurites are converted into the insoluble tellurium dioxide while the selenites stay in solution, (9.1.2).



The reduction to the metal is done either by electrolysis or by reacting the tellurium dioxide with sulfur dioxide in sulfuric acid, (9.1.3).



Physical properties

The physical properties of the Group 16 elements encompasses a gas (O_2), a non-metallic solid (S_2), and metals ($\text{Se}, \text{Te}, \text{Po}$), Table 9.1.4.

Table 9.1.4: Selected physical properties of the Group 16 elements.

Element	Mp (°C)	Bp (°C)	Density (g/cm ³)
O	-218.79	-182.95	1.429 g/L
S	115.21	444.6	1.819
Se	221	685	4.81 (gray), 4.39 (alpha), 4.28 (vitreous)
Te	449.51	988	6.24 (solid), 5.70 (liquid)
Po	254	962	9.196 (alpha), 9.398 (beta)

Vapor phase

The lighter Group 16 elements form X_2 dimers in the vapor phase. Sulfur also forms higher allotropes in the vapor phase (e.g., S_8 and S_6), while selenium and tellurium forms atomic vapor in addition to the dimmers. Unlike dihydrogen, however, the bonding is associated with the molecular orbital combination of the two π -orbitals (Figure 9.1.25). All of the dimeric X_2 molecules are paramagnetic.

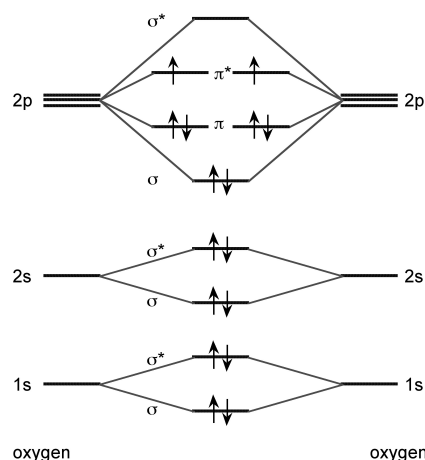


Figure 9.1.25: Molecular orbital diagram for the formation of O_2 .

Solid state

While sulfur forms over 30 allotropes, the common form of sulfur is cyclooctasulfur (S_8) has three main allotropes: S_α , S_β , and S_γ . The orthorhombic form (S_α) is more stable up to 95 °C, while the β -form is the thermodynamic form. The lone pairs of electrons make the S-S-S bend (108°), resulting in S_8 having the shape of a crown (Figure 9.1.26). When sulfur melts the S_8 molecules break up. When suddenly cooled, long chain molecules are formed in the plastic sulfur that, behave as rubber. Plastic sulfur transform into rhombic sulfur over time.

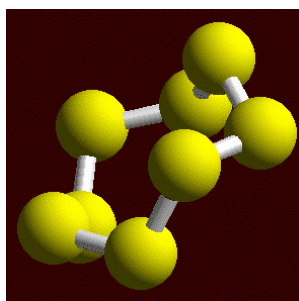


Figure 9.1.26: The structure of S_8 .

Elemental selenium produced in chemical reactions appears as the amorphous red form. When rapidly melted, it forms the black, vitreous form, which is usually sold industrially as beads. The most thermodynamically stable and dense form of selenium is the electrically conductive gray (trigonal) form, which is composed of long helical chains of selenium atoms (Figure 9.1.24). The conductivity of gray selenium is light sensitive and is hence used in photocopiers. Selenium also exists in three different deep-red crystalline monoclinic forms, which are composed of Se_8 molecules, similar to many allotropes of sulfur. Unlike sulfur, however, selenium does not undergo the changes in viscosity when heated.

Tellurium is a crystalline metal with a trigonal structure ($a = 4.4572 \text{ \AA}$, $c = 5.929 \text{ \AA}$). Polonium has a simple cubic structure in it's a form ($a = 3.359 \text{ \AA}$)

Compounds of the Group 16 elements.

The chemistry of the Group 16 elements is dominated by the stability of the -2 oxidation state and the noble gas configuration of the X^{2-} anion.

Oxidation state

The electronegativity of oxygen (3.5) results in it having predominantly -2 oxidation state, however, sulfur, selenium and tellurium all for compounds with higher oxidation states, especially with oxygen (Table 9.1.5).

Table 9.1.5: Examples of oxidation states in compounds of the Group 16 elements.

Element	-2	-1	+4	+6
O	Na_2O , H_2O	H_2O_2	-	-

S	H ₂ S	H ₂ S ₂	SO ₂	H ₂ SO ₄ , SO ₃
Se	H ₂ Se	H ₂ Se ₂	SeO ₂	SeF ₄
Te	H ₂ Te	^t Bu ₂ Te ₂	TeO ₂	Te(OH) ₆

Catenation

Catenation is the ability of a chemical element to form a long chain-like structure via a series of covalent bonds. Although oxygen shows this property only in the existence of ozone, sulfur is second only to carbon in exhibiting this mode of combination; the chalcogens beyond sulfur show it to diminishing degrees, polonium having no tendency to catenate.

When aqueous metal sulfide salts are heated with elemental sulfur a range of polysulfide ions are formed, (9.1.4). When alkali polysulfides dissolve in polar solvents (e.g., DMF or DMSO) a deep blue solution is formed. The absorption ($\lambda_{\text{max}} = 610 \text{ nm}$) is associated with the radical anion, S₃^{•−}. While, polyselenides and polytellurides are less common, the Se₃^{2−} and Te₃^{2−} ions are known.



The term *polysulfide* often refers to a class of polymers with alternating chains of several sulfur atoms and hydrocarbon substituents. The general formula is R₂Sn, where n ranges from 2 – 10. For the selenium and tellurium analogs the extent of catenation is far more limited.

Bibliography

- D. Barisic, S. Lulic, and P. Miletic, *Water Research*, 1992, **26**, 607.
- M. Davies, *History of Science*, 1989, **22**, 63.
- T. F. Kelley, *Science*, 1965, **149**, 537.
- M. B. Power, J. W. Ziller, A. N. Tyler, and A. R. Barron, *Organometallics.*, 1992, **11**, 1055.

This page titled [9.1: The Group 16 Elements- The Chalcogens](#) is shared under a [CC BY 3.0](#) license and was authored, remixed, and/or curated by [Andrew R. Barron \(CNX\)](#) via [source content](#) that was edited to the style and standards of the LibreTexts platform.

9.2: Ozone

Ozone (O_3) is an allotrope of oxygen that is much less stable than the diatomic molecule (O_2). Ground-level ozone is an air pollutant with harmful effects on the respiratory system, while the ozone layer in the upper atmosphere filters potentially damaging ultraviolet light from reaching the Earth's surface.

The structure of ozone is bent, with C_{2v} symmetry, similar to water (Figure 9.2.1a). The central oxygen has sp^2 hybridization with one lone pair. As a consequence of the bent structure, and the resonance hybridization (Figure 9.2.1b) ozone is a polar molecule (dipole moment = 0.5337 D).

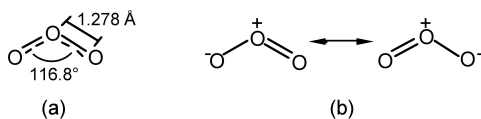
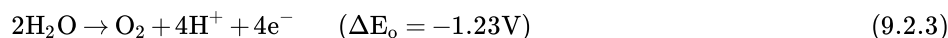
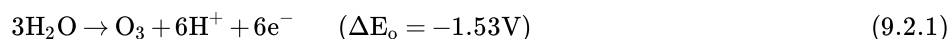


Figure 9.2.1: The (a) structural parameters of ozone and (b) its resonance hybridization.

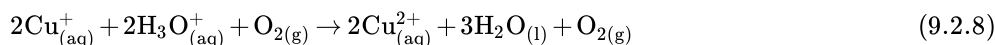
Ozone is made by the exposure of oxygen (O_2) to an electric discharge. Ozone has a characteristic smell can be commonly smelled after a lightening strike; in fact the name ozone comes from the Greek *ozein* meaning *to smell*. In the laboratory, ozone can also be produced by electrolysis using graphite rod cathode, a platinum wire anode, and sulfuric acid (3 M) electrolyte. The half cell reactions are as follows:



Ozone is also produced through photolysis of oxygen, (Equation 9.2.4 and 9.2.5), both in the laboratory and the atmosphere.



Ozone is a very strong oxidizing agent, and will readily oxidize a range of materials, e.g., Equations 9.2.6 and 9.2.7. It will also oxidize metals (except gold, platinum, and iridium) to their highest oxidation state, e.g., Equation 9.2.8.



Metal ozonides, which contain the ozonide anion (O_3^-) are explosive and must be stored at cryogenic temperatures. Ozonides for all the alkali metals are known. KO_3 , RbO_3 , and CsO_3 can be prepared from their respective superoxides.



Ozone as a modulator of life on Earth

The Earth's atmosphere acts as a source of O_2 and a repository of CO_2 , but it also acts as a shield for life. First, nearly all meteorites burn up on entry because of the high temperatures generated by the friction of the atmosphere. Second, the atmosphere acts as a shield for high energy UV radiation.

Although UV radiation converts 7-dehydrocholesterol into vitamin D3 in the skin (Figure 9.2.2), and is therefore useful, high energy UV destroys living cells. In fact the darkening we call a suntan is actually the body's mechanism for preventing further UV damage. Sun burn and skin cancer are caused by relatively weak UV light that reaches the Earth's surface, without the atmosphere we would be exposed to high energy UV that would be a hazard to all life on Earth. The Earth's "sun screen" is ozone (O_3). And without ozone in the upper atmosphere there would be no life on Earth.

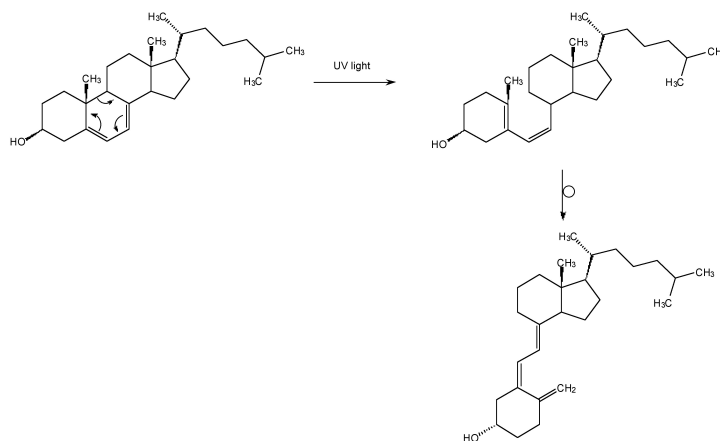


Figure 9.2.2: The conversion of 7-dehydrocholesterol (a derivative of cholesterol) to pre-vitamin D3 by photolysis by ultraviolet light, and its subsequent isomerization to vitamin D3.

The ozone layer is located in the lower portion of the stratosphere from approximately 10 km to 50 km above Earth, though the thickness varies seasonally and geographically. This layer contains over 91% of the ozone in Earth's atmosphere and absorbs 93-99% of the sun's high frequency ultraviolet light. The ozone decomposes photolytically to O_2 and molecular oxygen, (9.2.10), and it is this reaction that accounts for the UV protection of the atmosphere. Ozone is naturally regenerated by the exothermic reaction of the molecular oxygen with O_2 , (9.2.11).



The balance between ozone formation and destruction is thus an important mechanism for the protection of living organisms on the planet. While the ozone layer had been relatively constant on Earth for millions of years, the last 70 have seen a dramatic change including the increase in the polar hole in the ozone layer. The ozone hole is defined geographically as the area where the total ozone concentration is less than 220 Dobson Units.

One Dobson unit refers to a layer of ozone that would be 10 μm (micrometre) that is 1×10^{-5} m thick under standard temperature (25 °C) and pressure (1 atmosphere).

The ozone hole has steadily grown in size and length of existence over the past two and half decades. At present the size of ozone hole over Antarctica is estimated to be about 30 million sq.km (Figure 9.2.3).

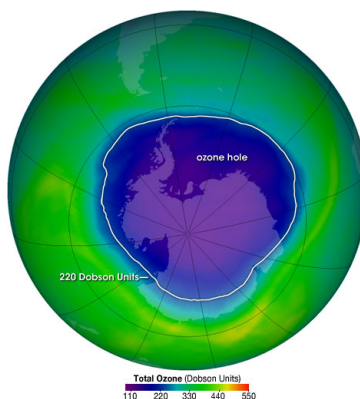


Figure 9.2.3: The concentration profile of ozone over Antarctica.

This page titled [9.2: Ozone](#) is shared under a [CC BY 3.0](#) license and was authored, remixed, and/or curated by [Andrew R. Barron \(CNX\)](#) via [source content](#) that was edited to the style and standards of the LibreTexts platform.

9.3: Water - The Fuel for the Medieval Industrial Revolution

Despite the greatest industrial complex of the Roman Empire being the imperial grain mill at Barbegal near Arles in what is now southern France (Figure 9.3.1), and the knowledge of gearing used for the mill, the waterwheel (the power source of the Barbegal's power) was little used in the ancient world. This was probably due to the high slave population obviating the need for labor saving devices. However, it may also be that because the Roman Empire was very centralized, they could provide flour on a large scale from a few highly mechanized locations. Upon the fall of the Roman Empire, the knowledge of water power would have been lost were it not for the writing departments of churches and monasteries that continued to operate through the subsequent Dark Ages.



Figure 9.3.1: The Barbegal mill as it stands today.

The Barbegal mill is probably the first example of industrial mass production. It consisted of eight pairs of waterwheels positioned on a 65-foot slope (Figure 9.3.2). The wheels were turned by water that fell from a reservoir, which in turn was fed by a magnificent aqueduct. The sixteen wheels each powered two grindstones using a set of gear that allowed the horizontal shaft from the wheel to turn a vertical shaft on which the grindstones were positioned. Grain for the mill was imported from as far as Egypt, and the flour production was eight times that required for the local population of 10,000, resulting in an export business. Unfortunately, upon the fall of Rome the technology of waterpower almost ceased since the small city-states set up had no need for industrial complexes.

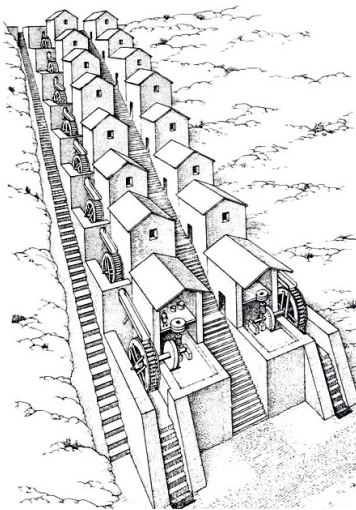


Figure 9.3.2: An artist's representation of the overshot waterwheels that are thought to have driven the 16 mills at Barbegal.

There are two general designs of waterwheel. The first is powered by water falling from above the wheel and is called an overshot wheel (Figure 9.3.3). The alternative design, the undershot wheel, relied on water flowing on a river or pond such that the current moved the paddles at the bottom of the wheel (Figure 9.3.4).

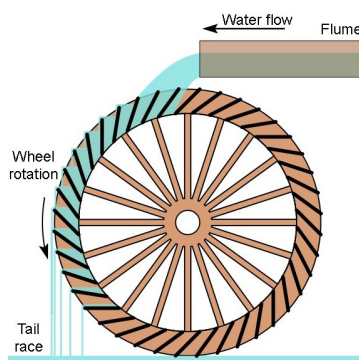


Figure 9.3.3: A schematic diagram of an idealized overshot water wheel.

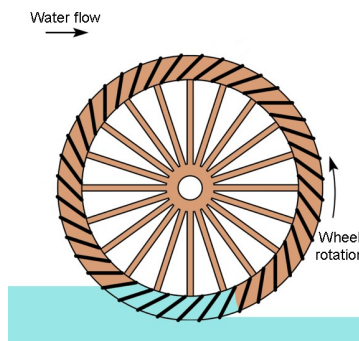


Figure 9.3.4: A schematic diagram of an idealized undershot water wheel.

Despite its fall from use, the waterwheel was not forgotten. Due to the writings of 14th century BC engineers, such as Vitruvius (Figure 9.3.5), whose texts had been preserved in the libraries in churches and monasteries across Europe, the waterwheel powered mills made a resurgence between the fifth and the tenth century. In most cases mills were owned by the church, since they had the knowledge (from ancient texts) to construct the mills and, possibly just as important, the literacy to develop the accounting system for their profitable use. The church would lease mills to farmers on a time usage, and they would take payment in flour. The owners of waterwheels and their mills were the first barons of industry post the Dark Ages. In fact, the fact that the Saxon word for an aristocrat is *Lord*, which means *loaf giver*, suggests the importance of the waterwheel. By the end of the tenth century the waterwheel was in widespread use across Europe. The Domesday Book (the nationwide census carried out by the Normans after the invasion of England) listed nearly six thousand grain mills in 1089.



Figure 9.3.5: A depiction of Vitruvius (right) presenting *De Architectura* to the Emperor Augustus.

Despite the large number of waterwheels, the gearing used up until the ninth century was little different to that described by Vitruvius and used at Barbegal. Then around 890 AD the monastery of St Gall a new device was attached to the waterwheel. Instead of gearing to transfer power from horizontal to vertical rotation, a piece of wood was set into the shaft driven by the waterwheel (Figure 9.3.6). What had been created was a cam, since as the shaft turns the protruding piece of wood its anything in its way. For example, the first recorded use, by the monks at St Gall, was to crush malt for beer. However, the cam could be made to trip a hammer with every rotation (pounding), or to act on a crank to turn a rotary motion into a horizontal back-and-forward motion (cutting), or to push down a level and activate a suction pump (raising water from a well), or operate a bellows (for a metal forge). The range of motions meant that waterpower could now be used for a wide range of industries. By the end of the tenth

century there were waterwheels powering forge hammers, oil and silk mills, sugar cane crusher, tanning mills pounding leather, grinding stones, ore crushing mills (Figure 9.3.7), and as fulling mills for the rapidly expanding trans-European textile industry.

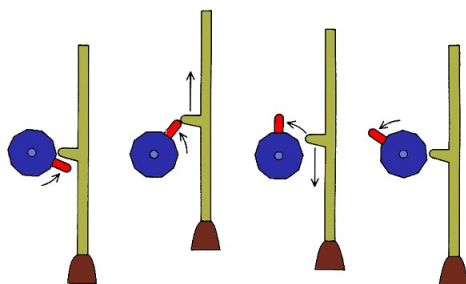


Figure 9.3.6: Schematic representation of the transformation of rotary motion into linear motion can be achieved by having a cam on the axle of the wheel



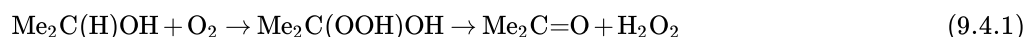
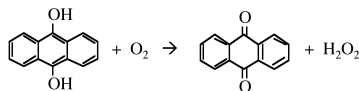
Figure 9.3.7: The cam principle as applied to a rock-crushing mill illustrated by Georgius Agricola in his book *De Re Metallica* (1556).

As a consequence of the waterwheel and the cam, the period between the tenth and fourteenth centuries has come to be known as the Medieval Industrial Revolution. It is interesting to note that water played a key role in the driving force during the next Industrial Revolution four hundred years later – the steam engine.

This page titled [9.3: Water - The Fuel for the Medieval Industrial Revolution](#) is shared under a [CC BY 3.0](#) license and was authored, remixed, and/or curated by [Andrew R. Barron \(CNX\)](#) via [source content](#) that was edited to the style and standards of the LibreTexts platform.

9.4: Hydrogen Peroxide

Hydrogen peroxide (H_2O_2) is a very pale blue liquid but appears colorless in dilute solution. It is prepared by the oxidation of anthraquinol (shown below). The hydrogen peroxide is extracted with water from the anthraquinone solution and the 20 - 40% solution is purified by solvent extraction. An alternative process involves the oxidation of isopropanol in either the vapor or liquid phase at 100 °C and *ca.* 15 atm, (9.4.1). The products are separated by fractional distillation.



In the gas phase H_2O_2 adopts a gauche conformation (Figure 9.4.1), but there is only a low barrier to rotation about the O-O bond.

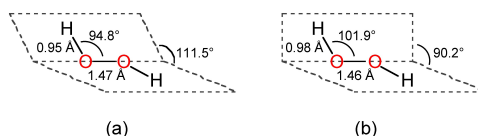


Figure 9.4.1: Structure of hydrogen peroxide in (a) the vapor phase and (b) the solid (crystal) phase.

Hydrogen peroxide is a liquid at standard temperature and pressure (25 °C, 1 atm) due to the presence of strong hydrogen bonding similar to found in water. In fact, the liquid range for H_2O_2 (Mp = -0.43 °C, Bp = 150.2 °C) is actually broader than water, and it is slightly more viscous than water. Hydrogen peroxide has a density of 1.44 g/cm³, and is 10⁶ times less basic than water.

As with water, H_2O_2 is a good solvent because of its polar nature and broad liquid temperature range, however, it is dangerous in its pure state due to its facile ($\Delta H = -99$ kJ/mol) auto decomposition, (9.4.2), as well as its strong oxidizing nature.



Hydrogen peroxide is usually sold as 3 - 12% solution for home use; however, laboratory and certain industrial applications require 30% solutions.

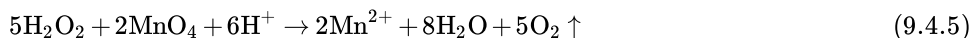
Note

Hydrogen peroxide should be stored in a cool, dry, well-ventilated area and away from any flammable or combustible substances. It should be stored in a container composed of non-reactive materials such as stainless steel or glass (other materials including some plastics and aluminum alloys may also be suitable). Because it breaks down quickly when exposed to light, it should be stored in an opaque container, and pharmaceutical formulations typically come in brown bottles that filter out light.

Aqueous solution are weakly acidic ($K = 1.5 \times 10^{-12}$), (9.4.3). However, there is no exchange of oxygen atoms between H_2O_2 and H_2O in the liquid phase.



As expected hydrogen peroxide is a strong oxidizing agent, (9.4.4), however, it can also act as a reducing agent, (9.4.5).



This page titled 9.4: Hydrogen Peroxide is shared under a CC BY 3.0 license and was authored, remixed, and/or curated by Andrew R. Barron (CNX) via source content that was edited to the style and standards of the LibreTexts platform.

9.5: Hydrogen Peroxide Providing a Lift for 007

In the pre-credit sequence of the 1965 film *Thunderball*, James Bond 007 (played by Sean Connery) uses a Jetpack to escape from two gunmen after killing Jacques Bouvar, SPECTRE Agent No. 6 (Figure 9.5.1). The Jetpack was also used in the *Thunderball* posters, being the "Look Up" part of the "Look Up! Look Down! Look Out!" tagline (Figure 9.5.2). The Jetpack returned in 2002 in *Die Another Day* (in which Pierce Brosnan played Bond) in the Q scene that showcased many other classic gadgets from previous Bond films.



Figure 9.5.1: James Bond 007 escaping from gunmen using a Jetpack (Copyright: Eon Productions).



Figure 9.5.2: Original poster for *Thunderball* (Copyright Danjaq, LLC and Eon Productions).

The Jetpack was actually a real fully functional device: the Bell Rocket Belt. It was designed for use in the US Army, but was rejected because of its short flying time of 21-22 seconds. Powered by hydrogen peroxide (H_2O_2), it could fly about 250 m and reach a maximum altitude of 18 m, going 55 km/h. Despite its impracticality in the real world, the Jetpack made a spectacular debut in *Thunderball*. Although Sean Connery is seen in close-up during the takeoff and landings (Figure 9.5.3), the main flight was actually piloted by Gordon Yeager (Fugre 4) and Bill Suitor (Figure 9.5.5).



Figure 9.5.3: Close-up shot of Sean Connery as James Bond landing the Jetpack. Note that the harness is not correctly attached, indicating this was a set-up shot for the film rather than a real flight. Presumably the crotch strap would have spoiled the lines of his suit. (Copyright: Eon Productions).



Figure 4: American pilot Gordon Yeager (1927 – 2005).



Figure 9.5.5: American rocket pack test pilot Bill Suitor (1944 -).

The Bell Rocket Belt is a low-power rocket propulsion device that allows an individual to safely travel or leap over small distances. All subsequent rocket packs were based on the construction design, developed in 1960-1969 by Wendell Moore. Moore's pack has two major parts:

1. Rigid glass-plastic corset (Figure 9.5.6a), strapped to the pilot (Figure 9.5.6b). The corset has a tubular metallic frame on the back, on which are fixed three gas cylinders: two with liquid hydrogen peroxide (Figure 9.5.6c), and one with compressed nitrogen (Figure 9.5.6d). When the pilot is on the ground, the corset distributes the weight of the pack to the pilot's back.
2. The rocket engine, able to move on a ball and socket joint (Figure 9.5.6e) in the upper part of the corset. The rocket engine consists of a gas generator (Figure 9.5.6f) and two pipes (Figure 9.5.6g) rigidly connected with it, which end with jet nozzles with controlled tips (Figure 9.5.6h). The engine is rigidly connected to two levers, which are passed under the pilot's hands. Using these levers the pilot inclines the engine forward or back and to the sides. On the right lever is the thrust control turning handle (Figure 9.5.6i), connected with a cable to the regulator valve (Figure 9.5.6j) to supply fuel to the engine. On the left lever is the steering handle, which controlled the tips of jet nozzles.

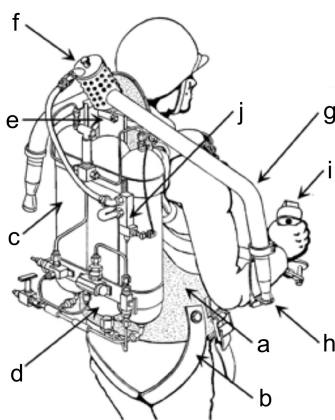


Figure 9.5.6: Diagram of the Bell rocket pack (Adapted from US Patent 3,243,144 (1966)).

The operating principle of the Jetpack is shown in Figure. The hydrogen peroxide cylinders and compressed nitrogen cylinder are each at a pressure of ca. 40 atm or 4 MPa). To operate the pilot turns the engine thrust control handle, and opens the regulator valve (3 in Figure 9.5.7). Compressed nitrogen (1 in Figure 9.5.7) displaces liquid hydrogen peroxide (2 in Figure 9.5.7), which enters the gas generator (4 in Figure 9.5.7). In the gas generator, the hydrogen peroxide contacts the catalyst and is decomposed. The catalyst consists of thin silver plates, covered with a layer of samarium nitrate. The resulting hot high-pressure mixture of steam and gas enters two pipes, which emerge from the gas generator. These pipes are covered with a layer of heat insulator to reduce loss of heat. The hot gas enters the jet nozzles, where first they are accelerated, and then expand, acquiring supersonic speed and creating reactive thrust. The whole construction is simple and reliable; the rocket engine has no moving parts. The pack has two levers, rigidly connected to the engine installation. Pressing on these levers, the pilot deflects the nozzles back, and the pack flies forward. Accordingly, raising this lever makes the pack move back. It is possible to lean the engine installation to the sides (because of the ball and socket joint) to fly sideways.

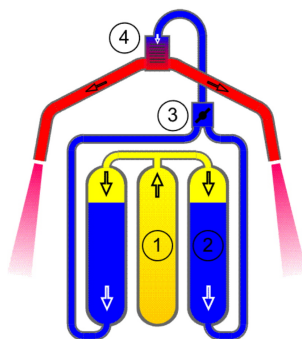


Figure 9.5.7: The operating principle of rocket engine.

This page titled [9.5: Hydrogen Peroxide Providing a Lift for 007](#) is shared under a [CC BY 3.0](#) license and was authored, remixed, and/or curated by [Andrew R. Barron \(CNX\)](#) via [source content](#) that was edited to the style and standards of the LibreTexts platform.

9.6: Comparison of Sulfur to Oxygen

Size

Table 9.6.1 summarizes the comparative sizes of oxygen and sulfur.

Table 9.6.1: Comparison of physical characteristics for oxygen and sulfur.

Element	Atomic radius (Å)	Covalent radius (Å)	Ionic radius (Å)	van der Waal radius (Å)
Oxygen	0.48	0.66	1.40	1.52
Sulfur	0.88	1.05	1.84	1.80

Electronegativity

Sulfur is less electronegative than oxygen (2.4 and 3.5, respectively) and as a consequence bonds to sulfur are less polar than the corresponding bonds to oxygen. One significant result is that with a less polar S-H bond the subsequent hydrogen bonding is weaker than observed with O-H analogs. A further consequence of the lower electronegativity is that the S-O bond is polar.

Bonds formed

Sulfur forms a range of bonding types. As with oxygen the -2 oxidation state prevalent. For example, sulfur forms analogs of ethers, i.e., thioethers R-S-R. However, unlike oxygen, sulfur can form more than two covalent (non-dative) bonds, i.e., in compounds such as SF₄ and SF₆.

Such hypervalent compounds were originally thought to be due to the inclusion of low energy *d* orbitals in hybrids (e.g., sp^3d^2 for SF₆); however, a better picture involves a combination of *s* and *p* orbitals in bonding (Figure 9.6.1). Any involvement of the *d* orbitals is limited to the polarization of the *p* orbitals rather than direct hybridization. In this regard SF₆ represents the archetypal hypervalent molecule. Finally, sulfur can form multiple bonds, e.g., Me₂S=O.

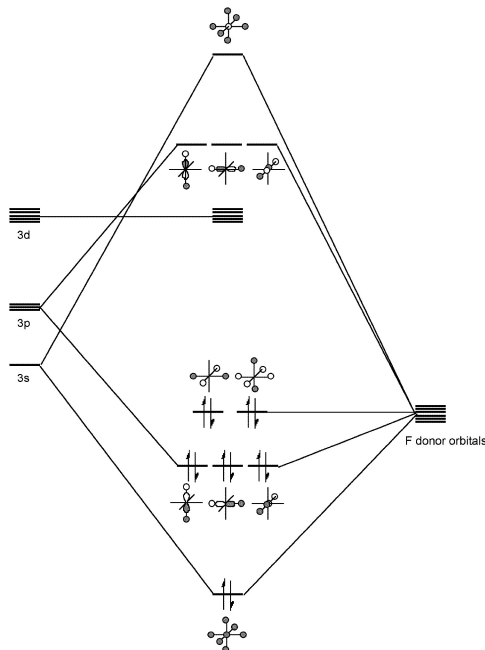


Figure 9.6.1: Molecular orbital diagram for SF₆.

Catenation

Catenation is defined as the ability of a chemical element to form a long chain-like structure via a series of covalent bonds. Oxygen's extent of catenation is limited to ozone (O₃) and peroxides (e.g., R-O-O-R). In contrast, the chemistry of sulfur is rich in the formation of multiple S-S bonds.

While elemental sulfur exists as a diatomic molecule (i.e., S_2) in the gas phase at high temperatures, sulfur vapor consists of a mixture of oligomers (S_3 to S_8) as a temperature dependant equilibrium. In the solid state the formation of S_n dominates, and sulfur exists as a range of polymorphs in which extended S-S bonding occurs in either rings of 6 to 20 atoms (e.g., Figure 9.6.2) or chains (catenasulfur).

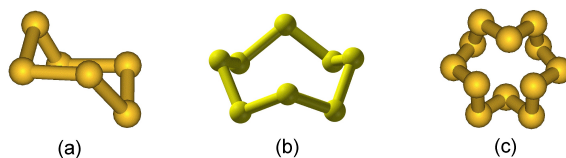


Figure 9.6.2: Structures of two polymorphs of sulfur: (a) cyclohexasulfur S_6 , (b) cyclooctasulfur S_8 , and (b) cyclododecasulfur S_{12} .

The higher level of catenation for sulfur is due to the greater strength of a S-S bond (226 kJ/mol) as compared to the O-O bond (142 kJ/mol). In general the homoleptic bond strength is expected to decrease going down a period of the Periodic Table. The reason for the unexpected weakness of the O-O bond is that the electronegative oxygen atoms repel each other and thus weaken the bond.

This page titled [9.6: Comparison of Sulfur to Oxygen](#) is shared under a [CC BY 3.0](#) license and was authored, remixed, and/or curated by [Andrew R. Barron \(CNX\)](#) via [source content](#) that was edited to the style and standards of the LibreTexts platform.

9.7: Chalconide Hydrides

Dihydrides

The hydrides of sulfur, selenium and tellurium are all extremely toxic gases with repulsive smells. Hydrogen sulfide (H_2S) is very toxic, in fact it is more than 5x as toxic as HCN (Table 9.7.1). Hydrogen sulfide is considered a broad-spectrum poison, meaning that it can poison several different systems in the body, although the nervous system is most affected. It forms a complex bond with iron in the mitochondrial cytochrome enzymes, thereby blocking oxygen from binding and stopping cellular respiration. Exposure to low concentrations can result in eye irritation, a sore throat and cough, nausea, shortness of breath, and fluid in the lungs. Long-term, low-level exposure may result in fatigue, loss of appetite, headaches, irritability, poor memory, and dizziness.

Table 9.7.1: Toxicity levels for hydrogen sulfide.

Concentration (ppm)	Biological effect
0.00047	Threshold.
10–20	Borderline concentration for eye irritation.
50–100	Eye damage.
100–150	Olfactory nerve is paralyzed and the sense of smell disappears, often together with awareness of danger.
320–530	Pulmonary edema with the possibility of death.
530–1000	Stimulation of the central nervous system and rapid breathing, leading to loss of breathing.
800	Lethal concentration for 50% of humans for 5 minutes exposure (LC50).
+1000	immediate collapse with loss of breathing, even after inhalation of a single breath.

Each of the hydrides is prepared by the reaction of acid on a metal chalcogenide, e.g., (9.7.1) and (9.7.2). The unstable H_2Po has been prepared by the reaction of HCl on Po metal.



The thermal stability and bond strength of the dihydrides follows the trend:



While H_2Se is thermodynamically stable to 280 °C, H_2Te and H_2Po are thermodynamically unstable.

All the dihydrides behave as weak acids in water. Thus, dissolution of H_2S in water results in the formation of the conjugate bases, (9.7.4) and (9.7.5), with dissociation constants of 10^{-7} and 10^{-17} , respectively.



Sulfanes

The propensity of sulfur for catenation means that while the hydrides of oxygen are limited to water (H_2O) and hydrogen peroxide (H_2O_2), the compounds H_2S_n where $n = 2 - 6$ may all be isolated. Higher homologs are also known, but only as mixtures. All of the sulfanes are yellow liquids whose viscosity increases with increased chain length.

A mixture of lower sulfanes is prepared by the reaction of sodium sulfides (Na_2S_n) with HCl, (9.7.6). From this mixture the compounds H_2S_n where $n = 2 - 5$ are purified by fractional distillation. However, higher sulfanes are made by the reaction of either H_2S or H_2S_2 with sulfur chlorides, (9.7.7) and (9.7.8).



This page titled [9.7: Chalcogenide Hydrides](#) is shared under a [CC BY 3.0](#) license and was authored, remixed, and/or curated by [Andrew R. Barron \(CNX\)](#) via [source content](#) that was edited to the style and standards of the LibreTexts platform.

9.8: Oxides and Oxyacids of Sulfur

Note

Alternative spellings of sulfurous and sulfuric acids are based upon the traditional UK spelling of sulphur, i.e., sulphurous and sulphuric acid.

Sulfur dioxide and sulfurous acid solutions

The combustion of sulfur results in the formation of gaseous sulfur dioxide, (9.8.1).



The bent structure of SO_2 is shown in Figure 9.8.1, and as a consequence of the sp^2 hybridization the molecule is polar.

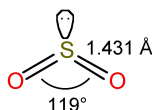


Figure 9.8.1: The structure of sulfur dioxide.

The modest boiling temperature of SO_2 (-10°C) means that it is readily liquefied and easily kept as a liquid at room temperature under a slight pressure. The liquid is associated by dipole-dipole attractions due to the polar nature of SO_2 . Liquid SO_2 is a good solvent due to the polarity of the molecule; as a consequence it readily solubilizes polar compounds and salts. It is also convenient since it is easy to remove from reaction products by evaporation.

Sulfur dioxide is soluble in water forming aqueous solutions where most of the SO_2 is maintained as a hydrogen-bonded hydrate, in a similar manner to that observed for aqueous solutions of carbon dioxide. At equilibrium in neutral water (no added base) a small fraction reacts, to give a mixture of bisulfite (HSO_3^- , Figure 9.8.2a) and sulfite (SO_3^{2-} , Figure 9.8.2b), (9.8.2). The free acid does not to exist.

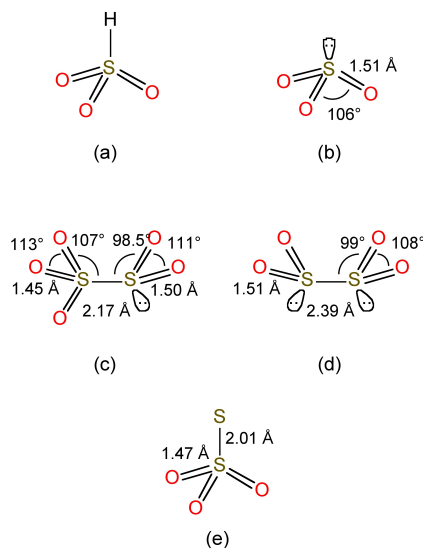
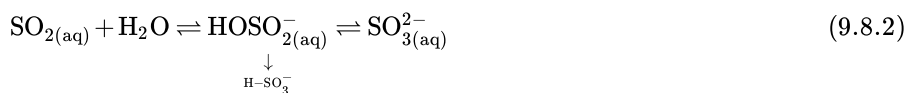


Figure 9.8.2: The structures of the (a) bisulfite, (b) sulfite, (c) disulfite, (d) dithionite, and (e) thiosulfate anions.

Bisulfite undergoes a further equilibrium, (9.8.3), to form disulfite, whose structure is shown in Figure 9.8.2c.



Salts of these anions are known, and complexes of the sulfite ion are known (Figure 9.8.3), while SO_2 itself can act as a ligand to heavy metals.

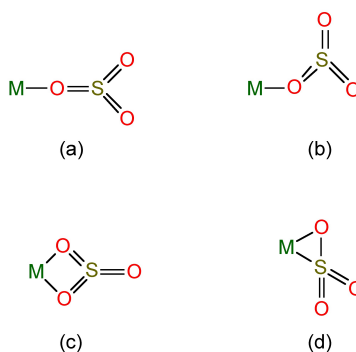
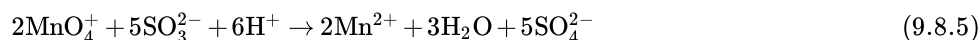
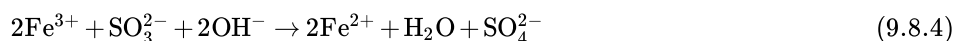


Figure 9.8.3: The structural modes of sulfite coordination.

The bisulfite ion has strong reducing properties, e.g., (9.8.4) and (9.8.5).



Bisulfite is also reduced by zinc in the presence of additional SO_2 , (9.8.6), to form the highly reducing dithionite anion (Figure 9.8.2d). Reaction of bisulfite with elemental sulfur yields the thiosulfate anion (Figure 9.8.2e), (9.8.7f).



Sulfur trioxide and sulfuric acid

Oxidation of sulfur dioxide in the presence of a catalyst (e.g., platinum) yields sulfur trioxide, (9.8.8), which may be condensed to a liquid at room temperature ($\text{Bp} = 45^\circ\text{C}$).



Liquid SO_3 exists as a mixture of monomer and trimers (Figure 9.8.4a and 4b), while as a solid ($\text{Mp} = 16.9^\circ\text{C}$) it forms polymers (Figure 9.8.4c).

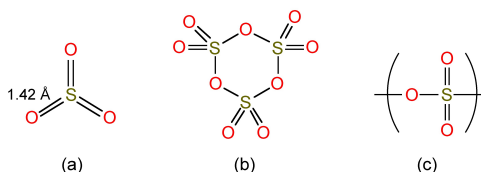


Figure 9.8.4: The structure of (a) monomeric, (b) trimeric, and (c) polymeric sulfur trioxide.

The reaction of SO_3 with water results in the formation of sulfuric acid, H_2SO_4 , as a viscous, hydrogen bonded liquid. Sulfuric acid is a strong protic acid, which in dilute solutions (in water) reacts as a dibasic acid, (9.8.9), forming bisulfate (HSO_4^-) and sulfate (SO_4^{2-}) anions. A large number of salts are known for both anions. In addition, sulfate is known to act as a monodentate or bidentate ligand in coordination complexes.



The dissolution of SO_3 in concentrated sulfuric acid yields very corrosive, *fuming* sulfuric acid, which contains some pyrosulfuric acid, (9.8.10).



WARNING

The corrosive properties of sulfuric acid are accentuated by its highly exothermic reaction with water. Burns from sulfuric acid are potentially more serious than those of comparable strong acids (e.g., hydrochloric acid), as there is additional tissue damage due to dehydration and particularly secondary thermal damage due to the heat liberated by the reaction with water.

Sulfur as a source of atmospheric pollution and acid rain

Sulfur dioxide is formed as a pollutant during the combustion of sulfur containing fuels, in particular coal. While the emission of SO_2 itself leads to concerns it is its conversion to sulfuric acid in the form of acid rain that has been of concern for several decades. The pathway for the formation of sulfuric acid in the atmosphere is dependant on whether the reaction occurs in dry atmosphere or in clouds and rain.

Gaseous reactions in a dry atmosphere

In the dry atmosphere, gaseous sulfur dioxide reacts with the hydroxide radical (formed by the photochemical decomposition of ozone, (9.8.11) and (9.8.12), in the presence of a non-reactive gas molecule such as nitrogen, (9.8.12). The sulfurous acid, thus formed reacts with oxygen to generate sulfur trioxide, (9.8.13), which reacts with water to form sulfuric acid, (9.8.14).



Measurements indicate that the conversion rate of SO_2 to H_2SO_4 is 4% per hour on a clear sunny day, but the rate is slower during the winter.

Liquid phase reactions in clouds and rain

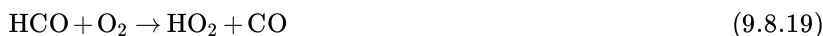
In the liquid phase SO_2 reacts directly with water, (9.8.15). The bisulfite (HSO_3^-) is oxidized by hydrogen peroxide forming a forming bisulfate (HSO_4^-) solution, (9.8.16).



Water soluble hydrogen peroxide is formed by the oxidation of water, (9.8.17).



The HO_2 radical is formed by the photolysis of organic carbonyl compounds, e.g., formaldehyde in (9.8.18) and (9.8.19).



The conversion rate is independent of pH is very fast: almost 100% per hour in summer. However, the conversion is limited by the supply of hydrogen peroxide, which is often present in much lower levels than SO_2 . Thus, a reduction in sulfur dioxide emissions does not always correlate with a reduction of wet acid deposition.

This page titled 9.8: Oxides and Oxyacids of Sulfur is shared under a CC BY 3.0 license and was authored, remixed, and/or curated by Andrew R. Barron (CNX) via source content that was edited to the style and standards of the LibreTexts platform.

9.9: Sulfur Halides

Sulfur hexafluoride

Sulfur hexafluoride (SF_6) is a gas at standard temperature and pressure (25 °C, 1 atm). The most common synthesis involves the direct reaction of sulfur with fluorine yields SF_6 .



It should be noted that while SF_6 is highly stable, SCl_6 is not formed. The explanation of this difference may be explained by a consideration of the Born-Haber cycle shown in Figure 9.9.1. A similar cycle may be calculated for SCl_6 ; however, a combination of a higher dissociation energy for Cl_2 and a lower S-Cl bond energy (Table 9.9.1) provide the rationale for why SCl_6 is not formed.

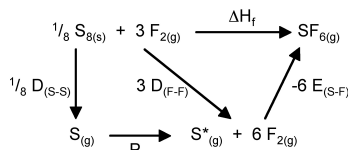


Figure 9.9.1: Born-Haber cycle for the formation (ΔH_f) of SF_6 : where $D_{(X-Y)}$ = dissociation energy for X-Y bond, $E_{(S-F)}$ = S-F bond energy, and S^* indicates 6 coordinate sulfur.

Table 9.9.1: Comparison of diatomic bond dissociation and S-X bond energy for the fluorine and chlorine analogs.

Bond dissociation energy	kJ/mol	Bond energy	kJ/mol
$D_{(F-F)}$	158	$E_{(S-F)}$	362
$D_{(Cl-Cl)}$	262	$E_{(S-Cl)}$	235

The S-F bond length (1.56 Å) is very short and consistent with π -bonding in addition to σ -bonding. Like SiF_6^{2-} , SF_6 is an example of a hypervalent molecule (Figure 9.9.2).

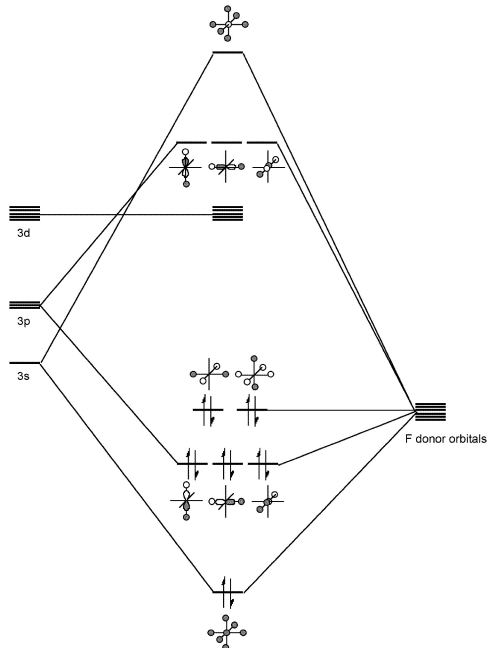


Figure 9.9.2: Molecular orbital bonding in SF_6 .

Sulfur hexafluoride is an unreactive, non toxic compound. Its inert nature provides one of its applications, as a spark suppressor. The hexafluoride is generally resistant to chemical attack, e.g., no reaction is observed with potassium hydroxide (KOH) at 500 °C. The low reactivity is due to SF_6 being kinetically inert due to:

- Coordination saturation precluding associative reactions with nucleophiles.

- Strong S-F bond (360 kJ/mol) limiting dissociative reactions.

Thermodynamically SF_6 should react with water ($\Delta H = -460$ kJ/mol), but the rate factors are too great. Sulfur hexafluoride can be reduced with sodium in liquid ammonia, (9.9.2), or with LiAlH_4 . In each of these reactions the mechanism involves the formation of a radical, (9.9.3). The reaction with sulfur trioxide yields SO_2F_2 , (9.9.4), however, the reactions with carbon or CS_2 only occur at elevated temperatures (500 °C) and pressure (4000 atm).



Sulfur monochloride pentafluoride

Although the hexachloride is unknown, it is possible to isolate the monochloride derivative (SF_5Cl) by the oxidative addition of Cl-F across SF_4 .



Sulfur monochloride pentafluoride is a gas (Bp = -21 °C), but unlike SF_6 it is fairly reactive due to the polarization of the S-Cl bond (Figure 9.9.3), and as a consequence it reacts with water, (9.9.6).



Figure 9.9.3: Polarization of the S-Cl bond in SF_5Cl .

Sulfur pentafluoride

Although SF_5 does not exist as a stable molecule, the gaseous dimer S_2F_{10} (Bp = 29 °C) may be isolated from the photochemical hydrogen reduction of SF_5Cl , (9.9.7).



While the sulfur is octahedral in S_2F_{10} (Figure 9.9.4a) the S-S bond is weak and long (2.21 Å versus an expected 2.08 Å for a single S-S bond). Despite the apparently weak S-S bond, S_2F_{10} shows almost no reactivity at room temperature; however, the S-S bond undergoes homoleptic cleavage at high temperatures. The resultant SF_5^\cdot radicals disproportionate to give highly reactive fluoride radicals, (9.9.8), which is the source of the highly oxidative properties of S_2F_{10} .

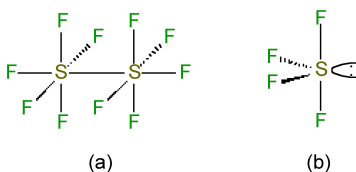


Figure 9.9.4: Structures of (a) S_2F_{10} and (b) SF_4 .

The SF_5^\cdot fragment is stabilized by the addition of an alkyl radical, and thus, there are a large number of RSF_5 derivatives known. Unlike, the chloride analog, these are very stable.

Sulfur tetrafluoride

Sulfur tetrafluoride (SF_4) is prepared from sulfur dichloride and sodium fluoride in acetonitrile solution at 70 - 80 °C.



The structure of SF_4 (and its substituted derivatives RSF_3) is based upon a trigonal bipyramidal structure with one of the equatorial sites being occupied by a lone pair (Figure 9.9.4b). Unlike the hexafluoride, sulfur tetrachloride is a highly reactive compound. It hydrolyzes readily, (9.9.10), and is a useful fluorinating agent (Figure 9.9.5).

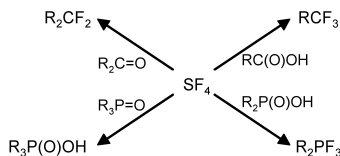


Figure 9.9.5: Examples of the use of SF_4 as a fluorinating agent.

Sulfur chlorides

The chlorination of molten sulfur yields the fowl smelling disulfur dichloride (S_2Cl_2). If the reaction is carried out with a catalyst such as FeCl_3 , SnI_4 or I_2 , an equilibrium mixture containing sulfur dichloride (SCl_2) is formed. However, the dichloride dissociates readily, (9.9.11), although it can be isolated as a dark red liquid if it distilled in the presence of PCl_5 . The reaction of chlorine at -80°C with SCl_2 or S_2Cl_2 allows for the formation of SCl_4 as a yellow crystalline compound which dissociates above -31°C . Sulfur chlorides are readily hydrolyzed. Sulfur chlorides are used to dissolve sulfur (giving species up to $\text{S}_{100}\text{Cl}_2$) for the vulcanization of rubber.



In the vapor phase S_2Cl_2 has C_2 symmetry (Figure 9.9.6a) while that of SCl_2 has C_{2v} symmetry (Figure 9.9.6b).

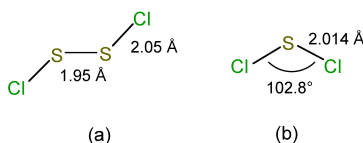


Figure 9.9.6: Structures of (a) S_2Cl_2 and (b) SCl_2 .

This page titled [9.9: Sulfur Halides](#) is shared under a [CC BY 3.0](#) license and was authored, remixed, and/or curated by [Andrew R. Barron](#) (CNX) via [source content](#) that was edited to the style and standards of the LibreTexts platform.

CHAPTER OVERVIEW

10: The Halogens

10.1: The Group 17 Elements- The Halogens

10.2: Compounds of Fluorine

10.3: Compounds of Chlorine

10.4: Oxyacids of Chlorine

10.5: Bromine Trifluoride as a Solvent

Thumbnail: Chlorine gas in an ampoule. (CC-BY-SA; W. Oelen (<http://woelen.homescience.net/science/index.html>))

This page titled [10: The Halogens](#) is shared under a [CC BY 3.0](#) license and was authored, remixed, and/or curated by [Andrew R. Barron \(CNX\)](#) via [source content](#) that was edited to the style and standards of the LibreTexts platform.

10.1: The Group 17 Elements- The Halogens

The Group 17 elements have a particular name: the *halogens* meaning *born of salt*. This is due to the formation of salts when they form compounds with a metal. Table 10.1.1 lists the derivation of the names of the halogens.

Table 10.1.1: Derivation of the names of each of the halogens.

Element	Symbol	Name
Fluorine	F	Latin <i>fluere</i> meaning <i>to flow</i>
Chlorine	Cl	Greek <i>khlôros</i> meaning <i>pale green</i>
Bromine	Br	Greek <i>brómos</i> meaning <i>stench</i>
Iodine	I	Greek <i>odes</i> meaning <i>violet or purple</i>
Astatine	At	Greek <i>astatos</i> , meaning <i>unstable</i>

Discovery

Fluorine

The mineral *fluorspar* (also known as *fluorite*) consists mainly of calcium fluoride and was described in 1530 by Agricola (Figure 10.1.1) for its use as a flux. Fluxes are used to promote the fusion of metals or minerals, and it was from this use that fluorine derived its name. In 1670 Heinrich Schwanhard found that when he mixed fluorspar with an acid the fumes produced (hydrogen fluoride) etched the glasses he was wearing. Despite many researchers investigating the chemistry of hydrogen fluoride (HF) the elemental form of fluorine was not isolated until 1886 when Henri Moissan (Figure 10.1.2) studied the electrolysis of a solution of potassium hydrogen difluoride (KHF_2) in liquid hydrogen fluoride (HF). The mixture was needed because hydrogen fluoride is a non-conductor. The device was built with platinum/iridium electrodes in a platinum holder and the apparatus was cooled to $-50\text{ }^{\circ}\text{C}$.



Figure 10.1.1: German author Georg Bauer (1494 - 1555), whose pen-name was the Latinized Georgius Agricola, was most probably the first person to be environmental conscious.



Figure 10.1.2: French chemist Ferdinand Frederick Henri Moissan (1852 - 1907) was awarded the Nobel Prize for his work with fluorine.

The generation of elemental fluorine from hydrofluoric acid proved to be exceptionally dangerous, killing or blinding several scientists who attempted early experiments on this halogen. The victims became known as *fluorine martyrs*.

Chlorine

Archaeological evidence has shown that sodium chloride (known as *table salt*) has been used as early as 3000 BC and brine (the saturated water solution) as early as 6000 BC. It is thought that hydrochloric acid was probably known to alchemist Jābir ibn Hayyān (Figure 10.1.3) around 800 AD, while aqua regia (a mixture of nitric acid and hydrochloric acid) began to be used to dissolve gold sometime before 1400 AD. Upon dissolving gold in aqua regia, chlorine gas is released along with other nauseating and irritating gases.



Figure 10.1.3: 15th century portrait of Abu Musa Jābir ibn Hayyān (721 - 815), also known by his Latinized name “Gerber”. He was a chemist, alchemist, astronomer and astrologer, engineer, geologist, philosopher, physicist, and pharmacist and physician.

Chlorine was first prepared and studied in 1774 by Carl Wilhelm Scheele (Figure 10.1.4), and therefore he is credited for its discovery despite his failing to establish chlorine as an element, mistakenly thinking that it was the oxide obtained from the hydrochloric acid. Regardless of what he believed, Scheele did isolate chlorine by reacting MnO_2 (as the mineral pyrolusite) with HCl , (10.1.1).

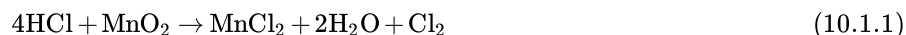


Figure 10.1.4: Swedish chemist Carl Wilhelm Scheele (1742 – 1786). Isaac Asimov called him "hard-luck Scheele" because he made a number of chemical discoveries before others who are generally given the credit.

Bromine

Bromine was discovered independently by two chemists Antoine Balard (Figure 10.1.5) in 1825 and Carl Jacob Löwig (Figure 10.1.6) in 1826.



Figure 10.1.5: French chemist Antoine Jérôme Balard (1802 - 1876).

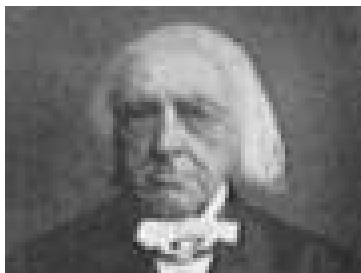


Figure 10.1.6: German chemist Carl Jacob Löwig (1803 - 1890).

Balard found bromide salts in the ash of sea weed from the salt marshes of Montpellier. The sea weed was used to produce iodine, but also contained bromine. Balard distilled the bromine from a solution of seaweed ash saturated with chlorine. The properties of the resulting substance resembled that of an intermediate of chlorine and iodine; with those results he tried to prove that the

substance was iodine monochloride (ICl), but after failing to do so he was sure that he had found a new element and named it *muride*, derived from the Latin word *muria* for brine.

In contrast, Löwig isolated bromine from a mineral water spring in Bad Kreuznach. Löwig used a solution of the mineral salt saturated with chlorine and extracted the bromine with Et_2O . After evaporation a brown liquid remained. Unfortunately, the publication of his results were delayed and Balard published first.

Iodine

Iodine was discovered by Bernard Courtois (Figure 10.1.7) in 1811 when he was destroying the waste material from the production of saltpeter (KNO_3) during gunpowder production. Saltpeter produced from French niter beds required sodium carbonate (Na_2CO_3), which could be isolated from seaweed washed up on the coasts of Normandy and Brittany. To isolate the sodium carbonate, seaweed was burned and the ash then washed with water; the remaining waste was destroyed by the addition of sulfuric acid (H_2SO_4). After adding too much acid, Courtois observed a cloud of purple vapor that crystallized on cold surfaces making dark crystals. Courtois suspected that this was a new element but lacked the money to pursue his observations. In supplying samples to his friends, Charles Desormes and Nicolas Clément, he hoped his research was to continue. On 29 November 1813, Desormes and Clément made public Courtois's discovery, describing the substance to a meeting of the Imperial Institute of France.



Figure 10.1.7: French chemist Bernard Courtois (1777 - 1838).

Astatine

The existence of *eka-iodine* had been predicted by Mendeleev (Figure 10.1.8), but astatine was first synthesized in 1940 by Corson (Figure 10.1.9), MacKenzie (Figure 10.1.10), and Segrè (Figure 10.1.11) at the University of California, Berkeley by bombarding bismuth with alpha particles.

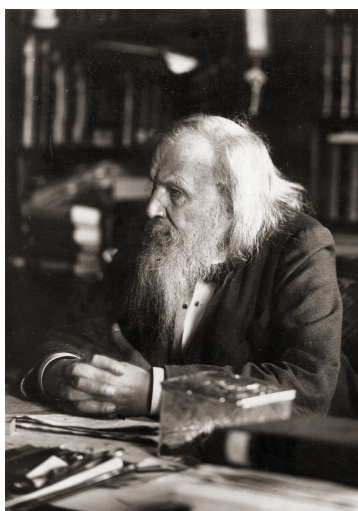


Figure 10.1.8: Russian chemist Dmitri Mendeleev (1834 - 1907).



Figure 10.1.9: Physicist and President of Cornell University, Dale R. Corson (1914 -).



Figure 10.1.10: Physicist Kenneth Ross MacKenzie (1912 - 2002).



Figure 10.1.11: Italian physicist Emilio Segrè (1905 - 1989).

Abundance

The abundance of the halogens is given in Table 10.1.2

Table 10.1.2: Abundance of the halogens.

Element	Terrestrial abundance (ppm)

F	950 (Earth's crust), 330 (soil), 1.3 (sea water), 6×10^{-4} (atmosphere)
Cl	130 (Earth's crust), 50 – 2000 (soil), 1.8×10^4 (sea water)
Br	0.4 (Earth's crust), 5 – 40 (soil), 65 (sea water)
I	0.14 (Earth's crust), 3 (soil), 0.06 (sea water), 60×10^{-3} (atmosphere)
At	Trace in some minerals

Isotopes

The naturally abundant isotopes of the halogens are listed in Table 10.1.3. All 33 isotopes of astatine are radioactive.

Table 10.1.3: Abundance of the major isotopes of the halogens.

Isotope	Natural abundance (%)
Fluorine-19	100
Chlorine-35	75.77
Chlorine-36	trace
Chlorine-37	24.23
Bromine-79	50.69
Bromine-81	49.31
Iodine-127	100%

While ^{19}F is the only naturally abundant isotope of fluorine, the synthetic isotope, ^{18}F , has half life of about 110 minutes, and is commercially an important source of positrons for positron emission tomography (PET). PET is a nuclear medicine imaging technique that produces a 3-D image of processes within the body. The system detects pairs of γ -rays emitted indirectly by a positron-emitting radionuclide (tracer), which is introduced into the body on a biologically active molecule.

Trace amounts of radioactive ^{36}Cl exist in the environment at about $7 \times 10^{-11}\%$. ^{36}Cl is produced in the atmosphere by the interaction of cosmic rays with ^{36}Ar . In the ground ^{36}Cl is generated through neutron capture by ^{35}Cl or muon (an elemental particle similar to an electron) capture by ^{40}Ca . ^{36}Cl decays with a half-life of 308,000 years making it suitable for geologic dating in the range of 60,000 to 1 million years. However, due to the large amounts of ^{36}Cl produced by irradiation of seawater during atmospheric detonations of nuclear weapons between 1952 and 1958, it is also used as an event marker for 1950s water in soil and ground water.

Iodine has 37 isotopes of iodine, but only one, ^{127}I , is stable. Of the radioactive isotopes, ^{129}I (half-life 15.7 million years) is used for radiometric dating of the first 85 million years of solar system evolution. ^{129}I is also a product of uranium and plutonium fission, and as a consequence of nuclear fuel reprocessing and atmospheric nuclear weapons tests, the natural signal has been swamped. As a consequence it can now be used as a tracer of nuclear waste dispersion into the environment. ^{129}I was used in rainwater studies to track fission products following the Chernobyl disaster.

Due to preferential uptake of iodine by the thyroid, isotopes with short half lives such as ^{131}I can be used for thyroid ablation, a procedure in which radioactive iodine is administered intravenously or orally following a diagnostic scan. The lower energy isotopes ^{123}I and ^{125}I are used as tracers to evaluate the anatomic and physiologic function of the thyroid.

Industrial production.

Industrial production of fluorine involves the electrolysis of hydrogen fluoride (HF) in the presence of potassium fluoride (KF) during which fluorine gas is formed at the anode and hydrogen gas is formed at the cathode (Figure 10.1.12). The potassium fluoride (KF) is converted to potassium bifluoride (KHF_2), (10.1.2), which is the electrolyte and intermediate to the fluorine and hydrogen, (10.1.3).

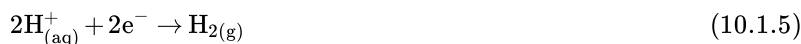


Figure 10.1.12: The fluorine cell room at F2 Chemicals Ltd, Preston, UK.

The HF is formed as a byproduct of the production of phosphoric acid, since phosphate-containing minerals contain significant amounts of calcium fluorides, which upon treatment with sulfuric acid release hydrogen fluoride, (10.1.4).



Chlorine is generally manufactured by electrolysis of a sodium chloride solution (brine). The production of chlorine results in the co-products caustic soda (sodium hydroxide, NaOH) and hydrogen gas (H_2). Chlorine can also be produced by the electrolysis of a solution of potassium chloride, in which case the co-products are hydrogen and caustic potash (potassium hydroxide). There are three industrial methods for the extraction of chlorine by electrolysis of chloride solutions, all proceeding by the same reaction at the cathode, (10.1.5), and anode, (10.1.6), which lead to the overall reaction, (10.1.7), where M = Na or K.



Bromine exists exclusively as bromide salts in the Earth's crust, however, due to leaching, bromide salts have accumulated in sea water, but at a lower concentration than chloride. The majority of bromine is isolated from bromine-rich brines, which are treated with chlorine gas, flushing through with air. In this treatment, bromide anions are oxidized to bromine by the chlorine gas, (10.1.8).



Two major sources of iodine are used for commercial production: the caliche (a hardened sedimentary deposit of calcium carbonate found in Chile) and the iodine containing brines of gas and oil fields in Japan and the United States. The caliche contains sodium nitrate (NaNO_3); in which traces of sodium iodate (NaIO_3) and sodium iodide (NaI) are found. During the production of sodium nitrate the sodium iodate and iodide is extracted. Iodine sourced from brine involves the acidification with sulfuric acid to form hydrogen iodide (HI), which is then oxidized to iodine with chlorine, (10.1.9). The aqueous iodine solution is concentrated by passing air through the solution causing the iodine to evaporate. The iodine solution is then re-reduced with sulfur dioxide, (10.1.10). The dry hydrogen iodide (HI) is reacted with chlorine to precipitate the iodine, (10.1.11).



Physical properties

The physical properties of the halogens (Table 10.1.4) encompasses gases (F_2 and Cl_2), a liquid (Br_2), a non-metallic solid (I_2), and a metallic metal (At).

Table 10.1.4: Selected physical properties of the halogens.

Element	Mp (°C)	Bp (°C)	Density (g/cm ³)
F	-219.62	-188.12	1.7×10^{-3} @ 0 °C, 101 kPa
Cl	-101.5	-34.04	3.2×10^{-3} @ 0 °C, 101 kPa

Element	Mp (°C)	Bp (°C)	Density (g/cm ³)
Br	-7.2	58.8	3.1028 (liquid)
I	113.7	184.3	4.933
At	302	337	ca. 7

Reactivity

All the halogens are highly reactive and are as a consequence of the stability of the X^- ion are strong oxidizing agents (Table 10.1.5).

Table 10.1.5: Electrochemical reduction potential for halogens.

Reduction	Reduction potential (V)
$F_2 + 2 e^- \rightarrow 2 F^-$	2.87
$Cl_2 + 2 e^- \rightarrow 2 Cl^-$	1.36
$Br_2 + 2 e^- \rightarrow 2 Br^-$	1.07
$I_2 + 2 e^- \rightarrow 2 I^-$	0.53

WARNING

Elemental fluorine (fluorine gas) is a highly toxic, corrosive oxidant, which can cause ignition of organic material. Fluorine gas has a characteristic pungent odor that is detectable in concentrations as low as 20 ppb. As it is so reactive, all materials of construction must be carefully selected and metal surfaces must be passivated. In high concentrations, soluble fluoride salts are also toxic and skin or eye contact with high concentrations of many fluoride salts is dangerous.

Use of chlorine as a weapon

Chlorine gas, also known as *bertholite*, was first used as a weapon in World War I by Germany on April 22, 1915 in the Second Battle of Ypres. At around 5:00 pm on April 22, 1915, the German Army released one hundred and sixty eight tons of chlorine gas over a 4 mile front against French and colonial Moroccan and Algerian troops of the French 45th and 78th divisions (Figure 10.1.13). The attack involved a massive logistical effort, as German troops hauled 5730 cylinders of chlorine gas, weighing ninety pounds each, to the front by hand. The German soldiers also opened the cylinders by hand, relying on the prevailing winds to carry the gas towards enemy lines. Because of this method of dispersal, a large number of German soldiers were injured or killed in the process of carrying out the attack. Approximately 6,000 French and colonial troops died within ten minutes at Ypres, primarily from asphyxiation and subsequent tissue damage in the lungs. Many more were blinded. Chlorine gas forms hydrochloric acid when combined with water, destroying moist tissues such as lungs and eyes. The chlorine gas, being denser than air, quickly filled the trenches, forcing the troops to climb out into heavy enemy fire.



Figure 10.1.13: The gas attack of the Second Battle of Ypres.

As described by the soldiers it had a distinctive smell of a mixture between pepper and pineapple. It also tasted metallic and stung the back of the throat and chest. The damage done by chlorine gas can be prevented by a gas mask, or other filtration method, making the fatalities from a chlorine gas attack much lower than those of other chemical weapons. The use as a weapon was pioneered by Fritz Haber (Figure 10.1.14) of the Kaiser Wilhelm Institute in Berlin, in collaboration with the German chemical conglomerate IG Farben, who developed methods for discharging chlorine gas against an entrenched enemy. It is alleged that Haber's role in the use of chlorine as a deadly weapon drove his wife, Clara Immerwahr, to suicide. After its first use, chlorine was used by both sides as a chemical weapon (Figure 10.1.15), but it was soon replaced by the more deadly gases phosgene and mustard gas.



Figure 10.1.14: German scientist and Nobel Prize winner Fritz Haber (1868 - 1934).



Figure 10.1.15: A poison gas attack, in World War I.

Vapor phase

All the halogens form X_2 dimers in the vapor phase in an analogous manner to hydrogen. Unlike dihydrogen, however, the bonding is associated with the molecular orbital combination of the two p-orbitals (Figure 10.1.16). The bond lengths and energies are given in Table 10.1.6

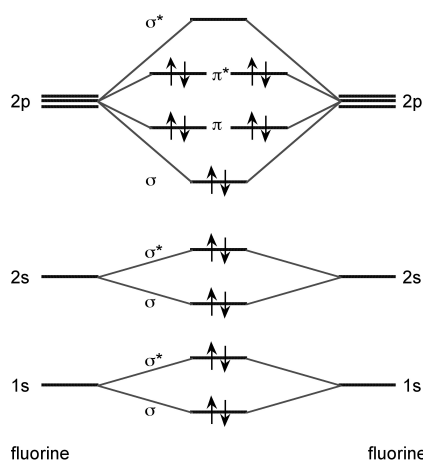


Figure 10.1.16: Molecular orbital diagram for the formation of F_2 .

Table 10.1.6: Bond lengths and energies for halogens.

Element	Bond length (Å)	Energy (kJ/mol)
F_2	1.42	158
Cl_2	1.99	243

Br ₂	2.29	193
I ₂	2.66	151

Solid state

Iodine crystallizes in the orthorhombic space group Cmca (Figure 10.1.17). In the solid state, I₂ molecules still contain short I-I bond (2.70 Å).

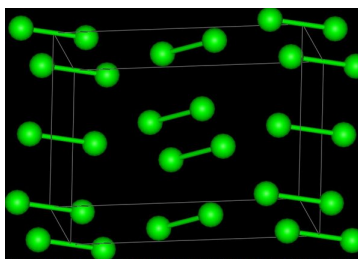


Figure 10.1.17: The solid state structure of I₂.

Compounds of the halogens.

The chemistry of the halogens is dominated by the stability of the -1 oxidation state and the noble gas configuration of the X⁻ anion.

Oxidation state

The use of oxidation state for fluorine is almost meaningless since as the most electronegative element, fluorine exists in the oxidation state of -1 in all its compounds, except elemental fluorine (F₂) where the oxidation state is zero by definition. Despite the general acceptance that the halogen elements form the associated halide anion (X⁻), compounds with oxidation states of +1, +3, +4, +5, and +7 are common for chlorine, bromine, and iodine (Table 10.1.7).

Table 10.1.7: Examples of multiple oxidation states for the halogens.

Element	-1	+1	+3	+4	+5	+7
Cl	HCl	ClF	ClF ₃ , HClO ₂	ClO ₂	ClF ₅ , ClO ₃ ⁻	HClO ₄
Br	HBr	BrCl	BrF ₃	Br ₂ O ₄	BrF ₅ , BrO ₃ ⁻	BrO ₄ ⁻
I	HI	ICl	IF ₃ , ICl ₃	I ₂ O ₄	IO ₃ ⁻	IO ₄ ⁻

Bibliography

- G. Agricola, *De Re Metallica*, Dover Publications, UK (1950)
- K. Christe, *Inorg. Chem.*, 1986, **25**, 3721.

This page titled [10.1: The Group 17 Elements- The Halogens](#) is shared under a [CC BY 3.0](#) license and was authored, remixed, and/or curated by [Andrew R. Barron \(CNX\)](#) via [source content](#) that was edited to the style and standards of the LibreTexts platform.

10.2: Compounds of Fluorine

Elemental fluorine (F_2) is the most reactive element. Fluorine combines directly with all other elements, except nitrogen and the lighter noble gases. It also reacts with many compounds forming fluorides, and many organic compounds inflame and burn in the gas. The highly reactive nature is due to the weak F-F bond (thermodynamically unstable), which provides a low activation energy to reactions (kinetically unstable). The ΔG for reactions is often large due to the strength of the resulting X-F bonds. The weak F-F bond (158 kJ/mol) is due to the small size (0.5 Å) and high nuclear charge of fluorine that result in a small overlap of the bonding orbitals and a repulsion between the non-bonding orbitals (lone pairs) on the two fluorine atoms.

Ionic salts

The ease of formation of F^- anion is due to the high electron affinity of fluorine (-322 kJ/mol). Since the fluoride ion is small (1.33 Å) and the least polarizable anion (i.e., *hard*) it is stable in ionic lattices with metal cations in a high oxidation state (high charge), e.g., MnF_4 and CrF_5 . In general the highest oxidation states for any metal are found with the fluoride salts. The large ionization energies needed to produce the cations are recovered by the high lattice energies.

Covalent compounds

The high electronegativity of fluorine means that it forms a single electron pair bond polar bond with a high ionic character. The polar nature of the bond means that there is a large inductive effect within a molecule. For example, perfluoroethanol (CF_3CF_2OH) has an acidity comparable to acetic acid.

The high strength of X-F bonds (Table 10.2.1) is also due to the high ionic character (up to 50%) that results in a high activation energy for bond breaking. In contrast, the low polarizability of the fluorine means that the inter-molecular van der Waals bonds are very weak. Thus, even with very high molecular weights the boiling point can be very low, e.g. WF_6 , Bp = 17 °C, Mw = 297.84 g/mol.

Table 10.2.1: Typical bond energies for X-F bonds.

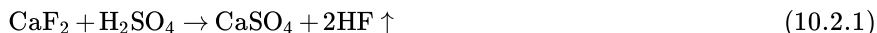
Bond	Bond energy (kJ/mol)
C-F	486
N-F	272
P-F	490

A wide range of fluoride complexes may be prepared from both metal (FeF_6^{3-} , RuF_6^- , PtF_6^{2-} , and SnF_6^{2-}) and non-metal (BF_4^- , SiF_6^{2-} , and PF_6^-) fluorides. While many fluorides are salts, when the metal is in its higher oxidation states (e.g., OsF_6 and WF_6), the formation of an ionic lattice with the appropriate cation (i.e., Os^{6+} and W^{6+} respectively) is energetically unfavorable.

Hydrogen fluoride

Hydrogen fluoride (HF) is converted to highly corrosive hydrofluoric acid upon contact with moisture. Pure hydrogen fluoride must be handled in metal or polythene vessels, while aqueous solutions will readily etch and dissolve standard laboratory glassware requiring the use of fluorinated polymer (e.g., Teflon) containers.

Hydrogen fluoride is synthesized by the reaction of a fluoride salt with a concentrated acid, (10.2.1). The HF vapor may be condensed, and then subsequently purified by distillation.



The H-F bonding in hydrogen fluoride involves an electron pair bond with a high degree of ionic character. This results in a very polar H-F bond and a large dipole moment (1.86 D).

In the vapor phase, hydrogen fluoride is monomeric above 80 °C, but at lower temperatures it associates into oligomers and small polymers, e.g., cyclic $(HF)_6$, as a consequence of strong intermolecular hydrogen bonds. As a pure liquid (Mp = -83 °C, Bp = 19.5 °C) hydrogen fluoride is extensively associated by strong hydrogen bonding to form zig-zag polymers (Figure 10.2.1).

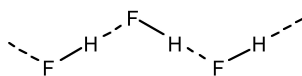
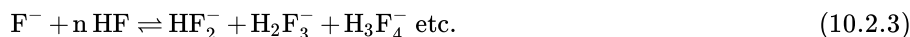


Figure 10.2.1: The hydrogen bonding in HF.

Hydrogen fluoride has a high dielectric constant (84.2) and as such is a good solvent for polar molecules. However, it is not a good solvent for salts (even fluorides) because it does not solvate cations too well. Despite this, it is useful as a solvent because it is non-oxidizing and easy to evaporate off products.

In a similar manner to water, hydrogen fluoride self-ionizes, (10.2.2). Salts of H_2F^+ are known and the F^- anion is further solvated by the HF to form a series of salts, (10.2.3). The complex anion HF_2^- is also formed in aqueous solutions of hydrogen fluoride ($\text{pK} = 0.7$).



Hydrogen fluoride is actually a weak acid in aqueous solution with a low $\text{pK} = 3.5$. In fact, HF is a weaker acid than the other halogen analogs:



This trend is despite the fluorine being more electronegative than the other halogens, but is consistent with the strength of the H-F bond (568 kJ/mol).

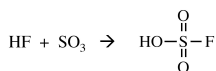
Hydrogen fluoride is used as a non-oxidizing acid for the hydrolysis of proteins and acid catalyzed condensation reaction. The stability of its salt (HF_2^-) allow for the study of very strong acids, (10.2.5) and (10.2.6).



The acidity of HF may be increased sufficiently by the addition of a fluoride acceptor (e.g., SbF_5) to facilitate the reaction with a weak base such as benzene, (10.2.7).



Finally, hydrogen fluoride can be used in the synthesis of other fluorine-containing compounds:



Organic fluorine compounds

Organic compounds in which some or all of the hydrogen atoms are replaced by fluorine have unique (and often important) properties. The high stability of fluorocarbon compounds is a consequence of the C-F bond energy (486 kJ/mol) in comparison with that of C-H (415 kJ/mol); however, while kinetically stable, fluorocarbons are not necessarily particularly thermodynamically stable.

Replacement of hydrogen with fluorine results in an increased density; since the small size of fluorine means that the minimal distortion or structural change occurs as a result of the substitution. As with metal salts, the weak inter-molecular forces means that completely fluorinated organic compounds have low boiling points. One attribute of the low inter-molecular forces is the low coefficient of friction for fluoropolymers such as polytetrafluoroethylene, commonly known as Teflon (Figure 10.2.2).

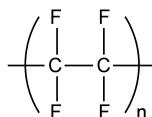


Figure 10.2.2: The structure of polytetrafluoroethylene (Teflon).

Synthetic routes to fluorocarbon compounds

The simplest route to a fluorocarbon compounds involves the direct replacement of another halogen by a metal fluoride, (10.2.9). The driving force for this reaction depends on the free-energy difference of MF and MCl, which is related to the difference in lattice energies. Thus, the larger the metal cation, the more favored the reaction. In this regard, AgF and CsF are the most effective fluorination agent.



Anhydrous hydrogen fluoride (HF) reacts with chlorocarbon compounds in the presence of a catalyst such as SbCl_5 or CrF_4 , (10.2.10). However, elevated temperatures (50 – 150 °C) and high pressures (50 – 500 psi) are required.



The direct replacement of hydrogen with fluorine is possible if the reaction is carried out under dilute conditions in the presence of a catalyst, (10.2.11).



Sulfur tetrafluoride (SF_4) is a particularly selective fluorination agent. It can be used to convert ketones to difluoro compounds, (10.2.12).



This page titled [10.2: Compounds of Fluorine](#) is shared under a [CC BY 3.0](#) license and was authored, remixed, and/or curated by [Andrew R. Barron \(CNX\)](#) via [source content](#) that was edited to the style and standards of the LibreTexts platform.

10.3: Compounds of Chlorine

Comparison to fluorine

To appreciate the chemistry of chlorine in comparison to that of fluorine it is necessary to appreciate the differences and trends between the elements. As may be seen in Table 10.3.1, chloride is significantly larger than fluorine. In addition while chlorine is an electronegative element its electronegativity is significantly less than that of fluorine, resulting in less polar bonding.

Table 10.3.1: Comparison of physical characteristics for fluorine and chlorine.

Element	Ionic radius (Å)	Covalent radius (Å)	van der Waal radius (Å)	Electronegativity
Fluorine	1.33	0.64	1.47	-4.1
Chlorine	1.81	0.99	1.75	-2.9

The X-Cl bond is an electron pair covalent bond with a highly polar nature. In this regard, chlorine is similar to fluorine. However, there are two key features with regard to chlorine's bonding that differentiates it from fluorine.

1. Unlike fluorine, chlorine can form multiple covalent bonds, e.g., ClO_4^- and ClF_3 .
2. Unlike fluorine, chlorine can form π -bonds with oxygen, i.e., $\text{Cl}=\text{O}$.

The chloride ion (Cl^-) forms salts with ionic lattices (e.g., NaCl) but also forms a wide range of complexes, e.g., $[\text{Fe}(\text{H}_2\text{O})_5\text{Cl}]^{2+}$ and $[\text{RhCl}_6]^{3-}$. Chloride also acts as a bridging ligand in which one, two or three chlorides can bridge two metal centers (Figure 10.3.1).

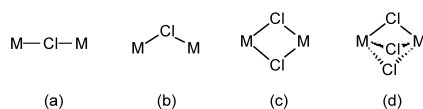


Figure 10.3.1: Structures of common halide bridging moieties.

Chloride (and bromide) bridges are usually bent, whereas fluoride bridges can be either linear or bent. As an example, BeF_2 and BeCl_2 are isostructural, consisting of infinite chains with bent bridges (Figure 10.3.2). In contrast, transition metal pentahalides show different structures depending on the identity of the halide. This, TaCl_5 dimerizes with bent bridges (Figure 10.3.3a), while TaF_5 forms a cyclic tetramer with linear fluoride bridges (Figure 10.3.3b).

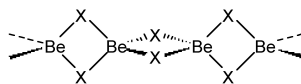


Figure 10.3.2: The solid state structure of BeX_2 ($\text{X} = \text{F}$ or Cl).

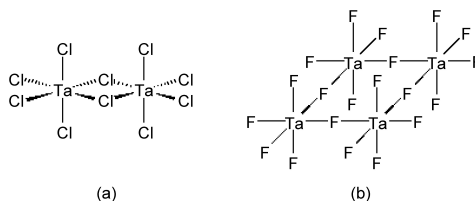


Figure 10.3.3: The solid state structure of (a) TaCl_5 and (b) TaF_5 .

The halide bridge

The bridging halide bonds can be described by both Lewis and molecular orbital (MO) theory. In a simple picture, the lone pair of a terminal halide can be thought to act as a Lewis base donor ligand to the second Lewis acidic metal center. Indeed some bridging halides are asymmetric consistent with this view; however, the symmetrical ones can be described by a resonance form. From a molecular orbital point of view, the bridging halide is represented by a combination of two metal centered orbitals with two halogen orbitals.

Hydrogen chloride

Hydrogen chloride (HCl) is prepared by the reaction of concentrated sulfuric acid (H_2SO_4) with either NaCl or concentrated HCl solution.

Hydrogen chloride is a polar molecule with a dipole of 1.08 D. However, the lower polarity as compared to that of hydrogen fluoride (1.91 D) is consistent with the physical and chemical properties. Hydrogen chloride is a gas at room temperature (Mp = -114.25 °C, Bp = -85.09 °C), and its low boiling point is consistent with weak hydrogen bonding in the liquid state. While self-ionization, (10.3.1), is very small, liquid HCl dissolves some inorganic compounds to give conducting solutions, (10.3.2).



Hydrogen chloride is soluble (and reacts) in water, (10.3.3). The pK_a of the reaction (-7.0) is larger than observed for fluorine (3.2) and as such HCl is a stronger acid than HF.



Oxides of Chlorine

Chlorine forms a series of oxides (Table 10.3.2) in which the chlorine has the formal oxidation states +1, +4, +6, and +7. The physical properties of the oxides are summarized in Table 10.3.2 While, the oxides of chlorine are not very stable (in fact several are shock sensitive and are prone to explode) the conjugate oxyacids are stable.

Table 10.3.2: Physical properties of the oxides of chlorine.

Compound	Mp (°C)	Bp (°C)
Cl_2O	-116	4
ClO_2	-5.9	10
Cl_2O_4	-117	44.5
Cl_2O_6	3.5	unstable
Cl_2O_7	-91.5	82

Dichlorine monoxide (Cl_2O , Figure 10.3.4a) is a yellowish-red gas that is prepared by the reaction of chlorine with mercury oxide, (10.3.4), or with a solution of chlorine in CCl_4 .

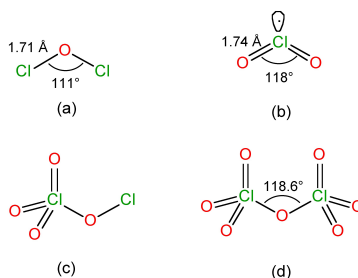


Figure 10.3.4: The structure of (a) Cl_2O , (b) ClO_2 , (c) Cl_2O_4 , and (d) Cl_2O_7 .

When heated or subject to a spark, Cl_2O explodes to Cl_2 and O_2 . Dichlorine monoxide reacts with water to form an orange-yellow solution of hypochlorous acid, (10.3.5).



Chlorine dioxide (ClO_2) is a yellowish gas at room temperature and is commonly used in industry as an oxidizing agent. The best synthesis of ClO_2 involves the reduction of potassium chlorate (KClO_3) by oxalic acid at 90 °C, since the CO_2 formed acts as a diluent for the highly explosive ClO_2 . On an industrial scale ClO_2 is made by the exothermic reaction of sodium chlorate with SO_2 in sulfuric acid, (10.3.6). The photolysis of ClO_2 yields a dark brown solid with the formula Cl_2O_3 ; however, its facile explosive decomposition precludes study.



The structure of ClO₂ (Figure 10.3.4b) is equivalent to SO₂ with one extra electron, resulting in a paramagnetic unpaired electron species. Unusually, despite the unpaired electron configuration, ClO₂ shows no tendency to dimerize. This is unlike the analogous NO₂ molecule.

Dichlorine tetraoxide (Cl₂O₄) is commonly called chlorine perchlorate as a consequence of its structure (Figure 10.3.4c). Dichlorine hexaoxide (Cl₂O₆) is an unstable red oil that has the ionic structure in the solid state: [ClO₂]⁺[ClO₄]⁻.

Dichlorine heptoxide (Cl₂O₇) is a relatively stable oil, that is prepared by the dehydration of perchloric acid at -10 °C, (10.3.7), followed by vacuum distillation. The structure of Cl₂O₇ (Figure 10.3.4d) has been determined by gas phase electron diffraction.



The reaction of Cl₂O₇ with alcohols and amines yields alkyl perchlorates (ROClO₃) and amine perchlorates (R₂NClO₃), respectively.

Fluorides of chlorine

Given the isolobal relationship between the halogens it is not surprising that the mixed dihalogens can be prepared, e.g., ClF, ICl, and BrCl. Chlorine fluoride is a highly reactive gas (Bp = -100.1 °C) that is a powerful fluorinating agent, and is prepared by the oxidation of chlorine by chlorine trifluoride, (10.3.8).



The higher electronegativity of fluorine as compared to chlorine (Table 10.3.1), and the ability of chlorine to form more than one bond, means that higher fluorides of chlorine are also known, i.e., ClF₃ and ClF₅. Chlorine trifluoride (CF₃, Bp = 11.75 °C) is a useful fluorinating agent, that is prepared by the high temperature reaction of elemental chlorine and fluorine, is a useful fluorinating agent. The gaseous pentafluoride (ClF₅, Bp = -31.1 °C) is prepared by the reaction of potassium chloride with fluorine, (10.3.10).



The structure of ClF₃ is T-shaped with two lone pairs on chlorine (Figure 10.3.5a), while that of ClF₅ is square pyramidal with a single lone pair on chlorine (Figure 10.3.5b).

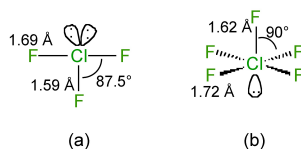
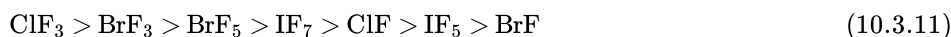


Figure 10.3.5: The structures of (a) ClF₃ and (b) ClF₅.

In general the halogen fluorides are very reactive; explosive reactions occur with organic compounds. They are all powerful fluorinating agents when diluted with nitrogen, and the order of reactivity follows:



Like most halogen fluorides, ClF, ClF₃ and ClF₅ all react with strong bases (e.g., alkali metal fluorides) to form anions, (10.3.12) and (10.3.13), and strong acids (e.g., AsF₅ and SbF₅) to form cations, (10.3.14), (10.3.15), and (10.3.16).



This page titled [10.3: Compounds of Chlorine](#) is shared under a [CC BY 3.0](#) license and was authored, remixed, and/or curated by [Andrew R. Barron \(CNX\)](#) via [source content](#) that was edited to the style and standards of the LibreTexts platform.

10.4: Oxyacids of Chlorine

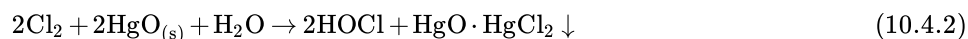
Table 10.4.1 lists the various oxyacids of chlorine. The relative strengths increase with the number of oxygen atoms since the more there are, the greater is the extent to which the negative charge on the resulting anion can be delocalized.

Table 10.4.1: Relative acidity of oxyacids of chlorine.

Oxyacid	Formula	pK _a
Hypochlorous	HOCl	7.5
Chlorous	HClO ₂	1.9
Chloric	HClO ₃	-2
Perchloric	HClO ₄	-10

Hypochlorous acid

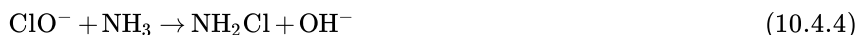
Hypochlorous acid (HOCl) can be made pure in the gas phase, (10.4.1), while strong acid solutions can be made from Cl₂O. In contrast, dilute aqueous solutions are obtained with a suspension of mercury oxide to remove the chloride, (10.4.2).



Solutions of the anion, OCl⁻, are obtained by electrolysis of brine solution; allowing the products to mix at low temperature, (10.4.3).

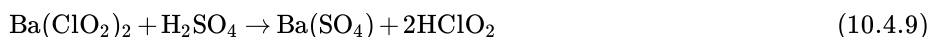
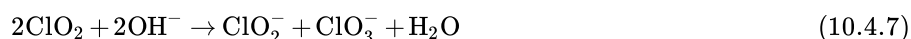


The anion (hypochlorite) is a good oxidant, (10.4.4) and (10.4.5), but can undergo disproportionation, (10.4.6); slowly at 25 °C, but fast above 80 °C.

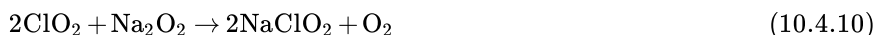


Chlorous Acid

Chlorous acid (HOClO) is prepared by the reaction of ClO₂ with base, (10.4.7), followed by the precipitation of the ClO₂⁻ salt with barium chloride, (10.4.8). The barium salt is dried and then reacted with a calculated amount of H₂SO₄, (10.4.9).



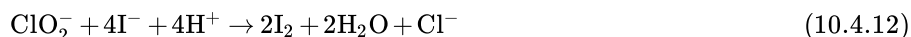
The pure acid is unknown since it is too unstable, however, salts can be prepared directly, e.g., (10.4.10).



The anion (ClO₂⁻) is stable in alkaline solutions but in acid solutions decomposition occurs, (10.4.11).



As with hypochlorite, the chlorite anion is a strong oxidant, (10.4.12).



Chloric Acid

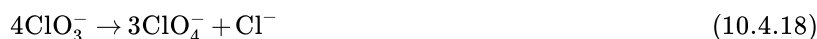
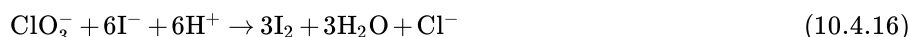
The chloric anion (ClO_3^-) is made from the reaction of chlorine gas with hot alkali (80 °C) or by the electrolysis of hot NaCl solution.



To obtain a solution of the acid, ClO_3^- is precipitated as the barium salt, (10.4.14), which is removed, dried, and suspended in water and treated with a calculated amount of H_2SO_4 , (10.4.15). The free acid cannot be isolated and a maximum concentration of only 40% can be obtained in water.



The ClO_3^- anion is pyramidal both in solid salts and in solution, and many salts are known; however, those with organic cations are explosive. The anion is a strong oxidizing agent, (10.4.16) and (10.4.17), and it disproportionates slowly in solution, (10.4.18).



Perchloric Acid

The perchlorate anion (ClO_4^-) is best made by electrolytic oxidation of chlorate in aqueous solution, (10.4.19). Fractional distillation can concentrate the solution to 72.5% which is a constant boiling mixture. This concentration is moderately safe to use, however, 100% perchloric acid may be obtained by dehydration with H_2SO_4 .



WARNING

Perchloric acid is a very dangerous liquid that will explode if traces of metal ions are present. It is also a very strong oxidizing agent that will convert organic compounds to CO_2 and H_2O .

Perchloric acid is a very strong acid that is fully ionized in aqueous solution, such that the salt $[\text{H}_3\text{O}][\text{ClO}_4]$ can be isolated. Many other perchlorate salts are known, but those with organic cations are explosive. Perchlorate salts of metals are often used when studying complex formation in aqueous solution, because ClO_4^- is a very weak ligand (PF_6^- is better) and unlikely to form complexes itself. However, perchlorate does complex with +3 and +4 cations.

This page titled [10.4: Oxyacids of Chlorine](#) is shared under a [CC BY 3.0](#) license and was authored, remixed, and/or curated by [Andrew R. Barron \(CNX\)](#) via [source content](#) that was edited to the style and standards of the LibreTexts platform.

10.5: Bromine Trifluoride as a Solvent

WARNING

Bromine trifluoride is a toxic, colorless, and corrosive liquid with a pungent choking smell that is soluble in sulfuric acid but explodes on contact with water and organic compounds. Vapors severely irritate and may burn the eyes, skin, and respiratory system. The liquid burns all human tissue and causes severe damage.

Bromine trifluoride (BrF_3) has a liquid range similar to water (Mp = 8.8 °C and Bp = 127 °C), and like water it auto ionizes, (10.5.1).



The products, like those of water's self-ionization, are an acid (BrF_2^+) and a base (BrF_4^-). However, unlike water, BrF_3 reacts with fluoride acids and bases not proton acids and bases. Thus, in BrF_3 a base is a salt that provides F^- , i.e., potassium fluoride (KF) is a base in BrF_3 solution in the same manner as potassium hydroxide (KOH) is a base in water. The product from the reaction of a fluoride donor salt with BrF_3 is the formation of the conjugate base, BrF_4^- , (10.5.2).



Other examples of this type of reaction include:



By analogy, an acid in BrF_3 solution is a compound that acts as a fluoride (F^-) acceptor, i.e., a Lewis acid, (10.5.5).



Exercise

What are the products from the reaction of HF with BrF_3 ?

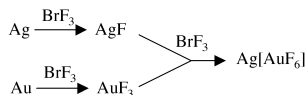
Answer



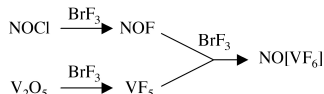
Bromine trifluoride as a fluorinating agent

Bromine trifluoride is a strong fluorinating agent that is able to convert a metal (e.g., vanadium) to its associated fluoride compound, (i.e., VF_5). A wide range of salts and oxides may be converted to fluorides with the metal in a high oxidation state. However, it should be noted that BeO , MgO , and Al_2O_3 form oxo fluorides rather than the fluoride.

The reaction of silver with BrF_3 yields the monofluoride, while the same reaction with gold yields the trifluoride, Eq. If the reactions are combined in BrF_3 solution a mixed metal fluoride salt is formed.



A similar reaction occurs with NOCl and V_2O_5 .



Exercise

What are the products from the reaction of BrF_3 with (a) Sb_2O_5 , (b) KCl , and (c) a mixture of Sb_2O_5 and KCl ?

Answer

(a) SbF_5 , (b) KF , and (c) $\text{K}[\text{SbF}_6]$.

Bibliography

- J. H. Simons, *Inorg. Synth.*, 1950, **3**, 184.

This page titled [10.5: Bromine Trifluoride as a Solvent](#) is shared under a [CC BY 3.0](#) license and was authored, remixed, and/or curated by [Andrew R. Barron \(CNX\)](#) via [source content](#) that was edited to the style and standards of the LibreTexts platform.

CHAPTER OVERVIEW

11: Group 18 - The Noble Gases

11.1: The Group 18 Elements- The Noble Gases

Thumbnail: Vial of glowing ultrapure neon. (CC SA; [Jurii](#) via <http://images-of-elements.com/neon.php>).

This page titled [11: Group 18 - The Noble Gases](#) is shared under a [CC BY 3.0](#) license and was authored, remixed, and/or curated by [Andrew R. Barron \(CNX\)](#) via [source content](#) that was edited to the style and standards of the LibreTexts platform.

11.1: The Group 18 Elements- The Noble Gases

The elements

The Group 18 elements have a particular name Noble gases. *Noble gas* is translated from the German noun *Edelgas*, first used in 1898 by Hugo Erdmann (1862 - 1910) to indicate their extremely low level of reactivity. The noble gases were often also called the *inert gases*, however, since noble gas compounds are now known this name is no longer used. Table 11.1.1 lists the derivation of the names of the Noble gases.

Table 11.1.1: Derivation of the names of each of the Group 18(VIII) elements.

Element	Symbol	Name
Helium	He	Greek <i>helios</i> meaning the <i>Sun</i>
Neon	Ne	From the Greek meaning <i>new one</i>
Argon	Ar	From the Greek meaning <i>inactive</i>
Krypton	Kr	From the Greek <i>kryptos</i> meaning <i>the hidden one</i>
Xenon	Xe	From the Greek <i>xenos</i>], meaning <i>foreigner, stranger, or guest</i>
Radon	Rn	From its <i>radioactive</i> nature

Discovery

Helium

The first evidence of helium was the observation by astronomer Pierre Janssen (Figure 11.1.1) on August 18, 1868 as a bright yellow line with a wavelength of 587.49 nm in the spectrum of the chromosphere of the Sun. On October 20 of the same year, English astronomer Norman Lockyer (Figure 11.1.2) observed a yellow line in the solar spectrum, which he named the *D3 Fraunhofer* line because it was near the known *D1* and *D2* lines of sodium. He concluded that it was caused by an element in the Sun unknown on Earth. Lockyer and Edward Frankland (Figure 11.1.3) named the element with the Greek word for the Sun, *helios*.

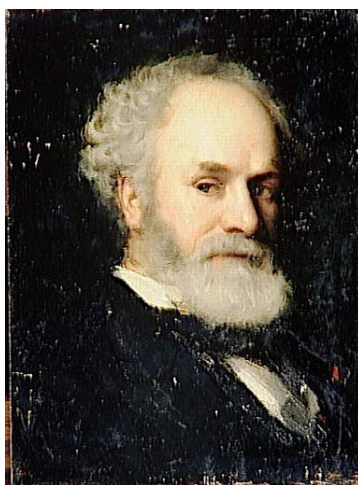


Figure 11.1.1: Portrait of French astronomer Pierre Jules César Janssen (1824 - 1907).



Figure 11.1.2: English scientist and astronomer Sir Joseph Norman Lockyer, FRS (1836 - 1920).

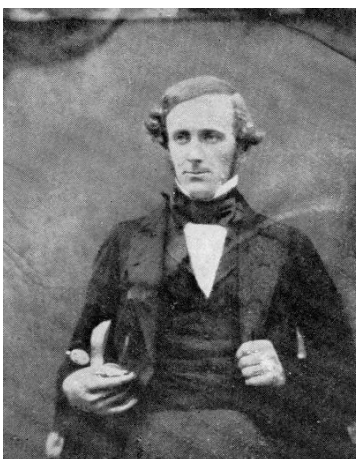


Figure 11.1.3: English chemist Sir Edward Frankland, KCB, FRS (1825 - 1899).

On March 26, 1895 British chemist Sir William Ramsay (Figure 11.1.4) isolated helium on Earth by treating the mineral cleveite (a radioactive mineral containing uranium and found in Norway) with mineral acids.

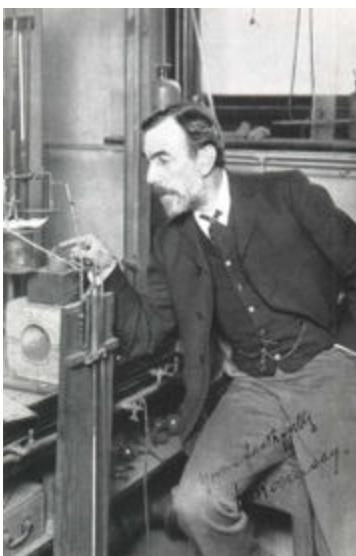


Figure 11.1.4: Scottish chemist Sir William Ramsay, KCB FRSE (1852 - 1916).

Neon

Neon was discovered in 1898 by Sir William Ramsay (Figure 11.1.4) and Morris Travers (Figure 11.1.5). When Ramsay chilled a sample of air until it became a liquid, then warmed the liquid and captured the gases as they boiled off. After nitrogen, oxygen, and

argon, the three gases that boiled off were krypton, xenon, and neon.



Figure 11.1.5: English chemist and founding director of the Indian Institute of Science, Morris William Travers (1872 - 1961).

Argon

In 1785 Henry Cavendish (Figure 11.1.6) suspected that argon was present in air but it was not isolated until 1894 by Lord Rayleigh (Figure 11.1.7) and Sir William Ramsay (Figure 11.1.4) in an experiment in which they removed all of the oxygen, carbon dioxide, water and nitrogen from a sample of clean air.



Figure 11.1.6: British scientist Henry Cavendish FRS (1731 - 1810).

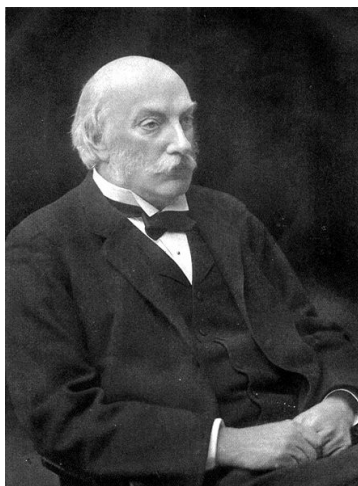


Figure 11.1.7: English physicist John William Strutt, 3rd Baron Rayleigh, OM (1842 - 1919).

Krypton

Krypton was discovered in 1898 by Sir William Ramsay (Figure 11.1.4) and Morris Travers (Figure 11.1.5) in residue left from evaporating nearly all components of liquid air.

Note

In 1960, an international agreement defined the *meter* (m) in terms of wavelength of light emitted by the ^{86}Kr isotope (wavelength of 605.78 nm). This agreement replaced the standard meter located in Paris, which was a metal bar made of a Pt-Ir alloy, and was itself replaced by a definition based on the speed of light, a fundamental physical constant. In October 1983, the *Bureau International des Poids et Mesures* defined the meter as the distance that light travels in a vacuum during $\frac{1}{299,792,458}$ s.

Xenon

Xenon was discovered by William Ramsay (Figure 11.1.4) and Morris Travers (Figure 11.1.5) on July 12, 1898, shortly after their discovery of krypton and neon.

Radon

Radon was the fifth radioactive element to be discovered after uranium, thorium, radium and polonium. Discovered in 1900 by Friedrich Dorn (Figure 11.1.8) after he noticed that radium compounds emanate a radioactive gas that he named *Radium Emanation* (*Ra Em*). Prior to these experiments, in 1899, Pierre and Marie Curie (Figure 11.1.9) observed that the *gas* emitted by radium remained radioactive for a month. Later that year, Ernest Rutherford (Figure 11.1.10) noticed variations when trying to measure radiation from thorium oxide. In 1901, he demonstrated that the emanations are radioactive, but credited the Curies for the discovery of the element.



Figure 11.1.8: German physicist Friedrich Ernst Dorn (1848 - 1916).



Figure 11.1.9: Pierre (1859 - 1906) and Marie Skłodowska-Curie (1867 - 1934) in their Paris laboratory.



Figure 11.1.10: British-New Zealand chemist and physicist Ernest Rutherford, 1st Baron Rutherford of Nelson, OM, FRS (1871 - 1937).

Abundance

The abundance of the Noble gases is given in Table 11.1.2

Table 11.1.2: Abundance of Group 18 elements.

Element	Terrestrial abundance (ppm)
He	8×10^{-3} (Earth's crust), 4×10^6 (sea water), 5 (atmosphere)
Ne	70×10^{-3} (Earth's crust), 0.2 (sea water), 18 (atmosphere)
Ar	1.2 (Earth's crust), 0.45 (sea water), 0.93×10^4 (atmosphere)
Kr	10×10^{-6} (Earth's crust), 80×10^{-6} (sea water), 1 (atmosphere)
Xe	2×10^{-6} (Earth's crust), 100×10^{-6} (sea water), 90×10^{-3} (atmosphere)

Isotopes

The naturally abundant isotopes of the Group 18 elements are listed in Table 11.1.3 All of the isotopes of radon are radioactive.

Table 11.1.3: Abundance of the non-synthetic isotopes of the Group 18 elements.

Isotope	Natural abundance (%)
Helium-3	0.000137
Helium-4	99.999863
Neon-20	90.48
Neon-21	0.27
Neon-22	9.25
Argon-36	0.337
Argon-86	0.063
Argon-40	99.600
Krypton-78	0.35
Krypton-80	2.25
Krypton-81	trace
Krypton-82	11.6

Krypton-83	11.5
Krypton-84	57
Krypton-86	17.3
Xenon-124	0.095
Xenon-126	0.089
Xenon-128	1.91
Xenon-129	26.4
Xenon-130	4.07
Xenon-131	21.2
Xenon-132	26.9
Xenon-134	10.4
Xenon-136	8.86
Radon-222	trace

Unlike most elements, helium's isotopic abundance varies greatly by origin, due to the different formation processes. The most common isotope, ^4He , is produced on Earth by a decay of heavier radioactive elements. It was also formed in enormous quantities during the *Big Bang*.

Naturally occurring ^{40}K with a half-life of 1.25×10^9 years, decays to stable ^{40}Ar (11.2%) by electron capture and positron emission, and also to stable ^{40}Ca (88.8%) via beta decay. These properties and ratios are used to determine the age of rocks.

With a half-life of 230,000 years ^{81}Kr is used for dating 50,000 - 800,000 year old groundwater. ^{85}Kr is an inert radioactive noble gas with a half-life of 10.76 years. It is produced in nuclear bomb testing and nuclear reactors. ^{85}Kr is released during the reprocessing of fuel rods from nuclear reactors.

Industrial production of the elements

Helium is extracted by fractional distillation from natural gas, which contains up to 7% helium. Since helium has a lower boiling point than any other element, low temperature and high pressure are used to liquefy nearly all the other gases. The resulting helium gas is purified by successive exposures to lowering temperatures. A final purification step with activated charcoal results in 99.995% pure Grade-A helium.

Argon is produced industrially by the fractional distillation of liquid air, a process that separates liquid nitrogen, which boils at 77.3 K, from argon, which boils at 87.3 K and oxygen, which boils at 90.2 K. Xenon is obtained commercially as a byproduct of the separation of air into oxygen and nitrogen.

Physical properties

The physical properties of the Group 18 elements are given in Table 11.1.4

Table 11.1.4: Selected physical properties of the Group 18 elements.

Element	Mp (°C)	Bp (°C)
He	-272.20	-268.93
Ne	-248.59	-246.08
Ar	-189.35	-185.85
Kr	-157.36	-153.22
Xe	-111.7	-108.12

Rn	-71.15	-61.85
----	--------	--------

All of the Noble gases show characteristic spectral lines (Figure 11.1.11– Figure 11.1.15).



Figure 11.1.11: Spectral lines of helium.



Figure 11.1.12: Spectral lines of neon.



Figure 11.1.13: Spectral lines of argon.



Figure 11.1.14: Spectral lines of krypton.

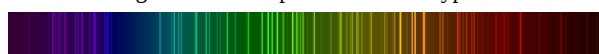
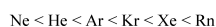


Figure 11.1.15: Spectral lines of xenon.

Compounds of the Group 18 elements.

Only a few hundred noble gas compounds have been formed. Neutral compounds of helium and neon have not been formed, while xenon, krypton, and argon have shown only minor reactivity. The reactivity follows the order:



Xenon compounds are the most numerous of the noble gas compounds. Oxidation states of +2, +4, +6, and +8 with electronegative elements, e.g., XeF_2 , XeF_4 , XeF_6 , XeO_4 , and Na_4XeO_6 . Compounds of xenon bound to boron, hydrogen, bromine, iodine, beryllium, sulphur, titanium, copper, and silver have also been observed but only at low temperatures in noble gas matrices, or in supersonic noble gas jets.

Although radon is more reactive than xenon it should form chemical bonds more easily than xenon, however, due to the high radioactivity and short half-life of radon isotopes, only a few fluorides and oxides of radon have been formed.

Krypton is less reactive than xenon, and oxidation states are generally limited to +2, KrF_2 . Compounds in which krypton forms a bond to nitrogen and oxygen are only stable below -60°C and -90°C , respectively. Krypton atoms chemically bound to other nonmetals (hydrogen, chlorine, carbon) as well as some late transition metals (copper, silver, gold), but only at low temperatures in noble gas matrices, or in supersonic noble gas jets. Similar conditions were used to obtain the first compounds of argon.

Noble gases also form non-covalent compounds, for example clathrates that consist of an atom trapped within cavities of crystal lattices of organic and inorganic compounds. Noble gases can form endohedral fullerene compounds, in which the noble gas atom is trapped inside a fullerene molecule (Figure 11.1.16).

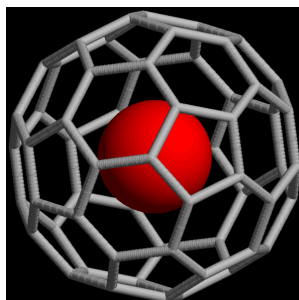


Figure 11.1.16: A skeletal structure of $\text{He}@C_{60}$.

Bibliography

- L. Pauling, *J. Am. Chem. Soc.*, 1933, **55**, 1895.
- M. Saunders, H. A. Jiménez-Vázquez, R. J. Cross, and R. J. Poreda, *Science*, 1993, **259**, 1428.

This page titled [11.1: The Group 18 Elements- The Noble Gases](#) is shared under a [CC BY 3.0](#) license and was authored, remixed, and/or curated by [Andrew R. Barron \(CNX\)](#) via [source content](#) that was edited to the style and standards of the LibreTexts platform.

Index

A

acetolysis

[1.8: Acids, Bases, and Solvents - Choosing a Solvent](#)

alcoholysis

[1.8: Acids, Bases, and Solvents - Choosing a Solvent](#)

alkaline earth metals

[4.1: The Alkaline Earth Elements](#)

aminoboranes

[6.10: Boron Compounds with Nitrogen Donors](#)

ammonation

[8.3: Hydrides](#)

ammonolysis

[1.8: Acids, Bases, and Solvents - Choosing a Solvent](#)

arsine

[8.3: Hydrides](#)

B

Beryllium

[4.3: Differences for Beryllium and Magnesium](#)

Boranes

[6.4: Boron Hydrides](#)

borohydride

[6.4: Boron Hydrides](#)

boron hydroxides

[6.7: Boron Oxides, Hydroxides, and Oxyanions](#)

boron oxides

[6.7: Boron Oxides, Hydroxides, and Oxyanions](#)

boron oxyanions

[6.7: Boron Oxides, Hydroxides, and Oxyanions](#)

Bridgman technique

[6.12: Electronic Grade Gallium Arsenide](#)

C

calcium

[4.2: Calcium the Archetypal Alkaline Earth Metal](#)

carbide lamp

[4.2: Calcium the Archetypal Alkaline Earth Metal](#)

combustion

[1.9: Chemical Reactivity - The Basics of Combustion](#)

crown ether

[3.2: Compounds of the Alkali Metals](#)

cryptands

[3.2: Compounds of the Alkali Metals](#)

D

diagonal effect

[3.3: The Anomalous Chemistry of Lithium](#)

double titration

[3.4: Organolithium Compounds](#)

G

Gallium

[6.11: Properties of Gallium Arsenide](#)

gallium arsenide

[6.11: Properties of Gallium Arsenide](#)

Grignard reagents

[4.4: Organometallic Compounds of Magnesium](#)

H

halide bridge

[10.3: Compounds of Chlorine](#)

heavy water

[2.8: Isotopes of Hydrogen](#)

hydride

[2.6: Hydrides](#)

hydrogen bond

[2.7: The Hydrogen Bond](#)

hydrogen bridged bond

[2.6: Hydrides](#)

I

interstitial hydrides

[2.6: Hydrides](#)

L

lithium

[3.3: The Anomalous Chemistry of Lithium](#)

M

Magnesium

[4.3: Differences for Beryllium and Magnesium](#)

mercuration

[5.4: Organomercury Compounds](#)

N

nuclear fusion

[2.9: Nuclear Fusion](#)

O

organolithium compounds

[3.4: Organolithium Compounds](#)

organomercury compounds

[5.4: Organomercury Compounds](#)

oxygen balance

[1.9: Chemical Reactivity - The Basics of Combustion](#)

Ozone

[9.2: Ozone](#)

P

Pentaborane(9)

[6.4: Boron Hydrides](#)

phosphines

[8.3: Hydrides](#)

Portland cement

[4.2: Calcium the Archetypal Alkaline Earth Metal](#)

S

skeletal electron pairs (SEP)

[6.5: Wade's Rules](#)

solvation

[1.8: Acids, Bases, and Solvents - Choosing a Solvent](#)

solvolysis

[1.8: Acids, Bases, and Solvents - Choosing a Solvent](#)

solvomercuration

[5.4: Organomercury Compounds](#)

specific solvation

[1.8: Acids, Bases, and Solvents - Choosing a Solvent](#)

W

Wade's Rules

[6.5: Wade's Rules](#)

Z

zinc

[5.3: Organometallic Chemistry of Zinc](#)

Index

A

acetolysis

[1.8: Acids, Bases, and Solvents - Choosing a Solvent](#)

alcoholysis

[1.8: Acids, Bases, and Solvents - Choosing a Solvent](#)

alkaline earth metals

[4.1: The Alkaline Earth Elements](#)

aminoboranes

[6.10: Boron Compounds with Nitrogen Donors](#)

ammonation

[8.3: Hydrides](#)

ammonolysis

[1.8: Acids, Bases, and Solvents - Choosing a Solvent](#)

arsine

[8.3: Hydrides](#)

B

Beryllium

[4.3: Differences for Beryllium and Magnesium](#)

Boranes

[6.4: Boron Hydrides](#)

borohydride

[6.4: Boron Hydrides](#)

boron hydroxides

[6.7: Boron Oxides, Hydroxides, and Oxyanions](#)

boron oxides

[6.7: Boron Oxides, Hydroxides, and Oxyanions](#)

boron oxyanions

[6.7: Boron Oxides, Hydroxides, and Oxyanions](#)

Bridgman technique

[6.12: Electronic Grade Gallium Arsenide](#)

C

calcium

[4.2: Calcium the Archetypal Alkaline Earth Metal](#)

carbide lamp

[4.2: Calcium the Archetypal Alkaline Earth Metal](#)

combustion

[1.9: Chemical Reactivity - The Basics of Combustion](#)

crown ether

[3.2: Compounds of the Alkali Metals](#)

cryptands

[3.2: Compounds of the Alkali Metals](#)

D

diagonal effect

[3.3: The Anomalous Chemistry of Lithium](#)

double titration

[3.4: Organolithium Compounds](#)

G

Gallium

[6.11: Properties of Gallium Arsenide](#)

gallium arsenide

[6.11: Properties of Gallium Arsenide](#)

Grignard reagents

[4.4: Organometallic Compounds of Magnesium](#)

H

halide bridge

[10.3: Compounds of Chlorine](#)

heavy water

[2.8: Isotopes of Hydrogen](#)

hydride

[2.6: Hydrides](#)

hydrogen bond

[2.7: The Hydrogen Bond](#)

hydrogen bridged bond

[2.6: Hydrides](#)

I

interstitial hydrides

[2.6: Hydrides](#)

L

lithium

[3.3: The Anomalous Chemistry of Lithium](#)

M

Magnesium

[4.3: Differences for Beryllium and Magnesium](#)

mercuration

[5.4: Organomercury Compounds](#)

N

nuclear fusion

[2.9: Nuclear Fusion](#)

O

organolithium compounds

[3.4: Organolithium Compounds](#)

organomercury compounds

[5.4: Organomercury Compounds](#)

oxygen balance

[1.9: Chemical Reactivity - The Basics of Combustion](#)

Ozone

[9.2: Ozone](#)

P

Pentaborane(9)

[6.4: Boron Hydrides](#)

phosphines

[8.3: Hydrides](#)

Portland cement

[4.2: Calcium the Archetypal Alkaline Earth Metal](#)

S

skeletal electron pairs (SEP)

[6.5: Wade's Rules](#)

solvation

[1.8: Acids, Bases, and Solvents - Choosing a Solvent](#)

solvolysis

[1.8: Acids, Bases, and Solvents - Choosing a Solvent](#)

solvomercuration

[5.4: Organomercury Compounds](#)

specific solvation

[1.8: Acids, Bases, and Solvents - Choosing a Solvent](#)

W

Wade's Rules

[6.5: Wade's Rules](#)

Z

zinc

[5.3: Organometallic Chemistry of Zinc](#)

Glossary

Sample Word 1 | Sample Definition 1

Detailed Licensing

Overview

Title: [Chemistry of the Main Group Elements \(Barron\)](#)

Webpages: 102

All licenses found:

- [CC BY 3.0](#): 81.4% (83 pages)
- [CC BY 1.0](#): 13.7% (14 pages)
- [Undeclared](#): 4.9% (5 pages)

By Page

- [Chemistry of the Main Group Elements \(Barron\) - CC BY 3.0](#)
 - [Front Matter - CC BY 3.0](#)
 - [TitlePage - CC BY 3.0](#)
 - [InfoPage - CC BY 3.0](#)
 - [Preface - CC BY 3.0](#)
 - [Table of Contents - Undeclared](#)
 - [Licensing - Undeclared](#)
 - [1: General Concepts and Trends - CC BY 3.0](#)
 - [1.1: Fundamental Properties - Oxidation State - CC BY 3.0](#)
 - [1.2: Fundamental Properties - Ionization Energy - CC BY 3.0](#)
 - [1.3: Fundamental Properties - Electron Affinity - CC BY 3.0](#)
 - [1.4: Fundamental Properties - Electronegativity - CC BY 3.0](#)
 - [1.5: Structure and Bonding - Valence Shell Electron Pair Repulsion \(VSEPR\) Theory - CC BY 3.0](#)
 - [1.6: Structure and Bonding - Crystal Structure - CC BY 3.0](#)
 - [1.7: Structure and Bonding - Stereochemistry - CC BY 3.0](#)
 - [1.8: Acids, Bases, and Solvents - Choosing a Solvent - CC BY 3.0](#)
 - [1.9: Chemical Reactivity - The Basics of Combustion - CC BY 3.0](#)
 - [1.10: Periodic Trends for the Main Group Elements - CC BY 3.0](#)
 - [2: Hydrogen - CC BY 3.0](#)
 - [2.1: Discovery of Hydrogen - CC BY 3.0](#)
 - [2.2: The Physical Properties of Hydrogen - CC BY 3.0](#)
 - [2.3: Synthesis of Molecular Hydrogen - CC BY 3.0](#)
 - [2.4: Atomic Hydrogen - CC BY 3.0](#)
 - [2.5: The Proton - CC BY 3.0](#)
 - [2.6: Hydrides - CC BY 3.0](#)
 - [2.7: The Hydrogen Bond - CC BY 3.0](#)
 - [2.8: Isotopes of Hydrogen - CC BY 3.0](#)
 - [2.9: Nuclear Fusion - CC BY 3.0](#)
 - [2.10: Storage of Hydrogen for Use as a Fuel - CC BY 3.0](#)
 - [3: Group 1 - The Alkali Metals - CC BY 3.0](#)
 - [3.1: The Alkali Metal Elements - CC BY 3.0](#)
 - [3.2: Compounds of the Alkali Metals - CC BY 3.0](#)
 - [3.3: The Anomalous Chemistry of Lithium - CC BY 3.0](#)
 - [3.4: Organolithium Compounds - CC BY 3.0](#)
 - [4: Group 2 - The Alkaline Earth Metals - CC BY 3.0](#)
 - [4.1: The Alkaline Earth Elements - CC BY 3.0](#)
 - [4.2: Calcium the Archetypal Alkaline Earth Metal - CC BY 3.0](#)
 - [4.3: Differences for Beryllium and Magnesium - CC BY 3.0](#)
 - [4.4: Organometallic Compounds of Magnesium - CC BY 3.0](#)
 - [5: Group 12 - CC BY 3.0](#)
 - [5.1: The Group 12 Elements - CC BY 3.0](#)
 - [5.2: Cadmium Chalcogenide Nanoparticles - CC BY 3.0](#)
 - [5.3: Organometallic Chemistry of Zinc - CC BY 3.0](#)
 - [5.4: Organomercury Compounds - CC BY 3.0](#)
 - [5.5: The Myth, Reality, and History of Mercury Toxicity - CC BY 3.0](#)
 - [6: Group 13 - CC BY 3.0](#)
 - [6.1: The Group 13 Elements - CC BY 3.0](#)
 - [6.2: Trends for the Group 13 Compounds - CC BY 3.0](#)
 - [6.3: Borides - CC BY 3.0](#)
 - [6.4: Boron Hydrides - CC BY 3.0](#)
 - [6.5: Wade's Rules - CC BY 3.0](#)
 - [6.6: Trends for the Oxides of the Group 13 Elements - CC BY 3.0](#)
 - [6.7: Boron Oxides, Hydroxides, and Oxyanions - CC BY 1.0](#)

- 6.8: Aluminum Oxides, Hydroxides, and Hydrated Oxides - *CC BY 1.0*
- 6.9: Ceramic Processing of Alumina - *CC BY 1.0*
- 6.10: Boron Compounds with Nitrogen Donors - *CC BY 1.0*
- 6.11: Properties of Gallium Arsenide - *CC BY 1.0*
- 6.12: Electronic Grade Gallium Arsenide - *CC BY 1.0*
- 6.13: Chalcogenides of Aluminum, Gallium, and Indium - *CC BY 1.0*
- 6.14: Group 13 Halides - *CC BY 1.0*
- 7: Group 14 - *CC BY 3.0*
 - 7.1: The Group 14 Elements - *CC BY 3.0*
 - 7.2: Carbon Black- From Copying to Communication - *CC BY 3.0*
 - 7.3: Carbon Nanomaterials - *CC BY 3.0*
 - 7.4: Nitrogen Compounds of Carbon - *CC BY 3.0*
 - 7.5: Carbon Monoxide - *CC BY 3.0*
 - 7.6: Carbon Dioxide - *CC BY 3.0*
 - 7.7: Suboxides of Carbon - *CC BY 1.0*
 - 7.8: Carbon Halides - *CC BY 1.0*
 - 7.9: Comparison Between Silicon and Carbon - *CC BY 1.0*
 - 7.10: Semiconductor Grade Silicon - *CC BY 1.0*
 - 7.11: Oxidation of Silicon - *CC BY 1.0*
 - 7.12: Applications for Silica Thin Films - *CC BY 1.0*
- 8: Group 15 - The Pnictogens - *CC BY 3.0*
 - 8.1: The Group 15 Elements- The Pnictogens - *CC BY 3.0*
 - 8.2: Reaction Chemistry of Nitrogen - *CC BY 3.0*
 - 8.3: Hydrides - *CC BY 3.0*
 - 8.4: Oxides and Oxoacids - *CC BY 3.0*
 - 8.5: Halides of Phosphorous - *CC BY 3.0*
- 9: Group 16 - *CC BY 3.0*
 - 9.1: The Group 16 Elements- The Chalcogens - *CC BY 3.0*
 - 9.2: Ozone - *CC BY 3.0*
 - 9.3: Water - The Fuel for the Medieval Industrial Revolution - *CC BY 3.0*
 - 9.4: Hydrogen Peroxide - *CC BY 3.0*
 - 9.5: Hydrogen Peroxide Providing a Lift for 007 - *CC BY 3.0*
 - 9.6: Comparison of Sulfur to Oxygen - *CC BY 3.0*
 - 9.7: Chalcogenide Hydrides - *CC BY 3.0*
 - 9.8: Oxides and Oxyacids of Sulfur - *CC BY 3.0*
 - 9.9: Sulfur Halides - *CC BY 3.0*
- 10: The Halogens - *CC BY 3.0*
 - 10.1: The Group 17 Elements- The Halogens - *CC BY 3.0*
 - 10.2: Compounds of Fluorine - *CC BY 3.0*
 - 10.3: Compounds of Chlorine - *CC BY 3.0*
 - 10.4: Oxyacids of Chlorine - *CC BY 3.0*
 - 10.5: Bromine Trifluoride as a Solvent - *CC BY 3.0*
- 11: Group 18 - The Noble Gases - *CC BY 3.0*
 - 11.1: The Group 18 Elements- The Noble Gases - *CC BY 3.0*
- Back Matter - *CC BY 3.0*
 - Index - *CC BY 3.0*
 - Index - *Undeclared*
 - Glossary - *Undeclared*
 - Detailed Licensing - *Undeclared*